

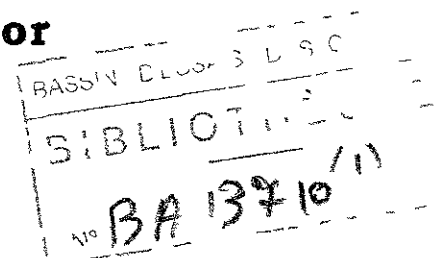


**Proceedings**  
**of the 6-th International Conference on**  
**STABILITY OF SHIPS**  
**AND OCEAN VEHICLES**

**Volume I**

**Peter A. Bogdanov, Editor**

**22 - 27 September 1997**  
**Varna, Bulgaria**



P. Bogdanov, Editor  
Proceedings of the 6-th International Conference on  
**Stability of Ships and Ocean Vehicles (STAB '97)**,  
held 22 - 27 September 1997 at Sunny Day Complex, St. St. Konstantine and Helena Resort,  
**Varna, Bulgaria**

**ORGANIZERS:**

Bulgarian Society of Naval Architects and Marine Engineers  
National Committee of Theoretical and Applied Mechanics  
National Marine Union  
Union of Bulgarian Scientists - Varna branch

**CO-ORGANIZERS:**

International Maritime Association of the Mediterranean (IMAM)  
Varna Free University (VFU)  
Varna Technical University (VTU)

*Additional copies of proceedings may be ordered from:*

**STAB '97 Conference Secretariat**  
27-B Gospodin Ivanov Str., 9000 Varna, Bulgaria,  
Phone: (+359 52) 229 710; Fax (+359 52) 244 030

*A catalogue record for this book is available from the National Library, Sofia*

**ISBN 954 715 039 1** Set of two volumes

**Copyright © 1997** by the editor. This work is subject to copyright. All rights reserved. No part of this publication may be reproduced, stored in a retrieval system or transmitted in any form by any means, electronic, mechanical, photocopying, recording or otherwise, without the prior written permission of the editor.

Printed by Bryag Print, Varna, **Bulgaria**.

In order to make this volume available as economically and rapidly as possible, the authors' papers have been reproduced and printed without any reduction, correction, etc., in a standard way for all papers submitted. The authors are fully responsible for all the information contained in their papers.

## PREFACE

STAB'97 is a follow-up Conference which continues the trend set by previous Conferences held in Glasgow (1975), Tokyo (1982), Gdansk (1986), Naples (1990) and Melbourne, Florida (1994). Being traditionally engaged with the most contemporary and important problems of stability and safety of ships and ocean vehicles, the STAB Conference is acknowledged as one of the most prestigious international events in the field of Marine Science, recognized not only by scientists, naval architects, shipbuilders and designers but also by officers of all branches of marine administration and control organizations, regulatory agencies, ship owners, marine consultants and operators, etc.

The topics of the Conference can be classified as follows

- Theoretical and Experimental Studies on Stability of Ships and Floating Marine Structures
- Advances in Experimental Technique for Investigations on Stability
- Stability criteria Philosophy and Research, Realistic Stability Criteria
- Operational Stability - the Influence of Environment
- Damage Stability
- Stability of Fishing Vessels
- Upgrading of Stability Qualities of Ro-Ro Ships
- Stability of Nonconventional Ship Types and Special Crafts
- Risk and Reliability Analysis in Stability and Capsizing
- Application of Expert Systems and On-board Computers Stability Monitoring and Control

The technical papers on these topics are distributed in two volumes of the Conference Proceedings. The second volume includes also State-of-the-Art Review Reports as well as written contributions subject of two Panel Discussions

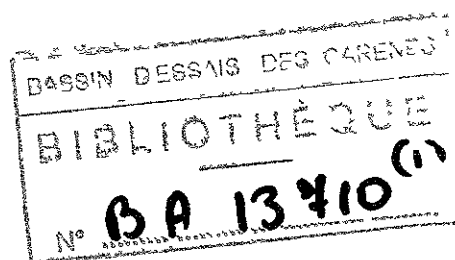
- 1 Damage Stability and Safety of Ro-Ro Vessels
- 2 Capsizing in Beam Seas - Chaos and Bifurcations

The Conference is organized by a local STAB'97 Secretariat with wide international participation. We are especially grateful to the members of the International Programme Committee and the International Advisory Board of STAB'97 as well as to the members of the ITTC Specialists Committee on Ship Stability for their considerable support and valuable contribution.

I would like to take this opportunity on behalf of the Organizers to thank the authors from about 30 countries having prepared interesting papers and written contributions in full accord with the objectives of the STAB'97 Conference.

We look forward to the continuing success of STAB Conferences in Australia and other countries in the future.

Peter A. Bogdanov  
President of the STAB'97 Conference



## INTERNATIONAL PROGRAMME COMMITTEE

Prof. Bruce Adee	University of Washington, Seattle, USA
Prof. R. Bhattacharyya	US Naval Academy, Anapolis, Maryland, USA
Prof. Dr. P. Bogdanov	Varna Free University, Varna, Bulgaria
Prof. P. Cassella	University of Naples, Naples, Italy
Prof. W.A. Cleary	Florida Institute of Technology, Melbourne, USA
Dr. E.A. Dahle	Det Norske Veritas, Høvik, Norway
Dr. A.V. Efimov	RUBIN Central Design Bureau, St Petersburg, Russia
Prof. A. Francescutto	University of Trieste, Trieste, Italy
Prof. M. Fujino	University of Tokyo, Tokyo, Japan
Dr. S. Grochowalski	National Research Council, Ottawa, Canada
Prof. G. Hearn	University of Newcastle upon Tyne, United Kingdom
Dr. H. Hormann	Germanisher Lloyd, Hamburg, Germany
Prof. A. Incecik	University of Glasgow, Glasgow, United Kingdom
Prof. Dr. S. Kastner	Bremen Polytechnic University, Bremen, Germany
Dr. R. Kishev	BSHC, Varna, Bulgaria
Prof. L. Kobylinski	SNEP Foundation, Gdansk, Poland
Prof. V.B. Lipis	CNIIMF, St. Petersburg, Russia
Prof. V.A. Nekrasov	State Maritime Technical University, Nikolaev, The Ukraine
Prof. Dr. M. A. S. Neves	State University of Rio de Janeiro, Brasil
Prof. A. Jucel Odabasi	Istanbul Technical University, Istanbul, Turkey
Prof. A. Papanicolau	National Technical University of Athens, Greece
Prof. N.M. Perez	University of Chile, Valdivia, Chile
Dr. N.N. Rakhmanin	Krylov Shipbuilding Institute, St. Petersburg, Russia
Prof. M.R. Renilson	Australian Maritime Research Centre, Australia
Prof. L. Perez-Rojas	Politecnical University Madrid, Spain
Prof. C. Sanguinetti	University of Chile, Valdivia, Chile
Prof. C. Guedes-Soares	Institute Superior Technico, Lisboa, Portugal
Prof. Dr. J. Sukselainen	VTT Manufacturing Laboratory, Espoo, Finland
Dr. S.G. Tan	MARIN, Wageningen, The Netherlands
Dr. N. Umeda	National Research Institute of Fisheries Eng., Ibaraki, Japan
Dr. D. Vassalos	University of Strathclyde, Glasgow, United Kingdom
Mr. H. Vermeer	Directorate of Shipping and Maritime Affairs, Rjswik, The Netherland
Prof. Xiu-Heng Wu	Wuhan Transportation University, Wuhan, China
Dr. Deuk-Joon Yum	Hyundai Maritime Research Institute, Ulsan, Korea

## INTERNATIONAL ADVISORY BOARD

Prof. D. Ananiev	State Technical University, Kaliningrad, Russia
Dr. P. Blume	HSVA, Hamburg, Germany
Prof. I.K. Boroday	Krylov Shipbuilding Institute, St. Petersburg, Russia
Mr. P. Cojeen	USCG, US Dept. of Transportation, Washington DC, USA
Prof. C.C. Hsiung	Dalhousie University, Halifax, Nova Scotia, Canada
Dr. I. Karaatanassov	Bulgarian Register of Shipping, Varna, Bulgaria
Dr. S.L. Karlinsky	RUBIN Central Design Bureau, St Petersburg, Russia
Prof. C. Kuo	University of Strathclyde, Glasgow, United Kingdom
Prof. R. Latorre	University of New Orleans, USA
Prof. Dr. R. Ozcan	Chamber of Shipping, Istanbul, Turkey
Dr. J.L. Montagne	Bassin d'Essais des Carenes, Paris, France
Prof. Y.I. Nechaev	Marine Technical University, St. Petersburg, Russia
Dr. A.H. Nielsen	Danish Maritime Institute, Lyngby, Denmark
Prof. G.L. Petrie	Webb Institute of Naval Architecture, Glen Cove, USA
Prof. W.G. Price	University of Southampton, United Kingdom
Prof. O. RutgerSSon	Royal Institute of Technology, Stockholm, Sweden
Prof. M. Santarelli	Buenos Aires, Argentina
Dr. J.S. Spenser	American Bureau of Shipping, New York, USA
Prof. Dr. M. Vantorre	University of Gent, Belgium
Prof. Dr. Y.L. Vorobyov	State Marine University, Odessa, The Ukraine
Prof. R. Yagle	University of Michigan, Ann Arbor, USA

## TABLE OF CONTENTS

	Page
<b>KEYNOTE ADDRESS</b>	
<i>on behalf of the 22nd ITTC Specialist Committee on Ship Stability:</i>	
<b>NUMERICAL AND PHYSICAL MODELLING OF SHIP CAPSIZE IN HEAVY SEAS: STATE OF THE ART</b>	
<i>D. Vassalos, M. Renilson, A. Damsgaard, A. Francescutto, H.Q. Gao, M. Hamamoto, J.O. de Kat, J. Matusiak, D. Molyneux, A. Papanikolaou . . . . .</i>	13
 <b>THEORETICAL AND EXPERIMENTAL STUDIES ON STABILITY OF SHIPS AND FLOATING MARINE STRUCTURES</b>	
<b>DYNAMIC TRANSVERSE STABILITY IN LONGITUDINAL WAVES: THEORETICAL AND EXPERIMENTAL RESEARCHES</b>	
<i>R. Nabergoj, G. Trincas, University of Trieste, ITALY D. Obreja, L. Crudu, L. Stoicescu, ICEPRONAV, Galati, ROMANIA . . . . .</i>	29
<b>PREDICTION OF SHIP CAPSIZE DUE TO BROACHING IN FOLLOWING AND QUARTERING SEAS</b>	
<i>N.Umeda, National Research Institute of Fisheries Engineering, Ibaraki, JAPAN D. Vassalos, Ship Stability Research Centre, University of Strathclyde, Glasgow, UK M. Hamamoto, Osaka University, Osaka, JAPAN . . . . .</i>	45
<b>A STUDY ON ROLL BEHAVIOUR OF SHIPS ON ASYMMETRIC WAVES</b>	
<i>H. Sadakane, Kobe University of Mercantile Marine, Kobe, JAPAN . . . . .</i>	55
<b>CAPSIZING OF SHIP IN LOW CYCLE RESONANCE</b>	
<i>V. Nekrasov, Ukrainian State Maritime Technical University, Nikolaev, The UKRAINE . . .</i>	65
<b>UNCERTAINTY ANALYSIS APPLIED TO THE PARAMETER ESTIMATION IN NONLINEAR ROLLING</b>	
<i>R. Penna, INSEAN, Roma, ITALY A. Francescutto, G. Contento, University of Trieste, ITALY . . . . .</i>	75
<b>THE NONLINEAR DYNAMICS OF BROACHING-TO INSTABILITY</b>	
<i>K. Spyrou, Centre for Nonlinear Dynamics and its Applications, University College, London, UK . . . . .</i>	83
<b>ON SHIP SURGING IN IRREGULAR WAVES</b>	
<i>V.B. Lipis, Central Marine Research and Design Institute, St. Petersburg, RUSSIA . . . . .</i>	93

## ADVANCES IN EXPERIMENTAL TECHNIQUE FOR INVESTIGATIONS ON STABILITY

### WIND HEELING MODEL TEST FOR THE DEVELOPMENT OF TALL SAILING VESSELS STABILITY

*J.Mlynarczyk*, Technical University of Gdansk, **POLAND** ..... 105

### EXPERIMENTAL INVESTIGATION ON CAPSIZING OF A PURSE SEINER IN BEAM SEAS

*C.I. Shin*, Nagasaki Institute of Applied Science, **JAPAN** ..... 113

### STUDY OF SHIP ROLL DECREMENT TESTS IN CALM WATER

*J.Valle*, Canal de Experiencias Hidrodinamicas de el Pardo, Madrid, **SPAIN**

*L.Perez-Rojas*, Escuela Tecnica Superior de Ingenieros navales, Madrid, **SPAIN** ..... 121

### EXPERIMENTAL RESULTS OF NONLINEAR ROLLING IN BIASED CONDITIONS IN BEAM SEAS

*G. Contento, A. Francescutto*, University of Trieste, **ITALY**

*L. Sebastiani*, CETENA, Genova, **ITALY** ..... 129

## OPERATIONAL STABILITY - THE INFLUENCE OF ENVIRONMENT

### LIQUID CARGO AND ITS EFFECT ON SHIP MOTIONS

*J. Journee*, Delft University of Technology, The **NETHERLANDS** ..... 137

### HEELING AND CAPSIZING OF SMALL VESSELS WHILE GREEN WATER SHIPPING IN FOLLOWING WAVES

*V. Yarisov*, Kaliningrad State Technical University, **RUSSIA** ..... 151

### PROBABILISTIC QUALITIES OF SEVERE SHIP MOTIONS

*V. Belenky*, National Research Institute of Fisheries Engineering, Ibaraki, **JAPAN**

*A.Degtyarev, A.Boukhanovsky*, Institute for High-Performance Computing and Data Bases,  
St. Petersburg, **RUSSIA** ..... 163

### PROBABILITY TO ENCOUNTER HIGH RUN OF WAVES IN THE DANGEROUS ZONE SHOWN ON THE OPERATIONAL GUIDANCE / IMO FOR FOLLOWING AND QUARTERING SEAS

*Y. Takaishi, K. Masuda*, Nihon University, Chiba, **JAPAN**

*K. Watanabe*, Yachiyo Engineering Co. Ltd., Meguro, Tokyo, **JAPAN** ..... 173

### ASSESSMENT OF SAFE STABILITY IN OPERATION

*L. Kobylinski*, Foundation for Safety of Navigaton and Environment Protection,

Polish Akademy of Sciences, Ilawa-Kamienka, **POLAND** ..... 181

### SHIP CRANKINESS IN FOLLOWING SEAWAY AND STABILITY REGULATION

*N. Rakhmanin, G. Vilensky*, Krylov Shipbuilding Research Institute,

St. Petersburg, **RUSSIA** ..... 191

### GUIDANCE TO THE MASTER FOR AVOIDING DANGEROUS SITUATIONS FOR A SHIP SAILING IN ROUGH FOLLOWING AND QUARTERING SEAS. CONCEPTION, CRITERIA, RATIONAL FORM OF REPRESENTATION

*A.I. Bogdanov*, Central Marine Research and Design Institute, St. Petersburg, **RUSSIA** ..... 201

**DAMAGE STABILITY****SURVIVAL TESTS OF DAMAGED FERRY VESSEL**

*A. Maron, J. M. Riola*, Canal de Experiencias Hidrodinamicas de el Pardo,  
Madrid, SPAIN ..... 223

**ON A 3-D MATHEMATICAL MODEL OF THE DAMAGE STABILITY OF SHIPS  
IN WAVES**

*G. Zaraphonitis*, MARTEDEC, Piraeus, GREECE  
*A. Papanikolaou, D. Spanos*, National Technical University of Athens, GREECE ..... 233

**STABILITY OF FISHING VESSELS****A STUDY OF THE SAFETY OF SMALL FISHING BOATS FOR THE SCALLOP  
HANGING CULTURE ON FISHING OPERATIONS IN SEVERE CONDITIONS**

*N. Kimura, K. Amagi*, Hokkaido University, Hakodate, JAPAN  
*K. Ueno*, Tokyo University of Fisheries, Tokyo, JAPAN ..... 247

**AN INVESTIGATION ON THE INFLUENCE OF STERN HULL SHAPE  
ON THE ROLL MOTION AND STABILITY OF SMALL FISHING VESSELS**

*M. A. S. Neves, L. Valerio*, Federal University of Rio de Janeiro, BRAZIL  
*M. Salas*, Institute of Naval and Marine Sciences, Austral University of Chile, CHILE ..... 259

**ON THE STABILITY SAFETY OF THE SHIPS**

*G. Boccadamo, P. Cassella, A. Scamardella*, University "Federico II" of Naples, ITALY ... 271

**A REVIEW OF DESIGN CHARACTERISTICS OF SOME FISHING VESSELS  
OPERATED IN TURKEY**

*G. Özmen*, Karadeniz Technical University, Trabzon, TURKEY  
*A. Alkan*, Yildiz Technical University, Istanbul, TURKEY  
*S. Ishida*, Ship Research Institute, Tokyo, JAPAN ..... 279

**DYNAMIC SIMULATION OF CAPSIZING FOR FISHING VESSELS  
WITH WATER ON DECK**

*Z.J.(Jerry) Huang, C.C. Hsiung*, Dalhousie University, Halifax, Nova Scotia, CANADA ... 287

**RISK AND RELIABILITY ANALYSIS  
IN STABILITY AND CAPSIZING****ANALYSIS OF A GENERAL CARGO SHIP LOST  
IN FRONT OF THE CATALONIA COAST**

*Richard Mari Sagarra, Juan Olivella Puig*, Universitat Politecnica de Catalunia,  
Barcelona, SPAIN ..... 303

**ON CAPSIZING RISK FUCTION ESTIMATION DUE TO PURE LOSS  
OF STABILITY IN QUARTERING SEAS**

*V. Belenky*, National Research Institute of Fisheries Engineering, Ibaraki, JAPAN ..... 315

**ON PROBABILITY OF SHIP CAPSIZING DUE TO BREAKING WAVES ACTION**

*V. Belenky*, National Research Institute of Fisheries Engineering, Ibaraki, JAPAN  
*S. Mordachev*, Kaliningrad State Technical University, RUSSIA ..... 323

## **APPLICATION OF EXPERT SYSTEMS AND ON-BOARD COMPUTERS FOR STABILITY MONITORING AND CONTROL**

### **SPECIALIZED SOFTWARE FOR STABILITY CONTROL ON BOARD RO-RO SHIPS**

*V. Rakitin, V. Chalakov, R. Kishev, BSHC, Varna, BULGARIA*

*N. Lyutov, Varna Free University, Varna, BULGARIA* ..... 337

### **FULL SCALE TEST OF THE INTELLIGENCE SYSTEM OF SHIP**

#### **SEAWORTHINESS ANALYSIS AND PREDICTION**

*V. Alexandrov, D. Rostovsev, A. Matlakh, Y. Nechaev, V. Polyakov,*

*State Marine Technical University, State Enterprise "Admiralty Shipyard",*

*St. Petersburg, RUSSIA* ..... 345

### **ANALYSIS OF EXTREMAL SITUATIONS AND SHIP DYNAMICS IN SEAWAY**

#### **IN AN INTELLIGENT SYSTEM OF SHIP SAFETY MONITORING**

*Y. Nechaev, State Marine Technical University, St. Petersburg, RUSSIA*

*A. Degtyarev, A. Boukhanovsky, Institute for High-Performance Computing and Data Bases,*

*St. Petersburg, RUSSIA* ..... 351

### **EXPERIENCES WITH ON BOARD COMPUTER (EXPERT) SYSTEMS FOR STABILITY**

#### **AND STRENGTH: OBJECTIVES FOR THE COMING YEARS**

*R. Kleijweg, SARC BV, Bussum, The NETHERLANDS* ..... 361

# **KEYNOTE ADDRESS**

**on behalf of**

*the 22nd ITTC Specialised Committee  
on Ship Stability*

# “Numerical and Physical Modelling of Ship Capsize in Heavy Seas: State of the Art”

by

D. Vassalos (Chairman), M. Renilson (Secretary), A. Damsgaard, A. Francescutto, H. Q. Gao, M. Hamamoto, J.O. De Kat, J. Matusiak, D. Molyneux and A. Papanikolaou  
The ITTC Specialist Committee on Ship Stability

## ABSTRACT

During the 21<sup>st</sup> ITTC, the Executive Committee approved the setting up of a ten-member Specialist Committee on Ship Stability. The main tasks recommended are to examine the techniques for carrying out model tests to investigate the capsizing of intact and damaged vessels and provide guidelines for such tests, and to assess the methods available for numerical simulations of capsizing of intact and damaged vessels. Such a committee is to provide a focal point for monitoring, reviewing and planning research, liaising with regulatory agencies, disseminating information and facilitating implementation and technology transfer. In this process, there are several issues to be addressed and questions answered. This paper is an attempt to identify, evaluate and present state-of-the-art developments concerning the numerical and physical modelling of ship capsizing in heavy seas and discuss the problems anticipated in the reduction of the relevant “tools” to practice (in the assessment of stability and in ship design, operation and management) as regards validation and standardisation. Preliminary plans by the committee for addressing these problems both in the immediate and in the foreseeable future are also presented.

## INTRODUCTION

Stability has always been treated empirically, mainly because of the inherent complexity of the problems associated with a meaningful treatment of it but also due to the fact that efforts expended towards an improved understanding of the subject were sporadic, discontinuous and uncoordinated, despite the fact that great minds have in the past devoted their lives to advancing knowledge in this area. As a result, a great many safety issues related to ship stability remain unresolved. The

number of serious casualties for Ro-Ro vessels alone still averages one per week [1], the stability problems with fishing vessels, pleasure and small craft are still at large and new challenging problems emerge with the plethora of unconventional high speed ship designs flooding the market at an ever increasing rate. Recent events, however, were to change this state of affairs. Firstly, the *Herald of Free Enterprise* tragic accident triggered a chain of events that raised stability awareness among researchers and the wider public alike. Secondly, and amongst debates

concerning suitability of stability measures, the *Estonia* disaster shook once more the foundations of the profession casting the final blow in the killing of the stability "abacus". Stability appears to have been reborn as a subject that commands the respect of the whole industry with researchers, regulators, administrators, designers, owners and operators working in tune to provide improved methodologies, procedures and measures to ensure safer ship designs that satisfy enhanced safety standards whilst competing effectively with other transportation modes. The road ahead to achieving this is filled with many obstacles but for the first time there is strong international co-operation and co-ordination of efforts with the subject attracting considerable investments centrally. In fact, the amount of research undertaken over the past few years far outweighs all research ever undertaken in this subject. More importantly, there are strong indicators that this is not a short-term surge that will fade away together with the memory of the recent tragic events. Long-term programmes have started world-wide and associations between researchers are being formed to ensure ship safety utilises fully state-of-the-art knowledge and evolves continuously with technological developments and social expectations.

Such concerted efforts by the international maritime community have forced stability to the forefront of developments, overcoming the inertia of the shipping industry and leading to scientific approaches to addressing stability. This, in turn, is paving the way to evolutionary changes in ship design, where fundamental aspects of safety are dealt with as central issues with serious economic implications rather than as simplistic compliance with prescriptive legislation. On the basis of the international stability climate alone, it requires little predictive powers to foresee intensified activities in the next five to ten years with a strong need for scientific support to resolve burning issues, currently on the International

Maritime Organisation's (IMO) regulating table, each with huge economic implications. For the first time, there is little doubt among the shipping community that decision making in the years ahead, concerning safety standards and safer ships, will have to be shaped by scientific arguments simply because developments happen faster than experience is gained, thus increasing the inherent potential for unsafe practice and inappropriate safety standards. Reliance on the ability of the scientific community to simulate raw data and experience needs to be cultivated and utilised effectively and suitable "tools" consolidated in preparation for the inevitable changes in ship design, operation and management.

The role of the ITTC in this prevailing situation can not be overemphasised. Setting up a specialist committee on ship stability offers a focal point for monitoring, reviewing and planning research, liaising with regulatory agencies, disseminating information and facilitating implementation and technology transfer. In this process, there are several issues to be addressed and questions answered. This overview is an attempt to guide discussion to those problems at hand that are relevant to ITTC.

#### **ITTC STABILITY COMMITTEE - TASKS, ISSUES AND KEY QUESTIONS**

Deriving from the above, the following tasks were recommended by the ITTC Executive Committee:

- examine the *techniques* for carrying out model tests to investigate capsizes of *intact* and *damaged* vessels and provide *guidelines* for such tests  
[physical model testing - test specification]
- assess the methods available for numerical simulations of capsizes of intact and damaged vessels

## [numerical modelling/testing]

The issues arising therefrom can be summarised as follows:

- Intact stability and operational safety
- Damage stability and survivability
- [Stability at speed] - this is clearly an area of concern currently being addressed by the HSMVs Committee.
- Validation of research results
- Reduction of results to practice
  - ⇒ Rules and criteria
  - ⇒ Operational guidelines
  - ⇒ Design practice

These, in turn, give rise to a number of key questions:

- Is understanding of ship capsize phenomena deep (clear) enough?
- Are time-domain simulation “tools” reliable enough?
- Are relevant experimental results accurate enough?
- Is standardisation of testing feasible? (numerical/experimental)

A brief overview on the above is presented in the following, leading to a number of points that merit careful discussion.

## MATHEMATICAL MODELLING OF SHIP CAPSIZE IN HEAVY SEAS

During the last four decades, research into ship behaviour at sea has, of necessity, been subdivided into three overlapping and inter-related areas which, nonetheless, have gone their separate ways in terms of theoretical and experimental work and associated progress deriving there from:

Seakeeping addressing ship behaviour in the longitudinal plane (mainly heave and pitch motions) in head seas.

Manoeuvring addressing ship behaviour on the horizontal plane (surge, sway, yaw motions) in still water.

Stability addressing extreme ship behaviour in the transverse plane (mainly roll motion) in waves.

Of the above, the subject of seakeeping has attracted the most effort, particularly at the early stages, mainly because it was more amenable to analysis by linear theory. As a result, the subject has progressed very rapidly, reaching the point where ship behaviour can be satisfactorily assessed even in extreme environments. The other two subject areas have simply staggered along, mainly because of severe non-linearities in the force mechanisms governing ship behaviour, relying heavily on support from experimental work using physical models. It is true to say, however, that due to limitations in computer capabilities, several research avenues have been explored, particularly in the area of stability, both at the conceptual (e.g. topological stability) and the working levels (e.g. capsizing sequences and modes). To this end, progress was achieved through a combination of theoretical, experimental and intuitive means based on careful thinking and a great deal of effort. The massive advances in computer technology recently, coupled with increased understanding in general ship dynamics, enabled researchers to delve into numerical simulation of ship behaviour at sea, using progressively more complex and, occasionally, more representative mathematical models of the dynamical system.

The influence brought upon research from these developments was threefold. Firstly, it affected a shift from physical model experiments to numerical experimentation without, of course, the physical understanding

afforded by the former. Secondly and, more importantly, it affected the research approach itself, in many ways substituting original thinking into the problem with undirected numerical exploration into ship dynamics. Thirdly, the traditional boundaries of the aforementioned three separate research areas started to become progressively more diffused, leading to researchers joining and expanding manoeuvring and seakeeping in order to study ship stability. Ship behaviour at sea, therefore, is progressively becoming a singular research topic, as indeed it should. Much as this state of affairs provides a cost-effective environment for experimentation, the need for creating a research-effective environment has somewhat been overlooked. A structured framework that would enable researchers to identify and define meaningful objectives and a focus on ship dynamics research, one that is based on clear thinking whilst utilising recent developments has now become more essential than forty years ago. A much needed boost in this direction, at least in terms of providing food for thought, has been given by the recent re-discovery of non-linear systems dynamics and its application to ship stability.

Considering the above, the state-of-the-art concerning mathematical/numerical modelling/testing of a vessel's stability can be summarised as follows:

### **Intact Stability**

6 D.O.F. coupled non-linear models with an auto-pilot based on some form of strip theory or 3D formulation, valid for zero to moderate speeds, containing some empirical information derived from model tests. Hydrostatic and F-K forces accurately calculated with diffraction forces less accurate. Interactive simulations in regular/irregular waves in the presence of wind and current are possible on PC with animation capabilities and ability to predicting a wide range of capsize modes. An example demonstrating state-of the-art capability is

shown in Figure 1, [2]. The polar diagram was derived from a large matrix of time-domain simulations in irregular waves for a ship in a given loading condition, indicating roll motion amplitudes as a function of ship speed and heading angle. Developments aim to provide bridge support. Other parameters include: likelihood of broaching, surf riding and capsizing. However impressive such developments might be, a great deal still remains to be done before these the derived "tools" are applied routinely to practice. For example, most auto-pilot models used in time-domain simulations are of relatively simple nature and these may not resemble present-day control algorithms on board ships. Furthermore, in extreme weather the helmsman is likely to take control of the wheel. Knowing that the auto-pilot model has a strong influence on the end results, such deficiencies must be accounted for before embarking on extensive simulations.

Results demonstrating the capability of the dynamical systems approach are shown in Figure 2, [3], referring to a surge-sway-yaw-roll model with an auto-pilot. Starting from a stationary state (in this case a steady surf-riding situation), it is possible to gain a feel of the global picture of what might ensue as a result of taking action, such as changing the propeller revolutions, in the whole range of heading angles. Considering that it represents only a "slice" from a 12D phase-space, this figure helps to provide only a hint of the complexity surrounding ship capsizes.

### **Damage Stability**

A similar model drifting at zero speed, coupled to a water ingress model. All terms in the coupled systems change with time in the presence of progressive flooding. An example demonstrating state-of-the-art capability is shown in Figure 3, [4]. The results show the capsize (roll motion) of a damaged RoRo vessel subjected to progressive flooding in

irregular waves with freeing ports on the RoRo deck (compartment 1: damage below the bulkhead deck; compartment 2: damage above the bulkhead deck).

### Discussion Points

- ship capsize physics not yet completely understood
- modelling of critical waves (wave packets) in extreme seas, i.e., understanding, realistic description and accurate numerical modelling of extreme sea conditions, estimate of probability of occurrence as well as fully non-linear methods of calculating extreme ship motions in these and probabilistic characterisation of the ensuing response are demanding challenges. Furthermore, probabilistic approaches can hide uncertainties in the modelling of hydrodynamic phenomena
- problems with new unconventional designs
- problems with high speed craft
- accurate modelling of water ingress and flood/water vessel interaction (water on deck intact - fishing vessels, water on deck following damage - RoRos, water over bulwark - open deck container ships)
- human factors
- conversion of numerical models to engineering "tools"

### PHYSICAL MODELLING OF SHIP CAPSIZE IN HEAVY SEAS

As indicated in the previous section, vast improvements in computer capacity and power, coupled with developments in non-linear systems and the continuously increasing level of awareness with regard to enhanced safety standards at sea, have provided the right nurturing environment for rapid developments in time domain simulation methods of extreme vessel behaviour in the marine environment. In parallel, the need for the use of experimental facilities re-directed itself towards a new focus. Namely, testing for vessel behaviour in

simulated extreme environments for prediction, validation, assessment, data generation purposes. For research into ship stability in extreme astern seas, all these aspects must be explored for achieving meaningful progress. This, normally involves the following:

### Type of Tests

- *captive/partially captive tests*  
to measure wave forces on the model in a range of conditions representative of extreme environments. In addition these facilitate both the understanding of the mechanisms involved and the development of time-domain simulation models.
- *free-running tests*  
to facilitate validation of computer simulation models as well as enhanced insight into the complex phenomena of ship capsize; measurement of motions, position and attitude of model; capsize events
- *free-drifting tests* (damage)  
measurement of water ingress, motions, position and attitude of model; capsize events; survival time
- *visualisation tests*  
enhanced insight and understanding of capsize physics and for analyses purposes
- *full-scale tests*  
seakeeping and manoeuvring data

An indication of the contribution of model experiment results to improving the stability and operational safety of ships is shown in Figure 4, [5], referring to model experiments in severe astern seas carried out in Japan during 1994-95, the results of which were used to support the draft IMO guidance to master for avoiding dangerous situations in astern seas. Capsize modes corresponding to parametric resonance, harmonic resonance, pure loss of stability and broaching-to have been recorded. Experimental investigations can be extremely useful in this respect but again a great deal must be accomplished towards standardising physical modelling/testing of ship capsize and

maximising the benefits that can be gained there from. For example, the accuracy of generating extreme waves from the superposition of harmonic waves and using this as a basis to characterise the probability of encountering dangerous situations and capsizing, merits further thought and discussion. Figure 5, [6], presents a comparison between results derived from time-domain simulations and those from physical model experiments, showing excellent agreement. However, the numerical models describing both the vessel motion and the water ingress are very simple, raising a series of questions in need of close scrutiny. Furthermore, the experimental results, because of the severe limitations in the cost and time required for model experiments, often rely on single outcomes to define a mean boundary of survivability in random waves. As a result, it is not uncommon for experimental data to provide erroneous information which needs to be carefully processed.

### Discussion Points

- representation of the extreme wave environment and characterisation of the extreme model response
- lack of special experimental techniques and procedures with strict requirements on accuracy
- (cheap) sensor technology
- dependence on initial conditions
- transient flooding (damage)

### STABILITY/SAFETY ASSESSMENT

A clear tendency of moving from prescriptive to performance-based safety regulations is emerging internationally. Introduction of performance standards is seen as beneficial from industry as these allow to consider alternative designs as well as a rapid implementation of technological innovation. In this respect, the analysis of alternative design solutions requires the development of a

standardised approach to demonstrate compliance with the requirements of intact and damage stability regulations by a combination of physical model experiments and numerical model tests whilst applying probabilistic techniques in the process of assessing stability. The trends emerging in terms of stability/safety assessment can be summarised as follows:

<p><b>Static stability + safety margin</b> (prescriptive criteria) - useful for comparative assessment of vessel safety but can be misleading as the physics governing static stability can be much different for the physics governing dynamic stability</p>	⇒	<p><b>Dynamic stability</b> (performance-based criteria) IMO - New Load Line Convention; Equivalence tests for RoRo vessels; New High Speed Craft Code</p>
<p><b>Deterministic Methods</b></p>	⇒	<p><b>Probabilistic Approaches</b></p>
<p><b>Single-level</b> (mode-specific approaches)</p>	⇒	<p><b>Multi-level</b> (multi-mode, integrated approaches/ systems)</p>

### VALIDATION/VERIFICATION

This, in itself, is a topic that merits wide ranging attention. For the purpose of this review, the following discussion points are put forward:

### Discussion Points

#### *What to validate?*

- mathematical model (equations)
- numerical model (algorithm)
- behaviour (motions, capsize modes, probability of occurrence)
- trends, relationships (parametric studies)
- criteria (limiting parameters)
- regulations (“equivalence” tests for RoRos)
- procedures (probabilistic damage stability)

*How to validate?* (define procedure, set standard?)

- ITTC efforts (container ship seakeeping benchmarks, semi-submersible drift force studies)
- deterministic tests using simple mathematical models
- sensitivity studies (discretisation mesh, time stepping procedure, duration of simulation)
- comparative studies (linear-approximate non-linear, fully non-linear, 2D, 3D)
- blind bench-marking for unknown cases and bench-marking of known cases.

## DESIGN/OPERATIONAL OUTLINES

Trends in this area can be briefly summarised as follows:

*design:* define key factors affecting ship safety against capsizing, establish relationships between ship design parameters, limiting stability and environmental parameters

*operation:* provide guidelines to avoid dangerous situations leading to capsize

## Discussion Points

The hydrostatic righting arm curve in calm water, continues still to provide the best platform for judging safety against capsizing *but* understanding vessel dynamics in extreme seas is now of paramount importance. In this respect, prescriptive criteria are giving way to performance-based standards and "Design for Safety" is slowly emerging as a priority area and a means for addressing ship safety in place of the traditional regulations-based approach.

## PROGRESS TO DATE AND FUTURE PLANS

The first meeting of the Stability Committee was held in Trondheim following the 21<sup>st</sup> ITTC, in September 1996, to discuss general issues and appoint a secretary. The second meeting was held in Osaka in conjunction with the Second International Workshop on the "*Stability and Operational Safety of Ships*". At this meeting the recommendations from the Executive Committee were discussed and the following internal working groups and coordinators established, with the first task of completing state-of-art review reports within the first year:

- Guidelines for model tests on intact stability (M. Hamamoto, Osaka University)
- Techniques for numerical simulation of intact stability (J.O De Kat, MARIN)
- Guidelines for model tests on damage stability (D. Molyneux, IMD)
- Techniques for numerical simulation of damage stability (A. Papanikolaou, NTUA)

The next meeting will be held in conjunction with the Third International Workshop on the "*Theoretical Advances in Ship Stability and Practical Impact*" in Crete. It is, in deed, the intention to use these round-table-discussion workshops as a platform for addressing in-depth the problems at hand with all known experts actively involved in the area invited to participate. Finally, liaison has been established and collaboration sought with a number of other specialist committees including: Loads and Responses, Manoeuvring, Safety of High Speed Marine Vehicles, Environmental Modelling and Model Testing of High Speed Marine Vehicles.

## CONCLUDING REMARKS

Considering the above, the following summary remarks can be made:

- Progress in understanding ship capsize phenomena and in developing numerical "tools" and experimental methods for

qualifying and quantifying the associated extreme behaviour has been impressive, particularly over the recent past.

- However, lack of complete understanding of ship capsizing physics, lack of standard procedures and methods and hence lack of appreciation of the effect of the unavoidably adopted “shortcuts” in addressing this problem cast serious doubts on the reliability of the developed “tools”.
- Many problems still remain in need of solution before a satisfactory answer can be provided to the questions raised.
- For the first time in Ship Stability Research, there is a focal point for co-ordinating efforts on an international scale, in the form of an ITTC Specialist Committee. There is much pride as there is enormous responsibility in undertaking this task, a fact readily acknowledged by all the Committee members.

## REFERENCES

- [1] Lloyd’s Register: “*World Fleet Statistics*” and “*Casualty Return*”.
- [2] De Kat, J.O.: “The Practical Role of Time Domain Capsizing Simulation”, International Workshop on *Numerical and Physical Simulation of Ship Capsizing in Heavy Seas*, Ross Priory, University of Strathclyde, July 1995.
- [3] Spyrou, K.: “Dynamic Instability in Quartering Seas - Part II: Analysis of Ship Roll and Capsizing for Broaching”, *Journal of Ship Research*, Vol. 40, No. 4, 1996, pp.326-336.
- [4] Letizia, L.: “Damage Survivability of Passenger Ships in a Seaway”, PhD Thesis, University of Strathclyde, Department of Ship and Marine Technology, 1996.
- [5] Hamamoto, M., Enomoto, T. and Sera, W.: “Model Experiments in Heavy Seas”, International Workshop on *Numerical and Physical Simulation of Ship Capsizing in Heavy Seas*, Ross Priory, University of Strathclyde, July 1995.
- [6] Vassalos, D., Pawlowski, M. and Turan, O.: “A Theoretical Investigation on the Capsizing Resistance of Passenger/Ro-Ro Vessels and Proposal of Survival Criteria”, Final Report, Task 5, The North West European R&D Project, March 1996.

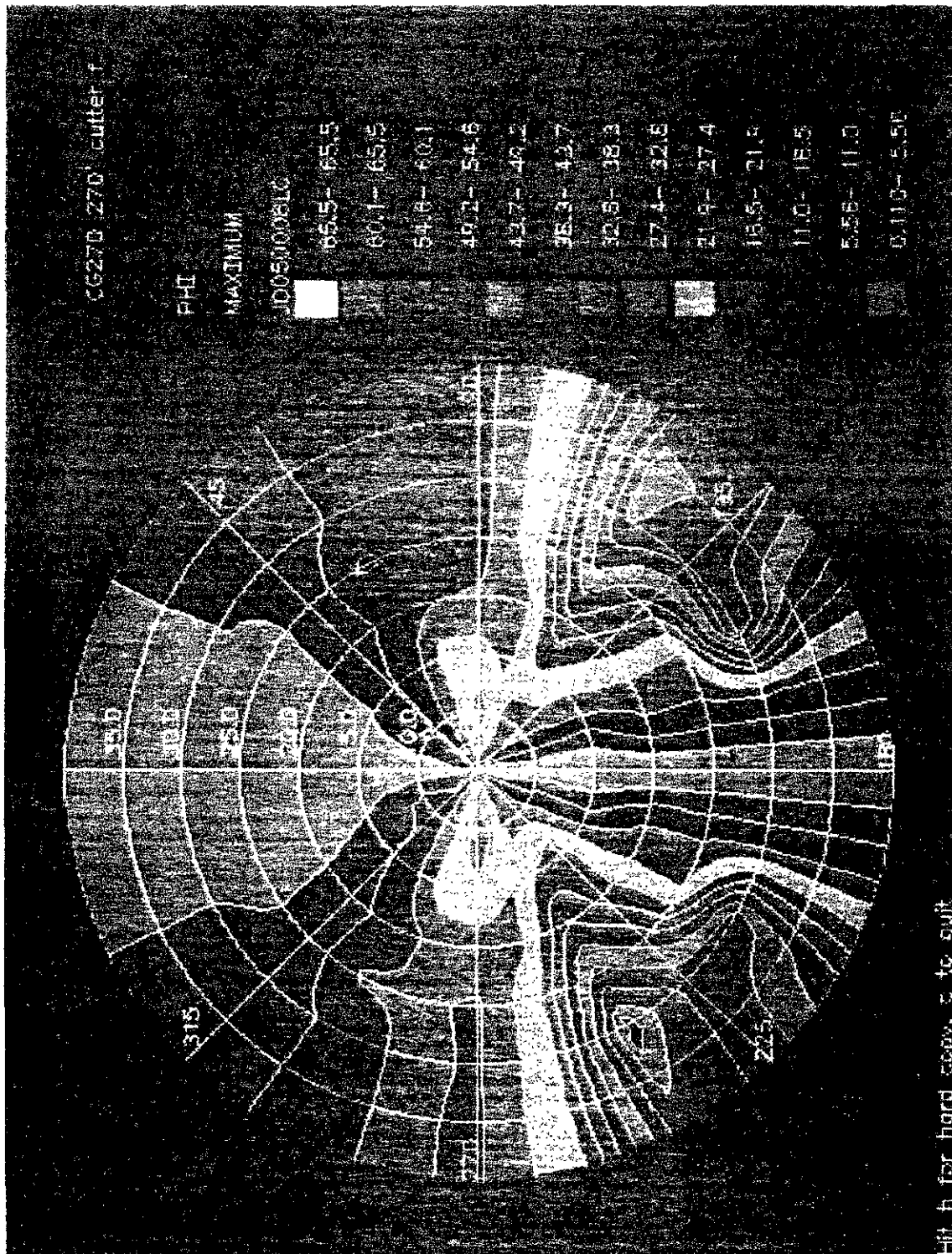


Figure 1: Roll Motion Amplitudes Polar Diagram, [2]

autopilot : (3,3,1),  $GM = 1.51\text{ m}$

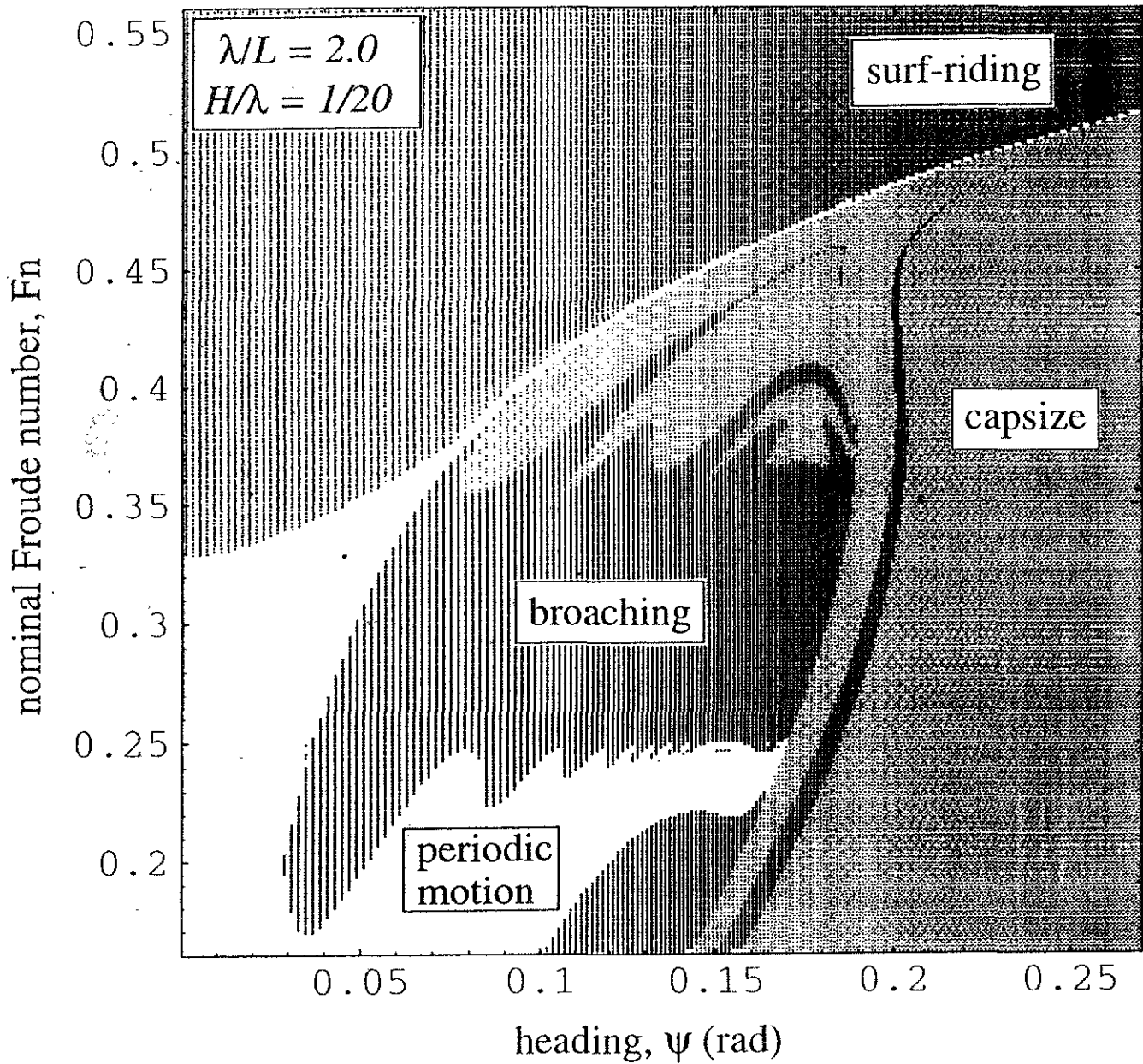


Figure 2: 'Multiple-effect' global analysis helps to locate the domains of surf-riding, periodic-motion, broaching and capsizing, [3]

Hs = 2.8 m; To=6.0; KG = 10.54 m; Freeboard = 0.7 m

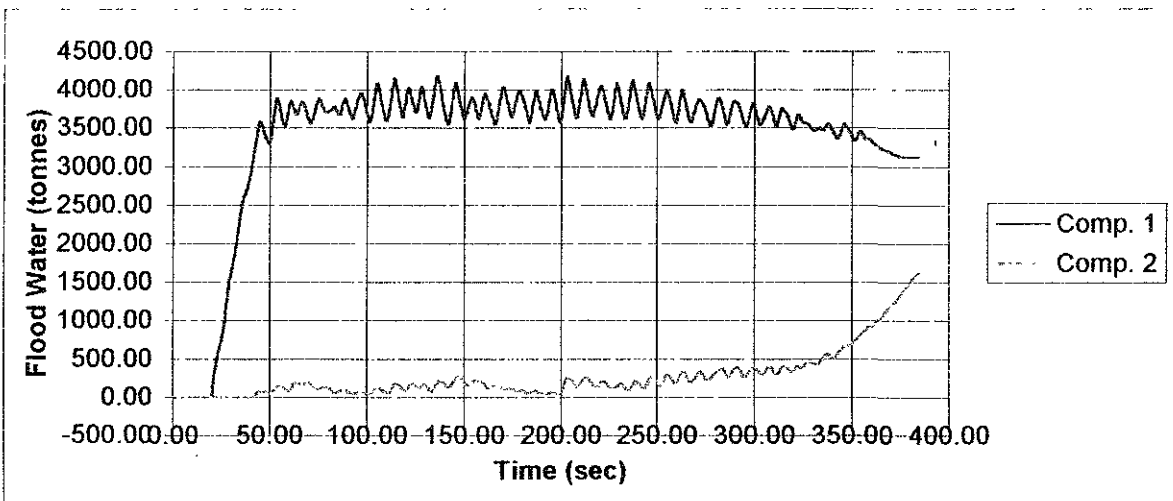
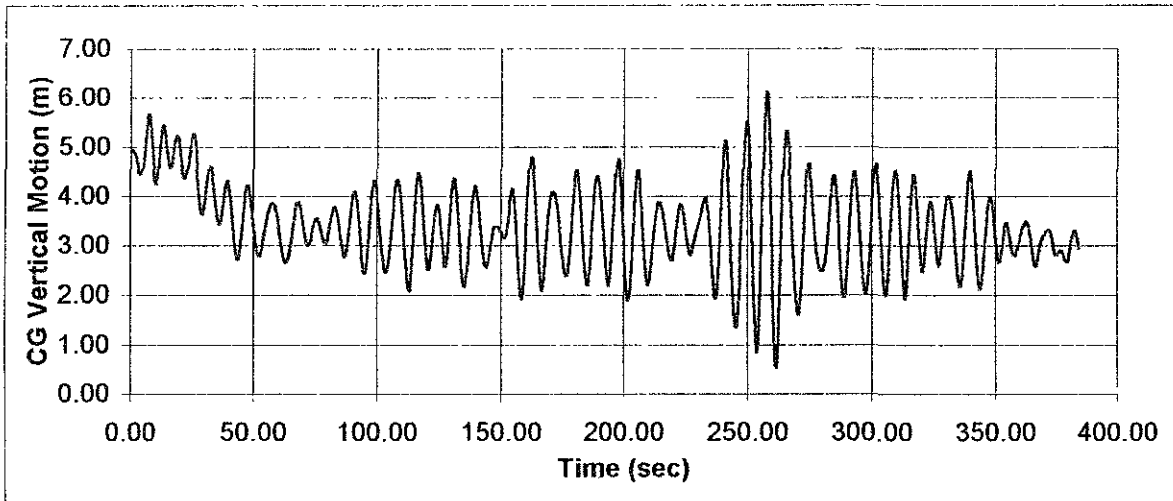
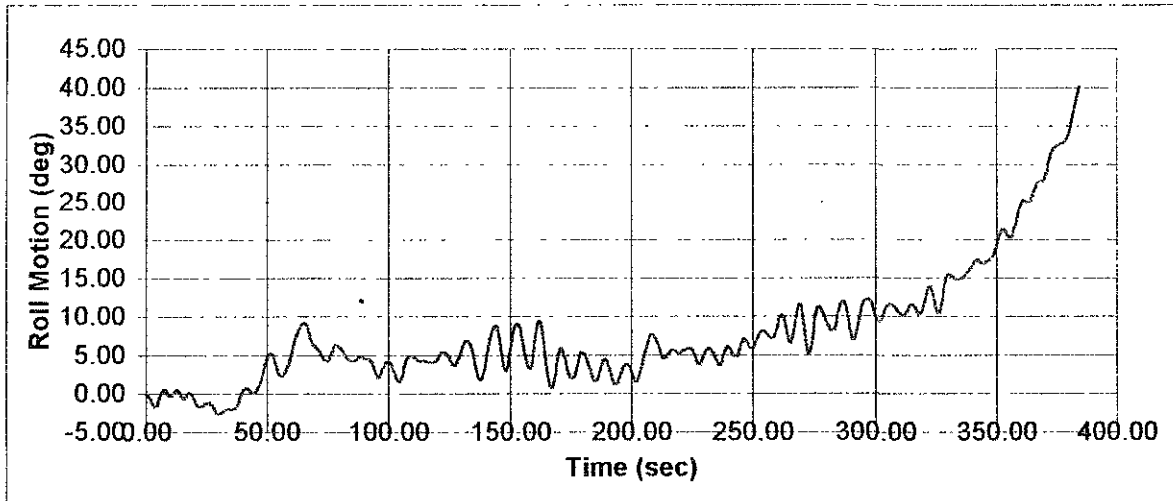
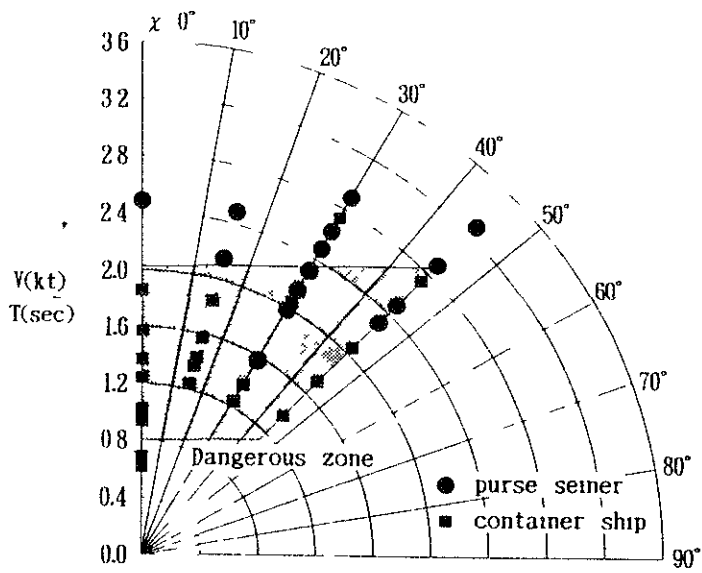
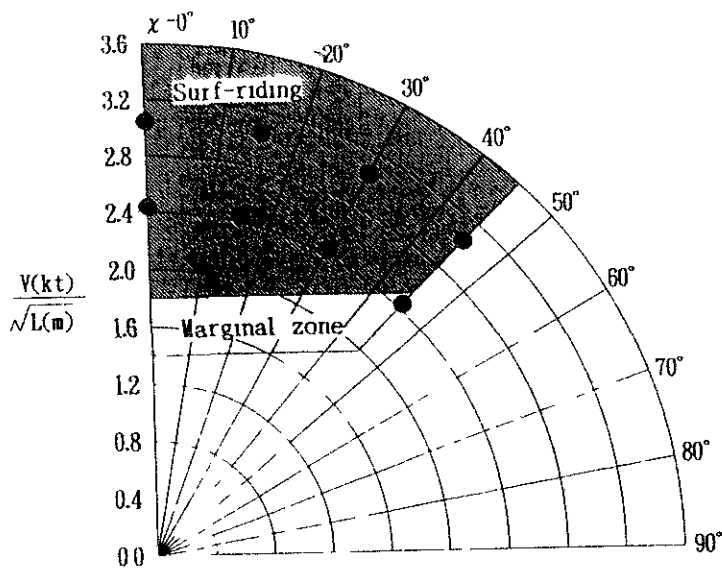


Figure 3:

Capsize of a Damaged RO-RO Subjected to Progressive Flooding.  
(Standard Penetration with Freeing Ports on the RO-RO Deck), [4]



(a) Examples of model capsizals in the dangerous zone



(b) Examples of model surf-riding in the dangerous zone due to surf-riding

Figure 4: Model Experiments in Severe Astern Seas, [5]

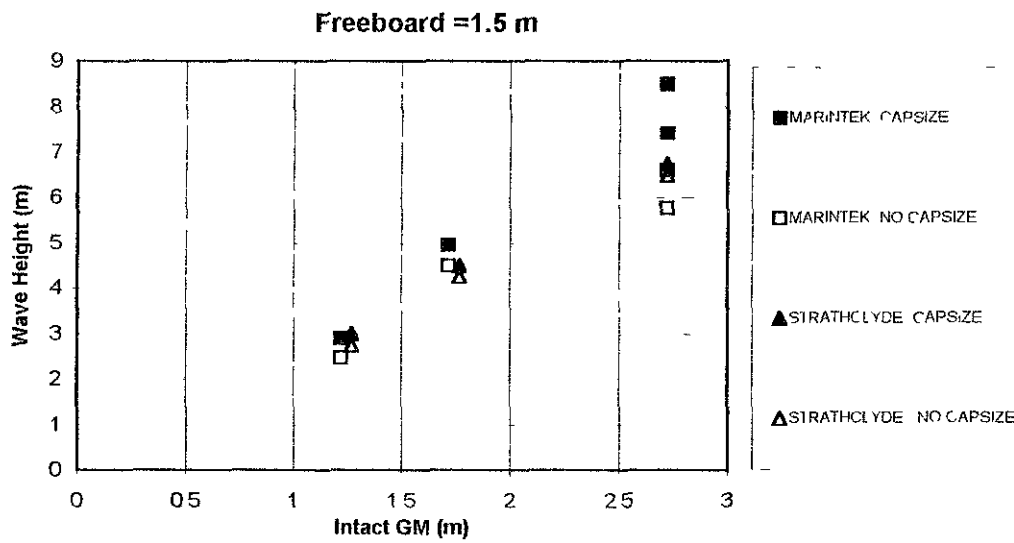
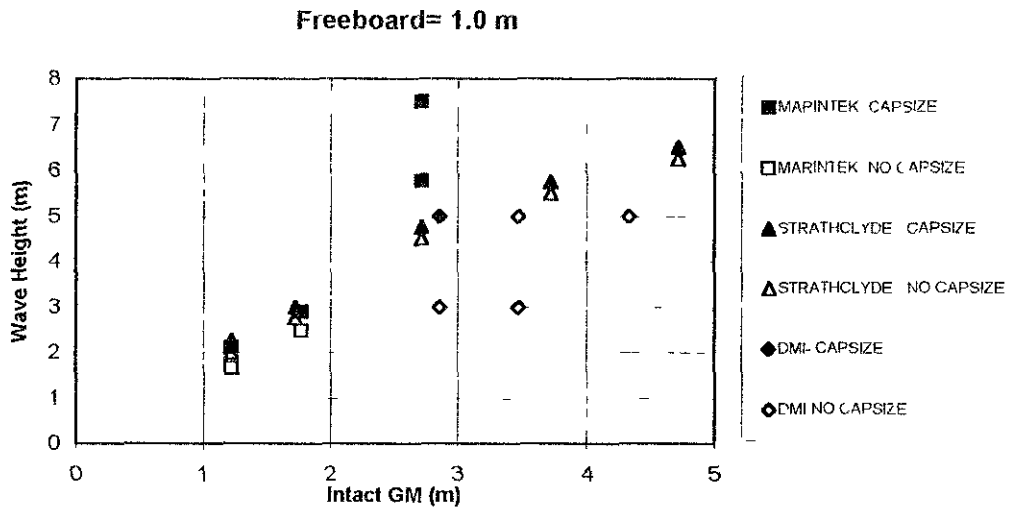
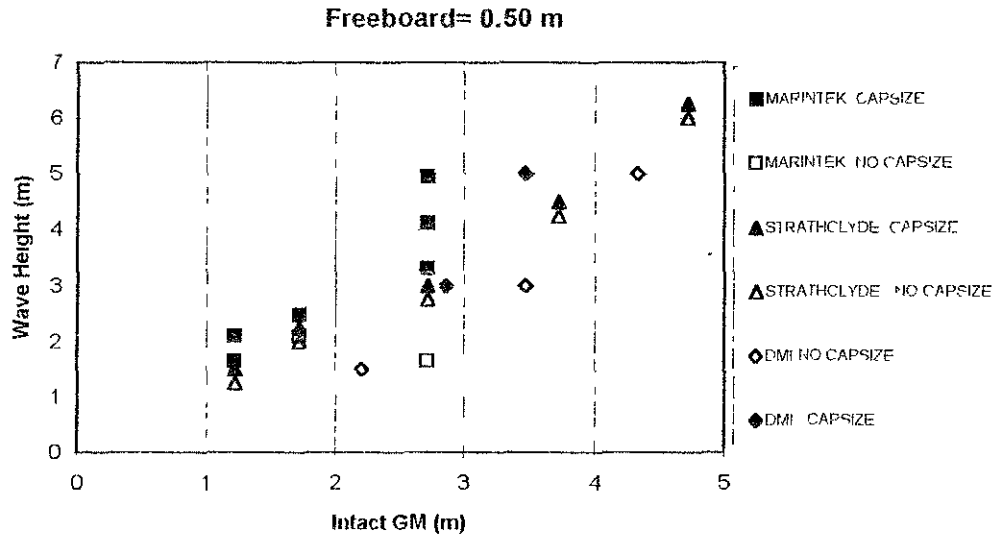


**Figure 5** SHIP2 - SIDE CASINGS - Comparison between theoretical and experimental results (The Joint North West European R&D Project), [6]

**THEORETICAL AND  
EXPERIMENTAL STUDIES  
ON STABILITY OF SHIPS  
AND FLOATING MARINE  
STRUCTURES**

## DYNAMIC TRANSVERSE STABILITY IN LONGITUDINAL WAVES : THEORETICAL AND EXPERIMENTAL RESEARCHES

R. Nabergoj (\*), D.C.Obreja (\*\*), G. Trincas (\*), L.Crudu (\*\*), L.Stoicescu (\*\*\*)

- (\*) Department of Naval Architecture, Ocean and Environmental Engineering, University of Trieste, Via A.Valerio 10, 34127 Trieste, Italy  
 (\*\*) Research and Design Institute for Shipbuilding, ICEPRONAV S.A., 19A, Portului Street, 6200 Galati, Romania  
 (\*\*\*) University "Dunarea de Jos", 47, Domneasca Street, 6200 Galati, Romania

### ABSTRACT

During the seakeeping tests carried out in the Ship Hydrodynamic Laboratories of ICEPRONAV S.A.Galati the occurrence of the induced roll motions of a 2700 dwt multipurpose cargo ship model was observed.

With the aim of a better understanding of the possible excitation sources of the induced roll motions and of the complex phenomenon of transverse stability in longitudinal waves, an experimental and theoretical scientific co-operation between the University of Trieste, ICEPRONAV S.A.Galati and University of Galati was developed.

The problems are formulated and solved within the linear hydrodynamic theory of a non-viscous fluid.

In order to reproduce the real physical phenomenon, free-running, semicaptive and captive model test were correlated.

The Ship Hydrodynamic Laboratories of ICEPRONAV S.A.Galati have performed the measurements for ship model motions, the radiation and diffraction hydrodynamic forces and moments and the restoring moment in longitudinal waves.

The results of this complex experimental program provides important data which should validate the specific theoretical modules as well as the general theoretical model of the ship behaviour in longitudinal waves, the comparison between theoretical and experimental results being presented.

### NOMENCLATURE

$A_{jk}$	added mass
$B_{jk}$	damping coefficient
$C_{jk}$	restoring coefficient
$D_{01}$	linear coefficient of damping
$D_{02}$	non-linear coefficient of damping
$F_n$	Froude number
$F_{3a}$	heave exciting force
$F_{4a}$	roll exciting moment
$F_{5a}$	pitch exciting moment
$I_4$	roll moment of inertia
$I_5$	pitch moment of inertia
$GM$	metacentric height (still water)
$K_B(t)$	function of time in Bernoulli equation
$K_3$	cubic restoring coefficient
$L$	length between perpendiculars
$M_D$	diffraction component of the restoring moment
$M_I$	Froude-Krylov component of restoring moment
$M_R$	radiation component of restoring moment
$M_U$	restoring moment component due to the pressure field changes when the ship is running in still water
$M_t$	total restoring moment in longitudinal waves
$U$	ship speed
$g$	gravitational constant
$h_w$	wave height
$K$	wave number
$m$	mass of body
$p$	fluid pressure

$p_0$	atmospheric pressure
$t$	time
$z$	heave motion
$\Phi$	velocity potential
$\Phi_I$	incident wave potential
$\Phi_D$	diffraction potential
$\Phi_R$	forced motion potential (radiation potential)
$\Phi_U$	velocity potential due to the steady motion in still water
$\lambda$	wave length
$\omega$	circular frequency of encounter
$\varphi$	roll amplitude
$\theta$	pitch amplitude
$\zeta_a$	wave amplitude

### 1. INTRODUCTION

The investigation of hydrodynamic qualities regarding the transverse stability of the ship on longitudinal waves represents a problem of an utmost importance. The theoretical model is rendered by considering the ship heeling when the velocity potential function of the fluid motion for an asymmetric body must be evaluated. Taking into account the hypothesis of the linear hydrodynamic model, the velocity potential may be written (Boroday, [1]) under the form

$$\Phi = \Phi_U + \Phi_I + \Phi_D + \Phi_R. \quad (1)$$

The sum of potentials  $\Phi_I$  and  $\Phi_D$  describes the diffraction problem, which is generated by the interaction of incident waves with the inclined ship hull, considered to be fixed in waves. The radiation potential describes the radiation problem, which is caused by ship forced motion in still water at fixed heel angle. The transverse stability of the ship in longitudinal waves is characterized by the restoring moment defined as equal and opposite to the hydrodynamic moment of the heeled ship as regard to the longitudinal central axis

$$M_r(\varphi, t) = M_U + M_I + M_D + M_R. \quad (2)$$

In order to develop performant computer programs for ship transverse stability evaluation in longitudinal waves, it was considered that an extensive experimental research is necessary for the investigation of the physical aspects of ship inclining.

During the seakeeping tests, carried out for the 2700 dwt cargo ship model, the occurrence of the induced motions on regular longitudinal waves were observed and measured, both for Froude numbers  $F_n = 0$  and  $F_n = 0.25$ .

Figs.1 and 2 bear the non-dimensional transfer functions of the induced roll motions on head waves and following waves respectively, as functions of  $L/\lambda$  ratio. The non-dimensional form is obtained by using the ratio  $\frac{\varphi}{K \cdot \zeta_a}$ . The

maximum response is obtained in the second instability domain that corresponds to the main resonance.

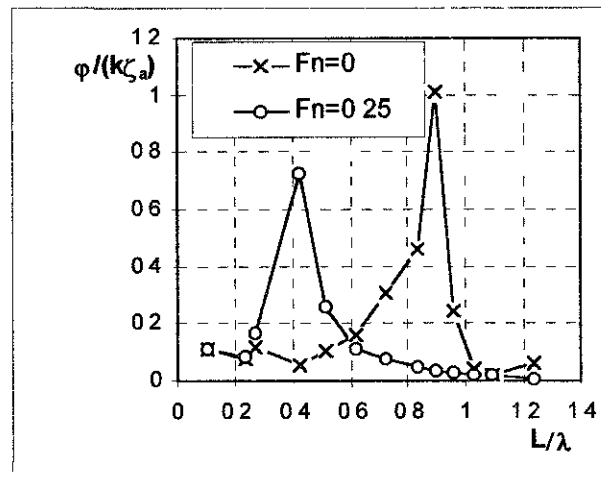


Fig. 1 Non-dimensional transfer functions of roll motion on head waves

When studying the ship's transverse stability in waves, two main directions could be identified : operational stability and capsizing.

The first is referred to the optimization of transverse stability characteristics so that the ship accomplish its aim in economical efficiency and safety conditions, being considered in moderate sea state. The second direction aims to ensure the ship's safety in storm conditions.

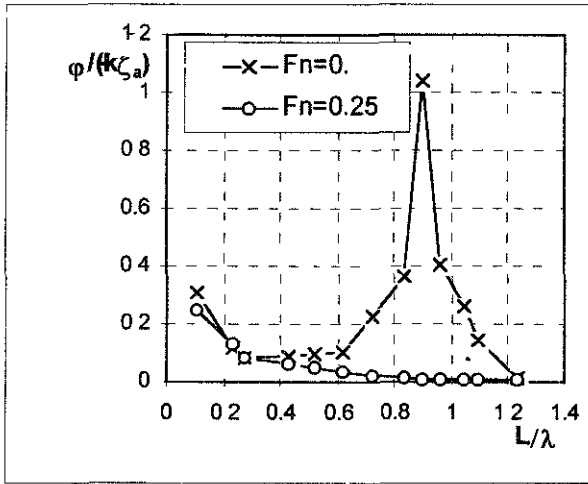


Fig. 2 Non-dimensional transfer functions of roll motion on following waves

The theoretical and experimental researches aspects presented in this paper are meant to solve the problem of operational stability at small heel angles, between  $0^\circ$  and  $15^\circ$ . The linear hydrodynamic model represents the basis for the theoretical and experimental investigation methods developed for solving the operational transverse stability problem.

## 2. RADIATION PROBLEM

The hydrodynamic coefficients for the ship in upright position have been calculated with the source distribution method by using the version suggested by W.Frank [2]. The method given by I.Elis [3] was applied to theoretically determine the hydrodynamic coefficients for the case of a heeled ship.

The experimental determination of hydrodynamic coefficients was performed on the basis of the forced harmonic oscillation tests of the ship model in still water by using a mechanical oscillator. The radiation hydrodynamic pressure field actuates on the model body. The radiation hydrodynamic forces and moments were measured by means of a six-component dynamometer mounted between the ship model and exciting legs of the mechanical oscillator. The hydrodynamic coefficients were calculated with the relations given by G.van Oortmerssen [4], by knowing the amplitude of

the imposed harmonic motion and the phase difference between excitation and the physical system response.

The experimental tests have included forced harmonic oscillation tests at zero speed with heave motions having the amplitudes of 1 cm, 2 cm and 3 cm and with pitch motions having the amplitudes of  $1^\circ$ ,  $2^\circ$  and  $3^\circ$ . Experimental measurements have been performed for heeling angles of  $0^\circ$ ,  $5^\circ$ ,  $10^\circ$  and  $15^\circ$ , within the frequency range between 0.4 Hz and 0.85 Hz. The table 1 lists the ship's main particulars and mechanical characteristics, at full load condition, as well as the ship model ones realized at 1/30 scale.

Examples regarding the evolution within the frequency range of the theoretical and experimental hydrodynamic coefficients, are given in figs.3 and 4. The non-dimensional hydrodynamic coefficients, independent of the ship's speed, are given on the ordinates and they are calculated with the following relations

$$\begin{aligned}
 A_{33ad}^\circ &= \frac{A_{33}^\circ}{m} & ; & & B_{33ad}^\circ &= \frac{B_{33}^\circ}{m \cdot \sqrt{g/L}} \\
 A_{55ad}^\circ &= \frac{A_{55}^\circ}{m \cdot L^2} & ; & & B_{55ad}^\circ &= \frac{B_{55}^\circ}{m \cdot L^2 \cdot \sqrt{g/L}} \\
 A_{35ad}^\circ &= \frac{A_{35}^\circ}{m \cdot L} & ; & & B_{35ad}^\circ &= \frac{B_{35}^\circ}{m \cdot L \cdot \sqrt{g/L}} \\
 A_{34ad}^\circ &= \frac{A_{34}^\circ}{m \cdot L} & ; & & B_{34ad}^\circ &= \frac{B_{34}^\circ}{m \cdot L \cdot \sqrt{g/L}} \\
 A_{45ad}^\circ &= \frac{A_{45}^\circ}{m \cdot L^2} & ; & & B_{45ad}^\circ &= \frac{B_{45}^\circ}{m L^2 \cdot \sqrt{g/L}} .
 \end{aligned} \quad (3)$$

On the graph abscissa, the non-dimensional circular frequency of harmonic motion is determined by the relation

$$\omega_{ad} = \omega \cdot \sqrt{L/g} . \quad (4)$$

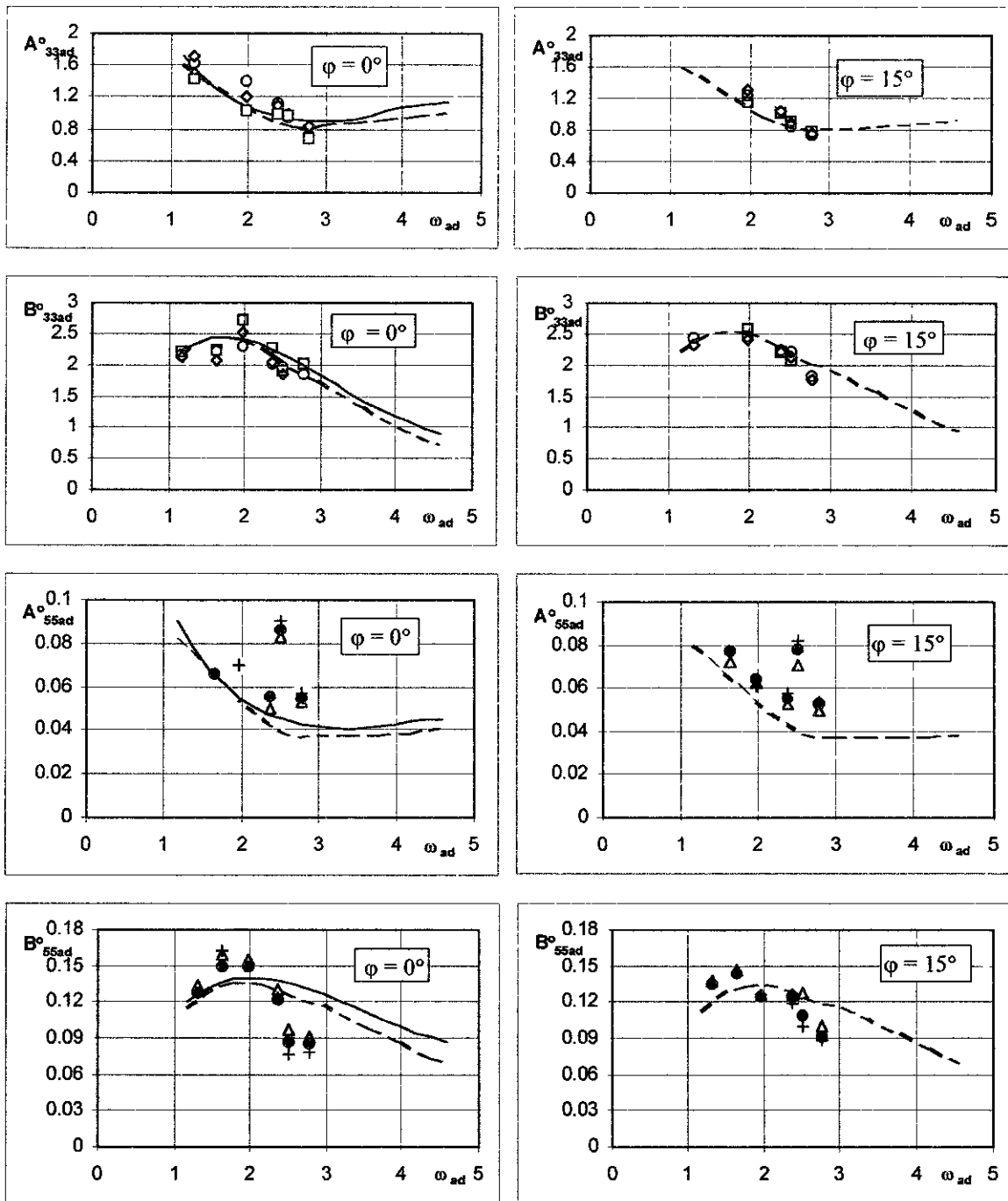


Fig. 3 Non-dimensional added mass and damping coefficients for heave and pitch motions

Symbols :      FRANK method      ————  
                   STAB program      - - - -  
 ICEPRONAV experiments:  $z_a = 1 \text{ cm}$      $\circ$  ;  $\theta_a = 1^\circ$  +  
    $z_a = 2 \text{ cm}$      $\diamond$  ;  $\theta_a = 2^\circ$  ●  
    $z_a = 3 \text{ cm}$      $\square$  ;  $\theta_a = 3^\circ$   $\Delta$

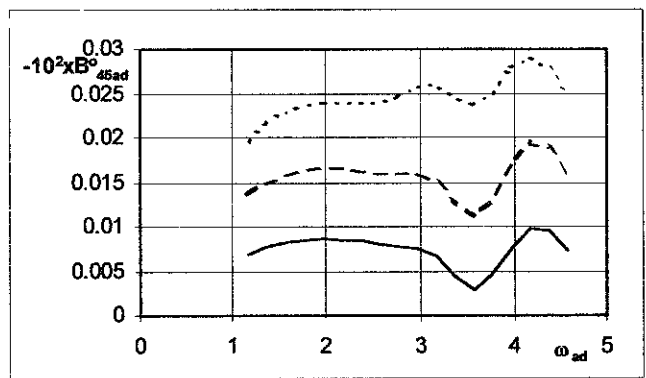
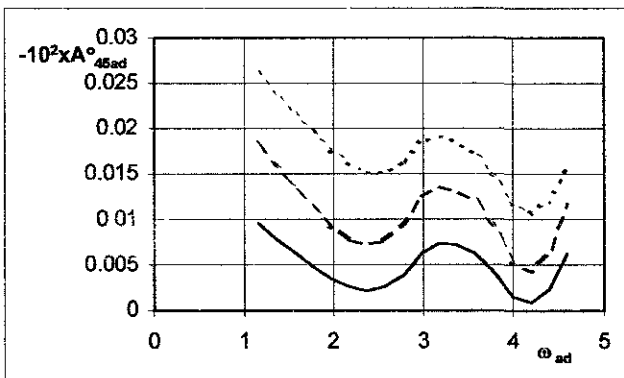
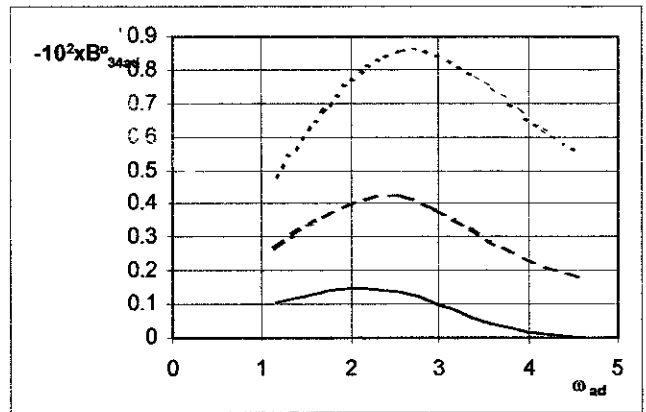
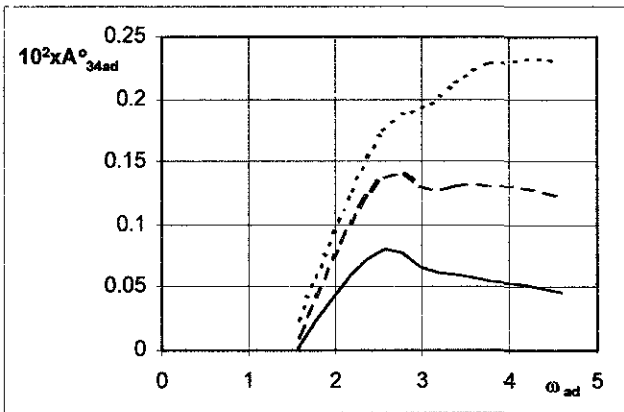
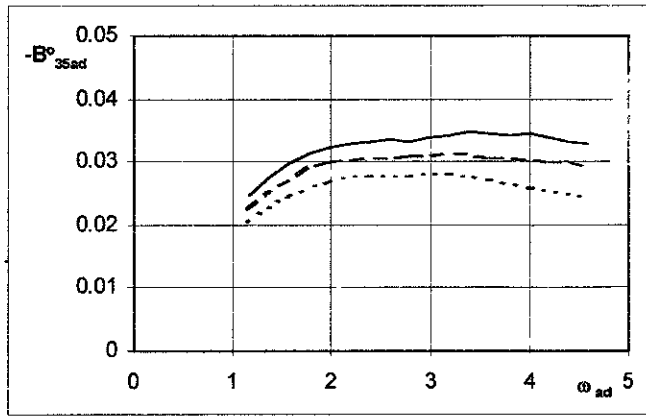
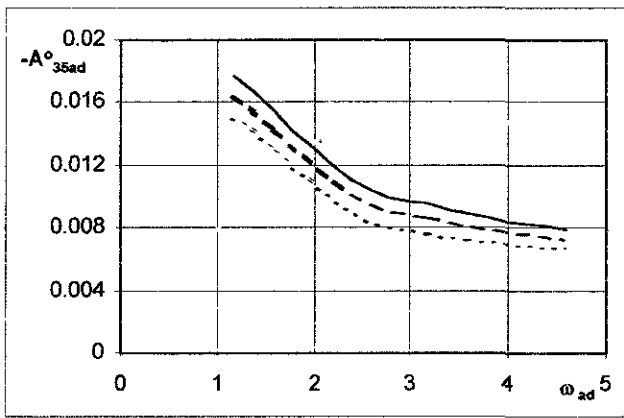


Fig. 4 Non-dimensional added mass and damping coefficients of inclined ship

Symbols :      $\varphi = 5^\circ$      —————  
                    $\varphi = 10^\circ$     - - - - -  
                    $\varphi = 15^\circ$     ········

An important aspect concerning the ship's transverse stability consists in evaluating the dependence of hydrodynamic coefficients against the imposed heeling angle. In the case of small heeling angles, between  $0^\circ$  and  $15^\circ$ , no significant dependence has been found. The coupled hydrodynamic coefficients depend on the heeling angle. However, the hydrodynamic forces and moments due to coupling effects are much lower than the main radiation hydrodynamic forces and moments.

At the same time, a maximum local value of the pitch added mass,  $A_{55ad}^\circ$ , near the circular frequency  $\omega_{ad} = 2.5$ , has been recorded experimentally, at all heeling angles. The phenomenon represents an expression of the local non-linearity of the hull response hydrodynamic characteristic at the pitch forced harmonic motion.

### 3. DIFFRACTION PROBLEM

To solve the diffraction problem means to determine Froude-Krylov hydrodynamic forces and moments as well as the diffraction ones. It has been carried out theoretically by extending the hydrodynamic linear model (Salvesen [5]), for the case of heeled ships. The calculation expressions for the excitation hydrodynamic forces and moments, generated by the longitudinal wave, indirectly depend on the ship's heeling angle by means of the sectional hydrodynamic coefficients.

The theoretical study of diffraction for the case of a ship in upright position has been performed on the basis of the hydrodynamic coefficients determined by W.Frank's method. For the heeled ship case, sectional hydrodynamic coefficients have been used, calculated in conformity with the tables presented by I.Elis [3], with a special module of the STAB computer program, performed at ICEPRONAV S.A.Galati (Stefanescu [10]).

The experimental methodology used for determining the excitation hydrodynamic forces and moments, has as a central support, a six-components dynamometer (Crudu [6]). The ship model was stiffly connected to the carriage

by a six-component dynamometer; therefore there is no freedom to move relative to the carriage. The experimental program was similar to that one used for solving the radiation problem.

The non-dimensional transfer functions of the heave excitation forces and pitch excitation moments, on following waves, for  $0^\circ$  and  $15^\circ$  heeled ships are exemplified in figs. 5 and 6, they are defined by the relation

$$F_{3ad} = \frac{F_{3a} \cdot L}{m \cdot g \cdot \zeta_a} \quad (5)$$

$$F_{5ad} = \frac{F_{5a}}{m \cdot g \cdot \zeta_a} .$$

For the case of zero speed, a satisfactory correlation of the theoretical and experimental results has been obtained. The differences registered at design speed are caused by the influence of the own wave, generated when the ship is running in still water. The adopted hydrodynamic model, does not take into account the interference of the own wave with the incident wave. The remarks performed during the experimental tests at a design speed for solving the diffraction problem, certifies an important decrease of the wave amplitude on the model body.

From the transverse stability viewpoint, the analysis of theoretical and experimental results shows that there is no significant dependence of excitation hydrodynamic forces and moments on longitudinal waves against the small heeling angles.

The experimental data analysis allowed the identification of some non-linear features of the pitch excitation moment. There is a local maximum for the ratio  $L/\lambda \cong 1$ , which can be regarded as a "compensation" of energy type of the minimum value of heave excitation force which appears at the same frequency.

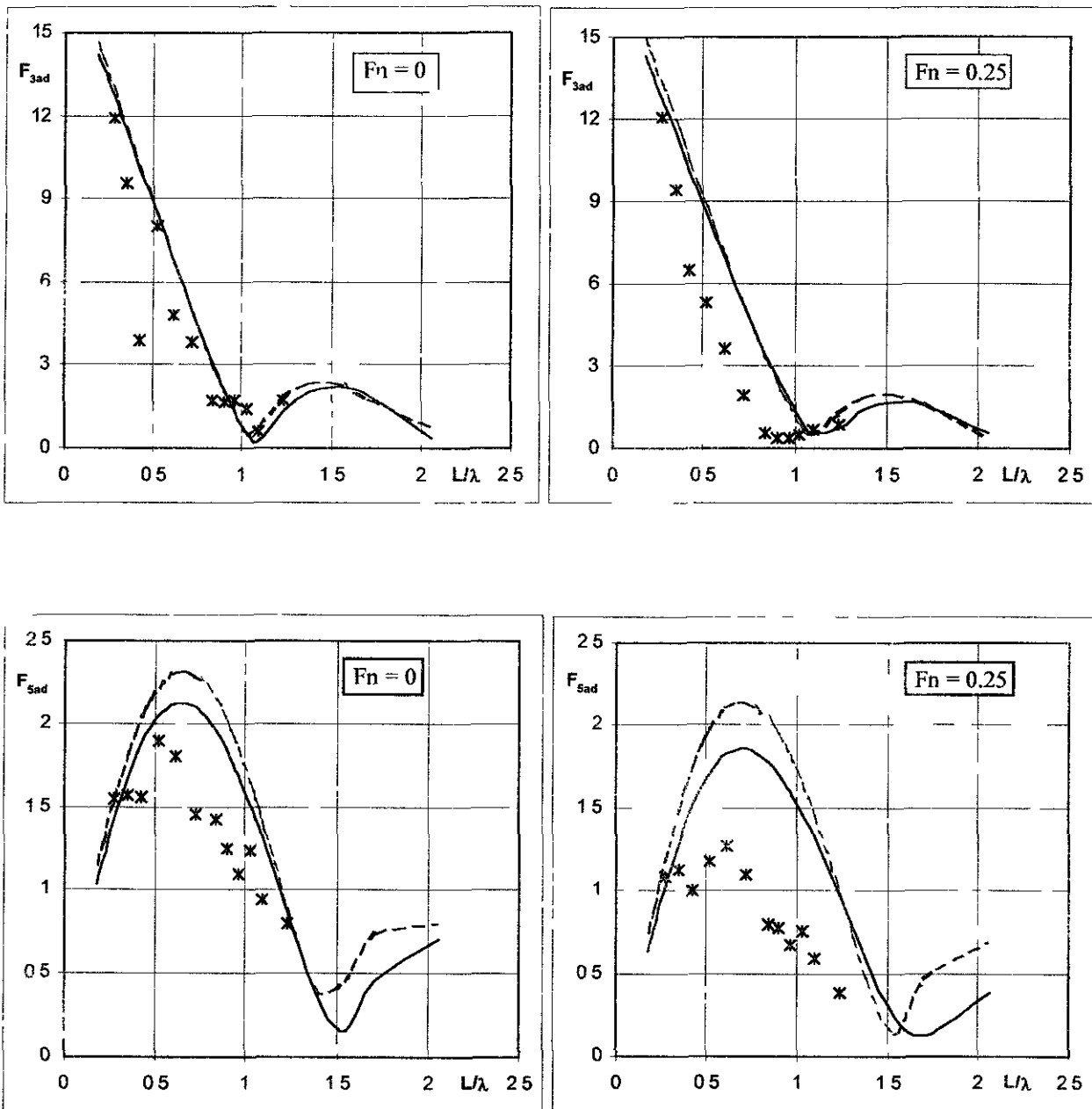


Fig. 5 Non-dimensional transfer functions of heave excitation force ( $F_{3ad}$ ) and pitch excitation moment ( $F_{5ad}$ ) on following regular waves, for zero heel angle

Symbols :      FRANK method  
                   STAB program  
                   ICEPRONAV experiments

—————  
 - - - - -  
 \*

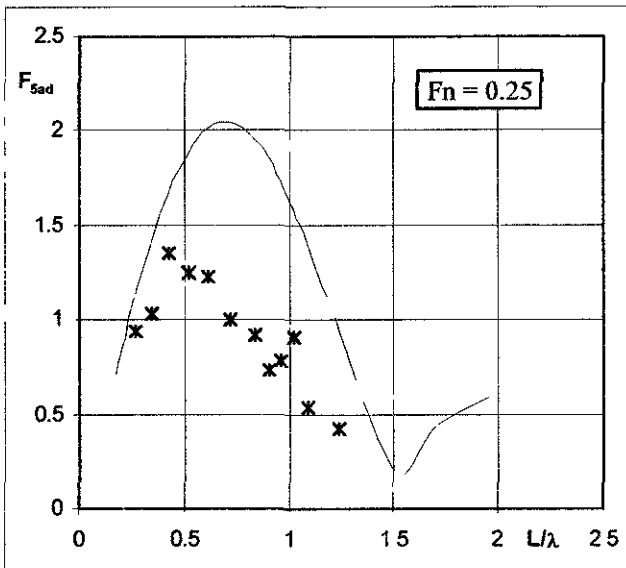
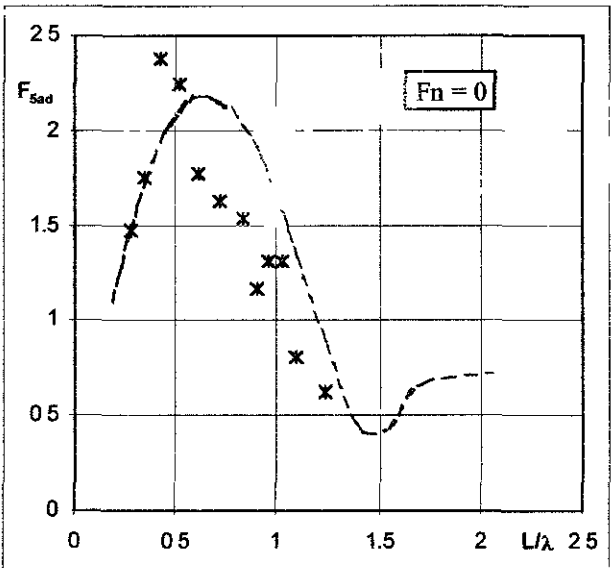
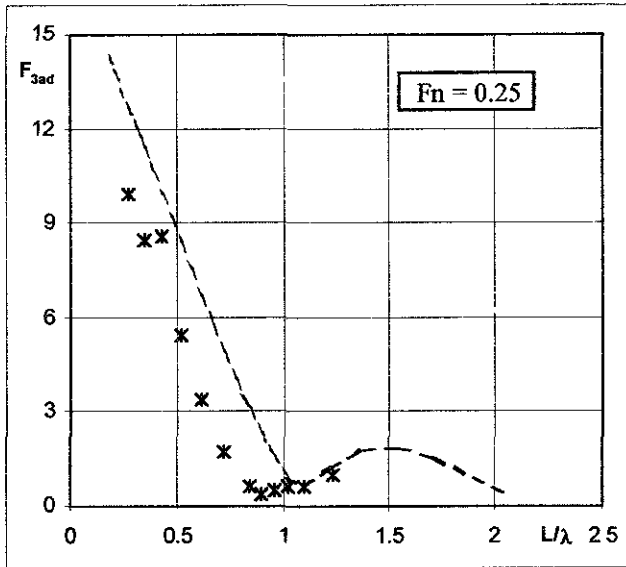
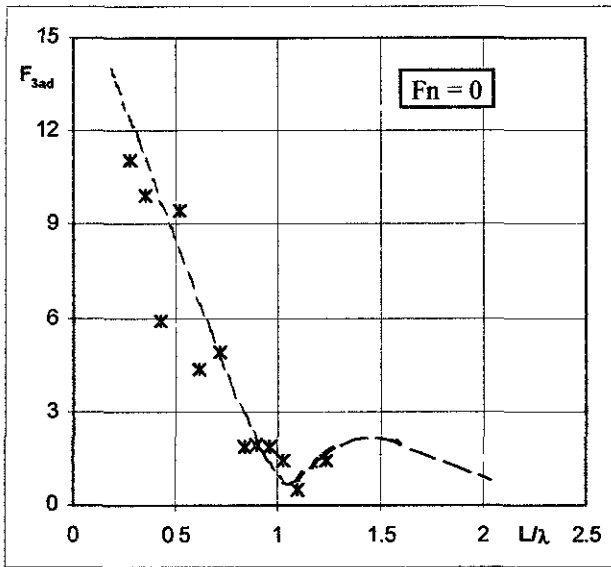


Fig. 6 Non-dimensional transfer functions of heave excitation force ( $F_{3ad}$ ) and pitch excitation moment ( $F_{5ad}$ ) on following regular waves, for heeling angle of 15 deg.

Symbols : STAB program  
ICEPRONAV experiments

— — — — —  
\*

#### 4. THE MAIN RESONANCE OF INDUCED ROLL MOTION

The induced rolling motion on longitudinal waves represents a real physical phenomenon, whose occurrence is determined by the following causes :

- continuous modification of the transversal metacentre position ;
- saturation energy phenomenon of the ship motions (heave or pitch, Nayfeh [7]) ;
- non-linear coupling of the heave and pitch motions with the induced roll motion (Nayfeh [8]).

The experimental solving of radiation and diffraction problems emphasized the existence of excitation hydrodynamic sources of the induced roll motion on longitudinal waves at main resonance, represented by local increases of pitch excitation moment and pitch added mass. The physical phenomenon can be explained by modifying the incident waves energy "distribution" as regard to the main components of the diffraction forces and moments as well as the radiated waves energy "distribution", as regard to the main components of the radiation forces and moments.

Due to the saturation phenomenon, the additional energy accumulated by the physical system for the pitch motion does not determine its amplitude increase, being transferred to the induced roll motion at the main resonance (in the second stability domain). There results that not only a main source of the induced roll motion (non-linearity of the ship's hull hydrodynamic characteristics) but also one of the main causes of the motion occurrence (the pitch motion saturation) have a hydrodynamic nature, imposing the necessity of studying the coupled differential equation system of heave, induced roll and pitch motions, having the following form

$$(m + A_{33}) \cdot \ddot{z} + B_{33} \cdot \dot{z} + C_{33} \cdot z + A_{34} \cdot \ddot{\phi} + B_{34} \cdot \dot{\phi} + A_{35} \cdot \ddot{\theta} + B_{35} \cdot \dot{\theta} + C_{35} \cdot \theta = F_{3a} \cdot \cos \omega t$$

$$A_{34} \cdot \ddot{z} + B_{34} \cdot \dot{z} + (I_4 + A_{44}) \ddot{\phi} + (D_{01} + D_{02} \cdot |\dot{\phi}|) \dot{\phi} + g \cdot m \cdot (GM \cdot \phi + K_3 \cdot \phi^3) + A_{45} \cdot \ddot{\theta} + B_{45} \cdot \dot{\theta} = F_{4a} \cdot \cos \omega t \quad (6)$$

$$A_{35} \cdot \ddot{z} + B_{35} \cdot \dot{z} + C_{35} \cdot z + A_{45} \cdot \ddot{\phi} + B_{45} \cdot \dot{\phi} + C_{45} \cdot \phi + (I_5 + A_{55}) \cdot \ddot{\theta} + B_{55} \cdot \dot{\theta} + C_{55} \cdot \theta = F_{5a} \cdot \cos \omega t .$$

The induced roll excitation moment modeling was based on the results obtained during the experimental solving of the diffraction problem, by adopting the following form

$$F_4(\phi, t) = F_{4a}(\phi) \cdot \cos \omega t = f_{4a} \cdot \phi \cdot \cos \omega t . \quad (7)$$

As regard to the coupled equations system, used by J.Hua [9], the system (6) explicitly separates the restoring coefficients in still water by the excitation hydrodynamic forces and moments and it considers the linear variation hypothesis of the coupled hydrodynamic coefficients :  $A_{34}$ ,  $B_{34}$ ,  $A_{45}$  and  $B_{45}$  with the heeling angle. In the linear analysis of the coupled motions in the frequency domain, the coefficients of the system (6) were considered as being independent of time.

To solve the system (6), the fourth-order Runge-Kutta method in the version modified by Gill, has been used. It was numerical modeled, the behaviour of a 2,700 d.w.t. cargo ship at zero speed on following waves (with a slope,  $h_w/\lambda = 1/50$  and with the frequency corresponding to the main resonance of the induced roll motion).

The experimental and numerical results are shown in fig.7, depending on the number of "i" cycles ; it was noticed a good concordance. A series of numerical tests were performed for identifying the nature of the hydrodynamic physical characteristic with decisive contribution for the induced roll motion appearance. It was observed that the modification of the induced roll excitation moment with 10% changes the numerical results, in the sense of the damping of the motion when the excitation moment decrease and of the infinite increase of the amplitude when the excitation moment increase.

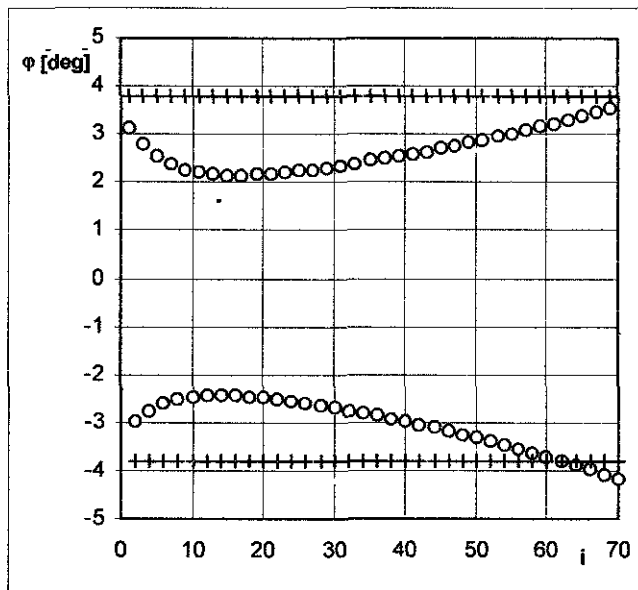
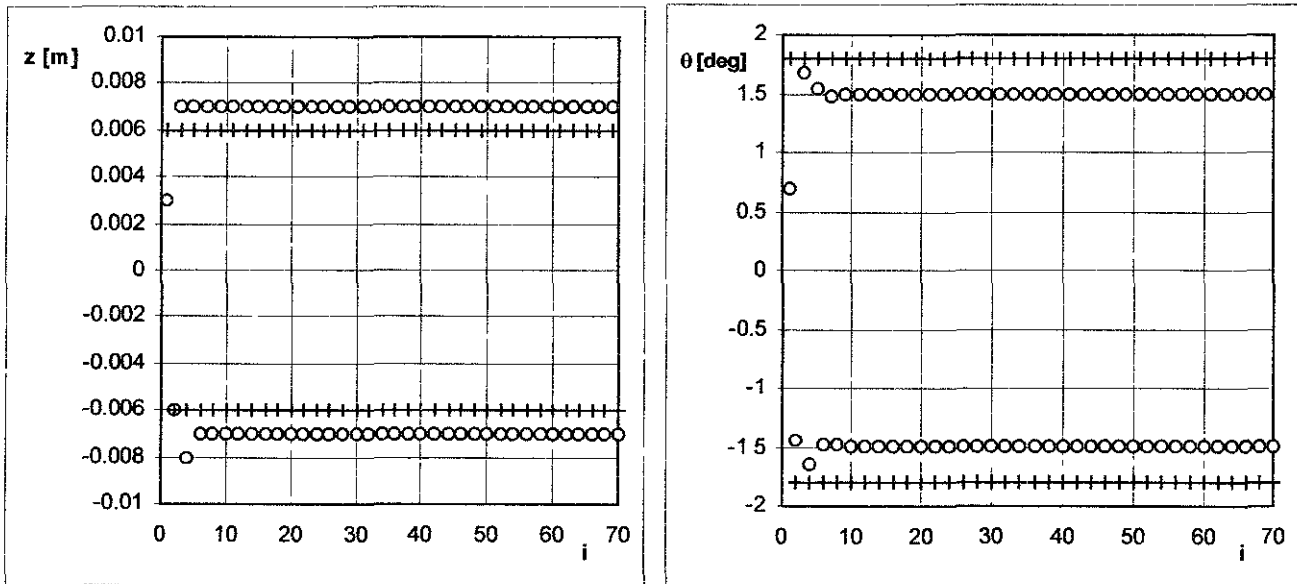


Fig. 7 Heave, pitch and induced roll motions in following waves at zero speed  
 $(h_w/\lambda = 1/50 ; L/\lambda = 0.896 ; \dot{\phi}/_{t=0} = 0.3)$

Symbols :    numerical solution (Runge - Kutta)    o  
                  ICEPRONAV experiments                    +

There results that the data obtained by solving the diffraction problem have an essential influence upon the physical phenomenon studied.

## 5. MINIMUM TRANSVERSE STABILITY DIAGRAM

When the inclined ship is running in longitudinal waves, there is a continuous variation of the restoring moment, as a result of the modification of the wetted surface, as well as of the pressure field distribution.

An important aim of the study on ship transverse stability in longitudinal waves is to determine the minimum transverse stability diagram, which allows the analysis of stability indicators on the basis of the minimum restoring moment of the heeled ship.

Thus, in conformity with the adopted hydrodynamic linear model, the STAB computer program as well as the experimental methodology for determining the restoring moment on longitudinal waves and its components were performed.

The non-dimensional transfer functions of the diffraction and radiation components of the restoring moment on following waves, obtained by the STAB computer program, are exemplified in fig. 8. The non-dimensional values were calculated by the ratio between the corresponding components amplitudes and the restoring moment values in still water, at zero speed, corresponding to the heeling angle taken into account. One can remark that the diffraction part brings a more important contribution in establishing the total value of the restoring moment on following waves, as regard to the radiation component within small heeling angles range.

The main part of the restoring moment is the Froude-Krylov component and it was calculated with a module of the STAB computer program, whose algorithm is based on the utilization of Bernoulli's equation written in linear form

$$p = p_0 - \rho \left[ \left( \frac{\partial}{\partial t} - U \frac{\partial}{\partial x} \right) \Phi_1 + g \cdot z \right] + K_B(t). \quad (8)$$

Fig.8 also shows the non-dimensional transfer functions of the Froude-Krylov component of the restoring moment on following waves, obtained by the STAB computer program. The Froude-Krylov component amplitude increases along with the heeling angle increase and it has maximum values for regular waves with a length close to the ship's length.

The total restoring moment on longitudinal waves is obtained by algebraic summing-up of the hydrostatic and hydrodynamic components, in conformity with the adopted hydrodynamic linear model.

To experimentally measure the restoring moment in longitudinal wave, a specific methodology was conceived ; it is based on the utilization of a one-component dynamometer which was located in the model centre of gravity (heeled with a pre-established angle). The ship model was carried to the design speed by means of a device which allows free heave and pitch motions. The experimental tests were drawn up in correlation with the radiation and diffraction experiments.

When the heeled ship model was running in still water, the  $M_U$  component of the restoring moment was also determined ; it represented about 3% of the restoring moments value, in still water, at zero speed, corresponding to that heeling.

Fig.9 presents a comparison of the theoretical and experimental results regarding the non-dimensional values of the minimum restoring moment on regular following waves.

The good agreement of theoretical and experimental results show that :

- within the small heeling angles range, between  $0^\circ$ ÷ $15^\circ$ , the superposition hypothesis of the effects is in accordance with the physical reality;
- it is important to utilize the contribution of each component when establishing the total restoring moment.

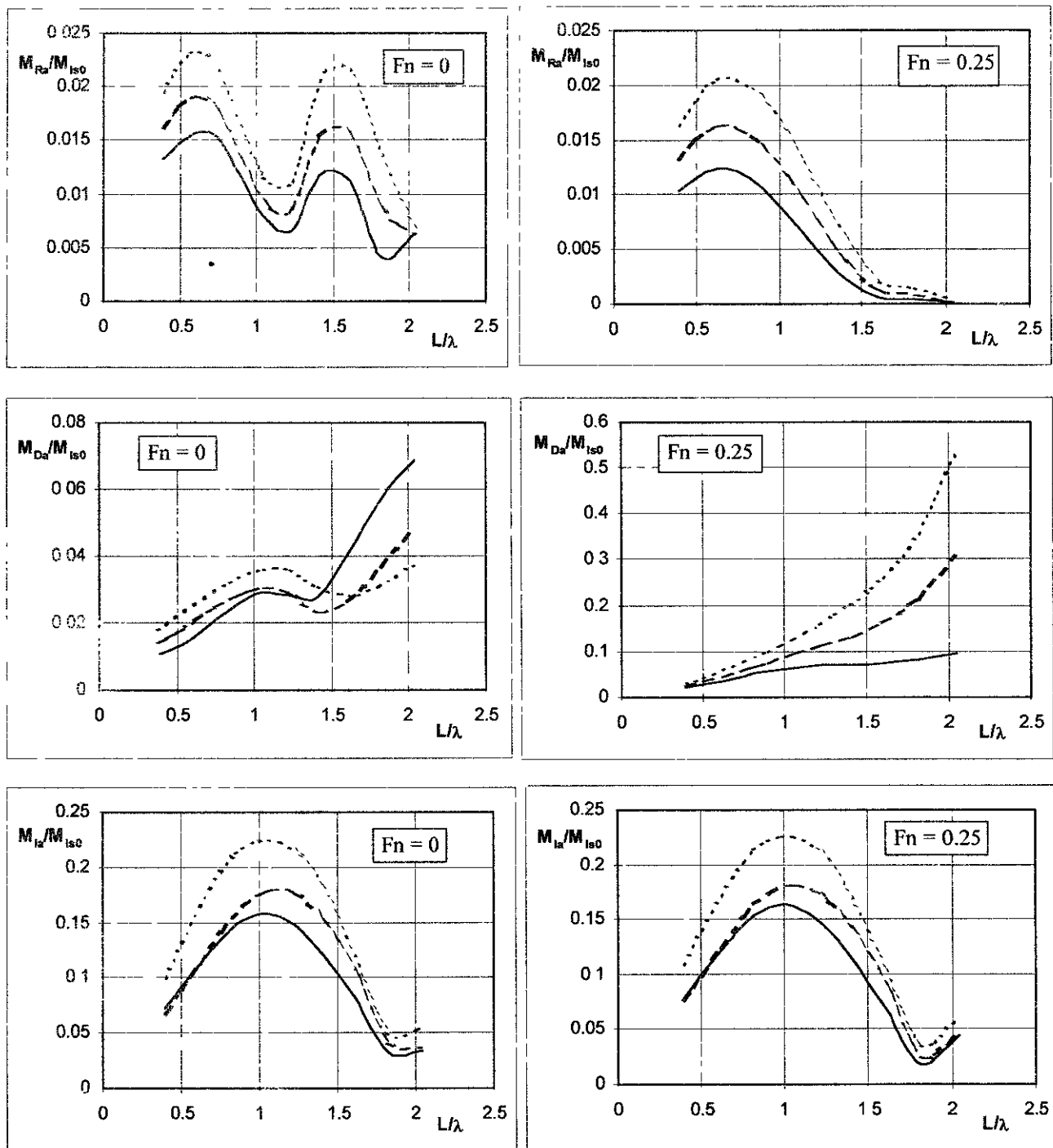


Fig. 8 Non-dimensional transfer functions of radiation, diffraction and Froude-Krylov components of the restoring moment in following waves

Symbols :  $\phi = 5^\circ$  ———  
 $\phi = 10^\circ$  - - - -  
 $\phi = 15^\circ$  ·····

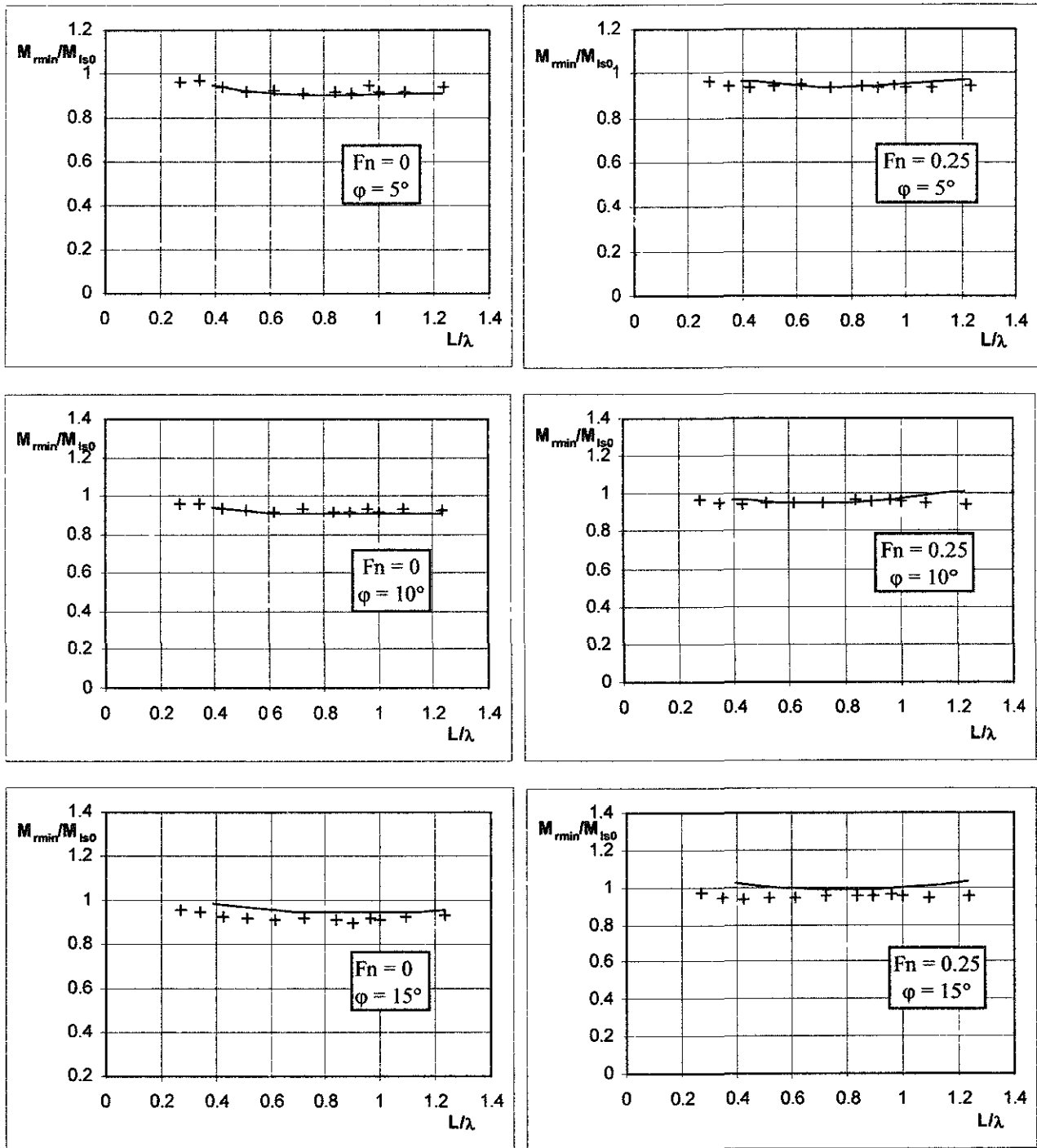


Fig. 9 Non-dimensional transfer functions of minimum restoring moment in following waves

Symbols : STAB program   
 ICEPRONAV experiments 

## 6. CONCLUSIONS

The structural integrity and hydrodynamic safety represents the main components of the ship safety. Two of the dangerous situations for the ships' transverse stability in longitudinal waves are related to :

- the parametric resonance of the induced roll motion ;
- the pure loss of stability .

A comprehensive theoretical and experimental research was conceived with the aim of clarifying :

- the induced roll motion excitation sources and causes ;
- the hydrodynamic mechanism accompanying the heeling phenomenon of the ship, when advancing in the incident waves field.
- the evaluation of the induced roll motion and the restoring moment amplitudes in longitudinal waves.

In case of small heeling angles, between  $0^\circ \div 15^\circ$ , the linear hydrodynamic model, suggested by Salvesen, was used ; it was also extended for the non-zero heel angles.

The experimental solving of radiation and diffraction emphasized the hydrodynamic excitation sources of the induced roll motion, represented by the local increases of the pitch excitation moment and of the pitch added mass in the second instability domain. The pitch motion saturation phenomenon represents a cause of hydrodynamic nature of the induced roll motion occurrence, the additional energy accumulated by the physical system in the pitch mode of ship motion being transferred to the induced roll motion, at the main resonance.

The agreement of the numerical solutions of the differential equations system of heave, induced roll and pitch motions, on longitudinal waves, with the experimental results of the towing tank tests represents a proof of modeling the physical mechanism which determines the existence of the induced roll motion.

Also, the satisfactory correlation of the theoretical and experimental results regarding the evaluation of the minimum restoring

moment on longitudinal waves demonstrates the possibility of using the linear hydrodynamic model adopted within the study of the operational transverse stability at small heeling angles. This hydrodynamic model can be improved by considering the effects of the incidental waves interaction with the system of own waves, generated when the ship is running in still water.

To know the diagram of the minimum restoring moment on longitudinal waves represents an important design element of the ship's operational transverse stability.

## ACKNOWLEDGEMENTS

The authors of this paper do thank to Mr.Dr. R.Kishev from BSHC - Varna for his special kindness to put the requested bibliographic reference at our disposal.

## REFERENCES

1. I.K.Boroday - "Ship Stability in Waves : on the Problem of Righting Moment Estimation for Ships in Oblique Waves", Proceedings of the STAB '90, Naples, Vol.2, 1990, pp.441-451.
2. W.Frank - "Oscillation of Cylinders in or Below the Free Surface of Deep Fluids", Naval Ship Research and Development Center, Washington, Report No.2375, 1967.
3. I.Elis - "Added Masses and Damping of Inclined Ship Sections", Annual Proceedings of Kaliningrad Technical Institute of Fisheries, 1980 (in Russian).
4. G.van Oortmerssen - "The Motions of a Moored Ship in Waves", Netherlands Ship Model Basin, Wageningen, Publication No.510, 1976.
5. N.Salvesen, E.O. Tuck, O.Faltinsen - "Ship Motion and Sea Loads", Transactions of the SNAME, New York, Vol.78, 1970, pp.250-279.

6. L.Crudu,R.Nabergoj,D.C.Obreja, G. Trincas- "Ship Stability in Following Waves : Theoretical and Experimental Investigations", Proceedings of the STAB '94, Melbourne, USA, 1994.

7. A.H.Nayfeh, D.T.Mook - "Nonlinear Oscillations", John Wiley & Sons, New York, 1979.

8. A.H.Nayfeh, I.G.Oh. - "Nonlinearly Coupled Pitch and Roll Motions in the Presence of Internal Resonance; Part I, Theory",

International Shipbuilding Progress, Vol.39, No.420, 1990, pp.295-324.

9. J.Hua - "A Study of the Parametrically Excited Roll Motion of a RoRo-Ship in Following and Heading Waves", International Shipbuilding Progress, Vol.39, No.420, 1992, pp.345-366.

10. S.Stefanescu, D.C.Obreja - "Program for Restoring Moment Evaluation in Longitudinal Waves", ICEPRONAV S.A.Galati, Report No. Ac 4077, 1997 (in Romanian).

## APPENDIX

MAIN PARTICULARS	Full scale	Model (1/30)
Length over all	86.04 m	2.864 m
Length between perpendiculars	79.84 m	2.661 m
Breadth	14.50 m	0.483 m
Draught aft	5.913 m	0.197 m
Draught forward	4.578 m	0.153 m
Depth	6.700 m	0.223 m
Dead weight	2.700 tf	100.0 Kgf
Displacement	4404.4 tf	163.1 Kgf
Speed	13.5 Kn	1.25 m/s
Longitudinal center of gravity from AP	38.702 m	1.290 m
Vertical center of gravity from BL	4.5 m	0.150 m
Metacentric height (still water)	1.6 m	0.053 m
Natural period of roll motion	7.55 s	1.38 s
Roll moment of inertia	82620.0 tm <sup>2</sup>	3.4 Kgm <sup>2</sup>
Pitch moment of inertia	1540620.0 tm <sup>2</sup>	63.4 Kgm <sup>2</sup>
Yaw moment of inertia	1433700.0 tm <sup>2</sup>	59.0 Kgm <sup>2</sup>

Table 1 Main particulars and mechanical characteristics at full load condition

# PREDICTION OF SHIP CAPSIZE DUE TO BROACHING IN FOLLOWING AND QUARTERING SEAS

N. Umeda\*, D. Vassalos\*\* and M. Hamamoto\*\*\*

\*National Research Institute of Fisheries Engineering,  
Hasaki, Kashima, Ibaraki, Japan

\*\*The Ship Stability Research Centre, University of Strathclyde,  
Glasgow, United Kingdom

\*\*\*Osaka University, Suita, Osaka, Japan

## ABSTRACT

This paper deals with stability of non-linear periodic motions of a ship running in following and quartering seas by making use of an averaging method. The motions discussed here include surge, sway, yaw and roll with an auto pilot. The effect of waves on the roll restoring moment is also taken into account. Numerical results based on this theoretical procedure are compared with existing results of free running model experiments. The comparison demonstrates that the calculated boundary for stable periodic motions allows for predictions of capsizing events due to broaching or those on a wave crest. Moreover, it is shown that capsizing due to broaching occurred in the experiments when a stable periodic motion does not exist and an unstable equilibrium point for surfing, with the maximum opposite rudder angle, exists near by.

## NOMENCLATURE

$A_R$  rudder area  
 $c$  wave celerity  
 $C_b$  block coefficient  
 $d_a$  aft draught

$d_f$  fore draught  
 $D_p$  propeller diameter  
 $F_n$  nominal Froude number  
 $g$  gravitational acceleration  
 $GM_b$  metacentric height  
 $GZ$  righting arm  
 $H$  wave height  
 $I_{xx}$  moment of inertia in roll  
 $I_{zz}$  moment of inertia in yaw  
 $J_{xx}$  added moment of inertia in roll  
 $J_{zz}$  added moment of inertia in yaw  
 $K_p$  hydrodynamic roll moment derivatives with respect to roll rate  
 $K_r$  hydrodynamic roll moment derivatives with respect to yaw rate  
 $K_R$  rudder gain  
 $K_v$  hydrodynamic roll moment derivatives with respect to sway velocity  
 $K_\delta$  hydrodynamic roll moment derivatives with respect to rudder angle  
 $K_\phi$  hydrodynamic roll moment derivatives with respect to roll angle  
 $K_w$  wave-induced roll moment  
l.c.b. longitudinal position of centre of buoy-

	ancy
L	ship length between perpendiculars
m	ship mass
$m_x$	added mass in surge
$m_y$	added mass in sway
n	propeller revolution number
$N_r$	hydrodynamic yaw moment derivatives with respect to yaw rate
$N_v$	hydrodynamic yaw moment derivatives with respect to sway velocity
$N_\delta$	hydrodynamic yaw moment derivatives with respect to rudder angle
$N_\phi$	hydrodynamic yaw moment derivatives with respect to roll angle
$N_w$	wave-induced yaw moment
p	roll rate
r	yaw rate
R	ship resistance
$S_F$	wetted surface area
t	time
T	propeller thrust
$T_D$	time constant for differential control
$T_E$	time constant for steering gear
$T_\phi$	natural roll period
u	surge velocity
v	sway velocity
$X_w$	wave-induced surge force
$Y_r$	hydrodynamic sway force derivatives with respect to yaw rate
$Y_v$	hydrodynamic sway force derivatives with respect to sway velocity
$Y_\delta$	hydrodynamic sway force derivatives with respect to rudder angle
$Y_\phi$	hydrodynamic sway force derivatives with respect to roll angle
$Y_w$	wave-induced sway force
$z_H$	height of centre of lateral force
$\delta$	rudder angle

$\kappa_{yy}$	gyro radius in pitch
$\kappa_{zz}$	gyro radius in yaw
$\lambda$	wave length
$\Lambda$	rudder aspect ratio
$\xi_G$	longitudinal position of centre of gravity from a wave crest
$\phi$	roll angle
$\chi$	heading angle
$\chi_c$	desired heading angle for auto pilot
$\omega_e$	averaged encounter frequency
$\zeta_w$	wave amplitude
$\zeta_{we}$	effective wave amplitude

## 1. INTRODUCTION

In model experiments, broaching, loss of transverse stability on a wave crest and low cycle resonance were identified as major causes for ship capsize in following and quartering seas, [1-2]. Among them, broaching is a phenomenon where a ship cannot maintain her desired course in spite of maximum steering effort and then suffers a violent yaw motion, [3]. The centrifugal force due to this yaw motion may cause the ship to capsize. Since factors related to this phenomenon covers a wide spectrum that includes ship stability, wave force prediction, manoeuvrability, non-linear dynamical systems, human factors and so on, a method for accurately predicting capsizing due to broaching has not yet been established.

The history of broaching investigation started with a manoeuvring model by ignoring the effects of roll motion. By using linear stability analysis, Davidson [4] firstly showed that even a ship that is directionally stable in calm water can be directionally unstable in following seas. Following that, time series of broaching were realised by time domain simulations of non-linear mathematical models with specific sets of initial conditions, [5,6]. These simulations are, however, limited in their ability to identify the

critical conditions for broaching because, like other non-linear phenomena, broaching depends critically on initial conditions, [6]. To overcome this difficulty, a non-linear dynamical approach was applied to broaching by Umeda and Renilson, [7,3]. They focused on equilibrium points, which correspond to surf-riding, and explained broaching as one of outstructures for unstable equilibria of surf-riding with the maximum rudder angle. For realising a transition from a normal periodic motion to an unstable equilibrium point, the periodic motion is required to be less stable, be unstable or disappear. This issue of the periodic motion was pursued by Umeda and Vassalos [8], who quantitatively confirmed that the periodic motion becomes unstable when the encounter frequency becomes small. These non-linear dynamical approaches provided deeper knowledge for understanding and predicting broaching but without considering the roll motion specifically.

Needless to say, the ultimate goal is to predict and prevent capsizing due to broaching. To predict capsizing due to broaching, it is essential to extend the manoeuvring mathematical model to the surge-sway-yaw-roll model, namely, to use a 4 DoF model. In this extension, the effect of waves on the roll restoring moment has a possibility to have a significant role. By using a linear analysis, Son and Nomoto [9] showed that instability on a wave upslope depends on roll. Renilson et al. [10] developed a non-linear 4 DoF mathematical model. Spyrou [11] investigated equilibria of a 4 DoF model and their instability with a similar manner to Umeda and Renilson [7] for a 3 DoF model. In this paper, periodic motions, as another steady state of a 4 DoF model, and their stability are discussed by extending the method by Umeda and Vassalos [8] with the effect of waves on the roll restoring moment taken into account. Then, the theoretical results are compared with experimental results by Hamamoto et al. [2] to examine the possibility for predicting capsizing

due to broaching.

## 2. MATHEMATICAL MODELLING

As can be seen in Fig 1, two co-ordinate systems are used: wave fixed with origin at a wave trough,  $\xi$  axis in the direction of wave travel; upright body fixed with origin at the centre of ship gravity, the  $x$  axis pointing towards the bow, the  $y$  axis to starboard and the  $z$  axis downwards. The latter co-ordinate system is not allowed to turn about the  $x$  axis. The symbols are defined in the nomenclature.

The state vector  $\mathbf{x}$  of this system is defined as follows:

$$\mathbf{x} = \{\xi_G / \lambda, u, v, \phi, p, \chi, r, \delta\}^T \quad (1)$$

The dynamical system can be represented by the following state equation: [8]

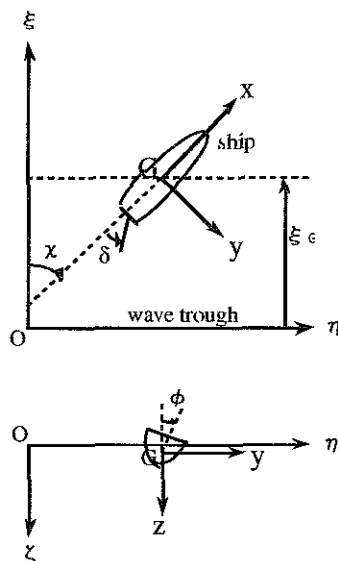


Fig. 1 Co-ordinate systems.

$$\dot{\mathbf{x}} = \mathbf{F}(\mathbf{x}) = \{f_1(\mathbf{x}), f_2(\mathbf{x}), \dots, f_8(\mathbf{x})\}^T \quad (2)$$

where

$$f_1(\mathbf{x}) = \{u \cos \chi - v \sin \chi - c\} / \lambda \quad (3)$$

$$f_2(\mathbf{x}) = \{T(u; n) - R(u) + X_w(\xi_G / \lambda, \chi)\} / (m + m_x) \quad (4)$$

$$f_3(\mathbf{x}) = \{-(m + m_x)ur + Y_v(u; n) + Y_r(u; n)r + Y_\phi(u)\phi + Y_\delta(\xi_G / \lambda, u, \chi; n)\delta + Y_w(\xi_G / \lambda, u, \chi; n)\} / (m + m_y) \quad (5)$$

$$f_4(\mathbf{x}) = p \quad (6)$$

$$f_5(\mathbf{x}) = \{m_x z_H ur + K_v(u; n)v + K_r(u; n)r + K_p(u)p + K_\phi(u)\phi + K_\delta(\xi_G / \lambda, u, \chi; n)\delta + K_w(\xi_G / \lambda, u, \chi; n) - mgGZ(\xi_G / \lambda, \phi, \chi)\} / (I_{xx} + J_{xx}) \quad (7)$$

$$f_6(\mathbf{x}) = r \quad (8)$$

$$f_7(\mathbf{x}) = \{N_v(u; n)v + N_r(u; n)r + N_\phi(u)\phi + N_\delta(\xi_G / \lambda, u, \chi; n)\delta + N_w(\xi_G / \lambda, u, \chi; n)\} / (I_{zz} + I_{zz}) \quad (9)$$

$$f_8(\mathbf{x}) = [-\delta - K_R(\chi - \chi_c) - K_R T_D r] / T_E \quad (10)$$

regarded as linear because its lift component is dominant in case of broaching where speed is high and frequency is very low, [14]. Although the righting arm in still water can be calculated without any problems, such geometric calculation cannot directly facilitate further analytical treatment. In this paper, the following fifth order polynomial is used to fit the calculated righting arm curve:

$$GZ(\phi) = GM_0 \phi + k_3 \phi^3 + k_5 \phi^5 \quad (11)$$

The wave effect on the righting moment can be estimated by integrating water pressure up to the wave surface, [15]. Since this effect is non-linear, calculated data are required, in principle, for all combinations of wave height, length and heading angle. To bypass this difficulty, this paper utilises a method based on Grim's effective wave concept, which has been well validated, [16]. Thus, the restoring arm in waves is modelled as follows:

$$GZ(\xi_G / \lambda, \phi, \chi; \zeta_w, \lambda) = \{GM_0 + a_1 \zeta_{we}^2 + (b_{11} \zeta_{we} + b_{12} \zeta_{we}^2) \cos 2\pi(\xi_G / \lambda)\} \phi + \{k_3 + a_3 \zeta_{we}^2 + (b_{31} \zeta_{we} + b_{32} \zeta_{we}^2) \cos 2\pi(\xi_G / \lambda)\} \phi^3 + k_5 \phi^5 \quad (12)$$

where

$$\zeta_{we} = \sqrt{\frac{\omega^2 L / g \cos \chi \sin(\omega^2 L / 2g \cos \chi)}{\pi^2 - (\omega^2 L / 2g \cos \chi)^2}} \zeta_w \quad (13)$$

$$\omega = \sqrt{\frac{2\pi g}{\lambda}} \quad (14)$$

Since the external forces are functions of the surge displacement but not time, this equation is non-linear and autonomous.

The wave forces and moments are predicted as the sum of the Froude-Krylov forces and hydrodynamic lift due to wave particle velocity by a slender body theory. This prediction has been well validated with a series of captive model experiments, [12]. The manoeuvring and propulsive coefficients are assumed to be independent of waves as a first order approximation, [13]. The roll damping moment can be

### 3. STABILITY OF PERIODIC MOTIONS

In a previous paper [8], using an inertia coordinate system travelling with a mean ship velocity,  $\bar{U}$ , and mean ship course,  $\bar{\chi}$ , the above autonomous model without the wave effect on restoring moment was transformed into a non-autonomous model, which is suitable for describing periodic motions. Then, an averaging method was applied to the transformed model, assuming that surge,  $\tilde{X}_G$ , sway,  $\tilde{Y}_G$ , roll,  $\tilde{\phi}$ , yaw,  $\tilde{\chi}$ , and rudder angle,  $\tilde{\delta}$ , are represented by the following harmonic motions:

$$\tilde{X}_G = r_1 \cos(\omega_e t - \varepsilon_1) \quad (15)$$

$$\tilde{Y}_G = r_2 \cos(\omega_e t - \varepsilon_2) \quad (16)$$

$$\tilde{\phi} = r_4 \cos(\omega_e t - \varepsilon_4) \quad (17)$$

$$\tilde{\chi} = r_6 \cos(\omega_e t - \varepsilon_6) \quad (18)$$

$$\tilde{\delta} = r_7 \cos(\omega_e t - \varepsilon_7) \quad (19)$$

In the present paper, similar analysis was carried out including the wave effect on the roll restoring moment. As a result, the following averaged equation is obtained:

$$\dot{\mathbf{v}} = \mathbf{G}(\mathbf{v}) = \{g_1(\mathbf{v}), g_2(\mathbf{v}), \dots, g_{10}(\mathbf{v})\}^T \quad (20)$$

where

$$\mathbf{v} = (u_1, v_1, u_2, v_2, u_4, v_4, u_6, v_6, u_7, v_7)^T \quad (21)$$

$$(u_1 \ v_1)^T = P(\tilde{X}_G \ \dot{\tilde{X}}_G)^T \quad (22)$$

$$(u_2 \ v_2)^T = P(\tilde{Y}_G \ \dot{\tilde{Y}}_G)^T \quad (23)$$

$$(u_4 \ v_4)^T = P(\tilde{\phi} \ \dot{\tilde{\phi}})^T \quad (24)$$

$$(u_6 \ v_6)^T = P(\tilde{\chi} \ \dot{\tilde{\chi}})^T \quad (25)$$

$$(u_7 \ v_7)^T = P(\tilde{\delta} \ \dot{\tilde{\delta}})^T \quad (26)$$

$$P = \begin{bmatrix} \cos \omega_e t & -1/\omega_e \sin \omega_e t \\ -\sin \omega_e t & -1/\omega_e \cos \omega_e t \end{bmatrix} \quad (27)$$

The difference between the previous and present procedures exists only in  $g_5(\mathbf{v})$  and  $g_6(\mathbf{v})$ .

The averaging theorem [17] indicates that, if an averaged equation has a hyperbolic fixed point,  $\mathbf{v}_0$ , the original equation possesses a unique hyperbolic periodic orbit of the same stability type as  $\mathbf{v}_0$ . Therefore, a harmonic motion of Eq. (2) corresponds to the  $\mathbf{v}_0$  that is defined as follows:

$$\mathbf{G}(\mathbf{v}_0) = \mathbf{0} \quad (28)$$

Then,  $\mathbf{G}(\mathbf{v})$  is linearised at  $\mathbf{v}_0$ , putting  $\mathbf{v} = \mathbf{v}_0 + \mathbf{q}$  to obtain the following equation:

$$\dot{\mathbf{q}} = D\mathbf{G}(\mathbf{v}_0)\mathbf{q} \quad (29)$$

where

$$D\mathbf{G}(\mathbf{v}) = \frac{\partial}{\partial v_j} (g_i(\mathbf{v})) \quad 1 \leq i, j \leq 10 \quad (30)$$

If an eigenvalue of  $D\mathbf{G}(\mathbf{v}_0)$  has a positive real part, the harmonic motion of the system described by Eq. (2) is unstable.

### 4. NUMERICAL RESULTS AND DISCUSSION

Numerical calculations based on the above method have been carried out for a 135 GT purse seiner, the principal particulars of which are shown in Table 1. In the previous paper [8], the calculated results of steady periodic mo-

tions were compared with the results of free running model experiments using a 1/15 scale model of the purse seiner [1] and reasonable agreement in periodic roll and yaw motions was shown. In these experiments, the model was set up for an overloaded condition, with draught is 2.99 m, to be relevant to an actual and recent capsizing accident of this type of vessel, where only capsizing events on a wave crest were observed. Following these experiments, Hamamoto et al. [2] realised also capsizing due to broaching by using the same model but in the full loaded condition, at a draught of 2.65 m. Therefore, the present investigation compares the stable boundary of periodic motions calculated by the above procedure with the experimental results from Hamamoto et al. [2] and discusses whether the theoretical results for the stable boundary of periodic motions can be used to predict capsizing due to broaching.

Table 1 Principal particulars of the purse seiner.

L	34.5 [m]	$k_{yy}/L$	0.316
B	7.6 [m]	$k_{zz}/L$	0.316
D	3.07 [m]	$GM_0$	0.75 [m]
$d_f$	2.50 [m]	$T_\phi$	8.9 [sec]
$d_a$	2.80 [m]	$A_R$	3.49[m <sup>2</sup> ]
$C_b$	0.597	$\Lambda$	1.84
l.c.b. (aft)	1.31 [m]	$T_E$	0.47[sec]
$S_f$	324. [m <sup>2</sup> ]	$K_R$	1.0
$D_p$	2.60[m]	$T_D$	1.24[sec]

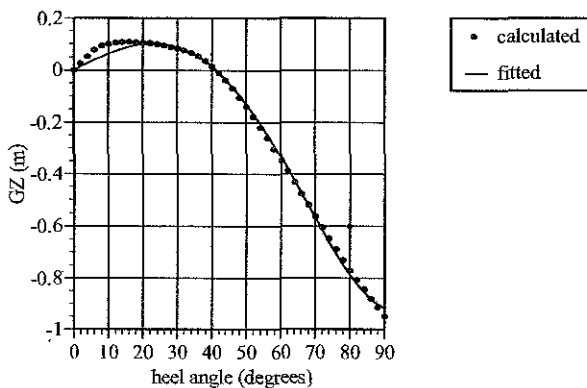


Fig. 2 Curve fitting of GZ curve in still water.

Because of difference in draught, captive experiments were conducted for the new loading condition. These involve resistance, propulsion, circular motion, rudder angle and heel angle tests. The added masses and moments of inertia were estimated theoretically or empirically. The roll damping moment was estimated with a linear component of the roll damping moment measured without a forward velocity and corrected empirically for forward speed. The restoring moment in still water had been fitted, in the previous paper, with a fifth order polynomial which has zero values at 0 degrees, 180 degrees and the vanishing angles. In this paper, to improve accuracy, the coefficients of Eq. (11) were determined to fit the values calculated directly from -90 degrees to 90 degrees. If the range of roll angle is extended, a higher order polynomial is required. As shown in Fig. 2, the accuracy of fitting is satisfactory. To account for the wave effect on the roll restoring moment, Eq. (12) was fitted to satisfy the following two requirements: the wave effect on the roll restoring moment should be zero at 180 degrees; the wave effect on the metacentric height should be accurately realised. The dependence of wave height can be modelled with 2nd order polynomials as shown in Fig. 3. An example of comparison presented in Fig. 4 indicates that modelling the wave effect on the roll restoring moment at large heel angles is not so satisfactory. Thus further improvement for curve fitting of this effect will be the future task.

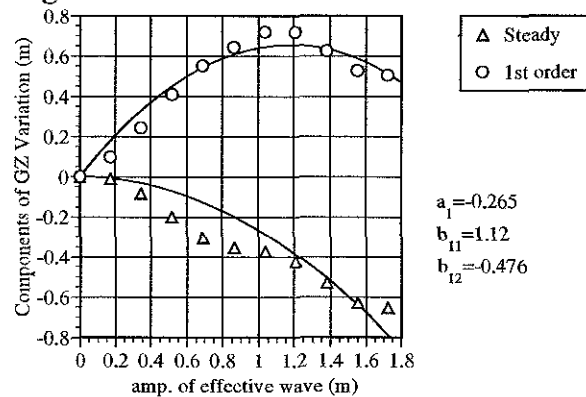


Fig. 3 Steady and first order components of the wave effect on the GZ curve. ( $H/\lambda=1/15$ ,  $\lambda/L=1.5$ )

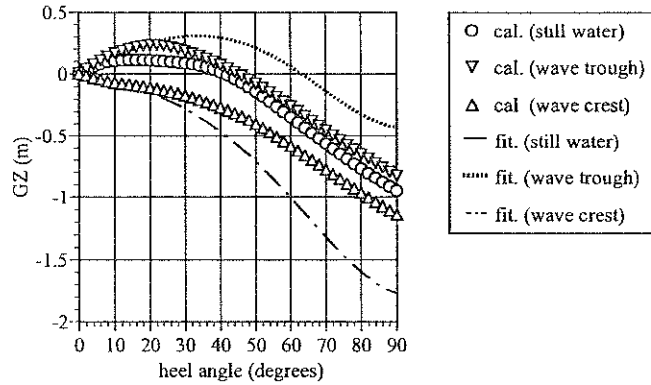


Fig. 4 GZ curves in transverse waves with  $H/\lambda=1/15$  and  $\lambda/L=1.5$ .

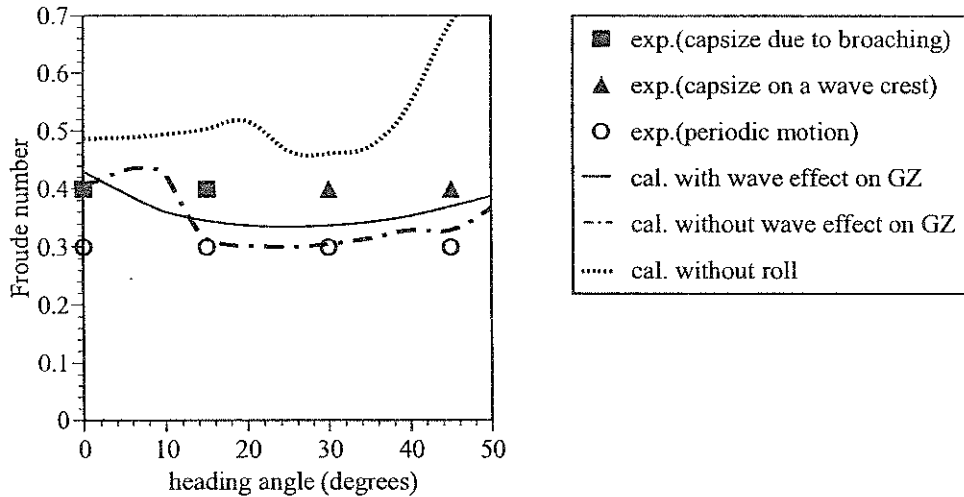


Fig. 5 Upper limit of stable periodic motions calculated by the present procedures and experimental results [2]. ( $H/\lambda=1/15$ ,  $\lambda/L=1.5$ )

The numerical results are shown in Fig. 5 together with the experimental results by Hamamoto et al, [2]. In the numerical calculation, Eq. (28) is solved by the Newton method using as the initial value the solution for a slightly lower Froude Number. Thus the solutions are determined in sequence from  $Fn=0.05$  to  $Fn=0.7$ . The step of increasing the Froude number is 0.001. In case of lower speed, a non-linear stable periodic motion exists with high encounter frequency, that almost coincides with a linear solution. [8] When the Froude number increases, the stability of periodic motion decreases. Then, when the Froude number exceeds a certain value, the periodic motion becomes unstable or cannot be found by the above pro-

cedure. This Froude number is regarded as an upper boundary of stable periodic motion, and is shown as a calculated value in Fig. 5. In some cases, amplitudes of rudder angles reach the maximum allowable. These cases are rather few but are also categorised as an upper boundary of stable periodic motion. The numerical calculations were carried out with the following three models:

- 1) the 3 DoF model (surge-sway-yaw model);
- 2) the 4 DoF model (surge-sway-roll-yaw model) without the wave effect on restoring roll moment;
- 3) the 4 DoF model (surge-sway-roll-yaw model) with the wave effect on restoring roll moment.

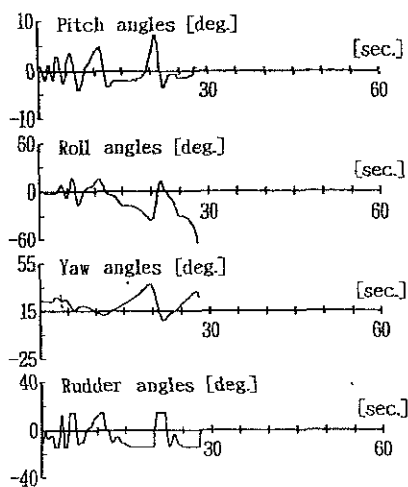


Fig. 6 Capsizing due to broaching recorded during experiments with 1/15 scaled model. ( $F_n=0.4$ ,  $\chi=15$  degrees,  $H/\lambda=1/15$ ,  $\lambda/L=1.5$ )

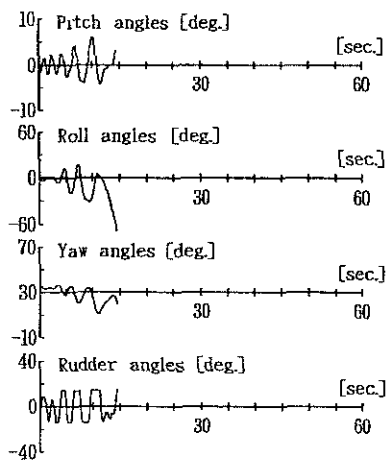


Fig. 7 Capsizing on wave crest recorded during experiments with 1/15 scaled model. ( $F_n=0.4$ ,  $\chi=30$  degrees,  $H/\lambda=1/15$ ,  $\lambda/L=1.5$ )

In the model experiments [2], capsizing due to broaching and capsizing on a wave crest were observed. In the former case, an example of which is shown in Fig. 6, when the rudder angle reached maximum negative angle, yaw rate was positive and pitch angle was almost constant and negative. Then the model capsized towards the port side. This direction corresponds to

that of centrifugal force due to the positive yaw rate. These facts indicate that the model nearly surf-ridden at the wave downslope and then, in spite of maximum steering effort, suffered a violent yaw motion, which resulted in capsizing. Therefore, this can be categorised as capsizing due to broaching as defined in the introduction of this paper. An example of the latter case of capsizing in the experiment is shown in Fig. 7. A harmonic roll motion developed and then the model trapped water on deck. Finally the model heeled due to trapped water and capsized when the ship centre met a wave crest.

The comparison between the experiments and calculations indicates that the boundary obtained by the 3 DoF model is not a good quantitative prediction for broaching. Because, it can be seen that capsizing due to broaching occurred in the stable zone calculated with the 3 DoF model. If roll motion is taken into account, the calculated boundary for stable periodic motions offers a useful prediction. In particular, the 4 DoF model with the wave effect on the roll restoring moment provides a better agreement with the experiments. However, these calculated boundaries for stable periodic motions exclude both capsizing due to broaching and that on a wave crest. To explain this result, it is worth while noting that the present calculation indicates only non-existence of a stable harmonic motion. If a stable harmonic motion cannot exist, the ship will attempt to find other steady states. Fig. 8 shows a zone for one of the other steady states, namely, unstable equilibria of surf-riding. These equilibria were calculated with the autonomous 3 DoF model, [7]. If a stable periodic motion does not exist and an unstable equilibrium with the maximum opposite rudder angle emerges near by, the ship is attracted by the equilibrium of surf-riding. Since this equilibrium point is unstable, the model is repelled in spite of maximum opposite rudder angle. This means an uncontrollable yaw motion. Such explanation on non-linear dynam-

ics of broaching have been proposed by Umeda. [7,3,8,13] In case of the experiment, it is presumed that the model capsized because the transverse stability could not counteract the centrifugal force due to yaw motion. On the other hand, the mechanism for the capsizing on

a wave crest still awaits explanation of quantitative evidence. It is necessary to investigate the effect of heel and trapped water from a viewpoint of non-linear dynamical system.

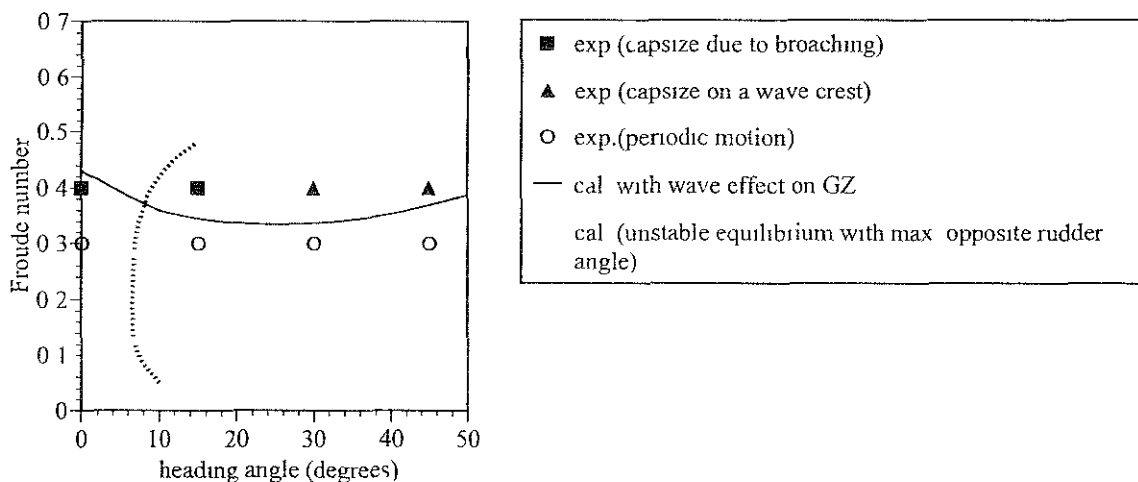


Fig. 8 Upper limit of stable periodic motions, unstable equilibria with the maximum opposite rudder angle and experimental results [2]. ( $H/\lambda=1/15$ ,  $\lambda/L=1.5$ )

## 5. CONCLUSIONS

The main conclusions from this work are summarised as follows:

- (1) The boundary for stable periodic motion obtained by the surge-sway-roll-yaw model quantitatively explains capsizing observed in model experiments, while that obtained by the surge-sway-yaw model does not.
- (2) The capsizing due to broaching in the model experiments occurred when a stable periodic motion did not exist and unstable equilibria potentially emerged near by in spite of maximum opposite rudder angle.
- (3) The wave effect on the roll restoring moment contributes to improve agreement with the experimental results.
- (4) An improvement in modelling the wave effect on the roll restoring moment and non-linear system dynamics on capsizing on a wave crest are among the tasks to be pursued in the near future.

## REFERENCES

1. Umeda, N., M. Hamamoto, et al. -Model Experiments of Ship Capsize in Astern Seas-, Journal of the Society of Naval Architects of Japan, 177, (1995), 207-217.
2. Hamamoto, M. et al. - Model Experiments of Ship Capsize in Astern Seas: 2nd Report- Journal of the Society of Naval Architects of Japan, 179, (1996), 77-87.
3. Umeda, N. and M.R. Renilson -Broaching of a Fishing Vessel in Following and Quartering Seas-, Proceedings of the 5th International Conference on Stability of Ships and Ocean Vehicles, Melbourne, 3, (1994), 115-132.
4. Davidson, K.S.M. -A Note on the Steering of Ships in Following Seas- Proceedings of the 7th International Congress of Applied Mechanics, London, (1948), 554-568.
5. Ananiev, D.M. and L. Roseva -Ship's Heeling During her Broaching and Manoeuvring in Following Seaway- Proceedings of Interna-

- tional Workshop on the Problems of Physical and Mathematical Stability Modelling, Kaliningrad, 1, 12, (1993), 1-15.
6. Matora, S., M. Fujino and T. Fuwa -On the Mechanism of Broaching-to Phenomena- Proceedings of the 2nd International Conference on Stability of Ships and Ocean Vehicles, Tokyo, (1982), 535-550.
  7. Umeda, N. and M.R. Renilson -Broaching : A Dynamic Analysis of Yaw Behaviour of a Vessel in a Following Sea- *Manoeuvring and Control of Marine Craft* (Wilson, P.A. eds.) / Computational Mechanics Publications (Southampton), (1992), 553-543.
  8. Umeda, N. and D. Vassalos -Non-Linear Periodic Motions of a Ship Running in Following and Quartering Seas- Journal of the Society of Naval Architects of Japan, No. 179, (1996), 89-101.
  9. Son, K. and K. Nomoto -On the Coupled Motion of Steering and Rolling of a Ship in Following Seas- Journal of the Society of Naval Architects of Japan, No. 152, (1983), 180-191, (in Japanese.)
  10. Renilson, M.R. and A.J. Tuite -Broaching Simulation of Small Vessels in Severe Following Seas- Proceedings of the International Symposium on Ship Safety in a Seaway: Stability, Manoeuvrability, Non-linear Approach, Kaliningrad, 1, 15, (1995), 1-14.
  11. Spyrou, K. -Geometrical Aspects of Broaching-to Instability- Proceedings of the 2nd International Workshop on Stability and Operational Safety of Ships, Osaka, (1996), 1-9.
  12. Umeda, N., et al. -Experimental Study for Wave Forces on a Ship Running in Quartering Seas with Very Low Encounter Frequency- Proceedings of the International Symposium on Ship Safety in a Seaway: Stability, Manoeuvrability, Nonlinear Approach, Kaliningrad, 1, 14, (1995), 1-18.
  13. Umeda, N. -Some Remarks on Broaching Phenomenon- Proceedings of the 2nd International Workshop on Stability and Operational Safety of Ships, Osaka, (1996), 10-23.
  14. Ikeda, Y., et al. -Effect of Forward Speed on Roll Damping of a High-Speed Craft- Journal of the Kansai Society of Naval Architects, 208, (1988), 27-34, (in Japanese).
  15. Umeda, N. et al. -Transverse Stability of a Ship in Following Sea- Journal of the Kansai Society of Naval Architects, 185, (1982), 49-56, (in Japanese).
  16. Umeda, N. et al. -Probabilistic Study on Ship Capsizing due to Pure Loss of Stability in Irregular Quartering Seas- Proceedings of the 4th International Conference on Stability of Ships and Ocean Vehicles, Naples, 1, (1990), 328-335.
  17. Guckenheimer, J. and P. Holmes -*Nonlinear Oscillations, Dynamical Systems, and Bifurcations of Vector Field*- Springer-Verlag, (New York), (1983).

#### ACKNOWLEDGEMENTS

This research was partly supported by the Grant-in-Aid for Scientific Research of the Ministry of Education, Science and Culture, Japan.

# A STUDY ON ROLL BEHAVIOR OF SHIP ON ASYMMETRIC WAVES

Hiroyuki SADAKANE

Faculty of Mercantile Marine, Kobe University of Mercantile Marine  
5-1-1, Fukae-minami, Higashi-nada, Kobe 658, Japan

## ABSTRACT

In this paper, the roll behavior of a ship on asymmetric waves is methodically studied by solving numerically a simplified equation of roll motion. The above asymmetric waves are described by deforming symmetric waves such as trochoidal waves.

The following results will be demonstrated;

- (1) On the single asymmetric waves, the wave asymmetry clearly influences the one-roll response of the ship, and increases the maximum roll angle.
- (2) In the case of the wave asymmetry being noticeable, a chaotic pattern appears in roll response both on single waves and on regular waves.

## NOMENCLATURE

$A, AA$ = deformation factor of wave crest	$k$ = wave number
$A_0$ = wave amplitude	$M_w$ = wave exciting roll moment
$B, BB$ = deformation factor under wave surface	$P_M$ = impulsive roll moment due to wave
$B$ = center of buoyancy of ship	$S$ = surface wave steepness, $H/W_L$
$GM$ = metacentric height	$T_R$ = natural roll period in small amplitude
$c$ = correction coefficient for $M_w$	$T_w$ = wave period
$H$ = wave height	$t$ = time
$I_x$ = virtual moment of inertia about the longitudinal axis of ship	$W_L$ = wave length
$k_r$ = coefficient of roll resistance	$\beta_3$ = nonlinear term of stability of ship
$K_r$ = damping coefficient of roll	$\eta$ = surface or subsurface wave elevation
	$\pi$ = ratio of the circumference of the circle to the diameter
	$\phi$ = absolute ship roll angle

- $\phi_a$  = apparent ship roll angle
- $\phi_w$  = wave slope angle
- $\phi_{alm}$  = maximum angle of one-roll due to single wave
- $\omega_R$  = natural angular frequency of ship roll

## 1. INTRODUCTION

The asymmetric extreme waves which occur unusually in the ocean can cause great damage to ships, but currently, influences of wave asymmetry on ship roll have not been examined methodically and reasonably.

Since we have up to now been mainly treating symmetric waves such as sinusoidal waves as the waves acting on ships, we can not sufficiently explain whether ship roll on the asymmetric waves increases more than that on symmetric waves. In order to consider the mechanism of capsizing and to examine the safety of ships, it is necessary to obtain some knowledge on the roll behavior derived from the wave asymmetry.

## 2. DESCRIPTION OF ASYMMETRIC WAVES [5]

### 2.1 From Symmetric Waves to Asymmetric Waves

We attempted to change symmetric wave forms into asymmetric wave forms, as shown in Fig.1, by using the following function.

$$f_a = A \cdot \exp(B(\eta - A_0)) \quad (1)$$

where  $\eta$ : the wave elevation from still water level,  $A_0$ : the wave amplitude,  $A$ : the deformation quantity at wave crest and  $B$ : the declining coefficient of deformation under water surface.

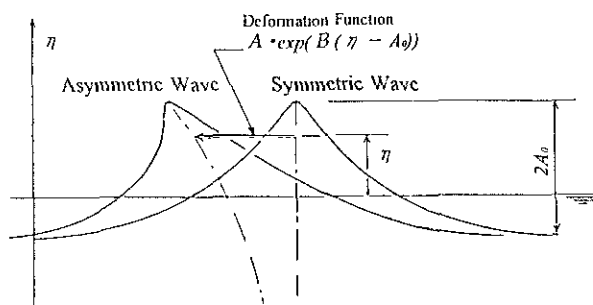


Fig.1 Means of deforming symmetric wave forms into asymmetric wave forms.

To generalize the above deformation factors, we express  $A$  and  $B$  as follows;

$$AA = A/W_L \quad (2)$$

$$BB = B/k \quad (3)$$

where  $W_L$  is the wave length, and  $k$  is the wave number  $W_L/(2\pi)$ . The above  $AA$  and  $BB$  are the non-dimensional deformation factors.

### 2.2 Subsurface in Asymmetric Waves

According to simple and basic theories, we understand that the roll moment due to waves is induced by the wave slope of the surface and subsurface in waves. And the pressure on water surface of waves is constant which is the atmospheric pressure. In the same manner,

we can suppose the subsurface being constant pressure, of which the wave height rapidly decrease with water depth [4].

Examples of subsurface in an asymmetric wave are shown in Fig.2, of which the surface wave steepness  $s=1/10$ . The surface and subsurface wave form of the asymmetric wave is described by deforming the trochoidal wave under  $AA=3.0$  and  $BB=2.0$  in eq.(1).

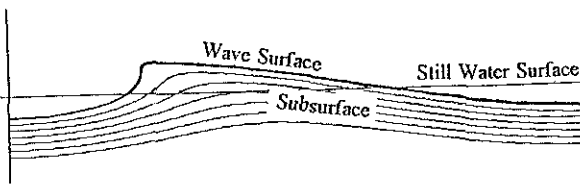


Fig.2 Subsurfaces in an asymmetric wave.

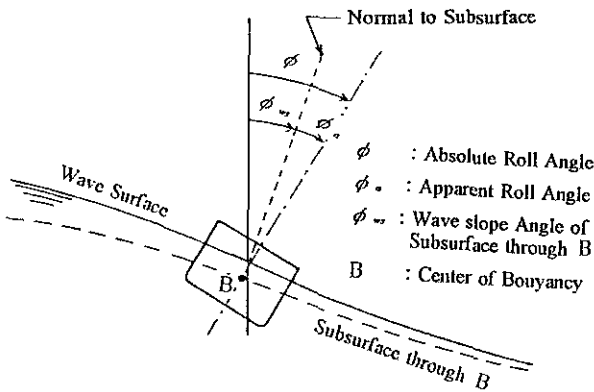


Fig.3 Co-ordinate system and B-subsurface that passes through the center of buoyancy B of a ship.

In order to search the qualitative influence of the wave asymmetry on the roll of a ship, we select a representative subsurface. The ship weight  $W$  is supported by the buoyancy acting on the ship. The resultant buoyancy acts

at the center of buoyancy B and its action line is normal to subsurface. We call the subsurface through B the B-subsurface.

In Fig.3 an example of the B-subsurface and a co-ordinate system are illustrated. The other symbols in Fig.3 will be denoted in the next chapter.

### 3. EQUATION OF ROLL MOTION

#### 3.1 Assumption of External Forces Acting on a Ship

Since the external forces acting on the ship on the steep and asymmetric waves can be very complex, we simplify the equation of roll motion by preparing the following assumptions.

- ① The motion of water particles in the waves has no influence on the ship hull.
- ② The virtual gravity works vertically on the B-subsurface.
- ③ The ship weight  $W$  remains constant. The fluctuation of  $W$  is not taken into account [6].
- ④ The wave exciting roll moment comes from the only slope angle of the B-subsurface.

#### 3.2 Equation of Roll Motion in Apparent Angle

The ship roll that arises under the assumptions of section 3.1 can be described using the

equation of the single-degree of freedom.

$$I_x \ddot{\phi} = -k_1 \dot{\phi}_a - W \cdot GM \cdot (1 - \beta_3 \phi_a^2) \phi_a \quad (5)$$

where  $\phi$  denotes the absolute roll angle of the ship,  $\phi_a$  the apparent roll angle,  $I_x$  the virtual moment of inertia about the longitudinal axis of the ship,  $k_1$  the coefficient of roll resistance,  $W$  the ship weight,  $GM$  the metacentric height, and  $\beta_3$  the coefficient of the nonlinear term of the stability.

The relationship among  $\phi$ ,  $\phi_a$  and  $\phi_{ws}$  is

$$\phi = \phi_a + \phi_{ws} \quad (6)$$

as shown in Fig.3.

Substituting (6) into (5), we obtain the equation of roll motion in the apparent roll angle.

$$\ddot{\phi}_a + K_1 \dot{\phi}_a - \omega_R (1 - \beta_3 \phi_a^2) \phi_a = -M_w \quad (7)$$

where  $\omega_R (= \sqrt{W \cdot GM / I_x})$  is the natural roll frequency in small amplitude,  $K_1 (= k_1 / I_x)$  the damping coefficient, and  $M_w$  the wave exciting roll moment,

$$M_w = c \phi_{ws} \quad (8)$$

where  $c$  is a constant correction coefficient. Eq.(7) is approximately reasonable for examining heavy roll [7], [1].

## 4. RESULTS OF NUMERICAL CALCULATION

### 4.1 Condition in Calculation

The ship used in calculation is a small model ship, because our study is the first step to make clear the influence of asymmetric waves on ship roll.

[The particulars of the ship model]

Length 80 cm, breadth 13 cm, draft 53 cm, weight 5.43 kgf, box shape with round bilge, the natural roll period  $T_R=0.65$  sec,  $K_1=1.0$  sec<sup>-1</sup>,  $\beta_3=1.0$  (the vanishing angle of stability 1.0 rad)

[The specifications of the waves]

Asymmetric wave form: Trochoidal wave form. Surface wave steepness:  $s=1/10$  or  $1/12$ .

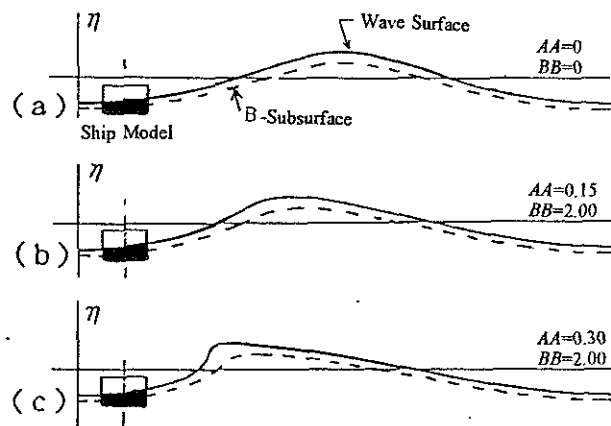


Fig.4 Examples of asymmetric waves deformed by  $AA$  and  $BB$  in eq.(1), and the dimensional comparison of the waves and the ship model (In case of the wave period  $T_w=1.0$  sec. and the surface wave steepness  $s=1/10$ ).

Deformation factor;  $AA=0, 0.15, 0.30, BB=2$  fixed. Examples of wave form are shown in Fig.4. Fig.4(a), (b) and (c) are the wave forms for  $AA=0, 0.15$  and  $0.30$  respectively.

In Fig.4, the rough section of the ship model is illustrated to compare with the dimension of the waves.

[ The specifications of numerical calculation ]

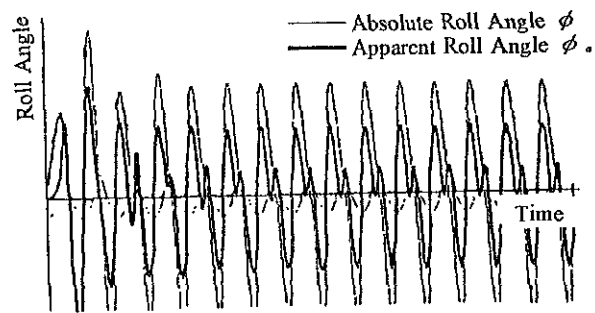
The initial condition: the ship model stands still at  $t=0$ . The numerical integration: Runge-Kutta method. Time step in calculation is  $T_w/200$  or  $T_w/400$ .

#### 4.2 Change of Roll Pattern Due to Wave form

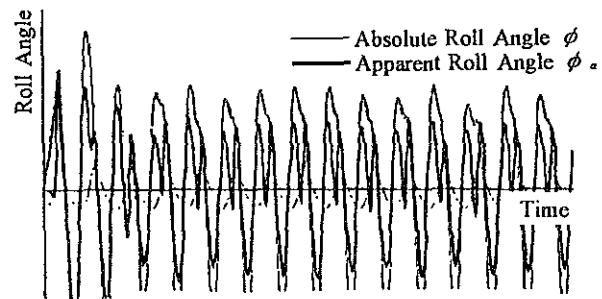
Examples of roll pattern on the waves are shown in Fig.5. Fig.5(a), (b) and (c) are the roll patterns on the waves corresponding to each wave form in Fig.4. In the case of Fig.5(a)  $AA=0$ , we can find transitional roll in the only initial stage and after a few rolls the roll amplitude converges on a constant value. The wide solid line in Fig.5 shows the apparent roll angle and a fine solid line the absolute roll angle. Fig.5(b) is the example of roll on asymmetric wave for  $AA=0.15$ , and in this case the roll amplitude does not converge on a constant value even after time has passed. Moreover, in the case of  $AA=0.30$ , the roll amplitude never converges as shown in Fig.5 (c).

The above irregular roll patterns on regular

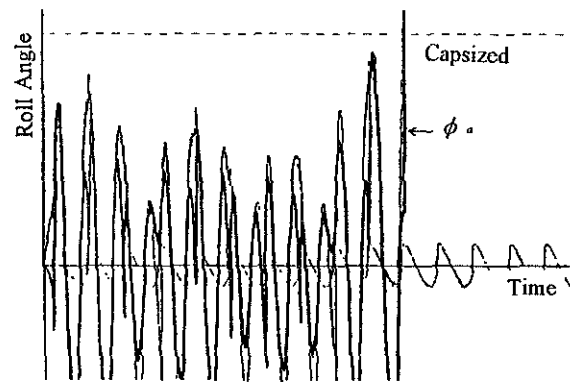
waves may be a chaotic phenomenon caused by the nonlinear stability term  $\beta_3$  in eq.(7) [3],[2]. Therefore we have to check the phenomenon from another viewpoint because the applied waves in Fig.5(b) and (c) are asymmetric. This is attempted in chapter 6. (2).



(a) Roll on the symmetric waves ( $AA=0, BB=0$ )



(b) Roll on the asymmetric waves ( $AA=.15, BB=2$ )



(c) Roll on the asymmetric waves ( $AA=.30, BB=2$ )

Fig.5 Variations of roll pattern on the symmetric waves and the asymmetric waves. (Each wave form is same in Fig.4)

Since we have illustrated strange roll patterns, the effect of such strange roll on the roll response for wave periods is examined in the following sections.

### 4.3 Roll response on Regular Asymmetric Waves

In Fig.6, the mean amplitudes of roll of the ship on regular waves are plotted on the axis of the wave period  $T_w$ . The surface

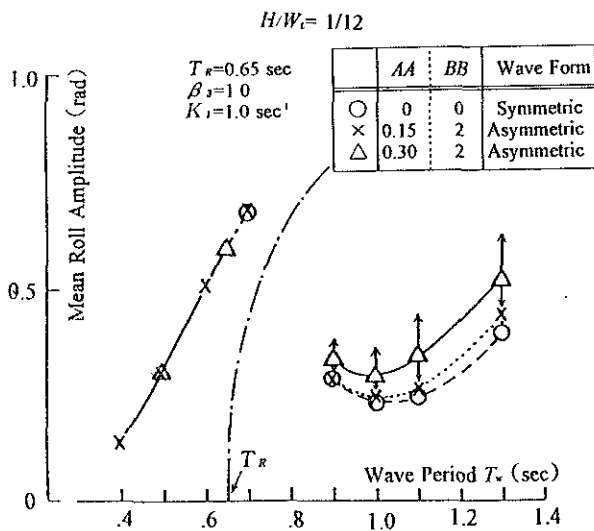


Fig.6 Difference of the roll response on the regular waves of which wave forms are symmetric or asymmetric.

wave steepness is  $1/12$ . Mark  $\circ$  is the mean amplitude for  $AA=0$ , mark  $\triangle$  for  $AA=0.15$  and mark  $\times$  for  $AA=0.30$ . From the results shown in Fig.6, we can summarize that the wave asymmetry does not clearly affect the mean roll amplitude. But the effect of the wave asymmetry appears somewhat in  $T_w > 0.8$  (sec). The marks of the arrows  $\uparrow$  and

$\downarrow$  in Fig.6 show that the roll motion does not converge on a constant amplitude.

### 4.4 One-roll Response on Single Asymmetric Waves

In this section, We pick up the one-roll due to the single asymmetric wave as shown in Fig.7. The transverse axis in the figure is the time or the position of the ship on waves. The wide solid line is the apparent roll angle  $\phi_a$  and the fine solid line the absolute roll angle  $\phi$ .

We are interested in  $\phi_{alm}$  being the maximum value of  $\phi_a$ . The dotted line is the B-subsurface. The curve of  $M_w$  is given from eq.(8). This curve is used in chapter 5 to discussion for the calculated results.

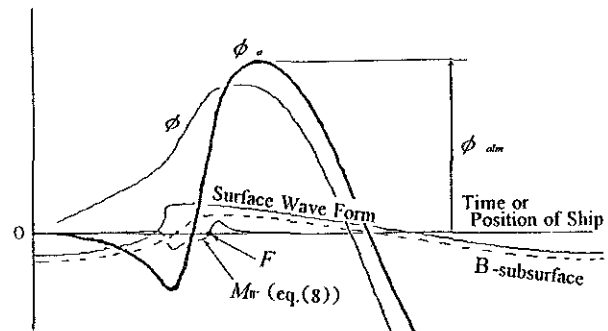


Fig.7 An example of one roll response on a single and asymmetric wave, and the definition of  $\phi_{alm}$ .

( $T_w=1.0 \text{ sec}$ ,  $s=1/10$ ,  $AA=0.3$  and  $BB=2$ .)

In Fig.8, a great deal of  $\phi_{alm}$ s for a large number of the wave periods changed very closely are continuously plotted. 3 kinds of  $\phi_{alm}$  curves are  $AA=0$ ,  $0.15$ , and  $0.30$ .  $BB=2$  and is constant. The one-roll response for  $AA=0.30$  becomes very complicated pattern.

From the calculated results, we can summarize as follows;

- (1) The wave asymmetry evidently affects the maximum roll angle  $\phi_{alm}$ . And the mean value of  $\phi_{alm}$  increases in rough proportion to  $AA$ .
- (2) The  $\phi_{alm}$  for  $AA=0.30$  drastically alters even in very close  $T_w$ . Namely, this response curve shows a chaotic pattern.

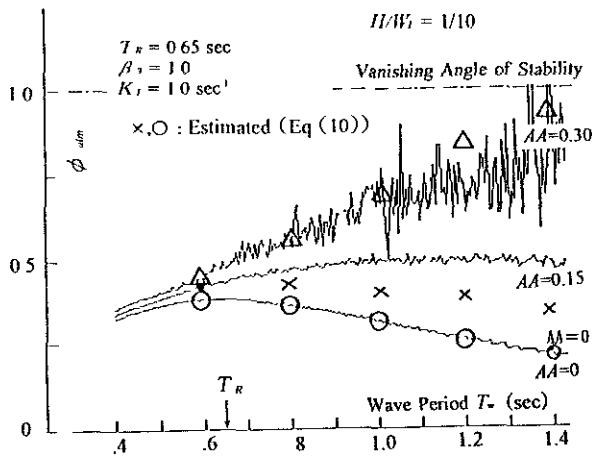


Fig.8  $\phi_{alm}$  responses for the wave period  $T_w$  changed closely. The influence of the wave forms on the  $\phi_{alm}$  responses appears remarkably.  $\phi_{alm}$  increases in rough proportion to  $AA$ , and the  $\phi_{alm}$  response for  $AA=0.30$  becomes a chaotic pattern.

In order to check the above chaotic pattern we set the time step in calculation more minutely. Then the chaotic pattern became more remarkable for  $AA=0.3$ , but for  $AA=0$  more smooth.

The dotted line in Fig.8 is the vanishing angle of stability of the ship.

## 5. DISCUSSIONS FOR CALCULATED RESULTS

From the calculated results in previous chapter, we can see the influence of the wave asymmetry and of the degree of the wave asymmetry on the roll response. Though at present, since we are not able to realize theoretically the results yet, we attempt to confirm the above influence from other viewpoints.

### (1) $\phi_{alm}$ Variation due to $AA$ (Fig.8)

$\phi_{alm}$  increased in rough proportion to  $AA$  as shown in Fig.8. The  $\phi_{alm}$  variation due to  $AA$  has to be caused by the wave exciting roll moment  $M_w$  in eq.(7). And, as  $\phi_{alm}$  is a kind of roll response occurring momentarily, the magnitude of  $\phi_{alm}$  probably depend on the strength of the impulsive moment  $P_M$  defined as follows;

$$P_M = \int_0^F M_w dt \quad (9)$$

where  $F$  is the time when  $M_w$  crosses zero near the wave crest of the B-subsurface (see Fig.7).

So let's estimate  $\phi_{alm}$ s by using  $P_M$ s for  $AA=0, 0.15, 0.30$  under the assumption that  $\phi_{alm}$  is in proportion to  $P_M$ . Namely,

$$[\phi_{alm}]_{AA=15, 30} = \frac{[P_M]_{AA=15, 30} [\phi_{alm}]_{AA=0}}{[P_M]_{AA=0}} \quad (10)$$

Marks  $\times$  and  $\Delta$  in Fig.8 are  $\phi_{alm}$ s for

$AA=0.15$  and  $0.30$ , which are obtained from eq.(10). Mark  $\circ$  is that for  $AA=0$ . We can see the estimated  $\phi_{alm}$  are plotted approximately on each response curve. This suggests that  $\phi_{alm}$  enable to be estimated from  $AA$ , because  $AA$  drives the variation of  $M_w$  and the  $M_w$  dominates the strength of  $P_M$ .

## (2) A Cause of Chaotic Roll

The chaotic pattern of roll in Fig.5(c) and of  $\phi_{alm}$  response in Fig.8 may occur owing to the effect of the nonlinear stability term  $\beta_3$  in eq.(7). However, we need to show that the nonlinearity of stability term is not the only cause of occurring chaotic roll. Namely, by putting  $\beta_3=0$ , we can examine the above subject. Fig.9 shows the  $\phi_{alm}$  response in the case of  $\beta_3=0$ . Though the stability term is linear, the chaotic pattern appears in the roll

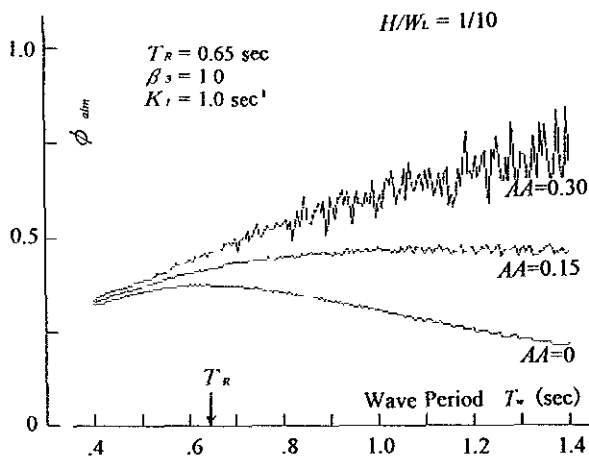


Fig.9  $\phi_{alm}$  responses in the case of the linear stability  $\beta_3=0$ . The specification of waves is same in Fig.8. The chaotic pattern appears in response regardless of the linear stability.

response. Judging from the results, we have to recognize that the nonlinearity of stability and also the wave asymmetry bring about chaotic roll and stimulate the occurrence of the chaotic phenomenon.

## 6. CONCLUDING REMARKS

The effects of the wave asymmetry on the ship roll were examined by solving numerically the roll equation taking into account the wave asymmetry.

The following results were obtained;

- (1) The wave asymmetry affected the roll motion.
- (2) The maximum roll angle due to the single asymmetric waves increased in rough proportion to the deformation factor  $AA$ . The increasing ratio was noticeable in the wave period over the natural roll period of the ship.
- (3) The mean roll amplitude on regular asymmetric waves was not different from that on the symmetric waves.
- (4) The wave asymmetry enable to bring about the occurrence of the chaotic roll.

## ACKNOWLEDGEMENTS

Part of this research was carried out while the author had been staying in The Norwegian institute of Technology. The author appreciates Prof. D. Myrhaug for his helpful encouragement, and Prof. M. Hamamoto,

Osaka University for his deep thoughtfulness.

The author note supplementally that this paper was prepared based on the reference [8] and on the results calculated after that.

## REFERENCES

- (1)S.Ishida, M.Yasuno and T.Takaishi: Model Experiment on the Mechanism of Capsizing of a Small Ship in Beam Seas, Jour. of the Society of Naval Architects of Japan, vol.167 (1990), pp.91-101.
- (2)M.Kan and H.Taguchi: Capsizing of a Ship in Quartering Seas (Part 3, Chaos and Fractal in Asymmetric Capsize equation), Jour. of the Society of Naval Architects of Japan, Vol.169(1991), pp.213-222
- (3)R.Kawashima: Ship Rolling Motion Analysis from the Nonlinear Dynamic's point of View - I , The Jour. of Japan Institute of Navigation, Vol.81(1989), pp.117-124.
- (4)S.Motora: Ship Dynamics, Kyouritu-Shupan (in Japanese), p.96, 1966
- (5)H.Sadakane: A Description of Wave Form of Solitary and Asymmetric Waves, The Jour. of Japan Institute of Navigation, Vol.92(1994), pp.151-156.
- (6)H.Sadakane: On the Rolling of a Ship on a Billow (1st Report, Fluctuation of apparent Ship-Weight),Jour. of the Kansai Society of Naval Architects, Japan, No.169 (1978), pp.83-93.
- (7)H.Sadakane: On the Rolling of a Ship on a Billow (3rd Report Heeling Moment), Jour.

of the Kansai Society of Naval Architects, Japan, No.180 (1981), pp.77-85.

- (8)H.Sadakane: A Study on Roll Behavior of Ship on Asymmetric Waves, The Jour. of Japan Institute of Navigation, Vol.93(1995), pp.141-148.

# CAPSIZING OF SHIP IN 'LOW CYCLE RESONANCE'

by V.A. Nekrasov, professor

Ukrainian State Maritime Technical University  
9, Geroev Stalingrada Av., Nikolaev  
327025, UKRAINE

## ABSTRACT

This paper deals with non-linear irregular motions of a ship in rough sea. It aims at creating a method of motion probabilistic characteristics' determination and stability investigation. Proposed method includes algorithms that are used for construction: equations of wind, wave and ship motions, equations of the motion probabilistic characteristics, stochastic analogs of Liapunov's functions and stochastic analogs of Liapunov's function derivatives. It also contains local stability criteria of ship dynamical states as stability criteria of stationary random processes of ship's oscillations. This allows to determine conditions of ship's non-local stability loss under the action of wind-waves excitations. An example of calculation of the non-linear roll motion probabilistic characteristics and their stability when a ship runs in the rough sea is presented.

## INTRODUCTION

General theorems of the stability theory emphasize a dependence of stability region boundary of non-linear dynamic system not only on the peculiarities of the system itself but on the character of external excitations as well. In order to consider non-local stability of the system these theorems require constructing Liapunov's functions and derivatives of Liapunov's functions. Therefore, an investigation of ship stability in a rough sea as stability of non-linear dynamic system must include the following:

a) description of given dynamic system behavior under action of given excitations;

b) construction of stochastic analogs of Liapunov's functions and derivatives of Liapunov's functions;

c) determination of stability region boundary in terms of the probabilistic theory.

Solution of all these questions under investigation of any type of non-linear ship motion is carried out by the given research.

A verification of the theory is fulfilled on an example of roll motion stability loss of a ship running in following and quartering seas when oscillations of ship potential pit strengthen this type of motion.

## 1. DESCRIPTION OF SHIP BEHAVIOR

A behavior of ship under action of random wind-waves excitations is presented in a general case by the solutions of the following differential equations

$$\frac{dY_k}{dt} = \varepsilon F_k(Y_1, \dots, Y_n; X_1, \dots, X_n; t);$$

$$k = 1, 2, \dots, n, \quad (1.1)$$

where  $X_k(t)$  are initial excitations, causing a motion of air and liquid, = given random functions of time, close to white noises;  $Y_k(t)$  are dynamical co-ordinates of system = displacements and velocities of certain points of the air and liquid and displacements and velocities of ship;  $\varepsilon$  is small parameter = ratio of acceleration of acting wind-waves excitations and free fall acceleration.

By introducing dynamical co-ordinates increments

$$Y_k(t) - Y_{k0} = H_k(Y_0) \equiv \\ \equiv H_k(Y_{10}, \dots, Y_{n0}; X_1, \dots, X_n; t),$$

where  $Y_{k0} = Y_k(t_0)$  are initial values of the dynamical co-ordinates, and their representing as

$$H_k(Y_0) = \varepsilon H_k^{(1)}(Y_0) + \varepsilon^2 H_k^{(2)}(Y_0) + \dots, \quad (1.2)$$

the components of solutions of the differential equations (1.1) can be written in the form

$$H_k^{(1)}(Y_0) = \int_{t_0}^t F_k(Y_0, t') dt';$$

$$H_k^{(2)}(Y_0) = \sum_{l=1}^n \int_{t_0}^t \frac{\partial F_k}{\partial Y_l}(Y_0, t') \times \int_{t_0}^{t'} F_l(Y_0, t'') dt'' dt'; \dots \quad (1.3)$$

An equation for characteristic function  $q_1(\lambda, t)$  of the considered processes of the ship motion and the motion of fluids is constructed on the basis of introduced representations [1]. For the case, when right parts of the motion equations (1.1) are represented by polynomials of dynamical co-ordinates, this equation is written in the form

$$\frac{\partial q_1(\lambda, t)}{\partial t} = \phi(\lambda; t, \frac{\partial}{i\partial\lambda}) q_1(\lambda, t). \quad (1.4)$$

For sufficiently large intervals of time  $\tau = t - t_0$  the operator  $\phi(\lambda; t, y) = \phi(\lambda; y)$  is determined by the expression

$$\phi(\lambda; y) = \sum_{k=1}^n i\lambda_k a_k(y) + \frac{1}{2} \sum_{k=1}^n \sum_{l=1}^n i\lambda_k b_{kl}(y) + \dots \quad (1.5)$$

Here

$$a_k(y) = A_k(y) + \sum_{k=1}^n A_{kl}^{(1)}(y) + \dots;$$

$$b_{kl}(y) = B_{kl}^{(1)}(y); \dots \quad (1.6)$$

and

$$A_k(y) = \varepsilon K[F_k(y)];$$

$$A_k^{(1)}(y, t) = \varepsilon^2 \int_0^\infty K\left[\frac{\partial F_k}{\partial y_l}(y), F_l(y, \tau)\right] d\tau;$$

$$\dots;$$

$$B_{kl}^{(1)}(y) = 2\varepsilon^2 \int_0^\infty K[F_k(y), F_l(y, \tau)] d\tau;$$

$$\dots \quad (1.7)$$

In considered expressions an operation

$$K[x, y] = M[(x - (M[x])(y - M[y]))]$$

is the operation of standardized averaging.

On the basis of the equation for characteristic function a system of equations for initial statistical moments

$$\alpha_{jk}(t) = M([Y_k(t)]^j)$$

is constructed. It is represented in the following form

$$\frac{d\alpha_j}{dt} = Q_j(\alpha_j, G_j, t); \quad j = 1, 2, \quad (1.8)$$

where  $G_j$  are vectors of intensity coefficients of the processes  $X_k(t)$ .

There exists a more simple method of construction of equations for statistical moments.

With the help of this method the equations for statistical moments of the first order are formed by application of the averaging operation  $M[\dots]$  to the equations (1.1).

Equations for statistical moments of the second order are formed after multiplication of equations (1.1) with  $Y_k(t)$ ,  $k = 1, 2, \dots, n$ , and application of the averaging operation  $M[\dots]$ , etc.

Fulfilling this operation it is necessary to take into account a correlation between processes  $Y_k(t)$  and excitations  $X_l(t)$ , understanding stochastic integrals of the

expressions (1.3) in Stratonovich sense [4]. Therefore, for any function  $R(y(t), x(t))$  included in (1.3)

$$M[R(y(t), x(t))] = \varepsilon M[R(y, x(t))] + \varepsilon^2 \int_0^\infty K \left[ \sum_{k=1}^n \frac{\partial R(y, x(t))}{\partial Y_k} F_k(y, x(t + \tau)) \right] d\tau + \dots \quad (1.9)$$

Here  $y$  is not function of time.

Determining characteristic function  $q_1(\lambda, t)$  up to  $\varepsilon^2$  corresponding equation for probability density  $f_1(y, t)$  of the processes  $Y_k(t)$  coincides with Fokker-Planck-Kolmogorov equation. This equation for non-linearities of  $(Y_k - Y_k^3)$  type, as is known, has only non-stationary solution. However, the searching of such solution has no sense because the problem of solution of the equations (1.1) is formulated correct to statistical moments of several first orders and must be solved on the same level. In this case a stationary solution of considered problem exists. It allows to determine limited quantity of statistical moments when including of any non-linearities in the equations of motion (1.1), of  $(Y_k - Y_k^3)$  type as well [1].

Limiting solution of the considered problem of the ship behavior determination under action of random wind-waves excitations on the level of statistical moments of the first two orders we come to necessity of solution of the following equations for moments

$$\frac{d\alpha_j}{dt} = Q_j(\alpha_1, \alpha_2, G_1, G_2, t); \quad j=1,2, \quad (1.10)$$

where  $\alpha_1(t)$ ,  $\alpha_2(t)$  are statistical moments of the processes  $Y_k(t)$ ;  $G_1(t)$ ,  $G_2(t)$  are intensity coefficients of the processes  $X_k(t)$ .

When forming of the equations (1.10) the processes  $X_k(t)$  are supposed to be close to white noises and  $Y_k(t)$  are Subgaussian random functions. Statistical moments of

higher orders included in these equations are expressed by moments of the first and the second orders with the help of relations, taking place for Subgaussian random functions [2] or, approximately, for Gaussian random processes.

For stationary random processes of acting on a ship wind-waves excitations the solution of problem of the ship behavior description is determined by solution of following nonlinear algebraic equations

$$Q_j(\alpha_1, \alpha_2, G_1, G_2) = 0; \quad j=1,2. \quad (1.11)$$

## 2. DESCRIPTION OF WIND-WAVES EXCITATIONS CHARACTER

Wind above sea may be considered as a stationary random process, velocity of which  $V(t)$  is determined by the term

$$V(t) = \bar{V} + \tilde{V}(t),$$

where  $\bar{V}$  is average velocity of wind on the level of sail center;  $\tilde{V}(t)$  are pulsations of wind velocity.

A spectral density  $S_{\tilde{v}}(\sigma)$  of the wind velocity pulsations  $\tilde{V}(t)$  in the domain of frequencies  $\sigma$ , on which the ship reacts, is not changed significantly. Therefore, the spectral density  $S_{\tilde{v}}(\sigma)$  in this interval of frequencies  $\sigma$  may be considered as a constant value. In this case, process  $\tilde{V}(t)$  is close to white noise  $\Psi_1(t) = X_1(t)$ . In more general case process  $\tilde{V}(t) = Y_1(t)$  is represented by the solution of the following stochastic differential equation

$$\dot{Y}_1 = Y_1 + X_1(t). \quad (2.1)$$

A spectral density of stationary sea  $S_{\zeta}(\sigma)$  in a system of co-ordinates connected with the ship is changed significantly. Therefore, random process  $\zeta(t) = Y_2(t)$  of irregular sea in this system of co-ordinates may be

represented by transformation of close to white noise random excitations  $\Psi_2(t) = X_2(t)$ ,  $\Psi_3(t) = X_3(t)$  in the dynamical system

$$\ddot{Y}_2 + 2\delta_1[1 + \varepsilon_1 X_2(t)]\dot{Y}_2 + 2\delta_3 \overset{.3}{Y}_2 + \omega_\zeta^2 [1 + \varepsilon_2 X_3(t)]Y_2 = 0, \quad (2.2)$$

on the output of which spectral density of process  $Y_2(t)$  changes depending on spectral moments of irregular sea  $\zeta(t)$ :

$$m_0 = \int_0^\infty S_\zeta(\sigma) d\sigma;$$

$$m_1 = \int_0^\infty \sigma S_\zeta(\sigma) d\sigma;$$

$$m_2 = \int_0^\infty \sigma^2 S_\zeta(\sigma) d\sigma.$$

One from possible version of the equation (2.2) coefficients representation is considered in the paper [2] in detail.

A choice of these coefficients is ensured by the fulfillment of the following conditions:

a) ordinates of process  $Y_2(t)$  have distribution close to the normal distribution;

b) amplitudes of process  $Y_2(t)$  have distribution close to the Rayleigh distribution;

c) dispersion of amplitude velocity

$A_2(t)$  of process  $Y_2(t)$  on the output of filter (2.2) equals dispersion of amplitude velocity of sea  $\zeta(t)$ , which represented by the spectrum  $S_\zeta(\sigma)$  in the moving system of co-ordinates;

d) dispersion of phase difference velocity

$\varphi_2(t)$  (dispersion of frequency fluctuations) of process  $Y_2(t)$  on the output of filter (2.2) equals dispersion of frequency fluctuations of irregular sea  $\zeta(t)$ , that is given by the spectrum  $S_\zeta(\sigma)$  in moving system of co-ordinates.

A random process of horizontal displacements of wave surface  $\eta(t) = Y_4(t)$

in moving system coordinates is formed similarly. It is determined by solution of equation

$$\ddot{Y}_4 + 2\delta_2[1 + \varepsilon_3 X_4(t)]\dot{Y}_4 + 2\delta_4 \overset{.3}{Y}_4 + \omega_\eta^2 [1 + \varepsilon_4 X_5(t)]Y_4 = 0, \quad (2.3)$$

where  $X_4(t)$  and  $X_5(t)$  are random processes close to white noises.

Intensity coefficients of processes  $X_k(t)$ ,  $k = 2, 3, 4, 5$ , are selected in such a way that non-correlation of processes  $Y_2(t)$  and  $Y_4(t)$ , taking place for progressive irregular sea, is ensured.

Filters (2.2) and (2.3) are related to self-oscillators. Their self-oscillations are caused by negative linear damping coefficients. Positive non-linear damping coefficients ensure the boundary character of oscillations amplitudes. Parameters  $\omega_\zeta, \omega_\eta$  characterize mean frequency of wave action on ship in moving system of co-ordinates.

### 3. CONSTRUCTION OF STABILITY CRITERIA

The equations for statistical moments of the second orders, belonging to the system (1.10) or (1.11), are equations of power (energy) transformations of the wind-waves actions into the processes of ship motion. Therefore, stationary solutions of the equations (1.11) cease to exist if in result of these transformations a developed kinetic energy exceeds potential resources of the ship or a occurrence of other resource restrictions takes place.

In this connection, a stability investigation of the stationary solutions of the non-linear equations for statistical moments (1.11) is fulfilled in region of existence of the solutions. This region is determined by an existence domain of real values of the equation (1.11) roots.

For the stability investigation of stationary process  $Y_k^{(s)}(t)$  with statistical moments  $\alpha_1^{(s)}$  and  $\alpha_2^{(s)}$  additional small perturbations  $\Delta\alpha_1$  and  $\Delta\alpha_2$  are introduced and equations for additional perturbations  $\Delta\alpha_1$  and  $\Delta\alpha_2$  are written in the form

$$\frac{d\Delta\alpha_1}{dt} = \frac{\partial Q_1}{\partial \alpha_1} \Big|_s \Delta\alpha_1 + \frac{\partial Q_1}{\partial \alpha_2} \Big|_s \Delta\alpha_2; \quad (3.1)$$

$$\frac{d\Delta\alpha_2}{dt} = \frac{\partial Q_2}{\partial \alpha_1} \Big|_s \Delta\alpha_1 + \frac{\partial Q_2}{\partial \alpha_2} \Big|_s \Delta\alpha_2.$$

Since equations for statistical moments of the second order are created with the help of quadratic forms of dynamical coordinates  $Y_k(t)$ , which are usually used for the construction of Liapunov's functions, the system of equations (1.11) may be considered as Liapunov's functions stochastic analog, that takes into account not only peculiarities of the non-linear dynamical system but a character of acting excitations also.

Then, a matrix of the first partial derivatives of the equations (1.11) right parts with respect to the statistical moments becomes by stochastic analog of Liapunov's function derivative and a stability region of the equations (1.11) solutions is determined by the domain of negative values of this matrix eigenvalues.

Therefore, a stability region boundary is defined by an equality to zero of the first partial derivatives' matrix determinant. This determinant, as is known, equals the multiplication of matrix eigenvalues  $\lambda_i$  :

$$\left| \frac{\partial Q}{\partial \alpha} \right| = (-1)^m \prod_{i=1}^m \lambda_i, \quad (3.2)$$

where  $m$  is quantity of statistical moments of the first two orders. Then, criteria of stability region are determined by the following non-equalities

$$\operatorname{Re}[\lambda_i] < 0, \quad i = 1, 2, \dots, m. \quad (3.3)$$

In addition to this it is necessary to note that a solution of the equations for statistical moments (1.11), defining the behavior of a ship under stationary random wind-wave actions, is realized by the methods of nonlinear programming. A determinant of the first partial derivatives' matrix and eigenvalues of this matrix are calculated with the help of an application of the traditional algorithms of linear algebra.

The solution of equations (1.11) as solution of nonlinear equations for the same wind-waves actions on a ship can have several branches. Therefore, the ship in the same condition can have several dynamical states each of them in a general case should not be stable.

#### 4. DIFFERENTIAL EQUATION OF NON-LINEAR ROLL MOTION

A simplest non-linear differential equation of roll motion of a ship running in a sea, composed up to  $\varepsilon$ , is represented in the form

$$\begin{aligned} & (I_x + \mu_{44})\ddot{\theta} + \lambda_{44}^{(1)}\dot{\theta} + \lambda_{44}^{(2)}\theta|\dot{\theta}| + \\ & + D[h_0\theta + h_1\theta|\theta| + h_2\theta^3] \times \\ & \times [1 - \kappa_\zeta(\sigma_p, \varphi_0)\zeta(t)] = \\ & = M_0 + \bar{M}_1 + \tilde{M}_1(t) + \\ & + D[h_0 + 2h_1|\theta| + 3h_2\theta^2] \times \\ & \times \kappa_\eta(\sigma_p, \varphi_0)f(\sigma_p^2)\eta(t), \end{aligned} \quad (4.1)$$

where  $\theta(t)$  is roll motion process;  $\zeta(t)$  and  $\eta(t)$  are processes of vertical and horizontal displacements of wave surface in the coordinate system connected with ship;  $M_0$  and  $\bar{M}_1$ ,  $\tilde{M}_1(t)$  are initial and wind heeling moments;  $\kappa_\zeta(\sigma_p, \varphi_0)$  and  $\kappa_\eta(\sigma_p, \varphi_0)$  are generalized reducing coefficients of exciting moment for two-dimensional wave actions. The first of them, as is known, takes

into account pulsations of restoring moment under the influence of ship's hull wetted surface variability:

$$\kappa_{\zeta}(\sigma_p, \varphi_0) \approx \frac{r_0}{h_0} \times \frac{3(1-\chi)}{\chi T} \times \\ \times \kappa_s(\sigma_p, \varphi_0) \cos^*(\varphi_0).$$

Here

$r_0$  and  $h_0$  are initial metacentric radius and initial metacentric height of ship;

$T$  is draft;

$\kappa_s(\sigma_p, \varphi_0)$  is reducing coefficient;

$\chi = \delta / \alpha$  ( $\delta$  is block coefficient and  $\alpha$  is waterline coefficient);

$\varphi_0$  is angle of waves' propagation direction

( $\varphi_0 = 0$  - following sea);

$\sigma_p$  is frequency of wave spectrum peak;

$\cos^*(\varphi_0)$  is an averaging component taking into account waves' propagation direction.

Together with the equations (2.2) and (2.3) of wave exciting motion the equation of ship roll (4.1) composes the system equations of the considered dynamical system motion. The wind in it is represented by a random process, close to the white noise.

## 5. DETERMINATION OF PROBABILISTIC CHARACTERISTICS OF MOTION AND STABILITY

On the basis of the motion equations (2.2), (2.3) and (4.1) a system of equations for statistical moments of the first  $\alpha_1(t)$  and the second  $\alpha_2(t)$  orders has been composed. This system contains 27 nonlinear algebraic equations.

A composition of these equations, their solution and investigation of solution stability has been carried out with the help of above method and modern number algorithms of nonlinear and linear algebra.

## 6. STABILITY INVESTIGATION

The example of such investigation is an analysis of "Patrulny" ship accident in June 1986 on the Low-Kama Water Reservoir. This ship, striving for the shelter, capsized in intensively growing quartering waves with  $h_{3\%} = 1.32H_{1/3} \approx 2.2$  m and average period  $\bar{\tau} \approx k_{\tau} \sqrt{h_{3\%}} \approx 4.0$  s,  $k_{\tau} \approx 2.7$ . The speed of the ship was about 3.0 m/s  $\approx$  6 knots.

Main dimensions and characteristics of ship:

$L_{pp} = 19$  m - length between perpendiculars;

$B_{WL} = 3.8$  m - breadth in WL;

$T = 1.17$  m - draught;

$\delta = 0.483$  - block coefficient;

$\alpha = 0.796$  - waterline coefficient;

$Z_G = 1.56$  m - applicate of gravity center;

$h_0 = 0.54$  m - initial metacentric height;

$l_{\max} = 0.289$  m - maximum of righting level (calm water);

$\theta_{\max} = 40^\circ$  - angle of righting level curve maximum (calm water);

$S_{CK} = 3.24$  m<sup>2</sup> - area of bilge keels.

Before accident, the ship was abeam to waves and the wind. Then, she began slowly to turn, changing a course angle  $\varphi_0$  from  $90^\circ$  to  $0^\circ$  and decreasing a wave action frequency.

Figs. 1-4 show possible consequences of such turning. In these figures a scale of wave spectrum peaks  $\sigma_p$  in a system of coordinates connected with the ship corresponds the scale of course angles  $\varphi_0$ . Besides, the following designations are introduced:

$\alpha_{11} = M[\theta]$  - statistical moment of the first order of heel angles;

$\alpha_{21} = M[\theta^2]$  - initial statistical moment of the second order of heel angles;

RP - real parts of corresponding eigenvalues;

$\sigma_{\theta}$  - natural frequency (frequency of the free small roll oscillations).

Thus, the figures represent moment-frequency characteristics of irregular roll motion [3].

Fig.1 shows moment-frequency characteristics of stable dynamical states of the ship. In this fig. a moment-frequency characteristic of  $\alpha_{21}$  is similar to usual amplitude-frequency characteristic of regular non-linear roll oscillations. For its left low-frequency part a corresponding phase lag defined by statistical moment  $M[\theta \eta]$  changes the sign in comparison with high-frequency right part. This corresponds the attribute of a lower branch of above mentioned amplitude-frequency characteristic.

Fig. 2 represents unstable dynamical states of a ship. These states take place in the domain of course angles from  $25^\circ$  to  $50^\circ$  under the influence of the statistical moment  $\alpha_{11} = M[\theta]$  (mean value of roll angles) stability loss. This fig. also shows that a solution of the considered problem ceases to exist in a region of real values of statistical moments that is determined by course angles from  $0^\circ$  to  $25^\circ$ .

Fig. 3 represents unstable dynamical states of ship as well. Now statistical moment  $\alpha_{12} = M[\dot{\theta}]$  (mean value of roll velocity) and some other correlation statistical moments lose stability in the same domain of course angles,  $25^\circ - 50^\circ$ .

For the left low-frequency parts of moment-frequency characteristics of statistical moment  $\alpha_{21}$  represented in figs. 2-3 phase lags defined by statistical moment  $M[\theta \eta]$  do not change signs in comparison with high-frequency right parts. This corresponds the attribute of upper ("resonant") branch of the above mentioned amplitude-frequency characteristic.

Fig. 4 summarizes a research made. It shows that a stability loss of statistical moments of the first order is accompanied by the roll motion amplitude increase. The dynamical states of a ship in this case correspond upper ("resonant") branch of the mentioned amplitude-frequency characteristic of regular oscillations. Therefore,

a considered phenomenon may be conditionally called as "capsizing of ship in 'low cycle resonance'". At the same time, a true name of this phenomenon is **capsizing of ship under the influence of low-frequency oscillations of its potential barrier**. In this case increasing amplitude does not lose stability. That function is realized by the mean values of roll and roll velocity.

## CONCLUSIONS

A proposed method allows to carry out a solution of all problems that are enumerated by the introduction to this paper. It also gives possibility to explain phenomena accompanying ship's motion in rough sea.

The research of roll motion stability of a ship running in irregular following and quartering seas shows that a stable solution of the problem, concerning mean value of roll angles, in determined conditions is placed between unstable solutions (fig.4). Therefore, any attempt to alter a ship position relatively to the stable mean heel angle, for example with the help of rudder, leads in these conditions to catastrophe.

## REFERENCES

1. Nekrasov V.A. Probabilistic problems of seakeeping of ships. - Leningrad: Sudostroenie, 1978.
2. Nekrasov V.A. "To the mathematical modeling of wave processes acting on a ship." Ship Hydrodynamics, Transactions of Nikolaev Shipbuilding Institute, 1990, pp. 30 - 38.
3. Nekrasov V.A. "Stochastic stability theory of ship motion". Proceedings of the 5th International Conference on Stability of Ships and Ocean Vehicles, Melbourne, 1994.
4. Stratonovich R.L. Selected questions of the fluctuation theory in radiotechnics. - Moscow, Sovetskoe Radio, 1961.

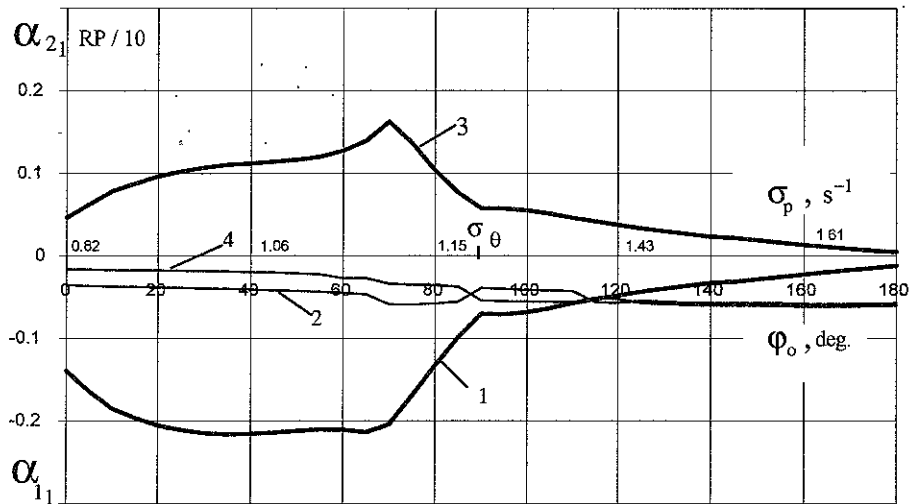


Fig. 1. Stable solution of problem of probabilistic characteristics determination and stability investigation for "Patrulny" ship running in rough sea

- 1 - moment-frequency characteristic of  $\alpha_{11} = M[\theta]$  (statistical moment of the first order of roll angles);
- 2 - real parts (RP) of  $\alpha_{11}$  eigenvalues;
- 3 - moment-frequency characteristic of  $\alpha_{21} = M[\theta^2]$  (initial statistical moment of the second order of roll angles);
- 4 - real parts (RP) of  $\alpha_{21}$  eigenvalues;
- $\sigma_\theta$  - natural frequency (frequency of the free small roll oscillations of the ship);
- $\sigma_p$  - frequencies of wave spectrum peaks;  $\varphi_0$  - course angles

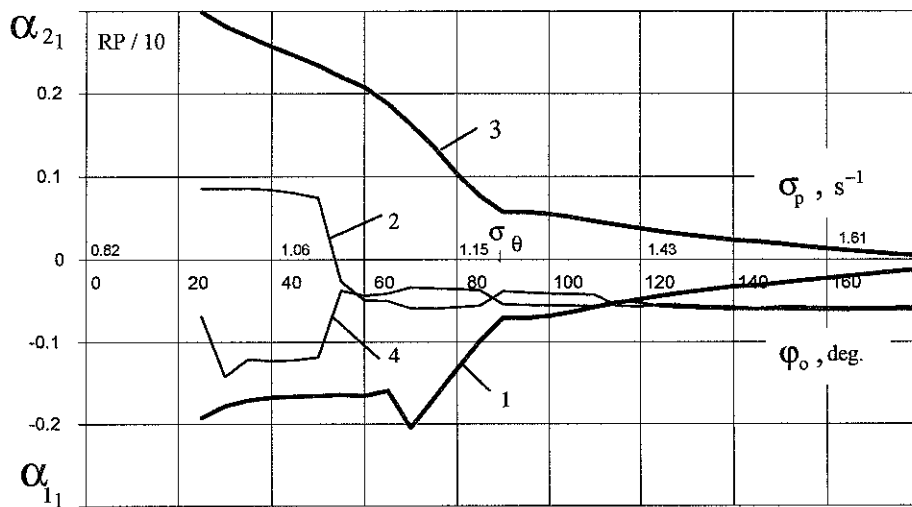


Fig. 2. The first unstable solution. Statistical moment  $\alpha_{11} = M[\theta]$  loses stability in the domain of course angles from  $25^\circ$  to  $50^\circ$

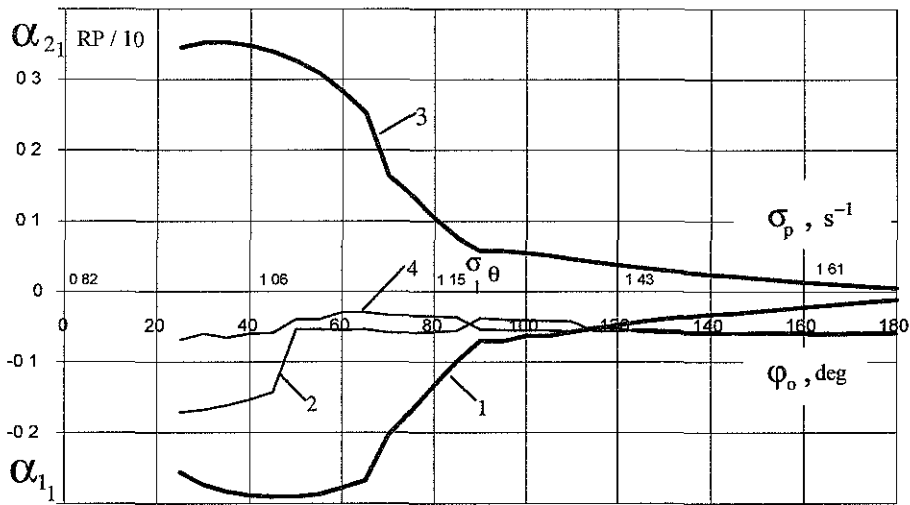


Fig. 3. The second unstable solution. Statistical moment  $\alpha_{12} = M [ d\theta/dt ] = 0$  loses stability in the same domain of course angles,  $25^\circ - 50^\circ$  (curve of real parts of this moment eigenvalues is similar to curve of real parts of  $\alpha_{11}$  eigenvalues, represented on fig.2)

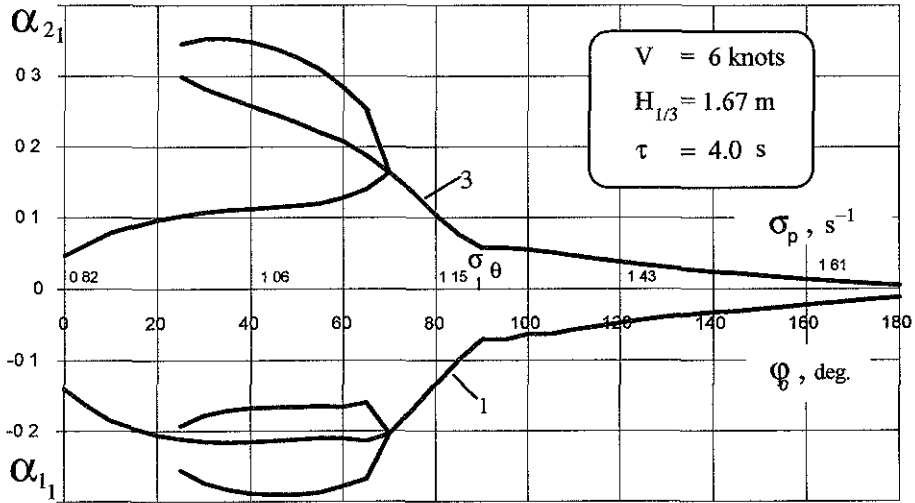


Fig. 4. The branching of solution (a reason of "Patrulny" ship capsizing under the influence of low-frequency oscillations of its potential barrier)

# UNCERTAINTY ANALYSIS APPLIED TO THE PARAMETER ESTIMATION IN NONLINEAR ROLLING

Roberto PENNA (\*), Alberto FRANCESCUTTO (\*\*) and Giorgio CONTENUTO (\*\*)

(\*)INSEAN -Italian Model Basin, Via di Vallerano 139, 00128 Roma, Italy

(\*\*) DINMA - University of Trieste, via A. Valerio, 10 - 34127 Trieste, Italy

e-mail: francesc@univ.trieste.it

## ABSTRACT

A MonteCarlo based methodology for the evaluation of the uncertainty connected with the parameter estimation from experimental results of large amplitude rolling motion in a regular beam sea has been developed. The application to two typical cases, a fishing vessel with quasi-linear righting moment and a frigate with highly nonlinear righting moment was considered. The results indicate that the separation capability between damping and excitation parameters is excellent, while that between different damping contributions is not completely satisfactory.

## INTRODUCTION

In the frame of ship safety, the present keywords are *design, training, operate for safety* [1,2]. This means the availability of high efficiency procedures for the simulation of ship behaviour in rough weather starting with large amplitude motions and special focus on rolling motion. Since theoretical methods for nonlinear hydrodynamics cannot at present give a satisfactory answer to this demand, researchers and designers have to resort very often to semiempirical approaches and experimental tests on scale models. With regard to experimental approaches, many different parameter identification techniques have been developed to estimate the values of the unknown parameters of the adopted mathematical model for rolling motion description. Due to the high nonlinearity of the equation of motion, most of these techniques are based on approximate solutions, usually obtained by means of perturbation methods,

which are *fitted* to the experimental records. Recently, following an indication by Haddara and Bennett [3], a new, high efficiency parameter estimation technique has been developed [4,5] which avoids the use of approximate solutions. While this approach improves both the generality (a perturbative solution has to be computed ex-novo any time the mathematical model is changed) and the precision of the estimation procedure, the question of the uncertainty connected with the estimated values remains to some extent an open, although a very important one [6].

A complete solution would require the availability of a great number of independent experimental records to be analysed, each taken in the same test conditions. The ordinary methods of error analysis [7] applied to the set of estimated parameter values would give their confidence interval. This process is money and time consuming, so that, following the idea of [8,9], a novel approach to the problem has been developed, based on MonteCarlo technique. A set of *independent numerical experimental outcomes* is generated by a computer starting from the one effectively obtained from experiments, by using a Gaussian random generation procedure with measured value and standard deviation. The set of so generated numerical *experimental* results is then analysed by the parameter identification procedure and uncertainty analysis is performed on the set of estimated parameter values. The procedure is still time consuming, but can be programmed to run automatically, so that there is no need to perform huge amounts of experimental tests. The procedure has been applied to the results of nonlinear rolling experiments in beam sea in

two typical conditions as regards the degree of nonlinearity. The results indicate the reliability of the estimated parameters (in this case linear and nonlinear damping coefficients and effective wave coefficients) and the difficulties connected with the separability of the different contributions (mainly the different damping terms).

## THE TESTED MODELS

Present analysis refer to the experimental tests conducted in a regular beam sea on two scale models of ships in the towing tank of the University of Trieste.

The first one refers to a fishing vessel presenting a quasilinear righting moment, so that the bending of the resonance peak is very small (Fig. 1). The solid line in Fig. 1 refers to the simulation obtained with estimated parameters. For clarity sake, the backbone curve (Eq. 4 below) giving the variation of resonant frequency with increasing the oscillation amplitude has also been reported.

The second series of tests refers to a frigate with highly nonlinear righting moment giving a strong bending to the resonance peak (Fig. 2). This last situation can be classified as 'pre- or quasi- bifurcating type', as is evident from the sharp vertical line in the low frequency side of the peak. The backbone curve exhibits, indeed a marked deviation towards low frequency as the amplitude of the motion is increased.

The tests have been conducted in a regular beam sea with constant wave steepness  $s_w = \frac{h_w}{\lambda_w} = \frac{1}{50}$ , being  $h_w$  and  $\lambda_w$  wave height and wavelength respectively. The model was restrained by soft elastic ropes so as to eliminate yaw and drift. Details on the models and on the experimental setup and procedure have already been reported elsewhere and will not be repeated here. Some details on the tested models and on the values adopted and identified for the parameters are given in Table. 1.

The results include uncertainty analysis in a standard way.

## MATHEMATICAL MODELLING OF THE NONLINEAR ROLL MOTION

The simulation procedure for large amplitude roll motion is here considered based on a single degree of freedom approach. While the coupling with vertical motions and with sway is of great interest in many respects, the adopted model is quite sufficient for the discussion of uncertainty in the estimated parameters.

In normalized form the roll motion can be described by:

$$\ddot{\phi} + 2\mu\dot{\phi} + \delta|\dot{\phi}|\dot{\phi} + \omega_0^2\phi + \sum_j \alpha_{2j+1}\phi^{2j+1} = e_w \cos \omega t \quad (1)$$

with

$$e_w = \alpha_0 \pi s_w \quad (2)$$

for the fishing vessel case, and

$$e_w = \pi s_w (\zeta_1 \omega_0^2 - \zeta_2 \omega^2) \quad (3)$$

for the frigate. This last excitation model was adopted for the frigate on the basis of [10] since no reasonable fitting of experimental data was possible with the very simplified expression (2), being in this case  $e_w$  frequency independent.

A perturbative analysis was conducted on the roll motion equation leading to analytical expressions for the steady state solutions and for the transient phases. The equivalent resonance frequency and linear damping were obtained in the traditional form:

$$\omega_{0_{eq}}^2 = \omega_0^2 + \frac{3}{4} a_3 C^2 + \frac{5}{8} a_5 C^4 + \frac{35}{64} a_7 C^6 + \frac{63}{128} a_9 C^8 + \dots \quad (4)$$

and

$$\mu_{eq} = \mu + \frac{4}{3\pi} \delta \omega_0 C \quad (5)$$

being  $C = C_0 \cos(\omega t + \psi)$  the approximate solution of Eq. 1 with  $C_0$  and  $\psi$  amplitude and phase.

Eq. 4 describes the curve known as backbone (Fig1 and Fig. 2).

### THE PARAMETER IDENTIFICATION PROCEDURE AND THE EVALUATION OF THE PARAMETER UNCERTAINTY

Haddara and Bennett [3] developed a Parameter Identification Technique (PIT) based on the least squares fitting of the numerical solution of the equation of motion to roll decrements of a ship in calm water. His method was specifically oriented to estimate damping coefficients. The extension of the method to the forced oscillations both for a single or even for a multi degree of freedom system [11] was developed by the authors. In the following we will refer to the single degree of freedom case applied to Eq. 2. Following this approach, the *best estimate* of the unknown parameters of the mathematical model can be found by minimizing the function  $S$  given by:

$$S(p_j, j = 1, N_{\text{param}}) = \sum_{i=1}^{N_{\text{data}}} (\varphi_{\text{num}_i} - \varphi_{\text{exp}_i})^2 \quad (6)$$

where  $p_j$  are  $N_{\text{param}}$  unknown parameters  $(\mu, \delta_1, \delta_2, \dots, \alpha_0, \dots)$ ,  $\varphi_{\text{exp}_i}$  are stationary experimental roll amplitudes measured at  $N_{\text{data}}$  wave frequencies  $\omega_i$ ,  $\varphi_{\text{num}_i}$  are the  $N_{\text{data}}$  stationary numerical solutions of the equation of motion adopted. The procedure runs step by step starting with given initial values of the parameters. Each successful step leads to a reduction of the sum of residuals or  $\chi^2$ . The procedure is stopped manually when the  $\chi^2$  or the iteration step are sufficiently small or steady.

The minimization process is evidently a strongly nonlinear one with the parameters resulting from a complex minimization

procedure of the deviations to the experimental data. As a consequence, the standard error propagation analysis cannot be applied to obtain the uncertainty of the estimated parameters in terms of the input data uncertainty and of the uncertainty connected with the use of the PIT. This is the reason why we resorted to the numerical generation of a large series of experimental outcome (average 1000 trials) starting from the effectively measured set of values *and of their standard deviation*. The procedure, known as MonteCarlo method, consists in the following steps:

1. Generation of a large number of independent set of experimental results by adding to the original set random deviations obtained by a Gaussian sampling procedure of assigned standard deviation;
2. Evaluation of the parameters to be identified from each set of independent experimental results by means of the PIT (Eq. 6);
3. Evaluation of the statistics (average and standard deviation) of the set of obtained parameter values after checking that the distribution is Gaussian. This last request is connected to the yet unspecified *large* number of independent outcomes.

There are, of course procedures (tests of hypotheses) for the evaluation of the statistical deviation of an obtained distribution from an assigned one. In the following, preliminary results are presented. These are based on the assumption that the experiments considered are in number sufficient to have a reliable evaluation of the statistics of the obtained random distribution. As we will see, this is certainly true, as it is evident from visual fit, for the excitation parameters and for the equivalent linear damping.

### RESULTS AND DISCUSSION

The results obtained by applying the MonteCarlo procedure to the experimental data of the two ship models are reported in Fig. 3 to Fig. 8 for the fishing vessel and in Fig. 9 to Fig.

16 for the frigate. All generated set of independent trials consisted in 1000 sets, with the exception of the fishing vessel with 5% Gaussian uncertainty level, where the number of trials was limited to 708 due to the high number of failures in the convergence procedure. The Figures report the histograms obtained from the analysis of the PIT outcomes together with the Gaussian distributions (continuous curves) calculated with the parameter average values and standard deviations. The procedure was made automatic, integrating the random generator and the PIT in the same code. The same set of initial values was used during the run. The stopping condition was set to 5 steps or to a threshold value for  $\chi^2$ , equal for all the runs of the same ship. The results are not necessarily the best estimate obtainable with the given input data, since sometimes the minimisation procedure requires much more than five steps to converge efficiently. In this sense, the obtained standard deviations can be considered as an upper bound to the best possible estimates. Finally, the runs leading to unacceptable values for the parameters (mainly one of the damping coefficients negative) were discarded.

#### Fishing vessel

Three different uncertainty levels have been considered for the generation of the independent sets of experimental results, namely 1%, 2% and 5% all Gaussian distributed. The results are shown in Table. 2 and synthetically in Fig 3, 4 and 5. The procedure indicated that the standard deviation of the excitation parameter (effective wave slope coefficient  $\alpha_0$ ) was much smaller than that of the two damping contributions, featuring a figure very close to the standard deviation of the input. The obtained distributions were bias-free. The dispersion of the damping contributions was quite high in all cases. The number of unacceptable trials was found to be higher the lower the quality of input data.

To have a closer insight into damping, the equivalent linear damping (Eq. 6) was computed and displayed in Fig. 6 to Fig. 8. This parameter exhibit a very small dispersion, as it

is to be expected by examining the dispersion of excitation coefficient, indicating a high negative correlation between the two separate contributions.

#### Frigate

In this case, only the 1% and 2% Gaussian uncertainty level was considered. Due to the complexity of the mathematical model to be fitted to the experimental data and particularly to the high nonlinearity of the righting arm leading sometimes the solution to a bifurcation level during the minimization procedure, the number of unacceptable results is higher than in the previous case.

The results are reported in Table. 3 and synthetically in Fig. 9 and Fig. 10. Here also the dispersion in separating the damping contributions is quite high. On the contrary, the distribution of both the excitation coefficients is very narrow banded, with a standard deviation close to that of the input data. The separate excitation contributions are shown in Fig. 11 to Fig. 14. They exhibit a distribution very close to the superimposed Gaussian (solid line), so that the evaluation of the statistics of these parameters is highly reliable. To have a better insight into the behaviour of damping contributions, In Fig. 15 and Fig. 16 the linear, nonlinear and equivalent linear damping results are shown in detail. Here also, the equivalent linear damping exhibits a very narrow banded distribution close to the Gaussian, while the separate linear and nonlinear contributions have high dispersion and correlation giving a distribution not very close to the Gaussian.

## CONCLUSIONS

The evaluation of the uncertainty connected with the application of a Parameter Identification Procedure to the analysis of large amplitude forced rolling was conducted with the aid of a MonteCarlo Procedure. The results indicate that the PIT exhibits extremely good separation capability between damping and excitation. Furthermore, its ability in separating different excitation contribution is excellent. On the contrary, the ability in splitting the equivalent linear damping in several

contributions, linear and nonlinear is still not completely satisfactory. This is an important point, since it means that separate values of the damping in nonlinear rolling possess an intrinsic high uncertainty.

#### ACKNOWLEDGEMENTS

This research has been partially supported by INSEAN under Contract Code 1/LR343/95.

#### REFERENCES

[1] Francescutto, A., "Is it Really Impossible to Design Safe Ships?", *Trans. RINA*, Vol. 135, 1993, pp. 163-173.

[2] Francescutto, A., "Towards a Reliability Based Approach to the Hydrodynamic Aspects of Seagoing Vessels Safety", *Proc. OMAE'92*, Calgary, 1992, Vol. 2, pp. 169-173.

[3] Haddara, M. R., Bennett, P., "A Study of the Angle Dependence of Roll Damping Moment", *Ocean Engng*, Vol. 16, 1989, pp. 411-427.

[4] Cardo, A., Coppola, C., Contento, G., Francescutto, A., Penna, R., "On the Nonlinear Ship Roll Damping Components", *Proc. Int. Symp. NAV'94*, Rome, 1994.

[5] Francescutto, A., Contento, G., Penna, R., "Experimental Evidence of Strongly Nonlinear Effects in the Rolling Motion of a Destroyer in Beam Sea", *Proc. Int. Conf. STAB'94*.

[6] Coleman, H. W., Steel, W. G. Jr, "Experimentation and Uncertainty Analysis for Engineers", Wiley & Sons, New York, 1990.

[6] Masia, M., Penna, R., "Quality of Experimental Data in Hydrodynamic Research", *Proc. Int. Symp. on "Advanced Mathematical Tools in Metrology"*, Berlin, 1996.

[8] Spouge, J. R., "Non-linear Analysis of Large-Amplitude Rolling Experiments", *Int. Shipb. Progress*, Vol. 35, 1988, pp. 271-320.

[9] Spouge, J. R., "A Technique for Estimating the Accuracy of Experimental Roll Damping Measurements", *Int. Shipb. Progr.*, Vol. 39, 1992, pp. 247-265.

[10] Blagoveschensky, S. N., "Theory of Ship Motions", Vol. I, Dover, New York, 1962.

[11] Francescutto, A., Contento, G., "An Investigation on the Applicability of Simplified Mathematical Models to the Roll-Sloshing Problems", *Proc. ISOPE'97*, Honolulu, 1997, Vol. 3, pp. 507-514.

	Fishing vessel	Frigate
Lbp (m)	2.000	2.400
B (m)	0.552	0.285
T (m)	0.214	0.081
$\Delta$ (kgf)	100.00	25.79
$\omega_0$	4.553	5.02
$\alpha_3$	0.2	-46
$\alpha_5$	-	120
$\alpha_7$	-	-110
$\alpha_9$	-	4
$\mu$	0.130	0.0626
$\delta$	0.270	0.151
$\alpha_0$	0.745	-
$\zeta_1$	-	0.576
$\zeta_2$	-	0.042

Table 1. Model data

err	runs	good	param	average	s.d.
1%	1000	1000	$\mu$	0.13	0.03
			$\delta$	0.27	0.05
			$\alpha_0$	0.746	0.007
			$\mu_{eq}$	0.310	0.004
2%	1000	958	$\mu$	0.135	0.06
			$\delta$	0.26	0.09
			$\alpha_0$	0.747	0.01
			$\mu_{eq}$	0.310	0.008
3%	708	467	$\mu$	0.15	0.05
			$\delta$	0.236	0.013
			$\alpha_0$	0.75	0.02
			$\mu_{eq}$	0.31	0.02

Table.2. Results for the fishing vessel

err	runs	good	param	average	s.d.
1%	1000	955	$\mu$	0.064	0.03
			$\delta$	0.15	0.03
			$\zeta_1$	0.576	0.006
			$\zeta_2$	0.042	0.006
			$\mu_{eq}$	0.213	0.003
2%	1000	792	$\mu$	0.08	0.05
			$\delta$	0.13	0.05
			$\zeta_1$	0.58	0.01
			$\zeta_2$	0.04	0.01
			$\mu_{eq}$	0.212	0.006

Table.3. Results for the frigate

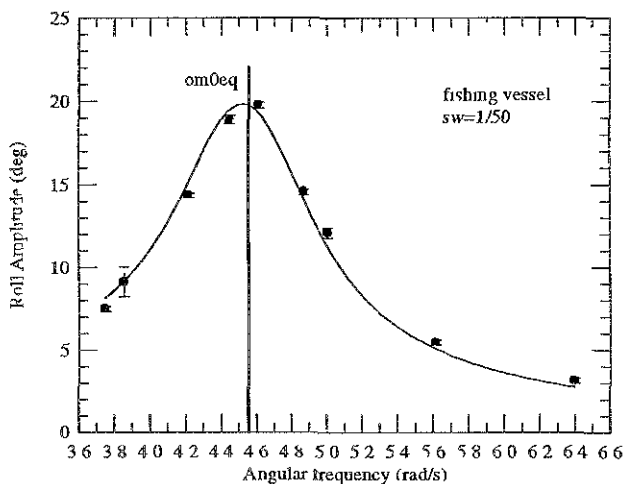


Fig. 1. Experimental data ● and best fit response curve (—) for the fishing vessel in beam sea.

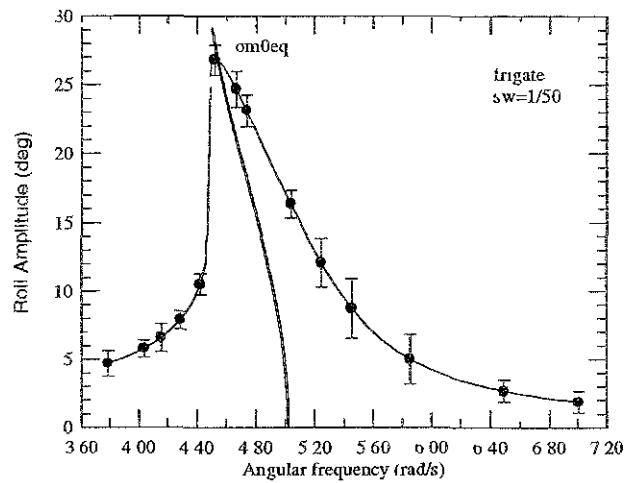


Fig. 2. Experimental data ● and best fit response curve (—) for the frigate in beam sea.

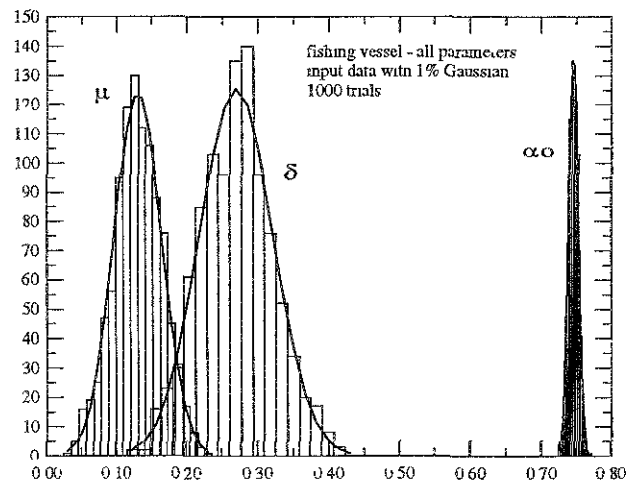


Fig. 3. Histograms of estimated parameter values and corresponding Gaussian distribution.

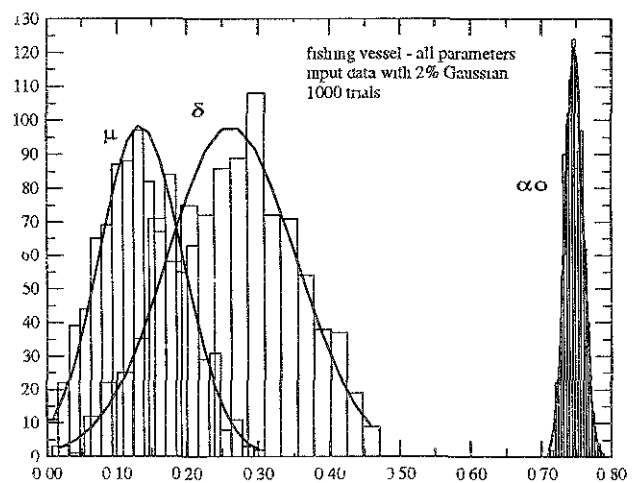


Fig. 4. Histograms of estimated parameter values and corresponding Gaussian distribution.

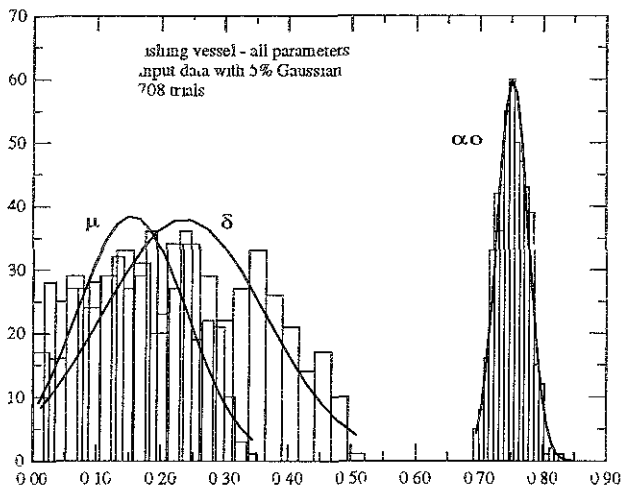


Fig. 5. Histograms of estimated parameter values and corresponding Gaussian distribution.

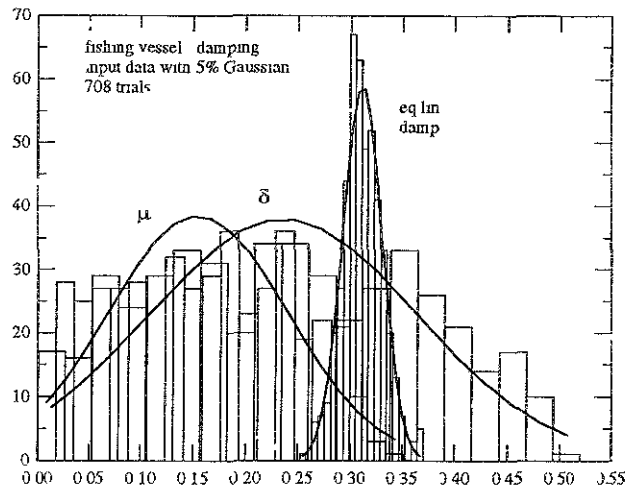


Fig. 8. Histograms of estimated parameter values and corresponding Gaussian distribution.

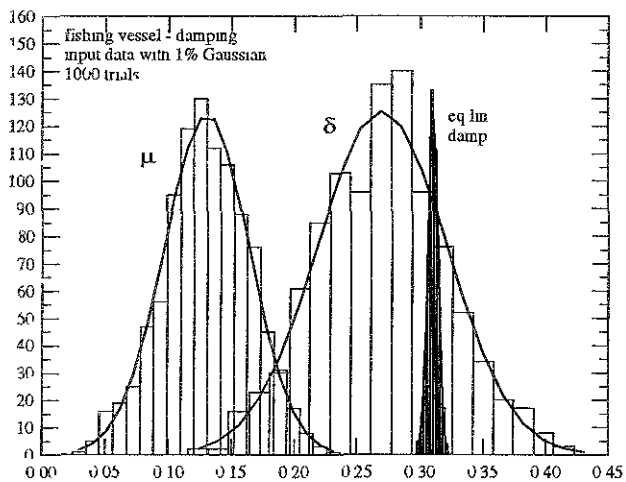


Fig. 6. Histograms of estimated parameter values and corresponding Gaussian distribution.

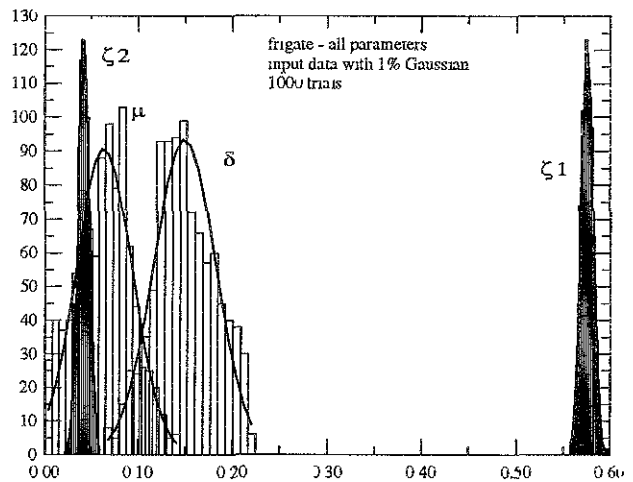


Fig. 9. Histograms of estimated parameter values and corresponding Gaussian distribution.

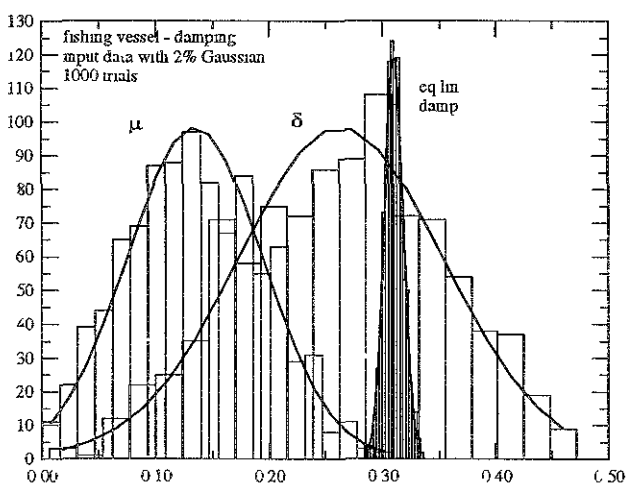


Fig. 7. Histograms of estimated parameter values and corresponding Gaussian distribution.

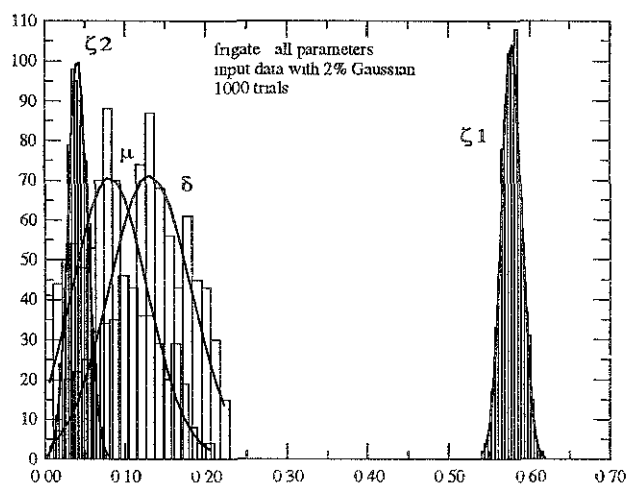


Fig. 10. Histograms of estimated parameter values and corresponding Gaussian distribution.

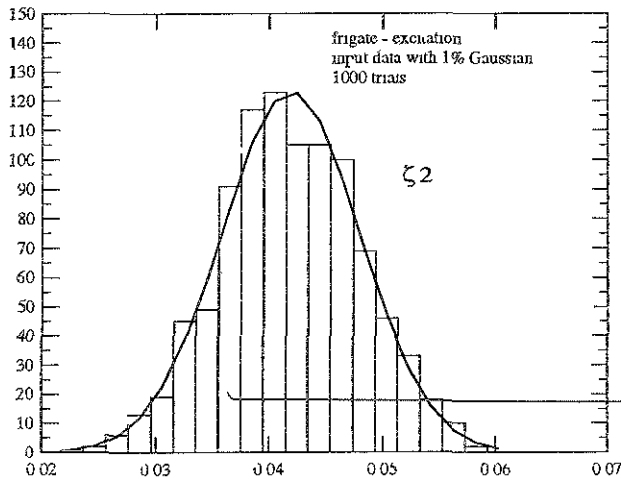


Fig. 11. Histograms of estimated parameter values and corresponding Gaussian distribution.

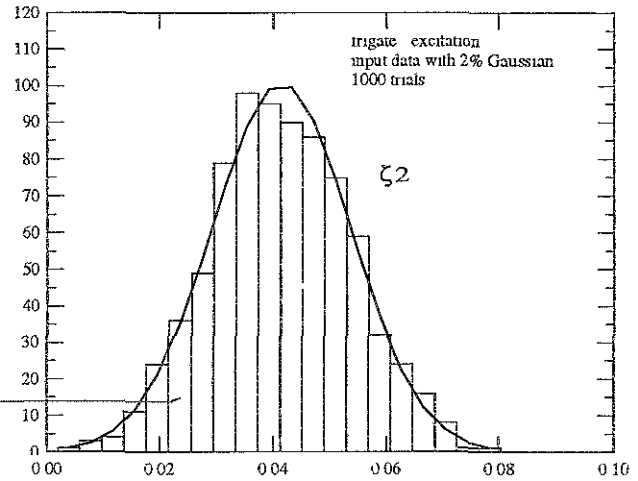


Fig. 14. Histograms of estimated parameter values and corresponding Gaussian distribution.

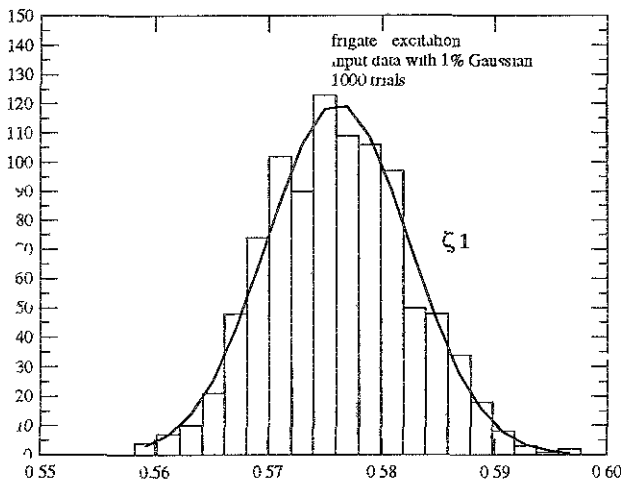


Fig. 12. Histograms of estimated parameter values and corresponding Gaussian distribution.

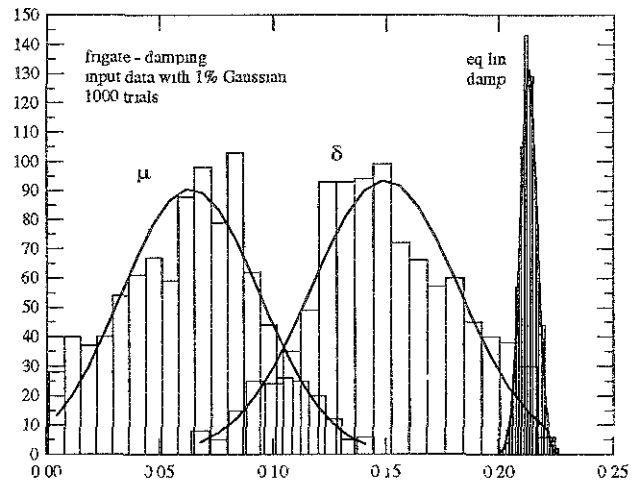


Fig. 15. Histograms of estimated parameter values and corresponding Gaussian distribution.

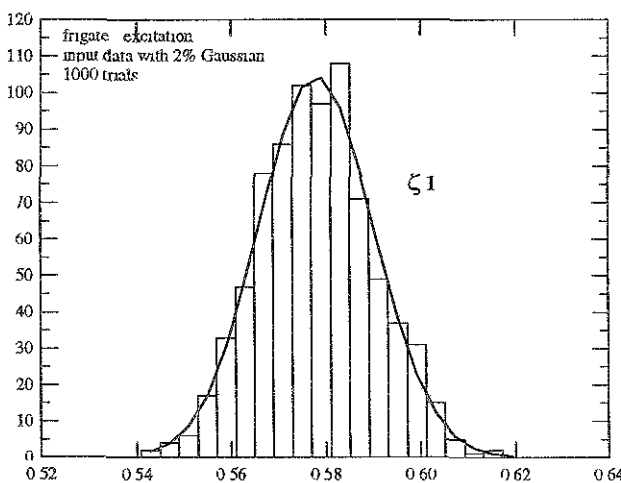


Fig. 13. Histograms of estimated parameter values and corresponding Gaussian distribution.

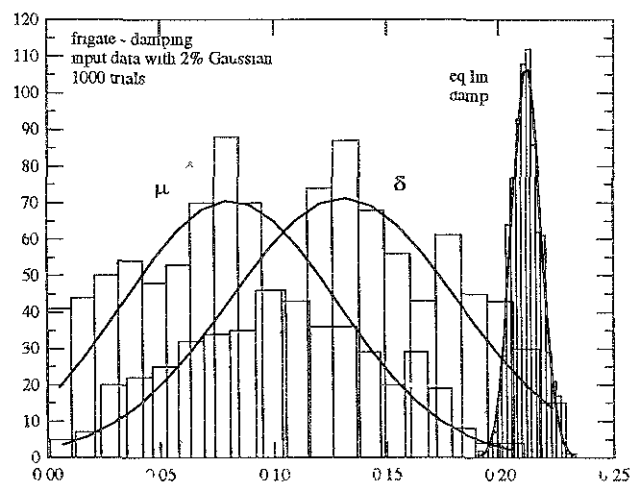


Fig. 16. Histograms of estimated parameter values and corresponding Gaussian distribution.

# A NEW METHOD TO ANALYSE ESCAPE PHENOMENA IN MULTI-DEGREE SHIP DYNAMICS, APPLIED TO THE BROACHING PROBLEM

Kostas Spyrou

Centre for Nonlinear Dynamics and its Applications  
University College London  
Gower Street, London WC1E 6BT, UK

## ABSTRACT

*A method to analyse the transients arising in broaching is presented. Currently, a proper framework for the systematic study of transient responses of multidimensional systems seems still to be lacking. This is even more true in the marine field where transient coupled motions are very rarely studied. The specific transition that is presently under study is the one triggered by a sudden control parameter variation effected in the vicinity of the threshold of surf-riding. This can lead to surf-riding, periodic motion, broaching or capsize. Each one of these types of behaviour is associated with a specific domain in the plane of actual or desired heading and nominal Froude number. The organisation on this plane is presented. This leads to the establishment of a simple procedure for quantifying the tendency of a ship towards broaching.*

## 1. OVERVIEW

Recently there is increasing awareness about the effect of nonlinearity on large-amplitude ship motions and, in particular, about the critical role that it can play for safety. The phenomena of ship capsize and broaching, both of an *escape* nature, are two characteristic examples of nonlinear behaviour that have been recently the subjects of in-depth studies, [1], [2].

The best known feature of nonlinearity is that it often allows the existence of multiple solutions, 'born' at *bifurcation* points. Bifurcations are basically smooth or discontinuous changes in the character of the response and they can be local or global. In their more critical versions, they are associated with sudden changes of response amplitude or with jumps towards remote

and usually undesirable destinations. A very useful summary and classification of the known types of bifurcation for energy-dissipating dynamical systems can be found in [3]. Quite often however, the knowledge of bifurcations, especially of the local ones, does not suffice in order to assess the safety margin of an engineering system. Given for example an initial state and a certain excitation level, one cannot say in general whether there will be an escape towards types of behaviour that are regarded as unacceptable. This represents a problem of *transient dynamics* which should be considered in parallel with the study of bifurcations of steady-state responses.

The possibility to predict ship motions beyond the realm of linear theory is obviously highly appealing, this however is confronted with shortcomings in two key areas: In solving the hydrodynamic problem which would allow calculation of the external loads acting on the ship; and in eliciting the variety of response patterns, the corresponding *manifolds* and the subsequent *state-space* organization for a dynamical system which, in general, is multi-degree.

It is well known that the accurate calculation of the forces acting on ships moving at high speed in large waves represents a very difficult problem for which practical, 'universally' accepted solutions will take some time to be produced. From the perspective of dynamical analysis, the standard method to get round this is through a judicious combination of ship theory, experiment and intuition with main objective the derivation of relatively simple mathematical models that, on the basis of the concept of *universality* of dynamical systems, present potential to capture the key features of system response.

Nonlinear ship motion analysis is 'traditionally' carried out in respect to the roll problem in beam seas. This corresponds to the single-degree

forced oscillator which has been under intensive investigation with analytical and numerical techniques for a number of years [4], [5], [6]. The study of other ship motions is however often severely restricted by the necessity to account for multidimensional dynamics in a global sense. By-and-large, this is still an unresolved matter. In the marine field even the most ambitious studies of multi-degree systems do not go much further than the stability analysis of steady-states and the occasional simulation, [7], [8], [9]. These approaches alone can offer however only limited insights into the nature of phenomena, broaching being here one typical example, where transient dynamics seem to play an important role.

An effort to develop a suitable framework for the study of broaching that would include steady state as well as transient analysis has been presented recently, [2], [10],[11], [12]. In the present paper we set in focus the transient motions that are connected with phenomena of capture to- and escape from surf-riding that have been shown earlier to lead to broaching, [2]. Some preliminary studies about the effect of autopilot gains on the boundary of the broaching and capture domains on a suitable plane of control parameters' are also reported.

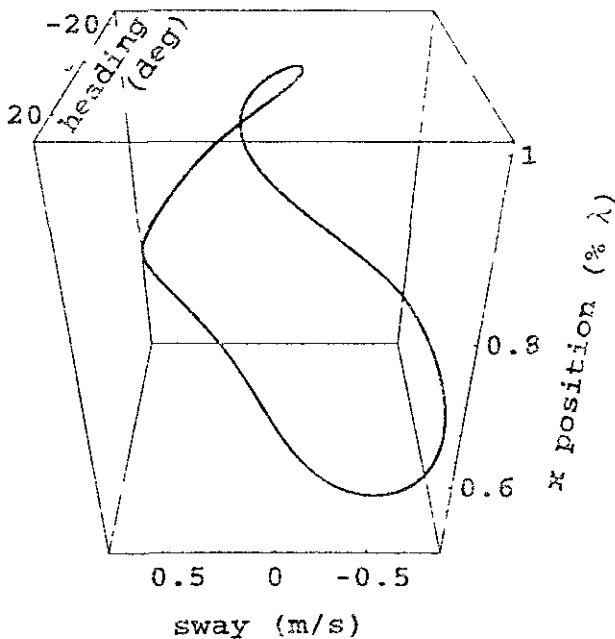


Fig. 1 : A 3-d projection of the stationary states of surf-riding

## 2. KEY ELEMENTS OF THE APPROACH

It is well established that in broaching motions in at least four different directions participate in the dynamics (surge, sway, yaw and roll, including also rudder control and assuming quasi-static equilibrium in the heave and pitch directions). This leads to an 8-dimensional, or higher, state-space which, obviously, one can visualize only through its 2-d or 3-d projections. It is reminded that by state-space we mean the 'enlarged' physical space that includes velocities in addition to displacements. The usual compact-form representation for an autonomous dynamical system is  $dz/dt = f(z; a)$  where  $z, a$  are re-

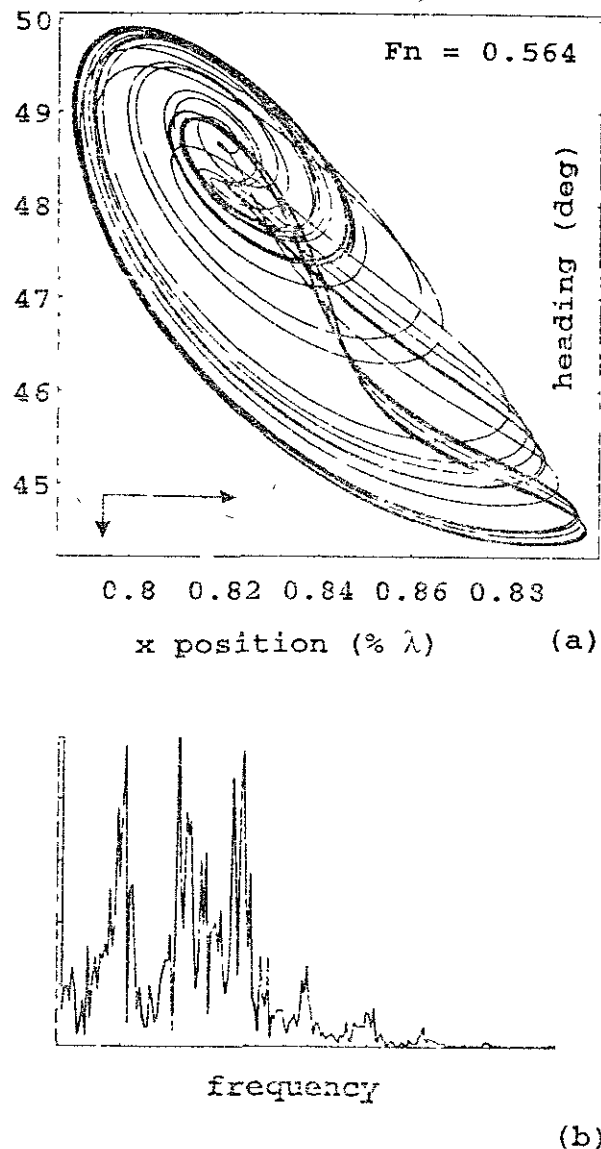


Fig. 2 : Chaotic surf-riding, [18]: (a) Phase-plot, and (b) power spectrum. The corresponding Lyapounov exponent is +0.01.

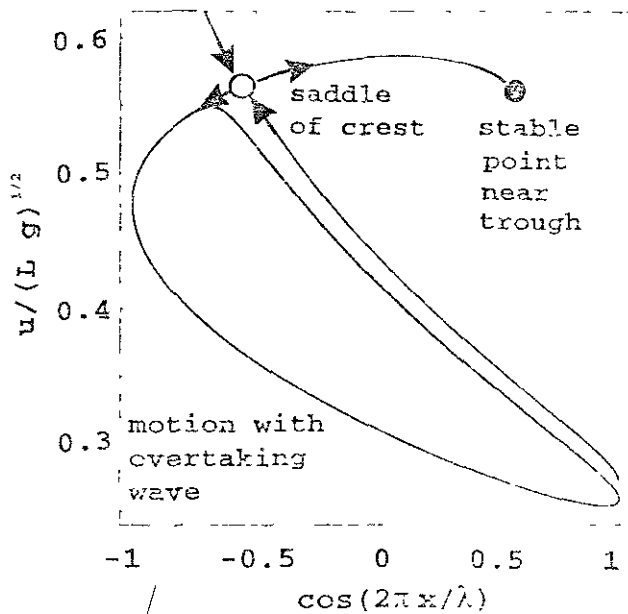


Fig. 3: Inset and outset of the saddle of crest that 'control' capture in surf-riding

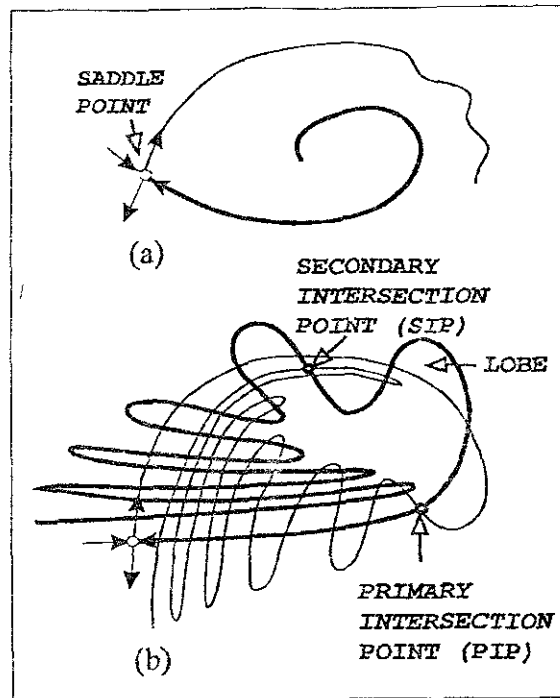


Fig. 4: Typical crossing of manifolds for a single saddle (homoclinic) on the Poincaré map for a 2-d system : (a) before and (b) after tangency of inset/ outset

spectively the state and control vectors;  $t$  is time; and  $f$  is a function that generates the *flow* (the geometric equivalent of the entirety of solutions of the vector differential equation) in the state-space. The detailed form of the mathematical model (in other words of the function  $f$ ) has been presented earlier and will not be repeated here, [2], [11]. It should only be mentioned that, in order to bring the equations into the autonomous form one has to present the wave loadings as dependent on the relative position of the ship on the considered regular wave rather than as functions of time. This can be done by using a system of coordinates moving with the wave celerity.

#### (a) Analysis of steady-states

Usually nonlinear analysis begins by locating the steady-states corresponding to the given vector equation. Very helpful tools for this are *continuation* (or *path following*) programs that can trace the dependence of steady states on one or more control parameters, see for example [13], [14], [15], [16]. It is usual to couple such algorithms with simultaneous eigenvalue analysis in order to know also the stability of each state identified. One step further, it is possible to follow also the evolution of bifurcation points, leading to the generation of bifurcation diagrams. Tracing equilibria, such the surf-riding states presented in Fig. 1, is the simplest possible application of continuation. The types of bifurcation associated with stationary surf-riding are, *saddle nodes* and *supercritical Hopf bifurcations*. Details about them are given in [2]. To analyse possible periodic, quasi-periodic and chaotic responses one needs to employ additional tech-

niques such as *Poincaré maps*, *power spectrum analysis*, calculation of *Lyapounov exponents* and others, Fig.2, [17], [18].

#### (b) Transient responses

Transient analysis will tell us what type of behaviour a ship will tend to adopt, when presently lying at an initial condition determined by the vector  $\mathbf{z}_0 = (u_0, v_0, r_0, p_0, \phi_0, \psi_0, x_0, \delta_0)^T$ ;  $u, v$ , are surge and sway velocities;  $r, p$  are yaw rate and roll velocity;  $\phi, \psi, \delta$  are angles of heel, heading and rudder;  $x$  is the position of the ship on a considered regular wave measured from a trough; the subscript  $_0$  indicates the values of variables at  $t = 0$ . It must be reminded here that, knowing the existing stable steady-states means only knowing what are the 'candidate' forms of long-term behaviour for the ship. Yet this information cannot be of any help towards predicting where exactly the ship will settle in response to a change in the setting of some control parameter. This can be extracted only by locating the *insets* of any existing saddle points (a pair for each saddle) in state-space, [19]. The insets define the boundaries of the basins of the attracting states. Equally important are also the *outsets* of the saddles that define the direction of the flow. The insets and outsets (or *invariant manifolds*) are rather unique objects that tend

asymptotically towards the saddle as  $t \rightarrow +\infty$  or  $-\infty$  respectively [for the 2-d system that corresponds to a simple, second order differential equation of a single variable, say  $y$ , they are orbits on the  $(y, dy/dt)$  plane, Fig.3]. However for a usual saddle of index- $m$  (that means only  $m$  positive eigenvalue-real-parts and all other negative) 'living' in a  $n$ -dimensional state-space, the inset would constitute a  $(n - m)$  - dimensional hypersurface and the outset a  $m$  - dimensional one. Even without considering the very intriguing phenomena in which the manifolds are often engaged (*homoclinic tangles* generating *chaotic transients* and *fractal boundaries*, see Fig. 4), [19], [20], [21], the difficulties involved in calculating their deployment in state-space are quite obvious. A sensible alternative is to proceed with a so-called *transient map*, that features repetitive integration from a "dense-enough" grid of initial conditions that span the whole state-space; or perhaps with a *cell-map* which is a refined version of the transient map with the addition that, one makes sure that the vicinity of any point ("cell") in state-space is not visited twice. However the number of initial conditions that need to be considered is overwhelming. An additional difficulty is that it is not exactly obvious what is the best presentation method.

In [10] it was advocated that 2-d intersections of state-space near its "interesting areas" can provide useful insights, particularly when there is no desire for restricting the range of possible initial conditions of the ship. Often however it is reasonable to assume that the change of state that the ship underwent due to a sudden variation of some control parameter (ship-based or exogenous) was effected upon a *nearly steady* initial motion pattern. Imagine for example a ship in steady periodic motion overtaken by following waves and operating 'unconsciously' near to the threshold of surf-riding; and then a group of steeper waves approaching it from behind; or the propeller rate to be set, for some reason, suddenly higher (in a Heav side function fashion); or finally, the desired heading to be suddenly modified. From a dynamical analysis point of view the assumption of steady state for the initial motion makes the difference between an unmanageable and a manageable problem.

The steady-states that we are interested about are fixed points and limit-cycles. In an extended state-control space and under the effect of some control parameter variation they will appear respectively as lines or as cylindrical surfaces. Both are relatively easily located from the steady-state analysis that precedes the investigation of transients. In [10] we assumed the initial

conditions lying on stable equilibria. This was done basically for the sake of simplicity and in order to make the first demonstration of the method easier. Such setup could be physically realized only if the ship had been captured in surf-riding. Now will be shown how the more general problem can be tackled, with the initial conditions lying either on stationary or, as is the far more usual, on periodic states.

### 3. THE MULTIPLE-EFFECT PROBLEM ARISING AT THE THRESHOLD OF SURF-RIDING

Let's consider once more a steered ship in stable periodic motion, as is overtaken from behind by sinusoidal waves of significant height. As stated earlier, the key assumption of the proposed approach is that the ship had been operating at steady-state at the moment when the selected control parameter was varied. This can be practically interpreted in two possible ways: The more obvious possibility is that the ship was in steady, overtaking-wave periodic motion. Then, the control parameter change could cause:

- (a<sub>1</sub>) a transition towards another *periodic* state,
- (a<sub>2</sub>) turning motion that cannot be checked (*broaching*),
- (a<sub>3</sub>) *capsize*,
- (a<sub>4</sub>) capture in the stationary condition of *surf-riding*.

The second scenario is that the ship had already been in surf-riding. Then the control change could potentially lead to:

- (b<sub>1</sub>) another stable *surf-riding* state,
- (b<sub>2</sub>) escape from surf-riding and return to *periodic* motion,
- (b<sub>3</sub>) escape from surf-riding followed by *broaching*,
- (b<sub>4</sub>) *capsize* en route to any of the above three destinations.

In either case, it is quite obvious that we are dealing with a rather unique for ship studies multiple-effect problem, resulting from the consideration of multi-degree dynamics. The primary effects may either be felt in surge (surf-riding), in yaw (broaching) or in roll (capsize). The determining factor is the initial state and the magnitude of change of the control parameter.

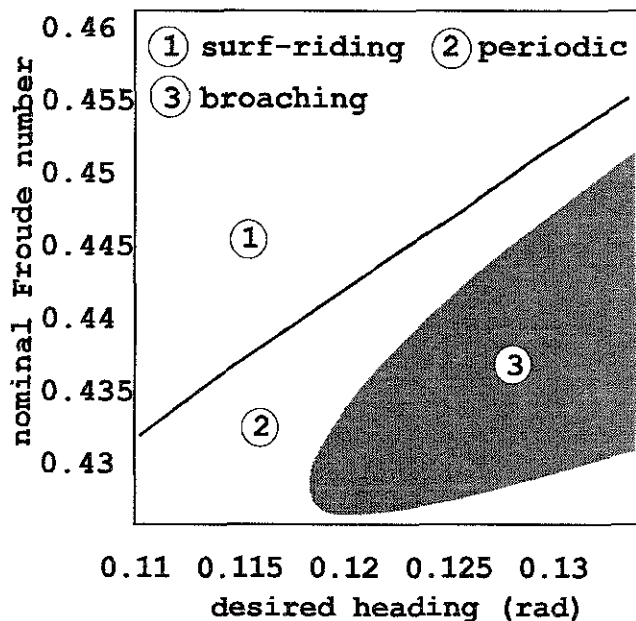


Fig. 5 : Organization of the domains of periodic motion, surf-riding and broaching. The initial motion type was periodic.

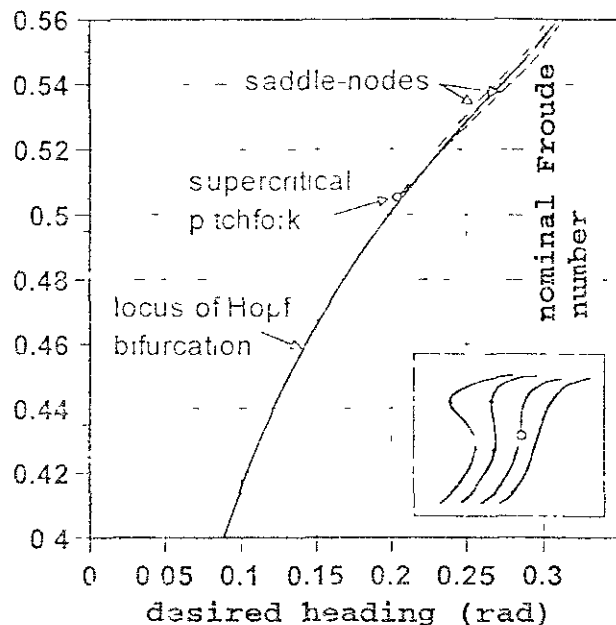


Fig. 7 : Loci of bifurcation points

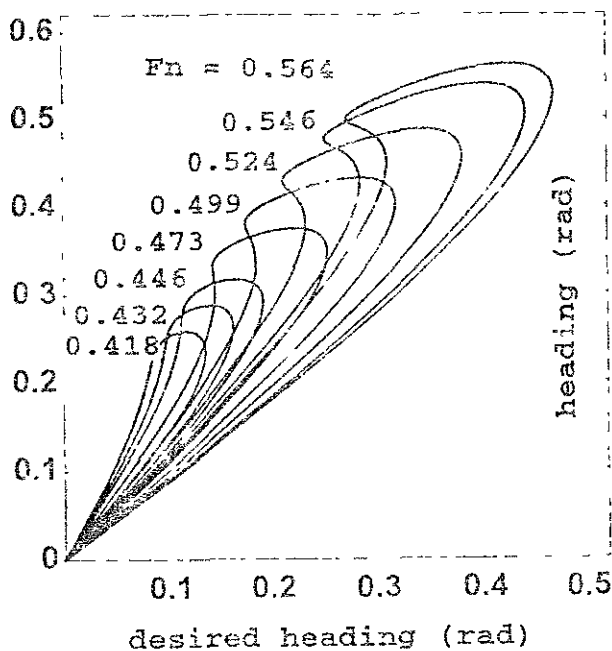


Fig. 6 : The evolution of the stationary surf-riding states with increasing  $F_n$

#### 4. PERIODIC INITIAL STATE

Consider now the ship sailing with nonzero encounter frequency and angle, and speed that brings it very near to the higher threshold of surf-riding. It has been pointed out that this threshold is basically a classic *homoclinic connection* where a limit cycle comes nearer and

nearer to a saddle point in state-space until the two collide, [2], [22]. A slight further increase of wave steepness is likely to cause the crossing of the inset of the saddle of crest, Fig. 3, which will generate in turn the usual jump associated with surf-riding. Although in a physical sense this is something relatively easy to imagine, a simple and hydrodynamically feasible method for modelling such change of the wave characteristics is not immediately obvious and this is a matter that is currently under investigation. However a qualitatively similar effect will be invoked if the propeller rate is suddenly stepped up and, at this stage, it is much simpler to let the propeller rate play the role of the varied control parameter. Here one must specify however with what phase, relatively to the periodic motion, the change of the control parameter setting is effected.

Ideally, one must find out at which point of the cycle the distance from the inset of the saddle of crest is minimum, Fig. 3. A rigorous mathematical solution to this problem will be discussed in another publication. Practically speaking however, it is known that it is more likely to be captured in surf-riding if the propeller thrust is increased when the ship centre lies in the vicinity of the trough, [2]. Also, as the higher threshold of surf-riding is approached (in general we shall name as *lower threshold* the nominal speed or Froude number at which equilibrium states come into existence; and as *higher threshold* the encounter of the homoclinic connection), the periodic motion tends to align itself with the inset of the saddle, Fig 3. In this case the distance may not be very sensitive to the phase.

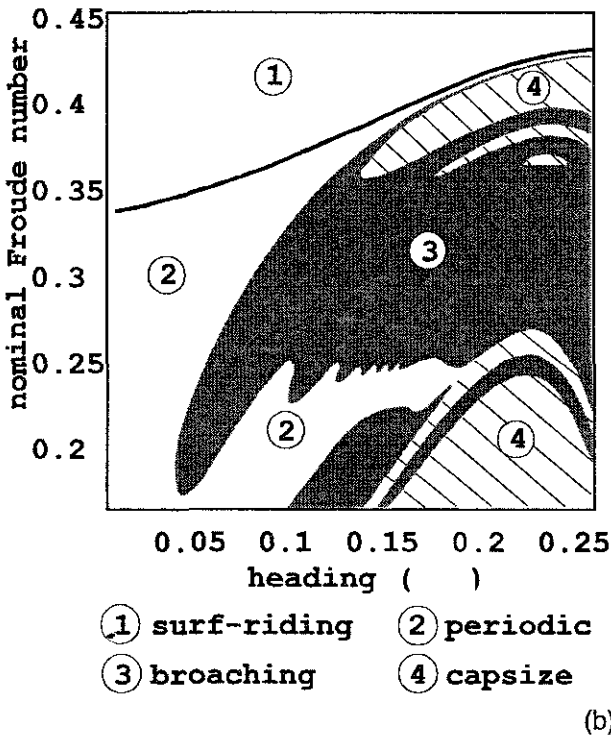
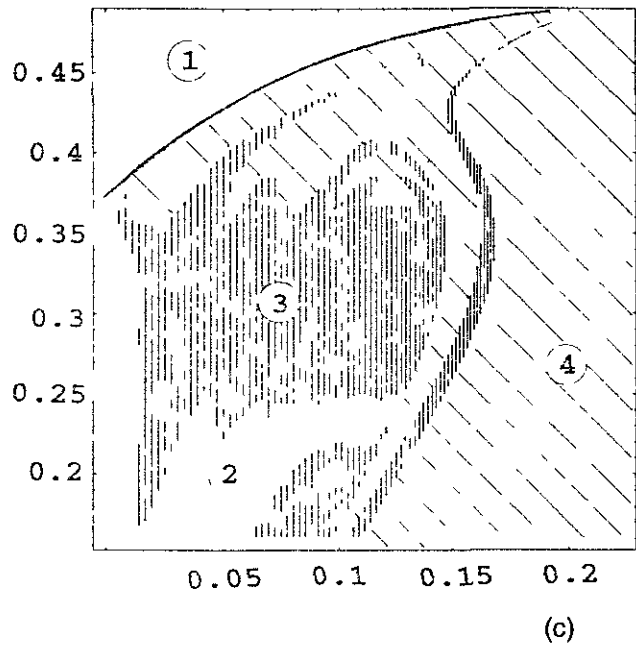
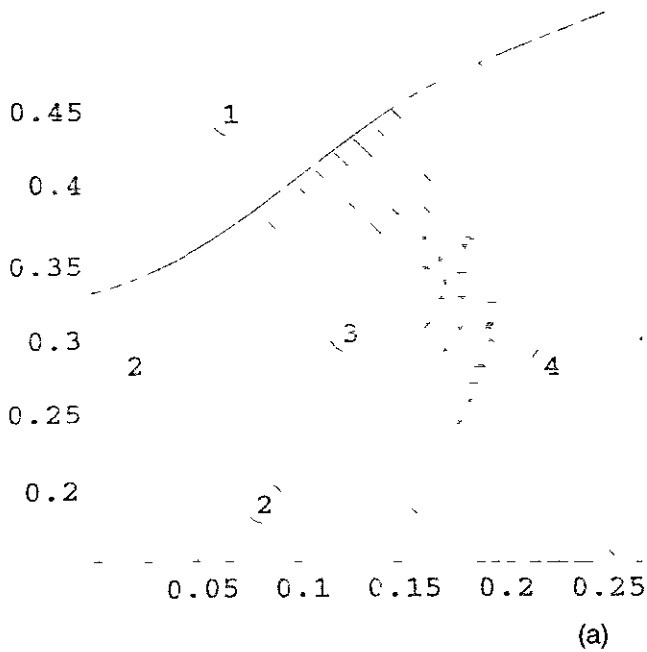


Fig. 8 : Escape from surf-riding :

- (a)  $a_w = 3, b_r = 1, t_\delta = 3$
- (b)  $a_w = 3, b_r = 3, t_\delta = 3$
- (c)  $a_w = 2, b_r = 1, t_\delta = 3$

number. Then, as the first trough is encountered, the propeller rate is increased leading to a higher nominal Froude number. Depending on the outcome the node under consideration is stored in the file of surf-riding, periodic motion, broaching or capsize. Then the numerical experiment is repeated for the next node until all the nodes have been examined.

The transition that is triggered by the change in the nominal Froude number is dynamically interesting for a number of reasons; not the least being that the periodic (overtaking wave) and the stationary (surf-riding) responses that correspond to the same desired heading have considerably different stability characteristics, even for the same or almost the same nominal Froude numbers. The autopilot gain values that guarantee stability for the one cannot necessarily do the same for the other, [12]. But even if the surf-riding point is stable in a steady-state sense, still, this cannot guarantee attraction there because there exists also the possibility of being engaged in turning.

The type of reference wave considered is simple sinusoidal of considerable steepness (the results presented in this paper are based on  $H/\lambda = 1/20$ ,  $\lambda/L=2.0$ ) where  $H$ ,  $\lambda$  are respectively, wave height and length; and  $L$  represents the ship length. In Fig.5 is shown how the domains of broaching, periodic motion and surf-riding are

The new method will be demonstrated through application to the purse-seiner that has been used extensively in our earlier studies ([2], [10]). The first step is to select a range for the desired heading,  $\psi_r$ , and nominal Froude number,  $Fn$ , and draw a grid on the plane of these two parameters. Then the nodes of this grid are considered sequentially for simulation : The first node is selected and simulation is carried out from a reference initial state until the ship settles into the steady periodic motion that corresponds to its desired heading and nominal Froude

arranged on the plane  $(\psi_r, Fn)$ , having deliberately set the metacentric height very high in order to avoid, at this stage, capsize. The domain of broaching is very clearly defined. In addition, in Fig. 6 we present the  $Fn$ -family of steady-state curves that are relevant to Fig. 5. We use projections on the plane  $(\psi_r, \psi)$ . The loci of the local bifurcation phenomena that would create instability for the steady-state responses can be seen in Fig. 7.

## 5. ESCAPE FROM SURF-RIDING

Here we consider, in a sense, the reverse scenario: The ship is assumed operating with nominal speed equal with the wave celerity  $c$ . If  $\lambda/L=2.0$  the corresponding Froude number of wave celerity is

$$Fn = \frac{c}{\sqrt{gL}} = \frac{\sqrt{(g\lambda/2\pi)}}{\sqrt{gL}} = \frac{1}{\sqrt{2\pi}} \sqrt{\frac{\lambda}{L}} = 0.564$$

As usual,  $g$  is the acceleration of gravity. For this  $Fn$  we derive through stationary-states continuation, with free parameter the desired heading, the curve of surf-riding equilibrium states. We store in a file those states near to the trough which are stable. It is reminded that a critical role in determining the length of the stable region in the vicinity of the trough is played by the autopilot gains, [2]: The proportional one defines the location of saddle-nodes; both however the proportional and differential gains have an effect on where the Hopf bifurcations may arise.

Each state stored in the file is represented by the corresponding desired heading  $\psi_r$  in the following way: Suppose that the autopilot equation is given by:

$$\frac{d\delta}{dt} = t_\delta [-\delta - a_\psi(\psi - \psi_r) - a_\psi b_r r]$$

where  $a_\psi$ ,  $a_\psi b_r$  are respectively proportional and differential gains; and  $t_\delta$  is the inverse time constant of the steering engine. At equilibrium the heading and rudder rates are zero and therefore the above equation reduces to a heading-error relation:

$$\psi - \psi_r = -\frac{\delta}{a_\psi}$$

The relation between  $\psi$  and  $\delta$  at equilibrium

requires solution of an algebraic system of equations which is done automatically in the continuation process. Since  $\psi_r$  is uniquely defined from the above equation, it can play the role of the representative of the equilibrium state. It should be remarked that the presence of large gain  $a_\psi$  will tend to minimize the heading error. Important is also the required rudder angle for achieving equilibrium, with small  $\delta$  leading to lower error.

Having defined the range of  $\psi_r$  to be between 0 deg and the largest desired heading where stable surf-riding is possible (we have assumed of course the rudder equally effective to port or starboard deflections), a similar range must be specified also for the second control parameter, that is the final nominal Froude number. This range should be as wide as possible and for our current studies that are based on  $\lambda/L=2.0$  we adopted the  $Fn$  range [0.164, 0.564].

In Figs. 8 (a), (b) and (c) we show the results of the investigation for three different pairs of autopilot gains. The four types of behaviour, surf-riding, periodic motion, broaching and capsize occupy respective domains of the  $(\psi_r, Fn)$  plane. Each one of these domains presents its own interesting structure. There is an intrusion of capsize into the broaching domain from larger headings. The boundary between periodic motion and broaching brings to mind a periodically forced Duffing-type oscillator, [10].

It is rather clear from Fig. 8 that either of the gains can affect considerably the locations of the boundaries. Yet, their qualitative characteristics do not seem to be seriously affected with the exception perhaps of a part of the broaching/periodic motion boundary (at low headings) which is under further investigation.

## 6. CONCLUDING REMARKS

A method to analyse the global dynamics of the transition between periodic motion and surf-riding has been put forward. The specific structure of the broaching and capsize domains, as they appear in the control parameters' plane  $(\psi_r, Fn)$ , has been shown for the first time. The proposed method uses the assumption of steady initial motion pattern for coping with the multi-dimensional character of the problem. On the basis of the current results, the method seems to provide a simple and effective means for quantifying the tendency of a ship for broaching. An additional advantage is that it can be used at the design stage.

In this paper we have focused on the link between surf-riding and broaching, the existence

of which was established theoretically in a previous publication, [2]. A classification of the hitherto understood broaching mechanisms is discussed in [2] and [22].

In general broaching does not necessarily need to involve surf-riding. It may also take place directly from the overtaking-wave periodic motion at relatively higher frequencies of encounter. This route seems to require however higher wave loadings and it may be more relevant to vessels of relatively large size since for these surf-riding should represent a very low probability event. Detailed analysis of the interesting dynamics underlying the loss of stability of the overtaking-wave periodic motions in a lateral sense is presented in [12].

## 7. REFERENCES

1. Thompson, J.M.T.: Designing against capsizing in beam seas, *Applied Mechanics Reviews*, 50, 5, 1997, pp. 307-325.
2. Spyrou, K.J. 1996 : Dynamic instability in quartering seas: The behavior of a ship during broaching, *Journal of Ship Research*, 40, 1, March 1996, pp. 46-59.
3. Thompson, J.M.T., Stewart, H.B. & Ueda, Y.: Safe, explosive and dangerous bifurcations in dissipative dynamical systems, *Physical Review E*, 49, 2, February 1994, pp. 1019-1027.
4. Minorsky, N.: *Nonlinear Oscillations*, 1962, D.Van Nostrand Company, Inc., Princeton, New Jersey.
5. Nayfeh, A.H. & Mook, D.T. : *Nonlinear Oscillations*, 1979, John Wiley & Sons, Inc., New York.
6. Thompson, J.M.T. : Global dynamics of driven oscillators: Fractal basins and indeterminate bifurcations, Chapter 1 in *Nonlinear Mathematics and its Applications*, 1996, Cambridge University Press, Cambridge, pp. 1-47.
7. Jiang, T. Schellin, T.E. & Sharma, S.D.: Manoeuvring simulation of a tanker moored in a steady current including hydrodynamic memory effects and stability analysis, *Proceedings, International Conference on Ship Manoeuvrability, Prediction and Achievement*, RINA, London, 1987.
8. Spyrou, K.J. : A new approach for assessing ship manoeuvrability based on dynamical systems' theory, PhD Thesis, University of Strathclyde, December 1990, Glasgow, UK.
9. Papoulias, F.A. & Riedel J.S. : Solution branching and dive plane reversal of submarines at low speed, *Journal of Ship Research*, 38, 3, September 1994, pp. 203-212.
10. Spyrou, K.J. : Dynamic instability in quartering seas-Part II: Analysis of ship roll and capsize for broaching, *Journal of Ship Research*, 40, 4, December 1996, pp. 326-336.
11. Spyrou, K.J. : Surf-riding and oscillations of a ship in quartering waves, *Journal of Marine Science and Technology*, 1, November 1995, Springer-Verlag, Tokyo, pp. 24-36.
12. Spyrou, K.J. : Dynamic instability in quartering seas-Part III: Nonlinear effects on periodic motions, *Journal of Ship Research*, 41, 3, September 1997.
13. Marek M., & Schreiber, I. : *Chaotic Behaviour of Deterministic Dissipative Systems*, 1995, Cambridge University Press, Cambridge.
14. Doedel E.J. & Kernevez J.P. : Software for continuation problems in ordinary differential equations with applications, Pasadena, California Institute of Technology, 1985
15. Seydel R. : *From Equilibrium to Chaos: Practical Bifurcation and Stability Analysis*, 1988, Elsevier, New York.
16. Foale, S. & Thompson, J.M.T.: Geometrical concepts and computational techniques of nonlinear dynamics, *Computer Methods in Applied Mechanics and Engineering*, 89, 1991, Elsevier Science Publishers, pp. 381-394.
17. Berge', P., Pomeau, Y. & Vidal, C.: *Order within Chaos*, 1984, John Wiley & Sons, New York.
18. Spyrou, K.J. : Homoclinic connections and period doublings of a ship advancing in quartering waves, *CHAOS : An Interdisciplinary Journal of Nonlinear Science*, June 1996, American Institute of Physics, 6, pp. 209-218.

19. Guckenheimer, J. & Holmes, Ph. : *Nonlinear Oscillations, Dynamical Systems and Bifurcation of Vector Fields*, 1983, Springer-Verlag, New York.

20. Wiggins, St. : *Global Dynamics, Phase Space Transport, Orbits Homoclinic to Resonances and Applications*, 1993, American Mathematical Society, Providence, Rhode Island.

21. Falzarano, J.M., Shaw, St. W. & Troesch, A.: Application of global methods for analysing dynamical systems to ship rolling motion and capsizing, *International Journal of Bifurcation and Chaos*, 2, 1, 1992 , pp. 101-115.

22. Spyrou, K.J. : Geometrical aspects of broaching-to instability, *Proceedings, Second Workshop on Stability and Operational Safety of Ships*, November 1996, Osaka University, Japan.

# On ship surging in irregular waves.

by

V.Lipis

Central Marine Research and Design Institute

Ship Hydrodynamics Laboratory

St Petersburg, Russia

## ABSTRACT

The mechanism of ship surging is considered as a longitudinal oscillations in condition of severe pitching motion caused not only by wave exciting Froude-Krilov force, but also by ship propeller trust oscillations with low - encounter frequency energy spectrum

The ship has an irregular running coming to a stop in a big wave conditions under severe pitching motion and propeller thrust brake due influence of air suction. Then the ship again accelerates in moderated waves and pitching

The ship motion is examined as the impulse process. The main speed loss and the main amplitude of speed oscillation depends upon the probability of propeller racing in waves conditions

## GENERAL

Mean speed in waves  $V_0$  is provided by mean propeller thrust ( $T_{e0}$ ) equal to mean resistance  $R_0$ , where the equation of ship longitudinal motion is as follows.

$$t_{s0} \frac{d\bar{V}}{dt} = \bar{T}_e(\bar{V}, t) - \bar{R}(\bar{V}, t),$$

where

$\bar{V} = V/V_0$ ,  $\bar{R} = R/R_0$ ,  $\bar{T}_e = T_e/T_{e0}$  and ship time constant:

$$t_{s0} = \left( \frac{\Delta}{g} + \lambda_{11} \right) \frac{V_0}{R_0}, \quad (1)$$

$\Delta/g$ ,  $\lambda_{11}$  - ship mass and added mass coefficient.

For ship of usual hullform with diesel power main engines at the qualitative analysis it is possible to believe:

$$\bar{R} = \bar{V}^2 + \bar{R}_\tau(V, t), \quad \bar{T}_e = 1 + \bar{T}_{e\tau}(V, t)$$

Here  $\bar{R}_\tau$ ,  $\bar{T}_{e\tau}$  - time-dependent resistance and thrust components determining oscillations of the speed  $\bar{V}_\tau$  in regard to its average value. By designating through  $\bar{Q}_\tau$  a variable part of hydrodynamic loads with a characteristic time interval  $t_0$  from (1) we have:

$$t_s \frac{d\bar{V}}{dt} + \bar{V}^2 = 1 + \bar{Q}_\tau \quad (2)$$

Where

$$\bar{Q}_\tau = \bar{T}_{e\tau} - \bar{R}_\tau \quad (3)$$

$\tau = t / t_0$ ,  $\mu_{11} = \lambda_{11} / \Delta/g$

$$t_s = \frac{t_{s0}}{t_0} = (1 + \mu_{11}) \frac{\Delta}{R_0} \left( \frac{V_0}{g t_0} \right) \quad (4)$$

Passing to moving system of coordinates and assuming  $\bar{V} = 1 - \bar{V}_\tau$ , we shall derive

$$t_s \frac{d\bar{V}}{dt} + 2\bar{V}_\tau - \bar{V}_\tau^2 = \bar{Q}_\tau(\bar{V}, \tau) \quad (5)$$

Usually linearized equation in respect to  $\bar{V}_\tau$ :

$$t_s \frac{d\bar{V}}{dt} + 2\bar{V}_\tau = \bar{Q}_\tau(\bar{V}, \tau) \quad (6)$$

What is the condition for this linearization?

We shall consider reaction on a load unit step in a moment  $\tau = 0$  [1].

$$\bar{Q}\tau = 1(\tau) \quad (7)$$

The equation (5) under of (7) has the solution

$$\bar{V}\tau_1 = \frac{\tau}{ts + \tau} 1(\tau) \quad (8)$$

From the equation (6) under condition of (7) we shall derive

$$\bar{V}\tau_2 = 1/2 [ 1 - \exp(-\frac{2\tau}{ts}) ] \quad (9)$$

On Fig. 1 transients  $\bar{V}\tau_1(\tau)$  (line 1,2,3) and  $\bar{V}\tau_2(\tau)$  (line 1'',2'',3'') are compared at three values  $ts$ . The lines 1,1'' relate to  $ts = 0,5$ , line 2,2'' - to  $ts = 5,0$ , line 3,3'' - to  $ts = 50$ . The error of the linear solution comes out in the dangerous direction (with underestimated  $V\tau$ ). And in a limit steady value of oscillations of speed on linear approach is twice less, than under the nonlinear solution. This circumstance, however, has practical meaning only at small  $ts$ , when the distinction between  $\bar{V}\tau_1$  and  $\bar{V}\tau_2$  has time to be displayed during, commensurable with a characteristic interval of load variation  $to$ . For example, as to accept natural period of a vessel then according to (4)

$$ts = \frac{1 + \mu_{11}}{2\pi} \frac{\Delta}{R_0} Fr(\omega_e \sqrt{L/g}) \quad (10)$$

Where

$$Fr = V_0 / \sqrt{gL}, \quad \omega_e = 2\pi / t_e, \quad t_e = t_0$$

The nonlinearity in fluctuations of speed at load step for period of motion can be essential for a small vessel on small speeds. For example, at  $ts = 0,5$  and  $\tau = 1$  the

exact solution  $\bar{V}\tau_1$  is greater than linear by 30%. Under condition of  $ts > 5 - 10$ , which is usually realized for medium and big vessels, the solutions  $V\tau_1$  and  $V\tau_2$  for  $\tau < 3 - 4$  practically coincide, so for an estimation of oscillations of speed in waves setting, for example, periodic load variation as

$$\bar{Q}\tau = \exp(i2\pi \bar{\omega}\tau) \quad (11)$$

Where  $\bar{\omega} = \omega / \omega_0$

We shall derive from (6) for stationary oscillations of surging speed the modulus of transfer function as

$$\Phi_V = \frac{1}{2} [ 1 + (\pi \bar{\omega} ts)^2 ]^{-1/2} \quad (12)$$

The function  $\Phi_V$  lies in zero frequency domain, so that the appreciable oscillations of speed are possible only in cases, when a vessel is either dynamically weak in inertia (small vessel at large loss of speed in waves), or the load oscillation spectrum is displaced in area of small frequencies. The last case is displaced brightest in condition of following waves, as the load oscillations  $\bar{Q}\tau$  can be generated by oscillations of resistance  $\bar{R}\tau$  on small encounter frequencies of waves  $\omega_e$

$$\bar{Q}\tau = - \bar{R}\tau = - \bar{R}_A \sin \omega_e t \quad (13)$$

Where the principle part of amplitude  $\bar{R}\tau$  is defined on a Krylov-Froude hypothesis

[ 3 ] The function  $\bar{R}_A$  has the greatest modulus value in head and following wave conditions. Encounter frequency.

$$\omega_e = \omega + V k \cos \beta = \omega_{e0} - k V \tau \beta \quad (14)$$

where

$V\tau\beta$  - surging speed projection to a direction of run of waves in moving coordinate system connected to a vessel,

$k = \omega^2 / g$  - wave number

Thus the average value of encounter frequency over speed  $V_0$  as is usual.

$$\omega_{e0} = \omega (1 + Fr \cos \beta / 0,4 \sqrt{\lambda/L}) \quad (15)$$

As  $kV\tau\beta \ll \omega_{e0}$  (the long waves or small  $V\tau\beta$ ) in (14) are possible to consider  $\omega_e = \omega_{e0}$ , and the equation (6) remains linear, so according (12), (13) for a spectrum of oscillations of speed of a vessel we have

$$S_V = \frac{1}{4} \frac{|\bar{R}_A|^2}{\zeta_A} S_w(\omega, \gamma) * [1 + (\pi \omega_{e0} \tau)^2]^{-1} \quad (16)$$

Where  $S_w(\omega, \gamma)$  - wave energy spectrum If  $kV\tau\beta$  is not small in comparison with  $\omega_{e0}$ , the equation (6) gets nonlinearity:

$$\tau s \frac{d^2 \bar{\xi} g}{d\tau^2} + 2 \frac{d \bar{\xi} g}{d\tau} = - \bar{R}_A \sin(\omega_{e0} \tau - kV\tau\beta t) \quad (17)$$

In following waves ( $\cos \beta \cong -1$ ) it is possible, that the vessel does not lose average speed and under condition of  $Fr \rightarrow 0,4 \sqrt{\lambda/L}$  according to (15)  $\omega_{e0} \rightarrow 0$ , so the load variation is defined by  $kV\tau\beta$  value and the nonlinearity is displayed in the greatest degree As  $V\tau\beta * t$  is equal to oscillations  $\xi g$  of a centre of a vessel in a direction of run of waves in regard to the origin of moving system of coordinates, the equation (17) can be written down as.

$$\tau s \frac{d^2 \bar{\xi} g}{d\tau^2} + 2 \frac{d \bar{\xi} g}{d\tau} = - \bar{R}_A \sin(\omega_{e0} \tau - kV\tau\beta t) \quad (18)$$

This nonlinear in relation to a load phase equation was investigated in details in many known works [3] - [7] and in others. The basic peculiarity is a possibility of so-called "surf-riding", when the instantaneous surging speed of a vessel reaches value of a wave phase speed, i.e.  $(V_0 + V\tau) \cos \beta = C$  and the vessel by jump is from a mode of oscillations of speed (surging) to a mode of riding on waves without speed oscillations.

**The goal of the present article** - not concerning this direction of researches to pay attention to other possible kind of a movement of a vessel in waves, when the nonlinear oscillations of speed occur in the small frequencies domain not in consequence of fluctuations of resistance  $R_t$ , but owing to fluctuations of thrust in conditions of propeller "racing" under heavy motions.

## 2. METHOD OF ANALYSIS OF PROPELLER RACING UNDER SHIP MOTIONS IN WAVES.

Ship motions cause time periodic variations hydrodynamic forces of propeller. The oscillations of the propeller near to a surface with blades water braking are accompanied by burst of air (atmospheric cavitation of blades), aeration of a flow and spraying. Thus an average thrust and torque moment of the propeller are much reduced, grow amplitude of its oscillations over period of motions. This phenomenon has name of propeller "racing". The physical picture of a flow of blades on such modes is rather complex. The hydrodynamic analysis

shows. that intensive periodic burst of air by propeller caution under motions arises only under condition of excess the propeller loading of some critical value. It is possible to characterize hydrodynamic propeller loading by  $K_d$  factor, which is defined under the formula.

$$K_d = V_0 (1 - W) D \sqrt{\rho} / T_{e0} \quad (19)$$

Where  $D = 2R$  - propeller diameter,

( $R$  - radius)

$W$  - wake factor

$\rho$  - density of water

The more is propeller load the less is  $K_d$  value. The mode of intensive burst of air suction to the propeller under motions comes under condition of .

$$K_d(J) \leq K^* d(\alpha) \quad (20)$$

These characteristics depend on propeller geometry and parameters of its operation, basic of which

- advance ratio

$$J = \frac{V_0 (1 - W)}{h_0 D}$$

- atmospheric cavitation number

$$\alpha = 2gh / (n_0 D)^2$$

In these parameters  $n_0$  - propeller RPM, and  $h$  - propeller axis immersion. In calm water the immersion  $\tilde{h}_0$  of the propeller develops of immersion  $h_0$  at standstill, stern wave ordinate  $Z_w$ , aft draught variation  $\Delta d_a$  and ordinate of propeller own wave system  $\delta h_0$

$$\tilde{h}_0 = h_0 + Z_w + \Delta d_a + \delta h_0$$

If the immersion  $h_0$  is less than  $R$ , above propeller will be formed wave trough and  $\delta h_0 < 0$ . In waves the propeller immersion varies in time

$$h(t) = \tilde{h}_0 - Z_p(t)$$

The relative vertical motion of the propeller  $Z_p(t)$  is defined at the rate of ship motions in waves with the account of diffraction effect. For occurrence of propeller blades water braking it is necessary, that a condition was carried out:

$$h_m = \tilde{h}_0 - Z_{pa} < R$$

Where  $h_m$  - minimum propeller axis immersion

$Z_{pa}$  - Instant value of positive amplitudes of oscillations  $Z_b(t)$

Working average of propeller load is defined by value of  $K_d$  factor depending on propeller ratio  $J$  advance and the critical  $K_d^*$  value depends, in basic, on atmospheric cavitation number over the minimum immersion

$$\alpha = 2g h_m / (n_0 D)^2$$

The hydrodynamic analysis gives the basis to consider  $K_d^*$  as a measure of activity of air suction influence for propeller under motions. This fact is fixed in a basis of settlement physical model of propeller racing for the first time developed in [1].

Let a vessel to be rather long on way in waves of invariable intensity and direction. An average added resistance results in reduction of average speed and propeller RPM, so that its average load is characterized by constant value  $K_d(J)$ . Owing to oscillations of propeller immersion there is the variation of its hydrodynamic forces.

If the waves and the motions are regular (Fig 2), then  $h_m$  is constant. Hence,  $K_d^*$  value is constant which in general is non-linear in relation to  $\alpha_m$ . Under condition of  $K_d > K_d^*$  the variation of propeller average hydrodynamic forces are small and are not accepted in propulsion analysis (Fig. 2a). It is considered, for

example, that the thrust  $T$  is constant and is equal to a thrust, which would be at the propeller in calm water. If  $K_d < K_d^*$ , on each period of oscillations the propeller in the top position sucks in the air, therefore there are the oscillations of a thrust and torque moment of large amplitude and the average value of a thrust and torque moment can will decrease on 40 - 60 % (Fig 2b)

This picture, however, is poorly similar to real process of propeller racing at which the large thrust and torque moment oscillations arise rather seldom and non-uniformly alternate through intervals of time, considerably large, than period of motions. The reason that in condition of irregular waves the dynamic propeller characteristics become random processes, and the spectral analysis of full scale and model tests results testifies to characteristic growth of intensity of propeller thrust and torque moment oscillations in small frequencies domain [1], [7]

These physical peculiarities are reflected by model of propeller action under motions as nonlinear pulsing system with random inputs (Fig 3). Oscillations of immersion  $h(t)$  and all dependent from  $h(t)$  the propeller characteristics are considered as random processes. Initial process  $h(t)$  has envelope  $hm(t)$ , which in general is followed up by fluctuations of parameter correspond  $\alpha_m(t)$ . Stochastic oscillations  $K_d^*$  correspond to this fluctuations. The zone of loads at which propeller heavily sucks in air, pulses, contracting and extending together with its border. While the trajectory of process  $K_d^*$  does not reach a constant level of  $K_d(j)$  the propeller mode is not captured by a zone of advanced atmospheric cavitation and the fluctuations of forces represent "continuous" stochastic processes on frequencies  $h(t)$ . In separate stochastic

moments of time the zone of critical loads "captures" a mode of propeller operation there are the sharp failures - pulses of average values of forces on frequencies  $hm(t)$ . The fluctuations of "continuous"  $T\tau$  and pulses of "average"  $T^*\tau$  of forces have spectra on various frequent ranges and are considered therefore as simultaneously proceeding independent stochastic processes. According to this scheme:

$$T\tau = T\tau (\Delta h(t) + T_r^*(hm(t))) \quad (21)$$

To the analysis of pulses of "average" forces the barrier-crossing theory of rejection is applied, thus random unit function is introduced

$$1(t) \equiv 1(K^*d - K_d) = \begin{cases} 1, & K^*d(t) \geq K_d \\ 0, & K^*d(t) < K_d \end{cases} \quad (22)$$

This function describes time parameters of propeller racing and

$$T^*\tau(t) = -q Teo 1(t) \quad (23)$$

In this expression the function  $q$  is defined under the hydrodynamic theory of the oscillating propeller (or on experiment results) depending on its parameters and "significant" value  $\alpha_m$  [2]. According to (22), (23) the propeller will nonlinearly transform process  $K_d^*(t)$  to a sequence of rectangular pulses with stochastic duration and pauses. As the initial process  $h(t)$  is normal random process and at its transformations is applied statistical linearization the total probability  $Pr$  of propeller racing under ship motions on waves is defined by expression:

$$P_r = \exp\left[-\frac{1}{2}\left(\frac{Kd - K_{ac}^*}{a\sigma_z}\right)^2\right] = \exp(-1/2\chi^2) \quad (24)$$

Where  $K^*_{do}$  - value  $K^*_d$  at average value  $\bar{h}_0$  dependent from  $\bar{h}_0$ .

$a$  - hydrodynamic factor.

On physical sense the probability  $P_r$  represents total relative time of propeller fraction on modes of advanced atmospheric cavitation (racing) for long time of a ship way in waves of constant intensity, i.e.

$$P_r = \lim_{t \rightarrow \infty} \left( \frac{1}{t} \int_0^t \mathbf{1}(t) dt \right) \quad (25)$$

Probability of racing  $P_r$  is always less than probability  $P_{em}$  of propeller emergence (propeller blades water braking):

$$P_{em} = \exp\left[-\frac{1}{2}\left(\frac{\bar{h}_0 - R}{\sigma_z}\right)^2\right], \quad \bar{h}_0 \geq R \quad (26)$$

As the characteristic of pulsing process  $P_r$  defines factor of filling of random pulses

$$P_r = \bar{\nu} \cdot \bar{\tau}_r$$

Where

$\bar{\nu}$  - average number of pulses in time unit

$\bar{\tau}_r$  - average duration of pulses

$$\bar{\tau}_r = \frac{\sqrt{2\pi}}{\omega_* \chi}$$

Where

$\omega_*$  - average frequency of envelope  $h(t)$ .

The order of values  $P_r$  and  $P_{em}$  for various conditions of head waves is demonstrated in table 1 on an example for the two-screw Ro-Ro ship by displacement

36000 t. It is visible, that the propeller racing can have high probability in waves more than 6 Bofort numbers even for a vessel in a load condition and this probability is much less, than probability of propeller emergences. Being limited the specified items of information on propeller action under motions we shall note in addition, that a spectrum of the process  $T^*e^{-\tau}(t)$  as (23) adjoins to zero frequency and quite reflects experimental data [1].

### 3. MOVEMENT OF A VESSEL WHEN AT PROPELLER RACING CONDITIONS IN WAVES.

The movement of a vessel in conditions of propeller racing is possible to consider as a consequence of pulsing process described in item 2 of thrust variation. The pulses of thrust reduction are repeated in average through intervals of time  $\frac{1}{\bar{\nu}}$ ,

which are several times as high as mean period of motions. Thus vessel is running nonstationary being braked on large waves, when the amplitude of motions is great and propeller sucks in the air, and then again accelerates while pass waves of the smaller sizes and motions small. For the purposes of practical account it is possible to use the following approximate approach. It is considered that the average characteristics of pulsing random process define some equivalent on influence on a vessel of nonrandom pulsing function of discrete relative time.

$$\bar{\nu} t = l + \varepsilon, \quad 0 \leq \varepsilon \leq 1, \quad l = 0, 1, 2 \quad (27)$$

The formula (22) accepts a kind

$$\mathbf{1}(t) = \mathbf{1}(\bar{\nu}t) = \begin{cases} 1, & 0 \leq \varepsilon \leq P_r \\ 0, & P_r < \varepsilon \leq 1 \end{cases} \quad (28)$$

The parameters of point function (28) serve the counter 1 to number of periods  $1/\tilde{V}$  occurrence of pulses and their relative duration  $Pr$ . According to (23) propeller thrust variations are defined as

$$\overline{T^* \tau}(\varepsilon) = -q \text{Teo } 1(\tilde{v}t) = q \overline{T^*} \mathbf{1}(l, \varepsilon) \quad (29)$$

The equation of a movement of a vessel according to (6), (29) is the nonlinear equation of the closed pulsing propeller-hull system. Offering, that the function does not depend upon  $\overline{V\tau}$  it is possible to use the equation of open pulsing system with a linear continuous part

$$\frac{P}{\alpha} \frac{d\overline{V\tau}}{d(\tilde{v}t)} - \overline{V\tau} = \frac{q_0}{2} \mathbf{1}(l, \varepsilon) \quad (30)$$

Where

$$\alpha = \frac{2\sqrt{2\pi}}{l_s \chi \omega_s}$$

The solution looks like:

$$\overline{V\tau} = \frac{q_0}{2} \left\{ \begin{array}{l} \left[ \frac{1 - \exp\left[-\frac{\alpha}{P_r}(1 - P_r)\right]}{1 - \exp(-\alpha/P_r)} \times \right. \\ \left. \times \exp\left[-\frac{\alpha}{P_r}\varepsilon\right] \right] \\ - \left[ \frac{1 - \exp(-\alpha)}{1 - \exp(-\alpha/P_r)} \times \right. \\ \left. \times \exp\left[-\frac{\alpha}{P_r}(\varepsilon - P_r + l + 1)\right] \right] \end{array} \right\} \quad (31)$$

$0 \leq \varepsilon \leq P_r$

$$\overline{V\tau} = \frac{q_0}{2} \frac{1 - \exp(-\alpha)}{1 - \exp\left(-\frac{\alpha}{P_r}\right)} \exp\left[-\frac{\alpha}{P_r}(\varepsilon - P_r)\right] \times \left\{ 1 - \exp\left[-\frac{\alpha}{P_r}(l + 1)\right] \right\}, \quad P_r \leq \varepsilon < l$$

The first expression describes variation of  $\overline{V\tau}$  during action of a thrust pulse, second - during its absence. This change occurs under the exponential law, and during a pulse of thrust the loss of speed is increased, and in an interval reduces, but with the time accrues on a sawtooth curve (Fig 4). The maximum values come at  $\varepsilon = Pr$  minimum at  $\varepsilon = 0$ . In a steady process:

$$\overline{V\tau}_{\text{max}} = \frac{q_0}{2} \frac{1 - \exp(-\alpha)}{1 - \exp\left(-\frac{\alpha}{P_r}\right)} \quad (32)$$

Double amplitude of oscillations:

$$\overline{V\tau}_a = \overline{V\tau}_{\text{max}} \left\{ 1 - \exp\left[-\frac{\alpha}{P_r}(1 - P_r)\right] \right\}$$

Additional average loss of ship speed caused by propeller racing under motions in waves:

$$\overline{V\tau}_m \approx \frac{q_0 \alpha}{4} \frac{1 + \exp(-\alpha/P_r)}{1 - \exp(-\alpha/P_r)} \approx \frac{q_0}{2} P_r \quad (33)$$

This elementary formula is especially evident. On Fig. 5 the diagrams  $V^*m$  depending on are resulted  $Pr(\chi)$  at change of relative average propeller immersion  $\tilde{h}_0$  (aft draught) for vessel ( $L = 140$  m,  $Cb = 0,70$ ,  $V_0 = 13,5$  kn,  $n_0 = 121$  1/min) in head seas with  $H_{1/3} = 4,5$  m.

REFERENCES

1. Lipis V.B. The screw Propeller Hydrodynamics on ships in waves Leningrad. "Sudostroenie" 1975, 263 p, (in Russian).
2. Lipis V.B., Remez Y.V The Safety Modes of the Ship Operation in Rough Seas. "Transport", Moscow, 1982, 118p, (in Russian).
3. Ship Theory Handbook. Ed. by Y.I.Voitkunski. In 3 vol., Leningrad "Sudostroenie", 1985 (in Russian).
4. Makoto Kan. Surging of Large Amplitude and Surf-riding of Ships in Following Seas. J.S.NA Japan, v. 162, 1987. v.165, 1989. v.166,1989.
5. Ananiev D.M. Determination the Boundaries of Surf-riding Domain Analyzing Surging stability. STAB' 94. Proc v.5. Florida, USA, 1994.
6. Boroday I.K., Netsvetaev Y.I. Seakeeping of Ships, Leningrad. "Sudostroenie", 1982, (in Russian).
7. Naiyo S, Nakamura S. Open water characteristics and Load Fluctuation of Propeller at Racing condition in waves. J. KSNA, Japan, 1979, N 172. p. 51-63.

Table 1

The characteristics of propeller racing under ship motions in waves

Characteristics			Service conditions						
			$d_a = d = 9,87$			$d_a = d = 8,6$		$d_a = 7,0$ $d = 6,25$	
Draught of ship	$d$	m							
Ship speed in still weather	$V_s$	kn	24,65			25,5		26,8	
Propeller RPM in still weather	ns	1/min	129,5			131,0		133,0	
Sea state (Bofourt numbers)	-	-	6	7	8	6	7	6	7
Significant wave height	$H_{1/3}$	m	4,5	6,5	8,5	4,5	6,5	4,5	6,5
Mean ship speed in head waves	$V_o$	kn	21,2	18,2	15,5	21,8	18,8	23,0	19,8
Mean propeller RPM in waves	no	1/min	125	119	113	126,5	122	128,5	124
Mean propeller RPM immersion	$h_o$	m	7,15	6,70	6,25	5,30	5,00	4,25	3,85
Mean amplitude of propeller immersion	$\Delta h_a$	m	1,69	2,48	3,2	1,72	2,50	1,75	2,50
Mean frequency of propeller immersion	$\omega_h$	1/s	1,40	1,17	0,97	1,43	1,16	1,45	1,20
Probability of propeller emergence	$P_{em}$	%	0,7	15,6	41,1	21,6	56,5	60,6	88,0
Probability of propeller racing	$P_r$	%	0,03	7,0	38,7	0,22	22,3	13,5	54,3

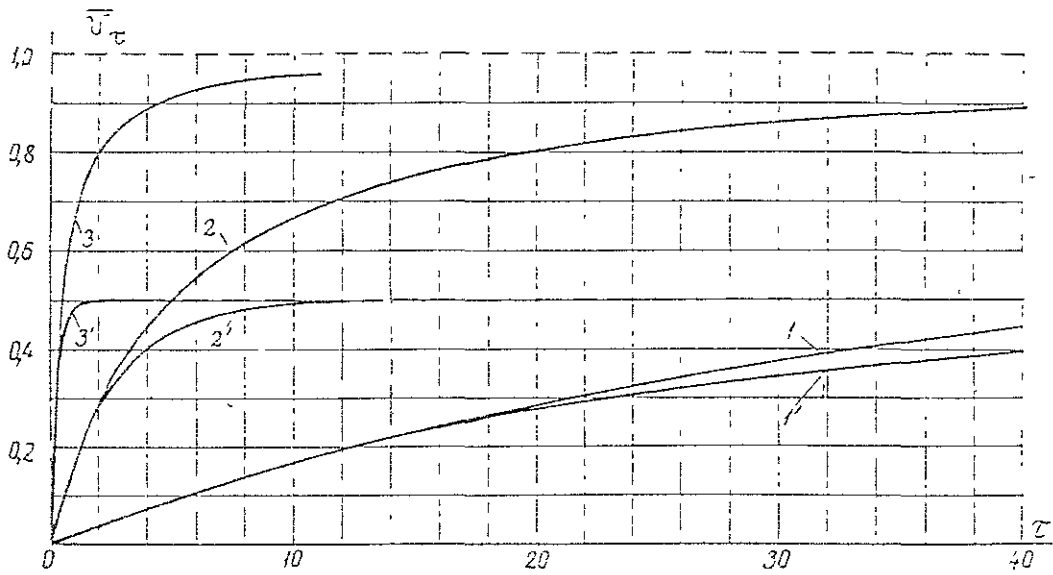


Fig. 1

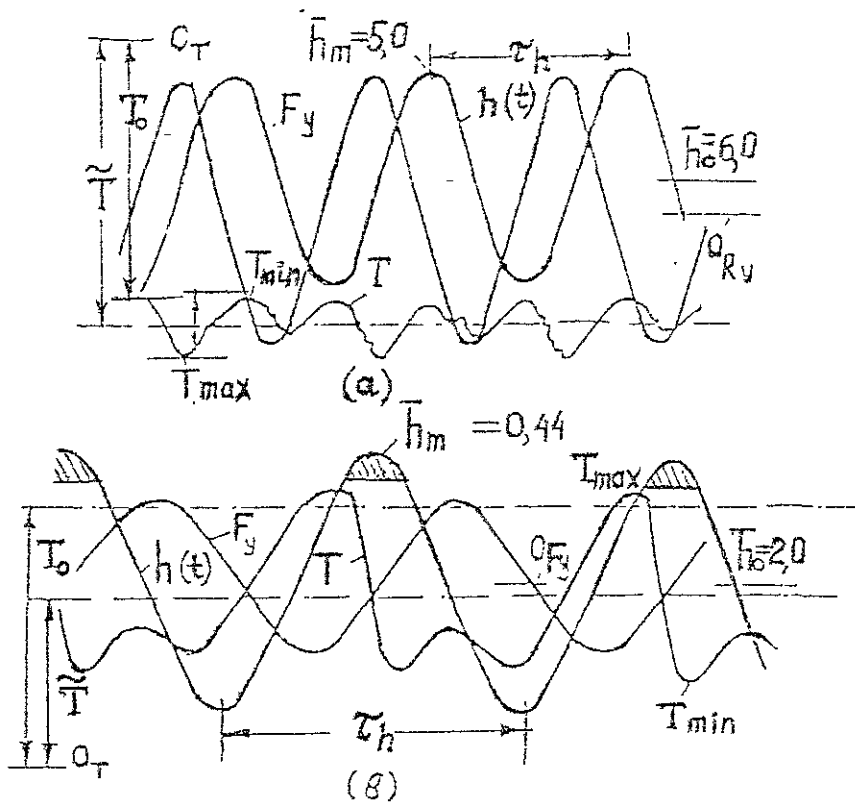


Fig. 2

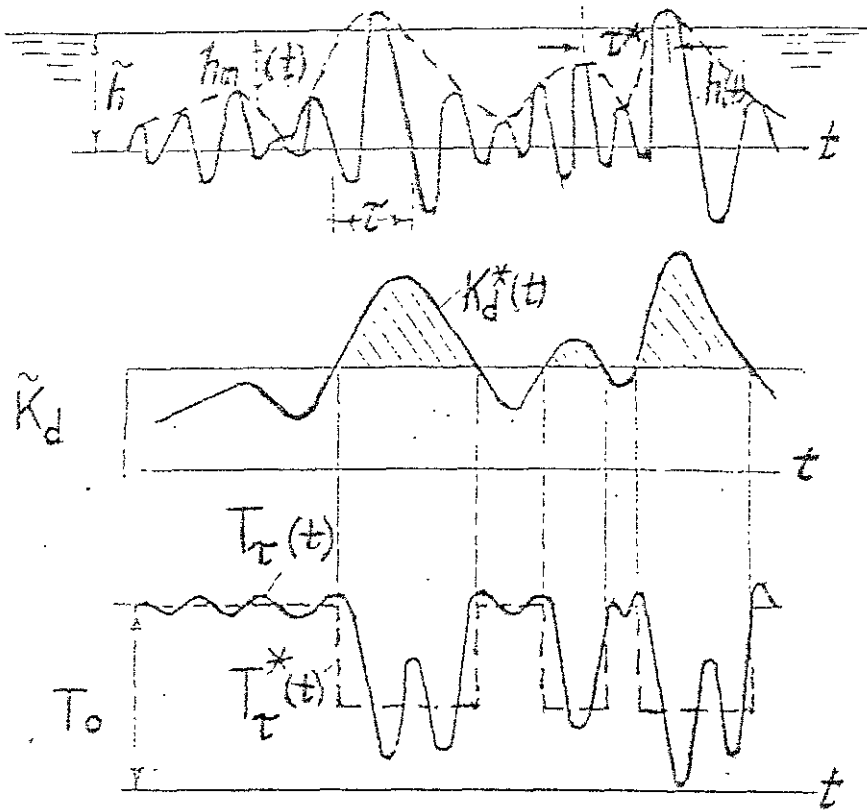


Fig. 3

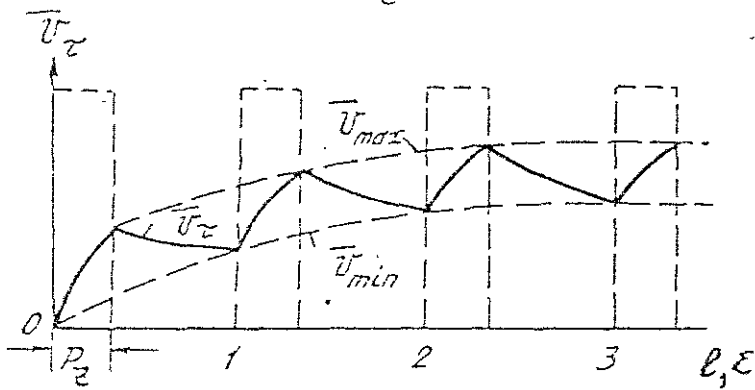


Fig. 4

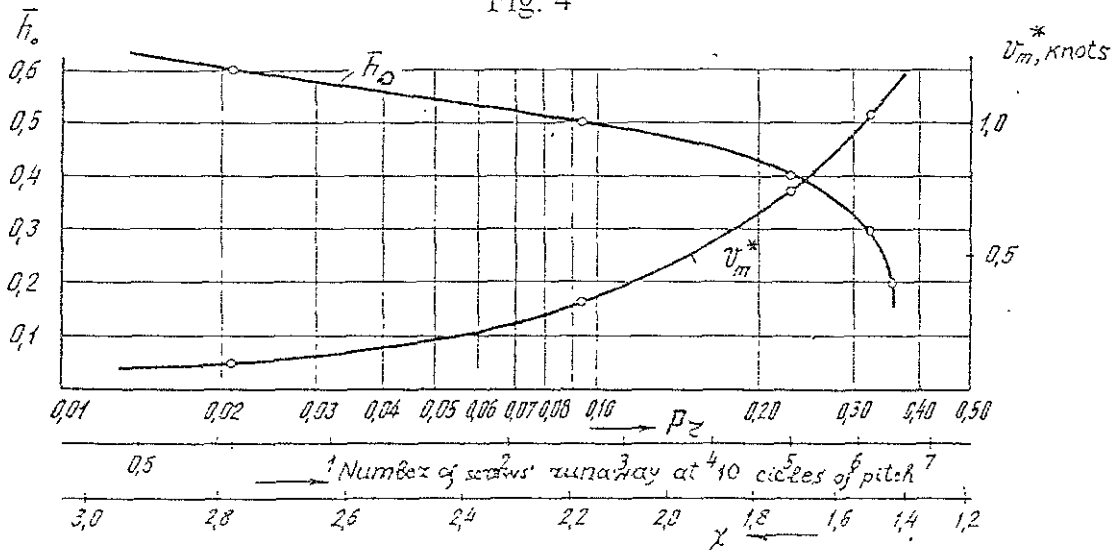


Fig. 5

**ADVANCES IN  
EXPERIMENTAL TECHNIQUE  
FOR INVESTIGATIONS  
ON STABILITY**

## WIND HEELING MODEL TEST FOR THE DEVELOPMENT OF TALL SAILING VESSELS STABILITY

J. Młynarczyk  
Faculty of Ocean Engineering & Ship Technology  
Technical University of Gdańsk

### ABSTRACT

A number of accidents and capsizings of sailing vessels confirms that existing stability criteria have to be improved. The weak point of these criteria is a simplicity of heeling moment calculation. To make these problems closer to real physical phenomena a series of aerodynamic model tests have been carried out.

The paper describes model tests of a sailing vessel USCGC EAGLE carried out in an aerodynamic tunnel of the Institute of Aviation in Warsaw. The problem of appropriate modeling is discussed. The paper is based on two research projects. One of them was sponsored by the US Coast Guard [8] and conducted by Science and Technology Corporation, US. The second project was sponsored by the Research Committee of the Polish Government and the Polish Register of Shipping and coordinated by the Faculty of Ocean Engineering & Ship Technology, Technical University of Gdańsk.

During the last fifteen years the Polish Shipyard of Gdańsk was the world leader in design and building of sailing vessels. Over a dozen or so sailing vessels were launched. It was a motive power for development of stability criteria.

### NOMENCLATURE

- $\alpha$  - angle of attack
- $\alpha_i$  - induced angle of attack
- $\alpha$  - wind gradient correlation coefficient
- $\alpha_s$  - angle of attack on the yard in the gap between two square sails
- $\beta$  - course angle according to apparent wind velocity direction
- $\gamma$  - course angle according to true wind velocity direction
- $\delta$  - sail trim angle

- $\lambda$  - drift angle
- $\Lambda$  - sail aspect ratio
- $b$  - span of sail
- $c$  - average chord of sail
- $D$  - sail drag
- $F$  - aerodynamic force of sail
- $L$  - sail lift
- $P$  - sail heeling force
- $R_n$  - Reynolds number of sail based on average chord
- $S$  - area of sail
- $S_{n-m}$  - gap between square sails working in stock - pile set
- $T$  - sailing thrust
- $V$  - wind speed
- $V_a$  - apparent wind velocity
- $V_{as}$  - apparent wind in the gap between sails
- $V_i$  - sail induced velocity
- $V_{ox}$  - true wind velocity measured at height above sea level
- $V_s$  - ship speed
- $z$  - height above sea level

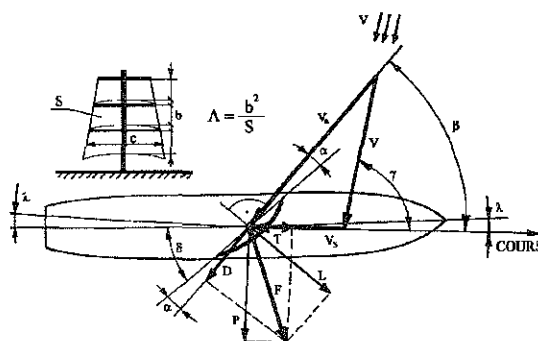


Fig.1 Angles, velocities and forces on sail profile.

## 1. INTRODUCTION

A stability is a critical element in the process of design and safety operation of sailing vessels. During her life the sailing ship is exposed to severe capsizing wind forces. In such condition the safety of vessels depends on an appropriate decision of the captain 'how to adjust the sails area to rapidly changing weather condition'.

To improve the stability criteria US Coast Guard decided to carry out wind heeling model test for the sailing vessel USCGC EAGLE at full scale and on a model test facility. The model test was carried out by the author in low speed tunnel of Aviation Institute in Warsaw under the contract of the Science and Technology Corporation (STC) [8]. An open working section of the closed circular wind tunnel is of 5 m.(16.4 ft) in diameter with max. speed 57 m/s (110 kt). The primary objective of the model test on USCGC EAGLE were the wind heeling moments measurements as function of apparent wind angle at the same sets and trims as in full scale test - the correlation test.

The second objective was the measurement of the wind heeling moment under the worst condition of sailing for heel angle from upright to as close to the knockdown condition as the testing allowed - the heeling moment versus heel angle test.

The main problem of such kind of test is scaling.

A false model scaling can give wrong results and conclusions. In described above set of tests the scale of model was 1:33.333.

The additional model test was carried out in the same wind tunnel under Polish Register of Shipping supervision. For this purpose the foremast of USCGC EAGLE with all sails in scale 1:17.5 was tested. The aerodynamic characteristic of each sail working separately and together have been established. The induced velocities in the vicinity of different sails were recorded. The main aim of these tests was to establish the mutual interaction between the sails. These data have been used to testing the procedures of computer program for simulating sailing vessels capsize in stable and gust condition [5] [6] [7].

The computer program is still under design.

## 2. WIND HEELING MOMENT MODEL TEST OF USCGC EAGLE

### 2.1 DESCRIPTION OF THE EAGLE

The USCGC EAGLE is a three-masted barque built in Hamburg, Germany, at the Blohm and

Voss Shipyard in 1936. She is the sail training ship for the U.S. Coast Guard Academy and the largest sailing ship in operation by the U.S. Government. An outboard profile of the USCGC EAGLE against the background of wind speed distribution as a function of height above the sea is presented on Fig. 2

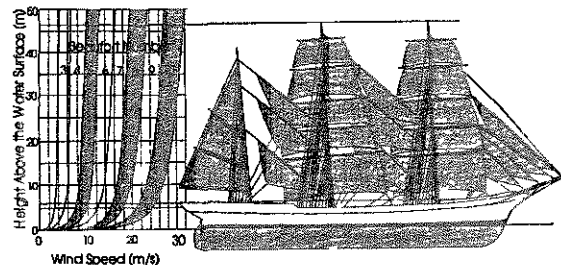


Fig. 2 Outboard profile of the EAGLE and wind speed distribution as a function of height above the sea

The principal characteristics of USCGC EAGLE:

Length Overall	- 89.9 m
Length on water line (LWL)	- 70.0 m
Beam	- 12.0 m
Draft	- 4.6 m
Sail Area	- 2066 m <sup>2</sup>
Mast Height above LWL	- 45.5 m

### 2.2 SCALING THE MODEL TEST

The following conditions have to be fulfilled in order to guarantee similarity between the flows over the sails in full and model test:

- geometry similarity
- kinetic similarity
- dynamic similarity

The geometry similarity was fulfilled by building the model of the hull, superstructure, sails and rigging based on plans of the full-scale ship, sail makers documentations of the sails, and pictures of the full-scale ship. The hull of the model was constructed of wood and the masts and yards were made of brass rods that were turned on a lathe to obtain an accurate reproduction of their shape. The mast fittings were made of steel or brass plate and mounted by brazing, brass soldering, or riveting them in place.

The sheets and square sail braces were made of steel wire to provide the proper stiffness and strength and were adjusted with small custom-made turnbuckles. The sail were made of dacron with a scaled shape taken from the documentation for the full-scale sails. The sail panels were marked with double seams.

The kinematic similarity was fulfilled by adequate modelling of sails flow conditions and apparent wind velocity gradient above the sea level.

When a thin airfoil with the sharp leading edge is placed in a flow, boundary layer separation on the leading edge appears frequently. In general, the flow around such a section is very sensitive to external flow conditions. In this case the maximum lift coefficient depends on

- the sum of the momentum losses incurred along the suction side
- the values of the skin friction drag coefficient
- the location of the boundary layer transition point along the suction side.

The boundary layer reattachment can occur in the laminar-turbulent transition zone where the critical value of the Reynolds number is exceeded locally. The secondary flow connected with the momentum dissipation in the region of flow separation affects the pressure field on the suction side and causes a decrease in the lift coefficient. The model test must be performed above the critical Reynolds number to fully develop a turbulent boundary layer and avoid this phenomenon. The critical Reynolds number value for thin airfoils is  $3 \cdot 10^5$  [2-4]. In the supercritical range of the flow parameters (turbulent flow), the behaviour of thin airfoils is not so sensitive to Reynolds number variation. Thus, exceeding the critical Reynolds number assures that proper aerodynamic force is established. Wind tunnel turbulence and airfoil surface roughness affect the turbulent boundary layer generation significantly. Apart from fulfilment supercritical conditions of the flow, turbulence conditions were induced by application of grinding powder along all the leading edges of the staysails and rigging. Thin wires were also added (0.5 mm (0.02 in.) in diameter) to span between the neighbouring yards in front of the square sails to generate Kármán vortices.

The local min. Reynolds number values for the least (flying jib) sail for full-scale and model was  $Rn=1,4 \cdot 10^6$  and for model test  $Rn=0,36 \cdot 10^6$ .

The wind velocity over the ocean is a function of the height above sea level. This velocity distribution with height is shown for different wind speeds in Fig. 1. Long-term measurements of the wind speed distribution over water have

led to the following equation for velocity as a function of height:

$$V(z) = V_{10} \cdot \frac{\ln\left(\frac{z}{0.05}\right)}{\ln\left(\frac{10}{0.05}\right)} \quad (1)$$

or approximating:

$$V(z) = V_{10} \cdot \frac{z^{0.1}}{10}$$

where  $V_{10}$  represents the value of standard velocity at 10 m (32.8 ft) above sea level and  $z$  is the height above sea level.

On a sailing ship, the apparent wind velocity is the superposition of the ship velocity and local wind true velocity, which varies with the height above sea level. Thus the upper sails work in higher velocities and generate higher loads. For the model tests, the model was to be stationary in a wind distribution that varied with height above the wind tunnel floor. The model-scale wind distribution used was based on apparent wind distribution at full scale, because forward speed of the full-scale ship would be modelled using the method describing below.

Neglecting the drift angle as a small value we obtain the relationships (see Fig. 1):

$$V = \frac{V_a \sin \beta}{\sin \gamma} = \frac{V_a \cos \beta - V_s}{\cos \gamma} \quad (2)$$

and:

$$V_a = \frac{V \sin \gamma}{\sin \beta} \quad (3)$$

It gives relationship:

$$V_a = V \cos(\gamma - \beta) + V_s \cos \beta \quad (4)$$

Since the difference between the true and apparent wind direction ( $\gamma - \beta$ ) is often small and the cosine of those angles is very nearly 1, the equation can be approximated as:

$$V_a = V + V_s \cos \beta \quad (5)$$

Wind sheer or drag near the free surface decreases the velocity from the free stream. The effects on the sailing ship is to decrease the apparent wind speed and direction closer to the deck. The equation that best fits actual measured data for wind speed as a function of height above the sea surface,  $z$ , is:

$$V(z) = V_{ox} \left( \frac{z}{10} \right)^c \quad (6)$$

For model testing, the wind speed is selected to maximise the loads on the dynamometer without exceeding its limits.

$V_{Tmax}$  = maximum free stream wind tunnel speed

This wind speed is the free stream wind speed, and screens will be added to slow down the flow toward the floor of the wind tunnel. This speeds corresponds to the apparent wind speed that was measured at the top of the foremast in the full-scale tests. If the model is to be exposed to the same shape of wind distribution wind height as the apparent wind distribution in full scale, the wind speed at any height must be in the same ratio to the free stream as the apparent wind speed at the corresponding height in full scale is to the masthead wind speed. At the sea surface, the true wind speed is zero and the only contribution to the apparent wind is from forward speed of the ship in full scale. Using Equation 4,

$$V_a(z) = V(z) + V_s \cos\beta \quad (7)$$

and at full scale:

$$V_a(z = 46.9m) = V_m = V(z = 46.9m) + V_s \cos\beta \quad (8)$$

and using Equation 5:

$$V_m = V_{ox} \left( \frac{z}{10} \right)^c + V_s \cos\beta \quad (9)$$

and

$$V_a(z = 0m) = V_s \cos\beta \quad (10)$$

For model scale:

$$V_a(z's = 46.9m) = V_{Tmax} \quad (11)$$

where  $s$  = scale ratio  
and  $z'$  = height above the wind tunnel floor (sea surface) at model scale

$$V_a(z's = 0m) = V_{Tmax} \cdot \alpha \quad (12)$$

where

$$\alpha = \frac{V_s \cos\beta}{V_m} \quad (13)$$

From Equation 9:

$$V_{ox} = \frac{V_m - V_s \cos\beta}{\left( \frac{46.9}{10} \right)^c} = \frac{V_m(1 - \alpha)}{\left( \frac{46.9}{10} \right)^c} \quad (14)$$

The corresponding model test relationship would be

$$V_{ox} = \frac{V_{Tmax}(1 - \alpha)}{\left( \frac{46.9}{10} \right)^c} \quad (15)$$

The general description of the wind speed versus height for the model test is then

$$V_a(z') = V_{Tmax} \cdot \alpha + V_{ox} \left( \frac{z's}{10} \right)^c \quad (16)$$

or

$$V_a(z') = V_{Tmax} \cdot \alpha + \frac{V_{Tmax}(1 - \alpha)}{\left( \frac{46.9}{10} \right)^c} \cdot \left( \frac{z's}{10} \right)^c \quad (17)$$

Then equation 16 becomes:

$$V_a(z') = V_{Tmax} \cdot \alpha + 0.9491 \cdot V_{Tmax} \cdot (1 - \alpha) \cdot (z')^{0.153} \quad (18)$$

The regression determined the value of the coefficient  $\alpha$  that best fits the apparent wind distribution. The distribution vary from test to test and with apparent wind angle for each correlation test data set. Therefore, a single test condition was selected from each of the eight correlation test data sets; the model-scale wind distributions were based on these individual events. The selection of the test condition in each data set was based on the event that had the highest heeling moment for those events where the ship was moving well in a close-hauled condition. The values of  $\alpha$  were similar for some of the tests so it was possible to use only three separate distributions (values of  $\alpha$ ) to cover all model-scale correlation tests. It was necessary to limit the number of distributions because developing a particular velocity distribution in the tunnel was the most time-consuming part of the testing. Each distribution was developed by iteratively varying comb-shaped piles and turbulence mixers placed upstream of the model until the measured and desired velocity profiles matched. The velocity distributions were designed Type 1, 2 and 3 wind profiles corresponding to values of  $\alpha$  of 0.2, 0.09 and 0.0 respectively. The correlation between the desired velocity distribution in the tunnel and the actual measured distribution for Type 1 wind profile is shown in Figs 3.

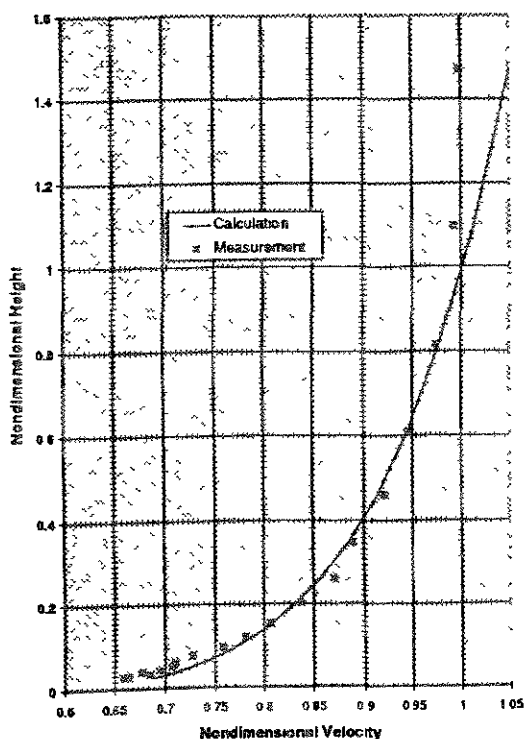


Fig. 3 Type 1 wind velocity distribution,  $\alpha = 0.2$ .

The dynamic similarity was fulfilled by matching an apparent wind gradient to full-scale test and preserved the same angle of attack on appropriate sails. In general a change of the true wind velocity, heading angle and vessel speed require additional apparent wind velocity distribution for correlation model test, according to eg. 18.

The adequate angle attack of each sail was fixed by adjustment of sail trim angles. In order to trim the model yards to the same angles as during the full-scale tests, thin brass plates of the appropriate size were attached to the mast above each yard and to the yards. These plates were shaped as half-circular sectors and had small holes drilled, enabling the yard position to be fixed as required at predetermined angles. Rows of sheet catches were distributed on deck to allow the staysails to be trimmed to the required angles; each staysail had its own row corresponding to the trim angles of the full-scale test conditions.

The square sails, yards and staysails sheets were equipped with stops to obtain quickly the required trim angles corresponding to the requested test data.

### 3. THE TEST FACILITY

The low speed wind tunnel at the Aviation Institute was selected for the test. This large aerodynamic tunnel has an open test section and an exhaust nozzle diameter of 5 m (16.4 ft). The maximum velocity of the air flow is 57 m/s (110 kt).

The measurement stand is shown in Fig 4. The floor of the tunnel had distributed turbulence mixers simulating the sea surface and was placed between the intake and diffuser exhaust nozzles. The model was placed on a turntable that was located in the centre of the tunnel floor and connected by brackets directly to a six degree - of - freedom strain gauge dynamometer. The construction of the rotating dynamometer base allowed the apparent wind to be simulated at any angle to the model.

The gap between the tunnel floor and the model hull surface was approximately 2 mm (0.08 in.). This narrow gap was achieved by using filler pieces that were templates of waterline at the heel angle being tested. The bottom part of the model hull and the measuring devices attached to the hull were protected from the flow by covers. The forces generated on the covers and the tunnel floor were not recorded by the strain gauge six degree - of - freedom dynamometer.

The forces and moments from the dynamometer

were recorded by an automated data acquisition system running on a personal computer. Data were collected at 400 samples/s for 2 s. A filtering system performed root - mean - square averaging of the data as they were collected. The time averaged measured quantities were transformed to dimensionless aerodynamic characteristics and presented on appropriate plots.

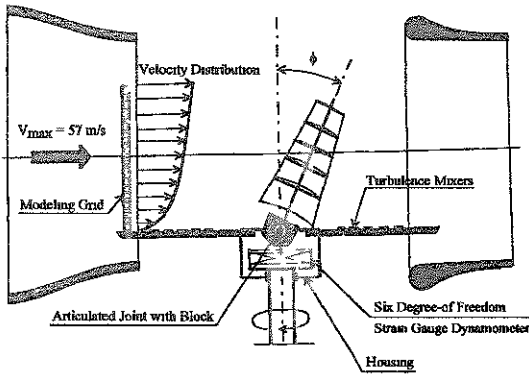


Fig. 4 The measurement stand for the model tests.

#### 4. MODEL SCALING

The following quantities place limits and therefore determine the model scale:

- The critical value of Reynolds number (Recrit) for the test conditions that enables the model test to occur in turbulent conditions. Recrit limits the minimum size of the model (maximum scale).
- The maximum value of blockage coefficient. The blockage coefficient limits the maximum model size (minimum scale). The blockage coefficient is the ratio of model lateral area to aerodynamic working section area. For values of the blockage coefficient higher than 10 percent of the drop in pressure from the highest level ahead of the model to the lowest level behind the model starts to affect the drag and lift generated on the model. The model lateral area is limited to approximately 2 m<sup>2</sup> (21.5 ft<sup>2</sup>) for the large, low speed wind selected at the Institute of Aviation.
- The maximum heeling moment recorded by the strain gauge dynamometer. For the dynamometer used, the maximum heeling moment could not exceed 800 N-m (590 ft-lb).
- The dimensions of the rotating part of the tunnel floor. These dimension limit the maximum value of the waterline length to

approximately 2.2 m (7.22 ft). The tunnel floor simulates the sea surface so the hull of the model must penetrate this surface.

- The strength of model rigging and mast. These model elements are not able to carry enormous load that is generated by large wind speed. Taking the pattern of the flow around the sails and all the above conditions into consideration, a model scale of 1 to 33.333 was chosen.

#### 5. THE TEST PERFORMED

Two types of model tests were performed. The first type was a replication of the full-scale measurements to establish the model to full-scale correlation. The second type of tests measured the wind heeling moment as a function of heel angle up to values approaching a 'knock-down'.

For the correlation tests, the model was placed at similar heel angles as in the measured full-scale tests and the sails were trimmed to the same angles to the wind as recorded in full scale. Data were recorded in approximately 10° increments of increasing apparent wind angle until the range of wind angles recorded at full scale was covered. The correlation tests were intended to show how the full-scale data compare with the model-scale data. The objective of the heeling angle tests was to generate curves of wind heeling moment versus heel angle that can be scaled to full scale for use in a stability assessment of the ship. Two sail arrangements were done: One at full sail (Fig 2) and one at reduced sail for heavy water (Fig. 5). The model was placed upright at an apparent wind angle that generated the maximum wind heeling moment. Then the heel angle was increased in increments of 10° until the model interfered with the wind tunnel floor (60° was the maximum angle).

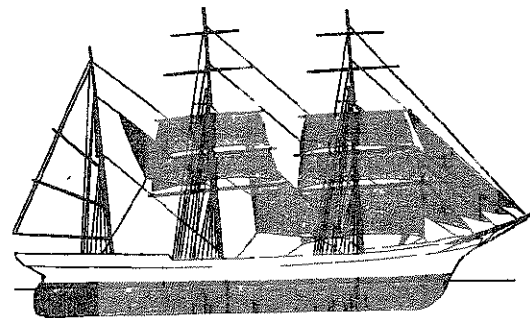


Fig. 5 Sail arrangement for heavy weather condition

The results for the heeling angle are present on Fig 6

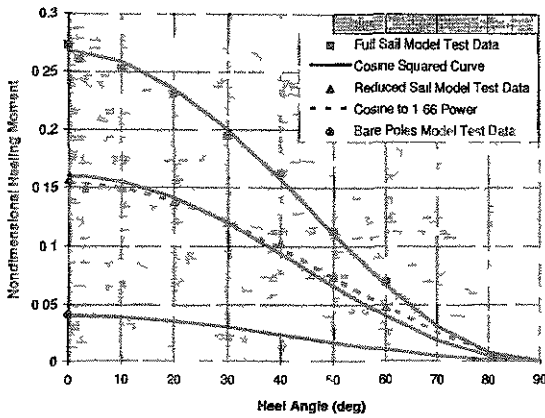


Fig 6 Results of the heeling angle test

## 6. THE SAILS INDUCED VELOCITY MEASUREMENTS

Under The Polish Register of Shipping supervision the computer program for simulating sailing vessels stability and capsize is under construction. The program is based on early theoretical works [5] [6] [7].

The hydrodynamic model is based on three dimensional equivalent inclination [7]. The aerodynamic model is based on thin airfoil theory [1]. The data base of aerodynamic characteristic of different shape of sail bases on the results of sails model tests [6].

USCGC EAGLE was selected as a one of the ships for testing the stability simulation program. For this purpose the additional aerodynamic test was carried out. Each sail of foremast was tested separately and next together for catching the mutual interaction on aerodynamic characteristics.

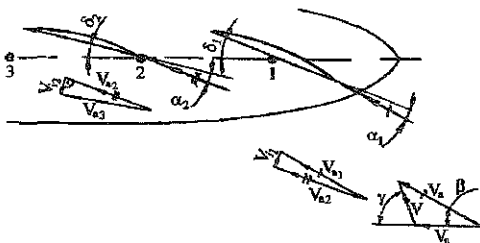


Fig 7 Influence of induced velocities on flow over the palisade of sails

Practically this influence depends on mutual induced velocities. The triangle set of sails are mainly affected in horizontal plane as shown on Fig 7.

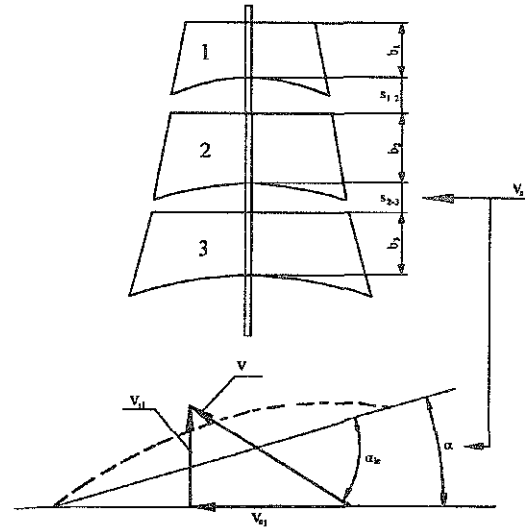


Fig 8 Influence of square sail stock pile on velocity field behind sails

The results show that the induced velocities in palisade sails are related to angle of attack on each sail and approximately equal to

$$\alpha_1 \approx 0.5 \alpha \quad (19)$$

It is valid for close hauled condition where the heeling moment is maximum.

The influence of induced velocities in square sail stock pile is mainly recognisable on velocity field behind the sails as shown on Fig 8.

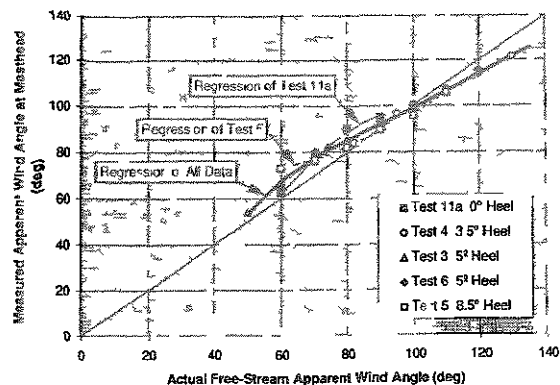


Fig 9 Difference in measured and actual apparent wind angle with upper sails set

shift of the fishing net on the deck.

## 2. OUTLINE OF THE CAPSIZING [1]

The purse seiner left for the East China Sea for fishing on February 17, 1993.

The Nagasaki marine observatory announced a gale warning in the whole area of the East China Sea near Kyushu in JAPAN at 5:35 p.m. on February 20.

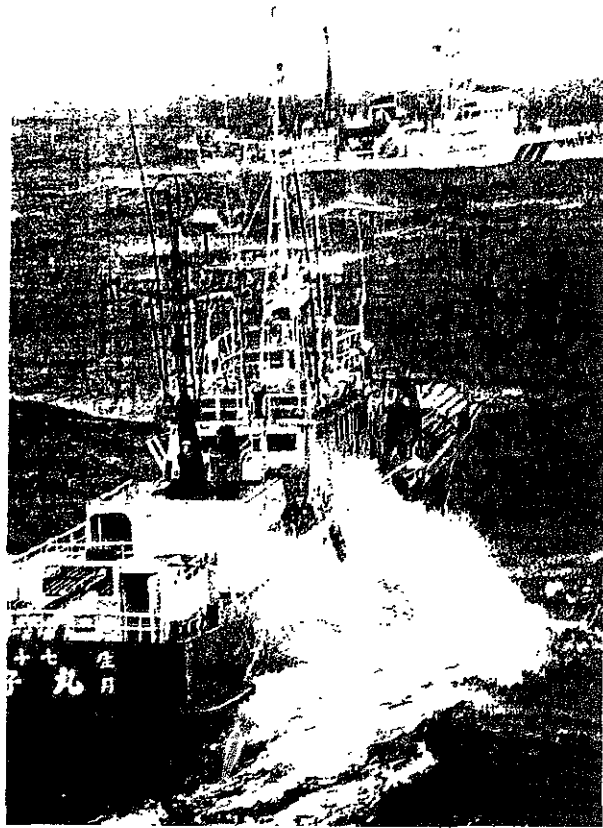
At about 11:40 p.m. the purse seiner gave up fishing, because the wind velocity became 10 m/sec and the wave height grew to 2 m high. Although the preparation for weathering the storm was made by crew, the fishing net was not fixed on the deck then.

At about 11:52 p.m. the purse seiner was navigating toward the east at a speed of 9 knots in the sea area of 328 degrees, 13 nautical miles from the Shira Se lighthouse. The wind velocity became 15 m/sec and the wave height grew to 2.5 m high. The purse seiner was rolling with an amplitude of 15 degrees in the starboard beam seas. A shipping spray on the deck occurred frequently, like that shown in Photograph 1, and the shipping water on the starboard deck occurred, causing the ship to roll largely to the starboard.

At about 0:05 a.m. on February 21, the purse seiner reached the sea area of 336 degrees, 12 nautical miles from the lighthouse. The direction of the current in that area had changed.

At about 0:20 a.m. the purse seiner was maintaining its direction and speed and was navigating waves which had grown to 3.5 m high.

At about 0:21 a.m. when the purse seiner rolled far to the starboard, the fishing net on the deck shifted in the same direction. Because of that, the ship was inclined to the



Photograph 1. Fishing Boat and Patrol Ship which were searching the capsized ship on Feb. 21, 1993.

(This is the photograph which was printed in the MAINICH news paper on Feb. 22, 1993)

starboard about 25 degrees and did not restore to the upright condition. And the engine was stopped.

A few of the crew were escaping from the crew space under the net space on the deck to the port of top of the deck house (see Figure 1). The ship was greatly inclining to the starboard immediately after that, because of a large quantity of shipping water on the starboard deck.

At 0:22 a.m. the purse seiner capsized in the sea area of 347 degrees, 11.3 nautical miles from the lighthouse.

## 3. MODEL EXPERIMENTS

The purpose of the model experiments is to find out the cause and the process of the capsizing of the purse seiner.

Therefore the experiments on the capsizing were carried out by using a model ship of the purse seiner in the same beam seas condition as the sea area where the ship capsized.

### 3-1. MODEL SHIP

The purse seiner is a single decker and the wheel house is located on the top of the deck house at the midship. A spacious flot storage of the fishing net is provided on the deck of the aft body. The general arrangement of the purse seiner is shown in Figure 1. The side deck of wooden plank used as a working area is characteristic of this ship, as shown in Figure 1.

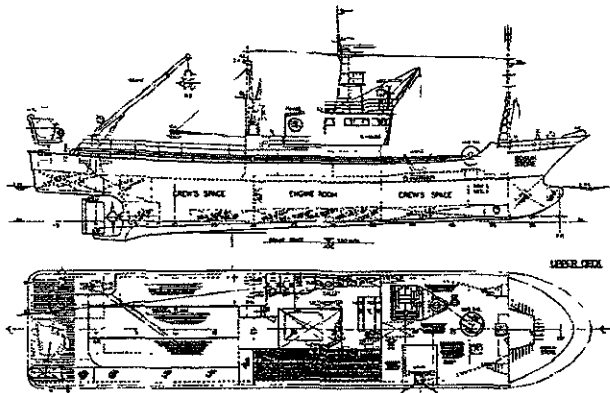


Fig.1 General Arrangement

The model ship was made according to that arrangement.

The principal particulars of full scale ship and 1/20 scale model of the purse seiner are shown in Table 1 and the body plan is shown in Figure 2.

Table 1. Principal Particulars of Full-Scale Ship and Model Ship

SHIP ITEM	FULL-SCALE SHIP	MODEL SHIP
Loa	36.90 m	1.845 m
Lpp	30.50 m	1.525 m
B	6.90 m	0.345 m
D	2.54 m	0.132 m
d	2.35 m	0.118 m
Displacement	260.76 ton	32.60 kg

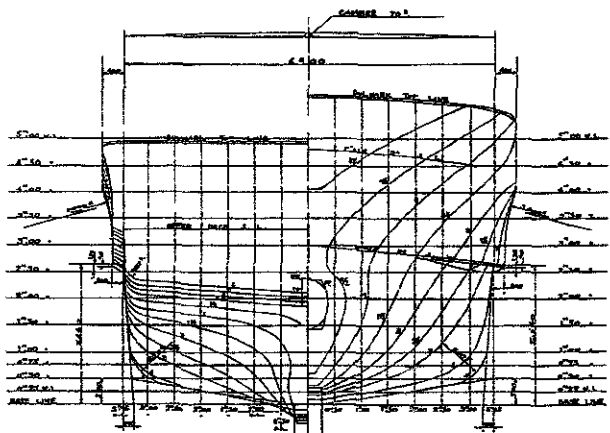


Fig.2 Body plan

### 3-2. EXPERIMENTAL CONDITION

#### •Metacentric Height GM

The experiments were carried out in three GM conditions of the model ship. One condition is a designed metacentric height,  $GM=6.85\text{cm}$  ( $KG=12.45\text{cm}$ ), and the others,  $GM=5.50\text{cm}$  ( $KG=13.80\text{cm}$ ) and  $4.45\text{cm}$  ( $KG=14.85\text{cm}$ ), are the assumed metacentric height which was reduced by the raised weight for this investigation. Each of the KG correspond to 2.49m, 2.76m and 2.97m in the full scale ship.

The stability curves in the three GM conditions of the purse seiner are shown in Figure 3.

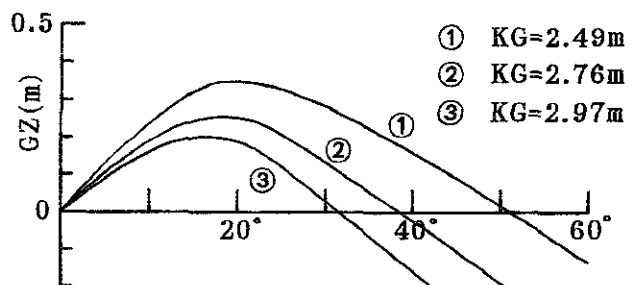
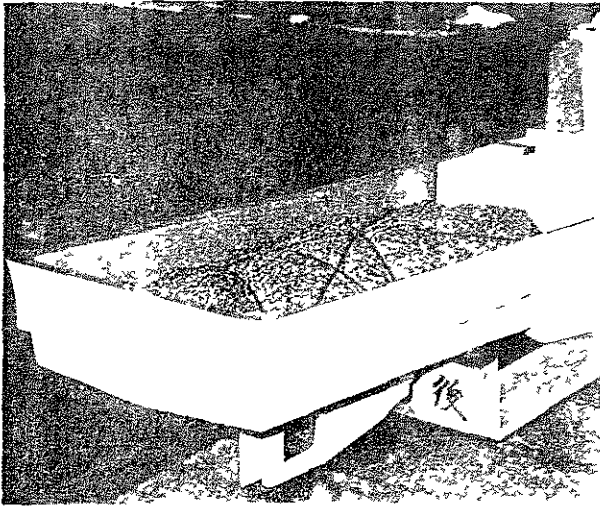


Fig.3 Stability Curves

#### •Fishing Net and Weight

The fishing net on the net space of the model ship was made with a net of chemical fiber and a sponge which can absorb water. The fishing net which was loaded on the deck is shown in Photograph 2.

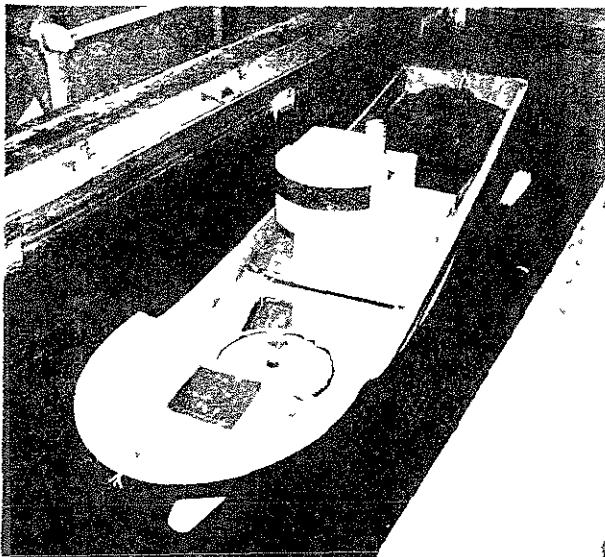


Photograph 2. Fishing Net which was loaded on the deck

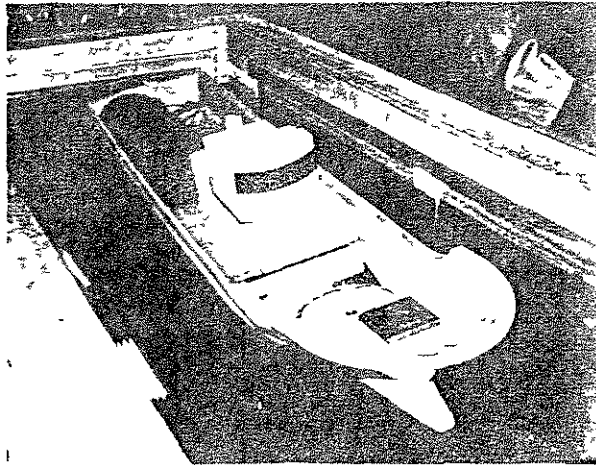
The weights of the fishing nets used in the experiments were 2.68 kg and 4.32 kg. The former was made up according to the rule in JAPAN, the latter is the designed net weight 3.33 kg plus the weight of the water soaked sponge which is 30% of the net weight.

#### •Inclination of Model Ship

In order to understand the cause and the process of the capsizing of the purse seiner, the model ship was tested not only in the upright condition (see Photograph 3), but also in the inclined condition (see Photograph 4). The author chose



Photograph 3. Upright Condition



Photograph 4. Inclined Condition with 10 degrees

two different inclined conditions, angle of 5 and 10 degrees respectively, the fishing net on the deck was adjusted to obtain the desired inclination.

#### •Wave Height and Period

The model ship was tested in three wave height conditions, 13.0cm, 15.0cm and 17.0cm. These heights correspond to the 2.6m, 3.0m and 3.4m wave heights in the sea area at the time of the capsizing.

The wave height was 2.6m in the sea area where the ship was navigating 30 minutes before the capsizing. Shipping water began to accumulate on the deck in this sea area.

The purse seiner capsized in the sea area with a wave height of 3.4m.

The wave height 3.0m is a intermediate condition between the 2.6m and 3.4m heights.

The wave periods used in the experiments were in increments of 0.1 second from 0.8 second to 1.6 seconds.

### 3-3.CAPSIZING EXPERIMENTS

The capsizing experiments were carried out in 54 different conditions of experimental conditions by varying GM, the weight of the fishing net, the floating

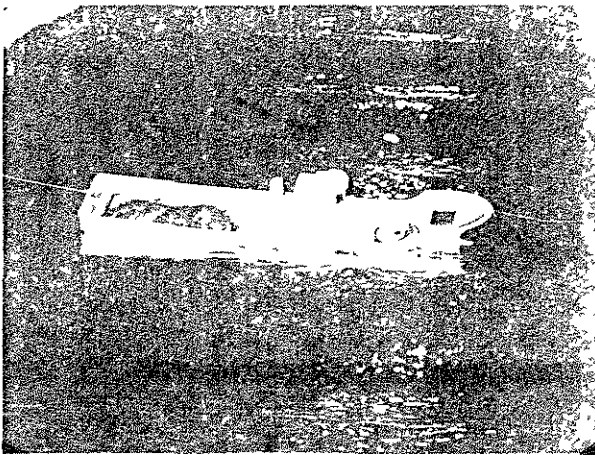
condition and the wave height  $H_w$ . These conditions are shown in Table 2.

Table 2. Experimental Conditions

Inclined Angle	0°	5°	10°
Weight of Fishing net	2.68 kg.	4.32kg	
K G (Full-Scale ship)	12.45cm, (2.49m)	13.80cm, (2.76m)	14.85cm, (2.97m)
G M (Full-Scale ship)	6.85cm, (1.37m)	5.50cm, (1.10m)	4.45cm, (0.89m)
$H_w$	13.0 cm	15.0 cm	17.0 cm

The model ship was exposed to regular transverse waves (see Photograph 5).

The behavior of the model ship in beam seas for each condition was recorded by video tape recorder.



Photograph 5. Model Ship in Regular Transverse Waves

### 3-4. RESULTS OF EXPERIMENTS

Results of the experiments on the capsizing are shown in Tables 3 to 8. In the Tables, triangles indicate that waves did not reach the deck over the bulwark top. In other words, the deck was dry. Double circles indicate that the shipping water got on the deck, but the model ship did not capsize. Black circles show that the model ship capsized due to the shipping water which had accumulated on the deck.

The shipping water on the

deck occurred at the shorter periods of incident waves than the natural rolling period  $T_R$  in the upright condition with different kinds of the metacentric height GM, but the model ship did not capsize in any GM condition, as shown in Tables 3 and 4.

Table 3. Experimental Results in Upright Condition with Fishing Net weighing 2.68kg

Initial Inclined Angle (deg.)	Weight of Fishing net (kg)	GM (cm)	$H_w$ (cm)	$T_w$ (sec)										
				$T_R$ (sec)	0.8	0.9	1.0	1.1	1.2	1.3	1.4	1.5		
0	2.68	6.85	1.037	1.3	○	○	○	△	△	-	-	-	-	-
				1.5	○	○	○	△	△	-	-	-	-	-
		1.7	○	○	○	△	-	-	-	-	-	-	-	
		1.9	○	○	○	△	-	-	-	-	-	-	-	
		2.1	○	○	○	△	-	-	-	-	-	-	-	
		2.3	○	○	○	△	-	-	-	-	-	-	-	
	5.50	1.11	1.5	○	○	○	△	△	-	-	-	-	-	
			1.7	○	○	○	△	△	-	-	-	-	-	
	4.45	1.28	1.3	○	○	○	○	○	△	-	-	-	-	
			1.5	○	○	○	○	○	○	△	△	-	-	
	1.7	○	○	○	○	○	○	○	△	△	-	-		

Table 4. Experimental Results in Upright Condition with Fishing Net weighing 4.32kg

Initial Inclined Angle (deg.)	Weight of Fishing net (kg)	GM (cm)	$H_w$ (cm)	$T_w$ (sec)										
				$T_R$ (sec)	0.8	0.9	1.0	1.1	1.2	1.3	1.4	1.5		
0	4.32	6.85	1.048	1.3	○	○	○	△	△	-	-	-	-	
				1.5	○	○	○	△	△	△	-	-	-	
		1.7	○	○	○	△	△	△	△	-	-	-		
		1.9	○	○	○	△	△	-	-	-	-	-		
		2.1	○	○	○	△	-	-	-	-	-	-		
		2.3	○	○	○	△	-	-	-	-	-	-		
	5.50	1.12	1.5	○	○	○	○	△	-	-	-	-		
			1.7	○	○	○	○	△	-	-	-	-		
	4.45	1.30	1.3	○	○	○	○	○	○	△	-	-		
			1.5	○	○	○	○	○	○	○	△	△		
	1.7	○	○	○	○	○	○	○	○	△	△			

In the inclined condition of 5 degrees, Tables 5 and 6 show that the model ship capsized in only the smallest GM condition although the shipping water got on the deck at just about the same range of wave period as in the upright condition in any GM.

Table 5. Experimental Results in Inclined Condition of 5° with Fishing Net weighing 2.68kg

Initial Inclined Angle (deg.)	Weight of Fishing net (kg)	GM (cm)	$H_w$ (cm)	$T_w$ (sec)										
				$T_R$ (sec)	0.8	0.9	1.0	1.1	1.2	1.3	1.4	1.5		
5	2.68	6.85	1.048	1.3	○	○	○	△	-	-	-	-		
				1.5	○	○	○	△	△	-	-	-		
		1.7	○	○	○	△	△	△	-	-	-			
		1.9	○	○	○	△	-	-	-	-	-			
		2.1	○	○	○	△	-	-	-	-	-			
		2.3	○	○	○	△	-	-	-	-	-			
	5.50	1.12	1.5	○	○	○	○	△	-	-	-			
			1.7	○	○	○	○	△	△	-	-			
	4.45	1.30	1.3	-	○	○	-	○	△	-	-			
			1.5	-	○	○	○	-	○	△	-			
	1.7	-	○	○	○	○	-	○	△	-				

Table 6. Experimental Results in Inclined Condition of 5° with Fishing Net weighing 4.32kg

Initial inclined Angle (deg.)	Weight of fishing net (kg)	GM (cm)	H <sub>w</sub> (cm)	T <sub>v</sub> (sec)									
				T <sub>v</sub> (sec)	08	09	10	11	12	13	14	15	
5	4.32	6.85 1.056	13	○	○	○	△	-	-	-	-	-	-
			15	○	○	○	△	△	-	-	-	-	
			17	○	○	○	△	△	-	-	-	-	
		5.50 1.07	13	○	○	○	△	△	-	-	-	-	
			15	○	○	○	△	△	-	-	-	-	
			17	○	○	○	○	△	-	-	-	-	
		4.45 1.30	13	-	●	●	●	○	○	△	-	-	
			15	-	-	-	●	○	○	△	-	-	
			17	-	-	-	●	○	○	△	-	-	

It is to be noticed that the model ship capsized at just about the same range of wave period in the upright condition and the 5 degrees inclined condition in any GM when the ship was inclining 10 degrees due to the shift of the fishing net. These results are shown in Tables 7 and 8.

Table 7. Experimental Results in Inclined Condition of 10° with Fishing Net weighing 2.68kg

Initial inclined Angle (deg.)	Weight of fishing net (kg)	GM (cm)	H <sub>w</sub> (cm)	T <sub>v</sub> (sec)								
				T <sub>v</sub> (sec)	08	09	10	11	12	13	14	15
10	2.68	6.85 1.049	13	○	○	○	△	-	-	-	-	-
			15	●	●	○	△	-	-	-	-	
			17	●	●	○	○	△	-	-	-	
		5.50 1.16	13	-	●	●	○	△	-	-	-	-
			15	-	●	●	○	△	-	-	-	-
			17	-	●	●	○	△	△	-	-	-
		4.45 1.35	13	-	●	-	-	●	●	△	-	-
			15	-	●	-	-	●	●	△	-	-
			17	-	-	-	-	-	●	△	△	-

Table 8. Experimental Results in Inclined Condition of 10° with Fishing Net weighing 4.32kg

Initial inclined Angle (deg.)	Weight of fishing net (kg)	GM (cm)	H <sub>w</sub> (cm)	T <sub>v</sub> (sec)							
				T <sub>v</sub> (sec)	08	09	10	11	12	13	14
10	4.32	6.85 1.03	13	○	○	○	△	-	-	-	-
			15	●	●	○	△	△	-	-	-
			17	●	●	○	△	△	-	-	-
		5.50 1.15	13	-	●	○	△	-	-	-	-
			15	-	-	●	○	△	-	-	-
			17	-	●	●	○	△	-	-	-
		4.45 1.37	13	-	-	-	-	●	●	△	△
			15	-	-	-	-	●	●	△	△
			17	-	-	-	-	-	●	△	△

#### 4. CONCLUSION

The conclusions that have emerged from considering the phenomena of the capsizing of the purse seiner in the model experiments are as follows:

1) The purse seiner in the upright condition does not capsize in the same sea area condition that the actual ship capsized in even if the range of the stability is decreased due to top heavy condition.

2) In case of the top heavy condition of the purse seiner, there is a strong possibility that a slight inclined condition due to a shift of the fishing net led to the capsizing.

3) The purse seiner with a large angle of inclination due to the shift of the fishing net capsizes easily even if the metacentric height is enough to maintain stability in the upright condition.

A process and a cause of the capsizing of the purse seiner became obvious from the phenomena of the capsizing in the model experiments and the abovementioned conclusions.

The author concludes that the purse seiner capsized through the following process:

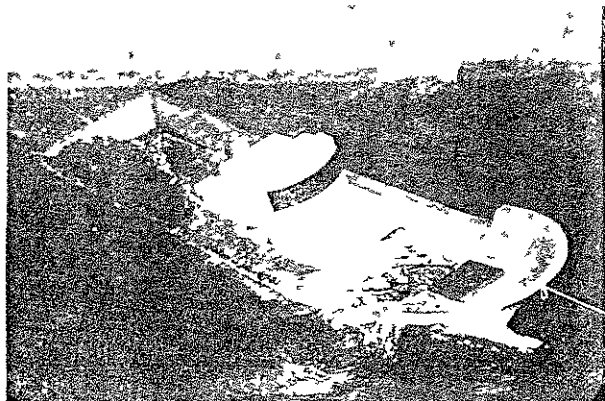
1st. the purse seiner was rolling with an amplitude of more than 15 degrees in starboard beam seas.

2nd. the shipping spray and water on the deck occurred on the starboard side frequently. The purse seiner was rolling and moreover was inclining to starboard due to the shipping water which had accumulated on the deck.

3rd. when the inclination of the purse seiner increased to the starboard due to the effect of accumulated shipping water, the fishing net on the deck shifted in the same direction.

4th. the ship was inclining more than 25 degrees to the starboard and did not restore

its upright condition (see Photograph 6).



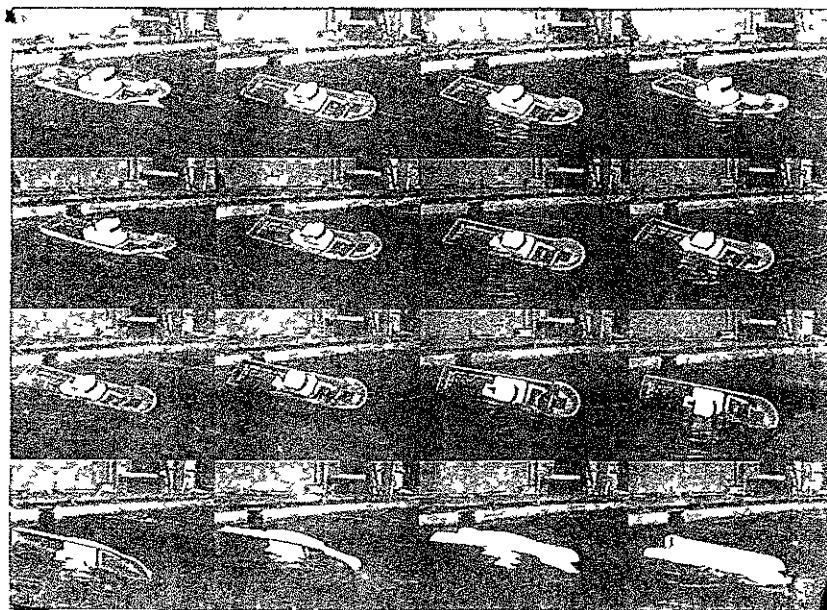
Photograph 6. Model Ship which was Inclining due to the Shipping Water on the Deck

And, finally, the purse seiner capsized because a large quantity or a long continuation of the shipping water on the starboard deck occurred (see Photograph 7).

Therefore the cause of the capsizing of the purse seiner is that the fishing net in the net space was not fixed on the deck.

#### 5. REFERENCES

1. 漁船 第7 蛭子丸転覆事件, 海と安全 '94-6, 日本海難防止協会 (The Japan Association of Marine Safety), No. 426, 1993. 6, pp 2~8



Inclination.  $10^{\circ}$   
KG = 14.85cm  
H<sub>w</sub> . 15.0 cm  
T<sub>w</sub> . 1.40sec.

Photograph 7. The capsizing phenomenon of the purse seiner at 0.3 second intervals in the experiments

#### ACKNOWLEDGEMENT

The author wishes to thank Mr. H. Inoshita, H. Miyazaki and N. Murai who are students of Nagasaki Institute of Applied Science for their assistance to these experiments.

The purpose of the present investigation is to provide some light in the problem of the scale effect on the ship roll damping coefficients by means of the results of free roll decrement tests in calm water at zero forward speed with different models and a full-scale ship using different linear and non-linear analysis methods.

## 1. ANALYSIS METHODS

Several decay experiments were carried out with models in the towing tank of the Escuela Técnica Superior de Ingenieros Navales of the Universidad Politécnica de Madrid and with a full-scale ship in Aldán (Pontevedra).

In roll decrement tests an initial heel is given to a model in calm water. Then the model is allowed to roll freely recording the decaying oscillations. A representation of heel angle versus time, figure 1, is obtained.

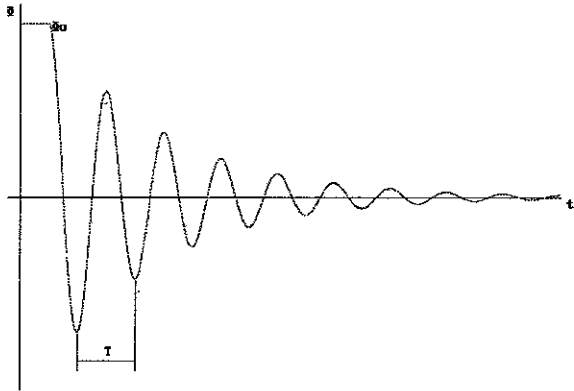


Fig 1.- Roll Decrement Calm Water Test

The analog signal obtained from the heeling sensor was digitized and recorded on the towing tank carriage computer.

Imposing the moment balance in the system, the roll decay equation for free roll decrement tests is obtained as follows

$$I \frac{d^2 \Phi}{dt^2} + M_{Rd} + c(\Phi)\Phi = 0 \quad (1)$$

where

- $I$  = total roll inertia
- $\Phi$  = roll angle
- $t$  = time
- $M_{Rd}$  = roll damping moment
- $c(\Phi)$  = roll stiffness coefficient

The roll stiffness coefficient can be calculated as

$$c(\Phi) = \rho g \nabla GZ(\Phi) \quad (2)$$

where

- $\rho \nabla$  = model mass
- $g$  = gravity acceleration
- $GZ(\Phi)$  = restoring lever

At this point, all the terms appearing in the equation are known excepting the roll damping moment.

Many different formulations have been used to represent the roll damping moment. Traditionally the following linear formulation with only one unknown coefficient was used

$$M_{Rd} = B_1 \frac{d\Phi}{dt} \quad (3)$$

The use of this linear equation is not correct due to the non-linear effects of the roll motion so non-linear analysis methods are requested.

In this investigation two non-linear methods, proposed in reference 1, were used. These methods make use of the peaks in the roll moment and roll angle time-histories to solve the following linear+ linear-quadratic and quadratic+ linear-cubic forms, each one with three unknown coefficients. In both cases second and fourth order interpolations were used.

linear+linear-quadratic

$$M_{rd} = B_1 \frac{d\Phi}{dt} + B_2 |\Phi| \frac{d\Phi}{dt} + B_3 \left| \frac{d\Phi}{dt} \right| \frac{d\Phi}{dt} \quad (4)$$

quadratic+linear-cubic

$$M_{rd} = B_1 \frac{d\Phi}{dt} + B_2 \Phi^2 \frac{d\Phi}{dt} + B_3 \frac{d\Phi^3}{dt} \quad (5)$$

To obtain the coefficients  $B_1$ ,  $B_2$  and  $B_3$  from equations (4) and (5), the process in reference 1 will be followed. A solution of the form:

$$\Phi(t) = A(t) \text{Cos}(W_d t) \quad (6)$$

is assumed, where  $A(t)$  represents the peaks of the roll angle history versus time.

By substituting this expression in equations (4) and (5) and averaging them over one period, the differential equations that solve the problem are obtained.

In the first non-linear method (4) the differential equation to be solved is

$$\frac{dA(t)}{dt} = - b_1 A(t) - \beta A(t)^2 \quad (7)$$

with

$$\beta = \frac{2}{3\pi} (b_2 + 2 b_3 W_d) \quad (8)$$

$A(t)$  = peaks of the roll angle - time history

$W_d$  = natural roll frequency

$b_1$  =  $B_1/I$

$b_2$  =  $B_2/I$

$b_3$  =  $B_3/I$

In the second non-linear method (5) the differential equation to be solved is

$$\frac{dA(t)}{dt} = - b_1 A(t) - \beta A(t)^3 \quad (9)$$

with

$$\beta = \frac{1}{8} (b_2 + 3 b_3 W_d^2) \quad (10)$$

$A(t)$  = peaks of the roll angle - time history

$W_d$  = natural roll frequency

$b_1$  =  $B_1/I$

$b_2$  =  $B_2/I$

$b_3$  =  $B_3/I$

## 2. EXPERIMENTS

The following decay experiments were carried in the towing tank of the Escuela Técnica Superior de Ingenieros Navales of the Universidad Politécnica de Madrid and Aldán (Pontevedra).

### 2.1.- VORTEX EFFECT EXPERIMENTS

In a previous investigation about the scale effects in roll damping coefficient (reference 2), three geometrically similar models (geosims) with 1 m., 1.5 m. and 2 m. length were used. These model had ship-like forms with corner bilge as represented in figure 2.

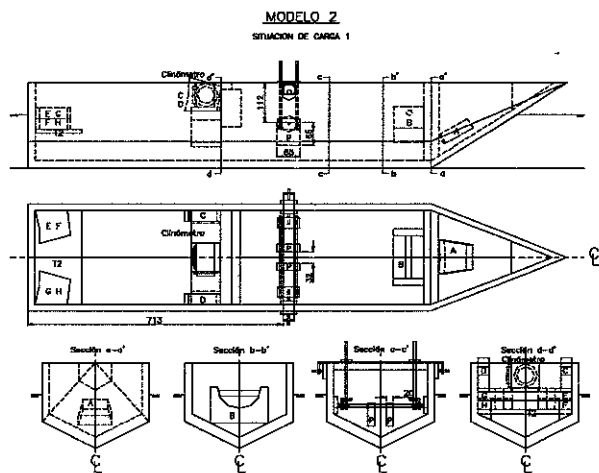


Fig. 2.- Ship-Like Form Corner Bilge Model

An ink test was made to the 1.5 m. length geosim. The ink test consisted in pumping ink with a syringe through the bilge corner of the model in the bow zone to visualize the vortex generation. As it was expected vortex were visualized.

It is reasonable that the vortex generation in the bilge zone of this model is owing to the great bilge angle. So, if a similar model with the same length, breadth, depth and wetted surface but with a smoother bilge zone is tested the bilge vortex will disappear. In that case the difference in the roll coefficient would be imputed to the bilge vortex generation.

A new model with 1.5 m. length was made changing the triangular lower section of the model with an elliptical one. The ellipse is calculated in such a way that, in each section, the new model has the same area, perimeter and breadth than the primitive one for 0.10 m. depth. For a depth greater than 0.10 m. the added section is the same in both cases, due to the vertical side. If the central section has the same area, perimeter and breadth in both cases, these parameters will be very similar in the bow sections.

The new model shape with rounded bilge is shown in figure 3.

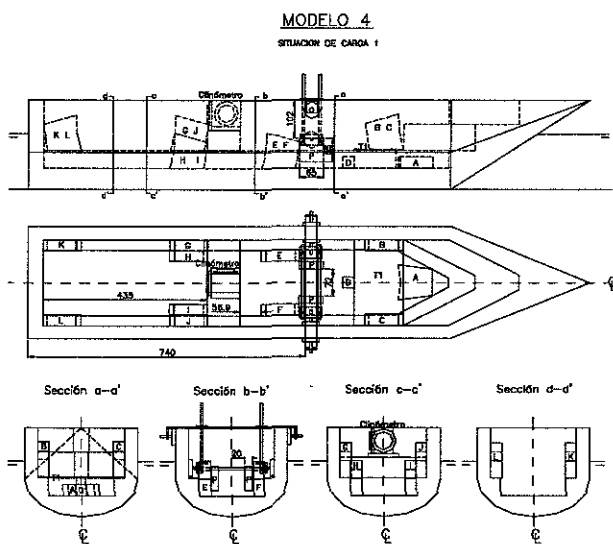


Fig. 3.- Ship-Like Form Rounded Bilge Model

These models were tested at similar loading conditions with equal transversal GM and inertia values. The equality of inertia was

controlled matching the natural roll period. A system of mobile weights with longitudinal, transversal and height movements was used to obtain the equality of GM and period. Fast calculation of GM and period was provided using a computer.

The cases studied are reflected in table 1 and were obtained combining two displacements, two transversal GM values and two inertial situations. These conditions were obtained placing the mobile weights in similar conditions.

Table 1

L (m.)	B(m.)	$\Delta$ (Kg.)	GM(m.)	Td (s.)
1.50	0.30	42.000	0.030	1.22
1.50	0.30	42.000	0.030	1.16
1.50	0.30	42.000	0.029	1.26
1.50	0.30	42.000	0.029	1.19
1.50	0.30	28.000	0.023	1.56
1.50	0.30	28.000	0.023	1.45
1.50	0.30	28.000	0.021	1.67
1.50	0.30	28.000	0.021	1.56

Each of these cases were tested in angles of 5°, 10°, 15° and 20° to port and starboard sides, so a total of 64 tests were carried out.

## 2.2.- SCALE EFFECT EXPERIMENTS

The scale effects in the roll damping coefficient in linear formulation (3) were studied previously in the investigation of the reference 2 for the three models with corner bilge forms presented before.

To have a greater knowledge of these scale effects, full scale tests were made in Aldán with the real vessel "Rebeca Dasilva".

"Rebeca Dasilva" is a fishing vessel that collect mussels over her deck. The load in these kind of vessels is situated very high, so, in order to have a good stability, they have a low length-breadth relation.

Main characteristics of "Rebeca Dasilva" are:

Length	= 18.74 m.
Breadth	= 6.50 m.
Draft	= 2.25 m.
Depth	= 1.75 m.
Displacement	= 100 Tons.

A wooden model was made in the towing tank to reproduce the same tests with a 1:10 scale model. The forms of this vessel are represented in figure 4.

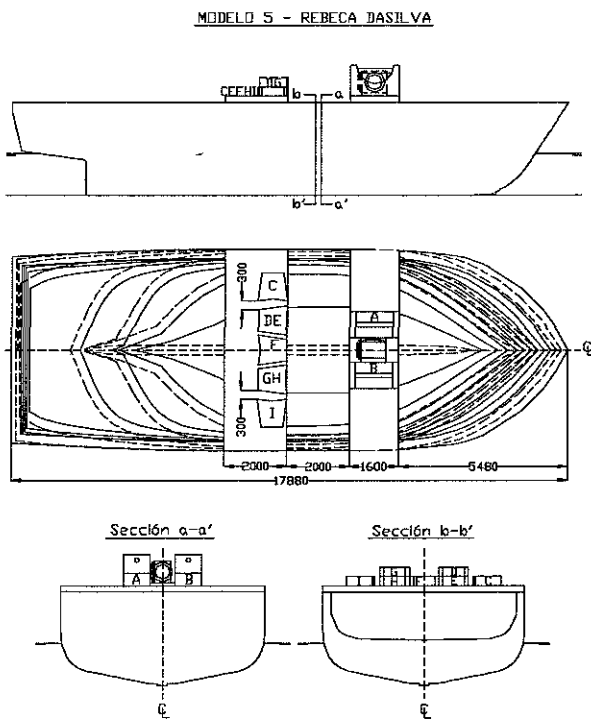


Fig. 4.- Rebeca Dasilva

The same computerized system was used to test the full scale vessel and the model.

To reproduce the free roll decrement test with the real ship a sunk 1.5 Tons. weight was localized. A person dived to fasten a rope to the weight. The other end of the rope was pulled up with the vessel crane and the weight hanged up from the side of the vessel. In that position a permanent heeling angle was obtained. When the angle was stabilized the rope was cut, the weight fell and the vessel started her roll motion which was registered.

Aldán is in an estuary in west northern Spain with very calm water. The trials were made in August with very good weather conditions so the influence of the external actions can be contempt.

The displacement of "Rebeca Dasilva" when the tests were done was 62060 Kg. A transversal stability test was done and a 2.678 m. transversal GM was measured. In that condition, the natural roll period was 3.8 seconds. The model was tested in similar conditions taking into account the scale, that means a displacement of 62 Kg., a transversal GM of 0.27 m. and a roll period of 1.2 seconds.

### 3. VORTEX EFFECTS

As it was expected, decay in the rounded bilge model is lower than decay in the corner bilge model because energy is spent in bilge vortex generation. Decay in the corner bilge model is around 1.6 times decay in the rounded bilge model and in some of the studied cases this difference arise to 3.

As an example, results obtained in the linear case are presented in figures 5 and 6. In these graphics linear coefficient B versus  $GM / \Delta^{1/3}$  is presented for the two studied models. The curves are marked with a R if they correspond to the rounded bilge model or with a C if they correspond to the corner bilge model. These letters are followed by a number that represents the initial angle of the free roll decrement test.

In order to obtain more clear graphics, data was separated in two different inertial cases, represented as cases A and B in figures 5 and 6. In case A the conditions in table 1 with lower periods (1.19 s. to 1.22 s.) are represented while case B contains the conditions with higher periods (1.45 s. to 1.67 s.). For each point represented in case A there is a point in case B with the same displacement, transversal GM and initial heeling angle but different period.

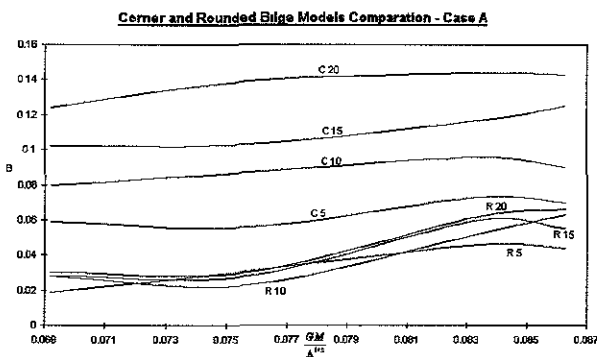


Fig. 5.- Model Comparison - Case A

Nevertheless, the same conclusions will be obtained.

In the following figures the roll angle time histories for a non-linear second order linear+linear-quadratic study are represented. In both cases the load situation is the same with transversal  $GM = 0.031 \text{ m}$ ,  $T = 1.22 \text{ s}$ . and initial angle  $10^\circ$ .

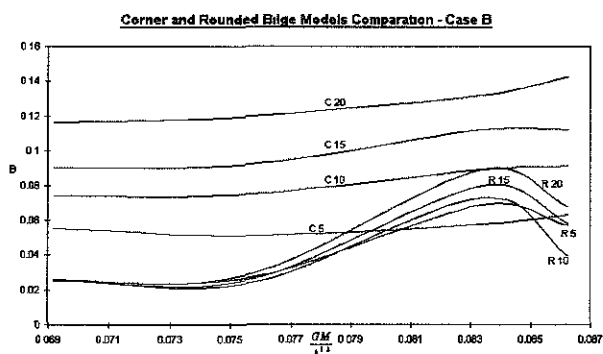


Fig. 6.- Model Comparison - Case B

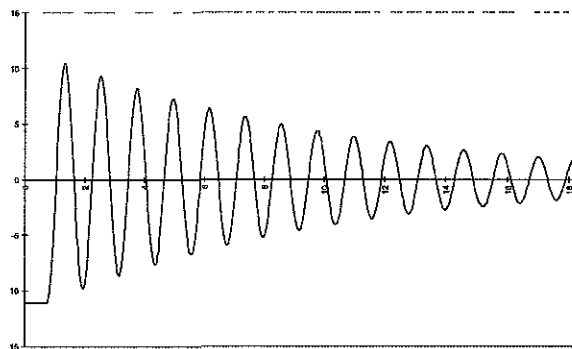


Fig. 7.- Corner Bilge Model - Roll Angle vs Time

In the last graphics an important influence of the initial heeling angle is found for the corner bilge case, in which the viscous effects are very important as it was shown in the ink test, while this influence is not as great in the rounded bilge case. This change in the damping coefficients with the initial heeling angle evidence the non-linearity of the roll motion, especially in the corner bilge case. When different analysis methods are used, non-linear methods fit the experimental data better in the corner bilge model while linear method is better in the rounded bilge model. As a conclusion of this, it is possible to say that many non-linear effects appear with vortex generation. So, the greater number of the non-linear effects in the roll damping coefficient seem to appear with vortex generation.

Results obtained in the non-linear cases have the same trends than in the linear cases but the use of three coefficients difficult their representation.

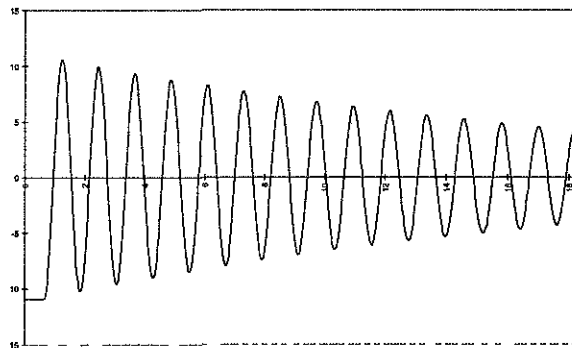


Fig. 8.- Rounded Bilge Model - Roll Angle vs Time

Corner and rounded bilge models were designed in such a way that all the parameters are the same excepting the vortex generation. So, it is assumed that the added dissipation moments appearing in the corner bilge model become from vortex generation.

In the following table the contribution of the eddy generation to the damping coefficient,  $B_{EO}$ , for  $10^\circ$  initial heeling angle is represented.

Table 2

$B_{EO}$ [Nms]	Draft [m]	$\omega$ [ $s^{-1}$ ]	$C_R$ [m/ $^\circ$ ]
0.033	0.1500	5.150	$2.907 \times 10^{-3}$
0.027	0.1500	4.987	$2.456 \times 10^{-3}$
0.020	0.1500	5.280	$1.718 \times 10^{-3}$
0.012	0.1500	5.417	$1.000 \times 10^{-3}$
0.041	0.1125	3.762	$1.562 \times 10^{-2}$
0.041	0.1125	4.028	$1.459 \times 10^{-2}$
0.035	0.1125	4.027	$1.246 \times 10^{-2}$
0.029	0.1125	4.333	$0.960 \times 10^{-2}$

In reference 3 there is a method to calculate  $B_{EO}$  using the formula

$$B_{EO} = \frac{4\rho d^4 \omega \Phi_A}{3\pi} C_R \quad (11)$$

where  $\rho$  is the fluid density,  $d$  the draft,  $\omega$  the roll frequency,  $\Phi_A$  the initial heeling angle and  $C_R$  a coefficient depending on the hull shape and the position of the gravity center.

In the studied loading cases, for each draft there are four gravity center positions, so four different  $C_R$  values are obtained. The obtained  $C_R$  values are coherent with the values in reference 3.

#### 4. SCALE EFFECTS

To compare the results obtained in the model and the full-scale tests, non-dimensional forms of the coefficients were used. For linear coefficient  $B_1$  (3) and non-linear coefficients  $B_1$  and  $B_2$  (4) (5), the same non-dimensional form presented in references 2 and 3 were used, it is

$$Bx_a = \frac{Bx}{\rho V B^2} \sqrt{\frac{B}{2g}} \quad (12)$$

For non-linear coefficient  $B_3$  (4) (5), the following non-dimensional form was used

$$Bx_a = \frac{Bx}{\rho V B^2} \quad (13)$$

The coefficients obtained for the model and the full-scale tests are

Table 3

Linear case	$B_{1a} \times 10^{-3}$
Full-Scale	7.601
Model	2.582

Table 4

Non-Linear case	$B_{1a}$	$B_{2a}$	$B_{3a}$
Linear+Linear-Quadratic Second Order	$\times 10^3$	$\times 10^3$	$\times 10^3$
Full-Scale	8.996	-354	-1.058
Model	3.290	-174	-496

Table 5

Non-Linear case	$B_{1a}$	$B_{2a}$	$B_{3a}$
Linear+Linear-Quadratic Fourth Order	$\times 10^3$	$\times 10^3$	$\times 10^3$
Full-Scale	8.238	-153	-457
Model	3.360	-160	-458

Table 6

Non-Linear case	$B_{1a}$	$B_{2a}$	$B_{3a}$
Quadratic +Linear-Cubic Second Order	$\times 10^3$	$\times 10^3$	$\times 10^3$
Full-Scale	8.400	-2.644	.247
Model	2.978	-1.236	-.004

Table 7

Non-Linear case	$B_{1a}$	$B_{2a}$	$B_{3a}$
Quadratic +Linear-Cubic Fourth Order	$\times 10^3$	$\times 10^3$	$\times 10^3$
Full-Scale	7.731	-746	.007
Model	3.124	-1.513	-.004

As a consequence of these results it is clear that an scale effect exists to extrapolate damping coefficients to the full-scale cases. In almost all

cases the coefficients for the full scale tests are around three times greater than in the model.

The non-linear, linear+linear-quadratic, fourth order study, in table 5, is the most accurate study. In this case coefficients  $B_{2a}$  and  $B_{3a}$  have the same value for the model and the full-scale ship and the coefficient  $B_{1a}$  is 2.45 times greater in the full-scale ship than in the model. In the linear case the coefficient  $B_{1a}$  is 2.94 times greater in the full-scale ship than in the model.

Comparisons using only one full-scale and one model tests do not allow a definitive conclusion and more exhaustive tests have to be made in order to obtain more comparison points. Nevertheless, scale effects exist and the use of an extrapolation method taking into account the viscous effects, very important in the roll motion, seems to be necessary. Reynolds number corresponding to the angular velocity of the roll motion when the rolling ship pass the  $0^\circ$  angle will be used in the extrapolation method in order to take the viscous effects into account.

## 5. CONCLUSIONS

From the results obtained in the previous points, the following conclusion will be taken from this investigation:

- The greater number of the non-linear effects in the roll damping coefficient seem to appear with vortex generation.
- Contribution of the eddy generation to the damping coefficient,  $B_{EO}$ , depends on the hull geometry and gravity center position.
- Contribution of the eddy generation to the damping coefficient,  $B_{EO}$ , measured in the model tests are coherent with the theoretical calculations in reference 3.

- Results obtained from linear method have the same trends than results obtained from non-linear methods.
- Scale effect exist comparing a full-scale ship and a model.
- A more exhaustive study of the scale effects seems to be necessary in order to obtain an extrapolation method taking into account the viscous effects.

## 6. REFERENCES

1. Cardo A., Francescutto A., Nabergoj R. - "On Damping Models in Free and Forced Rolling Motion" - Ocean Engineering - Pergamon Press - Volume 9, No. 2, 1982 - Pages 171 -179.
2. Pérez-Rojas L., Zamora R. - "Some Contributions to the Scale Effects on the Ship Roll Damping Coefficient" - WORKSHOP on Physical and Mathematical Modeling on Vessel's Stability in a Seaway, OTRADNOYE '93 - 1993 - Page 4.1 - 4.16.
3. Himeno, Y. - "Prediction of Ship-Roll Damping - State of the Art" - University of Michigan - Report no 239 - September 1981.

## AKNOWLEDGEMENTS

It is an utopia to think that a research work can be done by only one person. At present, any research work needs help from many people, and the one presented in this paper does not escape from this maxima. Authors want to thank Nodosa and Daso Mar staff, especially Mr. Manuel Dopico and Mr. Melchor Dasilva for their worthy help in the full-scale tests. Our gratitude for all ETSIN and CEHIPAR staff who collaborated in the different points of this work.

## EXPERIMENTAL RESULTS OF NONLINEAR ROLLING IN BIASED CONDITIONS IN BEAM WAVES

Giorgio CONTENTO (\*), Alberto FRANCESCUTTO (\*) and Luca SEBASTIANI (\*\*)

(\*) *DINMA - University of Trieste, via A. Valerio, 10 - 34127 Trieste, Italy*  
fax: +39-40-6763443 - e-mail:francesc@univ.trieste.it

(\*\*) *CETENA SpA, Via Savona 2, 16129 Genova, Italy*

### ABSTRACT

To highlight the behaviour of a ship in critical conditions in beam waves, a campaign of experiments have been conducted on the scale model of a RoRo. Two loading conditions and transversal inclinations following SOLAS'90 were analysed in different wave intensities. The results evidence a slightly greater roll amplitude in the bias into the waves condition. This condition appears to be the worse also for water on deck. The problems connected with the simulation of the large amplitude motions are discussed by means of a parameter identification technique.

### INTRODUCTION

A ship at sea can lose her upright equilibrium position under the action of many different causes ranging from external inclining actions (for example wind) to internal ones (shifting of cargo or asymmetric flooding). In the following we will shortly refer to a 'biased ship' as a ship that has lost her transversal upright equilibrium. The motions of a biased ship at sea are relevant to both intact stability (weather criterium) and damage stability (SOLAS) codes, especially in the light of the discussions following the SOLAS'95 Convention. Rolling motion of a biased ship has also been considered of great interest from a theoretical point of view both in longitudinal and in beam sea inasmuch as it discloses complex dynamic and chaotic features. On the other hand, only few experimental results have been reported in literature and the results are often contradictory

and of no help in view of improving the roll motion modelling.

Kobayashi [1] concluded that roll amplitude of a biased ship is greater than that of a non biased one. Furthermore the roll amplitude is greater when the ship is inclined weather side.

Lee & Kim [2] concluded that the roll amplitude is greater when the ship is inclined lee side.

Cao & Li [3] found that there is no definite conclusion, but in some cases the roll amplitude was greater in the presence of a lee side bias.

Wright & Marshfield [4] found that the roll amplitude is greater when the bias is towards lee side, while the capsizing probability is greater in the opposite bias condition.

Many authors stress the importance of the coupling between roll and vertical motions to explain the unsymmetrical behaviour and the connection between bias and capsizing probability.

These are the reasons why an extensive set of experiments has been planned and executed at the hydrodynamic laboratories of the University of Trieste.

### TESTED MODEL AND EXPERIMENTAL RESULTS

A scale model of a Ro-Ro in two different loading conditions ship has been tested in a regular beam sea. The principal dimensions and the mechanical data are given in Table. 1, while in Fig. 1 a schematic drawing of the body plan of the ship is shown.

Following the indications of SOLAS'90, the model has been tested with zero bias, with 7

and 12 degrees bias weatherside and leeside. The righting arm curve has been computed both in the fixed and in the free trim conditions. The comparison of the righting arms (fixed trim - model scale) between the three inclination conditions and the two loading is given in Fig. 2 and Fig. 3 with bias to port (coinciding with weather side in the experimental configuration) and angles measured from the actual equilibrium position.

The model was ballasted to the required displacement and transversal inertia moment. A movable weights device was installed on the deck to allow quick and easy transversal offset of the center of gravity to have the required transversal inclination.

The model was restrained by soft elastic strings to eliminate drift and yaw. Different tensioning was tried until a satisfactory setup was obtained.

The tests have been conducted at constant wave steepness at several frequencies, such as to cover completely the resonance peak. Wave steepness ranged from 1/90 to 1/20 to cover a wide range of sea states. The vertical motions, the lateral motion, the encounter frequency and the cases of water on weather deck have been recorded. Full details on the experimental results are given in [5]. Here only a sinthetical description will be reported.

The stationary roll amplitudes, measured around the actual centre of oscillation, are shown in Fig. 4 to Fig. 8, whereas in Fig. 9 and Fig. 10 the cases where water on deck was observed are evidenced. The model was not fitted with bulwark, so that no water accumulation on deck and sloshing was allowed.

## ANALYSIS OF THE EXPERIMENTAL RESULTS

The results have been analysed both in qualitative terms to get information on weather bias direction is most dangerous and in quantitative terms.

The following qualitative conclusions can be drawn:

1. There is a high degree of saturation due to the high nonlinear damping contribution given by the actual hull shape. This is evident by the flattening of the curve of maximum amplitudes as a function of the wave steepness (Fig. 11).
2. There is a good symmetry of the oscillation about the centre of oscillation.
3. In general there is no clear dependence of measured roll amplitude on the direction of bias relative to waves. When there is a marked difference, the roll amplitude is greater in the weather side bias (bias into waves) condition.
4. Water on deck was observed only in the high loading condition. Here again the worst bias condition is the bias into waves.

Finally, the experimental results were analysed in quantitative terms in the light of the development of a simulation procedure for large amplitude rolling in the different environmental condition for a ship in intact or critical conditions. This last part has been performed by means of the application of an efficient parameter identification technique [6,7] to obtain informations on the best mathematical modelling and on the proper values to be assigned to the coefficients of linear and non linear terms.

The mathematical model initially considered was a one degree of freedom roll motion equation:

$$\ddot{\phi} + 2\mu\dot{\phi} + nld(\phi, \dot{\phi}) + \omega_0^2\phi + nlr(\phi) = \pi \frac{H}{\lambda} (\zeta_1 \omega_0^2 - \zeta_2 \omega_e^2) \sin(\omega_e t) \quad (1)$$

with  $nld(\phi, \dot{\phi})$  and  $nlr(\phi)$  respectively nonlinear damping and restoring moments. The excitation was written in the above form to account for frequency dependence. The nonlinear part of the righting arm was represented in normalized terms in one of the following forms:

$$nlr(\phi) = \alpha_0 + \alpha_2\phi^2 + \alpha_3\phi^3 + \alpha_4\phi^4 + \alpha_5\phi^5 \quad (2)$$

for a model with bias and

$$\text{nlr}(\phi) = \alpha_3\phi^3 + \alpha_5\phi^5 + \alpha_7\phi^7 + \alpha_9\phi^9 \quad (3)$$

for a model without bias. Both mathematical models are written with angles measured from the upright position independently on its being an equilibrium one. The constant term in Eq. 2 accounts for bias, while the even terms are responsible for the loss of symmetry of the righting arm in biased conditions.

The Parameter Identification Technique based on the least squares fitting of the numerical solution of Eq. 1 to the experimental results was tried on all the cases, but it resulted successful only in several ones. In many cases either convergence was not possible or the best estimates of the parameters, damping and excitation coefficients, was not physically consistent (negative damping or excitation coefficients exceeding unity). In any successful case it was found that:

5. A delicate dependence on the righting arm coefficients ( $\omega_0, \alpha_i$ 's) is intrinsic to this approach, with strong indications that the quasi-free trim condition was the more reliable.

6. The following strongly nonlinear angle dependent damping model:

$$2\mu + \delta_1(\phi - \text{bias})^2 \dot{\phi} \quad (4)$$

had the best fitting capability:

Then a modified one degree of freedom model was tried:

$$\begin{aligned} \ddot{\phi} + 2\mu\dot{\phi} + \text{nlr}(\phi, \dot{\phi}) + \omega_0^2\phi [1 + a \cos(\omega t + \varepsilon)] + \text{nlr}(\phi) \\ = \pi \frac{H}{\lambda} (\zeta_1 \omega_0^2 - \zeta_2 \omega_e^2) \sin(\omega_e t) \end{aligned} \quad (5)$$

The mathematical model expressed by Eq. 4 includes a rough description of the effect of a vertical motion on roll motion. This approach is typical of the studies devoted to the parametric resonance in following waves and was tried also in beam seas to explain the unsymmetrical behaviour of a biased ship. The application of the Parameter Identification Procedure allowed

to obtain estimates of amplitude and phase of this disturbance. Unfortunately not all the cases could be successfully analysed in terms of this approach.

## CONCLUSIONS

The study, performed on a RoRo in different biased conditions permitted to obtain important informations on the behaviour and mathematical modelling for large amplitude roll motion simulations of a ship in critical conditions in different meteorological environment. Due to the high saturation phenomenon, the rolling motion did not attain sufficiently large amplitude rolling motion to 'sample' the righting arm curve beyond its maximum and thus exhibiting strong dependence on the relative bias-wave directions and possibly capsizing.

At the same time, it seems that it is quite difficult to obtain a reliable description of roll motion by means of a one degree of freedom equation. This corroborates the indications of previous authors on the need to take into account vertical motions when extreme rolling is concerned.

Future developments of the research will then be in the following directions

a) Considering a ship with larger bias and/or lower initial metacentric height.

b) Developing a Parameter Identification Technique able to deal with more degrees of freedom.

## ACKNOWLEDGEMENTS

This research has been developed with the financial support of CETENA SpA in the frame of Research Plan CETENA 1994/96.

## REFERENCES

- [1] Kobayashi, M., "Hydrodynamic Forces and Moments Acting on Two-Dimensional Asymmetrical Bodies", Proc. STAB'75, Glasgow, 1995.
- [2] Lee, C. M., Kim, K-H., "Prediction of Motions of Ships in Damaged Conditions in

Waves", Proc. STAB'92, Tokyo, 1992, pp. 287-301.

[3] Cao, Z-H., Lee, J-X., "Model Experiments on Inclined Ship in Waves", Proc. STAB'86, Gdansk, 1986.

[4] Wright, J. H. G., Marshfield, B. W., "Ship Roll Response and Capsize Behaviour in Beam Seas", Trans. RINA, Vol. 122, 1980, pp. 129-148.

[5] Francescutto, A., Contento, G., "Experimental Results of Nonlinear Rolling in Biased Conditions in Beam Waves", Technical Report 1/96, DINMA/CETENA, 1996.

[6] Cardo, A., Coppola, C., Contento, G., Francescutto, A., Penna, R., "On the Nonlinear Ship Roll Damping Components", Proc. Int. Symp. NAV'94, Roma, 1994.

[7] Francescutto, A., Contento, G., Penna, R., "Experimental Evidence of Strongly Nonlinear Effects in the Rolling Motion of a Destroyer in Beam Sea", Proc. STAB'94, Melbourne, FL, USA.

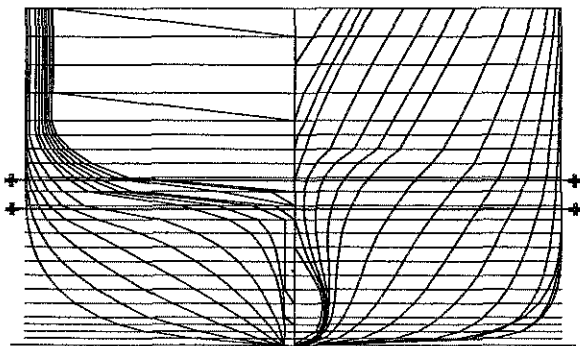


Fig. 1. Schematic plot of the body plan of the RoRo

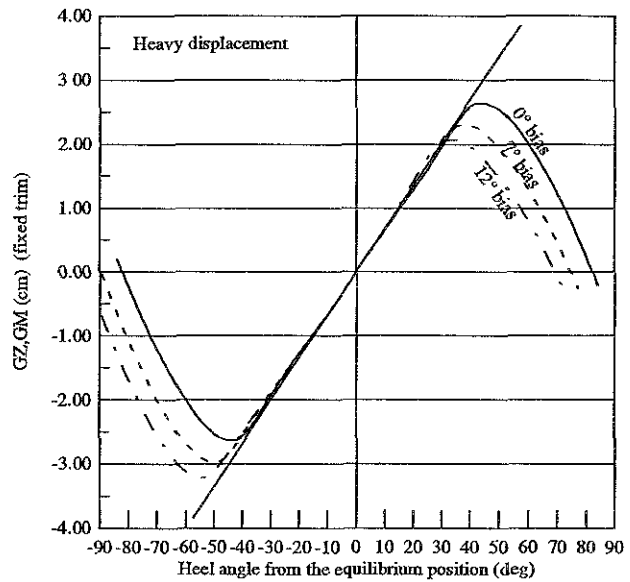


Fig. 2. Righting arm curves in the upright equilibrium condition and in the two biased conditions for the model in the heavy displacement.

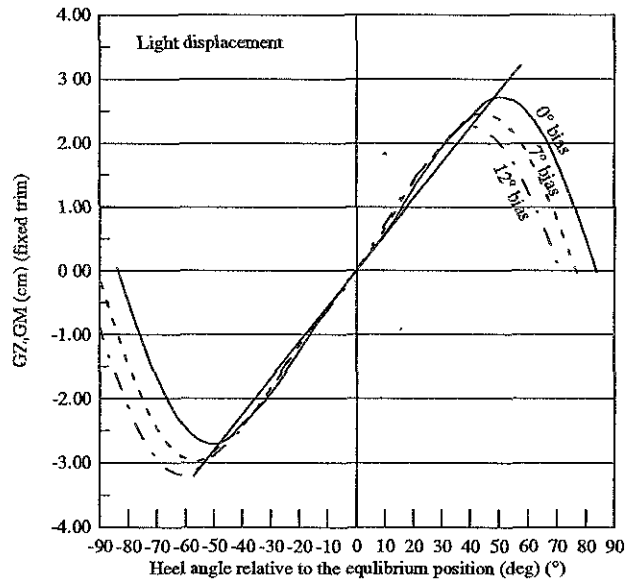


Fig. 3. Righting arm curves in the upright equilibrium condition and in the two biased conditions for the model in the light displacement.

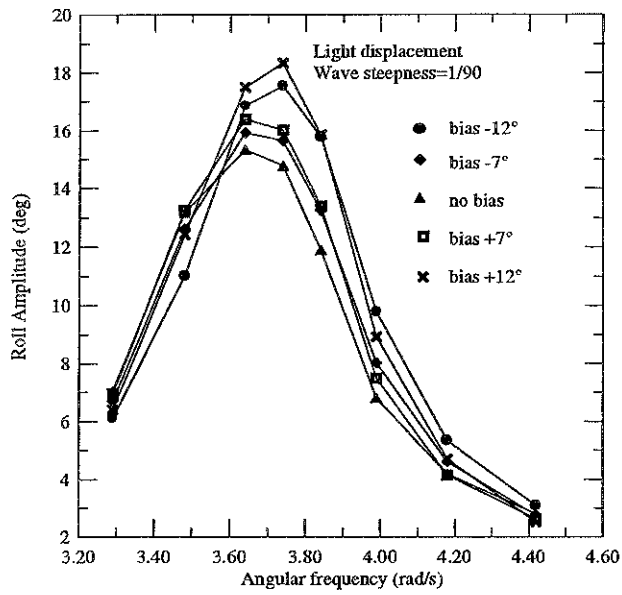


Fig. 4. Stationary roll amplitude in a regular beam sea with wave steepness 1/90

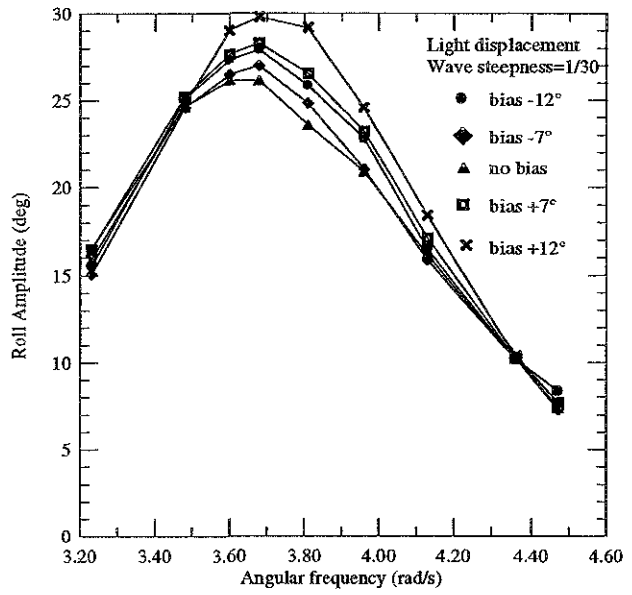


Fig. 6. Stationary roll amplitude in a regular beam sea with wave steepness 1/30

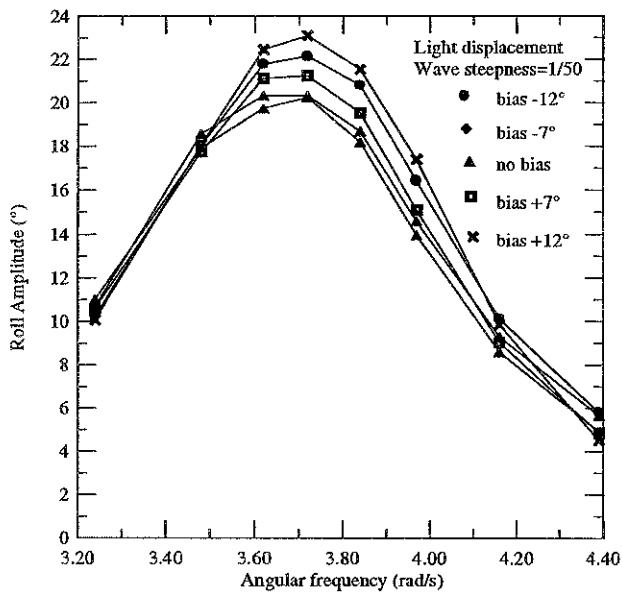


Fig. 5. Stationary roll amplitude in a regular beam sea with wave steepness 1/50

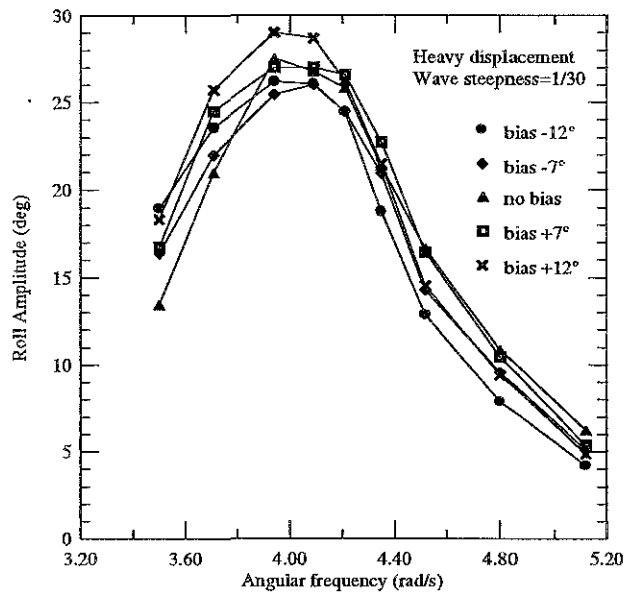


Fig. 7. Stationary roll amplitude in a regular beam sea with wave steepness 1/30

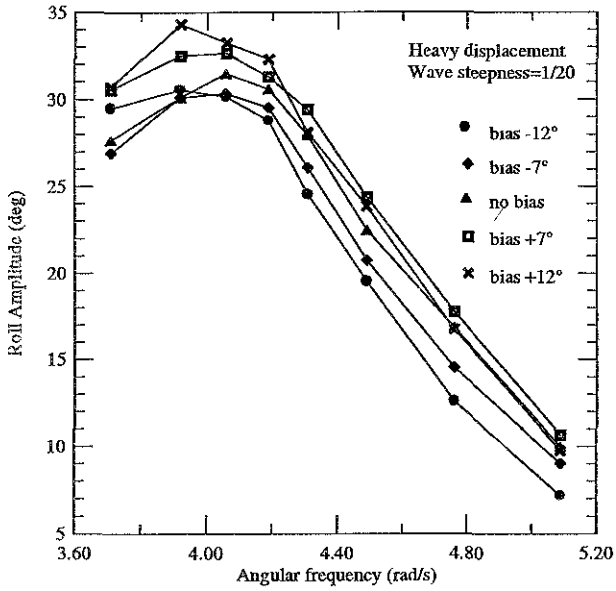


Fig. 8. Stationary roll amplitude in a regular beam sea with wave steepness 1/20

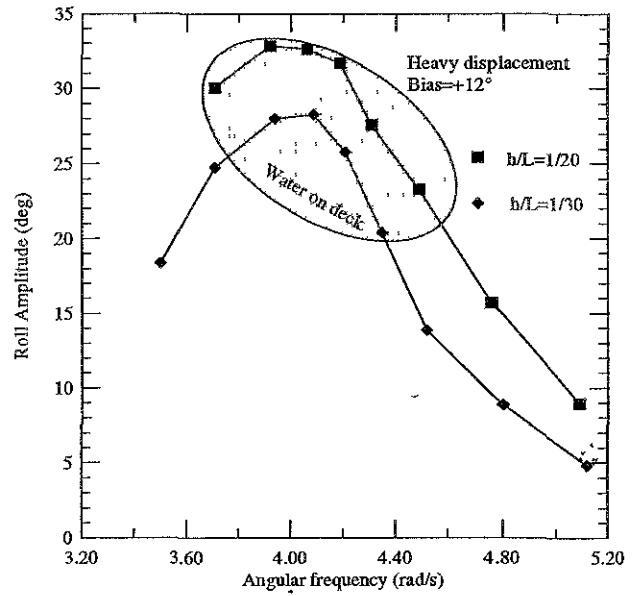


Fig. 10. Water on deck in the bias-into-the-waves condition.

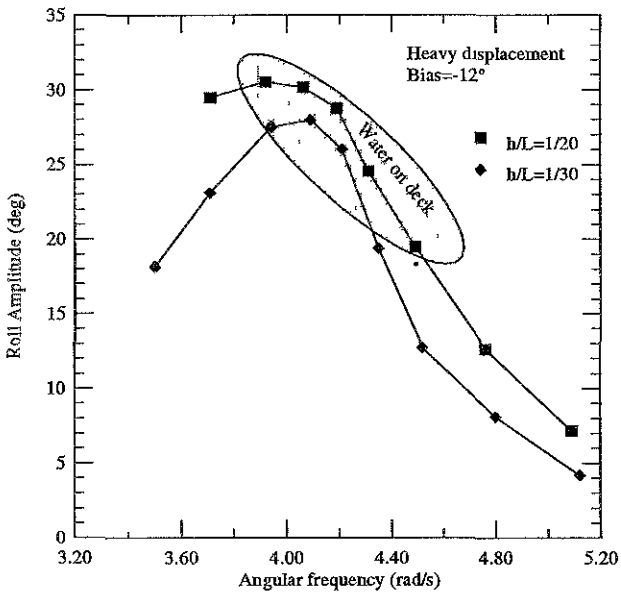


Fig. 9. Water on deck in the leeward bias condition.

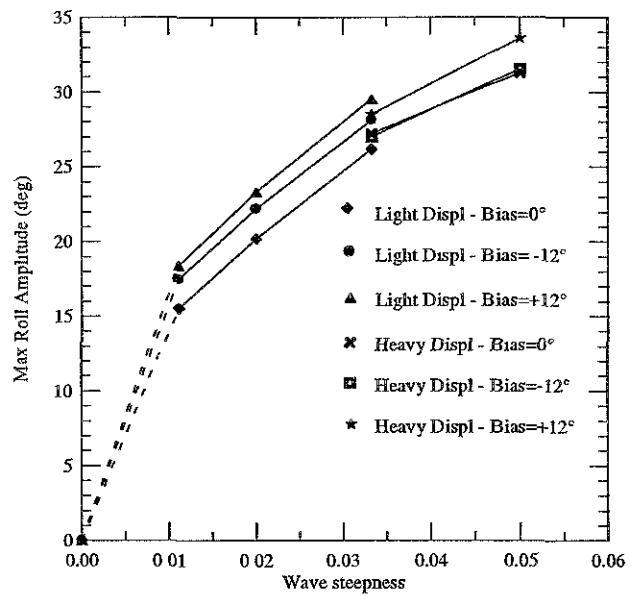


Fig. 11. Maximum roll amplitude vs wave steepness.

**OPERATIONAL STABILITY -  
THE INFLUENCE  
OF ENVIRONMENT**

# LIQUID CARGO AND ITS EFFECT ON SHIP MOTIONS

J.M.J. Journée  
Delft University of Technology

## SUMMARY

When a double bottom tank, a cargo tank or a space in a rolling vessel contains a fluid, gravity waves will appear at the surface of this fluid. These gravity waves will cause exciting roll moments on the vessel. At lower water depths, resonance frequencies can be obtained with high wave amplitudes. A hydraulic jump or bore, which is a strongly non-linear phenomenon, travels periodically back and forth between the walls of the tank. A theory, based on gasdynamics for the shock wave in a gas flow, has been used to describe the motions of the fluid. At higher water depths, the behaviour of the fluid tends to be more linear. Then, a linear potential theory, as used in strip theory ship motions computer programs, is used to describe the motions of the fluid in the tank.

Available experimental data on the behaviour of the fluid in free surface anti-rolling tanks have been used to verify the theoretical approaches for low water depths.

Also, forced roll oscillation tests were carried out with a 2-D model a cargo tank of an LNG carrier for a wide range of filling levels. These experimental data have been used to verify the theoretical results for all water depths.

Finally, a ship model was equipped with liquid cargo tanks and it has been tested

in beam waves at zero forward speed. The measured roll data of the model have been compared with the results strip theory calculations.

It has been concluded that the approaches given in this paper, based on theories developed already in the sixties, can be used to include the effect of non-viscous liquid cargo in ship motions calculations.

## 1 INTRODUCTION

When a tank which contains a fluid with a free surface is forced to carry out roll oscillations, resonance frequencies can be obtained with high wave amplitudes at lower water depths. Under these circumstances a hydraulic jump or bore is formed, which travels periodically back and forth between the walls of the tank. This hydraulic jump can be a strongly non-linear phenomenon. A theory, based on gasdynamics for the shock wave in a gas flow under similar resonance circumstances, as given by Verhagen and van Wijngaarden (1965), has been adapted and used to describe the motions of the fluid. For low and high frequencies and the frequencies near to the natural frequency, different approaches have been used. A calculation routine has been made to connect these regions. Available experimental data on the behaviour of the fluid in free surface anti-rolling tanks, obtained from van den Bosch and Vugts (1966), have

been used to verify this approach. At higher waterdepths, the behaviour of the fluid tends to be more linear. Then, the linear potential theory with the pulsating source method of Frank (1967), as used in strip theory ship motions computer programs, has been used to describe the motions of the fluid in the tank. Forced roll oscillation tests were carried out with a 2-D model of a cargo tank of an LNG carrier, to measure the exciting moments for a wide range of filling levels and frequencies and to compare these with theoretical predictions. Finally, a ship model was equipped with three of these liquid cargo tanks and tested in beam waves at zero forward speed. Several filling levels and two regular wave amplitudes were used to investigate the effect on the roll behaviour of the ship. The measured data have been compared with the results of 2-D potential calculations.

## 2 LIQUID CARGO LOADS

Observe a rectangular tank with a length  $l$  and a breadth  $b$ , which has been filled until a water level  $h$  with a fluid with a mass density  $\rho$ . The distance of the bottom of the tank above the centre of gravity of the vessel is  $s$ . Figure 1 shows a 2-D sketch of this tank with the axis system and notations.

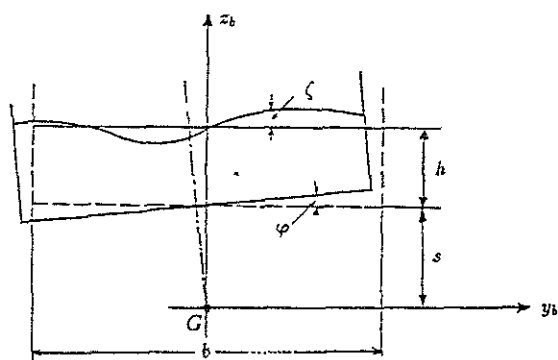


Figure 1: Axis system and notations of an oscillating tank

The natural frequency of the surface waves in a harmonic rolling tank appears as the

wave length  $\lambda$  equals twice the breadth  $b$ , so:  $\lambda_0 = 2b$ .

With the wave number and the dispersion relation:

$$k = \frac{2\pi}{\lambda} \quad \text{and} \quad \omega = \sqrt{kg \tanh(kh)}$$

it follows for the natural frequency of surface waves in the tank:

$$\omega_0 = \sqrt{\frac{\pi g}{b} \tanh\left(\frac{\pi h}{b}\right)}$$

### 2.1 THEORY OF VERHAGEN

Verhagen and van Wijngaarden (1965) have investigated the shallow water wave loads in a rolling rectangular container, with the centre of rotation at the bottom of the container. Their expressions for the internal wave loads are rewritten and modified in this paper to be useful for any arbitrary vertical position of the centre of rotation. For low and high frequencies and the frequencies near to the natural frequency, different approaches have been used. A calculation routine has been made to connect these regions.

#### Low and high frequencies

The harmonic roll motion of the tank is defined by:

$$\phi = \phi_a \sin(\omega t)$$

In the axis-system of figure 1 and after linearisation, the vertical displacement of the tankbottom is described by:

$$z = s + y\phi$$

and after linearisation, the surface elevation of the fluid is described by:

$$z = s + h + \zeta$$

Relative to the bottom of the tank, the linearised surface elevation of the fluid is described by:

$$\xi = h + \zeta - y\phi$$

Using the shallow water theory, the continuity and momentum equations are:

$$\frac{\partial \xi}{\partial t} + v \frac{\partial \xi}{\partial y} + \xi \frac{\partial v}{\partial y} = 0$$

$$\frac{\partial v}{\partial t} + v \frac{\partial v}{\partial y} + g \frac{\partial \xi}{\partial y} + g \phi = 0$$

In these formulations,  $v$  denotes the velocity of the fluid in the  $y$ -direction and the vertical pressure distribution is assumed to be hydrostatic. Therefore, the acceleration in the  $z$ -direction, introduced by the excitation, must be small with respect to the acceleration of gravity  $g$ , so:

$$\phi_a \omega^2 b \ll g$$

The boundary conditions for  $v$  are determined by the velocity produced in the horizontal direction by the excitation. Between the surface of the fluid and the bottom of the tank, the velocity of the fluid  $v$  varies between  $v_s$  and  $v_s / \cosh kh$  with a mean velocity:  $v_s / kh$ . However, in very shallow water  $v$  does not vary between the bottom and the surface. When taking the value at the surface, it is required that:

$$v = -(s+h)\dot{\phi} \quad \text{at: } y = \pm \frac{b}{2}$$

For small values of  $\phi_a$ , the continuity equation and the momentum equation can be given in a linearised form:

$$\frac{\partial \xi}{\partial t} + h \frac{\partial v}{\partial y} = 0$$

$$\frac{\partial v}{\partial t} + g \frac{\partial \xi}{\partial y} + g \phi = 0$$

The solution of the surface elevation  $\xi$  in these equations, satisfying the boundary values for  $v$ , is:

$$\xi = h - \frac{b\omega_0 \left\{ 1 + \frac{(s+h)\omega^2}{g} \right\}}{\pi\omega \cos\left(\frac{\pi\omega}{2\omega_0}\right)} \sin\left(\frac{\pi\omega y}{b\omega_0}\right) \phi$$

Now, the roll moment follows from the quasi-static moment of the mass of the

frozen liquid  $\rho l b h$  and an integration of  $\xi$  over the breadth of the tank:

$$M_\phi = \rho g l b h \left( s + \frac{h}{2} \right) \phi$$

$$+ \rho g l \int_{-b/2}^{+b/2} \xi y dy$$

This delivers the roll moment amplitude for low and high frequencies at small water depths:

$$M_{a_\phi} = \rho g l b h \left( s + \frac{h}{2} \right) \phi_a$$

$$+ \rho g l b^3 \left\{ 1 + \frac{(s+h)\omega^2}{g} \right\} \cdot \left\{ 2 \left( \frac{\omega_0}{\pi\omega} \right)^3 \tan\left(\frac{\pi\omega}{2\omega_0}\right) - \left( \frac{\omega_0}{\pi\omega} \right)^2 \right\} \phi_a$$

For very low frequencies, so for the limit value  $\omega \rightarrow 0$ , this will result into the static moment:

$$M_\phi = \rho g l \left\{ b h \left( s + \frac{h}{2} \right) + \frac{b^3}{12} \right\} \phi$$

The phase lags between the roll moments and the roll motions have not been obtained here. However, they can be set to zero for low frequencies and to  $-\pi$  for high frequencies:

$$\epsilon_{M_\phi \phi} = 0 \quad \text{for: } \omega \ll \omega_0$$

$$\epsilon_{M_\phi \phi} = -\pi \quad \text{for: } \omega \gg \omega_0$$

### Natural frequency region

For frequencies near to the natural frequency  $\omega_0$ , the expression for the surface elevation of the fluid  $\xi$  goes to infinity. Experiments showed the appearance of a hydraulic jump or a bore at these frequencies. Obviously, then the linearised equations are not valid anymore.

Verhagen and van Wijngaarden solved the problem by using the approach in gas dynamics when a column of gas is oscillated at a small amplitude, e.g. by a piston. At frequencies near to the natural frequency at



defined the complex potential at  $z$  of a pulsating point source of unit strength at the point  $\zeta$  in the lower half plane, as given in figure 2.

Take the  $x$ -axis to be coincident with the undisturbed free surface. Let the cross sectional contour  $C_0$  of the submerged portion of the cylinder be in the lower half plane and the  $y$  axis, positive upwards, being the axis of symmetry of  $C_0$ . Select  $N+1$  points  $(\xi_i, \eta_i)$  of  $C_0$  to lie in the fourth quadrant. Connect these  $N+1$  points by successive straight lines. Then,  $N$  straight line segments are obtained which, together with their reflected images in the third quadrant, yield an approximation to the given contour as shown in figure 2.

The coordinates, length and angle associated with the  $j$ -th segment are identified by the subscript  $j$ , whereas the corresponding quantities for the reflected image in the third quadrant are denoted by the subscript  $-j$ , so that by symmetry  $\xi_{-j} = -\xi_j$  and  $\eta_{-j} = -\eta_j$  for  $1 \leq j \leq N+1$ . Potentials and pressures are to be evaluated at the midpoint of each segment and for  $1 \leq i \leq N$  the coordinates of the midpoint of the  $i$ -th segment are:

$$x_i = \frac{\xi_i + \xi_{i+1}}{2} \quad y_i = \frac{\eta_i + \eta_{i+1}}{2}$$

In the translational modes, any point on the cylinder moves with the velocity:

$$\mathbf{v}^{(2)} = -iA^{(2)}\omega \sin \omega t \quad \text{for sway}$$

$$\mathbf{v}^{(3)} = -jA^{(3)}\omega \sin \omega t \quad \text{for heave}$$

The length of the  $i$ -th segment and the angle made by this segment with the positive  $x$ -axis are:

$$s_i = \sqrt{(\xi_{i+1} - \xi_i)^2 + (\eta_{i+1} - \eta_i)^2}$$

$$\alpha_i = \arctan \left\{ \frac{\eta_{i+1} - \eta_i}{\xi_{i+1} - \xi_i} \right\}$$

In here  $\alpha_i$  is defined as:  $-\frac{\pi}{2} \leq \alpha_i \leq +\frac{\pi}{2}$ .

If the denominator is negative, depending on the sign of the nominator  $\pi$  has to be added or subtracted, so that  $\alpha_i$  will be defined as:  $-\pi \leq \alpha_i \leq +\pi$ .

The outgoing unit vector normal to the cross section at the  $i$ -th midpoint  $(x_i, y_i)$  is:

$$\mathbf{n}_i = \mathbf{i} \sin \alpha_i - \mathbf{j} \cos \alpha_i$$

where  $\mathbf{i}$  and  $\mathbf{j}$  are unit vectors in the directions  $x$  and  $y$ , respectively.

The roll motion is illustrated in figure 2 and considering a point  $(x_i, y_i)$  on  $C_0$ , an inspection of this figure yields:

$$R_i = \sqrt{x_i^2 + (y_i - y_0)^2}$$

$$\theta_i = \arctan \left\{ \frac{y_i - y_0}{x_i} \right\}$$

In here  $\theta_i$  is defined as:  $-\frac{\pi}{2} \leq \theta_i \leq +\frac{\pi}{2}$ . If the denominator is negative, depending on the sign of the nominator  $\pi$  has to be added or subtracted, so that  $\theta_i$  will be defined as:  $-\pi \leq \theta_i \leq +\pi$ .

By elementary two-dimensional kinematics, the unit vector in the direction  $\theta$  is:

$$\boldsymbol{\tau}_i = -\mathbf{i} \sin \theta_i + \mathbf{j} \cos \theta_i$$

so that:

$$\mathbf{v}^{(4)} = S^{(4)}\boldsymbol{\tau}_i R_i$$

$$= -\omega A^{(4)} R_i (\mathbf{i} \sin \theta_i - \mathbf{j} \cos \theta_i) \sin \omega t$$

The normal components of the velocity

$$v_i^{(m)} = \mathbf{n}_i \cdot \mathbf{v}^{(m)}$$

at the midpoint of the  $i$ -th segment  $(x_i, y_i)$  are:

$$v_i^{(2)} = -\omega A^{(2)} \sin \alpha_i \sin \omega t$$

$$v_i^{(3)} = +\omega A^{(3)} \cos \alpha_i \sin \omega t$$

$$v_i^{(4)} = +\omega A^{(4)} R_i \cdot$$

$$\cdot (\sin \theta_i \sin \alpha_i + \cos \theta_i \cos \alpha_i) \sin \omega t$$

Defining:

$$n_i^{(m)} = \frac{v_i^{(m)}}{A^{(m)}\omega \sin \omega t}$$

then, consistent with the previously mentioned notation, the direction cosines for the three modes of motion are:

$$n_i^{(2)} = -\sin \alpha_i$$

$$n_i^{(3)} = +\cos \alpha_i$$

$$n_i^{(4)} = +\sin \theta_i \sin \alpha_i + \cos \theta_i \cos \alpha_i$$

A set of two coupled integral equations are applied by Frank at the midpoints of each of the  $N$  segments and is assumed that over an individual segment the complex source strength remains constant, although it varies from segment to segment. Then, the set of coupled integral equations becomes a set of  $2N$  linear algebraic equations in the unknowns.

The hydrodynamic pressure  $p^{(m)}$  along the cylinder is obtained from the velocity potential by means of the linearised equation of Bernoulli, where  $p_a^{(m)}$  and  $p_v^{(m)}$  are the hydrodynamic pressures in phase with the displacement and in phase with the velocity, respectively.

The potential as well as the pressure is a function of the oscillation frequency  $\omega$ . The hydrodynamic force or moment per unit length on the cylinder, necessary to sustain the oscillations, is the integral of  $p^{(m)} \cdot n^{(m)}$  over the submerged contour of the cross section  $C_0$ .

It is assumed that the pressure at the  $i$ -th midpoint is the mean pressure for the  $i$ -th segment, so that the integration reduces to summation, whence:

$$M^{(m)}(\omega) = 2 \sum_{i=1}^N p_a^{(m)}(x_i, y_i, \omega) n_i^{(m)} |s_i|$$

$$N^{(m)}(\omega) = 2 \sum_{i=1}^N p_v^{(m)}(x_i, y_i, \omega) n_i^{(m)} |s_i|$$

for the potential mass and damping forces or moments, respectively.

Frank's method is suitable for the computation of the potential mass and damping of symmetric 2-D shapes, in or below the surface of a fluid. This method has been incorporated in a lot of 2-D ship motions computer codes, all over the world. Starting from the keel point of the cross section, the input data of the off sets have to be read in an upwards order. Then, the (outward) normal on the elements of the cross section will be defined to be positive in the direction of the fluid outside the cross section.

Easily, this method can be used to calculate the linear loads due to a potential fluid in an oscillating symmetrical tank too. Starting from the intersection of the free surface with the tank wall, the offsets of the tank have to be read in a downwards order, so in an opposite direction as has to be done for the cross sections of a ship. When doing this, the (inward) normal on the elements of the cross section of the tank will be defined to be positive in the direction of the fluid in the tank. Then, the calculated potential mass and damping delivers the in and out phase parts of the loads due to the moving liquid in the tank.

With this, the in and out phase parts of the 2-D excitation forces and moments about the origin in the water surface of the fluid in a rectangular tank are found with:

$$X_{2c} = \omega^2 M^{(2)} x_{2a}$$

$$X_{2s} = -\omega N^{(2)} x_{2a}$$

$$X_{3c} = \omega^2 M^{(3)} x_{3a}$$

$$X_{3s} = -\omega N^{(3)} x_{3a}$$

$$X_{4c} = \omega^2 M^{(4)} x_{4a}$$

$$+ \rho g \left\{ bh \left( s + \frac{h}{2} \right) + \frac{b^3}{12} \right\} x_{4a}$$

$$X_{4s} = -\omega N^{(4)} x_{4a}$$

This very simple approach can be carried out easily with many existing 2-D, but also 3-D, ship motions computer programs.

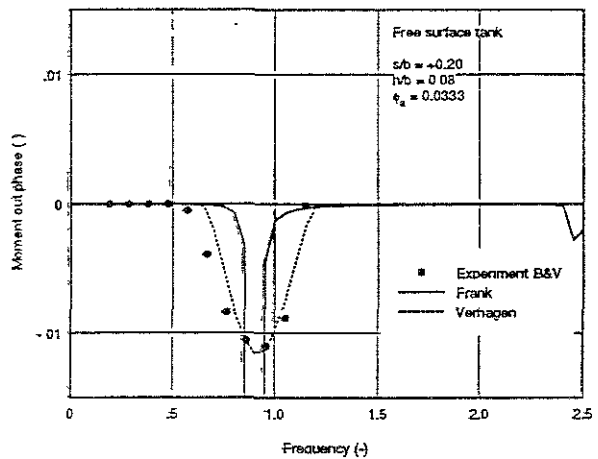
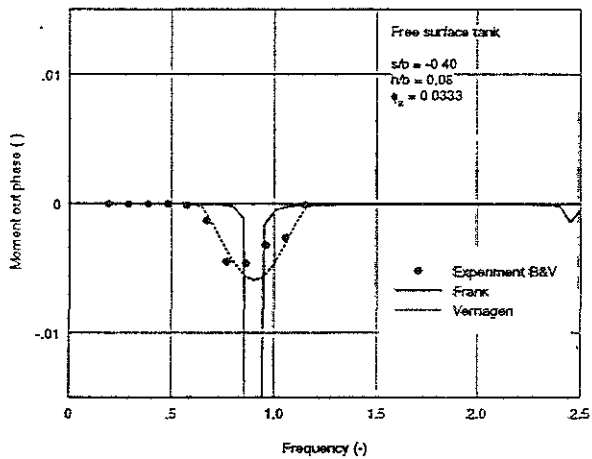
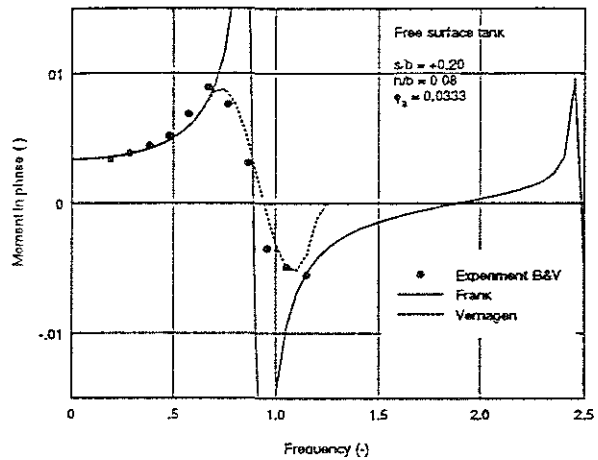
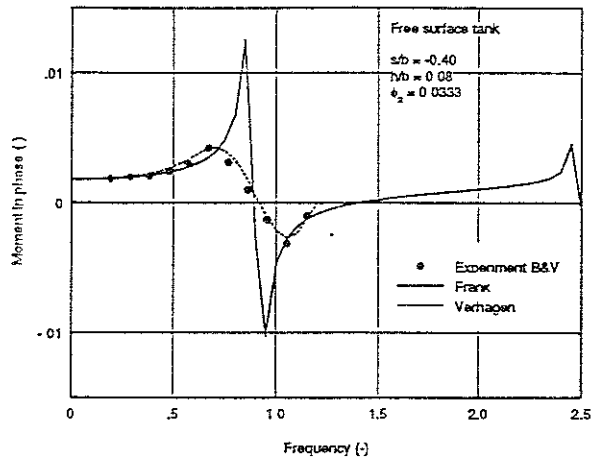


Figure 3: In and out phase moments of a free surface anti-rolling tank (Tank bottom below  $G$ )

Figure 4: In and out phase moments of a free surface anti-rolling tank (Tank bottom above  $G$ )

However, one should keep in mind that in the calculation routine of Frank, the angles  $\alpha$ ; and  $\theta$ ; have to be defined well in all four quadrants.

### 2.3 VERIFICATIONS

Three different validations were performed to verify the validity of using Frank's pulsating source method for obtaining the moments caused by the motions of liquids in oscillating tanks.

Firstly, results of extensive model experiments on rectangular free surface anti-rolling tanks, carried out in the past by van den Bosch and Vugts (1966), have been used.

Figure 3 and 4 show a few comparisons between calculated and measured in and out phase parts of the first harmonic of the roll moments for very small water depths in the tank.

The comparisons are given here for one filling level ( $h/b = 0.08$ ) and one roll amplitude ( $\phi_\alpha = 0.0333$  rad). Two positions of the bottom with respect to the rotation point, i.e. the centre of gravity  $G$  of the vessel, have been taken: 40 per cent of the tank width below the axis of rotation ( $s/b = -0.40$ ) and 20 per cent above it ( $s/b = +0.20$ ). The roll moment has been made non-dimensional by dividing this moment through  $\rho g l b^3$ . The non-dimensional frequency parameter has been obtained by di-

viding the frequency through  $\sqrt{g/b}$ . Outside the natural frequency area, the figure shows a good agreement between Frank's method and the experiments. But, for frequencies close to the natural frequency, a very poor prediction has been found. Because of the appearance of a hydraulic jump or a bore at these frequencies, the linearised equations are not valid anymore. The calculated phase lags between the roll moments and the roll motions have a step of 180 degrees at the natural frequency, while the calculated roll moment amplitudes go to infinity. Because of a distinction between frequencies close to the natural frequency and frequencies far from it, the shallow water method of Verhagen and van Wijngaarden shows a good prediction at all frequencies.

Secondly, forced roll oscillation experiments have been carried out with a 2-D model of a cargo tank of an LNG carrier. A sketch of this 1:25 model of the tank is given in figure 5.

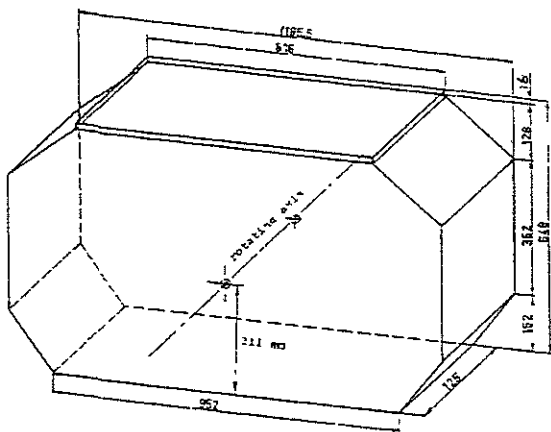


Figure 5: 1:25 model of an LNG tank

At filling levels of 15, 45, 70, 90, 97.5 and 100 per cent of the depth of the tank, the exciting roll moments have been measured for a range of oscillation frequencies and one roll amplitude ( $\phi_a = 0.10$  rad) of the tank. Because of the shape of this tank, a strong non-linear behaviour was expected at the lowest and highest free surface levels.

Figures 6a and 6b show the measured and predicted in and out phase parts of the first harmonic of the roll moments of the LNG tank as a function of the frequency. The roll moment has been made non-dimensional by dividing this moment through  $\rho g l b^3$ . The non-dimensional frequency parameter has been obtained by dividing the frequency through  $\sqrt{g/b}$ .

Except at the natural frequency of the fluid in the tank, a fairly good prediction has been found with Frank's method.

Again, the shallow water method of Verhagen and van Wijngaarden gives a good prediction for all frequencies at the lowest filling level of the tank.

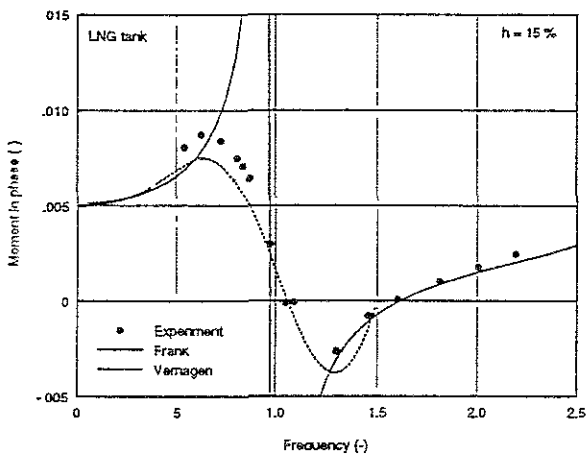
Thirdly, a fully filled rectangular tank has been observed.

It is obvious that the ratio between the effective and the solidified mass for sway or heave of the fluid in fully filled tanks is 1.0. The ratio between the effective and the solidified moments of inertia for roll of the fluid in a fully filled rectangular tank as a function of the aspect ratio  $h/b$  of the tank was given by Graham and Rodrigues and published later by Silverman and Abramson (1966) as:

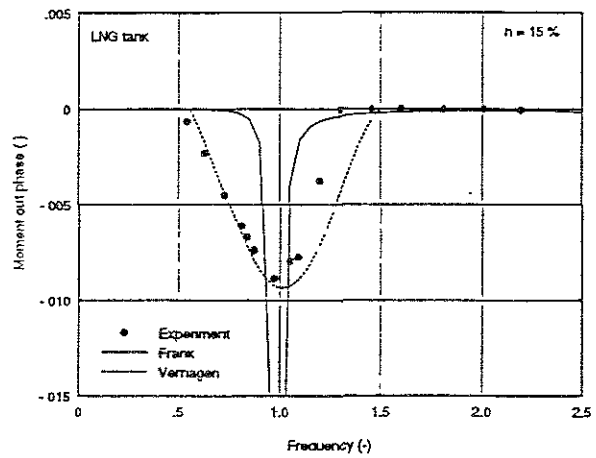
$$c_e = 1 - \frac{4}{1 + \frac{h^2}{b^2}} + \frac{768}{\frac{\pi^5 h}{b} \left(1 + \frac{h^2}{b^2}\right)} \cdot \sum_{n=0}^{\infty} \frac{\tanh \left[ (2n+1) \frac{\pi h}{2b} \right]}{(2n+1)^5}$$

This expression had been obtained from results of space vehicle studies carried out by NASA. The contributions of frequencies higher than the first order are very small and can be neglected.

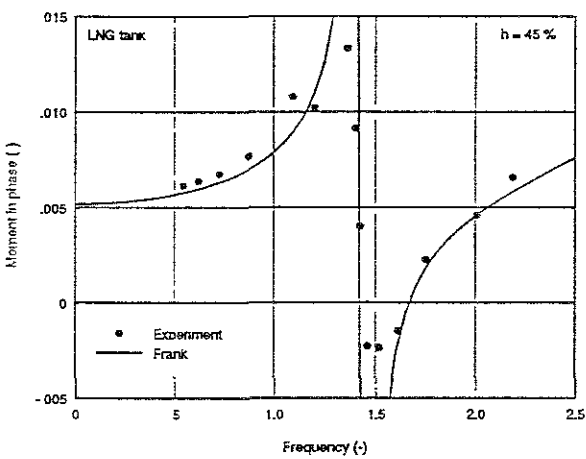
Calculations have been performed with the 2-D computer code SEAWAY of Journée (1996), which includes Frank's pulsating source method. Also, 3-D calculations have been carried out with the DELFRAC computer code of Pinkster (1996). The results are given in figure 7.



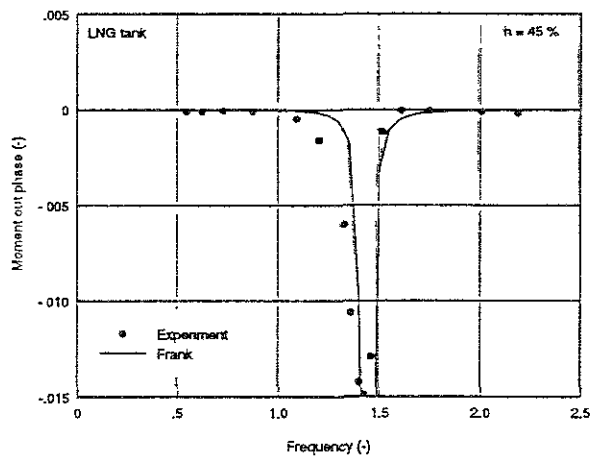
Filling level: 15 %



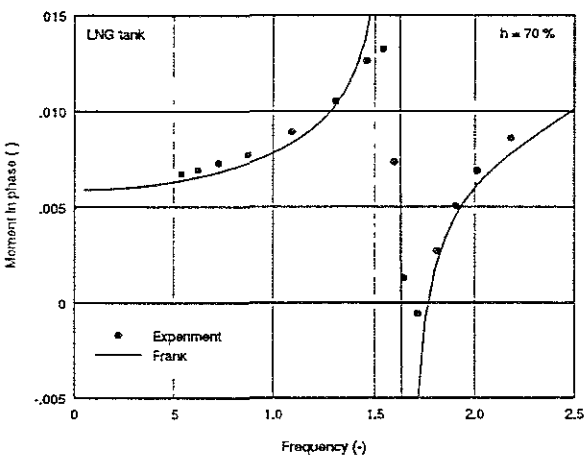
Filling level: 15 %



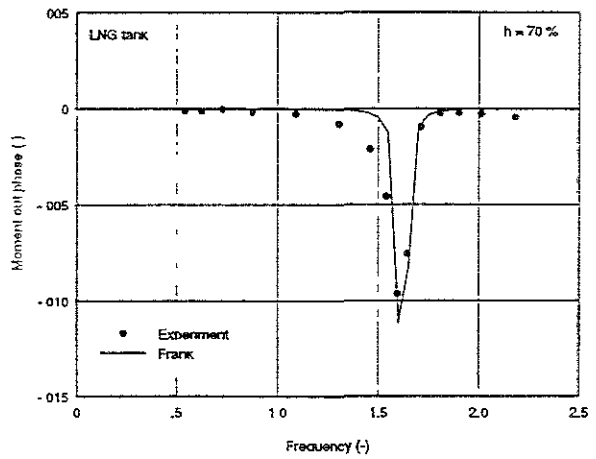
Filling level: 45 %



Filling level: 45 %

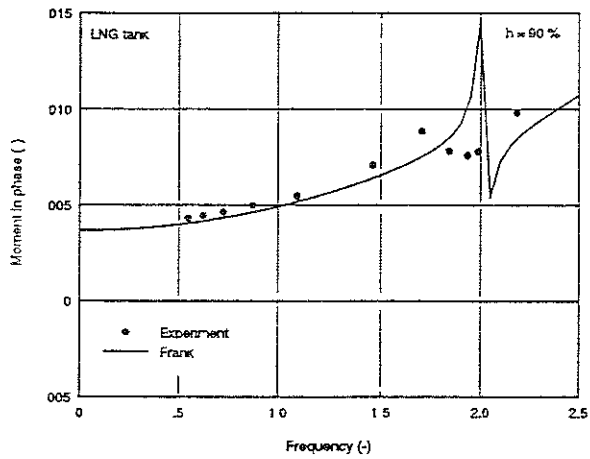


Filling level: 70 %

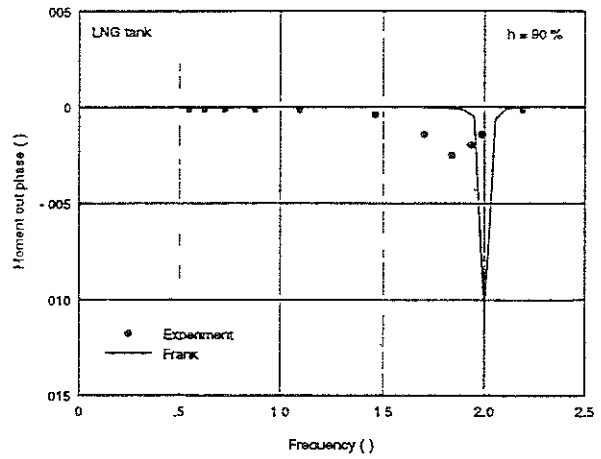


Filling level: 70 %

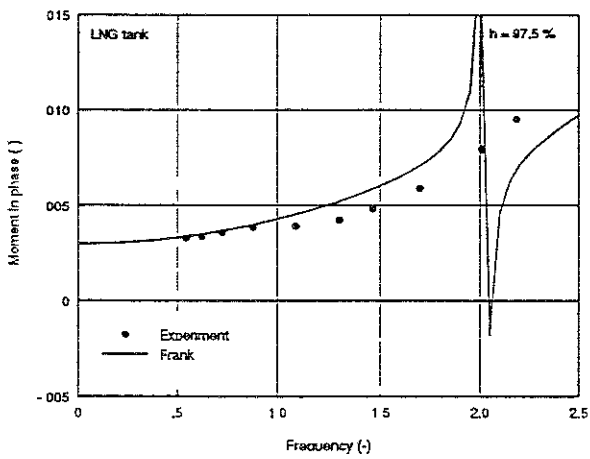
Figure 6a: In phase and out phase moments of an LNG tank



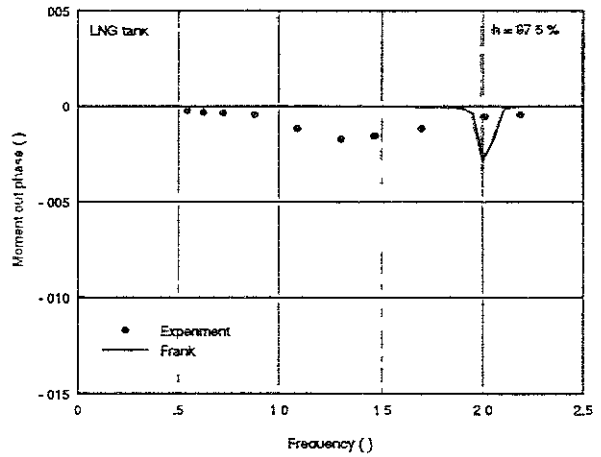
Filling level: 90 %



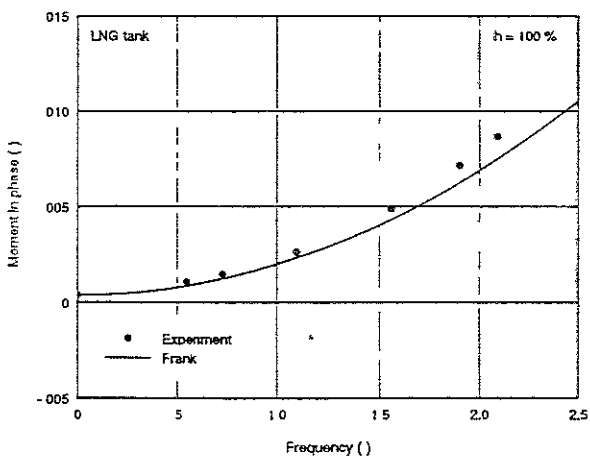
Filling level: 90 %



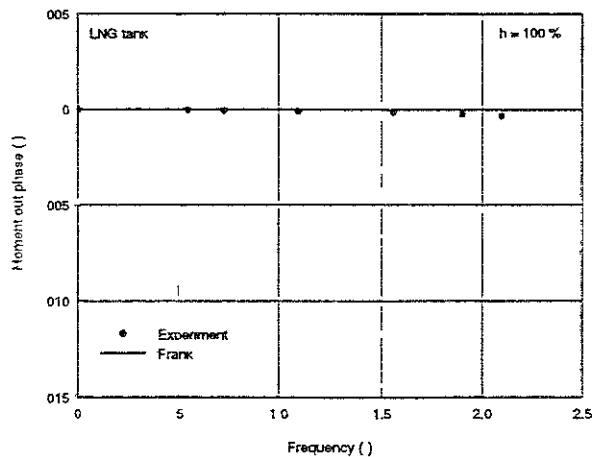
Filling level: 97.5 %



Filling level: 97.5 %



Filling level: 100 %



Filling level: 100 %

Figure 6b: In phase and out phase moments of an LNG tank

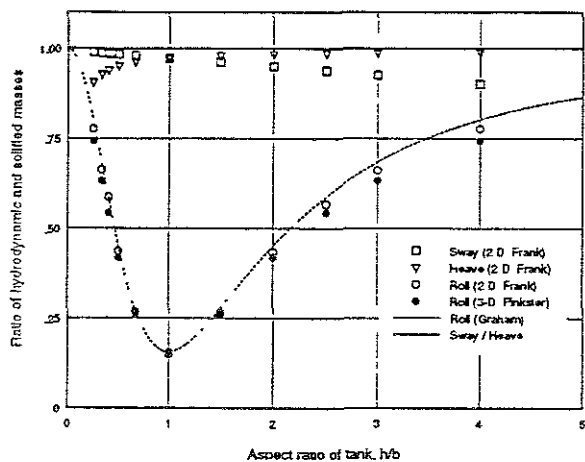


Figure 7: Ratio  $c_e$  between effective and solidified moment of inertia of fully filled rectangular tanks

Figure 7 shows a fairly good agreement between these results. For small and large aspect ratios deviations can be expected, caused by the limited number of 16 line elements in SEAWAY or 30 panels in DELFRAC on the contour of half the cross section of the tank.

### 3 SHIP MOTIONS

To investigate the effect of free surface (liquid cargo) tanks on the roll motions of a ship, three tanks as given in figure 5 were build in a 1:60 model of an LNG carrier. The body plan of this vessel is given in figure 8.

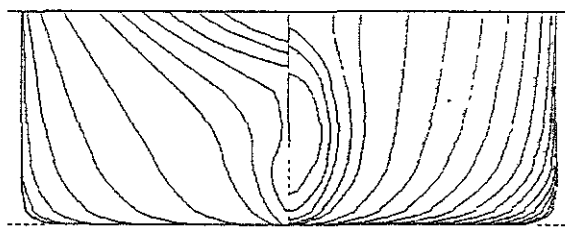


Figure 8: Body plan of LNG carrier

Static heel tests and roll decay tests in still water and roll motion measurements in regular beam waves with two different wave amplitudes were performed at zero

forward ship speed. These tests were carried out in Towing Tank I of the Ship Hydromechanics Laboratory of the Delft University of Technology with a length of 142 metre, a breadth of 4.22 metre and a water depth of 2.50 metre. The model was placed transversal in the towing tank at half the length of the tank and the spacing between the model and the tank walls was about 0.70 metre. The model was free to move in 6 degrees of freedom and the roll damping waves could propagate over a long distance before they were reflected to the model by the tank-ends.

The main dimensions of the ship are given in table 1.

LNG carrier			
Length bpp	$L_{pp}$	m	164.00
Breadth	$B$	m	32.24
Draught	$d$	m	12.60
Trim	$t$	m	0.00
Volume	$\nabla$	$m^3$	51680
Block coefficient	$C_B$	-	0.776
Length of bilge keels	$l_{bk}$	m	69.70
Height of bilge keels	$h_{bk}$	m	0.30
Gyradius for yaw	$k_{zz}$	m	45.43

Table 1: Main dimensions of ship

The length of each of the three cargo tanks was 13.45 metre and the distance of the bottom of the tanks above the ship's base line was 2.00 metre.

With the exception of these midship cargo tanks 3, 5 and 7, all other cargo tanks are supposed to be filled up to 97.5 per cent of the inner tank height with a stowage factor of 1.00  $ton/m^3$ . This was simulated in the experiments by solid ballast weights and an adaption of the radius of inertia for roll of the ship.

For the cargo tanks 3, 5 and 7 three loading conditions have been chosen:

- Condition I: frozen liquids (45-45-45%)  
The three cargo tanks are equally filled up to 45 % of the inner tank height

with homogeneous frozen liquid cargo with a stowage factor of 1.00 ton/m<sup>3</sup>, simulated by solid ballast weights.

- Condition II: liquids (45-45-45%)  
This condition is similar to condition I after unfreezing the liquid cargo, so the three tanks are partially filled with water.
- Condition III: liquids (45-70-15%)  
This condition is similar to condition II, but the filling levels of the three tanks are 45 %, 70 % and 15 %, respectively.

The results of the static heel angle tests and the roll decay tests are given in table 2.

Condition		I	II	III
$\nabla$	m <sup>3</sup>	51680	51680	51360
$KG$	m	10.48	10.42	10.60
$GM$	m	2.75	2.81	2.62
$GG'$	m	0.00	1.69	1.59
$k_{xx}$	m	10.14	9.38	9.49
$T_{\phi}$ -meas.	s	13.70	21.30	23.00
$T_{\phi}$ -calc.	s		21.18	22.82

Table 2: Loading conditions of the ship

The measured non-dimensional roll damping coefficients  $\kappa$  are presented in figures 9, 10 and 11.

These data have been compared with predicted values obtained with the semi-empirical method of Ikeda.

For condition I, with frozen liquid cargo, a very good agreement has been found.

For conditions II and III, with liquid cargo, the predicted roll damping coefficients are somewhat underestimated at smaller roll angle amplitudes. But at larger roll angle amplitudes, which are of interest in more dangerous circumstances, the figure shows a fairly good agreement.

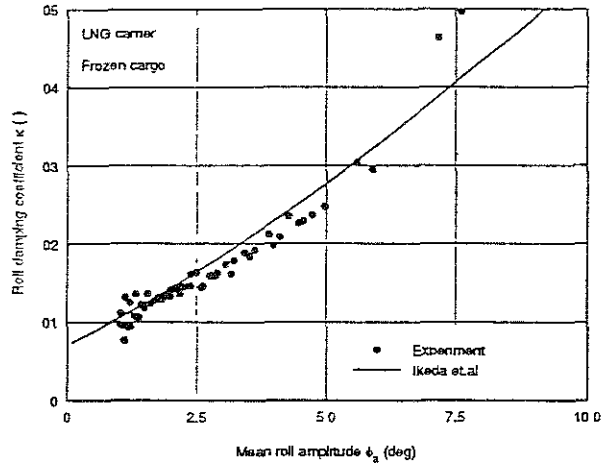


Figure 9: Roll damping coefficients (Condition I)

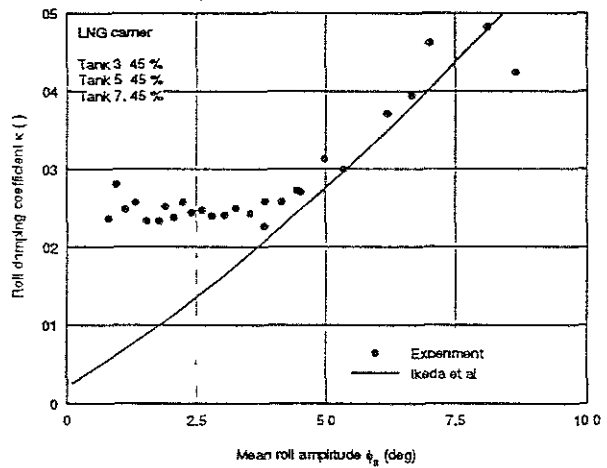


Figure 10: Roll damping coefficients (Condition II)

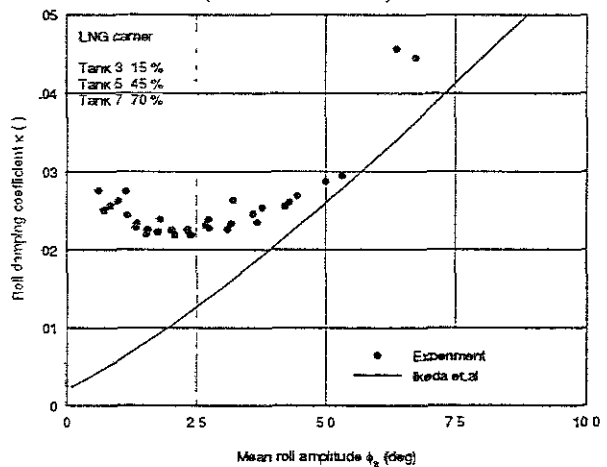


Figure 11: Roll damping coefficients (Condition III)

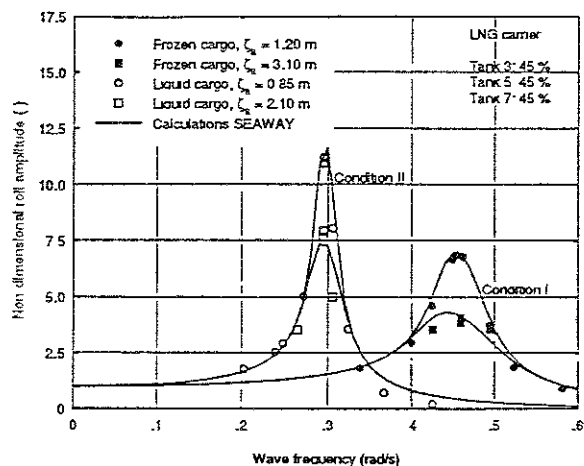


Figure 12: Roll motions of an LNG carrier (Conditions I and II)

Figures 12 and 13 show a comparison of the measured and predicted roll amplitudes at two different wave amplitudes for each loading condition.

For loading condition I, the non-potential roll damping has been obtained by the method of Ikeda. The radius of inertia for roll of the ship's mass has been obtained from the measured natural roll period of 13.7 seconds and calculated hydromechanic coefficients. The figure shows a good agreement between experiments and predictions.

For the loading conditions II and III, the non-potential roll damping has been obtained by the method of Ikeda et. al. (1978) too. The radius of inertia for roll of the ship's mass has been obtained from the radius of inertia of the ship with the frozen liquid cargo of condition I and a theoretical correction for unfreezing this cargo. The deviating volume of liquid cargo in condition III has been accounted for too. The exciting roll moments due to the liquid cargo have been obtained with Frank's method.

So, for the loading conditions II and III, the roll motions have been calculated without using any experimental data of these loading conditions. Table 2 shows a very good agreement between the predicted and the measured natural roll frequencies; the deviation is less than 1%. Nevertheless

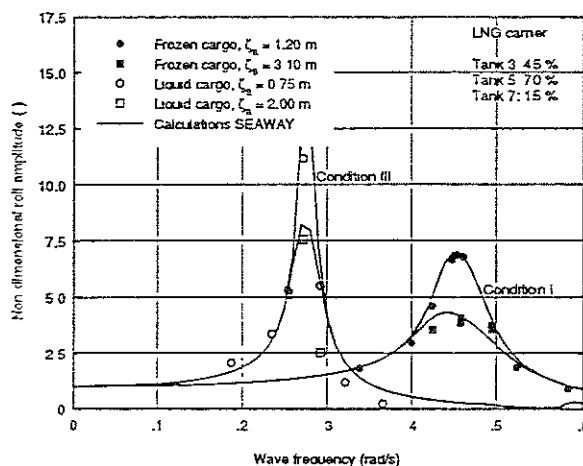


Figure 13: Roll motions of an LNG carrier (Conditions I and III)

some overestimation at higher frequencies, figures 12 and 13 show a very good agreement between the predicted and the measured response amplitude operators for roll. However, it may be noted that for the loading conditions II and III, the natural roll frequency of the ship is about half the lowest natural frequency of the fluid in the three cargo tanks. When these frequencies are close to each other, non-linear effects caused by the bore or the hydraulic jump at the surface of the fluid in the tanks will play a much more important role.

#### 4 CONCLUSIONS

From the calculations and the experiments, the following conclusions can be drawn:

1. At very low filling levels of the tank, the method of Verhagen and van Wijngaarden predicts the exciting roll moments fairly good. Because this theory is given for shallow water only, the method fails for higher filling levels.
2. With the exception of frequencies near to the natural frequency of the fluid in the tank, the potential theory of Frank predicts the exciting roll moments fairly good for all filling levels of the tank.

3. An addition of these roll moments in the right hand side of the equation of motions of the ship, results in good predictions of the roll motions of the ship.
4. The non-linear roll damping of the ship plays an important role in these roll motions. Linearisation results in a good prediction of the harmonic roll motions.

The pulsating source method of Frank, as included in many strip theory ship motions computer programs, can be used easily to include the effect of non-viscous liquid cargo in ship motion calculations. Also, 3-D calculation techniques for calculating potential mass and damping of ships can be used for this purpose.

## 5 REFERENCES

- Bosch, J.J. van den and Vugts, J.H. (1966), Roll Damping by Free Surface Tanks, Report No. 83-S, 1966, NSRC-TNO, Delft, The Netherlands.
- Frank, W. (1967), Oscillation of Cylinders in or below the Free Surface of Deep Fluids, Report No. 2375, October 1967, NSRDC, Washington D.C., U.S.A.
- Ikeda, Y., Himeno, Y. and Tanaka, N. (1978), A Prediction Method for Ship Rolling, Report No. 00405, December 1978, Department of Naval Architecture, University of Osaka Prefecture, Japan.
- Journée, J.M.J. (1996), The Behaviour of Ships in a Seaway, ISBN 90-370-0142-4, Report No. 1049, May 1996, Ship Hydromechanics Laboratory, Delft University of Technology, The Netherlands.
- Pinkster, J.A. (1996), Hydrodynamic Aspects of Floating Offshore Structures, ISBN 90-370-0154-8, Report No. 1050,

May 1996, Ship Hydromechanics Laboratory, Delft University of Technology, The Netherlands.

- Silverman, S. and Abramson, H. (1966), The Dynamic Behavior of Liquids in Moving Containers, Edited by H.N. Abramson, Chapter 2: Lateral Sloshing in Moving Containers, Report No. NASA SP-106, 1966, Scientific and Technical Information Division, National Aeronautics and Space Administration, Washington D.C., USA.
- Verhagen, J.H.G. and van Wijngaarden, L. (1965), Non-linear Oscillations of Fluid in a Container, Journal of Fluid Mechanics, 1965, Volume 22, Part 4, Pages 737-751.

## HEELING AND CAPSIZING OF SMALLER VESSEL WHILE GREEN WATER SHIPPING IN FOLLOWING WAVE

Vladimir V. Yarisov

Doctor of Naval Architect Department, Kaliningrad State Technical University  
of Russian Federal Fishery Committee, 1 Sovietsky avenue, Kaliningrad 236000, Russia  
tel (0112) 46-52-25, fax (0112) 27-36-04

### ABSTRACT

The main reasons and features of failures of smaller vessels because of stability loss in green water shipping conditions of a deck in following and quartering waves are determined in the paper

Influence on stability of separate architectural and constructive elements and parameters of static stability of a typical smaller fishing vessel has been determined during its movement in following and quartering waves in green water shipping conditions of a deck from the stern. Qualitative and quantitative evaluation of this influence have been made

The research of rolling and stability has allowed to develop mathematical model of behaviour of a vessel in following and quartering waves in green water shipping conditions of a deck and to identify its parameters, as well as to take into account the dominant factors of the process of dangerous heeling

On the basis of theoretical and experimental researches a simple physical approach has been developed. On the basis of that approach a practical technique of determination of critical rise of the centre of gravity of a vessel has been realized and verified experimentally. Stability criteria have been singled out

### NOMENCLATURE

L - length of a vessel between perpendiculars,  
B - width of vessel along the current waterline,  
D - height of board,  
d - draft,  
 $\Delta$  - weight displacement,  
 $\delta$  - coefficient of general fullness,  
 $\alpha$  - coefficient of waterline fullness,  
 $\beta$  - coefficient of middle-frame fullness,  
 $\chi$  - coefficient of vertical fullness,  
 $\varphi$  - coefficient of longitudinal fullness,  
f - height of freeboard,  
 $h_f$  - height of bulwark,  
 $S_{wl}$  - area of upper deck,  
 $S_w$  - given area of deck well,  
 $\alpha_x$  - relative coefficient of deck well ( $S_{wl}/S_w$ ),  
 $t_r$  - time of complete removal of water from the upper deck,  
A - total area of storm scuppers (per one board),  
 $\mu$  - coefficient of permeability of upper deck,  
z - distance from initial level of water in deck well up to the level of top edge of scupper,  
 $f_m(\varepsilon, Fr, h_w/\lambda_w)$  - average level of water in deck well of a vessel depending on a course angle of a vessel in relation to dispersion of water, Froude number and steepness of water,  
 $z_g$  - elevation of the gravity centre of a vessel above the basic plane,  
 $h_o$  - initial metacenter height,

$l(\theta)$  - arms of the initial diagram of static stability,

$l_{\max}$  - maximum of arm of static stability,

$\theta_{\max}$  - angle of maximum of the diagram of static stability,

$\theta_v$  - angle of rolling lap of the diagram of static stability,

$\overline{l(\theta)}$  - average value of arm of static stability on a wave,

$\Delta l(\theta)$  - amplitude value of periodic part of arm of static stability on a wave,

$\theta_f$  - angle of immersing of the edge of bulwark into the water,

$\varepsilon$  - course angle of a vessel in relation to the dispersion of water measured from the stern part of diametrical plane of a vessel clockwise,

$Fr$  - Froude number,

$h_w$  - height of a wave,

$\lambda_w$  - length of a wave,

$\varphi_0$  - initial phase of water,

$\sigma_k$  - apparent frequency of water,

$\tau_k$  - apparent period of a wave,

$\theta$  - angle of onboard roll,

$\dot{\theta}$  - speed of onboard roll.

$\ddot{\theta}$  - acceleration of onboard roll,

$I_x$  - moment of inertia of a vessel in relation to longitudinal central axis,

$M_R(\theta, t, \varepsilon)$  - restoring moment,

$M_{IN}(\theta)$  - moment of hydrodynamical forces of inertia,

$M_D(\dot{\theta})$  - moment of resistance forces,

$Q^*(\theta, t, \varepsilon)$  - main part of the perturbing moment caused by water,

$M_w(\theta, t, \varepsilon)$  - heeling moment caused by the water in deck well,

$l_w$  - arm of the heeling moment caused by the water in deck well,

$\mu_{\theta\theta}$  - joined moment of inertia,

$W$  - coefficient of resistance,

$W_Q$  - relative coefficient of resistance,

$\alpha_{mo}$  - effective angle of wave slope,

$n$  - number of a period when the water floods the upper deck,

$m$  - number of periods for which the flood water flows down from the upper deck

## INTRODUCTION

The necessity of taking into account the flood of a deck in following wave was marked in works of V V Garkavy, I K Boroday, S Grokholovskiy, T Chishia, K Kavashima, N Takaisha, M Kan, N Umeda and other researchers

Flood of a deck by sea water and its accumulation on the upper deck is widely recognized as danger for stability of a vessel. Especially it is important for smaller vessels.

Therefore, purpose of the present paper was development (and experimental test) of technique of estimation of vessels stability in conditions of flood of a deck in following wave, and also estimation of influence of upperworks architecture features of smaller vessels on stability at the movement in following wave in conditions of flood of a deck.

## THEORETICAL AND EXPERIMENTAL RESEARCHES

According to the collected and analysed by the author results of capsizing statistics [1] of fishing and cargo vessels depending on the cause of failure, course angle of a vessel, it is possible to assert that the significant part of vessels (more than 30%), which were lost because of capsizing, is for smaller vessels accepted plenties of sea water on a deck in following wave or at course angles close to following, where the precondition of dangerous heeling and capsizing is periodic decrease of stability in the following wave and the heeling moment caused by the water flooded a deck of a vessel from stern. These facts were confirmed by experimental way [2,3].

According to the results of emergency statistics the data on types of vessels (in Fig 1 are given architectural and constructive types of the vessels which had failures), geometrical characteristics of cases, stability, speed of a course, height of freeboard, bulwark and deck well are analysed.

$$\begin{aligned}
L &= 16.9 \dots 40 \text{ m}; & L/B &= 2.82 \dots 5.19; \\
L/D &= 6.01 \dots 10.2; & B/D &= 1.73 \dots 2.50; \\
B/d &= 2.04 \dots 4.00; & D/d &= 1.14 \dots 1.64; \\
\alpha &= 0.715 \dots 0.86; & \beta &= 0.640 \dots 0.70; \\
\delta &= 0.474 \dots 0.91; & z_g/D &= 0.79 \dots 0.935; \\
h_o &= 0.400 \dots 0.818; & h_o/B &= 0.072 \dots 0.156; \\
l_{\max} &= 0.114 \dots 0.316; & \theta_{\max} &= 19.0 \dots 30.6^\circ, \\
\theta_v &= 42.8 \dots 70.6^\circ; & Fr &= 0.078 \dots 0.340; \\
h_f &= 0.50 \dots 1.1; & h_f/B &= 0.10 \dots 0.14;
\end{aligned} \tag{1}$$

$$\begin{cases}
\frac{f}{B} \leq 0.143 + \frac{h_f}{2B}, 0 \leq \frac{h_f}{B} \leq 0.065 \\
\frac{f}{B} \leq 0.199 - 0.55 \frac{h_f}{B}, 0.065 \leq \frac{h_f}{B} \leq 0.100 \\
\frac{f}{B} \leq 0.244 - \frac{h_f}{B}, 0.100 \leq \frac{h_f}{B} \leq 0.300
\end{cases}$$

$$\alpha_k = 0.030L - 0.450$$

Here it would be necessary to note, that about 40% of the vessels which had failures, met the requirements for stability of the Russian Sea Register of Navigation.

Subject to research in the present paper were smaller vessels, with limited distance from shelter port, with length up to 40 m, with relatively large deck well, having stern part of a deck not protected by poop and other stern superstructures, and also continuous bulwark with the characteristics (1).

The basic assumptions at solving of the given tasks are the following:

- being examined the stability of an intact vessel, i.e. the opportunity of flood of internal premises during failure is not taken into account;

- vessel is controlled; arising at heeling developing moments are compensated by handling of a rudder; the course of a vessel is kept constant;

- being examined onboard roll of a smaller vessel in following and sidelong wave to the system of free incoming waves; the liquid, surrounding a vessel, is considered ideal, heavy, incompressible, having unlimited depth; the amplitudes of incoming waves are considered relatively small;

- influence of diffraction component of the perturbing moment is neglected, as the

mode being examined shows itself essentially on long in relation to a vessel waves, when diffraction component of the perturbing moment is small in relation to the main one;

In the Fig.2 the used system of coordinates is given.

At the movement in following and sidelong following wave the vessel will have periodic change of stability characteristics. It is considered that the waves with length close to the length of a vessel are most dangerous. As more often direction of wind coincides with general direction of waves run, and angular fluctuation of wind are small, the wind heeling moment was not taken into account, but the heeling moment caused by water on a deck of a vessel from stern was taken into account [1], (in Fig.3. the scheme for determination of the heeling moment caused by water in deck well is given). At the movement in following and sidelong following wave is characteristic sporadic flood of deck well with large amounts of sea water (this is testified by eloquent descriptions of failures). After passing such wave the vessel with filled by water partially or entirely deck well makes dynamic inclination because of action of the heeling moment created by this water as by liquid load accepted on the upper deck. Flood of the upper deck occurs when the crest of a wave is on stern perpendicular of a vessel, the heeling moment arising under such circumstances practically does not change (this is shown by the data given in Fig.4 on calculation of time of water outflow from deck well) and appears to be close to capsizing, during movement the vessel appears to be in adverse phase in relation to water, i.e. at the top of a wave, and this circumstance results in capsizing.

On the basis of the analysis of the moments of forces acting on a vessel in following and sidelong following wave in conditions of flood of a deck [2] the mathematical model of onboard roll with assumptions about neglect of influence of keel vertical roll, and also about an invariance of an angle of course which is applicable to courses

initial small crosswise impulse which corresponds to the small initial angle of heeling  $\theta(0) = \theta_0$ ,  $\dot{\theta}(0) = \dot{\theta}_0$ . In a certain period of time after application of initial external force the system comes to the steady mode  $\theta_0 \approx \theta_{st}$  and further they are already considered as initial conditions. The results of the analysis allowed to watch laws of change of amplitude of onboard fluctuations and to establish the dependence of its maximum value from the perturbing moment caused by water on a deck. The worst in relation to stability in conditions of flood of a deck of a vessel in following water is the case when  $\theta(0) = \theta_{st} = 13... 18^\circ$ ,  $\dot{\theta}(0) = 0$ , (Froude numbers in this case accordingly are: 0.05... 0.23), that this initial condition corresponds to the influence of external heeling moment caused by water on a deck at situation of stern perpendicular of a vessel on a crest of a wave. With the growth of course angle the amplitude of onboard roll is insignificantly increased. The account of irregularity of water as a rule results in higher values of minimal arms of stability for the worst situation of a vessel on profile of a regular wave of the same length and height. The consideration of the characteristics of attachment and stability of a vessel on profile of regular, not deformed wave provides some reserve of stability, i.e. for real conditions of navigation results in error to the safe side.

For improvement and estimation of adequacy of mathematical model of behaviour of a vessel, and also for study of influence of upper works architecture, there was in a proper way planned physical experiment which consisted in the following:

- determination of water level in deck well depending on load, speed of movement of model, course angle and parameters of water;
- experimental check of the founded theoretical results;
- determination of frequency of capsizing of model of a vessel with various upper works architecture in strong collapsing water;

- estimation of influence of applicate size of gravity centre of a vessel on safety of navigation in conditions of abrupt and collapsing following water;

- study of influence of bulwark installation in stern of a vessel ("stern gate") on flood ability of model at its movement in following water.

As object of experiment was chosen smaller shrimping trawler MKTM "Batella" B 275 with typical contours.

The basic variant of the developed self-propelled model was made in scale 1:15 (in Table 1 and 2 the basic geometrical characteristics of model are given, in Table 2 are also the characteristics of stability of model), for realization of necessary measurements the complete set of John & Railhofer equipment was used, as well as gauges specially developed for it).

The basic and additional series of models (in Fig.5 are presented architectural and constructive types of models of vessels). The series of models of vessels A, B, C, D was developed in such way that one variant of a vessel differs from any other only by one architectural and constructive element. Architectural and constructive variants of vessels A, B, C, D in certain degree cover the basic types of smaller vessels which are in use nowadays.

In Fig.6 the effective moments during realization of tests are presented.

The tests have shown the following:

- that the installation of bulwark in stern reduces (approximately by 15%, 17%) the flood ability of a model;

- the change of speed, course angle and characteristics of water influences on flood ability of a deck rather strongly, for the approximate quantitative estimations it is necessary to use experimental dependence found on the basis of results of experiments on above trawler in a range of Froude numbers from 0 till 0.15, steepness of water from 1/11 up to 1/15 and course angles of water  $\varepsilon$  from 0 up to 25 degrees,  $\alpha_k = 0.35... 0.50$ ,  $f/B = 0.08$ ,  $h_f/B = 0.14... 0.10$ ;

deviating from strictly following not more than for 25° was created.

The moment of heeling caused by water in deck well according to the scheme given in Fig.3 can be put down as:

$$M_w = P_w l_w = P_w [(Y_B - Y_F) \cos \theta + \dots + (Z_B - Z_F) \sin \theta], \quad (2)$$

For determination of the heeling moment caused by water on a deck it is possible to take advantage of the approach developed by V.V.Garkavy [4], thus having specified level of water in deck well depending on a course angle, speed of vessel's movement and characteristics of water.

The heeling moment caused by water on a deck is presented as empirical dependence:

$$M_w(\theta, t, \varepsilon) = \dots \begin{cases} D l_w(t, Fr, h_w / \lambda_w) \sin \frac{\pi}{\theta_f} \theta, & -\theta_f < \theta < \theta_f \\ 0, & |\theta_f| \geq \theta \end{cases}, \quad (3)$$

where the arm of the heeling moment caused by sea water on a deck is found from the following expression:

$$l_w(t, Fr, h_w / \lambda_w) = 0.21 \alpha_k \frac{B}{T} \frac{1}{\chi} F(t, Fr, h_w / \lambda_w), \quad (4)$$

The function which is taking into account discharge of water after flood of a deck looks like a kind of empirical dependence:

$$F(t, Fr, h_w / \lambda_w) = f_m(Fr, h_w / \lambda_w) \varphi(t) e^{-\frac{307}{\tau_k}(t - n\tau_k)}, \quad (5)$$

$$\varphi(t) = \begin{cases} 0, & 0 < t < n\tau_k \\ 1, & n\tau_k < t < (n+m)\tau_k \end{cases}, \quad (6)$$

$$m\tau_k > t_r, \quad (7)$$

$$t_r = \frac{S_w}{A\mu} \sqrt{\frac{z}{2g}}, \quad (8)$$

For the moment of damp forces is used square-law approximation at in discrete steps varied coefficient of resistance:

$$M_D(\dot{\theta}) = -W \dot{\theta}^2 \text{sign} \dot{\theta}, \quad (9)$$

$$\text{where } W = kW_Q, \quad (10)$$

$k = 1$ , if the board of a vessel has not come into water ( $|\theta| < \theta_f$ );  $k = 2$ , if the board of a vessel has come into water ( $\theta \geq \theta_f$ ) and both the signs of acceleration and speed of onboard roll coincide;  $k = 4$ , if the board of a vessel has come into water and both signs of acceleration and speed of onboard roll do not coincide. The values of coefficients are determined experimentally by V.V.Garkavy [4] and are confirmed by the results of our physical experiment [3].

The restoring moment is presented by harmonic function according to the method of Y.I.Nechaev [5]:

$$M_R(\theta, t, \varepsilon) = -\Delta [\overline{l(\theta)} + \Delta l(\theta) \cos(\sigma_k t - \varphi_0)], \quad (11)$$

The main part of the perturbing moment caused by waves is presented by dependence:

$$Q^*(\theta, t, \varepsilon) = \Delta^* l(\theta) \alpha_{m0} \sin \sigma_k t, \quad (12)$$

The mathematical model of onboard roll of a vessel in sidelong following regular water in conditions of episodic flood of a deck from stern with length of a wave equal to the length of a vessel, with use of dependences (2-12) will be presented by the differential equation:

$$(I_x + \mu_{\theta\theta}) \ddot{\theta} - M_D(\dot{\theta}) - M_R(\theta, t, \varepsilon) = Q^*(\theta, t, \varepsilon) + \dots + M_w(\theta, t, \varepsilon), \quad (13)$$

In a range of relatively low frequencies distinctive for tasks of the theory of the ship, the adequacy to discrete model is revealed with use of numerical methods of integration of initial continuous model (in the differential form) only in case when accuracy of the mentioned numerical methods is not below fourth order (for example, method of RK-4 order).

Initial conditions, when time = 0, are the following: it is considered that in the initial moment of time to the system is applied the

$$f_m(Fr, h_w/\lambda_w) = [0.10Fr - 2.10Fr^2 + 0.756] * \dots \\ \dots * [13.2(h_w/\lambda_w) - 0.10], \quad (14)$$

- at impact on a vessel of a collapsing following wave - most safe is the vessel "D" - a smooth deck vessel with forecastle (the forecastle is up to the 7th theoretical frame), without bulwark, and "B" - a smooth deck vessel with forecastle (the forecastle is up to the 4th theoretical frame), without bulwark. The installation of bulwark on the main deck of a vessel (variants "A" and "C") results in sharp increase of probability of capsizing (in Table 3 the results of experimental research in collapsing following water are presented).

- the mathematical model without account of keel and pitch fluctuations, which uses rather strong schematization of nonlinear effects at flood of deck well, gives satisfactory numerical results and is suitable for the approximate quantitative estimations;

In Fig.7 the curves of experimental records in absolute coordinates of onboard roll and calculated curves found for mathematical model of behaviour of a vessel in following and sidelong following water in conditions of flood of a deck with the same characteristics as for physical model are shown in comparison. From comparison we can see that the calculated data deviate from experimental data to the side of some overestimate of roll amplitudes. This deviation can be explained by influence of longitudinal roll, and also by difference of real values of decrement coefficient and joined moment of inertia from accepted in account (especially after coming of a deck into water);

- the amplitudes of onboard roll turn out to be insignificant, about 10 - 13° for following water and is a little bit higher or of the order for sidelong following water;

- the tests have confirmed the possibility of parametrical resonance of onboard fluctuations occurrence in sidelong following water;

- the capsizing of model in irregular water occurs after some fluctuations at impact of group of high waves of approximately

identical intensity, that is batches of waves close to regular;

- the tests have shown that stability of smaller fishing vessels which meets the Requirements of the Russian Sea Register of Navigation does not guarantee safety of navigation in following wave in conditions of flood of a deck from stern,

## BASIC RESULTS

On the basis of the carried out theoretical and experimental researches the practical technique of determination of the critical diagram of stability was developed, where, against the traditional schemes, in a case of flood of a deck the amplitude roll is not calculated, but the work of the heeling moment caused by water in deck well and the restoring moment are compared at situation of a vessel on the top of a following wave with an assumption of static character of inclination of a vessel and flow of water (as it is offered by Tsutomu Tshichiya [6,7,8], N.N.Rakhmanin [9,10,11], V.V.Garkavy [4]). In this case free surface of the liquid is supposed to be rectilinear (flat).

For a regular wave with the length equal to the length of a vessel ( $\lambda_w = L$ ), with steepness  $h_w / \lambda_w = 1/11$ , by the results of systematic tests of Y.I.Nechaev [5] we determine addition of arm static stability at the top of a wave ( $|\Delta l_w|$ ) depending on angle of roll, width of a vessel, parameters of the form  $L/B$ ,  $B/d$ ,  $D/d$ , Froude number ( $Fr = 0$ ) and course angles ( $\epsilon = 0$ ).

The ordinates of the calculated diagram of stability for situation of a vessel on the top of a following wave are determined by the following expression:

$$l_r(\theta) = l(\theta) - |\Delta l_w(\theta)|, \quad (15)$$

In Fig.8 the scheme for determination of critical elevation of the applicate of gravity centre of a vessel is presented.

The critical position of applicate of gravity centre of a vessel is determined from condition of equality of the areas "a" and "b" (condition of equality of works of the restoring

and heeling moments). By the method of consecutive approximation we achieve the equality of the areas "a" and "b" and find the required diagram of static stability. The value of applicator of gravity centre of a vessel in examined situation will be critical.

The offered technique of determination of critical elevation of applicator of gravity centre of a vessel has recommended itself during experimental check (about this testifies the experimental material presented in Fig.9) and can be recommended for practical application in case when the steepness of water does not exceed 1/11. The generalization of technique in case of water of any steepness does not have principle difficulties.

The basic practical conclusions and recommendations for increase of safety of navigation of the above smaller vessels, found in the paper, consist in the following.

- bulwark, which forms deck well, is a dangerous construction, the installation of bulwark of the required height in the area of long deck well is inadmissible. It is necessary to apply a bulwark of detachable design, variable in length, or to replace it with life line or mesh protection. Storm scupperes of the sizes required by standards are of small effect while flood of a deck.

- water-proof superstructures which are symmetric in relation to diametrical plane of medium length essentially increase safety of navigation in examined situation.

## GRAPHIC MATERIAL

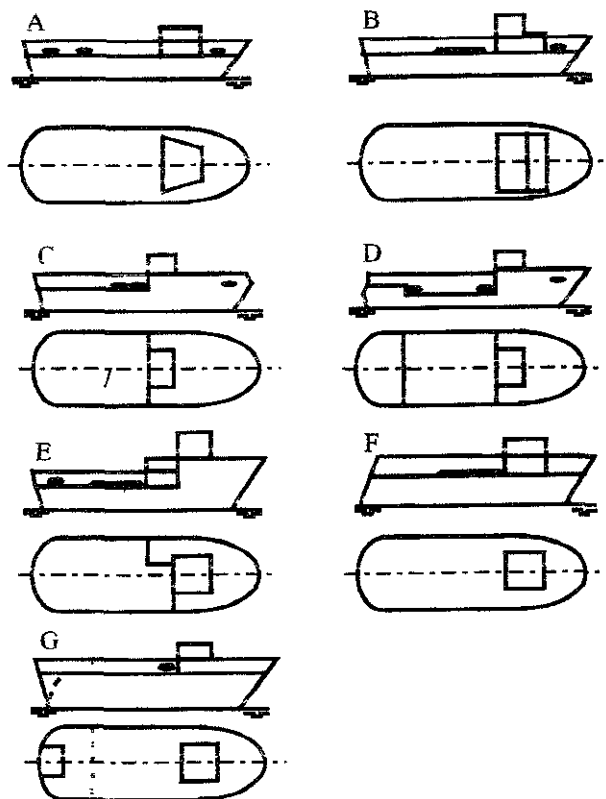


Fig.1. Architectural and constructive types of vessels which had failures.

- A - smooth deck vessel with one-stepped cabin in nose,
- B - smooth deck vessel with raised cabin in the middle part,
- C - one-decker with forecastle and cabin in the middle part;
- D - one-decker with forecastle and quarter-deck, with a cabin of the second step in nose;
- E - one-decker with forecastle transforming into cabin of the left board, and with a cabin of the second step,
- F - two-decker with one-stepped cabin;
- G - shelter-deck vessel opened from stern and with the closed shipping deck.

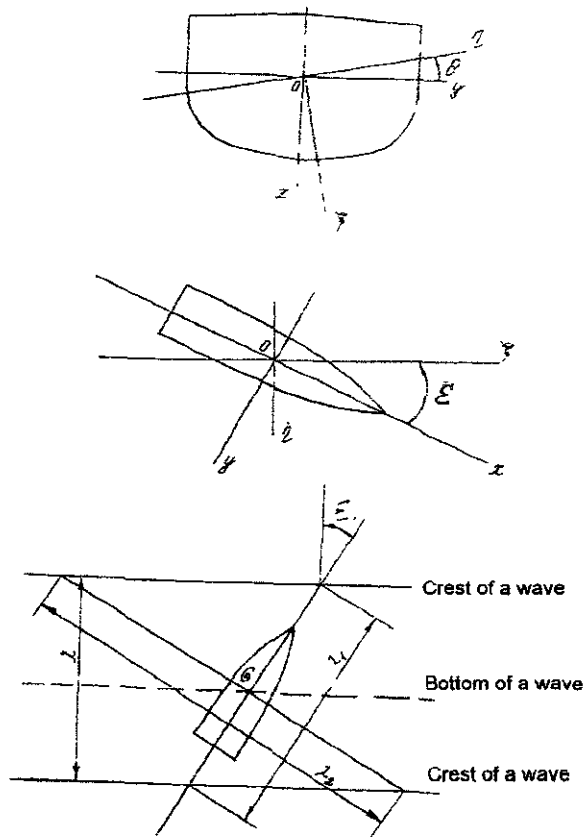


Fig.2. Used system of coordinates.

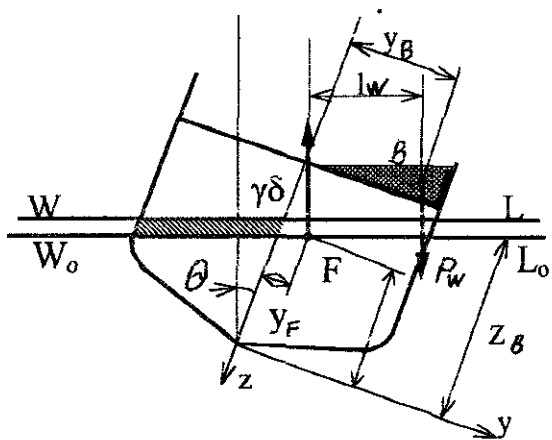


Fig.3. Scheme for determination of the heeling moment caused by water in deck well of a vessel

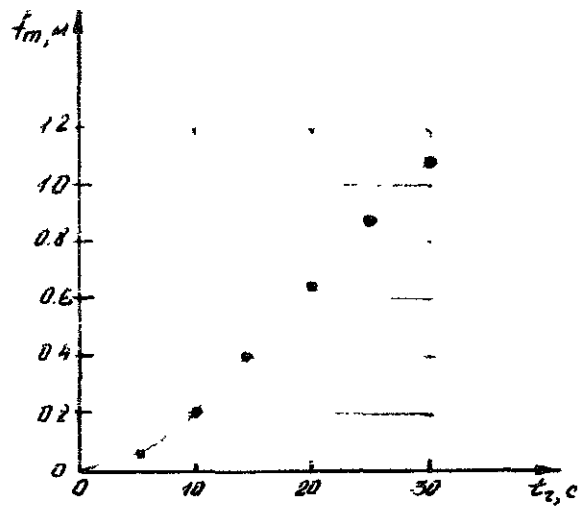


Fig.4. Dependence of water outflow time from deck well through storm scupperes of vessel MKTM "Batella"

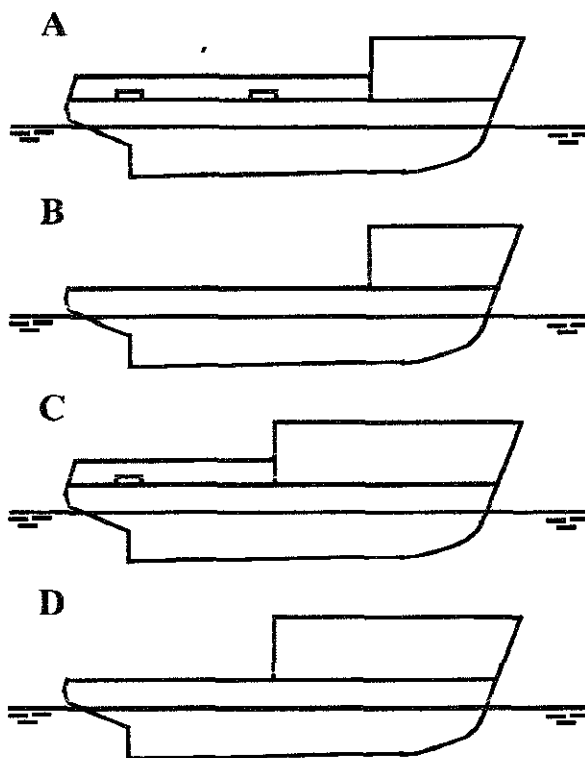


Fig.5. Architectural and constructive types of models of vessels

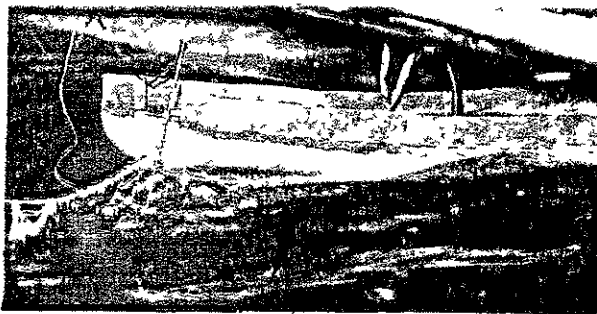
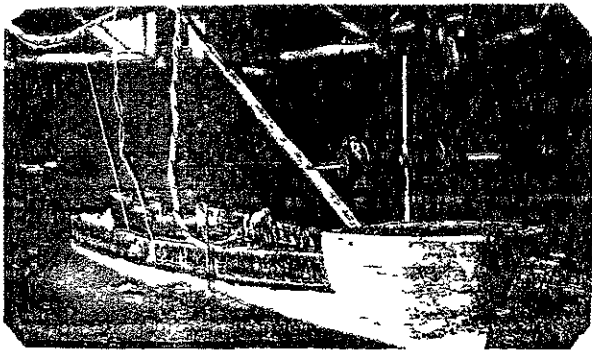


Fig 6. Effective moments during realization of tests

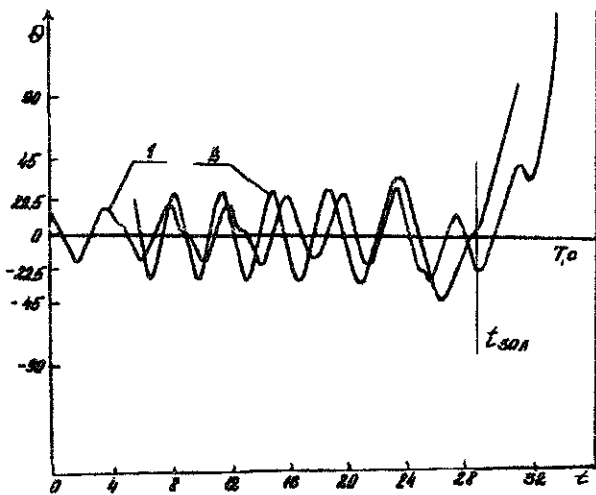


Fig.7. Comparison of results of account and experiment (model-variant "A", II variant of stability,  $\varepsilon=0^0$ ,  $V \approx 0.25$  m/s,  $\lambda_w \approx 2.1$  m,  $h_w \approx 0.24$  m,  $t_{30\%}$ - the moment of time when the water floods the upper deck) The curves under number "1" represent experimental record, and the curves under number "2" - calculated.

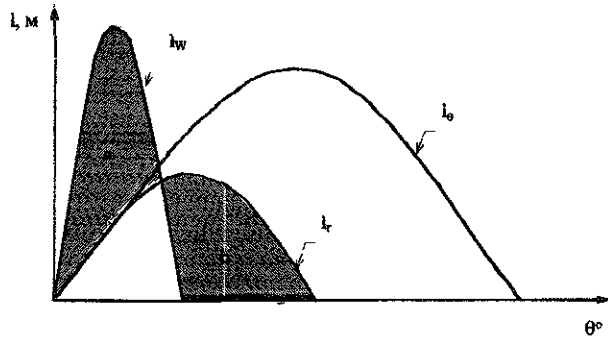


Fig.8. Scheme for determination of critical elevation of the applicate of gravity centre of a vessel

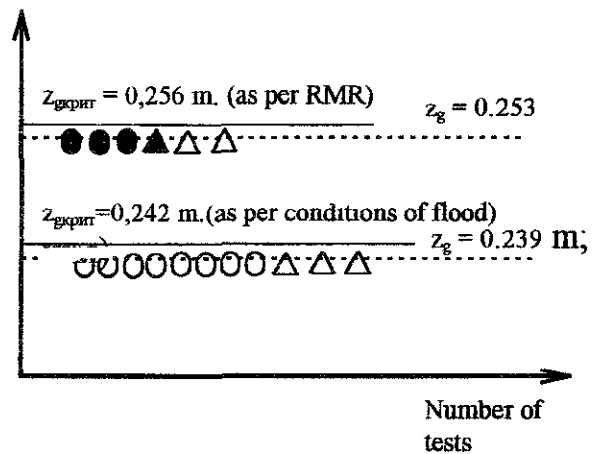


Fig.9 Experimental check of the offered criterion of stability

MTKM «Batella» (Variant A),  $D = 108$  kg,  $z_g^I = 0.239$  m,  $z_g^{II} = 0.253$  m,

○ - Results related to the tests in following regular water ( $h_w/\lambda_w \approx 1/11 \div 1/12$ ,  $F_r = 0 \dots 0.15$ ,  $\varepsilon = 0 \dots 25^0$ ),

△ - Results related to the tests in following irregular water ( $\tau_{cp} = 2.01$  c,  $h_{3\%} = 0.21$  m,  $F_r = 0 \dots 0.15$ ,  $\varepsilon = 0^0$ )

TABLES

Table 1

Designation	Unit of measure	Real vessel	Model
L	m	26	1.733
B	m	8	0.538 3
d	m	3.26	0.237
d <sub>n</sub>	m	2.79	0.186
d <sub>x</sub>	m	3.71	0.247
D	m	3.90	0.260
α		0.778	0.778
β		0.800	0.800
χ		0.707	0.707
δ		0.560	0.560
Δ	t	379.0	0.108

Table 2

	$\bar{z}_g = z_g/D$	$h_0/B$	$l_{max}/B$	$\theta_{max}$	$\theta_c$
I	0.919	0.077	0.054	51	76
II	1.020	0.033	0.031	50	65

Table 3

Type of a vessel (variant of load)	General number of tests, N	Number of capsizing n	Frequency of capsizing %
A(I)	34	23	67.6
A(II)	32	32	100
B(I)	32	3	9.4



Profile of a collapsing wave at the moment of impact on a vessel.

(Height along forward slope  $h^I \approx 450$  mm (7 m for a mock-up vessel), along back slope  $h^{II} \approx 630$  mm (9.3 m))

REFERENCES

1. Ярисов В.В. Анализ аварий рыболовных судов от потери остойчивости в условиях заливания палубы. // Проектирование и нормирование мореходных качеств судов: Труды КТИРПХ, 1994, -с. 114-130. (Russia)
2. Ярисов В.В. Исследование остойчивости, качки и заливаемости судов на попутном волнении в условиях заливания палубы с помощью математического и физического экспериментов. // Проектирование и нормирование мореходных качеств судов. Труды КТИРПХ, 1994, - с.130-144.
3. Ярисов В.В. Исследование качки и остойчивости рыболовных судов на попутном волнении в условиях заливания палубы с кормы. Отчет о НИР/КТИРПХ, руководитель В.В.Гарькавый. 91-51.1.1, - Калининград, 1992, - 274 с
4. Гарькавый В.В. Разработка теоретико-экспериментальных способов оценки остойчивости судов снабжения морских буровых установок и уточнение влияния воды в трубах на остойчивость. Отчет о НИР / КТИРПХ , руководитель Н.Б.Севастьянов. - 80 - 2.2.9 , N ГР 55580505. - Калининград, 1982. - 186 с. (Russia)
5. Нечаев Ю.И. Моделирование остойчивости на волнении. Ленинград: Судостроение, 1989, - 238 с. (Russia)
6. Approximate Calculation of the Loss of Stability Caused by Deck Water at Calm Sea, Fishing Boat Laboratory, Tokyo, Japan, March, 1961.
7. Tshuchiya T. Theoretical approach for the Stability Criterion of Fishing Boats. Technical Report of Fishing Boat, vol.25 , serial 57, Tokyo, Japan, March, 1971.
8. Tshuchiya T., Minory A., Yasuyuki Ya. Study on the transverse stability and freeboard of Coastal fishing boat Fishing Boat Laboratory, vol.27, serial N 61-62, Tokyo, Japan, March, 1974.
9. Rakhmanin N.N. On the definition of the concept of "Low-built vessel". IMO, STAB/INF.54, 29, March, 1971.

10. Рахманин Н.Н. О динамической устойчивости судов с водой на палубе// Доклад науч.-техн. конф. по теории корабля, вып.73. Ленинград: Судостроение, 1966, с.211-217. (Russia)

11. Рахманин Н.Н. Приближенная оценка безопасности плавания низкобортного судна при залипании палубы забортовой водой в условиях волнения: В сборнике: Мореходность и управляемость судов, вып. 105, Ленинград, 1968. (Russia)

# PROBABILISTIC QUALITIES OF SEVERE SHIP MOTIONS

V.L. Belenky

National Research Institute of Fisheries Engineering,  
Ebidai, Hasaki, Kashima, Ibaraki, 314-04, Japan

A.B. Degtyarev and A.V. Boukhanovsky

Institute for High- Performance Computing and Data Bases.  
PO. Box 71, St.Petersburg, 194291 Russia

## ABSTRACT

The paper is devoted to probabilistic characteristics of nonlinear ship response to irregular seas. The authors examined nonlinear stochastic rolling in vicinity of principal resonance and found that probabilistic characteristics calculated by different realisations are substantially different. The physical reason of this phenomenon is fold bifurcation or jumps between high and low energy levels of roll response in vicinity of principal resonance. Practical calculation of nonlinear irregular rolling with regard to this phenomenon is considered.

## NOMENCLATURE

$\alpha_3$  nonlinear coefficient in GZ approximation  
 $m_2$  nonlinear coefficient in roll excitation  
 $h_{3\%}$  wave height of 3% probability of exceeding  
 $F_a$  wind excitation force  
 $F_w$  wave excitation force  
 $I_x$  transversal inertia moment  
 $K_\phi$  correlation function of rolling  
 $k$  wave number  
 $M_a$  wind excitation moment  
 $M_w$  wave excitation moment  
 $M_R$  restoring moment  
 $M$  ship mass  
 $M_{22}$  added mass 22  
 $M_{24}$  added mass 24

$M_{44}$  added mass 44  
 $O(\varepsilon)$  neglected terms  
 $P$  impulse stochastic process  
 $S_\alpha$  roll excitation spectral density  
 $S_\zeta$  3D wave heights spectral density  
 $V$  Variance / Variance operator  
 $W$  Width of confidence band  
 $u = k \sin \chi$  parameter of 3D wave spectrum  
 $v = k \cos \chi$  parameter of 3D wave spectrum  
 $y$  relative horizontal movement of ship's center of gravity  
 $\alpha_m$  effective angle of wave slope  
 $\varepsilon$  bookkeeping / small parameter  
 $\gamma$  phase angle of rolling  
 $\lambda_{1,2}$  stochastic amplitudes of non-canonical presentation of stochastic process  
 $\Lambda_{22}$  horizontal damping coefficient  
 $\Lambda_{24}$  cross damping coefficient  
 $\Lambda_{44}$  angle damping coefficient  
 $\kappa_\phi$  coefficient of roll excitation  
 $\phi$  absolute angle of heel  
 $\phi_r$  relative angle of heel  
 $\phi_L$  quasi - linear process of rolling  
 $\phi_a$  amplitude of rolling  
 $\omega$  frequency of excitation (stochastic frequency of non-canonical presentation)  
 $\chi$  course of a ship relative to general direction of wave propagation.  
 $\varphi$  initial phase angle of the excitation

## 1. INTRODUCTION

The problem of estimation of probabilistic characteristics of nonlinear irregular rolling is unavoidable if we are interested in probability of capsizing and correct estimates of ship stability in operation. The authors encountered this problem while one of them was working on a practical application of piecewise linear approach to capsizing probability estimation [1]. To complete calculation of capsizing probability it was necessary to know distribution density of roll angles and velocities for a ship with given GZ curve. Attempts to obtain such distributions by direct numerical simulations failed: sometimes it was not possible to reproduce the same results with the same input data once again. The reason was simple: different realisations produced different output. It was not a surprise from the pure theory point of view: it is known that linear dynamic system generates ergodic stationary response having ergodic stationary excitation. (Ergodic property can be considered in regard to stationary stochastic process only and means that probabilistic characteristics obtained from the whole ensemble of realisations are the same as they were calculated using one realisation that is «long enough»). Analogous property is unknown for nonlinear systems, so we have no rights to expect that statistical estimates obtained by one realisation is correct because a stochastic process is presented by the whole ensemble of its possible realisations.

This simple statement [2] generated question to be answered before we can go ahead with further development of probabilistic stability assessment: what is the physical reason of the above phenomenon in case of nonlinear rolling and are there any method that allows to calculate rolling distribution, other than direct simulation of a big number of realisations?

Further researches [3, 4] allowed to uncover the physical reason of the above phenomenon that here is named as «cyclic non-stationary quality» and to approach to the practical methods of working with response of nonlinear system under stochastic excitation. State of the art review can be found in [4] and is missed here.

## 2. DIRECT SIMULATION

We shall call «direct» such kind of numerical simulation when we are calculating state of the dynamic system step by step in time having some realisation of the excitation process as the simulation input. Then we repeat all the calculation for another realisation of the stochastic excitation process until we get enough statistics for reliable estimation.

The excitation was simulated by well known Longuet-Higgins sea wave model using Fourier series with stochastic initial phase angles. The following system of differential equations was used to describe a ship:

$$\begin{cases} (M + M_{22})\ddot{y} + \Lambda_{22}\dot{y} = F_w(t) + F_a(t) \\ (I_x + M_{44})\ddot{\phi}_r + \Lambda_{44}\dot{\phi}_r + M_R(\phi_r) + \\ + M_{24}\ddot{y} + \Lambda_{24}\dot{y} = M_w(t) + M_a(t) \end{cases} \quad (1)$$

Wind here is also considered as stationary ergodic stochastic process presented by Fourier series, for details see [1] or [4]

The results of the simulation are presented on fig. 1 in form of so-called «cumulative variance estimates» vs. time. This means that we calculate variance estimate as of certain time passes.

Different curves mean different realisations of the rolling process. It could be clearly seen that during 20000 seconds these curves showed no tendency to stay within interval width of which would decreasing with time. Contrary to the same curves calculated for the same system (1)

stationary quality of severe rolling. Usage of this tool is illustrated by the following example.

We consider nonlinear rolling described by the following differential equation

$$\ddot{\phi} + 2\delta\dot{\phi} + \omega_{\phi}^2\phi + a_3\phi^3 = (\omega_{\phi}^2 + m_2\phi^2)\alpha_m(t) \quad (2)$$

We calculate estimated variance of each realisation and then average them finding width of confidence band with the give confidence probability. All these calculations were repeated for different values of nonlinear coefficient  $a_3$ . Details of this calculation can be found in [3] or [4]. The result is given in fig.3 (solid line).

If the stochastic process is ergodic, the estimate variance of the variances obtained by one realization could be defined by [5]:

$$V(V_{\phi}) = \frac{4}{T} \int_0^{\infty} K_{\phi}^2(\tau) d\tau \quad (3)$$

The error will be not so big if we substitute the correlation function in (3) by its estimate obtained by one of the realizations [4]. The value of width of confidence band yielded by the variance (3) gives us some measure of error caused by finite number of statistics only. This value is shown be dashed line on fig. 3

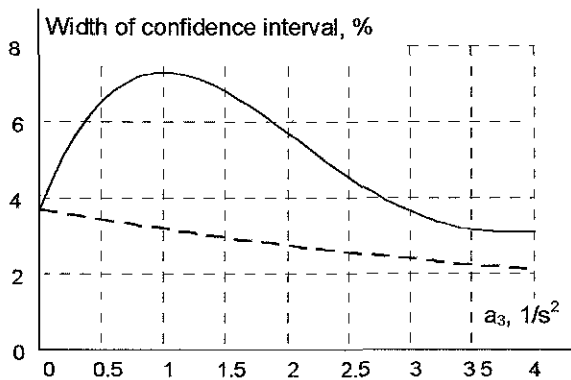


Fig. 3 Confidence band for variance with (dashed line) and without (solid line) ergodic assumption

It could be clearly seen that only linear system ( $a_3=0$ ) is ergodic. A spread of estimated variances could not be explained just by insufficient number of statistics anywhere else except the point ( $a_3=0$ ). So the difference between two confidence bands could be chosen as a measure of cyclic non-stationary quality - the tool we need to proceed our study.

#### 4. PHYSICAL REASON

What are the physical reason of the cyclic non-stationary quality of nonlinear dynamic system describing severe rolling? It is possible to show that the reason is fold bifurcation - existence of two responses at the same excitation frequency [3, 4]. When frequency band where fold bifurcation is possible coincides with a peak of the excitation spectrum frequent «jumps» can be observed, see fig.4. These «jumps» between low and high energy level seems to be responsible for cyclic nonstationary quality of rolling.

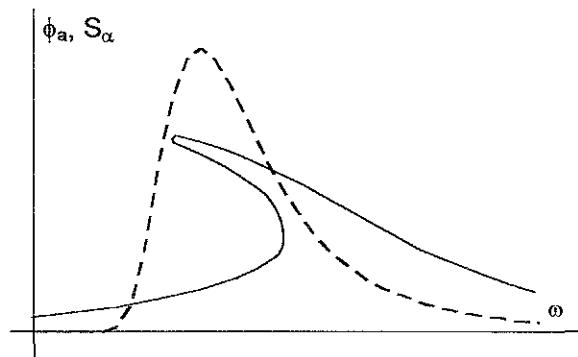


Fig. 4 Bifurcation area and excitation frequency band

Let's examine fig.3. With the increasing of nonlinear coefficient  $a_3$  the measure of cyclic non-stationary is increasing until certain value of the coefficient and then decreasing. Changing of the nonlinear coefficient leads to changing of form of nonlinear GZ curve and as a result to shifting the bifurcation area form the peak of the excitation [4].

This idea can be tested easily. Let's take the white excitation, so any response curve shifts

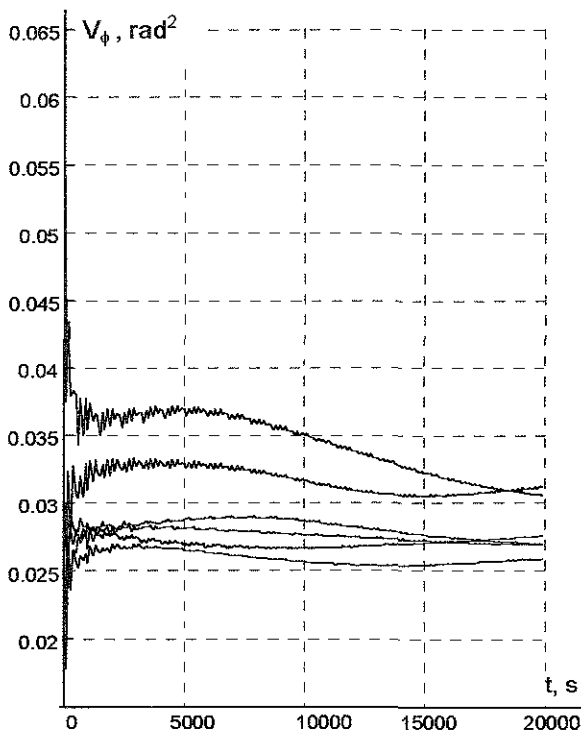


Fig. 1 Cumulative variance estimate vs. time for nonlinear system (1) taken from [4]

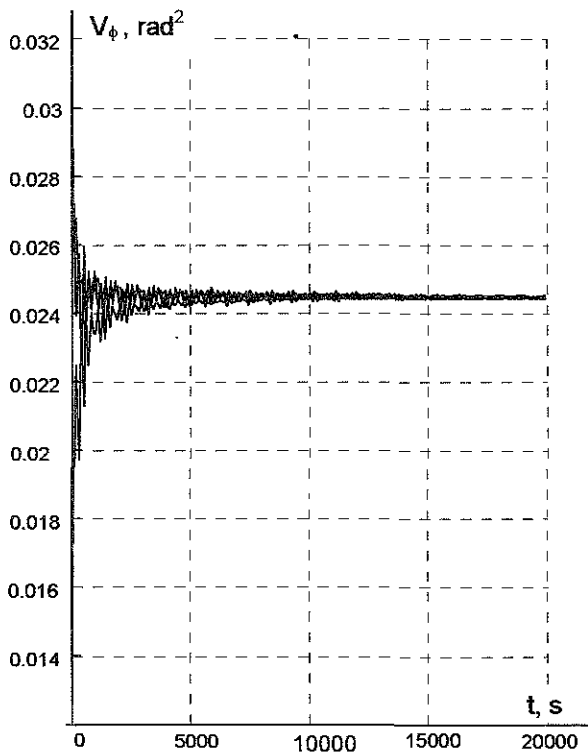


Fig. 2 Cumulative variance estimate vs. time for linear system

where real GZ curve is substituted by metacentric formula (in other words for linear system) show evident tendency to stay within such an interval, see fig. 2.

Formally this example does not give us a right to state that the stochastic process that corresponds to curves on fig. 1 is not ergodic, because all judgements on stochastic process can not be done during finite time. Probably if we could proceed calculations we could see these the cumulative curves within the interval, but we never have infinite realisations in engineering practice. Having in mind that certain sea state conditions also could not be constant in time, we always have some limitation in time duration. This means that despite we did not prove that the process is not ergodic we cannot use ergodic hypothesis in practice anymore. To avoid misunderstanding in terms we called this property of the rolling process «cyclic non-stationary quality»

### 3. TOOLS FOR STUDY

To proceed our study we need some tools. As it is well known, any estimate obtained by statistics is a stochastic value. So estimated variance, for example, as any other stochastic value, has its own mean value and variance. The estimates of these figures also can be obtained from statistics in real engineering practice. So we have to work with statistical estimates of statistical estimates. This concept may be clarified by a simple example. Each realisation of rolling process on fig 1 or 2 yields some estimate of variance. A set of realisations produces a set of estimated variances and we can estimate variance of this set. The result is estimated variance of the whole ensemble of realisations that could be found with certain probability to be within confidence band as any other statistical characteristic. The width of confidence band reflects an error of estimation of the characteristics. This value could be used as a tool for study of defined above non-

should not affect on cyclic nonstationary if we the above hypothesis is correct - see fig. 5.

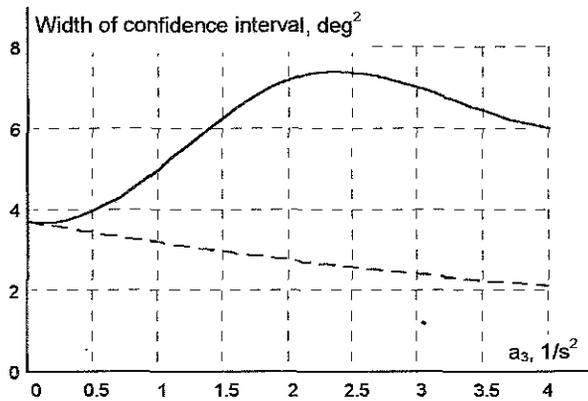


Fig. 5 Confidence interval for variance with (dashed line) and without (solid line) ergodic assumption

One could see that increasing of the measure of cyclic nonstationary is slower in fig. 5 rather than in fig. 3. This can be explain that the bifurcation area is initially small and jumps are rare. With the further increasing of nonlinear coefficient  $a_3$  the bifurcation area stays in high excitation frequency all the time and the measure is practically constant. This result does not disapprove the above hypothesis, for more details see [3] or [4].

## 5. MATHEMATICAL MODEL

We agreed that the reason of cyclic non-stationary phenomenon is the fold bifurcation. Existence of two responses at one excitation frequency leads to «jumps» from high amplitude mode to low one and vice versa. The above description could be used for formulating mathematical model of cyclic non-stationary phenomenon.

Let's consider the stochastic process of severe rolling as multiplication of quasi-linear stochastic rolling and some impulse stochastic process that models «jumping»:

$$\phi(t) = \phi_L(t) \cdot P(\varepsilon t) \quad (4)$$

Majority of available knowledge on «jumps» or fold bifurcation concerns stable state motion of dynamic system with one frequency excitation. Fold bifurcation is associated with certain frequency band where two stable periodical responses co-exist. So to be able to use this knowledge we have to present linearized rolling  $\phi_L(t)$  as a single harmonic function and to keep all stochastic properties at the same time.

Such a model was proposed by the authors in [4]. The idea of this is to use non-canonical presentation of the excitation [6]:

$$\alpha(t) = \lambda_1 \sin \omega t + \lambda_2 \cos \omega t \quad (5)$$

Here we have three stochastic values: amplitudes  $\lambda_1$  and  $\lambda_2$  have Gaussian distribution and stochastic frequency  $\omega$  has a distribution density in a form of normalised wave spectrum:

$$f(\omega) = \frac{S_\alpha(\omega)}{V_\alpha} \quad (6)$$

If we set the time  $t$  constant and simulate excitation by generation of stochastic values  $\lambda_1$ ,  $\lambda_2$  and  $\omega$ , we obtain a set independent realisations corresponding to the above time  $t$ . The main advantage of the non-canonical presentation is a possibility to get averaging by realisations without step-by-step generation of stochastic process, see [4] for details and [6] for theoretical background. This feature also makes it possible to use conventional quasi-linear methods for roll response calculation because the excitation is harmonic in each realisation (practical method will be considered further).

To simulate «jump» we divide all frequency band in three zones, see fig.6. While the only response exists in zones I and III, two stable responses could be found in zone II. If the frequency  $\omega_1$  occurs in zone II, we should propose an algorithm of the response choice.

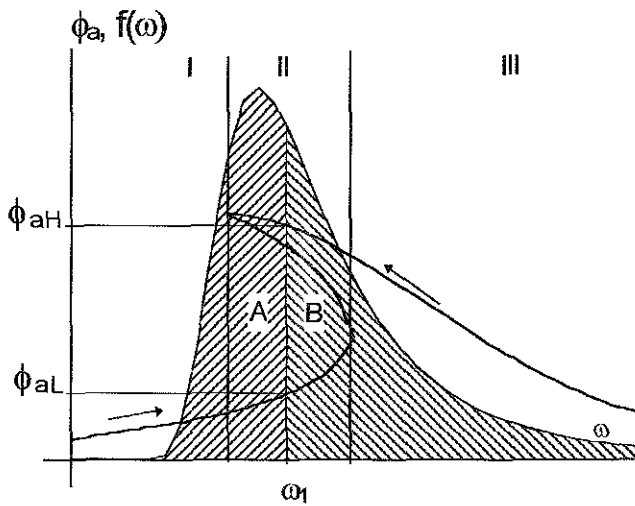


Fig. 6 On the probability of high or low response in bifurcation area

This choice depends on previous history of the oscillation expressed in initial conditions and initial phase angle of the excitation. To avoid of history consideration, the following method is used. oscillations start on higher (or lower) frequency where the only response exist. Then the frequency is altered slowly to pull the system in the bifurcation area. The choice is finally determined by the way how we reach the point. If we system reaches bifurcation area from high frequencies high amplitude response is chosen, if the area is reached from low frequencies, the low amplitude response is chosen, see fig 6

If the frequency  $\omega_1$  is a stochastic value, probability of the choice of high amplitude response can be associated with the distribution density area from the right of  $\omega_1$ .

$$P(\phi_a(\omega_1) = \phi_{aH}(\omega_1)) = \int_{\omega_1}^{\infty} f(\omega) d\omega, \quad (7)$$

and probability of the choice of low frequency amplitude response can be associated with the distribution density area from the left of  $\omega_1$

$$P(\phi_a(\omega_1) = \phi_{aL}(\omega_1)) = \int_0^{\omega_1} f(\omega) d\omega \quad (8)$$

The proposed algorithm allows to find out what kind of response we shall get in bifurcation zone, however, this is just a hypothesis, that seems to have some physical background. Probabilistic qualities of «jumps» during nonlinear stochastic rolling are the subject for further study.

## 6. PRACTICAL CALCULATION OF CYCLIC NON-STATIONARY QUALITY

Here we try to develop practical algorithm of taking into account the influence of cyclic non-stationary quality. Proposed criteria of cyclic non-stationary significance could be expressed as.

$$C = \frac{W_{V\phi}}{V_{\phi H} - V_{\phi L}} \cdot 100\% \quad (9)$$

Here  $W_{V\phi}$  is the width of confidence band of variance estimate obtained by numerical simulation and the values  $V_{\phi H}$  and  $V_{\phi L}$  are estimated variances calculated only with respect high and low amplitude modes correspondingly.

The question how small this difference should be to consider the process as ergodic is open. We propose to set up the significance level (the threshold after crossing of which we cannot assume that the process is still ergodic) by expert estimate as the first expansion.

Calculation of the width of confidence band  $W_{V\phi}$  without ergodic assumption is suggested to use multiplication model of «jumps» as it was described above.

We use non-canonical model of the excitation, but we need to generalise it for consideration of any given course of a ship relative waves:

$$\alpha_x(t) = \lambda_1 \sin \vartheta t + \lambda_2 \cos \vartheta t; \quad (10)$$

To take into account 3-dimensional character of sea wave, we introduce new stochastic value

$$\mathfrak{g} = \sqrt[4]{g^2(u^2 + v^2)}, \quad (11)$$

the variance of stochastic amplitudes:

$$V_\lambda = \int_0^\infty \int_0^\infty u^2 S_\xi(u, v) du dv, \quad (12)$$

and the distribution of the parameters

$$f(u, v) = \frac{u^2 S_\xi(u, v)}{V_\alpha}; \quad (13)$$

Using Gaussian generator of random numbers we get two values  $\lambda_1$  and  $\lambda_2$ , their variance should be in accordance with formula (12).

Then we use special generator to get the parameters  $u$  and  $v$  in accordance with the distribution density (13)

Having the set of these three value we are able to get an amplitude of ship response by solving the following rolling differential equation, that is just some generalisation of equation (2):

$$\ddot{\phi} + 2\delta\dot{\phi} + \omega_\phi^2\phi + a_3\phi^3 + a_5\phi^5 = (\omega_\phi^2 + m_2\phi^2 + m_4\phi^4)\kappa_\phi(\omega, \chi)\alpha_x(t) \quad (14)$$

The equation (14) can be solved by any appropriate quasi-linear method. We used the method of multiple scales see [7], [8] and [4].

We introduce time scales in accordance of power of bookkeeping parameter:

$$T_0=t, \quad T_1=\varepsilon t, \quad T_2=\varepsilon^2 t \dots, \quad (15)$$

time derivatives can be expressed as:

$$\frac{d}{dt} = D_0 + \varepsilon D_1 + \varepsilon^2 D_2 + \dots$$

$$\frac{d^2}{dt^2} = D_0^2 + 2\varepsilon D_1 D_0 + \varepsilon^2 [2D_0 D_2 + D_1^2] + \dots$$

$$\text{where } D_i = \frac{\partial}{\partial T_i}$$

The solution is searched in following form:

$$\phi = \phi_0(T_0, T_1, \dots) + \varepsilon \phi_1(T_0, T_1, \dots) + \dots, \quad (16)$$

where  $\phi_0, \phi_1, \dots$  are the solutions of corresponding expansions.

Then we substitute the solution (16) into the equation (14) and transform it into the system of linear differential equations accordingly to power of the bookkeeping parameter. To do that we should present coefficients of the equation (14) as:

$$\varepsilon \delta = \mu; \quad \varepsilon b_3 = a_3; \quad \varepsilon b_5 = a_5, \quad (17)$$

$$\varepsilon c_i = m_i;$$

Assuming harmonic form of the solution

$$\phi = \phi_a(t) \cos(\omega t - \gamma(t) - \varphi) + O(\varepsilon) \quad (18)$$

and using further exponential form for harmonic function we obtain the following system.

$$\varepsilon^0: \quad D_0^2 \phi_0 + \omega_\phi^2 \phi_0 = 0$$

$$\varepsilon^1: \quad D_0^2 \phi_1 + \omega_\phi^2 \phi_1 = -2D_0 D_1 \phi_0 - 2\mu D_0 \phi_0 - 2\mu D_0 \phi_0 - b_3 \phi_0^3 - b_5 \phi_0^5 + (c_0 + c_2 \phi_0^2 + c_4 \phi_0^4) r e^{i(\omega t - \varphi)} \quad (19)$$

The solution of the first equation (19) is trivial. Substitution of this solution into the second equation of (19) yields the following system of differential equations relative to  $\phi_a(t)$  and  $\gamma(t)$ , see system (20).

We are interested stable state mode - therefore we assume  $\dot{\phi}_a = 0$  and  $\dot{\gamma} = 0$ , that transform the nonlinear differential equation (20) into algebraic one. Solution of the algebraic equations yields requested numerical value for amplitude, phase and ordinate of the process at the given moment of time.

$$\left\{ \begin{aligned} \dot{\phi}_a \omega_\phi &= -\mu \phi_a \omega_\phi + \\ &+ \left( c_0 + \frac{c_2}{4} \phi_a^2 + \frac{3c_4}{16} \phi_a^4 \right) \sin(\gamma) \\ \phi_a \omega_\phi \dot{\gamma} &= \omega \phi_a - \frac{3}{8} b_3 \phi_a^3 - \frac{5}{16} b_5 \phi_a^5 + \\ &+ \left( c_0 + \frac{c_2}{4} \phi_a^2 + \frac{3c_4}{16} \phi_a^4 \right) \cos(\gamma) \end{aligned} \right. \quad (20)$$

If our stochastic excitation frequency occurs in fold bifurcation area and we get two values for amplitude and phase and, respectively, two ordinates instead of one we use the procedure based on mathematical model described in chapter 5. Then we come back to the presentation (10), generate new set of stochastic values and repeat all the calculation again and again until we gather enough statistics. Having enough statistics we calculate variance and borders of confidence band.

Then we calculate the variance estimates for high and low amplitude response modes and finally obtain the value of criterion of cyclic non-stationary quality in accordance with formula (9)

## 7 FULL SCALE TRAILS AND CYCLIC NON-STATIONARY QUALITY

The problem of cyclic non-stationary quality is not only pure theoretical or methodological. Contemporary intellectual shipborne seakeeping systems use to measure rolling to display current characteristics of safe operation. Accuracy of rolling judgement could be critical in this case.

Described above method was used for estimation of significance of errors in judgement caused by cyclic non-stationary quality of severe rolling. Data of general cargo ship «Never» was used for these calculations: see table 1.

The results of calculations are shown in form of circular diagrams, see figures 7 and 8. Pierson-Moskowitz spectrum was used.

Table 1

Data on ship «Never»	
Length, L, m	109.8
Breadth, B, m	14.8
Draught T, m	3.1
Total depth H, m	5.0
C <sub>B</sub>	0.84
C <sub>w</sub>	0.88
GM, m	1.44
Weight displacement, t	4260
KG, m	5.2
BM, m	5.1
CB, m	1.6
Natural frequency $\omega_\phi$ , s <sup>-1</sup>	0.82
Damping coefficient: $\delta / \omega_\phi$	0.1

## 8. CONCLUSIONS AND COMMENTS

There is a phenomenon of cyclic non-stationary quality of severe irregular rolling. It is expressed in impossibility to obtain statistical characteristics from one realisation of stochastic process.

A relative difference of confidence band width with and without ergodic assumption can be used as a measure of the above phenomenon

The physical reason of cyclic non-stationary quality is fold bifurcation.

Non-canonical presentation of stochastic excitation in combination with method of multiply scales allows to develop the practical algorithm for calculation of the above measure.

Cyclic non-stationary quality can significantly affect on full scale measure especially when recording time is short. It seems to be necessary to take into account this quality when choosing course and speed for the full scale measurements. The circular diagrams can be used as some guide for that.

The authors think that further study of probabilistic qualities of «jumps» would be useful as well as generalisation of the proposed

approach for statistics of higher order and any types of probability distributions.

## REFERENCES

1. Belenky, V.L. Piece-wise linear methods for the probabilistic stability assessment for ship in a seaway, *Proc. of 5th STAB Conference*, vol. 5, Melbourne, Florida, 1994.
2. Belenky, V., Degtyarev, A. and Boukhanovsky, A. On probabilistic qualities of severe rolling, *Proc 5th STAB Conference*, vol. 6, Melbourne, Florida, 1994
3. Belenky, V., Degtyarev A. and Boukhanovsky, A. Probabilistic qualities of severe rolling, Proc. of Int. Symp. in memory of Prof. Sevastianov "Ship Safety in a Seaway: Stability Maneuverability, Nonlinear Approach" (Sevastianov Symposium) Kaliningrad 15-19 May 1995, Vol.1, Paper 7
4. Belenky, V.L., Degtyarev, A.B., Boukhanovsky, A.V., Probabilistic qualities of nonlinear stochastic rolling, *Ocean Engineering*, 1997, Vol. 25, pp. 1-25 in press
5. Bendat J.S., Piersol A.G. Random data. (Analysis and Measurement Procedures). Wiley-Interscience, New York, 1986.
6. Chernecki, V.I. Analysis of accuracy of nonlinear control systems. Mashinostroenie, Moscow, 1968. (in Russian)
7. Nayfeh, A.H., Introduction to perturbation techniques. Wiley-Interscience, New York, 1981
8. Degtyarev, A.B. Mathematical modeling of the ship motion with the help of interpolation method, Proc of CRF'92, S.Petersburg, 1992, pp. 254-261

## ASKNOWLEDGEMENT

Figures 1, 2, 4 and 5 are reprinted from «Ocean Engineering», Vol. 25. Belenky, V.L., Degtyarev, A.B., Boukhanovsky, A.V., «Probabilistic qualities of nonlinear stochastic rolling» Pages 1-25. Copyright 1997, with permission from Elsevier Science Ltd., The Boulevard, Langford Lane, Kidlington OX51GB, UK

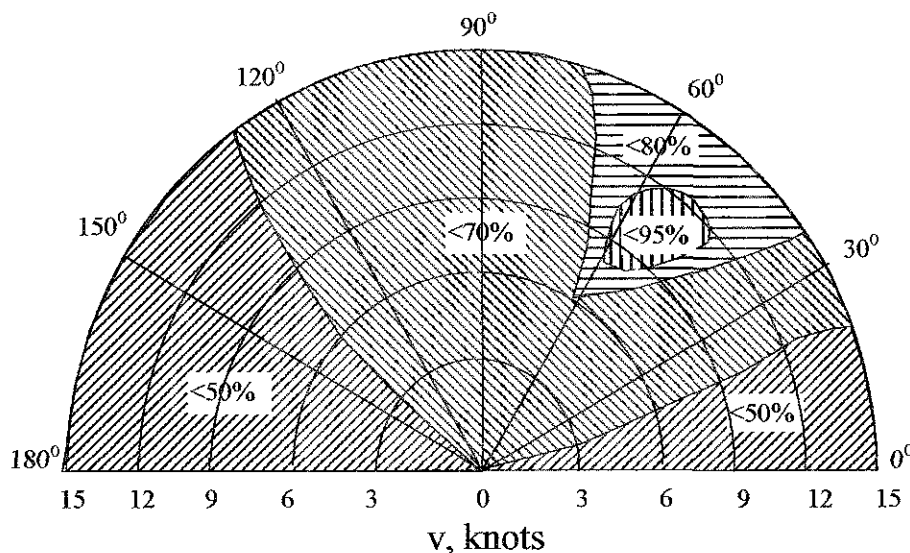


Fig. 7 Circular diagram of non-stationary cyclic quality, Sea state 6 point.  
 $h_{3\%} = 7.0$  m,  $V_{WAVE} = 1.75$  m<sup>2</sup>,  $\omega_{mean} = 0.615$  s<sup>-1</sup>

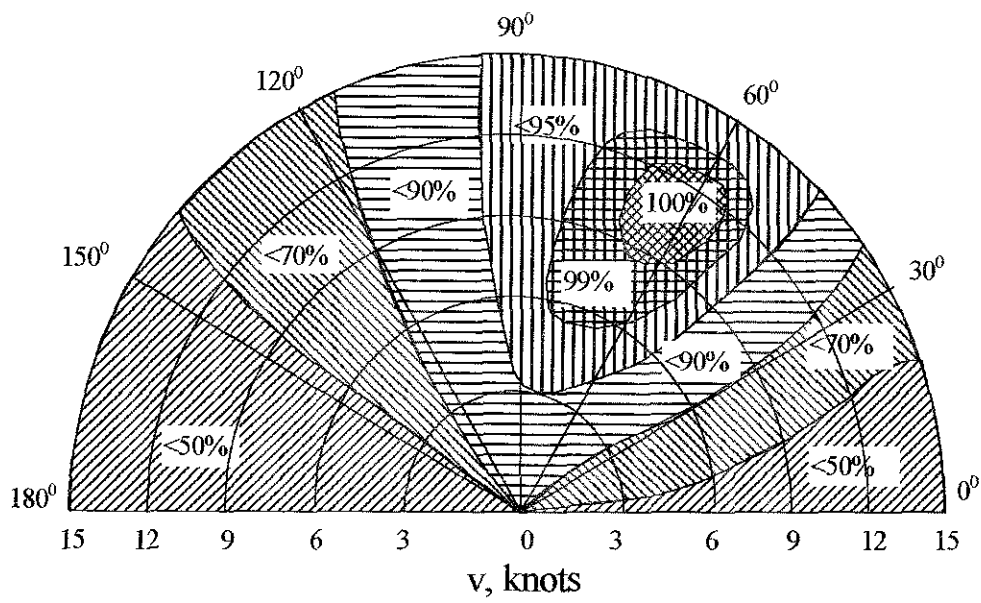


Fig. 7 Circular diagram of non-stationary cyclic quality, Sea state 6 point.  
 $h_{3\%} = 10.0 \text{ m}$ ,  $V_{\text{WAVE}} = 3.58 \text{ m}^2$ ,  $\omega_{\text{mean}} = 0.533 \text{ s}^{-1}$

# PROBABILITY TO ENCOUNTER HIGH RUN OF WAVES IN THE DANGEROUS ZONE SHOWN ON THE OPERATIONAL GUIDANCE/IMO FOR FOLLOWING/QUARTERING SEA

Y Takaishi\*, K Watanabe\*\*, K Masuda\*

\* College of Science and Technology, Nihon University  
7-24-1 Narashinodai, Funabashi, Chiba 274, Japan

\*\* Yachiyo Engineering Co., Ltd  
1-10-23 Nakameguro, Meguro, Tokyo 153, Japan

## ABSTRACT

The time history of encounter waves differs from the wave record at a fixed point, i.e. the groupiness of encounter waves varies according to ship course and speed. The groupiness of ocean wave itself had been estimated statistically by using characteristic values of wave spectrum. This method has been applied to the encounter waves, and the probability to encounter high run is shown as functions of  $V/T$  and number of runs. It is concluded that the groupiness or probability to encounter high run becomes higher in the range of  $V/T$  between 1.0 and 2.0 (kt/sec). The danger of encountering such high run is confirmed by model test results on capsizing.

## 1. INTRODUCTION

A ship will encounter occasionally a group of high waves, i.e. high run, when navigating in following/quarterming seas. One of the present author had been explained this phenomena by introducing a concept of the wave energy concentration ratio which is determined on the encounter wave spectrum, and he has proposed the dangerous zone to encounter high run on the V/T-Diagram[1]. This idea is now included in the "Guidance to the Master for Avoiding Dangerous Situations in Following and Quarterming Seas", which recently was adopted as the MSC/IMO Circular[2]. However, this V/T-diagram gives no quantitative information on the degree of encountering high run. Then, the authors have tried to derive the statistical properties of this encounter wave grouping phenomena in following/ quaterming seas to quantify the probability of occurrence of high runs in wave group, applying the Longuet-Higgins' method[3] that the groupiness of

ocean wave itself depends on the characteristic values of energy spectrum. A band-width parameter, which is calculated for the encounter wave spectrum transformed from the ocean wave spectrum, is used to estimate the probability of wave group length or high run to be appeared in encounter waves of a ship. The results have been confirmed by the statistical analysis of simulated time series of encounter waves that the probability of occurrence of high runs in following sea becomes higher in the range of  $V/T = 1.0 - 2.0$  with the highest value at  $V/T = 1.45$ . The influences of directional distribution of wave energy, i.e. the effects of short-crestedness of ocean waves have been also investigated and it has been shown that the increment of encounter wave groupiness is less, as the directional distribution of wave energy becomes wider. The danger to encounter such high run has been demonstrated on the V/T-diagram by using experiment results on capsizing for various ship models.

## 2. STATISTICAL ANALYSIS OF WAVE GROUP

### 2.1 Longuet-Higgins' Method

The run is the number of successive wave train in a group, all of which exceed a level  $\rho$ , as shown in Fig 1. According to Longuet-Higgins, the mean length of wave group,  $\bar{l}$ , the mean values of wave number and run in a group,  $\bar{G}$  and  $\bar{H}$ , are represented by the following formulae as the functions of the band-width parameter,  $\nu$ , of the wave spectrum

$$\bar{l} = \left\{ \mu, l / (2\pi) \right\}^{1/2} (\mu_0 / \rho) e^{\rho^2 / (2\mu_0)} \quad (1)$$

$$\bar{G} = (2\pi)^{-1/2} [(1 + \nu^2)^{1/2} / \nu] (\mu_0^{1/2} / \rho) e^{\rho^2 / (2\mu_0)} \quad (2)$$

$$\bar{H} = (2\pi)^{-1} [(1 + \nu^2)^{-1/2} / \nu] \mu_0^2 / \rho \quad (3)$$

where  $\nu$  is derived from the  $n$ -th moment of the spectrum,  $m_n$ , as follows,

$$\nu = \sqrt{m_n m_0 - m_1^2} / m_1 \quad (4)$$

$$\mu_0 = m_0, \quad \mu_1 = 0, \quad \mu_2 = m_2 - m_1^2 / m_0 \quad (5)$$

provided that the components of the spectrum in higher frequency range than  $1.5 f_p$  as well as the lower frequency range than  $0.5 f_p$  are ignored, where  $f_p$  is the peak frequency of the spectrum

The probability density functions of  $L$ ,  $G$  and  $H$  are represented by an exponential function, respectively, as follows

$$p(L) = \bar{L}^{-1} e^{-L/\bar{L}} \quad (6)$$

$$p(G) = \bar{G}^{-1} e^{-G/\bar{G}} \quad (7)$$

$$p(H) = \bar{H}^{-1} e^{-H/\bar{H}} \quad (8)$$

The probability that the run exceeds  $H$  is calculated by equation (9)

$$P(H) = \int_H^\infty p(H) dH = e^{-H/\bar{H}} \quad (9)$$

The probability,  $P(H)$ , takes the same value for the same  $H/\bar{H}$  value, or  $\rho$ . It means that the increased number of run and the increased level of wave height of run have the same effect

## 2.2 Application to Encounter Wave

The encounter wave spectrum is obtained by transformation of wave spectrum in wave frequency domain  $\omega$  into encounter wave frequency domain  $\omega_e$ , i.e.

$$S(\omega_e, \chi) = S(\omega) / |1 - 2\omega V \cos \chi / g| \quad (10)$$

where  $V$  is ship speed,  $\chi$  is encounter angle, and

$$\omega_e = \omega - \omega^2 V \cos \chi / g \quad (11)$$

The Longuet-Higgins' method is applied to the encounter wave spectrum. The spectrum of Pierson-Moskowitz type is used for calculation of long-crested sea, as shown by the non-dimensional equation (12) and Fig. 2

$$S'(\omega') = \frac{2\pi S(\omega)}{T_{01} H_{1/3}^2} = 0.11 \omega'^{-5} \exp\{-0.44 \omega'^{-4}\} \quad (12)$$

where  $\omega' = \omega / \omega_0$ ,  $\omega_0 = 2\pi / T_{01}$ ,  $T_{01}$  mean wave period,  $H_{1/3}$  the significant wave height. The short-crested wave spectrum is shown by equation (13),

$$S(\omega, \theta_i) = S(\omega) D(\omega, \theta_i) \quad (13)$$

with the energy distribution function  $D(\omega, \theta)$ , as equation (14)

$$D(\theta) = \frac{1}{\sqrt{\pi}} \frac{\Gamma(1+n/2)}{\Gamma(1/2+n/2)} \cos^n \theta \quad (14)$$

The encounter wave spectrum in short-crested waves is represented by summing the component wave spectrum in various directions, as equation (15),

$$S(\omega_e, \chi) = \sum_{i=1}^I S(\omega_{e_i}, \chi) \quad (15)$$

$$= \sum_{i=1}^I \frac{S(\omega, \theta_i) \Delta \theta_i}{|1 - 2\omega V \cos(\chi - \theta_i) / g|}$$

where

$$\omega_{e_i} = \omega - \omega^2 V \cos(\chi - \theta_i) / g \quad (16)$$

The band-width parameters of encounter wave spectra have been calculated for navigation conditions as shown in Fig. 3, where  $V/T$  (kt/sec) is taken as the unique factor to govern the encounter wave grouping. Figures 4, 5 and 6 show the encounter spectra of following sea for various exponents of directional distribution function,  $n = \infty, 10$  and  $4$ , respectively. Figures 7(a), (b) and (c) show the band-width parameter  $\nu$  versus  $V/T$ . Then, the characteristic values of encounter wave groupiness such as  $\bar{L}$ ,  $\bar{G}$ , and  $\bar{H}$  are derived by using equations (1), (2) and (3) for the significant wave height, i.e.  $\rho / m_0^2 = 2$  or  $\rho = H_{1/3}^2 / 2$ , as shown in Fig. 8 and 9. From these figures it is clearly recognized that the encounter wave groupiness increases remarkably in the range of  $V/T = 10 \sim 20$  and it becomes highest at  $V/T = 14.5$ .

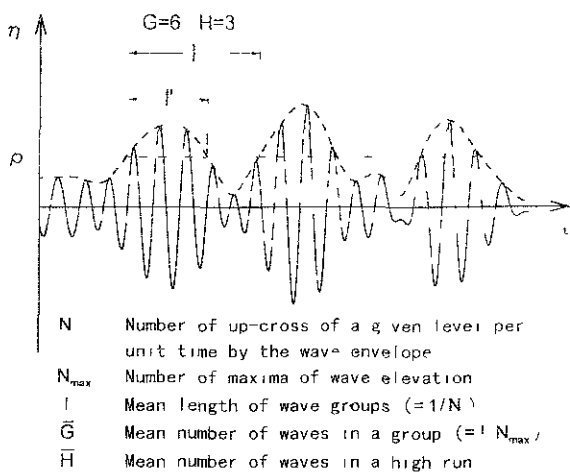


Fig.1 Definition of wave group and high run

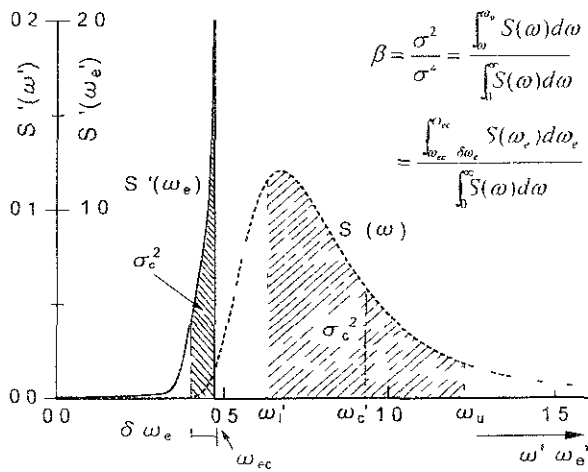


Fig.2 Wave spectrum (P-M type), encounter wave spectrum and definition of wave energy concentration ratio,  $\beta$

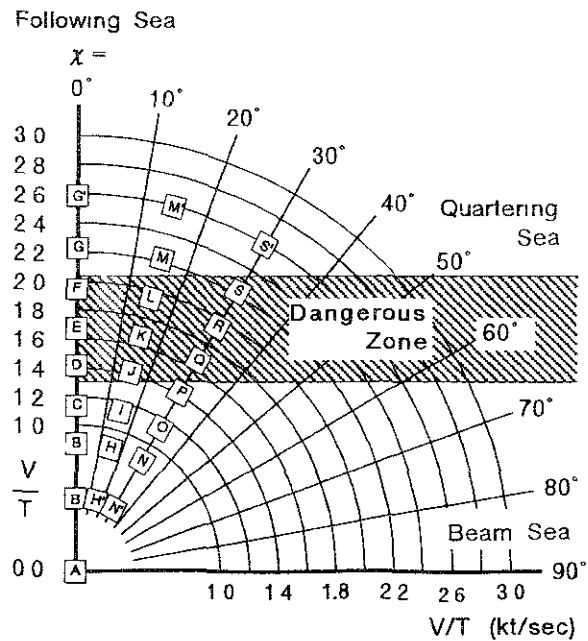


Fig.3 Encounter conditions on V/T-Diagram

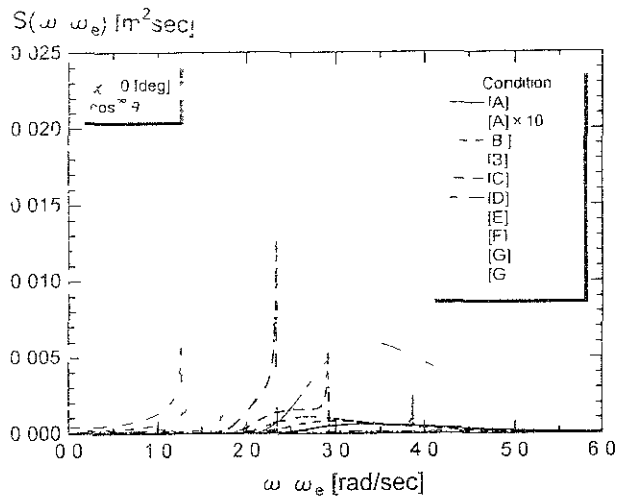


Fig.4 Transformation of wave spectra of long-crested waves  $S(\omega)$  into spectra of encounter wave  $S'(\omega_e)$  in following seas,  $\cos^2 \theta$ ,  $\chi = 0$  [deg]

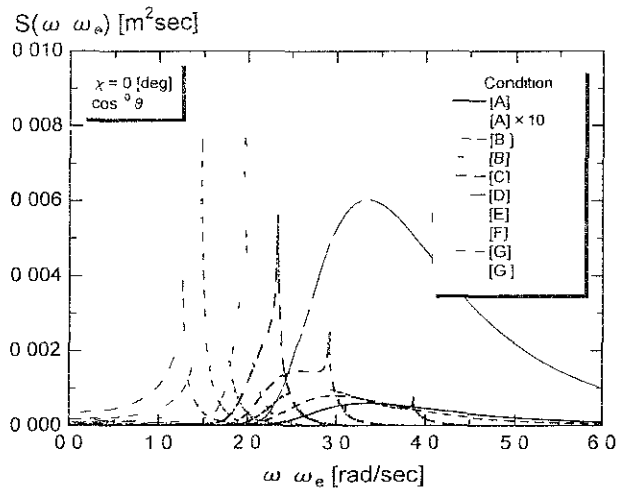


Fig.5 Transformation of wave spectra of short-crested waves  $S(\omega, \theta)$  into spectra of encounter wave  $S'(\omega_e)$  in following seas,  $\cos^4 \theta$ ,  $\chi = 0$  [deg]

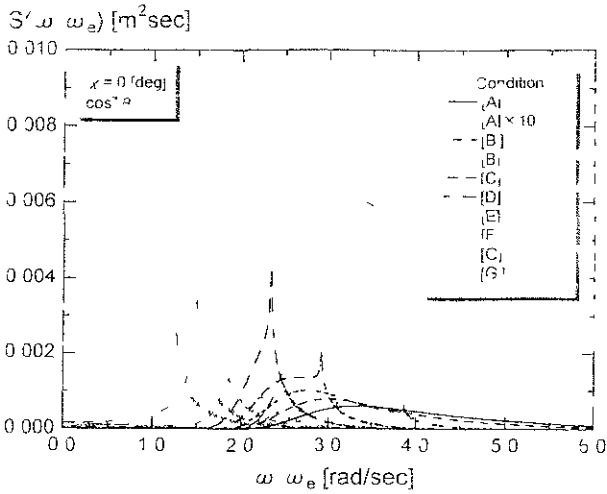


Fig.6 Transformation of wave spectra of short-crested waves  $S(\omega_e)$  into spectra of encounter wave  $S'(\omega_e)$  in following seas,  $\cos^4 \theta$ ,  $\chi = 0$  [deg]

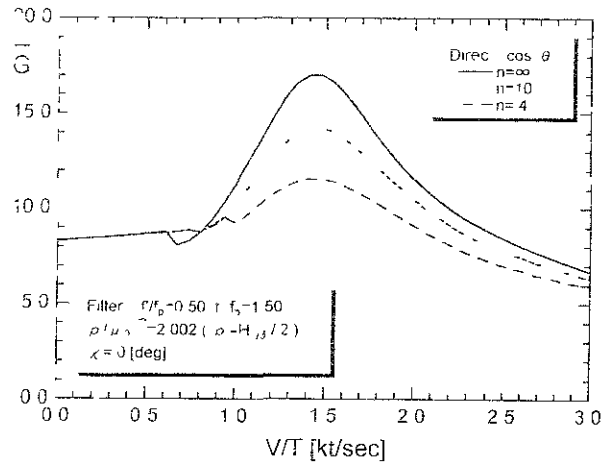


Fig.8 Mean number of waves in a group vs.  $V/T$  for the significant wave height

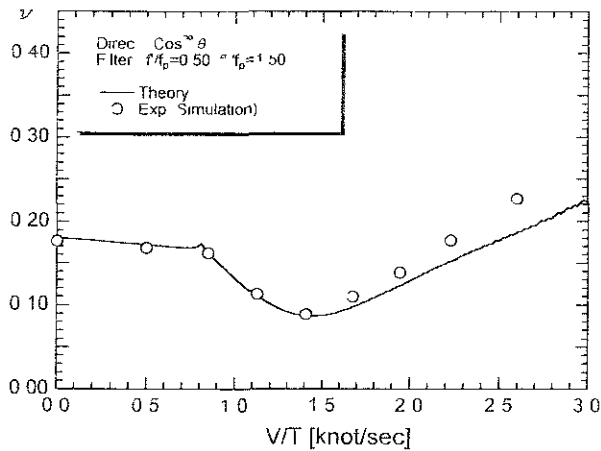


Fig.7 Band width parameter  $\nu$  vs.  $V/T$  in following sea, Long-crested wave,  $n = \infty$

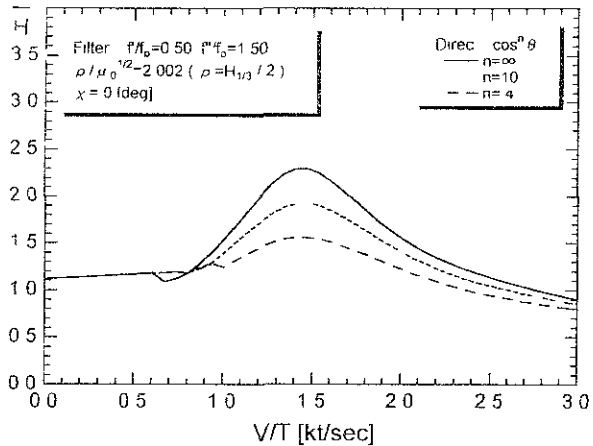


Fig.9 Mean number of waves in a high run exceeding the significant wave height vs.  $V/T$

Table 1 Probability of runs greater than  $H$  obtained by simulation

Cond	A		B		C		D		E		F		G	
	N	P(H)	N	P(H)	N	P(H)	N	P(H)	N	P(H)	N	P(H)	N	P(H)
1	1267	0.81374	945	0.86777	580	0.92084	378	0.89786	340	0.87855	344	0.84108	385	0.81607
2	385	0.24727	365	0.33517	331	0.52540	233	0.55344	174	0.44961	161	0.39364	139	0.29387
3	68	0.04367	57	0.05234	142	0.22540	154	0.36560	101	0.26098	77	0.18826	55	0.11628
4	17	0.01092	10	0.00918	48	0.07619	81	0.19240	63	0.16279	36	0.08802	16	0.03383
5	2	0.00129	1	0.00092	15	0.02381	42	0.09976	47	0.12145	22	0.05379	6	0.01269
6	1	0.00064	0	0.00000	8	0.01270	21	0.04988	32	0.08269	14	0.03423	3	0.00634
7	1	0.00064	0	0.00000	3	0.00476	7	0.01663	23	0.05943	11	0.02690	1	0.00211
8	0	0.00000	0	0.00000	2	0.00318	5	0.01188	14	0.03618	9	0.02201	0	0.00000
9	0	0.00000	0	0.00000	0	0.00000	2	0.00475	8	0.02067	9	0.02201	0	0.00000
10	0	0.00000	0	0.00000	0	0.00000	1	0.00238	6	0.01550	5	0.01223	0	0.00000
$M_0$ [m SEC]	0.0010929		0.0014062		0.0013826		0.00143098		0.0013334		0.0011938		0.00113237	
$H_1$ [m]	0.064083		0.073212		0.073196		0.0746493		0.072582		0.068045		0.065601	
$\nu$	0.8299		0.16334		0.11256		0.0859457		0.10074		0.11791		0.15733	

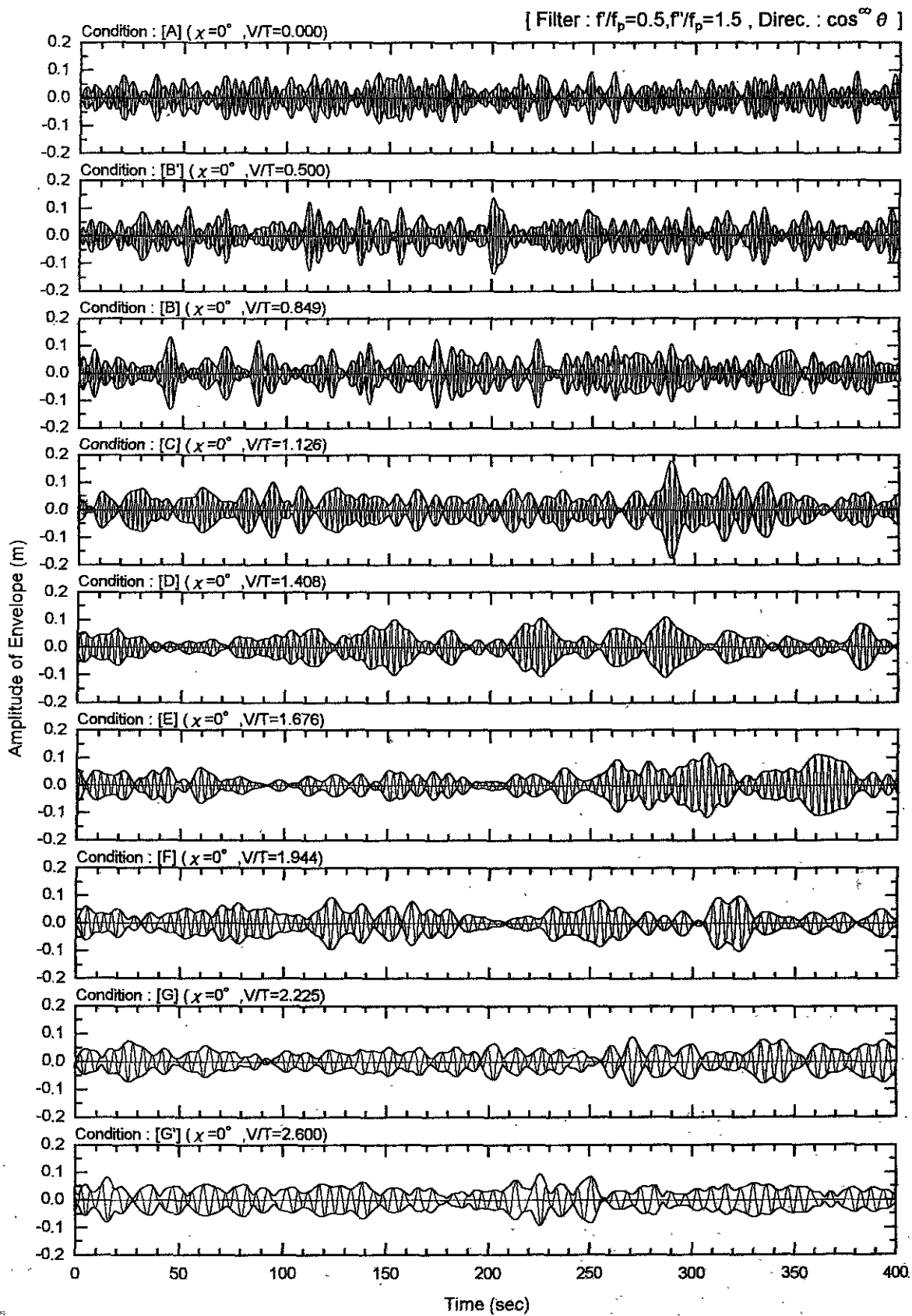


Fig.10 Filtered encounter waves and its envelope in following seas of long-crested waves

### 2.3 Statistical Analysis of Encounter Waves Obtained by Simulation

The time series of encounter wave in short-crested sea can be obtained by time-domain simulation as double summation of elemental waves as equation (17),

$$\eta(\mathbf{x}, t) = \sum_{i=1}^I \sum_{j=1}^J a_{ij} \cos(\omega_i t - \mathbf{k}_{ij} \cdot \mathbf{x} + \varepsilon_{ij}) \quad (17)$$

where

$$\begin{aligned} a_{ij} &= \sqrt{2S(\omega_i, \theta_j) \Delta\omega_i \Delta\theta_j} \\ \mathbf{k}_{ij} \cdot \mathbf{x} &= k_i (x(t) \cos \theta_j + y(t) \sin \theta_j) \\ (x(t), y(t)) &= (x_0 + V \cos \chi \cdot t, y_0 + V \sin \chi \cdot t) \end{aligned} \quad (18)$$

The time series of encounter waves in long-crested sea are shown in Fig.10 for various  $V/T$  values. The envelope of wave amplitudes are drawn on the figure.

### 3. STATISTICAL PROPERTIES OF ENCOUNTER WAVE GROUP AND EFFECTS OF PARAMETERS

The envelopes of time series of encounter waves have been analyzed by statistical manner and the probability that number of run exceeds  $H$  has been obtained as shown in Figures 11, 12 as well as Table 1. The influence of directional distribution of wave spectrum is also shown by chain or broken lines in the figures. From these results, the qualitative features of encounter wave grouping are concluded as follows.

(1) Theoretical calculation and numerical simulation give almost the same tendency that the encounter wave groupiness increases remarkably in the speed range of  $V/T$  between 1.0 and 2.0, see Fig. 11.

(2) The probability of exceedance,  $P(H)$ , that the number of waves in a run is greater than  $H$  can be represented by a straight line on Fig. 12. Therefore, by using Fig. 11 and 12, we can estimate  $P(H)$  for any conditions of  $V/T$  and  $H$  as well as  $\rho$ .

(3) The increase rate of encounter wave groupiness in the range of  $V/T=1.0 \sim 2.0$  will become greater, as the value of  $H$  increases, as shown in Fig.13.

(4) The increment of encounter wave groupiness in the above-mentioned range of  $V/T$  is less, as the directional distribution of wave energy becomes wider.

### 4. COMPARISON WITH MODEL TEST RESULTS

The capsizing rates of two model ships in following/quartering seas[1] again are plotted on the V/T-diagram together with the curve representing the probability to encounter high run,  $P(H \geq N)$ , where number of run,  $N$ , is assumed 4, as shown in Fig.14. From these results, it is clearly shown that the probability to encounter to high run correlates closely the danger of capsizing events of ships in following/quartering seas, as one of the present authors already has shown by using the wave energy concentration ratio which was defined on the encounter wave spectrum. The degree of danger could be assumed to be proportional to the probability,  $P(H)$ . Note that the capsizing rates for larger GM show a better correlation to  $P(H)$ .

As the results of this study, the authors recommend the followings:

(1) The dangerous zone shown in the operational guidance/MSB circular/IMO (1995) may be classified according to the probability, i.e.  $P(H)$  values, from the most dangerous zone near  $V/T = 1.5$  to the marginal zone lower than 1.0 and higher than 2.0.

(2) The model test in following/quartering seas, i.e. in irregular waves should include such dangerous conditions defined by the mean wave period and ship speed[5]. The V/T-diagram is useful to find such conditions. In performing the model test in such conditions, it is necessary to encounter the model to high wave runs, i.e. the design of test conditions is important. The numerical simulation of encountering waves beforehand the test will be effective. The examples of such model tests were carried out by Umeda et al. [6] and Hamamoto et al. [7].

### 5. CONCLUSIONS

By statistical analyses of encounter waves both in frequency and time domain, the remarkable increase of groupiness in following/quartering seas has been shown qualitatively as the function of  $V/T$  and number of waves in a high run. The degree of danger to encounter high run can be classified in the dangerous zone indicated in the operational guidance, and this result will be useful to evaluate ship stability against capsizing by probabilistic approach.

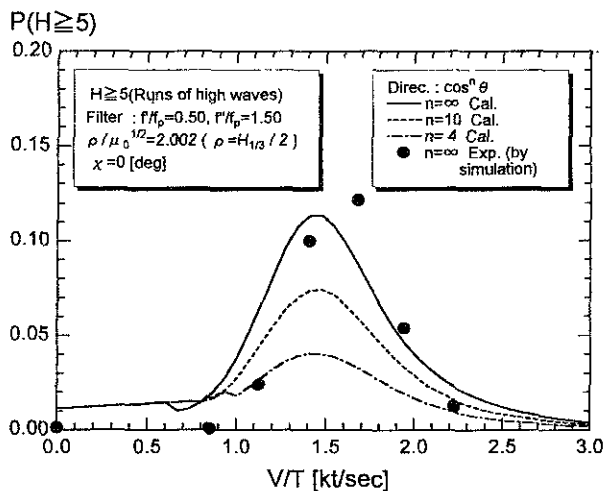


Fig.11 Probability of runs greater than 5

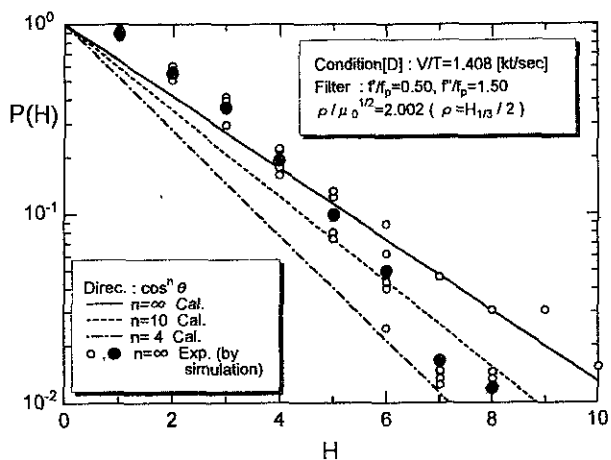


Fig.12 Probability of runs greater than H

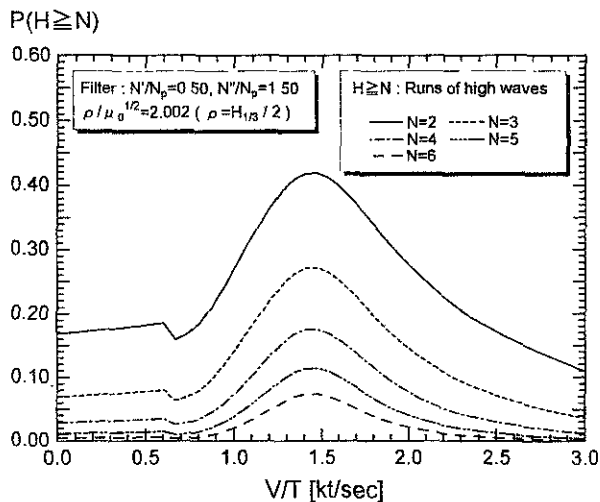


Fig.13 Probability of runs greater than N, N=2,3,4,5,6

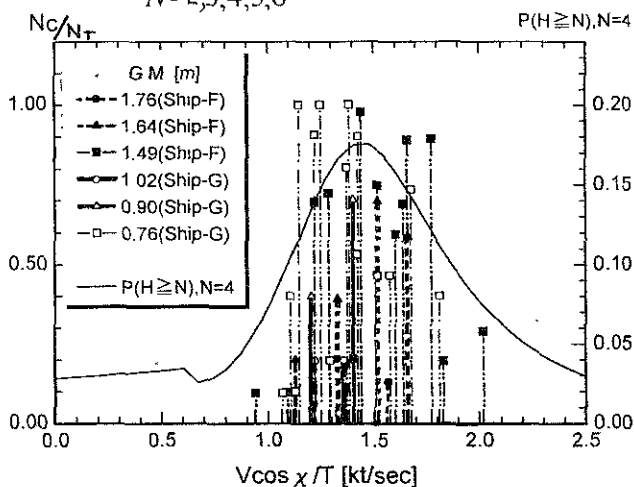


Fig.14 Capsizing rate ( $N_c/N_T$ ) and probability of runs ( $P(H \geq N=4)$ )

## 6. REFERENCES

- [1] Takaishi, Y.; Dangerous encounter wave conditions for ships navigating in following and quartering seas, Proc. of 5th STAB, Florida, (1994)
- [2] MSC Circular/IMO; Guidance to the master for avoiding dangerous situations in following and quartering seas, (1995)
- [3] Longuet-Higgins, M.S.; Statistical properties of wave groups in a random sea state, Phil. Trans. R. Soc. London, A 312, (1984), pp.219-250
- [4] Takaishi, Y., Watanabe, K., Masuda, K.; Statistical properties of encounter wave grouping phenomena in following and quartering seas, J. Society of Naval Architects of Japan, Vol.181, (1996), pp.283-294
- [5] Takaishi, Y. et al.; On wave condition for model experiments of ships in following and quartering seas, Journal of the Kansai Society

- of Naval Architects, Japan, Vol.225, (1996), pp.107-114
- [6] Umeda, N. et al.; Model experiments of ship capsizing in astern seas, J. Society of Naval Architects of Japan, Vol.177, (1995), pp.207-217
- [7] Hamamoto, H. et al.; Model experiments of ship capsizing in astern seas, 2nd Report, J. Society of Naval Architects of Japan, Vol.179, (1996), pp.79-87

## 7. ACKNOWLEDGEMENT

This work has been performed as a part of the research project RR 24 organized in the Shipbuilding Research Association of Japan. The authors would like to thank the advises and discussions given by Committee members, chaired by Prof. M. Fujino, The University of Tokyo.

# ASSESSMENT OF SAFE STABILITY IN OPERATION

Lech K. Kobylński

Foundation for Safety of Navigation and Environment Protection

Polish Academy of Sciences

14-200 Hawa-Kamionka, Poland

## ABSTRACT

During last decades a great deal of work was devoted to the development of design stability standards. They were finally adopted by IMO resolutions although ship designers and operators are fully aware that they do not constitute the ultimate solution. At present much attention is devoted to the operational aspects of stability including human factor, because it is well known that 70 to 80 per cent of casualties are caused by human failure. The author considers operational aspects of stability including human factor and discusses a set of methods and measures necessary to deal with the situation in order to safeguard safe operation in various weather conditions.

## 1. INTRODUCTION

During the last quarter of the century much more attention was paid to safety at sea and marine environment protection. In spite of the fact, that the number of serious accidents is constantly reducing, and, according to statistics of fatalities it could be seen that seafaring is not particularly dangerous enterprise in comparison with other activities, it is general feeling that shipping is not safe enough. Actually the probability of losing life during sea voyage is smaller than in road transport but still 15 to 20 ships of the total capacity of more than 100000 gross tonnage capsize each year (Lipis & Salov, [1]).

The most dangerous accidents at sea are those, where ships are lost, because usually in such casualties there are also numerous fatalities. Analysis of causes of such accidents reveals, that about 2/3 of ships are lost in casualties of the type CRG (collisions, rammings, groundings). In the second place there are fires

and explosions, in the third (about 19%) capsizings. The last although not the most frequent usually result in many fatalities because there is not enough time for rescue action. Quite often capsizing is a result of collision or fire.

Great deal of work was devoted during last decades to the development stability standards aimed at increasing safety at sea. In particular IMO was very active in developing and adopting recommendations on intact and damage stability standards, as e.g. Resolutions A.167, A.168, A.562. IMO developed also Code of Intact Stability for all Types of Ships (Resolution A.749), where all existing requirements concerning stability were incorporated. This resulted in the substantial progress in safety against capsizing. With a great deal of work devoted to developing design standards, much less attention was paid to operational factors which in majority of accident play the vital role. Therefore in this paper attention is drawn to the operational aspects of stability including effect of human factor.

## 2. BASIC PHILOSOPHY OF STABILITY STANDARDS

The existing stability standards including standards adopted by IMO are substantially design standards, i.e. they are supposed to be used when designing ships. However, if ships constructed satisfy the standards it does not mean automatically that they are safe. Analysis of stability accidents reveals, that ships which capsize sometimes satisfy standards; this is also obvious from the way how, for example, IMO standards were developed (Kobylinski, [2]). In order to reduce the probability of capsizing standards should be increased, this is, however,

impracticable from various reasons and even may cause dangerous behaviour in a seaway.

It was stressed by many authors and legislators, that from the point of view of stability to design fool-proof ships is unrealistic (Krappinger & Hormann, [3]) and that the problem of developing safety measures for stability of ships in a seaway is too complicated that it would be impossible to solve it once for all. This situation could be compared with the situation regarding estimation of ship resistance, where in spite of the fact that William Froude when constructing his first towing tank promised to solve problem of ship resistance in two years and we well know that more than hundred years later this problem is far from being solved.

Present international standards, as e.g. IMO Resolution A.167(ES.IV), are based on statistical comparison of design stability parameters for ships considered safe in operation and for those which capsized. In both cases stability levers were compared calculated for calm water condition in certain assumed loading condition, which is purely stipulated condition. Similarly, standard included in the Resolution A.562(14) (weather criterion) is also based on assumed wind pressure and wave slope values. If a ship is satisfying those standards in assumed worst loading condition intended by the owner it is supposed to be safe enough to be allowed to put into operation. The regulations require also that the position of the centre of mass of the ship has to be calculated on the basis of inclining test performed when the construction is finished.

The authors of the standards realised, however, that compliance with the standards is not sufficient for maintaining safety, and operation of the ship is vitally important as Res. A.167 (ES.IV) included the following statement:

„Compliance with the stability criteria does not ensure immunity against capsizing regardless of the circumstances or absolve the master from his responsibilities. Masters should therefore exercise prudence and good seamanship having regard to the season of the year, weather forecasts and the navigational zone and should

take the appropriate actions as to speed and course warranted by the prevailing circumstances” (IMO, [4])

The above statement reveals that operational factors were recognised as important issues in ensuring safety against capsizing. Nevertheless, rather few operational requirements were included into stability recommendations. It is clear, that operation of the ship depends on human abilities, i.e. so called „human factor” plays important role.

### 3. SYSTEM APPROACH TO SAFETY AND IMPORTANCE OF OPERATIONAL FACTORS

It is clear that in order to achieve safety it is not sufficient that the ship satisfies stability standards. It is necessary to consider safety as a system. This was proposed by the author several years ago (Kobylnski, [5], other scientists expressed the same opinion (Kastner, [6]). This idea was also adopted by IMO when Code of Stability for all types of Ships was developed (Kobylnski, [7]).

System of safety from the stability point of view should include at least four elements as proposed by Kastner [6], i.e. ship, cargo, environment and operation. These four elements are strongly interconnected and influencing each other as it is seen from Venn's diagram shown in Fig. 1.

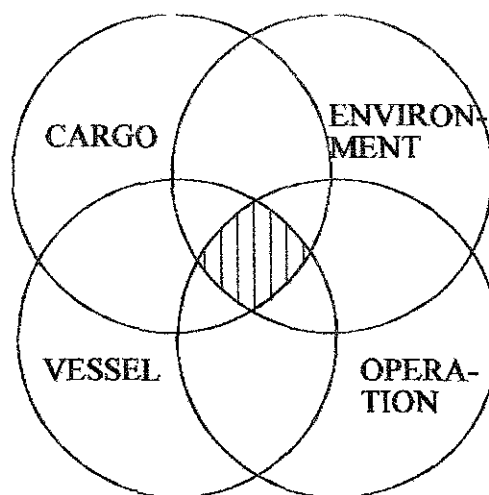


*Fig. 1. Venn's diagram showing four-fold interaction of elements in safety system [8].*

Operation is understood as human control of ship's stability and its safe handling. Therefore operation is related to human factor. Operation affects stability, which is also affected by environment and cargo. Kastner [6] defined operational stability in the following way: „Operational stability defines the actual stability status of the ship during her voyage, which varies in time due to changes in cargo and ballast of the ship, and due to changing environmental conditions at sea”

The role of human operator is to control the operational stability and take appropriate action in order to ensure safety.

Operation which includes human factor, according to some authors is responsible for 60 to 80% of all stability accidents (Manum, [9]), other sources stress definitely that about 80% of major maritime accidents are result of human and organisational errors (Bea, [10], U S Coast Guard [11]). The United Kingdom P&I Club performed an analysis of the claims filled in 1993 and estimated human errors to be primary cause of 62% of those accidents (Fig.2) (Boniface, [12]). From this it is clear that operation must be considered as the most important factor in achieving safety.

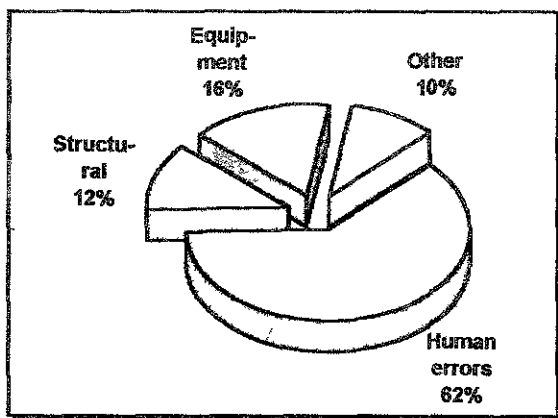


*Fig.2. Causes of major (>\$100 000 US) claims for all classes of commercial vessels*

The importance of operation factors has begun being recognised by international shipping community. IMO included human factor issue in its programme of work and already,

recognising organisation and management as being source of many human errors it adopted Safety Management (ISM) Code, which requires vessel operators to develop and implement a safety management system starting from 1998 (IMO, [13]). Also IMO recognised the necessity to introduce formal safety assessment in shipping as a way to increase safety at sea and a special working group was created to consider this issue which includes also human element (IMO, [14]). How it would be possible to introduce human factor, at least partially, to formal safety assessment in relation to stability was shown by the author (Kobylnski, [15]).

#### 4. FACTORS IN OPERATIONAL STABILITY.

Analysis of causes of serious accidents at sea reveals that in the majority of cases (about 80%) they can be attributed to human and organisational errors (HOE). The remaining 20% could be attributed to material and construction failures due to force majeure or other causes. Causes of marine accidents could be classified as shown in fig.3 (Payer, [16]). HOE could result from design, construction or operational factors. Design and construction are responsible for about 20% of all HOE failures, the rest are direct result of operation. HOE failures are influenced by the following factors:

- society - culture
- organisation
- individual
- system

##### Society-culture:

There is a strong influence of the society and its culture on the acceptable risk in human activity. In general, there is a pressure to reduce safety requirements and consequently to reduce safety factor and to increase risk on economic grounds because obviously safety costs more. From the pure economy there is, however, certain optimum safety index, because it must be taken into account that with the increased safety index investment and

operational costs also increase, but failure related costs decrease (see fig 4, Hutchinson, [17])

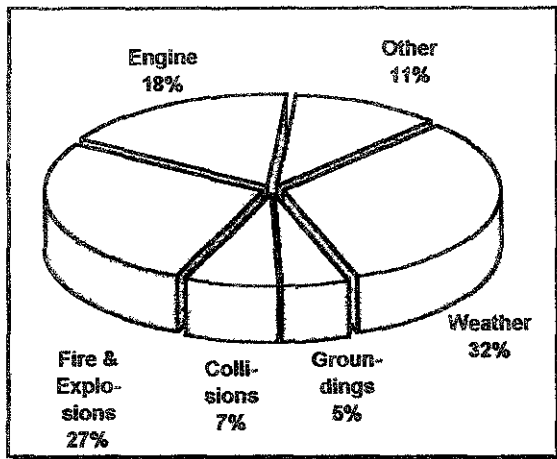


Fig. 3. Causes of serious accidents in percentage of the tonnage [16]

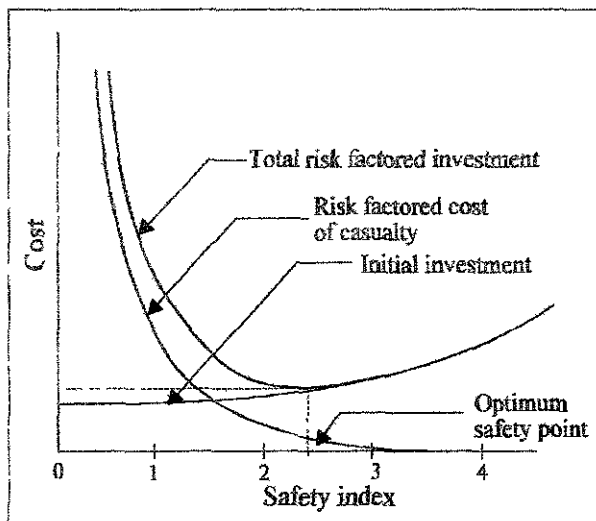


Fig. 4. Risk factored costs [17].

However safety index or risk calculated on the basis of pure economy might be intolerable from other reasons. Public opinion is a very mighty factor. Public opinion tend to tolerate many single fatalities, as e.g. car accidents but does not tolerate single accidents with number of fatalities (examples: HERALD OF FREE ENTERPRISE or ESTONIA casualties). Following the two casualties mentioned there was enormous pressure of public opinion moved by the great number of casualties to

revise and increase safety requirements. This was in spite of the fact, that as it may be seen from the statistics of fatalities sea transport is not particularly risky. (see Table 1) Public opinion must be considered as a very important factor influencing adoption of tolerable risk. However, the reaction of the public depend on where the casualty happened and what kind of people were involved. For example, the worst ever casualty at sea, the collision, fire and foundering of DONA PAZ ferry, where more than 4000 people died was hardly noticed by the public of the western world, because the casualty happened in Eastern Asia. Risk is the product of probability (or frequency) of accidents and their consequences, i.e.,

$$R = P \times C$$

For the estimation of tolerable risk ALARP (as low as reasonably practical) principle is applied. Method of application of ALARP principle is shown in fig 5

Table 1. Hourly mortality rates (FAR) for various activities (Data in this table were taken from [18&19])

Activity	FAR x 10 <sup>8</sup>
World fleet as a whole	11.8
Passenger aviation - crew	14.0
Aviation - passengers	1.4
Agriculture	10
Fishery	35
Coal mining	40
Car driving	70
Off-shore industry	76
Climbing	4000
30 years old men- all causes	15

### Organisation

A number of casualties are caused by mismanagement or bad organisation. Bad organisation may mean:

- lack of supervision
- lack of procedures

- lack of assisting means
- lack of activity of the administration
- lack of operational manuals
- lack of safety policy and motivation

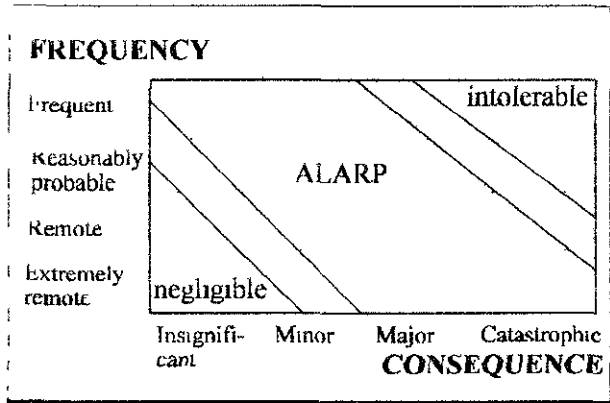


**Fig.5 Application of the ALARP principle**

The problems of organisation were well recognised by IMO which recently adopted already mentioned International Ship Management Code (IMO, [13]) The adoption of the ISM Code is to some extent closing the existing gap in safety requirement and certainly will increase safety, although this code is not directly mentioning stability

**Individual**

Errors of operators are often obvious cause of accidents. As the human error is well known, there is a tendency to make operators responsible for casualties. However, usually the casualty is the result of combination of individual and organisational errors. Moreover, the action of operator which depends largely on individual features of human being depends also on external conditions. There are many causes of human failure which are listed below

- fatigue
- negligence
- ignorance
- envy
- arrogance
- wishful thinking
- misjudgement
- bad intention

- slackness
- laziness
- boredom
- physical limits
- alcohol/drugs
- not seriousness
- lack of education

The above list by no means is exhaustive. The human failures increase under pressure and panic, they depend also on stress. Factors which influence decisions taken by operator depend on

- physical predisposition
- physical predisposition
- character, morale, integrity
- knowledge and experience
- training degree

The effect of personnel selection and training on crisis management is shown in fig 6 (Ship Structure Committee, [10])

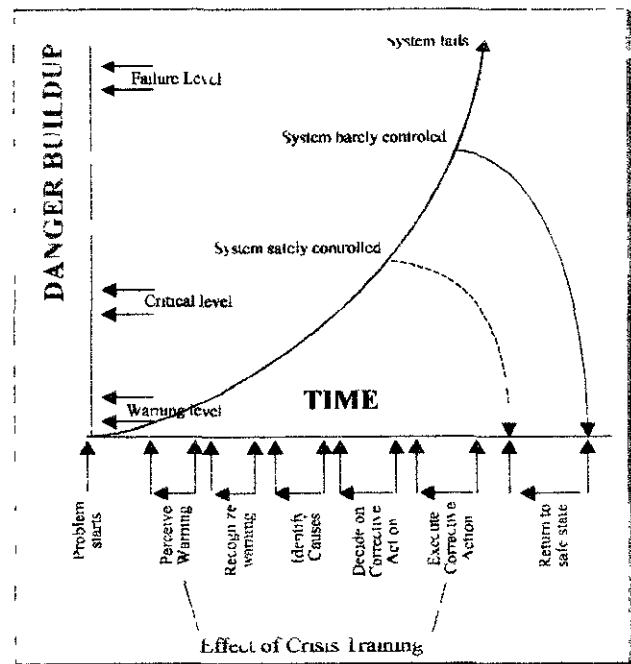


**Fig.6 Effect of personnel selection and training on crisis management.**

Reaction of the controller to critical situation could be divided in three phases: warning-considering of the decision-handling. System can not be controlled if the decision is taken to

late or the warning is too late or false or assessment of the situation is wrong

Human failures can not be eliminated entirely, but training, education, experience of the man at control can considerably reduce their number

### System

Safety system of stability consists of elements such as design stability standards, operational stability, stability control during operation, stability information and weather forecast and information. Also constructional features of the ship and securing of cargo form parts of the system

Design stability should satisfy standards established, so does operational stability as defined above. However, the important element of the system is the possibility to control the operational stability. Information on the actual stability during the voyage allows proper judgement of safety. There are several possibilities of control of stability in operation. They will be discussed in the following paragraphs. In some ways this is related to the information concerning stability supplied to the master. Such information is required by the provisions of SOLAS and also Load Lines Conventions, but the traditional form of such information requires improvement and modernisation.

Weather forecast and information constitutes important element of the safety system, because it allows the master to adopt appropriate tactics in avoiding heavy weather.

Stability safety system includes also Formal Safety Assessment (FSA), which in itself could form a basis for development of more rational stability standards. FSA includes hazard identification, overall risk evaluation, assessment of tolerable risk, development of safety requirements on this basis and safe operation (IMO, [20]). This is, however, a separate subject which is not discussed here. It might be only mentioned, that quite recently IMO decided to start work on requirements concerning FSA and a special working group for this purpose was created (IMO, [21]).

## 5. STABILITY CONTROL IN OPERATION

There are several possibilities to control ships stability during service. They are well summarised by Lipis & Salov, [1], who divided those possibilities in two large groups, namely methods utilising calculation based on recorded cargo data and methods utilising instruments to measure actual ship stability. The first group could be further subdivided in personal means (manual calculations or computer calculations), and special devices for assessment of stability (mechanical devices, electro-simulators, cargo loading computers etc.)

All methods involving calculation, whether manual or using special devices i.e. the first group are based on data on the position of centre of gravity of the empty ship and on cargo mass and distribution. They are therefore encumbered by errors in estimation both quantities. In particular mass and position of centre of gravity of the empty ship is changing with its age. It is also changing during the voyage because of consumption of fuel, water and storage. All devices in this group facilitate only estimation of stability but in fact they do not allow assessment actual stability during the voyage.

There are many types of instruments available based on measurement of certain ships parameters during the voyage or when leaving the port. Parameters measured at sea could be rolling amplitude, rolling period, acceleration and inclining moment (executed by using water tanks or other means). The simplest method is measurement of rolling period of the ship before commencing the voyage. This method was recommended by IMO. This method is, however, not very accurate because of the uncertainty concerning radius of inertia of the ship. Conventional inclining test belongs to this category but it is usually performed before ships commissioning or after major alterations. Kaps and Kastner [22] proposed to perform inclining test before commencing each voyage. They call it operational inclining test (OSI). Fig 7 shows that operational stability estimated

this way is much more accurate than normally used estimation based on calculations

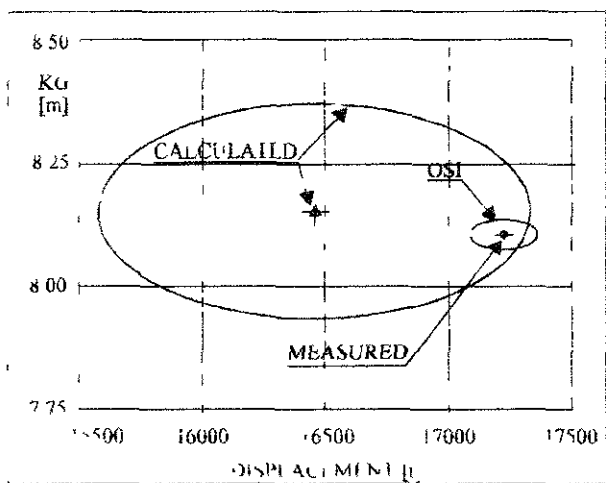


Fig 7. Random error ellipses at 95% confidence level for KG versus displacement (after [22]).

This very simple method not requiring elaborate instrumentation could be recommended as a measure to increase safety

## 6. INFORMATION AVAILABLE ONBOARD

As already mentioned, SOLAS and Load Lines Conventions require that information concerning stability has to be supplied to the master. They do not, however, specify the content and form of such information. Resolution A 167(ES IV) of IMO is more specific in this respect, so is recently adopted Code of Stability for all Types of Ships (IMO, [23]). It is obvious, that information on stability is vital for the master to operate his ship safely. The format of this information should be such, that necessary data could be obtained in the easiest possible way which is important especially in emergency situations. IMO has still in its work programme the subject of stability information. Within this item there should be also considered, apart from traditional format of a booklet, application of various instruments and computers facilitating calculations

There is, however, other aspect of information. This consists of information on how to navigate in adverse weather conditions. First of all master should adopt tactics of avoidance heavy weather which could bring the ship in a dangerous situation. This requires long term weather forecast provided by weather service. In most seas such service already does exist, the problem is the accuracy of forecasts.

Once the ship is sailing in confused seas, the master should adopt tactics of avoiding dangerous combination of ship heading against waves and speed. The danger may consist of excessive (resonant) rolling, slamming, excessive deck wetness, loss of control, etc. Quite recently IMO adopted the recommendation in the form of a diagram showing dangerous combinations of ship heading and speed where excessive rolling may occur (IMO, [24]). This is, however, the first step in this direction, further effort is anticipated and in future probably computer systems will be developed allowing to assess properly and accurately situations from the point of view of all adverse effects.

It seems that in the future the information provided for the master and crew on stability will be much more elaborate. For future large vessels, especially for high speed ships the pattern adopted in commercial aviation might be useful. Definite proposal was made by Jullumstroe, [25] in this respect. The information according to this proposal should consist of

- pilot manual
- operation manual
- routing manual
- transport manual

## 7. TRAINING

The impact of training and education of operators is well recognised. Nevertheless, recently adopted STCW Code (IMO, [26]) when specifying minimum standards of competence for officers in charge of navigational watch on ships of 500 gross tonnage and over, mentions in respect of stability only three items

- working knowledge and application of stability and stress tables, diagrams and stress calculating equipment
- understanding of fundamental actions to be taken in the event of partial loss of intact buoyancy, and
- understanding of the fundamentals of watertight integrity

The same Code requires little more from masters and chief mates, namely

- understanding fundamental principles of ship construction and the theories and factors affecting trim and stability and measures necessary to preserve trim and stability,
- knowledge of the effect on trim and stability of a ship in the event of damage to and consequent flooding of a compartment and counter measures to be taken, and
- knowledge of IMO recommendations concerning ship stability

This hardly sufficient, because no special training on stability matters is anticipated such, as for example, is required with respect to manoeuvrability. It seems, that special courses on stability have to be required, possibly using stability simulators simulating behaviour of ships in heavy weather conditions. Such simulators do not exist at present, but nothing prevents their development and marketing in near future. It is important that they should simulate emergency situations as the most important part of the training should be management of emergency situations

## 8. REFERENCES

[1] Lipis, V B, Salov, V Y Problem of the Stability Control of Transport Ships in Operation, Fourth International STAB'90 Conference Proceedings, p 66, Naples 1990

[2] Kobylinski, L K Safety of Ships Against Capsizing, Third International Congress on Marine Technology, Athens'84, Vol I, p 387, 1984

[3] Krappinger, O, Hormann, H Problemstellung und Lösungsansätze Jahrbuch der STG, Vol 78, p 205, 1984

[4] Recommendation on Intact Stability for Passenger and Cargo Ships under 100 metres in Length, IMO, Resolution A 167(ES) IV 1968

[5] Kobylinski, L K Philosophische und Hydrodynamische Probleme der Internationalen Kenterkriterien von Schiffen, Internationales Schiffstechnisches Symposium Rostock, 1984

[6] Kastner, S Operational Stability of Ships and Safe Transport of Cargo Through International STAB'86 Conference Proceedings, Vol I, p 207, Gdansk 1986

[7] Kobylinski L K Code of Stability for all Types of Ships Based on System Approach Fourth International PRADS'89 Conference Varna 1989

[8] Kastner, S Inclusion of Theoretical Achievements on Ship Stability in Ship Design Process and in Ship Operation, Fourth International STAB'90 Conference Proceedings, Vol II, p 677

[9] Manum, I A What Have Guided International Activities on Intact Stability Problems so Far? Are Chances Needed? In what Direction? Fourth International STAB'90 Conference, Proceedings, Vol II p 667

[10] Bea, R The Role of Human Error in Design, Construction and Reliability of Marine Structures, Ship Structure Committee Report SSC-378, Washington, DC, 1994

[11] US Coast Guard Prevention Through People Quality Action Team Report Department of Transportation, Washington DC, 1995

[12] Boniface, D E, Bea, R G Assessing the Risk of and Countermeasures for Human and Organisational Error, SNAME Proceedings, 1996

[13] International Ship Management Code IMO, 1996

[14] Formal Safety Assessment Draft guidelines for FSA application to the IMO rule-making process, IMO, doc MSC 08/14 1996

[15] Kobylinski, L K Possibility of Application of Safety Assessment to the Development of Stability Criteria, US Coast

- Guard Vessel Stability Symposium. New London, 1995
- [16] Payer, H G Schiffssicherheit und das menschliche Versagen, Hansa-Schiffahrt-Nachrichten, Vol 131 Nr 10 1994
- [17] Hutchinson B L Cargo Mechanics (Application of Seakeeping- Revisited), Marine Technology, Vol 23, No 3, 1986
- [18] Caldwell, J B Prospects of a Rational Approach to Marine Safety, The Fourth International Shipbuilding and Ocean Engineering Conference, Helsinki 1986
- [19] Fitzgerald, B P, Grant McD M A Practical Methodology for Risk Assessment of Offshore Installations, Offshore Operations Post Piper Alpha Conference, 1 Mar L/RINA, 1991
- [20] Formal Safety Assessment Submitted by United Kingdom IMO, doc MSC 66/14, 1996
- [21] Formal Safety Assessment Draft Guidelines for FSA application to the IMO rule-making process, IMO, doc MSC 67/13, 1996
- [22] Kaps, H, Kastner, S On the Determination of Ship Stability during Service, fourth International STAB'90 Conference, Proceedings, Vol I, p 226, Naples 1990
- [23] Code of Intact Stability for all Types of Ships Covered by IMO Instruments, IMO, Resolution A 749(18), 1995
- [24] Guidance to the Master for Avoiding Dangerous Situations in Following and Quartering Seas IMO, MSC Circular 1995
- [25] Jullumstroe, E Stability of High Speed Vessels, Fourth International STAB'90 Conference, Proceedings Vol I, p 522, Naples 1990
- [26] International Convention on Standards of Training, Certification and Watchkeeping for Seafarers 1978 Seafarers' Training, Certification and Watchkeeping (STCW) Code, IMO, 1995

# SHIP CRANKINESS IN FOLLOWING SEAWAY AND STABILITY REGULATION

by Prof. N. Rakhmanin, Dr. G. Vilensky  
Krylov Shipbuilding Research Institute,  
St. Petersburg, Russia

## ABSTRACT

Below the analysis is given in relation to existing approaches to development of stability criteria for the case of ship sailing in following seas. Ship crankiness is considered on the basis of modern theory of ship motions and the corresponding numerical measure for this phenomena is found. Namely it is assumed to use the amplitude of steady parametric rolling motion as such a measure. Finally it is suggested the new idea to check ship stability in following seaway condition by means of the criterion which supposes to restrict above mentioned parametric roll amplitude.

## NOMENCLATURE

$L$  — ship length,  
 $V$  — ship speed,  
 $\lambda$  — wave length,  
 $\zeta$  — wave ordinate,  
 $H_{1/3}$  — significant wave height,  
 $\chi$  — wave heading angle,  
 $GM_0$  — metacentric height,  
 $\Delta GM$  — metacentric height increment in waves,

$GZ_{\max}$  — maximal arm of stability curve,  
 $\phi_v$  — vanishing angle of stability,  
 $\phi$  — instant roll angle,  
 $\omega_e$  — encounter frequency,  
 $n_\phi$  — natural roll frequency,  
 $n$  — integer,  
 $\nu_{\phi_0}$  — nondimensional roll damping coefficient,  
 $\phi_0^{par}$  — z parametric roll amplitude,  
 $(\phi_0^{par})_{\max}$  — maximal parametric roll amplitude,  
 $\phi_0^{norm}$  — agreed margin for parametric roll amplitude

## 1. INTRODUCTION

The problem of providing for safe ship navigation while sailing in following seaway is still actual today, although it started to draw the attention of the specialists as far back as in the mid-fifties. A great deal of knowledge has been accumulated in the field of stability and ship behaviour dynamics under the conditions of following seaway, the unfavourable and dangerous situations which the navigator may meet at sea have been systematized, and certain recommendations which help the captain to escape

some dangers of navigation under such conditions have been found. However, the variety of mentioned dangerous situations and the difficulty of their mathematical description create not a few obstacles on the way of searching for practically acceptable standards of ship safety in following seaway. These standards must reflect the most essential connections between safety criteria and those ship constructional characteristics the change of which on a design stage permits to eliminate the capsizing.

Even not full enumeration of the names of scientists who dealt with the problem shows its complexity and variety. In Russia - S.N. Blagoveschensky, I.K. Borodai, V.V. Lugovskoy, N.V. Sevastianov, Y.I. Netchaev, D.M. Ananiev, N.Y. Maltsev, V.N. Saltovskaya, Y.L. Makov, in other countries - B. Arndt, K. Vendel, O. Grim, J. Paulling, S. Kastner, S. Motora and in recent years S. Renilson, N. Umeda, G. Thomas, M. Kan have made a great contribution to the investigation of the problem. Reviews of works and publications on the discussed theme are available in books [4,7] and in proceedings of the International Conference on Stability of Ships and Ocean Vehicles of 1990 and 1994, e.g. [27].

The fact of stability reduction when a ship is on the crest of a wave is wellknown. The stability decrease influences the whole range of heeling angles and can entail the capsizing of a ship. In this respect the situation is the most dangerous when the ship's speed and length are equal to the wave's speed and length. This happens when the Froude numbers are close to 0.4.

The phenomenon of "broaching" of a ship, which is joint riding and broaching on a following wave, presents another danger for a ship in following seaway [8]. Waves give an additional

energy to a ship which moves on quartering waves. When a ship's length equals to a wave's length, this energy could be sufficient for a ship to move together with the wave. In a riding position the ship may lose its course stability and spontaneously turn beam to the waves. Large dynamic heels fraught with a capsizing often arise at this. However, these heels are by no means related with stability decrease on the wave crest and are the result of external dynamic moments which arise in the process of spontaneous broaching.

This situation is especially important for small fishing vessels or ships of other types (with the length  $L \leq 60$  m) in connexion with their relatively high Froude numbers and frequent operation under seaway conditions of  $\lambda \geq L$ . The Rules of Register [14] (see 3.9.11 part IV "The Stability") for Small Vessels provide for speed limitation in a following wave, which length is equal or more than the vessel's length, to  $1.4 \sqrt{L}$  in knots for this reason. At this the vessel's speed will be 0.58 or less of wave phase speed and as a rule the riding on wave could be avoided [12].

According to [4], "except for two above mentioned factors which accompany the ship's sailing in following seaway, namely the stability decrease and course instability with broaching, in some cases parametrically excited roll may present a certain danger for the ship safety".

It was generally accepted [10] in the end of seventies, that with parametric excitation the rolling motion amplitudes do not increase infinitely according to the well-known solution of Mathieu equation for unstable region but stay limited because of nonlinearity of the restoring and the

damping moments. In other words the parametric rolling in following seaway was considered only as a circumstance decreasing the ship's resistance to external heeling moments but not as a direct danger for its safety [4,10].

It appeared as a result at present time that with rare exception most of the national rules of stability are lack of criteria which reflect directly the physics of those dangerous situations which arise from sailing in quartering waves. As a rule indirect recommendations could be found like in the 3.9.11 part IV "The Stability" of the Rules [14], which deal with the option of safe speed and wave heading angle or one can find common warnings in general. For example we can refer to the IMO Code of Intact Stability for All Types of Ships [17] and IMO Guidance for a Captain with recommendations for ship operation in order to escape dangerous situations while sailing in quartering waves [27].

The first evidence of that following seaway can create troubles for large modern ships of merchant fleet with the length  $L \geq 100$  m have appeared in IMO on the border of seventies and eighties, when the Organization started its work on review of the stability requirements for transport ships on the basis of introduction of a weather criterion to the international practice. The German Delegation has repeatedly drawn the attention of the IMO Subcommittee on Stability and Load Lines to the dangerous crankiness of containerships in following seaway and to the necessity of this problem to be researched for large ships. The Head of the Ship Safety Division, Germanischer Lloyd Mr. W. Hausler, the Member of German Delegation for the Subcommittee has repeatedly spoken about the reports the Division received

about container losses in the open sea because of unexpected heeling angles about  $30^\circ - 45^\circ$ . Against the back-ground of the usual small rolling motion typical for sailing in following seaway [6] these heels without a visible reason (such as a wind squall or riding on wave which is unlikely for large ships) could throw the crew down into panic. And it must be noted that it is not without the reason.

In the middle of the eighties the sufficiently reliable experimental and gained with numerical simulation theoretical data appeared confirming the possibility of the ship's capsizing in the strictly following seaway only as a result of roll in the regime of parametric resonance, which arises because of periodical stability alterations. In particular Prof. Paulling [26] demonstrated the danger of the main parametric resonance by means of seaway dynamics analysis of the "Mariner" type ship with the stability curve that meets all the IMO requirements for intact condition. Fig.1 gives an idea of the capsizing dynamics, the calculation results are shown with dots, and the model test

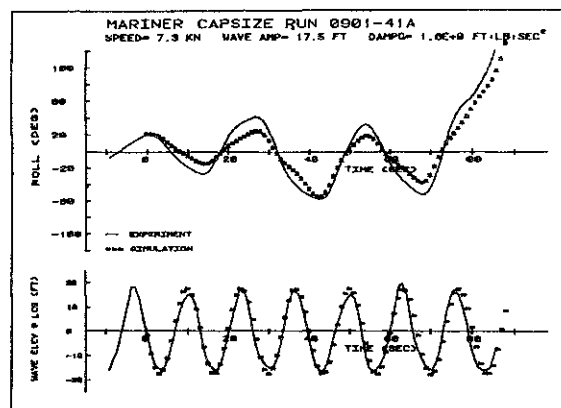


Fig.1. The results of experimental and numerical determinations of rolling motion amplitudes in the following seaway in the regime of main parametric resonance [26]:

— - the experiment; ■ - modelling;

data are shown with continuous lines. As it could be seen the fatal inclination can occur after 3 - 4 roll double amplitudes and it is practically impossible to escape it by changing the ship's course.

Analogous results were received during the tests with radio-operated self-propelled models in the Sevastopol Bay [9] and in seakeeping basin [20].

It followed from these tests that during sailing under storm conditions with medium wave lengths equal to ship's length the risk of dangerous inclination of a ship subjected to crankiness may appear rather high, within the limits of 1/100 to 4/1000, if the significant waves (exceedance probability  $\sim 14\%$ ) are taken for large ones. This is much higher than the probability of a road accident for a car passenger within a 1 year period ( $\sim 10^{-3}$ ).

In spite of all mentioned the design situation assuming the ship sailing on the following wave crest, with the wave's length approximately equal to the ship's length, nowadays finds its direct reflection only in the National Standards for the German Navy ships [18], [19], [22].

This situation is not formulated in the Rules of Russian Shipping Register, but it follows from the Annex explaining the principles of composing these Rules [13], where the lower limit for maximum curve arm is recommended. One can find analogous requirements in the Japanese Rules of Stability for passenger ships.

Besides it is necessary to mention a number of proposals, which didn't find their reflection in the practical Rules, but which are instructive from the methodical side [3, 15, 16, 21, 23, 24]. Most of them are connected with the efforts to create the criteria of sailing safety in

following seaway on the basis of using the main weather criterion idea [2]. The extreme strictness of criteria that have been found in this way prevented from their practical use.

The second group of works [3], [21] paid attention to the alterations of ship's hydrostatic characteristics under the conditions of sailing in following seaway without additional external actions. As a whole the criteria established in this case being useful as a generalization of certain experience bear rather relative character and not always help to correctly foresee the danger connected with following seaway. Striving for evaluation of the latter danger on the basis of dangerous phenomena characteristic of sailing under these conditions leads either to unjustified severity of stability requirements [21] or, on the contrary, permits the reduction of stability to rather low limits excusing this possibility with its short duration if the course and speed [3], [11] are properly chosen.

This approach may appear to be inadmissible for a cranky ship. Resonance roll excited by means of short-term but deep alterations of the restoring moment under the conditions of following seaway together with an insufficient level of stability in such seas may itself as it has been mentioned lead the ship to capsizing in the course of several cycles of oscillations. In this case the crew will have no time to alter the course or the speed for safe ones.

## 2. SHIP CRANKINESS

Crankiness as a characteristic of a ship to show big inclinations to the side without visible external reasons can be explained fully enough from positions of the modern ship motions theory

by the ship's heeling dynamic instability which originates as a result of periodical alterations of her stability while sailing in seaway. It especially reveals itself when the ship moves in following or quartering waves.

The problem of roll caused by the variability of the restoring moment comes to well-known Mathieu equation, which has been repeatedly discussed in shipbuilding literature [1], [4], [25], [26]. From the theory of these equations it is known, that under certain combination of its parameters characterizing the roll damping  $\nu_{\phi_0}$ , the natural roll frequency  $n_{\phi}$  and the depth of stability modulation  $\Delta GM/GM_0$  the unstable, prone to increase roll oscillations may appear. The regions of unstable equation solutions pointing to the ship crankiness are located in vicinities the following relative frequencies:

$$\frac{\omega_e}{2n_{\phi}} = \frac{1}{n} \quad (1)$$

where  $n = 1, 2, 3 \dots$

The case, when  $1/n = \infty$ , i.e. the apparent frequency of encounter  $\omega_e \rightarrow 0$ , corresponds to the static equilibrium condition of a ship with reduced or lossed stability. This is reflected by an evident relation for static instability

$$\frac{\Delta GM}{GM_0} \geq 1 \quad (2)$$

For small values of initial stability  $GM_0/B < 0.02-0.03$ , which is characteristic for cranky ships, this relation is realized with a high degree of probability.

When the value of apparent frequency  $\omega_e$  differs from zero the possibility of realization of different unstable solutions of the Mathieu equation is not the same. For small roll damping values  $\nu_{\phi_0}$  and small disturbance levels  $\Delta GM/GM_0$  the width of unstable regions is proportional correspondingly to  $(\Delta GM/GM_0)^n$ , and the depth of stability modulation necessary for unstable roll evolution (the threshold of parametric roll excitation) appears to be proportional to the 1-st or 1/2 degree of roll damping coefficient. In particular, the excitation threshold for the main parametric resonance ( $n=1$ ) is determined by condition [1].

$$\frac{\Delta GM}{GM_0} \geq 4\nu_{\phi_0} \quad (3)$$

For monohull ships without bilge keels the nondimensioned linear roll damping coefficient  $2\nu_{\phi_0}$  is within the limits of 0.05-0.10, therefore condition (3) seems to be easier realized than the static instability condition (2) and manifests itself in a rather wide range of the parameter  $\Delta GM/GM_0$  values.

Not only the above mentioned results which determinethe crankiness presence or absence and the frequency regions where parametric role may occur are know nnowadays, but the calculation techniques to determine the amplitudes of such rolling motion are developed, which give an idea of crankiness degree and its danger [5, 16, 25, 26].

J. Kerwin [25] calculated the rolling motion amplitudes in the main parametric resonance regime on the basis of Mathieu equation and has taken into consideration the nonlinear

character of roll damping by means of binomial formula use with linear and quadratic terms for resistance law. Specialists from Poland [16] considered the nonlinear character of the restoring moment at the linear law of roll damping. J. Paulling [26] researched the nonlinear in damping and restoring moment roll equation numerically having taken the stability alteration in seaway into consideration, and got satisfactory agreement with the test (see Fig.1). G. Vilensky [5] established general analytical solution of nonlinear roll equation for the case of ship sailing in regular following and quartering waves. Here the stability curve form and its modulation were expanded successfully into trigonometrical series, and the disturbing wave moment and static wind moment were taken into consideration.

Calculated research [5] and model tests in seakeeping bassin demonstrated that under the conditions of purely following seaway the parametric roll with frequency  $\omega_e$  is significantly lower than the roll which occurs with frequency  $\omega_e/2$ . However, the parametric excitation with

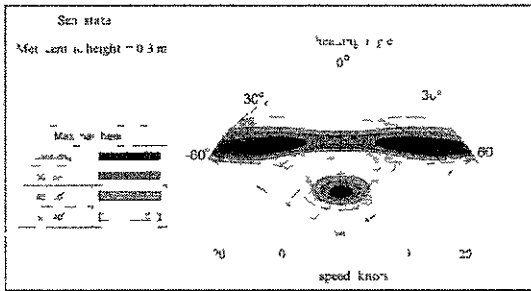


Fig.2. Relation between maximal heeling angles during the parametric roll  $(\phi_o^{par})_{max}$  and ship's speed and course angle  $\chi$  to the wave:  $GM = 0,3 \text{ m}$  - metacentric height;  $H_{1/3} = 6,5 \text{ m}$  - significant wave height.

frequency  $\omega_e$  in the stern quartering waves can be summed up with the resonance effect of the exciting moment. This case of combinational resonance (see Fig.2) doesn't coincide with known solutions of equation and may lead to dangerous heeling angles ( $\sim 60^\circ$ ). The essential part of zero harmonic (a constant component) is characteristic for this mode of resonance. The considerable constant component increasing the ship crankiness appears even without the wind[5].

Recent experimental and calculation research by means of analytical method [5] executed in the Krylov Research Institute confirmed the known facts, that rolling motion parametrically excited in following seaway can be developed right up to the capsizing. It was found

that with the relation  $\frac{\Delta GM}{GM_o}$  increase and the coefficient  $\nu$  decrease maximal inclinations or crankiness of a ship increases, the range of apparent frequencies of encounter at which the mentioned roll regimes exist widens, and the rate of their amplitudes growth increases.

Known opinion has been confirmed that the parametric resonance in the regime of  $\omega_e/2$  is not dangerous in head seas. In this case it arises with a sufficiently high stability and consequently relatively small  $\Delta GM/GM_o$ , high natural frequencies  $\Omega$  and occurs with small amplitudes or doesn't occur at all. On the contrary, rolling motion that arises in the main parametric resonance regime in following seaway is as a rule several times higher in amplitudes than the usual one caused by the exciting moment and serves as an indication of dangerous ship crankiness.

As an illustration for above said Fig.3

demonstrates the results of a three-meter multipurposed bulkcarrier model test under unfavourable loading case connected with container transportation on the upper deck ( $GZ_{max} = 0,35$  m, vanishing angle of stability

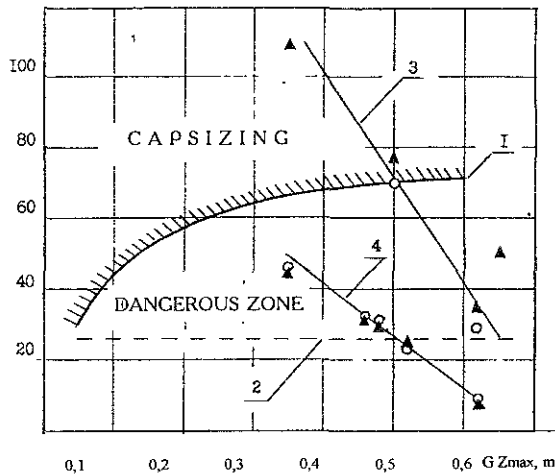


Fig.3. Relation between maximal parametric roll amplitudes in following seaway and the stability curve maximal arm value in calm water according to test — ( o ) and to calculation [25] — ( ▲):

1 - vanishing angle line; 2 - line of agreed heeling angles limitation; 3 - data for models without bilge keels; 4 - data for models with keels.

curve -  $65^\circ$  and  $GM_0 = 0,67$  m). The tests were carried out to evaluate a ship's crankiness with various modifications of the constructional elements and model loading, and also in order to work out the recommendations for limitations of crankiness during sailing in purely following waves of sea state wave ( $H_{1/3} = 6,5$  m). The experimental data correlate quite well with the maximal roll amplitude values in the main parametric resonance regime calculated with consideration of Kerwin's recommendations [25]. Fig.4 demonstrates the

variation of parametric rolling motion amplitudes versus the ship's speed, and the calculated values for the amplitudes of 3% exceedance probability of usual forced ship roll in irregular quatering seaway while sailing at resonance course angles.

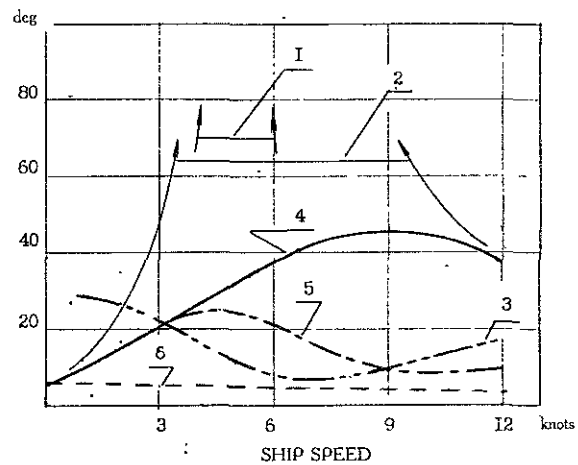


Fig.4. Relation between parametric roll amplitudes in following seaways and ship's speed according to model test data:

1 - the range of capsizing with  $GZ_{max} = 0,5$  m and without keels; 2 - the same with  $GZ_{max} = 0,35$  m; 3 - the curve for a ship without keels with  $GZ_{max} = 0,62$  m; 4 - the ship with keels and  $GZ_{max} = 0,35$  m; 5 - the ship with keels and  $GZ_{max} = 0,62$  m; 6 - maximal forced roll amplitudes at resonance course angles.

The analysis of data shown in Fig.3 and Fig.4 demonstrates that:

Firstly, the amplitudes of parametric roll are appreciably higher than the amplitudes of forced rolling motion. At resonance conditions this difference can achieve 10 times, if the rolling motion is not completed with capsizing;

Secondly, it is seen that the amplitudes of parametric roll are rather sensitive to the alteration

of parameters characterizing the rolling motion excitation threshold (3), and for this reason it is very convenient to use them as a measure for ship's crankiness. The latter can be controlled at the design stage by the rational selection of a hull form (in order to reduce the relative depth of stability curve modulation), by means of the bilge keels area increase, and during the operation - by means of stability increase and as well by means of rational alterations in speed and course angle;

Thirdly, the possibility and the expediency of maximal parametric roll amplitude values limitation becomes clear.

It is evident, that ship's crankiness may be considered as a safe one, if its measure  $(\phi_o^{par})_{max}$  does not exceed reasonable limitations (Fig.3).

The authors consider that in this way the real enough and physically well-founded criterion for the following seaway may be achieved as

$$(\phi_o^{par})_{max} \leq \phi_o^{norm} \quad (4)$$

At this the following value can be taken as a norm of crankiness:

$$\phi_o^{norm} = k \cdot \phi_{lim}$$

where  $\phi_{lim}$  - is maximal allowed heeling angle, for instance equal to the stability curve vanishing angle, or to shift cargo angle, or to flooding angle and so on depending on which is less;

$k$ - is coefficient which takes into account the inaccuracy of roll amplitudes calculation scheme, in particular the error in roll damping coefficient

determination, stability alterations in seaway or test errors in the case of experimental amplitude determination  $(\phi_o^{par})_{max}$ .

The criterion proposed takes into consideration rather important specific character of rolling motion in the following and quatering course angles and head wave course angles either. The meeting this criterion does not exclude the possibility of additional ship stability check-up under the conditions of durable decrease of the restoring moment at sailing in following seaway using other rational criteria or the requirements official Stability Rules. At the same time it may be expected that with reasonably selected crankiness level the ship's safety will increase to some degree also in other hard situations related to following seas, for example in the situations of broaching or riding on wave.

#### Literature

1. Basin A.M. Ship Motions. Moscow: Transport, 1969, 272 p.
2. Blagoveschensky S.N. National requirements to intact stability. In coll. "Theoretical and practical questions of stability and subdivision of ocean ships, Register of USSR, Moscow - Leningrad: Transport, 1965, pp.3-52.
3. Bogdanov A.I. Regression formula for calculation of stability alteration in following seaways coefficient, Reports thesises. Scientific and Technical Conference "Krylov's Readings-93", St. Petersburg, 1993, pp.71-74.
4. Borodai I.K., Netsvetaev Y.A. Ship Seakeeping. Leningrad: Shipbuilding, 1982. 288p.
5. Vilensky G.V. Reasons of dangerous roll in

- following seaway. In proceed. of International Shipbuilding Conference on centenary of Krylov Research Institute. Section V - Hydrodynamics of ships. St. Petersburg: 1994 , pp.265-271.
6. Kublanov Y.M. , Rakhmanin N.N. On the question of angle energetical surface waves spectrum and its utilization in shipbuilding calculations. Scientific and Technical coll.: The Questions of Shipbuilding, seria: "Ship Design". Issue 10. Leningrad: Scientific Research Institute "Rumb", 1976, pp.3-12.
7. Lugovsky V.V. Nonlinear problems of ship seakeeping. Leningrad: Shipbuilding, 1966, 235 p.
8. Lipis V.B., Remez Y.F. Safe regimes of ship navigation in the storm. Moscow: Transport, 1982, 117 p.
9. Medved A.F. The research of general behaviour and capsizing of radio-controlled models in natural seas. Cybernetics on the ocean transport. Issue 9 . 1980, pp.55-60.
10. Netchaev Y.I. Ship stability in following seaway. Leningrad: Shipbuilding, 1978, 272 p.
11. Nogid L.M. Ship's stability and ship's behaviour in seaway. Leningrad: Shipbuilding, 1967, 241 p.
12. Sevastyaniov N.V. Fishing vessels stability. Leningrad: Shipbuilding, 1970, 255 p.
13. The Register of the USSR. Rules for classification and building of ocean going ships, part IV "The Stability". Leningrad: Transport, 1977.
14. The Register of the USSR. The Rules of Classification and Building of Ocean Going Ships. Leningrad: Transport, 1990, pp.406-496.
15. The Register of the USSR. The method of stability evaluation in following seaway. Leningrad: Transport, 1977.
16. Register of Ships of Poland. The development of calculation and evaluation methods for intact ship stability in following seaway. Theme 5.4 m-1, plan N 5. Gdansk, 1984.
17. Code of Intact Stability for all Types of Ships Covered by IMO Instruments. Annex to Report of Ad hoc Intact Stability working Group, SLF-36/3, July 1991.
18. Arndt B. Ausarbeitung einer Stabilitätsvorschrift für die Handelsmarine. Jahrbuch der STG, 59 Band, 1965.
19. Arndt B., Brandl H., Vogt K. 20 Years of Experience Stability Regulations of the West-German Navy. 2nd International Conference on Stability of Ships and Ocean Vehicles, proceedings. Tokyo: 1982, hh.765-775.
20. Allievi A.G., Calisal S.M., Rohling G.F. Motions and Stability of a Fishing Vessel in Transverse and Longitudinal Seaways, proceedings. 11th Ship Technology and Research (STAR) Symp., 1986.
21. Blume H., Hattendorf H. An Investigation on Intact Stability of Fast Cargo Liners, proceedings. 2nd International Conference on Stability of Ships and Ocean Vehicles. Tokyo: 1982, pp.171-183.
22. Grim O. Rollschwingungen , Stabilität und Sicherheit im Seegang, Schiffstechnik. V.1, 1952, S.10-15.
23. Helas G. Intact Stability of Ships in Following Waves, proceedings. 2nd International Conference on Stability of Ships and Ocean Vehicles. Tokyo: 1982, pp.669-700.
24. Martin J., Kuo Ch., Welaya Y. Ship Stability Criteria Based on Time-Varying Roll Restoring Moments, proceedings. 2nd International Conference on Stability of Ships and Ocean Vehicles. Tokyo: 1982, pp.227-242.

25. Kerwin J.E. Notes on Rolling in Longitudinal Waves. International Shipbuilding Progress. V.2, n 16, 1955, pp.3-27.

26. Paulling J.R. A Comparison of Stability Characteristics of Ships and Offshore Structures, proceedings. 2nd International Conference on Stability of Ship and Ocean Vehicles. Tokyo: 1982, pp.581-588.

27. Umeda N. Operational Stability in Following and Quatering Seas: A Proposed Guidance and its Validation, proceedings. 5th International Conference on Stability of Ships and Ocean Vehicles. V.2. Florida: 1994, pp.71-85.

# GUIDANCE TO THE MASTER FOR AVOIDING DANGEROUS SITUATIONS FOR A SHIP SAILING IN ROUGH FOLLOWING AND QUARTERING SEAS. CONCEPTION. CRITERIA. RATIONAL FORM OF REPRESENTATION.

A.I. Bogdanov

Central Marine Research & Design Institute Ltd.  
193015, St. Petersburg, Kavalergardskaya Str., 6, Russia

## ABSTRACT

Guidance to the master for avoiding dangerous situations for a ship sailing in rough following and quartering seas, acting in Russian sea fleet is described. It is shown that for guaranteeing of sufficient level of safety, the conception of such document should ensure account for the actual ship features of: hull form, loading and stability conditions, characteristics of sea state and parameters of a ship movement, as well as totality of the most dangerous phenomena capable arise with the ship during sailing in such conditions. Five dangerous phenomena and appropriate them criteria of safety are considered. Rational form representation of information to the master with account of human factor influence, in the form of documentation and on-board PC program, is discussed.

## NOMENCLATURE

FQS - following and quartering seas.

WCA - wave-to-course angle.

MCH - metacentric height.

SSD - static stability diagram.

SC - stability criterion.

d.i. - dangerous inclination.

## 1. INTRODUCTION

For the ship-operators and ship-builders a dangers of storm navigation in following and quartering seas (FQS), connected with unexpected occurrence of a large heel angles and even with

a capsizing of various types and sizes ships, satisfied to the national stability requirements and the IMO requirements, are well known. That testified about necessity of the special additional requirements development, reflecting peculiarities of navigation in a FQS. The problem of safety ensuring in these conditions are intensively investigated in the world and remains important on the present time. Various criteria of safety [1-10 and others] were offered, however they have not yet received application in a stability Regulations of the conventional ships.

The variety of the dangerous phenomena, possible at navigation in following wave-to-course angles (WCA) and complexity of their theoretical description, is left not enough hope for development of the only universal criterion of safety. The analysis of the existing offers on a various ships stability normalising shows, that safety of a particular vessel in these conditions it is difficult (and, probably, it is practically impossible) to ensure only by constructive means and on the basis of consideration of some the only dangerous situation, similar to IMO weather criterion. This problem not only scientific, but also operational and technical. Therefore for ensuring of safety in this conditions was needed and was offered a complex approach [11-12], which stipulated fulfilment of the following measures:

- Consideration and joint account simultaneously of all the most dangerous phenomena, capable to arise at storm navigation in a FQS

for creation of a complete picture of dangers menacing to a vessel;

- Development of a system rather simple criteria, correctly displaying general laws of the most dangerous phenomena;

- Development and introduction in the national and IMO Rules of the appropriate stability requirements, used at designing of a ships;

- Development of a Guidance to the master (included in the Stability booklet) on prevention of dangerous situations at navigation in a FQS, and also a special software for on-board computer, used at operation of a ship;

- Training ship-operators to physical bases of the dangerous phenomena and rules of safe navigation in storm conditions on a FQS;

- Sharing the whole complex of set forth above measures.

Thus, for realisation of the complex approach the work on ensuring of safety should be conducted on a three interconnected and adding each other directions: stability Regulations, Guidance to the master, training of ship-operators.

In the article the decision of an operational safety ensuring problem is considered. That is the safety of a ship already constructed and adopted for navigation, which will satisfy to the stability requirements currently in force.

In this case the safety is ensured:

- By knowledge and quality of a crew preparation for navigation in FQS conditions;

- By presence, quality, completeness and convenience of use of a Guidance to the master, specially developed for a given purpose;

- By presence of the special program for on-board computer and skill to it using (at presence on-board PC).

Such a problem was set and is solved in Russia under the orders of Sea Transport Department [11-13]. From 1988 the ships of Russian sea fleet are supplied by a special Guidance to the master, adding the Stability booklet, and then also a software for on-board PC, taking into account specificity of conventional ships navigation in FQS WCA. The technique of a Guidance is authorised by the Russian Federation Sea Transport Department, is adopted by the Rus-

sian Sea Register of Shipping (further the Register) and at the moment it is in force in the advanced and more perfect second edition [14]. A purpose of the given article - to acquaint of the experts with the basic provisions of a Russian Guidance and accepted conception of safety ensuring.

## 2. CONCEPTION OF SAFETY ENSURING FOR THE CONVENTIONAL SHIPS OPERATION IN ROUGH FOLLOWING AND QUARTERING SEAS

2.1 For the decision of a safety ensuring complex problem for a ships storm navigation in FQS it was supposed, that the development of a stability Regulations and Guidance to the master should be realised through of the Register Rules as follows:

At the designing stage - check of ship safety on the criteria reflecting the most dangerous phenomena and allowing to adjust safety by constructive measure should be made.

In case such criteria are carried out not completely, and high level of safety without infringement of the ship voyage time-table is required, should be a ship design parameters (hull form, centre of gravity location, bilge keels and others) changed so, that the criteria were carried out.

If the infringement of a ship voyage time-table (caused compelled for preservation of safety by changes of a course, speed, draught, stability etc.) is allowable, its design characteristics can remain previous, but in the Stability booklet the appropriate operational restrictions should be included.

At the stage of operation - in the Stability booklet the information, describing a danger degree of storm navigation of a particular ship in FQS, should be included. If such danger exists, a Guidance to the master, containing the recommendations for a rational loading in a port with a purpose of possible reduction of this danger yet before voyage, and also on choice of safe modes of storm navigation during voyage, with a purpose of an emergency situations occurrence prevention for all possible for the

given ship dangerous phenomena, up to prohibition with FQS WCA navigation in certain conditions, should be developed.

2.2 The most of undertaken earlier attempts to normalise a ship's stability in following WCA were based on research and establishment of capsize / non-capsize border. The scenarios analysis of known wrecks shows, that for the conventional ships in these navigation conditions such criteria are not sufficient. Inclination to much smaller heel angles can be a first reason for them and result to such dangerous consequences in storm conditions, as, for example: cargo shifting, infringement of the engine work and to stop it, with subsequent turning of a moveless ship to the beam sea and wind, destruction by a wave of illuminators, windows, air pipes, hatchway closings, flooding through openings etc. That already subsequently, even after change of a course and speed can result to wreck of a ship from loss of a stability, buoyancy or as result of severe rolling (ship "Komsomolets Kirgisi" and others). For ensuring of safety it is necessary to exert influence upon the first reason.

Therefore it was offered to normalise the meaning of a maximum permitted heel angles and condition of sufficient safety on the FQS was formulated - ship's stability and rolling characteristics should be those, that an opportunity of ship inclining on an angle of dangerous inclination -  $\theta_{d.i.}$  was excluded. [11-14]. To prevent occurrence of the listed above consequences of a such inclination, the heel angles should not surpass  $40^\circ$ .

Was marked, that primary factors, distinguishing navigation in the FQS from all other and having influence to safety in the greatest degree, are essential increasing (up to  $\infty$  at Froude number  $Fr_L=0,4$ ) of a wave apparent period  $\tau_{app}$ , in a combination with significant changes (including possible reduction up to negative meanings) of stability diagram arms for this period. That raises time of a ship staying with a lowered stability so, that makes it commensurable with own rolling period  $\tau_s$ ; allows to give a vessel sufficient time, to be captured by a wave,

and also adequately to react by change of a roll to change of a stability. In these conditions rather important factor for safety is a ratio of a lowered stability existence time for apparent wave period  $t_{(-)}$  and time, required vessel to dangerous inclination on one board  $t_{d.i.}$ . The listed factors should without fail be taken into account at the safety criterion in FQS development.

2.3 In view of above-stated, for the decision of a complex problem was formulated and was accepted the following conception of safety ensuring for the conventional ships navigation in rough FQS:

1. Was considered, that the proper level of safety of a ship can be ensured in the event that methods and decisions, fixed in a basis of a stability Regulations and of the Guidance to the master take into account:

- Individual characteristics of a particular ship (type, sizes, hull form etc.);

- Actual loading condition, draught, trim, stability, own rolling period in view of static stability diagram non-linearity influence;

- Parameters of designed, the most dangerous sea state (in Regulations), and parameters of actual sea state and sea depth (in the Guidance);

- The most dangerous phenomena, the physical bases of which allow to change the constructive decisions at the designing stage (in the Regulations), and simultaneously all the most unfavourable and dangerous phenomena, which are probable for the given ship in considered navigation conditions (in the Guidance).

2. Should be considered and take account at least 5 dangerous phenomena, capable to arise at stern sea operation and representing the greatest potential of danger concerning occurrence of accident in result of a ship inclination to a dangerous heel angle:

- Significant reduction or loss of a transverse stability at passage of a wave along of ship length (for apparent period of a wave),

- Main rolling resonance, when the wave apparent period  $\tau_{app}$  is close to or is equal to own ship rolling period  $\tau_s$ ;

- Parametric rolling resonance, when

$$\tau_{app} \sim \tau_s / 2;$$

- Capture by a wave, manoeuvrability loss and the inadvertent dynamic turning of a ship at high speed (broaching);

- Deterioration of manoeuvrability, wave impacts and pooping on small speeds.

.3 Was supposed, that stability criteria, based on an establishment of the fact of capsizing / non-capsizing of a ship (i.e. wreck / not of wreck) result to a too low level of safety. Therefore as a condition of sufficient safety for the conventional ships in FQS it is offered to consider such at which a ship will not has an opportunities of inclination on the dangerous heel angles which are in limits of  $40^\circ$ .

.4 Was taken into account, that the significant and long periodic reduction of a transverse stability has large influences to a ship behaviour in all dangerous situations. It is the important factor, determining safety of ship navigation in following seas and distinguishing it from navigation by other WCA (An example of a stability diagram arms changing during of apparent wave period for a ship of 119m length is shown on fig. 1).

If this factor is not accounted or is accounted insufficiently full, the recommendations of the Regulations or the Guidance cannot ensure of sufficient safety

.5 Was considered, that the recommendations of the Guidance, based on the incomplete account of simultaneously all possible for a ship dangerous phenomena can result in a wrong estimation by the master of a general situation and to acceptance of the decision, leading to a ship accident or wreck. Therefore such recommendations should be excluded.

.6 Was accepted in attention, that to correctly take into account in the Guidance all listed important factors, remaining on a position of the "universal" or "non-tailor-made" storm diagrams (not depending on the individual characteristics and loading conditions of a ship and actual parameters of sea state) practically is impossible. Therefore the "non-universal" or "tailor-made" diagrams, taking into account the whole complex of the listed above characteristics, phenomena and factors influencing on safety, should be offered.

.7 Recognise the importance of simplicity

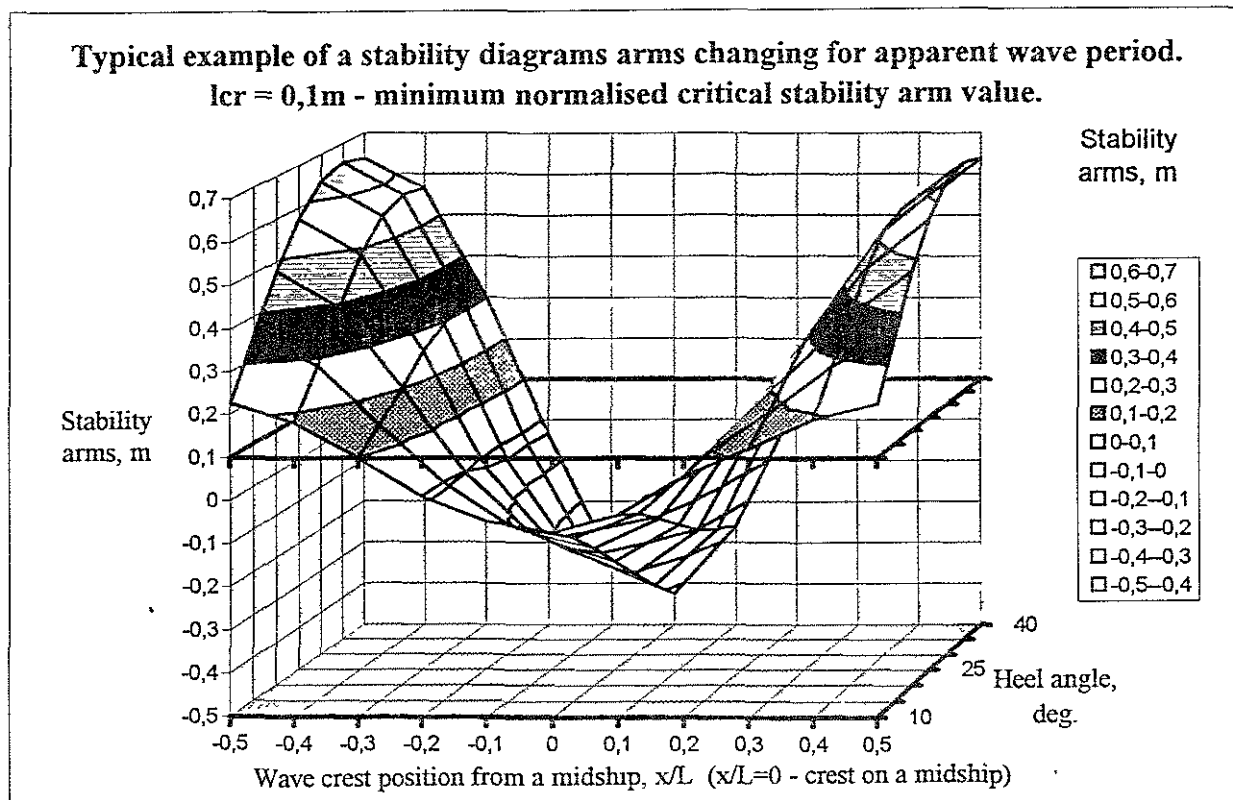


Fig 1

and convenience of the Guidance use, was nevertheless considered, that it should be without detriment to reliability and safety. The main concept of the ship's document on safety should be completeness of the information about a condition of a ship and trapping its dangers and guarantee of a necessary level of safety ensuring after fulfilment of the recommendations of such document. The recommendations of the Guidance should not bring in unreasonable change of a ship course and speed.

.8 Good addition to the Guidance is preparation of the appropriate to it program for on-board PC, allowing to the master more operatively to estimate safety and well-founded to choose safe modes of navigation. Presence of a such program should not exempt from necessity to have the Guidance.

.9 Guidance and the program for on-board PC should take into account "the human factor" and to cover all ship's loading cases and sea conditions, possible at normal operation of the ship.

### 3. DANGEROUS PHENOMENA, DESIGN SITUATIONS AND SAFETY CRITERIA

#### 3.1 Design dangerous situations.

To follow the accepted concept, for purposes of normalisation in Register Rules it is possible to use three of first five described in 2.3.2 dangerous phenomena, as they depend on a stability (i.e. design) of the ship and to them, in this or that degree, it is possible to affect during designing. Three criteria of safety could accordingly be developed: stability, roll in a modes of main and of parametric resonance. Taking into account above-stated, for this purpose were simulated and are accepted as designed the following situations [11-14]:

.1 The ship, making rolling, caused by influence of waves or any other reasons, operate with designed speed by a following course and gets on a wave with the most unfavourable concerning a stability parameters. At passing this wave along a ship hull at the time moment, when the stability characteristics decrease below than normalised critical level, the ship with

the maximum angular speed pass through a vertical position and then makes complete inclination to one board. The amplitude of such inclination should not reach dangerous value.

.2 Ship on the most unfavourable concerning its stability a following seas operate with speed corresponding to the rolling in a mode of the main resonance. The maximum rolling amplitude should not reach a dangerous values.

.3 The same for a parametric resonance.

#### 3.2 Stability criterion in a following waves

$K_{fw}$ .

Proceeding from the first design situation, for normalisation purposes and inclusion in Rules was substantiated and was offered a stability criterion in a following waves  $K_{fw}$  [11,12,15].

It is based on the thesis, that the stability of a ship is considered insufficient, and its operation is potentially dangerous, if in the specified situation for apparent wave period a time  $t_{( )}$  will be more time  $t_{d.i.}$ , where:

$t_{( )}$  - time, during which the arms of a ("momentary") stability diagrams, appropriate to various ship locations on a wave profile during apparent period, in a range of heel angles 10-40° decrease below than normalised critical level ( $l_{cr}$ );

$t_{d.i.}$  - time of dangerous inclination. The minimum time, for which in these conditions it is possible for the given vessel to incline from a vertical position to an angle of dangerous inclination.

The stability of a vessel in a following sea on criterion  $K_{fw}$  is considered sufficient, if at worst concerning a stability loading case at a movement with design speed in a direction of distribution of a design following wave a condition will be satisfied

$$K_{fw} = t_{d.i.} / t_{( )} = \tau_s / (4 * k_\tau * \tau_{app.}) \geq 1,0 \quad (1)$$

Where:  $k_\tau$  - non-dimensional designed factor (change of a stability in a following seas), showing, which share of wave apparent period  $\tau_{app.}$  the stability arms of the given ship in a range of heel angles 10-40° are reduced below than normalised critical value  $l_{cr}$ . It can be de-

terminated precisely by calculation under the complete scheme [14], or under the specially received simple regression formula [15].

$\tau_s$  - own ship rolling period on still water, designed in view of non-linearity of the stability diagram [14-15].

$\tau_{app.} = \lambda / (c - v_f)$  - apparent period of a designed wave, sec.;

$\lambda$  and  $c$  - accordingly, length and speed of a designed wave;

$v_f$  - designed speed, accepted equal 0,8 from full speed in still water, m/sec. For ships, specially intended for work in heavy storm conditions, and also for ships of length less 60m., the value is subject to special consideration by the Register. Thus it is recommended, that factor should be more than 0,8.

$l_{cr}$  - choose by the greatest of the follow values 0,1m., 0,6 $l_w$ ,  $l_c$ . Where  $l_w$  and  $l_c$  - accordingly, arms of heeling moment of a beam wind pressure for unlimited region of navigation and of heeling moment due to a steady circulation in [16];

The criterion takes into account change of a stability, draught and trim in various moment of time for apparent period of a designed wave. The satisfaction to criterion  $K_{fw}$  testifies that the characteristics of a stability and roll of a ship are those, that at a movement on a following seas with given speed and hit in the most unfavourable rolling phase on the most dangerous concerning of a stability loss (or other given) wave the ship has no enough time to make inclination on a dangerous angle of heel.

The more detailed description of the criterion, physical sense and method of calculation is contained in [11,12,14,15].

Inclusion of a stability criterion  $K_{fw}$  in the Register Rules, in addition to existing, will allow yet at the stage of ship designing to take into account dangerous change of its stability in a following seas and, if necessary, to accept the appropriate constructive or other measures. It was transformed into criterion of safety for assignment of operational restrictions in the Guidance, as will be described below.

### 3.3 Criterion of a resonant rolling.

The condition of rolling resonant modes occurrence is defined by expression:

$$\tau_{app.} = \tau_s * n/2, \quad \text{where } n = 1, 2, 3, 4... \quad (2)$$

In 3.1 we are stipulate consideration and account only of modes really meeting in practice, main  $\tau_{app.} = \tau_s$  ( $n=2$ ) and parametric  $\tau_{app.} = \tau_s / 2$  ( $n=1$ ) resonances.

Rather wide range of the workers MCH, speeds and WCA, possible at the conventional ships operation testifies that normalisation of a stability characteristics does not allow to provide the conditions, excluding an opportunity of occurrence at least of one of resonant roll modes. It is clear also, that roll can represent danger to a ship only when its amplitudes or acceleration exceed permitted value. However it was not represented possible to estimate them quantitatively, due to absence of an approved and reliable methods of roll calculation in a following seas.

Therefore the rolling criteria in the Regulations were not offered by us, and for a required level of safety ensuring at the given stage, was decided to include into the Stability booklet (in the Guidance) the operational restrictions and recommendations for a ship-operators at the choice of such speeds and WCA, which would not be dangerous concerning occurrence of a rolling of a vessel in a mode both main, and parametric resonance. The rolling criteria fixed in their basis are described in item 4.1.4. The borders accepted in the Guidance as near-resonant zones should be considered as conditional, from which the rolling can adversely influence on ship behaviour and to it is necessary to pay raised attention of a ship-operator.

The hydrodynamic problem about ship rolling in FQS is difficult for theoretical study and only in the most last time by V.V.Lugovsky [17] and N.N.Rakhmanin, G.V.Vilensky [18] two various variants of its solution, allowing to approach to practical development of rolling criteria of ships in these navigation conditions, are for the first time offered. If such criteria will be developed, they could be included in the Reg-

ister Rules in addition to of a stability criterion  $K_{fw}$  and on their basis the more substantiated recommendations on rolling in the Guidance, instead of nowadays existing approximate could be developed.

### 3.4 Account of the broaching-to phenomenon and unfavourable phenomena on low speed.

The broaching-to phenomenon can also result in an inclination on a dangerous heel angle or to a capsize and arises on waves, length and speed of which are close to length and speed of a ship. Such situation is probable for small or rather high speed large ships. This phenomenon is not connected rigidly to a stability and cannot arise if there are not enough conditions for capture of a ship by a wave (surf-riding). Such conditions are established for small ships in the Register Rules [16] and there correspond speeds in knots, equal  $1,4\sqrt{L}$  or Froude number 0,23. This value was accepted for a basis of broaching-to criterion in the Guidance.

Also nor depend on a stability and unfavourable phenomena on low speeds, listed in 2.3.2. They do not usually arise, when ship speed exceeds 3-5kn. The meaning of this speed is nominated in the Guidance in view of peculiarities of a particular ship and results of it sea-worthy tests.

## 4. GUIDANCE TO THE MASTER FOR AVOIDING DANGEROUS SITUATIONS IN FOLLOWING AND QUARTERING SEAS

### 4.1 Basic provisions of the Russian Guidance.

**4.1.1 Purpose.** At ship operation in a following and quartering sea occurrence of the dangerous phenomena, resulting in accidents or a capsize of a ship, is possible. The Guidance has a purpose to help master to prevent occurrence of emergencies and allows to decide the following problems:

.1 At a load of a ship before voyage: - to receive the recommendations for rational draft, trim and stability, at which the unfavourable in-

fluence of a following sea in voyage will be minimum.

.2 At an actual ship loading case in a voyage: - to estimate a danger degree of storm navigation at actual sea parameters, depth of the sea and WCA; - to receive the recommendations at the choice of safe modes of storm operation in the stern WCA, and at a significant danger - on a safe course changing and safe sailing up to a beam sea; - to receive the recommendations for required change of draft, trim and stability with a purpose of reduction of unfavourable influence of a following WCA.

#### 4.1.2 Area of distribution.

.1 Vessel. The methodology of Guidance preparation is distributed to all types of conventional ships, satisfying to the Register Rules. Each Guidance is developed in view of peculiarities of a particular ship and can be used only on ships of one series.

.2 Sea conditions. The stern wave-to-course angle (WCA) - means, that the direction of waves distribution makes with a ship course an angle from 0 (by a wave) up to  $45^\circ$ . The Guidance is applied in a range of WCA from 0 up to  $90^\circ$  at all possible in operation sea parameters and sea depth. The actual waves can be set irregular (3% or 1/3 probability) or regular (swell wave). Depth of the sea is taken into account. The Guidance is recommended to use, if the parameters of actual waves get in zones of unfavourable or dangerous for a ship following sea, determined on the graph of roughness,

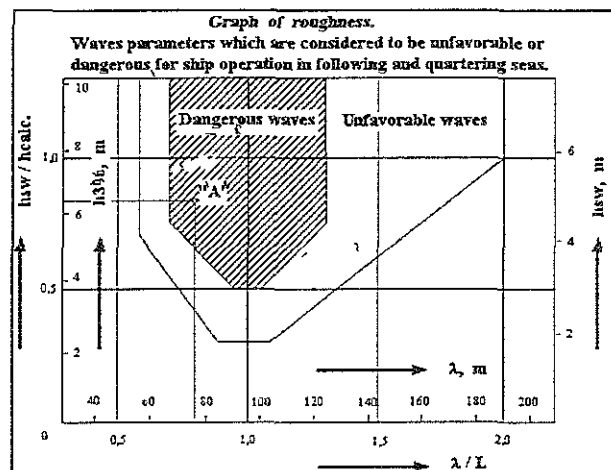


Fig. 2

received on the basis of the analysis of emergency statistics, results theoretical and experimental researches (Graph of roughness in non-dimensional co-ordinates, and also in dimensional, for a vessel of length 96m is represented on fig. 2. Where  $h_{calc.}=0,22*L^{0,715}$  - height of a designed wave.). Otherwise the navigation in the stern WCA is considered favourable and to apply the Guidance there is no necessity.

3 Loading condition. Cover the whole range of possible in operation loading cases at which storm navigation is allowed.

4.1.3 Definitions: L - ship length between perpendiculars, m.; B, d - breadth and draught on a midship, m.;  $\Delta$  - ship displacement, t.;  $h_{sw}=0,22*\lambda^{0,715}$ ,  $h_{3\%}=1,336h_{sw}$ ,  $h_{1/3}=1,004h_{sw}$  - accordingly average height of a swell and irregular waves of 3 % and 1/3 probability, m.;  $\lambda$  - average waves length, m.; c - wave speed, m/sec.; H - sea depth, m.;  $\tau_{app}$  - wave apparent period, c.;  $\tau_s$  - own ship roll period on still water in view of non-linearity of SSD, c.; h - initial MCH in view of free surfaces of liquid goods, m.. Corresponds to a horizontal axis of "Diagrams" on fig. 3-4; -  $V_s$  - ship speed, kn.; -  $V_{res.}$  - speed, appropriate to the main rolling resonance, when  $\tau_{app} = \tau_s$ , kn.;  $V_m$  - minimum speed at which ship is yet capable to be operated in conditions of a following sea, kn.;  $k_b = 1,4$ . As agreed with Administration for ships of length  $L > 40m$ . this factor can be increased, but no more than 1,8.

#### 4.1.4 Dangers of stern seas and criteria of safety.

The Guidance simultaneously takes into account 5 kinds of dangerous and unfavourable for a ship phenomena, probable at storm navigation in the stern WCA. To each phenomenon there corresponds a certain zone on "tailor-made" "Diagrams for a ship sailing in rough following and quartering seas " (further "Diagrams"), submitted on fig. 3-4.

1 Significant reduction or loss of a transverse stability at wave passage along a ship (1st dangerous zone - insufficient stability, constructed on the basis of criterion  $K_{fw}$ ).

Criterion of safety:

$$V_s < (c - 4*k_{\tau} * \lambda / \tau_s) / (0,514 * \cos \beta), \text{ kn.} \quad (3)$$

2 The intensive rolling in a main resonance mode, when wave apparent period  $\tau_{app}$  is close to own ship rolling period  $\tau_s$  (2nd dangerous zone - main rolling resonance).

Criterion of safety:

$$V_s \left\{ \begin{array}{l} < 1,3 \\ > 0,7 \end{array} \right\} (c - \{ \} \lambda / \tau_s) / (0,514 * \cos \beta), \text{ kn} \quad (4)$$

(Note: here and further in figured brackets are specified the top and bottom borders of a zones.)

In case the ship has not goods, dangerous concerning a shifting, criterion of safety:

$$V_s \left\{ \begin{array}{l} < - \\ > + \end{array} \right\} (c - \lambda / \tau_s) / (0,514 * \cos \beta) \left\{ \begin{array}{l} \\ \end{array} \right\} 2 \text{ kn, kn.} \quad (5)$$

3 Intensive rolling in a mode of a parametric resonance, when  $\tau_{app} \sim \tau_s / 2$  (3rd dangerous zone - parametric rolling resonance).

Criterion of safety:

$$V_s \left\{ \begin{array}{l} < 2,1 \\ > 1,9 \end{array} \right\} (c - \{ \} \lambda / \tau_s) / (0,514 * \cos \beta), \text{ kn.} \quad (6)$$

4 Movement of a ship with high speed, when its capture by the wave, loss of manoeuvrability and spontaneous uncontrollable dynamic turning broad-side to a wave and wind - "broaching-to" is probable (4th dangerous zone - "broaching-to"). Criterion of safety:

$$V_s < k_b * \sqrt{L} / \cos \beta, \text{ kn.} \quad (7)$$

5 Ship movement with low speed, when it is poorly listened of a rudder, is more subject to impacts of stern waves and pooping (5th, unfavourable zone, - insufficient manoeuvrability).

$$\text{Criterion of safety: } V_s > V_m, \text{ kn.} \quad (8)$$

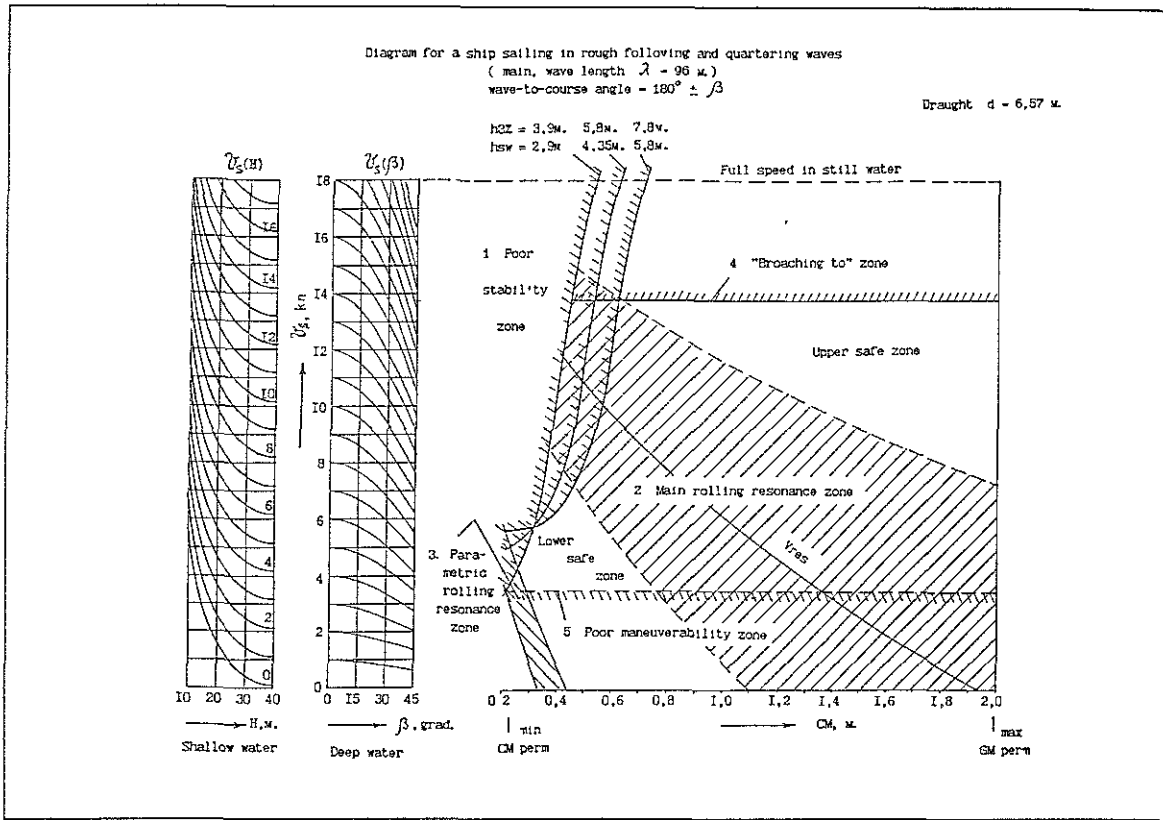


Fig 3. Example one of the main "Diagrams" for the wave length 96 m. and draught 6,57 m.

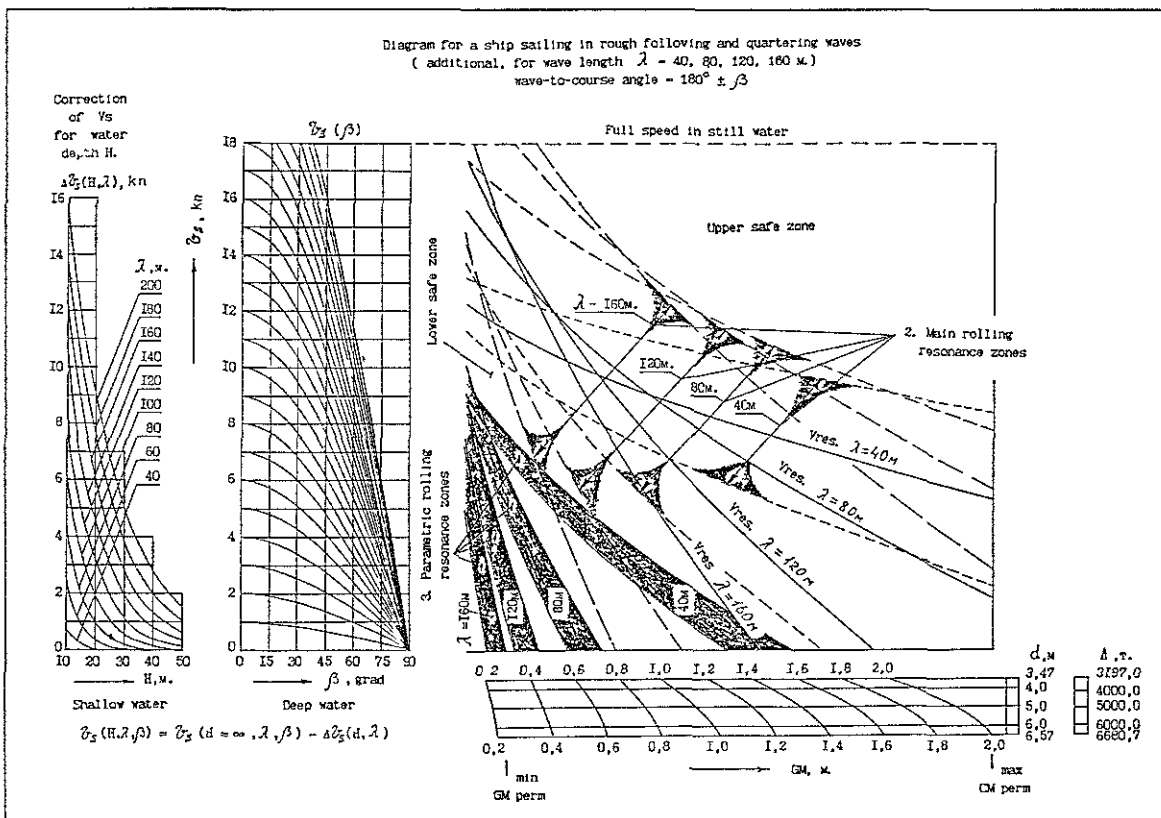


Fig 4 Example one of the additional "Diagrams" for the wave length range 40-160 m.

#### 4.1.5 Necessary data to safety estimation.

.1 At a ship loading before voyage.

d (or  $\Delta$ ), Xg - prospective on loading conditions a midship draught (or displacement) and centre of gravity on ship length position;  $h_{\min}$ ...  
 $h_{\max}$  - range of initial MCH possible change under the given loading conditions;  $h_{\text{calc}}$  - height of a designed wave.

.2 At storm navigation during voyage.

d (or  $\Delta$ ), Xg - actual midship draught (or displacement) and Xg; h - actual initial MCH in view of free surfaces of liquid goods influence;  $V_s$  - log ship speed;  $\beta$  - wave-to-course angle (WCA); H - sea depth; ( $h_3\%$ ,  $h_{1/3}$  or  $h_{sw}$ ),  $\lambda$  - height and average length of observable waves; - presence on a ship of goods dangerous concerning shifting (yes/no).

#### 4.1.6 Diagrams for a ship sailing in rough following and quartering seas.

.1 The estimation of safety of ship storm navigation is made under the set of "Diagrams", example two of which for a ship with length 96m. is submitted on fig. 3-4. They are conditionally divided on main and additional.

.2 Main "Diagrams" (fig.3), calculated in a range of WCA from 0 up to 45° for three-four loading cases, at which there is a 1st dangerous zone. At each meaning of loading, the wave lengths (in a range the most dangerous concerning a stability  $\lambda = 0,7L-1,3L$ ) and their heights (no less than three meanings in a range 0,5-1,5 from designed wave height  $h_{\text{calc}}$ ) are vary. The main "Diagrams" characterise the most unfavourable combination of a lowered stability and phenomena, described in 4.1.4. They are intended for: a choice of optimum draught, a trim and a stability during ship loading; estimations of safe modes of navigation on all 5th dangerous zones simultaneously at wave parameters, corresponding of a dangerous waves on fig. 2; to an approached estimation of the 1-st dangerous zone borders at operation in the field of unfavourable roughness on the graph of roughness.

.3 Additional "Diagrams" (fig. 4) are constructed in the whole range of loadings for a number of chosen wave lengths, is more significant distinguished from ship length. Are in-

tended for an estimation of operation safety under the relation to 2nd and 3rd resonant zones of a rolling at  $0,7L > \lambda > 1,3L$ . Contain a wider WCA range - from 0 up to 90°, for convenience of ship course change determination from following and up to a beam wave, in case of necessity to avoid resonant kinds of a rolling.

.4 In a field of "Diagrams" 5 zones, designed at  $\beta = 0$  and  $H = \infty$ , are constructed. The transition to other  $\beta$  and H is made according to vertical axes  $V_s(\beta)$ ,  $V_s(H)$  or  $\Delta V_s(H, \beta)$ .

.5 The choice of safe modes of navigation at intermediate meanings of an actual sea and loading parameters is made by a linear interpolation between their adjacent meanings under "Diagrams".

#### 4.1.7 Estimation of safety.

.1 The estimation of safety under "Diagrams" is carried out in case the point ("A"), appropriate to actual parameters of sea state on the graph of roughness gets in area of unfavourable or dangerous roughness.

.2 To safe modes of navigation there corresponds a points of "Diagrams", not belonging of any from 5th zones listed in items 4.1.4.

.3 To permitted modes of navigation there correspond points of 2-nd dangerous zone - main rolling resonance, differ from a  $V_{\text{res.}}$  curve more, than on 2-3 knots, if the ship does not transport goods, dangerous concerning shifting. Short-term navigation inside of the 5th, unfavourable zone is allowed also, if the point  $V_s(\beta, H)$  is not simultaneously in 2-nd or 3rd a dangerous zone of main "Diagrams".

.4 The greatest danger to a ship is represented the navigation, when MCH, speed, WCA and H are those, that the appropriate point is simultaneously in several dangerous zones of "Diagrams".

#### 4.2 Substantiation of the "tailor-made" storm diagrams form of representation.

The information can formally be submitted to a ship operator in the various graphic form. However unsuccessful choice of such a form can essentially reduce, to reduce to zero and

even to bring in negative consequences in efficiency of practical use of the information. That especially important at development of a "tailor-made", more exact diagrams and, if a purpose - a safety ensuring, when the speech goes about life of the passengers and crew, safety of goods and vessel.

It is represented obvious, that first of all, with the maximum accuracy and graphical clearness should be displayed the information about influence of the most important, for achievement of a given purpose, parameters. Our purpose - a safety ensuring in relation of an inclination on a dangerous heel angle (which, in a final result, can bring to the subsequent capsizing). The main contribution into its achievement, for the majority of conventional ships, is brought by the safety criteria (SC) (3-6), dependent upon a stability. Is possible to show, that from parameters, usually used for construction of the storm diagrams, the most important for a given purpose is a stability characteristic (MCH - h), second - speed of a ship V, third - WCA, fourth - sea depth etc.

Actual MCH in a voyage cannot be determined precisely. Its relative error usually makes no less than 10-15 %, and it grows with reduction of absolute meaning of h and can reach 50, 70 and even more than 100 % [19-21]. As with reduction MCH grows and danger of a wreck, for the correct and duly of a ship operator warning about of the phenomena dangerous concerning a capsizing, the storm diagrams should reflect SC dependence on important parameter h with taking into account of influence of a probable error of its practical determination +/-dh.

For a substantiation of the storm diagrams form choice which is the most answering for a put purpose, comparison of the alternate diagrams was carried out: offered multi-parametric diagram in co-ordinates V-h-WCA-H and known diagram in polar co-ordinates V-WCA, distinguished by absence in an obvious kind the most important parameter h (see fig. 5, where the axes H from place economy reason are not placed). Each polar diagram is designed only for one meaning of MCH, sea depth and sea parameters. The receive information corresponds only to one point of a multi-parametric diagram V-h-WCA-H (Fig. 3-4).

Dependent from a stability SC (3-6) have an identical structure

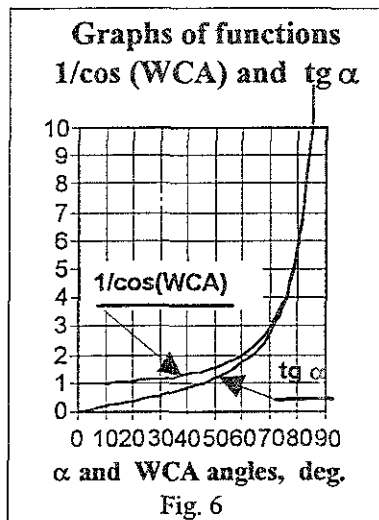
$$V = f(h) / \cos(WCA) \quad (9)$$

To estimate influence only the forms of diagrams representation was considered, that: - is considered the arbitrary SC, depending from a stability and having a structure (9); - all parameters on both diagrams are equally determined; - the border of criterion on the diagram V-h-WCA-H is linear on a considered piece; - the ship point "S", appropriate to a ship location, is in a safe zone in direct affinity from a line of border SC, but does not belong to it. In this simplified case function  $f(h) = f(\alpha)$ . Where -  $\alpha$  an angle of an inclination of a SC line to a positive direction of an axis h on the diagram V-h-WCA-H, which can change from 0 up to  $\pm 90^\circ$  and characterises a degree of SC dependence ("rigidity") from a stability.

The determination of safe speed error, caused by an error dh of determination h in voyage

$$dV(dh) = m \cdot dh \cdot \operatorname{tg} \alpha / \cos(WCA), \quad (10)$$

is directly proportional to product  $\operatorname{tg} \alpha$  on  $1/\cos(WCA)$ , where m - scale of the diagram V-h-WCA-H. These functions heavily grow, accordingly from 0 and 1, up to  $\infty$  at change of  $\alpha$  and WCA from 0 up to  $90^\circ$ , i.e. at increase of SC rigidity from h and with approach to a beam sea course (See fig. 6). In these cases a significant



errors in determination of safe speed V are possible, which easy to see and them easily to estimate and to take into account under the multi-parametric diagrams V-h-WCH-H. In polar co-ordinates V-WCH they are latent, therefore their use lead to closes of a master's eyes on a possible affinity of a danger, that can result to indefinitely large errors of a ship operator at determination of safe speed, including errors to the dangerous side (see Fig. 5) and acceptance of the decision, bringing near to a dangers or aggravating an emergency situation.

Comparison of a safe speed  $V$  estimation results, determined by a ship operator under the V-h-WCA-H diagram and the polar diagram V-WCA at various dependence ( $\alpha$  angle) of arbitrary safety criterion (cases 1, 2, 3, 4) from the metacentric height  $h$  and possible errors  $\pm dh$  of its determination in operation

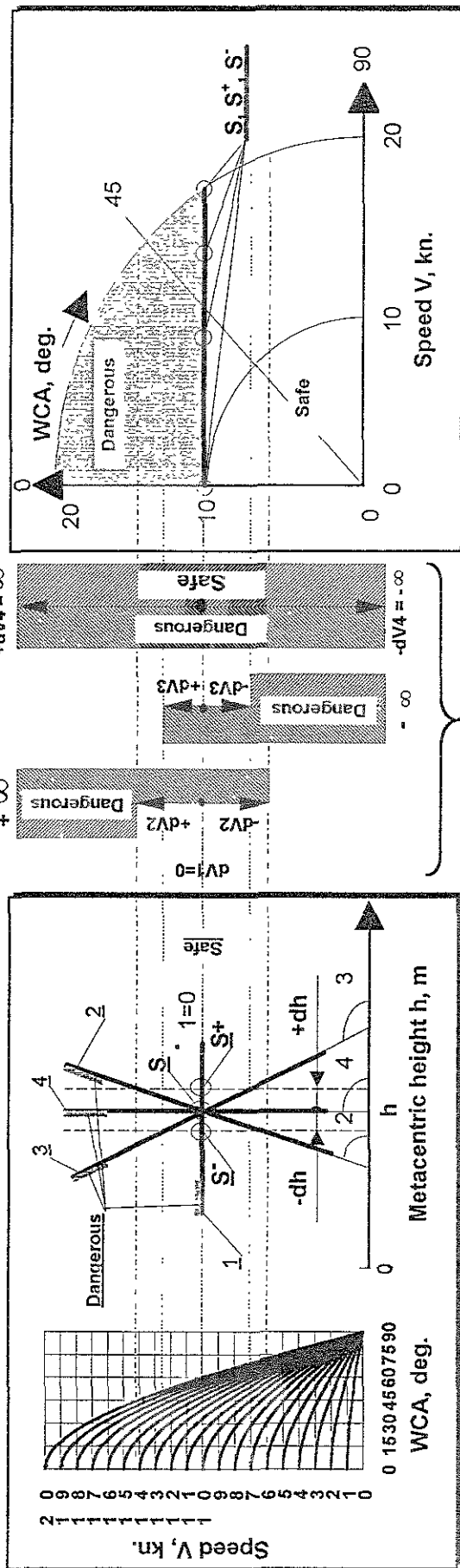


Diagram in a polar co-ordinates V-WCA

Ranges of possible errors  $\pm dh$  in a safe speed  $V$  determination, which are clearly visible on the V-h-WCA-H diagram and non visible on the polar diagram V-WCA

Diagram in a V-h-WCA-H co-ordinates

S - point, appropriated to a ship location in a safe zone for an actual  $h$  value.  
 S-, S+ - actual location of this point, if the  $h$  value determined with an error  $-dh$  or  $+dh$   
 $-dV$ ,  $+dV$  - errors of a safe speed  $V$  determination, corresponding to this points.  
 $\alpha_1, \alpha_2, \alpha_3, \alpha_4$  - angles of a safety criterion lines inclination to an  $h$  axis.

Fig. 5

It was represented important to determine in which cases it is possible to apply the polar diagrams and in which it is impossible. With this purpose a numerical research of meanings of non visible in the polar diagram V-WCA of an error  $\pm dV$ , depending on an angles  $\alpha$  and WCA values, was carried out. All possible combinations WCA meanings, changing in a range from 0,1 up to 1,0m and angles  $\alpha$  and WCA in a range from 0 up to  $90^\circ$ , were considered. The calculation was made under the formula (10) (where scale  $m = 10$  is accepted, as it is usual 1sm. of the diagrams V-h-WCA-H corresponds to change of speed on 1kn. and WCH on 0,1m.). The example of calculations for a case, when actual MCH  $h=1,0m$  is determined with (minimum possible in voyage) a relative error 10 % ( $dh=0,1m$ ), is brought on fig. 7. The level of a permitted absolute error of determination of safe speed in rough sea is accepted equal 0,5kn. Possible consequences of the polar diagrams application by the ship operator are analysed.

Results of numerical research have allowed to make the following conclusions:

.1 The error in determination of safe speed ( $dV$ ) heavily grows with increase of an angle  $\alpha$  (degree of SC dependence from a stability), increase of a WCA and an errors of MCH determination ( $dh$ ). It aspires to infinity at  $\alpha=90^\circ$  and  $WCA=90^\circ$  and reaches the maximum meanings at a combination of these values;

.2 Area of permitted errors ( $dV < 0,5 \text{ kn.}$ ) corresponds to small meanings of angles (from 0 up to 28grad., when is away or SC dependence from a stability is weak), and is limited by WCA curves from 0 up to  $85^\circ$ . (fig. 7). In these cases both forms of representation of the diagrams, as polar V-WCA, and V-h-WCA-H can successfully be applied;

.3 Area of inadmissible high errors ( $dV > 0,5 \text{ kn.}$ ) is extends with increase of an angle  $\alpha$  and exists at the whole WCA, from following ( $WCA=0$ ) and up to a beam sea ( $WCA=90^\circ$ ). It covers about 90% of all possible in practice variants of combinations  $\alpha$  and WCA. In these cases application of the polar diagrams V-WCA can result in dangerous consequences and, therefore, it is not recommended;

.4 The so wide area of inadmissible high errors is a characteristics of polar co-ordinates system V-WCA, is caused only by the form of the diagrams representation and does not depend more of any other factors;

.5 The diagrams form in polar co-ordinates V-WCA can be safely used only for problems, SC of which do not practically depend on a stability, or for construction of the less exact "non-tailor-made" diagrams or for the bow WCA;

.6 For an estimation of safety of navigation in all possible in ship operation cases of changing  $\Delta$ ,  $Xg$ ,  $h$ ,  $\lambda$ ,  $h_w$ , WCA and H in the Guidance no more than 30 diagrams V-h-WCA-H, including main and additional is enough to include. To reach the similar result and accuracy with use of the diagrams in polar co-ordinates V-WCH it is required with a small step on  $h$  to construct a few hundreds such a diagrams;

.7 At the decision of problems of ship safety providing from a capsizing on the whole WCA, it is recommended to make an estimation of a used SC dependence degree from a stability. At presence of high such dependence it is necessary to pass to the V-h-WCA-H system of co-ordinates.

Above-stated has served as a substantiation of a "non-tailor-made" diagrams representation form choice in the Russian Guidance [14,23], satisfying to the requirements showed to it (item 2.3), taking into account "the human factor" and ensuring the greatest efficiency of a ship safety in stern WCA storm navigation. For this purpose the Diagrams are submitted in co-ordinates system V-h-WCA-H, free from lacks of the polar form V-WCA diagrams.

#### 4.3 Program for on-board PC and illustration of its work on emergency examples.

At presence on a ship of on-board PC, a safe modes of storm navigation choice preferably to carry out with the help of the special software. For this purpose the program Following Waves Safe Sailing (FWSS) is developed which corresponds to the described above Guidance provisions and allows more operatively and precisely to decide the worth problems. It is developed according to [14] and corresponds to the IMO recommendations.

The dialogue with the program is extremely simple. Common skills of work on IBM PC compatible computers and some ship operator experience are required only. It can be used

Estimation of allowable area application to a diagrams in polar co-ordinates "V-WCA",  
 for a ship storm navigation safe modes choice on criteria, dependent on a stability.  
 Range of an angles  $\alpha$  and WCA change is from 0 up to 90 deg.

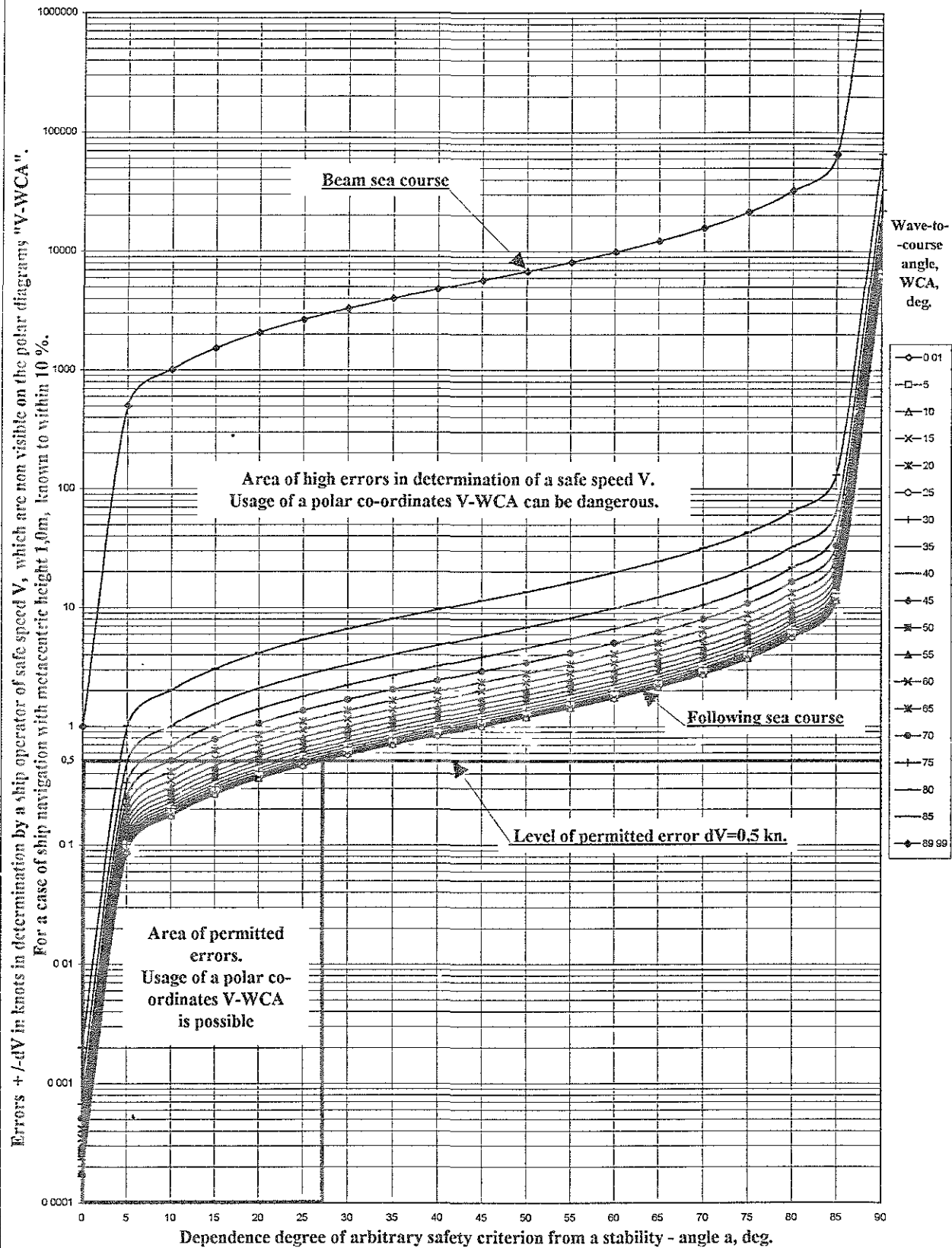


Fig. 7

also as a simulator for training of ships officers and cadets-ship operators to methods of safe navigation in storm following sea.

The main MENU FWSS contains the items: HELP, DATA, LOADING, VOYAGE, RECOMMENDATIONS, PRINT and EXIT.

The HELP - contains the minimum information, necessary for the right use by the program.

The DATA - contain two submenu, in which a ship and sea state data, listed in item 4.1.5 are entered.

At activation of item the LOADING one of the "Diagrams" is calculated, appropriate to an entered data on a ship and parameters of a designed wave  $\lambda = L$  and  $hw = 0,22 * \lambda^{0,715}$ , the most dangerous concerning loss of a stability. The diagram allows during a ship loading to choose a such stability, at which the range of safe speeds in voyage will be greatest.

At activation of item the VOYAGE occurs calculation of the Diagram, appropriate to an entered data on a ship and actual sea state. Varying these parameters it is possible to determine a safe speeds and WCA. On the Diagram also displayed the graph of roughness (in the right top corner) by which it is possible to estimate a danger degree of a given roughness for the ship, and also current data on a ship and roughness.

In menu item the RECOMMENDATION, depending on location of a current point "S" of a ship relatively the dangerous zones, at a screen is displayed the information about condition of a ship safety and recommendation about possible actions of the master for prevention of a dangerous situation.

The diagram, corresponds to the chosen decision can be printed on the printer with the help of a key a PRINT and can be included in the voyage report.

The EXIT item - corresponds to an exit from the program.

The results of a ship operator dialogue with the program FWSS are submitted on fig. 8-11 on examples of accidents cases of two various ships.

The diagrams on fig. 8-9 correspond to probable conditions of wreck in 1970 of the ship "Poronaisk" (length of 96m), on which in conditions a roll at storm force 10-12 has taken place a goods shifting. A static heel in  $20^\circ$  was formed, continuing to be increased. That has result to an engine stop, turning broad-side to a wave and to subsequent capsizing of a unmoved ship. As it is visible from fig. 8, at sailing by the stern WCA a ship could simultaneously be in a two dangerous zones - insufficient stability and main rolling resonance, and at in-

creasing of speed at 1 kn. - also in a broaching-to zone. Joint influence of these three dangerous phenomena could quite result to inclinations on a dangerous heel angles and lead to a goods shifting, with all following consequences. In these conditions it was necessary to reduce speed essentially up to 5-6 kn., or to change the WCA to  $30-50^\circ$ . According to fig. 9, the situation even was more aggravated, when a vessel has lost a speed and was turned to a beam sea. Thus it got in a dangerous zone of a roll in a parametric resonance mode, as could serve as the reason of the subsequent capsizing.

The diagrams on fig. 10-11 correspond to probable wreck conditions in 1993 the ship "Polesk" (length 140m), at which in conditions of rolling in roughness 5-8 numbers has also taken place a goods shifting. There was appeared the static heel in  $30-35^\circ$  with roll swing up to  $52^\circ$ . The engine has stopped, vessel has lost a speed, was turned a broad-side to a wave and subsequently has capsized. According to fig. 10, at sailing by the stern WCA the ship was in a dangerous zone of the main rolling resonance, on separate waves with length 100-120m and height 10-12m could simultaneously get yet in a zone of a insufficient stability, and at increase of speed only on 0,5kn. - in a broaching zone. That could result to inclinations on a dangerous concerning goods shifting heel angles. With account of possible error of MCH determination, the further scenario and the reasons of a ship wreck without a speed broad-side to a wave are similar described above for the ship "Poronaisk".

The given examples show clearness and convenience of application of the diagrams V-h-WCA-H for the detailed analysis of an emergency simultaneously on all dangerous phenomena. The master sees the whole picture in function of important parameter - stability and it is easily to him to estimate, which dangers are threaten and what it is necessary to undertake, if the error in MCH determination is possible in the large or smaller side. It is visible, that in the area of a beam sea WCA a line of roll SC border are close to a vertical (fig. 9,11) and even the small MCH error can result in very large er-

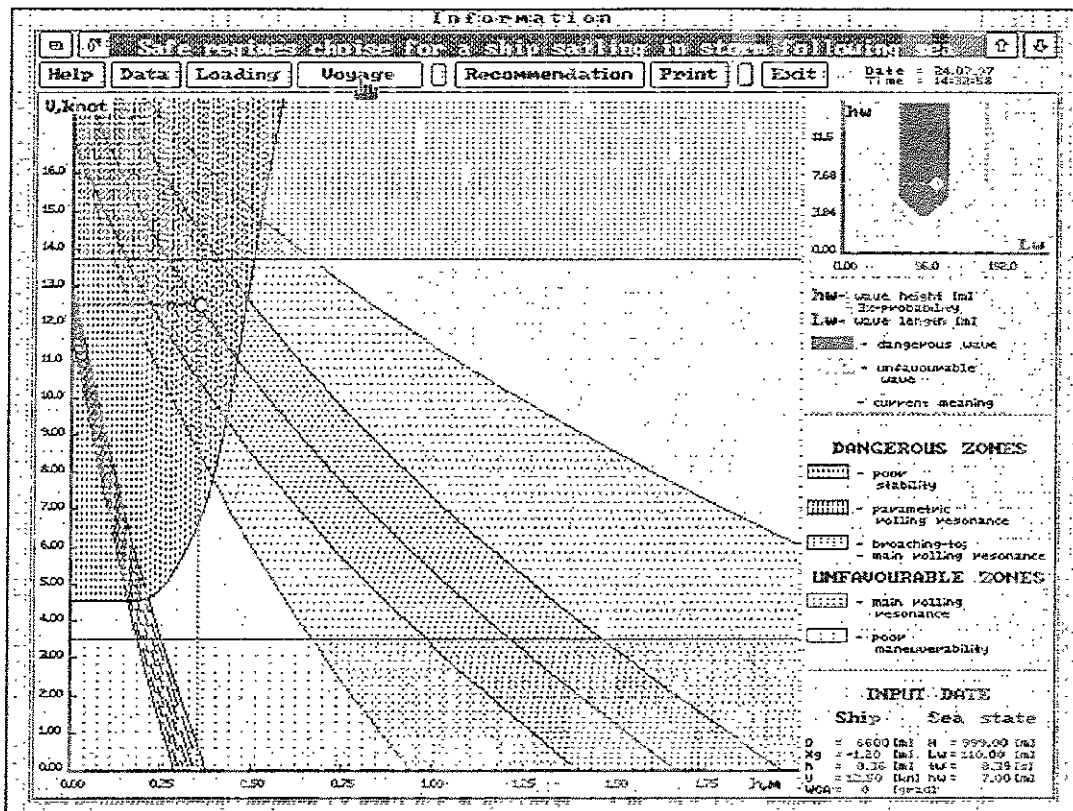


Fig. 8. Analysing of the ship "Poronaisk" probable wreck conditions. WCA=0°, V=12,5 kn.

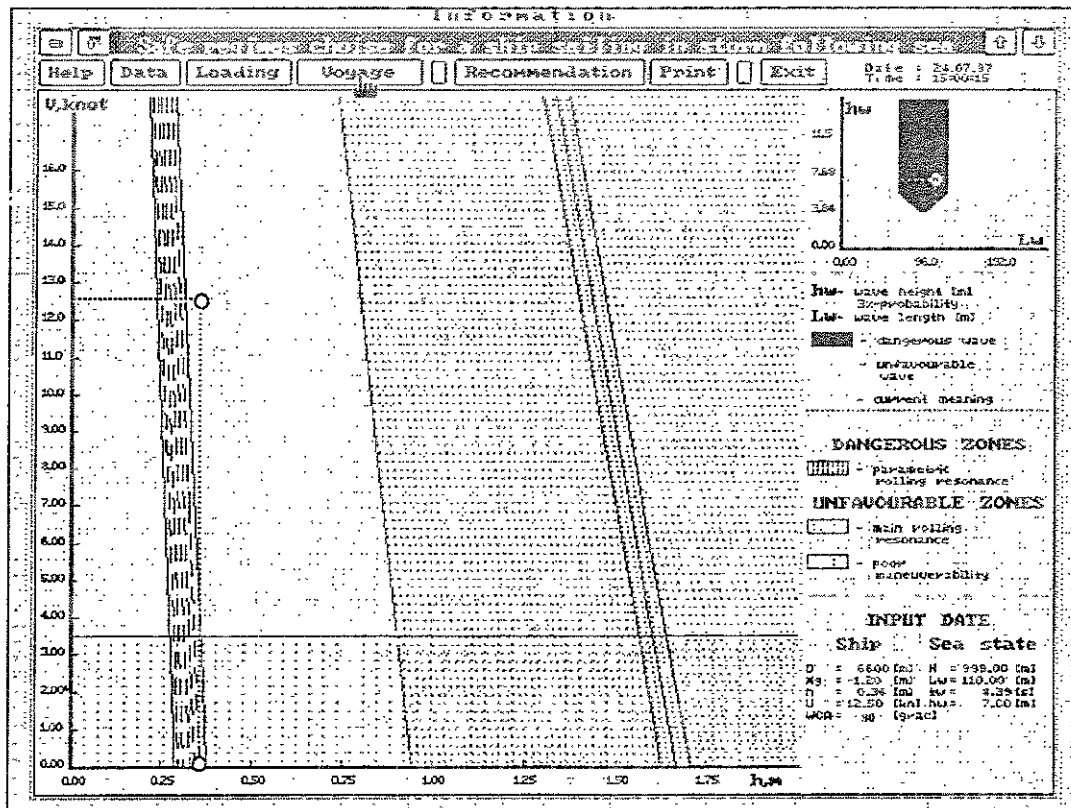


Fig. 9. Analysing of the ship "Poronaisk" probable wreck conditions. WCA=80°, V=0 kn.

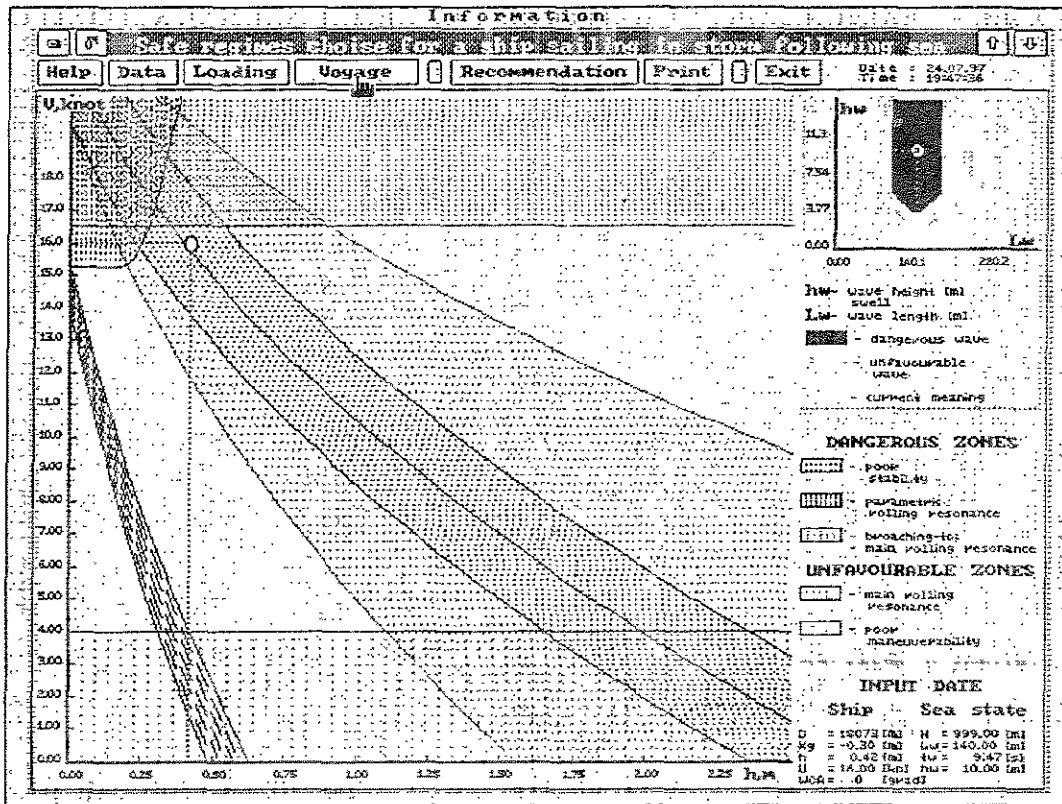


Fig. 10. Analysing of the ship "Polesk" probable wreck conditions. WCA=0°, V=16,0 kn.

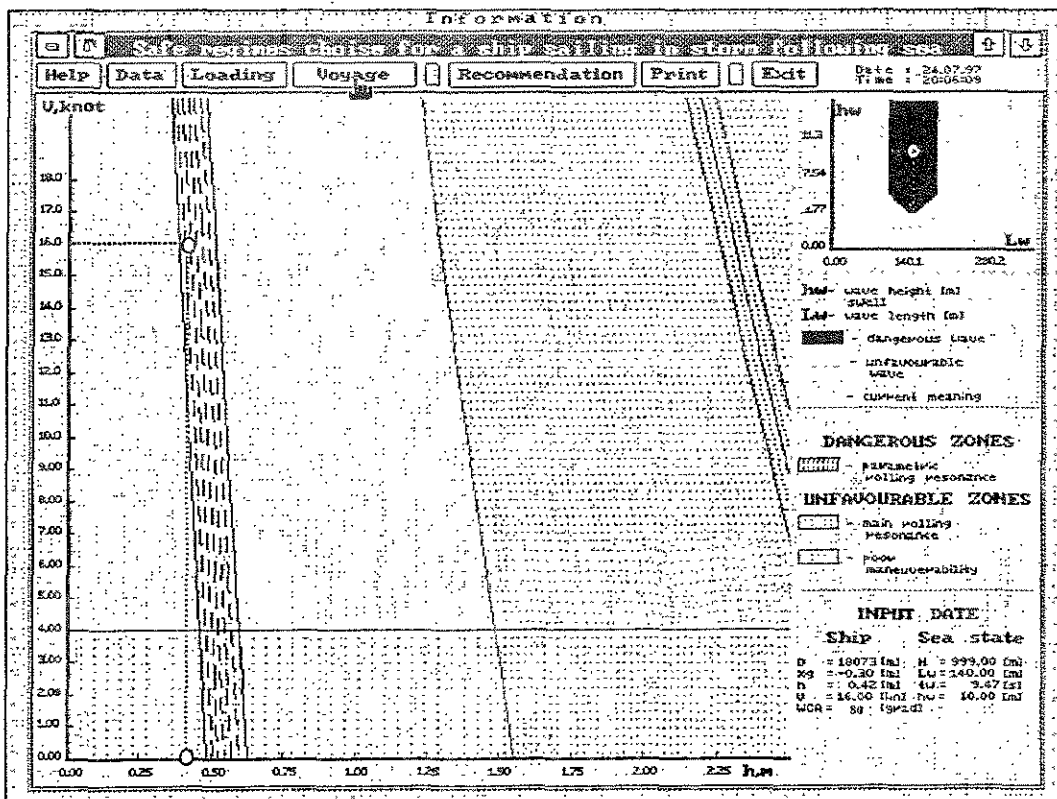


Fig. 11. Analysing of the ship "Polesk" probable wreck conditions. WCA=80°, V=0 kn.

rors in determination of the safe speed of a ship. Having such complete information the master can well-founded to accept the decision leading away from danger on important SC, dependent from a stability. That not allow to do of the polar diagrams V-WCA.

Reliability of a technique of the Guidance and the programs FWSS are repeatedly checked at the wrecks analysis of a various ships

## 5. DEVELOPMENT OF THE IMO GUIDANCE

In 1991 under the initiative of Japan in the agenda of IMO SLF Sub-Committee a question on development of the IMO "Guidance to the master for avoiding dangerous situations in following and quartering seas" was included. International correspondence group under the direction of Japan (co-ordinator - Prof. M. Fugino) was organised. In work of which from Russian Federation Prof. V.B.Lipis and author was participated. The offers of Japan [22], Russia [23], Poland [24] and Canada [25] were considered. The Japanese offers are based on results of systematic model tests of a fishing and several container ships for the phenomenon of surf-riding and broaching, and also on influence of a successive high wave attack. In tests the facts of capsize / non-capsizes were registered. The two simple "non-tailor-made (universal)" diagrams of safety in polar co-ordinates  $(V/\sqrt{L})$ -WCA and  $(V/T)$ -WCA were offered, used for all ships and cases of navigation. Where  $V$  - ship speed in knots,  $L$  - ship length in meters, and  $T$  - wave period in seconds. With the Japanese offers corresponds a similar on essence of Canada and Poland offers.

The offers of Russia, based on the concepts described in the article of the complete account of the individual characteristics of a ship and its load, parameters of actual sea state, "tailor-made" diagrams and technique [14], have received a positive estimation. With interest was perceived in IMO and demonstration of the on-board PC program FWSS. However, complexity of preliminary calculations and labour input of preparation of such Guidance and the software for an individual ship, requiring of pres-

ence a special methods and programs of calculations, have not allowed them to accept at the given stage. Was decided to accept the Guidance, using the less exact "non-tailor-made" diagrams, but based on a more simple and not requiring realisation of preliminary calculations, the offers of Japan. Which were much revised and are complemented in view of the main provisions of the Russian offers and remarks of other countries: the initial sizes and form of dangerous zones are changed, roll in a mode of the main and parametric resonances [26] etc. was added.

However the dangerous phenomenon of essential reduction of a stability on a wave, in an obvious kind, was not accounted. Irrespective of the ship characteristics and of a voyage conditions was considered, that this phenomenon is always inside dangerous zones of the "non tailor-made" diagrams and outside its boundaries a ship will be obviously safe concerning of a stability loss on a wave [27]. About mistaken of this statement, in our opinion, opportunity of a zone of a insufficient stability existence in a wide range of MCH, speeds and WCA beyond the scope of all other dangerous zones on the "tailor-made" diagrams of emergency ships, showed by us on fig. 3, 8, 10, convincingly testifies. Which are constructed at the complete account of actual parameters of a ship and roughness. The author of the Japanese offers has subsequently tried to take into account this phenomenon [28,29]. However his offer nor was accepted in IMO.

In the draft MSC circular about approve of the IMO Guidance [26] was especially marked, that the accepted Guidance does not take into account the actual stability and dynamic characteristics of an individual ship, but provides a general boundary of safe and unsafe combination of the operational parameters for all types of conventional ships covered by IMO instruments. It is not the criteria to guarantee of the safety absolutely, since the vessel can be unsafe even outside the dangerous zone, if the stability of the ship is insufficient and the dangerous phenomena happen simultaneously. Is decided to review the Guidance in the future in a view

to improving it, especially concerning large ships. It is recommended to encourage use of the special developed software for on-board PC for the account of the actual characteristics of an individual ship and real voyage conditions.

## 6. CONCLUSION

Summarising of done work it is possible to conclude.

1 Concept and technique of decision the problem of a safety ensuring for the ship navigation in a stern WCA, based on the complex approach is developed

2 Stability criterion in a following seas  $K_{fw}$  (in the Regulations) and a system of safety criteria (in the Guidance) is offered. Methods of their calculation are developed.

3 Diagrams of storm navigation are offered, allowing to the master to see a complete picture of totality probable for the given ship dangers, to choose safe modes of navigation in a WCA range from following seas up to a beam sea at actual loading condition of an individual ship and sea state. The form of representation of these diagrams in co-ordinates V-h-WCA-H, the most adequate to safety ensuring concerning a capsizing is validated.

4 Managing document [14], approved by the Register and Sea Transport Department, in a sea fleet of Russia in force at the moment, is developed. The training on practical application of its recommendations is carry out in a shipping companies and is include in the working programs of educational institutions on ship operator's, ship mechanic's and a ship builder's specialization, and also on ships officers qualification improvement courses.

5 Software for on-board PC, approved by the Register and allowing to ship operators more operatively to choose a safe modes of navigation in these conditions is developed.

6 Complex of carried out work has allowed successfully to decide at the given stage an important operational problem of safety ensuring for a conventional ships storm navigation in following and quartering seas. From 1988 the ships of a Russian transport fleet supplies with

addition to a stability booklet (Guidance) according to [14], and from 1994 also of a special software for on-board PC, allowing to ship operators receive the reasonable recommendations for safety in these complex conditions of navigation

7 The accumulated usage experience of the Russian Guidance and on-board PC software, based on the described above safety concept can be useful for improving and revising in future of the Russian and the IMO Guidances accepted at the given stage.

## 7. REFERENCES

1. Germany, "Improved Stability Criteria", SLF 35/3/3, IMO, 1990.
2. Netherlands, "Improved Stability Criteria", SLF 36/3/2, IMO, 1991.
3. Grim O., "Beitrag zu dem Problem der Sicherheit des Schiffes im Seegang" Schiff und Hafen, 6, 1961, pp.490-497, in German.
4. Tomas G.A. and Renilson M.R., "Surf-Riding and Loss of Control of Fishing Vessels in Severe Following Seas", Spring Meeting of the RINA, 1991.
5. Umeda N. and Ikeda Y., "Rational Examination of Stability Criteria in the Light of Capsizing Probability", Proceedings of the 5<sup>th</sup> International Conference on Stability of Ships & Ocean Vehicles, Melbourne, 1994, 9p.
6. Nechaev Y.I., "Ship Stability in Following Seas", Leningrad, Sudostroenie, 1978, 272p., in Russian.
7. USSR Register, "Method of Ship Stability in Following Seas Estimation", Leningrad, Transport, 1977, in Russian.
8. Arndt B., "Ausarbeitung einer Stabilitätsvorschrift für die Handelsmarine. Jahrbuch der STG, 59 Band, 1965.
9. Arndt B., Brandl H., Vogt K., "20 Years of Experience Stability Regulations of the West-German Navy.", Proceedings of the 2<sup>nd</sup> International Conference on Stability of Ships and Ocean Vehicles, Tokyo, 1982, pp. 765-775.
10. Martin J.E., Kuo Ch., Welaya Y., "Ship Stability Criteria Based on Time-Varying Roll restoring Moments", Proceedings of the 2<sup>nd</sup> International Conference on Stability of Ships

- and Ocean Vehicles, Tokyo, 1982, pp. 227-242.
11. Bogdanov A.I., "Stability Criterion. Safe Speed and Wave-to-Course Angle Diagrams For a Ship Sailing in Storm Following Seas", 18 SMSSH, 6 National Congress of Theoretical and Applied Mechanics, Actual Problems in Ship Hydro- and Aerodynamics, v.3, p.81-1 - 81-9, BSHC, Varna, Sept., 1989.
  12. Bogdanov A.I., "Stability Regulation. Safe Speed and Wave-to-Course Angle Diagrams For a Ship Sailing in Storm Following Seas", USSR Register, proceedings, v.17, 1991, pp 20-44, in Russian.
  13. RD 31.00.57.1-88 "Choice of Safe Speeds and Wave-to-Course Angles For a Ship Sailing in Storm Following Seas.", Moscow, Morteinformreclama, 1988, 40p. , in Russian.
  14. RD 31 00.57 2-91 "Choice of Safe Speeds and Wave-to-Course Angles For a Ship Sailing in Storm Following Seas.", Moscow, Morteinformreclama, 1993, 59p. , in Russian.
  15. Bogdanov A.I., "Regression Formula for Calculations of Ships Stability in Following Seas Factor",. Thes. of Conference "XXXVI Krylov Readings -1993", St. Petersburg, 1993, pp. 71-74, in Russian.
  16. Russian Register of Shipping, "Rules of Sea Ships Classifications and Constructions", Part IV "Stability", v.1, 1995, 464p, in Russian.
  17. Lugovsky V.V., "History of Development and Directions of Perfection the Stability Regulations of Russian Sea Register of Shipping", St. Petersburg, Russian Sea Register of Shipping, proceedings, v.19, 1996, pp. 83-93, in Russian.
  18. Rakhmanin N.N., Vilensky G.V., "Following Seaway and Ship Crankness", St. Petersburg, Russian Sea Register of Shipping, proceedings, v.19, 1996, pp. 122-140, in Russian.
  19. Aksiutin L.R., "Probable mistakes at a ship-board stability calculations", EIMT, Seria "Ship operation, communication and maritime safety", v. 9(304), 'Moscow, Morteinformreclama, 1994, pp. 1-5, in Russian.
  20. Salov V.E., "Providing of Stability Control Quality for the Conventional Ships in Operation", CNIIMF proceedings, St. Petersburg, 1992, pp.154-167, in Russian.
  21. Russian Federation, "Problem of the stability control of transport ships in operation", SLF 37/3/7, IMO, 1992.
  22. Japan, "Safety Operational Manual in Following and Quartering Waves", SLF 36/3/4, 1991.
  23. Russian Federation, "Safety Operational Manual for Avoiding Dangerous Conditions in Following and Quartering Seas", SLF 37/3/5, IMO, 1992.
  24. Poland, "Safety Operational Manual for Avoiding Dangerous Conditions in Following and Quartering Seas", SLF 38/3, IMO, 1993.
  25. Canada, "Guidance to the Master for Avoiding Dangerous Situations in Following and Quartering Seas", SLF 38/3, IMO, 1993.
  26. Draft MSC circular, "Guidance to the Master for Avoiding Dangerous Situations in Following and Quartering Seas", SLF 39/18, IMO, 1995.
  27. Japan, "Safety Operational Manual in Following and Quartering Waves", SLF 37/3/2, 1992.
  28. Japan, "Guidance to the Master for Avoiding Dangerous Situations in Following and Quartering Seas", SLF 38/INF.10, IMO, 1994.
  29. Umeda N. Operational Stability in Following and Quartering Seas: A proposed Guidance and its validation, proceedings. 5<sup>th</sup> International Conference on Stability of Ships and Ocean Vehicles. V.2. Florida, Melbourne, 1994, pp. 71-85.

# SURVIVAL TESTS OF A DAMAGED FERRY VESSEL

J.M. Riola, A. Marón

Canal de Experiencias Hidrodinámicas de El Pardo (Spain)

## ABSTRACT

In August 1995 an association of Spanish shipowners and shipbuilders asked the "El Pardo Model Basin" (CEHIPAR) to carry out a series of seakeeping tests of a damaged passenger ferry vessel.

The main aim of the tests was to contribute to a better understanding of the effect on stability and survivability of the water inflow in the garage deck after a side damage. The tests were also useful to develop a methodology for future tests of this kind.

## 0.- INTRODUCTION

The ship forms were based in the J.J. Síster, a typical Spanish ferry vessel owned by Compañía Transmediterránea. A side damage near amidships was reproduced. The model was loaded so as to achieve different residual freeboards with an upright and evenkeel after damage condition.

For each loading condition several GM's were tested including the minimum SOLAS'90 requirement.

The model was subjected to three different wave conditions for each combination of residual freeboard and GM. These corresponded to 1.5, 2.75 and 4 meters significant wave height.

The test set-up, test cases and results obtained are described in the following paragraphs.

## 1.- MODEL DESCRIPTION

The model scale was 1:24. Table I shows the main particulars of the ship and model corresponding to the moulded draft.

Table I. Main Particulars

	Ship	Model
Length overall (m)	140.8	5.867
Length between perp. (m)	125.0	5.208
Maximum breadth (m)	22.0	0.917
Moulded draft (m)	6.0	0.250
Depth to garage deck (m)	8.1	0.338
Garage deck area (m <sup>2</sup> )	2300	3.993

The model was made of wood. The model arrangement together with its instrumentation is shown sketched in figure 1.

The rudder and bilge keels of the actual ship were reproduced in the model. The model was fitted with four holds to contain the varying ballast weights. Reserve buoyancy was put over the upper deck to avoid complete capsizing of the model.

A garage deck was reproduced at 8.1 meters over the baseline without any obstruction, casings or trunks. This garage deck had no sheer in the model for simplicity of construction.

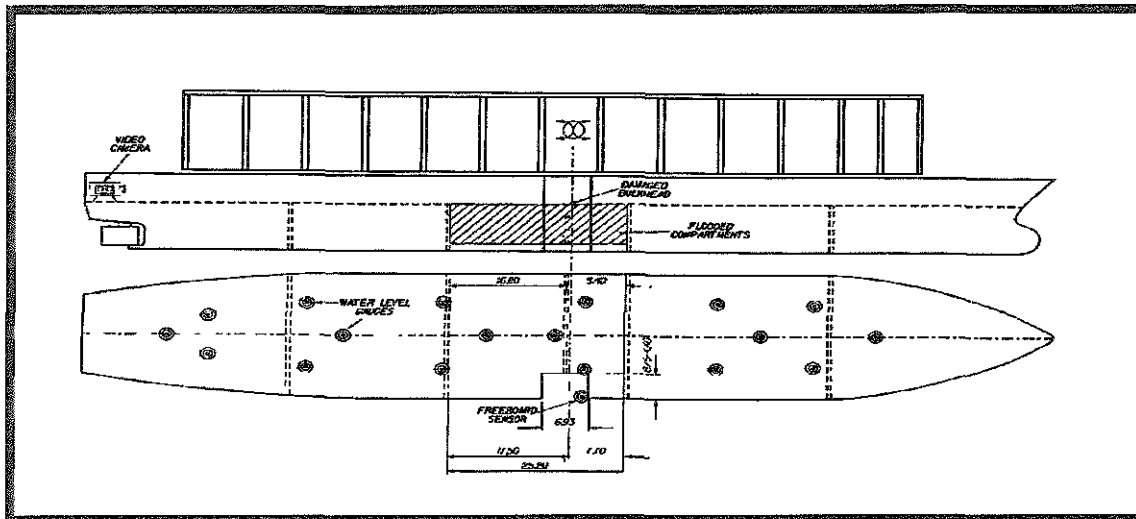


Figure 1

A damage extending  $0.03 L_{wl} + 3$  meters  $0$  in length and with a penetration of  $B/5$  was cut on the starboard side. The vertical extension was from the bottom to the upper deck.

This damage produced the flooding of the two largest adjacent compartments of the real ship (the main engine room and the auxiliary machinery room) extending a total of 20.2% (25.2 m) of the ship's length.

The double bottom was not flooded in these tests, although its complete flooding was simulated with additional ballast. The damaged bulkhead was reproduced except for the damage extension.

The different loading conditions and GM's were obtained by varying the ballast distribution in the holds and upper deck.

The drafts were checked against draft marks with the ship in water.

The GM's were adjusted to the target values by means of inclination tests before and after damage.

The transversal radius of gyration of the model was measured prior to the tests and the total transversal radius of gyration of the model plus ballast was checked to be within 5% of  $0.35 B$ .

The model was fitted with instrumentation to measure:

- Roll angle.
- Water elevation at 18 points distributed uniformly on the garage ro-ro deck as shown in figure 1.
- Water elevation at the damage opening, giving an indication of the instantaneous freeboard.

A waterproof video camera was installed inside the garage space to record the ingress of water through the damage. Two external video cameras recorded the model motions.

All the signals were digitised and sampled at a rate of 20 Hz (4.08 Hz at full scale) and recorded in hard disk.

## 2.- TESTS PERFORMED

Nine different loading conditions were proposed initially in order to study the influence of residual freeboard and stability in the ship behaviour after damage. All the loading conditions were such that the ship will stay upright and evenkeel after damage because this was expected to be the worse condition from the point of view of water ingress.

The nine conditions were the combinations of three residual freeboards at the damage (2.00, 1.15 and 0.81 meters) and three effective metacentric heights after damage. One of the metacentric heights was the minimum required by SOLAS'90 for each of the three drafts. The other two metacentric heights were 0.5 and 1 meters over this minimum value.

The 0.81 meters residual freeboard would correspond to the real ship maximum draft after the damage considered in these tests.

Actually, for the 0.81 meters residual freeboard it was not possible to increase the GM more than 0.8 meters over the minimum required GM.

Therefore the ship was tested with 0.8 and 0.4 meters of additional GM instead of the 1 and 0.5 meters originally intended. Also, due to time constraints, the tests with 2 meters freeboard and minimum GM was skipped and therefore the corresponding results are not available for this report. Looking at the results obtained for 2 meters freeboard and other GM's, it seems that this condition is not very dangerous for the ship.

Table II resumes the eight different loading conditions tested:

**Table II. Loading Conditions**

GM	Residual freeboard		
	2.0 m	1.15 m	0.81 m
SOLAS'90		X	X
SOLAS'90 + 0.5	X	X	X(*)
SOLAS'90+1 m	X	X	X(*)

(\*) The actual GM's were 0.4 and 0.8 meters over the minimum required SOLAS'90 value due to model constraints.

The displacements and drafts before and after the damage for each residual freeboard and the minimum GM required by SOLAS 90 are given in tables III and IV.

**Table III. Displacements and drafts before and after damage**

		Residual Freeboard		
		2.0	1.15	0.81
Intact Cond.	Displac. (mt)	6423	7860	8475
	Mean draft (m)	4.57	5.29	5.59
	Trim (m)	0.37	0.8	0.89
Damage Cond.	Mean draft (m)	6.1	6.95	7.29
	Trim (m)	0.0	0.0	0.0

**Table IV. GM's before and after damage (SOLAS 90 requirement)**

Residual Freeboard (m)	Min. GM before damage (m)	Min. GM after damage (m)
2.00	0.851	0.494
1.15	1.296	1.517
0.81	1.980	2.403

A roll extinction test was performed for each loading condition in order to determine the natural roll period. Table V gives the measured rolling periods.

**Table V. Natural rolling periods (seconds)**

GM	Residual freeboard		
	2.00 m	1.15 m	0.81 m
SOLAS'90		13.82	11.34
SOLAS'90 + 0.5	18.60	12.76	10.76
SOLAS'90+1	15.16	10.92	9.80

For each of the loading conditions, the model was subjected to irregular long crested seas corresponding to wave spectra with three different significant wave heights ( $H_s$ ).

Following the recommendations of the IMO Panel of Experts, Jonswap spectra with a peak period of  $4\sqrt{H_s}$  and a peak enhancement factor of 3.3 was used.

The three different combinations of significant wave height and peak period are given in table VI

Table VI. Wave characteristics

Significant wave height (m)	Peak period (s)
1.50	4.90
2.75	6.63
4.00	8.00

For each sea state two different realisations were tested with a duration corresponding to half an hour each at full scale. Therefore, a total of 48 runs were made corresponding to a duration of 24 hours at full scale.

The wave tests were performed in the large CEHIPAR seakeeping model basin. This basin is 150 m long, 30 m wide and 5 m deep so that no depth or wall side effects can be expected.

Each run was started with the model parallel to the wave crests and with the damaged side (starboard) to the incoming waves.

The model was free to drift with the waves and to move in the six degrees of freedom.

Two rope lines were tied to the bow and the stern near the waterline in order to restrain the model from turning away from the waves.

These ropes proved to be unnecessary as the model remained almost parallel to the wave crests during all the runs and therefore they kept completely slack not influencing ship motions.

The data acquisition was started after the wave pattern was fully developed.

The computerised planar motion carriage (C.P.M.C.) was moved following the model drift so that the umbilical cable was kept as slack as possible.

### 3 - ANALYSIS OF RESULTS

The observation of the video recordings and the numerical results indicates a homogeneous behaviour of the model in all the runs. After a few waves have produced a massive inflow of water into the garage, the ship heels away from the incoming waves (to port) accumulating water in the port side and increasing the actual freeboard at the damage point.

Further groups of high waves produce additional ingress of water augmenting the port side heel and the freeboard presented to the waves.

The frequency and amount of water inflow diminishes with time as the waves have more difficulty in exceeding the freeboard at the damage until some stable condition is reached.

Eventually a big wave or group of waves forces the model to heel to the waves (starboard side). In such cases the final result is that a substantial amount of the water accumulated previously leaves the ship through the damage taking advantage of the relatively mild waves following the high wave group.

After that, it takes a short time for the model to heel again to the port side and the cycle of increasing water accumulation begins again until either the stable condition is reached or a new ingress of water with a starboard heeling occurs.

The time the ship heels to the waves is generally of a very short duration lasting a few wave cycles, just until the next high waves come.

Only on one occasion ( $H_s=2.75$  m,  $F_b= 1.15$  m,  $GM=SOLAS + 0.5$  m) the ship stayed for a long time (about half the run duration of 30 minutes full scale) heeling to the starboard side.

In such a case a smaller amount of accumulated water was observed because more water left the model through the damage than was introduced by the waves.

As a consequence, the mean heel angle toward the waves was smaller than when heeling to the opposite side.

The tables and figures at the end of this report present same results obtained during these tests. The following three variables have been considered:

- The mean list in the last five minutes (full scale) of the run. This is considered to be the final stable condition for the ship due to the wave induced heel and the heel caused by the accumulated water on the side opposite to the waves.
- The maximum roll angle in the full duration of the test.
- The mean water level in the garage in the last five minutes (full scale) of the run. This value is obtained as an average of the measurements obtained from the 18 water level sensors installed on the garage deck.

The results given correspond to the worst case of the two runs for each load condition and sea state.

Figures 2, 3 and 4 represent the three variables as a function of relative GM after damage. They show some tendency for a higher list and mean water level for the intermediate GM. This is especially clear for the 0.81 m freeboard case.

It can be seen that the maximum mean list during these tests was 12 degrees corresponding to the 1.15 m of freeboard with a significant wave height of 2.75 m and a GM of 0.5 m over the SOLAS 90 requirement.

The maximum roll recorded was 32 degrees.

The dependence on sea state is shown in figures 5, 6 and 7 where the significant wave height is the independent variable. It can be observed that the maximum list occurs generally for the intermediate sea state of 2.75 meters, decreasing

for the higher waves of 4 m. The same happens to the water accumulated on deck. On the other hand, the maximum roll angle is always increases with the wave height.

Figure 8 represents the variation of mean water level as a function of residual freeboard at the damage and compares it with the values proposed by the IMO panel of experts.

It can be seen that the measured water accumulation is similar but a little higher than the values given by the formula proposed by the IMO panel of experts.

#### **4.- STATIC STUDIO**

Apart from the damage stability basin tests carried out at the Ship Dynamics Laboratory further research was undertaken via computer simulation from both static stability and probabilistic calculus. The study focussed on two different areas:

##### **4.1.- PROBABILISTIC METHOD**

Probabilistic method of damage stability was calculated with the module F6/4P of the FORAN naval architecture computer program.

The ship is not of recent construction and therefore unlikely to conform to rule 6/7 of IMO A.265 (VIII) for ferry vessels.

With a subdivision length of 134.82 meters and a total of 930 passengers of which 345 could be allocated in boats, the final indexes required (R) and attained (A) were calculated.

The value of the necessary required index is 0.66322 and the attained one does not reach 0.6:

##### **4.2.- WATER ON DECK**

The "FLOOD" module of FORAN calculates the stability curve taking into account the flooding of the auxiliary machinery room, the main engine room and the ro-ro garage deck.

Table VII summarizes the results for the worse case, i.e. minimum freeboard.

The table shows the cases in which the SOLAS'90 requirements are satisfied considered various levels of water on deck. In this table C/N means compliance/not compliance with the requirements.

**Table VII. Stability for 0.81 m of freeboard**

GM	Mean Water on Deck (m)					
	0	.1	.2	.3	.4	.5
SOLAS'90	C	N	N	N	N	N
SOLAS+0.5	C	C	C	C	C	C
SOLAS+1	C	C	C	C	C	C

It can be observed that the cases of GM plus 0.5 or 1 meter are safe enough.

In the worst case (GM = 0.49 and freeboard = 0.81 m) a total amount of .45 m of water was measured during the tests, for which the stability is far from complying with the SOLAS'90 requirements. Even so the maximum and mean roll angles were below the limits suggested by the Panel of Experts.

## 5.- CONCLUSIONS

The following conclusions can be drawn from these tests:

- In all the cases, with this symmetrical flooding, the model tends to heel to the side opposite to the incoming waves increasing the real freeboard at the damage side.
- The heeling to the side opposite to the waves increases progressively until the freeboard at the damage is large enough to avoid further ingress of water.
- Big waves can produce a temporary and short heel towards the waves. The result will be a

decrease in the amount of water accumulated on the deck.

- A larger GM will generally result in a larger accumulation of water but with a final mean list similar to the case of lower GM's. The reason is, probably, that to obtain a large freeboard, a larger amount of water is needed when the GM is higher.
- The amount of water accumulated on the garage deck for waves of 2.75 and 4 m significant wave height is very similar to that given by the formula of the IMO Panel of Experts.
- Even with this amount of water accumulated on the garage deck, the model, with a GM as required by SOLAS 90 or higher, is able to withstand waves up to 4 m significant height with no capsizing (mean list less than 20°, maximum roll less than 40° and 30° of list not exceeded during more than 20 % of the time).
- Further research seems recommendable. Variables such as wave period damage size and position, effect of obstructions on the deck, initial list, casings and so on, should be further investigated.

## 6.- REFERENCES

1. Model tests carried out at El Pardo Model Basin, 1995.
2. VASSALOS, D., "Capsizal Resistance of Damage ro-ro Ferries", WEGEMT, 1995.
3. VASSALOS, D., PAWLOWSKI, M. and TURAN, O., "Criteria for Survival in Damaged Condition", The safety of Passenger Ro-ro vessels, London, 1996.
4. ARIAS, C., "Revision al Concepto de Seguridad", Ingenieria Naval, Oct-1995 (in Spanish).

5. MARON, A. and RIOLA, J. M. "Ensayos de Estabilidad después de averías en Buques Roro Ferries", pub. N° 135 CEHIPAR, Feb-1996.

## AKNOWLEDGEMENTS

Authors want to thank to José L. Martin his cooperation and the Ship Dynamics Laboratory personnel for their daily work.

**TESTS OF DAMAGED FERRY**

Mean list in the last 5 minutes

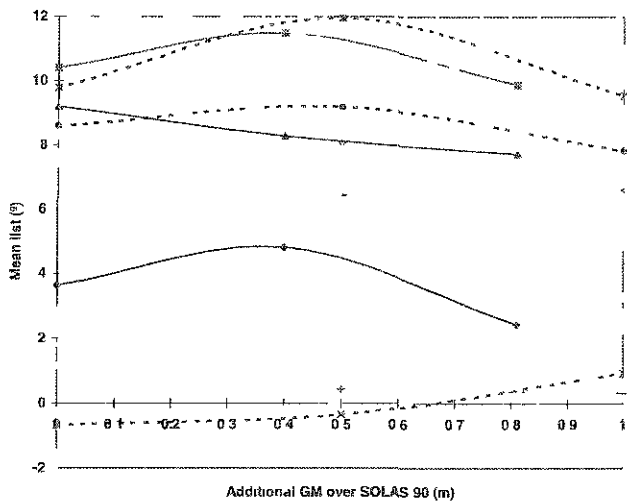


Figure 2

**TESTS OF DAMAGED FERRY**

Mean water level in garage in the last 5 minutes

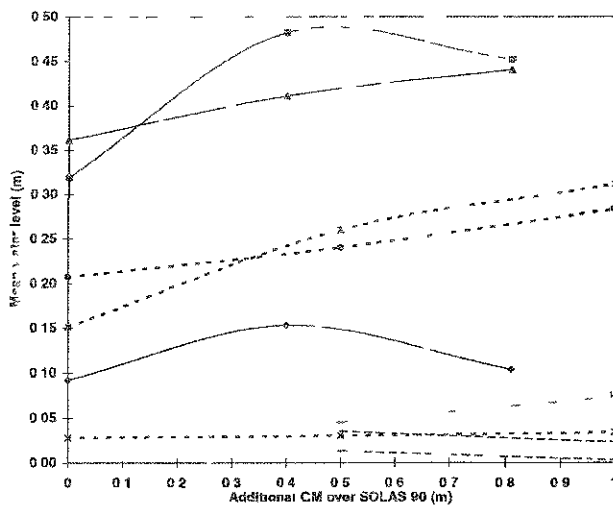


Figure 4

**TESTS OF DAMAGED FERRY**

Maximum roll angle

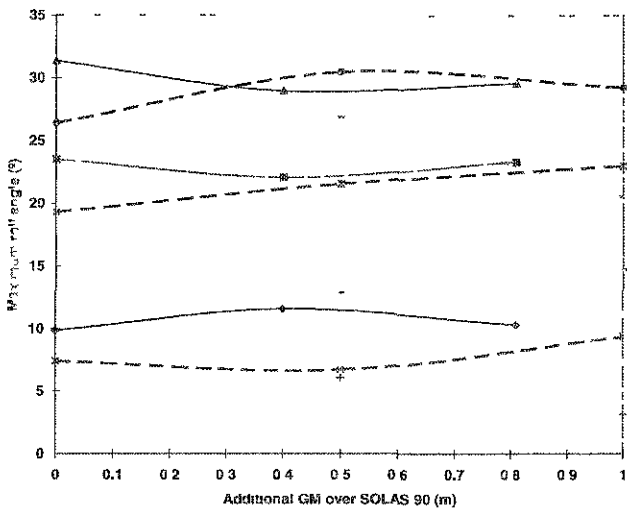
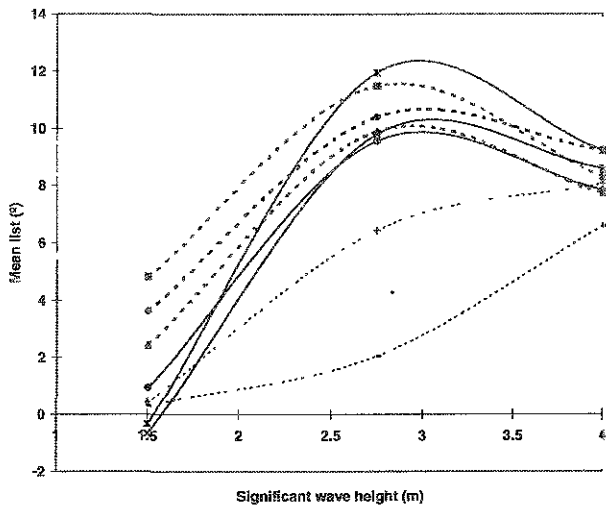


Figure 3

- ◆— fb=0.81 Hs=1.50
- fb=0.81 Hs=2.75
- ▲— fb=0.81 Hs=4.00
- ×— fb=1.15 Hs=1.50
- \*— fb=1.15 Hs=2.75
- fb=1.15 Hs=4.00
- +— fb=2.00 Hs=1.50
- fb=2.00 Hs=2.75
- fb=2.00 Hs=4.00

**DAMAGED FERRY TESTS**  
**Mean list in the last 5 minutes**



**Figure 5**

**DAMAGED FERRY TESTS**  
**Maximum roll angle**

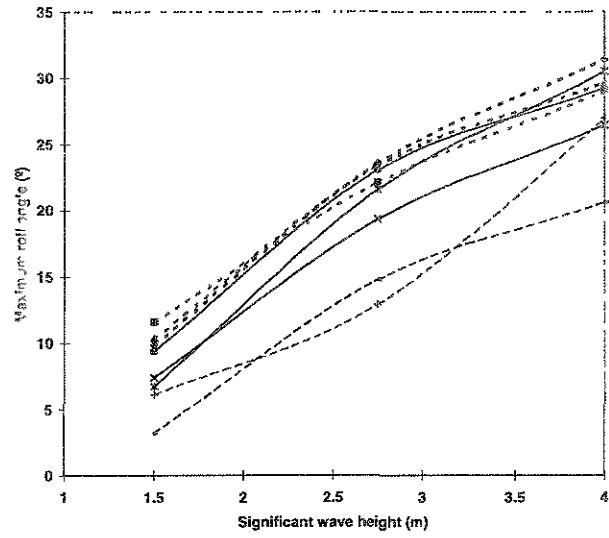


**Figure 6**

**DAMAGED FERRY TESTS**  
**Mean garage water level in last 5 minutes**

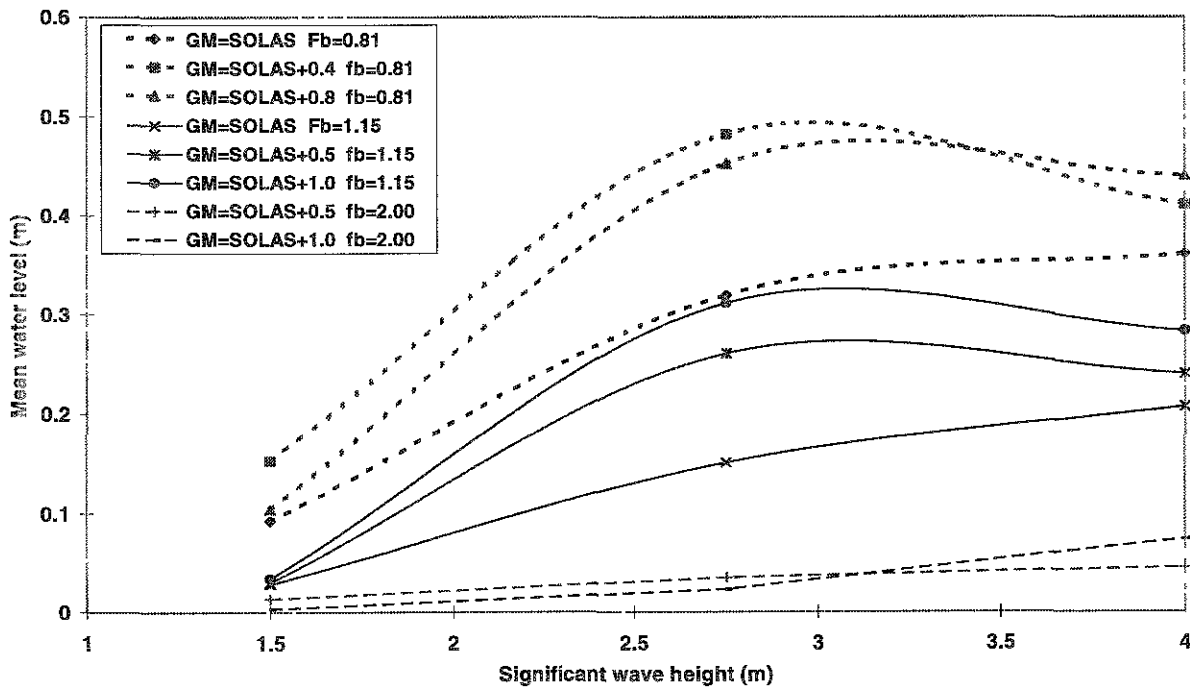


**Figure 7**

**DAMAGED FERRY TESTS**  
**Mean water level in the last 5 minutes**

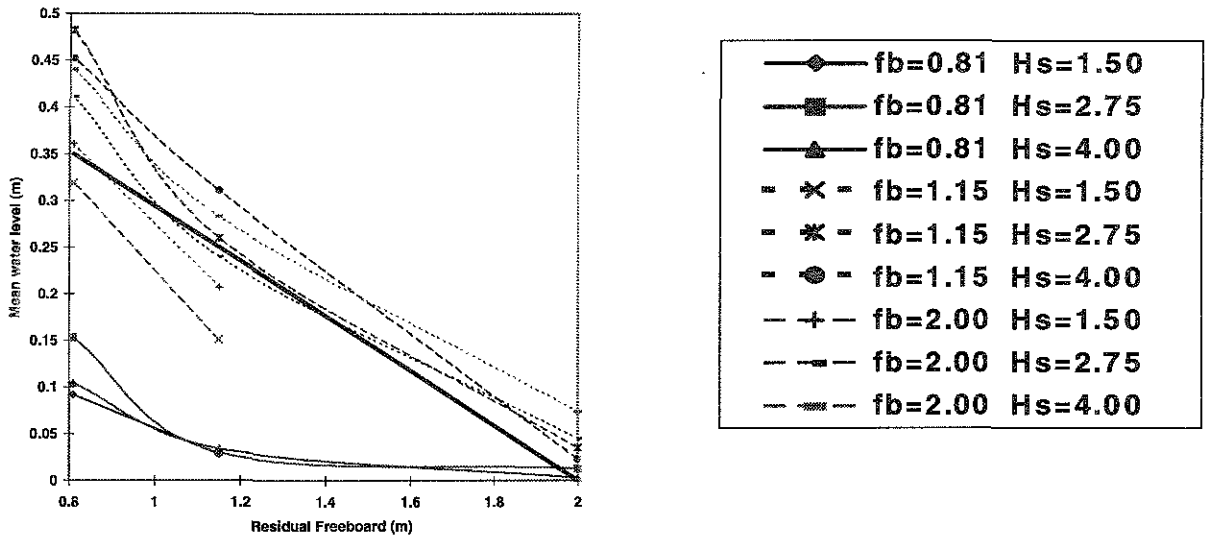


**Figure 8**

**ON A 3-D MATHEMATICAL MODEL  
OF THE DAMAGE STABILITY OF SHIPS IN WAVES**

G. Zaraphonitis<sup>1</sup>, A.D. Papanikolaou<sup>2</sup>, D. Spanos<sup>3</sup>  
<sup>1</sup>Dr.-Eng., MARTEDEC S A., <sup>2</sup>Professor, NTUA, <sup>3</sup>Dr.-Eng. Cand., NTUA

Ship Design Laboratory, National technical University of Athens  
 Heroon Polytechniou 9, 15 773 Zografou, Athens, GREECE

**ABSTRACT**

The formulation of a three dimensional, six degrees of freedom, mathematical model for the simulation of large amplitude motions and capsize of a damaged ship at zero forward speed in waves is presented. The employed numerical solution and the related computer algorithm are explained and results from an application of the developed method to an existing Ro-Ro Passenger ferry are presented and discussed.

**NOMENCLATURE**

$A_y^\infty$  infinite frequency added mass coefficients ( $i, j = 1, \dots, 6$ )  
 $B_y(\sigma)$  damping coefficients ( $i, j = 1, \dots, 6$ )  
 $\bar{F}$  sum of external forces  
 $F'_{Di}(t)$  diffraction forces ( $i = 1, \dots, 6$ )  
 $F'_{Rj}(t)$  radiation forces ( $i = 1, \dots, 6$ )  
 $I$  intact ship inertia matrix  
 $G$  intact ship centre of gravity.  
 $Gx'y'z'$  body-fixed coordinate system  
 $K_y(\tau)$  kernel function ( $i, j = 1, \dots, 6$ )  
 $\bar{M}_C, \bar{M}_G$  sum of external moments about points  $C$  and  $G$  respectively  
 $m_S$  intact ship mass  
 $m_w$  flood water mass  
 $OXYZ$  inertial coordinate system  
 $R$  coordinate transformation matrix  
 $t$  time

$W$  flood water centre of gravity.  
 $\bar{X}_G$  position vector of  $G$  with respect to the inertial coordinate system  
 $\bar{X}_W$  position vector of  $W$  with respect to the inertial coordinate system  
 $\beta$  wave heading in the inertial coordinate system  
 $\beta_i$  wave heading in the body-fixed coordinate system  
 $\theta, \phi, \psi$  Euler angles ( $\theta$  roll,  $\phi$  pitch and  $\psi$  yaw)  
 $\sigma$  wave frequency  
 $\tau$  time lag  
 $\bar{\omega}$  angular velocity vector expressed in the inertial coordinate system  
 $\bar{\omega}'$  angular velocity vector expressed in the body-fixed coordinate system

**INTRODUCTION**

The present paper derives from current research at the Ship Design Laboratory of NTUA on the damage stability of Ro-Ro passenger ships in waves, in view of recent regulatory developments of IMO (SOLAS 95, Regional agreement, Reg. 14) to allow the physical modelling of the damage stability of Ro-Ro passenger ships in waves as an alternative to the so-called 'water on deck' penalty concept. In the light of these developments, it becomes evident that the availability of proper computer algorithms, allowing the theoretical simulation of the capsize of a damaged ship in waves,

provides the necessary flexibility and efficiency to address systematically alternative design measures, in order to improve the survivability of the ship and to ensure compliance with SOLAS regulations

Based on previous work of the Ship Design Laboratory of NTUA in the field of linear and nonlinear ship motions (Zaraphonitis and Papanikolaou [11]), a six degrees of freedom mathematical model for the ship motions in waves, at zero forward speed, has been formulated and solved numerically, in the time domain, allowing the theoretical-numerical simulation of large amplitude ship motions and the prediction of capsizing under specific environmental conditions.

The nonlinear, 6 DOF equations of ship motions, accounting for the effect of flooding in case of ship damage, have been formulated based on large amplitude rigid body dynamics. In order to simplify the formulation and subsequent solution of the equations, the effect of the flood water is treated assuming the mass concentrated at the centre of volume occupied by the fluid. A semi-empirical water ingress/outflow model is used for the estimation of the flow of water into and out the damaged compartments. Radiation and wave diffraction forces are calculated using hydrodynamic coefficients from application of a 3D computer code in the frequency domain, and by employing the impulse response function concept for the calculation of forces in the time domain. Froude-Krylov and hydrostatic forces are calculated by direct pressure integration over the instantaneous wetted surface.

An advanced numerical integration method has been developed, based on the extrapolation numerical integration technique, which proved to be very efficient. The developed algorithm has been implemented at a DEC 3000 Alpha workstation.

## 2. MATHEMATICAL MODEL

### 2.1 Coordinate Systems

Four coordinate systems will be used to express the equations of motion. Let  $OXYZ$  be an inertial coordinate system, with  $OZ$  vertical and positive upwards and  $Gx'y'z'$  a body-fixed coordinate system with  $G$  located at the centre of gravity of the intact ship. We introduce also a coordinate system  $OX'Y'Z'$  which is always parallel to the body-fixed coordinate system and  $Gxyz$  which is always parallel to the inertial coordinate system.

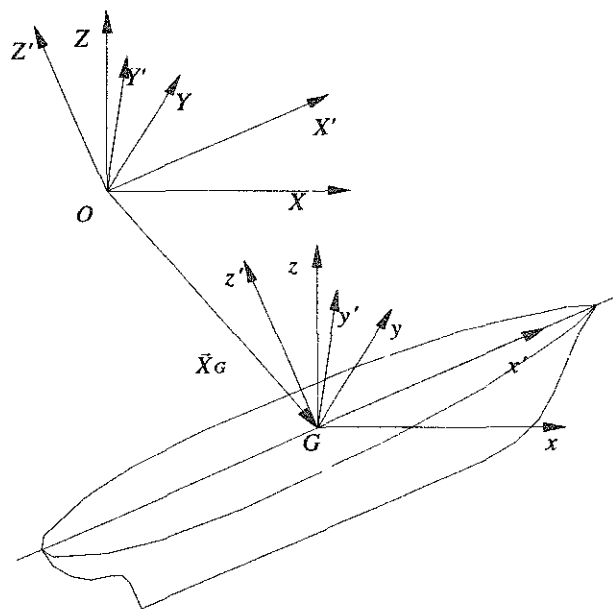


Fig. 1. Coordinate systems

When the ship is at rest, point  $O$  coincides with  $G$  and all coordinate systems coincide with each other. The instantaneous position of the ship is uniquely defined by the position vector  $\vec{X}_G$  of point  $G$  with respect to the inertial coordinate system and the three Euler angles (yaw, pitch and roll).

Let  $P$  be a point in space and  $\vec{X}$  its position vector with respect to the inertial coordinate system. Let  $\vec{X}'$ ,  $\vec{x}$  and  $\vec{x}'$  be the position vectors of point  $P$  with respect to systems  $OX'Y'Z'$ ,  $Gxyz$  and  $Gx'y'z'$  respectively

These vectors can be transformed to each other using a coordinate transformation matrix  $\mathbf{R}$

$$\bar{X} = \mathbf{R} \bar{X}' = \bar{X}_G + \bar{x} = \bar{X}_G + \mathbf{R} \bar{x}' \quad (1)$$

The full expression for the coordinate transformation matrix  $\mathbf{R}$  is given in appendix A.

In the following, all vectors or matrices expressed with respect to  $OXY'Z'$  or  $Gx'y'z'$  will be marked with an ( $'$ ), while one or two dots over a variable or function denote first or second order time derivative

## 2.2 Equations of Motion

We consider the complete dynamic system consisting of the intact ship and the flood water. In order to simplify the derivation and solution of the motion equations of the above dynamic system, the mass of the flood water is assumed to be concentrated at its centre of gravity. This is a rather reasonable assumption, since as already discussed in previous work (see e.g. Vassalos [10]), the effect of sloshing is expected to be weak. Sloshing can induce considerable dynamic effects when the excitation frequency is close to the natural frequency of the flood water. However, the possibility of resonance is rather small, since the roll natural frequency of Ro-Ro ferries is usually much lower than the natural frequency of the flood water, unless the flood water layer is thin. In this latter case, sloshing will be naturally negligible, due to the small mass of oscillating water involved.

According to Newton's second law

$$\bar{F} = \frac{d}{dt} \iiint_V \rho \dot{\bar{X}} dV \quad (2)$$

For the angular motion the expression is

$$\bar{M}_C = \frac{d}{dt} \iiint_V \rho \bar{X} \times \dot{\bar{X}} dV \quad (3)$$

where  $\bar{F}$  and  $\bar{M}_C$  are the sum of all external forces and moments (about  $C$ ) applied to the dynamic system consisting of the intact ship and the flood water, expressed in the inertial coordinate system.

Let  $W$  be the centre of gravity of the flood water and  $\bar{X}_W$  its position vector, expressed with respect to the inertial coordinate system. Equation (2) can take the form

$$\bar{F} = m_s \ddot{\bar{X}}_G + m_w \ddot{\bar{X}}_W + \dot{m}_w \dot{\bar{X}}_W \quad (4)$$

where  $m_s$  is the mass of the intact ship and  $m_w$  is the mass of the flood water.

It can be easily proved that:

$$\iiint_V \rho \bar{X} \times \dot{\bar{X}} dV = m_s \bar{X}_G \times \dot{\bar{X}}_G + \mathbf{R} (\mathbf{I} \dot{\bar{\omega}}') + m_w (\bar{X}_G + \bar{x}_w) \times (\dot{\bar{X}}_G + \dot{\bar{x}}_w) \quad (5)$$

where  $\bar{x}_w$  is the position vector of  $W$ , expressed in  $Gxyz$ . Let  $\bar{M}_G$  be the sum of all external moments about point  $G$ , also expressed in  $Gxyz$

$$\bar{M}_G = \bar{M}_C - \bar{X}_G \times \bar{F} \quad (6)$$

Introducing equations (5) and (6) in (3) and after some manipulations, the equation of angular motion takes the following form:

$$\bar{M}_G = \mathbf{R} (\mathbf{I} \dot{\bar{\omega}}' + \bar{\omega}' \times (\mathbf{I} \bar{\omega}')) + m_w \bar{x}_w \times (\ddot{\bar{X}}_G + \ddot{\bar{x}}_w) + \dot{m}_w \bar{x}_w \times (\dot{\bar{X}}_G + \dot{\bar{x}}_w) \quad (7)$$

The details of the derivation of the above equations can be found in Zaraphonitis [12]. In Appendix B, equations (4) and (7) are transformed in a form more suitable to be used in a numerical integration scheme

### 2.3 Exciting Forces

The external forces and moments consist of the following parts:

- Froude-Krylov and hydrostatic forces

Froude-Krylov and hydrostatic forces and moments are calculated by direct numerical integration of the incident wave pressure and hydrostatic pressure respectively over the instantaneous wetted surface. Integration is extended up to the instantaneous free surface, taking into account the ship's motions and the free surface elevation due to the incident wave. The distortion of the free surface due to the diffraction of the incident wave system and due to radiation is omitted.

- Radiation forces

Radiation forces and moments are associated with the disturbance of the flow due to the motion of the ship. Ignoring the nonlinearity of the problem and following Cummins procedure ([1]), radiation forces and moments are calculated from the added mass and damping coefficients of the ship (see, also, de Kat and Paulling [3]):

$$F'_{R,i}(t) = -A_y^\infty \ddot{X}'_{G_j} - \int_0^\infty K_y(\tau) \dot{X}'_{G_j}(t-\tau) d\tau, \quad i, j=1, \dots, 6 \quad (8)$$

and

$$K_y(\tau) = \frac{2}{\pi} \int_0^\infty B_y(\sigma) \cos(\sigma\tau) d\sigma \quad (9)$$

where  $A_y^\infty$  is the infinite-frequency added mass coefficient and  $B_y(\sigma)$  is the frequency-dependent damping coefficient of the ship. These coefficients are calculated in the frequency-domain by the three-dimensional computer program NEWDRIFT (Papanikolaou, [6]). The integral of equation (9) for the Kernel

functions is calculated numerically using Filon's method. Due to the very fast decay of the Kernel functions, the integration of the convolution integral in equation (8) is truncated at an appropriate upper limit.

Finally, a quadratic roll damping model is used to correct the employed inviscid flow model for viscous effects, therefore ensuring realistic roll motion responses at resonance.

- Diffraction forces

Diffraction forces and moments are approximated by superposition of the elementary diffraction forces associated with each of the component waves composing the ship exciting wave train:

$$F'_{D,i}(t) = \text{Re} \sum_{n=1}^N F_i^D(\sigma_n, \beta_i) \zeta_n(X_G, Y_G, t), \quad i=1, \dots, 6 \quad (10)$$

where  $F_i^D(\sigma_n, \beta_i)$  is the frequency-dependent diffraction coefficient of mode  $i$ ,  $\zeta_n(X_G, Y_G, t)$  is the instantaneous wave elevation at point  $G$  of wave component  $n$  and  $\beta_i$  is the relative wave heading ( $\beta_i = \beta - \psi$ ).

### 2.4 Water Ingress Model

The flow rate of flood water  $\dot{m}_w$  into respectively out of the damaged ship compartment is calculated by integration over the surface  $A$  of the opening:

$$\dot{m}_w = \iint_A dQ \quad (11)$$

$dQ$  is expressed by a semi-empirical formula (Hutchinson, [2]):

$$dQ = gK \text{sign}(H_{out} - H_{in}) \sqrt{|H_{out} - H_{in}|} dA \quad (12)$$

where  $K$  is an empirical weir flow coefficient,  $H_{out}$  is the height of the external free surface and  $H_{in}$  is the height of the internal free surface at the damage opening.

### 2.5 Natural Seaway Modelling

Two different approaches are used for the modelling of the incident wave spectrum by a finite number of harmonic waves. According to the first approach, we introduce a lower and an upper limit for the wave frequency  $\sigma_{min}$  and  $\sigma_{max}$ . The continuous incident wave spectrum is discretized by a number of  $N$  harmonic wave components of frequency:

$$\sigma_n = \sigma_{min} + n\Delta\sigma \quad (13)$$

and amplitude:

$$a_n = \sqrt{2S(\sigma_n)}\Delta\sigma \quad (14)$$

where:

$$\Delta\sigma = \frac{\sigma_{max} - \sigma_{min}}{N} \quad (15)$$

Following the second approach, the area under the incident wave spectrum curve between  $\sigma_{min}$  and  $\sigma_{max}$  is subdivided into  $N$  parts of equal area  $ds$ . The incident wave spectrum is decomposed into  $N$  harmonic wave components of equal amplitude  $a = \sqrt{2ds}$  and frequency, corresponding to the centre of the  $n$ th elementary part. In both cases, the phase angles of the regular waves are randomly distributed in the entire range  $[0, 2\pi]$ .

The wave energy of the discretized wave systems resulting from the above two approaches, obviously equals the wave energy of the incident irregular seaway. In figures 2 and 3 a JONSWAP spectrum with significant wave height  $H_s = 4.0m$  and peak period  $T_p = 8sec$  is presented, along with its

discretization calculated by the two approaches (amplitudes and corresponding frequencies of the individual harmonic waves).

Let  $m_n$  be the  $n$ th order moment of the continuous wave spectrum. The comparison of the calculated moments of order  $n = -1, \dots, 4$  for the continuous wave spectrum and for the discretized wave systems is also presented in figures 2 and 3. It can be seen that for  $n \geq 2$  the first approach gives better results, which could be expected, since there are more waves in the high frequency range. On the contrary, the second approach gives better results for the moments of negative order.

Let  $T_{-1}$  be the average period of the continuous wave spectrum,

$$T_{-1} = 2\pi \frac{m_{-1}}{m_0} \quad (16)$$

and  $T_1$  the period corresponding to the average frequency of the continuous wave spectrum:

$$T_1 = 2\pi \frac{m_0}{m_1} \quad (17)$$

The calculated values of  $T_{-1}$  and  $T_1$  for the continuous spectrum and for the approximate discrete wave systems, resulting from the above two approaches, are given in the following table:

Table 2. Average Wave Periods

	$T_{-1}$	$T_1$
Cont. Wave Spectrum	7.29048	6.86722
Approach A	7.29656	6.86722
Approach B	7.28516	6.86722

Since in the first approach the frequencies  $\sigma_n$  of the harmonic wave components are equally spaced in the interval  $[\sigma_{min}, \sigma_{max}]$ , the resulting wave system is almost periodic. In order to simulate an irregular seaway for a long time, the

number  $N$  of the harmonic wave components should be quite large. On the other hand, since the frequencies  $\sigma_i$  of the harmonic wave components calculated by the second approach are not equally spaced, the resulting wave system gives a closer simulation of an irregular seaway even with a few wave components. Figure 4 presents the wave elevation calculated by the two methods. The difference in the graphs, as far as the reproduction of aperiodicity for the modelled seaway is concerned, is evident. Therefore, the second approach is adopted, because it gives a better representation of the irregular incident seaway.

### 3. NUMERICAL SOLUTION

The resulting system of differential equations is integrated numerically in the time domain, using an advanced integration method based on an extrapolation scheme described in more details by Stoer and Bulirsch [9]. This method is found very fast and accurate, especially for this specific type of problems. It allows relatively large time stepping and therefore significant reduction of the number of calculations for the right hand side of the equations.

The basic aspects of the adopted numerical procedure for the calculation of the exciting forces and for the implementation of the simulation scheme are presented in more detail in Spanos et al. [7].

For the time being, the computer program runs on a DEC-3000 Alpha deck station. Simulation time is about 15 times slower than real time in case of one compartment flooding, considering an incident wave train consisting of 20 wave components.

### 4. DISCUSSION OF RESULTS

Simulation records for the motion of an existing Ro-Ro passenger vessel, in service between the Greek mainland and the Aegean islands, are

presented. The main characteristics of the Test Ship are presented in Table 1.

Table 1 Test Ship Main Characteristics

$L_{BP}$	142.00	m
B	22.80	m
T	6.40	m
$D_{MAIN DECK}$	8.00	m
$D_{UPPER DECK}$	12.90	m
LIGHT SHIP	7884	t
DISPLACEMENT	11354	t
KG	9.874	m

In figure 5 the discretization of the vessel by  $2 \times 177$  panels is presented. The discretization concerns the vessel's bottom, sides and the first watertight upper deck.

The incident wave is described by a JONSWAP spectrum with  $H_s = 4.0m$  significant wave height and  $T_p = 8sec$  peak period (fig. 3). The initial wave heading  $\beta$  is equal to  $90^\circ$ . The continuous spectrum is approximated by a wave system consisting of 20 elementary waves.

The simulation of the ship's motion is performed for two cases. At first the ship is considered intact, floating freely at the free surface with zero forward speed. In the second case, one compartment of 66m length, ranging crosswise over the entire ship's breadth and vertically from the main to the upper deck, located 3m in front of the intact ship's LCG, is considered flooded. The flood water mass is equal to 10% of the intact ship's displacement and is kept constant throughout the simulation (no water inflow or outflow is considered).

In fig. 6 the simulation records for both cases are presented. In the uppermost graph, the free surface elevation at the centre of gravity of the intact ship is presented (point C), followed by results for the heave, roll and pitch motion. In the last four graphs, the results for the second case (ship with flooded compartment) are presented. Capsize occurs after about 250sec. The fifth graph from the top shows the free

surface elevation at point *C*. Note that, although the incident wave system remains the same in both cases, the free surface elevation given in the first graph differs from that in the fifth one. This is because, in the inertial coordinate system, point *C* is moving in different ways in the two cases, following the motion of the ship. In figures 7 to 12 the same results are presented in the form of phase diagrams.

## 5. CONCLUSIONS

A mathematical model and the corresponding numerical solution procedure for the simulation of large amplitude motions and capsize of a damaged ship are presented, followed by numerical results from the application of the method to a typical Greek Ro-Ro vessel. Further work is now underway in NTUA-SDL towards the refinement and validation of the mathematical model and the developed computer algorithm, as well as to their flexibility for applications to various ship types. A series of model experiments tank are scheduled for late 1997 at NTUA's towing (Laboratory of Marine Hydrodynamics) aiming at the systematic validation of the developed theoretical-numerical method.

Concluding, it is obvious that the presented simulation model will be eventually a valuable tool in the process of designing a Ro-Ro vessel, since it will enable the designer to analyse the impact of damage stability on different design solutions and to maximise the survivability of the vessel, before proceeding to the experimental investigation, following the Equivalent Model Test Method according to SOLAS 95, Res. 14.

## 6. ACKNOWLEDGEMENTS

The authors wish to acknowledge the support to the present research by the Greek Secretariat

General for Research and Technology (code IIENEΔ 1995)

The study is also supported through technical information provided by the Greek Shipowners Association for Passenger Ships, the Union of Greek Coastal Passenger Shipowners and the Hellenic Chamber of Shipping.

## 7. REFERENCES

1. Cummins, W. E., 'The impulse response function and ship motions', Schiffstechnik, vol. 9, no. 47, pp. 101-109, June 1962
2. Hutchinson, L., 'Water on-deck accumulation studies by the SNAME ad hoc Ro-Ro safety panel'. Workshop on Numerical & Physical Simulation of Ship Capsize in Heavy Seas, University of Strathclyde, 1995
3. de Kat J. O., Paulling, J. R., 'The simulation of ship motions and capsizing in severe seas', Trans. SNAME, vol. 97, pp. 139-168, 1989
4. de Kat, J. O., 'Large amplitude ship motions and capsizing in severe sea conditions', Ph.d. Dissertation, Dep. of Naval Architecture and Offshore Engineering, University of California, Berkeley, July 1988
5. Letizia, L., Vassalos, D., 'Formulation of a non-linear mathematical model for a damaged ship subject to flooding', Proc. of the Sevastianov Symposium, Kaliningrad, May 1995
6. Papanikolaou, A. D., 'NEWDRIFT: The six DOF three dimensional diffraction theory program of NTUA-SDL for the calculation of motions and loads of arbitrarily shaped bodies in regular waves', NTUA-SDL, Internal Report, Athens 1988
7. Spanos, D., Papanikolaou, A.D., Zaraphonitis, G., 'On a 6DOF mathematical model for the simulation of ship capsize in waves', to appear in the Proc. of the 8th Int. Congress on Marine Technology, Istanbul, November 1997.

8. Spanos, D., 'Theoretical-numerical modelling of large amplitude ship motions and of capsizing in heavy seas', Dr. Eng. Thesis, Dep. of Naval Architecture, NTUA, in progress.
9. Stoer, B., Bulirsch, R., 'Introduction to numerical analysis', Springer-Verlag, New York, 1980
10. Vassalos, D., 'A realistic approach to assessing the damage survivability of passenger ships', Trans. SNAME, vol. 102, pp. 367-394, 1994
11. Zaraphonitis, G., Papanikolaou, A. D., 'Second order theory and calculations of motion and loads of arbitrarily shaped 3D bodies in waves', Journ. Marine Structures, vol. 6, 1993
12. Zaraphonitis, G., 'Formulation of the equations of motion for a damaged ship in waves', NTUA, Ship Design Laboratory Internal Report, 1997

#### APPENDIX A COORDINATE SYSTEMS TRANSFORMATION

When the ship is at rest, point  $O$  coincides with  $G$  and all coordinate systems coincide with each other. When the ship is moving, the position and the orientation of the body-fixed coordinate system with respect to the inertial one is uniquely defined by the position vector  $\vec{X}_G$  and the set of the three so-called Euler angles: roll ( $\theta$ ), pitch ( $\varphi$ ) and yaw ( $\psi$ ).

To obtain the body-fixed coordinate system from the inertial one, the later is supposed to be translated to  $Gxyz$  and then rotated by an angle  $\psi$  about the yaw axis, then by an angle  $\varphi$  about the new pitch axis and finally by an angle  $\theta$  about the new roll axis.

The transformation matrix between the inertial and the body-fixed coordinate system is given by:

$$\mathbf{R} = \begin{bmatrix} \cos\varphi\cos\psi & \sin\theta\sin\varphi\cos\psi & \cos\theta\sin\varphi\cos\psi \\ & -\cos\theta\sin\psi & +\sin\theta\sin\psi \\ \cos\varphi\sin\psi & \sin\theta\sin\varphi\sin\psi & \cos\theta\sin\varphi\sin\psi \\ & +\cos\theta\cos\psi & -\sin\theta\cos\psi \\ -\sin\varphi & \sin\theta\cos\varphi & \cos\theta\cos\varphi \end{bmatrix} \quad (18)$$

The derivation of (18) can be found in [12].

Let  $\vec{\omega}$  and  $\vec{\omega}'$  be the angular velocity vector expressed with respect to the inertial and the body-fixed coordinate systems respectively:

$$\vec{\omega} = \mathbf{R}\vec{\omega}' \quad (19)$$

It can be proved (see [12]) that:

$$\vec{\omega}' = \mathbf{B} \begin{bmatrix} \dot{\theta} & \dot{\varphi} & \dot{\psi} \end{bmatrix}^T \quad (20)$$

where:

$$\mathbf{B} = \begin{bmatrix} 1 & 0 & -\sin\varphi \\ 0 & \cos\theta & \sin\theta\cos\varphi \\ 0 & -\sin\theta & \cos\theta\cos\varphi \end{bmatrix} \quad (21)$$

#### APPENDIX B EQUATIONS OF MOTION

In order to proceed with the numerical integration of the equations of motion, equations (4) and (7) must be transformed to a more appropriate form.

From eq. (4) we derive:

$$(m_s + m_w)\ddot{\vec{X}}_G = \vec{F} - m_w\ddot{\vec{x}}_w - \dot{m}_w \left( \dot{\vec{X}}_G + \dot{\vec{x}}_w \right) \quad (22)$$

From eq. (7) it can be proved that:

$$\begin{aligned} \vec{M}_G = & \mathbf{R} \left( \mathbf{I} \dot{\vec{\omega}}' + \vec{\omega}' \times (\mathbf{I} \vec{\omega}') \right) + \frac{m_W}{m_S + m_W} \vec{x}_W \times \vec{F} + \\ & + \frac{m_S m_W}{m_S + m_W} \vec{x}_W \times \ddot{\vec{x}}_W + \frac{m_S \dot{m}_W}{m_S + m_W} \vec{x}_W \times \left( \dot{\vec{X}}_G + \dot{\vec{x}}_W \right) \end{aligned} \quad (23)$$

and from eq. (20):

$$\dot{\vec{\omega}}' = \mathbf{B} \begin{bmatrix} \ddot{\theta} \\ \ddot{\phi} \\ \ddot{\psi} \end{bmatrix} + \dot{\mathbf{B}} \begin{bmatrix} \dot{\theta} \\ \dot{\phi} \\ \dot{\psi} \end{bmatrix} \quad (24)$$

Inserting (24) in (23) and after some manipulation we derive:

$$\begin{aligned} \mathbf{I} \cdot \mathbf{B} \begin{bmatrix} \ddot{\theta} \\ \ddot{\phi} \\ \ddot{\psi} \end{bmatrix} = & \vec{M}'_G - \vec{\omega}' \times (\mathbf{I} \vec{\omega}') - \\ & - \mathbf{I} \begin{bmatrix} -\dot{\phi} \dot{\psi} \cos \theta \\ -\dot{\theta} \dot{\phi} \sin \theta + \dot{\theta} \dot{\psi} \cos \theta \cos \phi - \dot{\phi} \dot{\psi} \sin \theta \sin \phi \\ -\dot{\theta} \dot{\phi} \cos \theta - \dot{\theta} \dot{\psi} \sin \theta \cos \phi - \dot{\phi} \dot{\psi} \cos \theta \sin \phi \end{bmatrix} - \\ & - \frac{m_W}{m_S + m_W} \vec{x}'_W \times \vec{F}' - \frac{m_S m_W}{m_S + m_W} \mathbf{R}^T \left( \vec{x}_W \times \ddot{\vec{x}}_W \right) - \\ & - \frac{m_S \dot{m}_W}{m_S + m_W} \mathbf{R}^T \left( \vec{x}_W \times \left( \dot{\vec{X}}_G + \dot{\vec{x}}_W \right) \right) - \end{aligned} \quad (25)$$

Let  $\vec{\xi}$  be a 13-dimensional vector, with:

$$[\xi_1 \quad \xi_2 \quad \xi_3]^T = \vec{X}_G \quad (26a)$$

$$[\xi_4 \quad \xi_5 \quad \xi_6]^T = [\theta \quad \varphi \quad \psi]^T \quad (26b)$$

$$\xi_i = \dot{\xi}_{i-6}, \quad i=7, \dots, 12 \quad (26c)$$

and

$$\xi_{13} = m_W \quad (26d)$$

The equations of motion (eq. 22 and 25) can take the form:

$$\dot{\xi}_i = \xi_{i+6}, \quad i=1, \dots, 6 \quad (27a)$$

and

$$\dot{\xi}_i = f(\xi_1, \dots, \xi_{13}, t), \quad i=7, \dots, 12 \quad (27b)$$

Finally, from eq. (11) and (12) we can derive:

$$\dot{\xi}_{13} = f(\xi_1, \dots, \xi_{13}, t) \quad (27c)$$

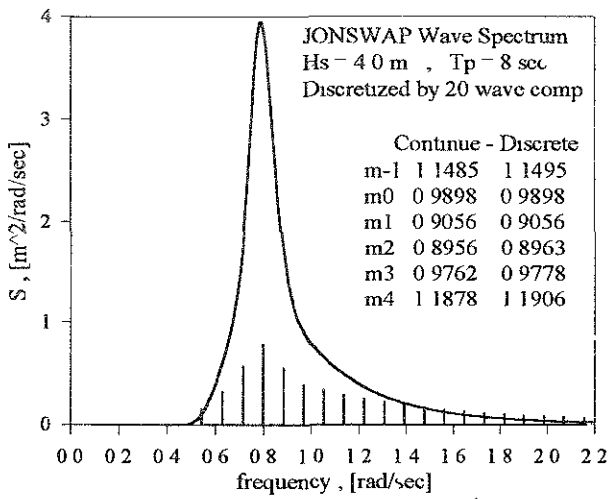


Fig 2 Spectrum discretization - 1<sup>st</sup> approach

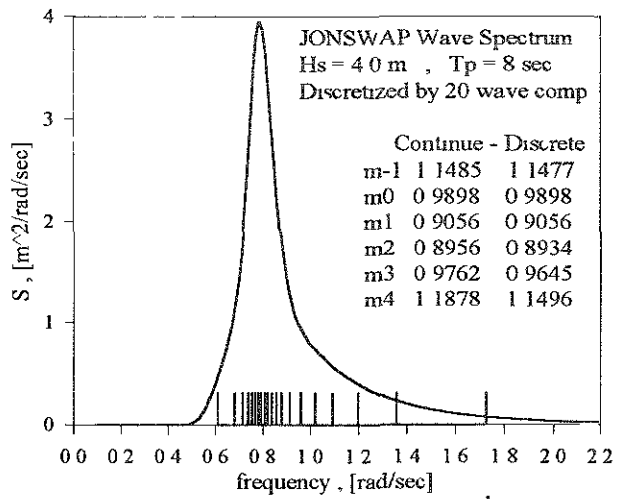


Fig 3 Spectrum discretization - 2<sup>nd</sup> approach

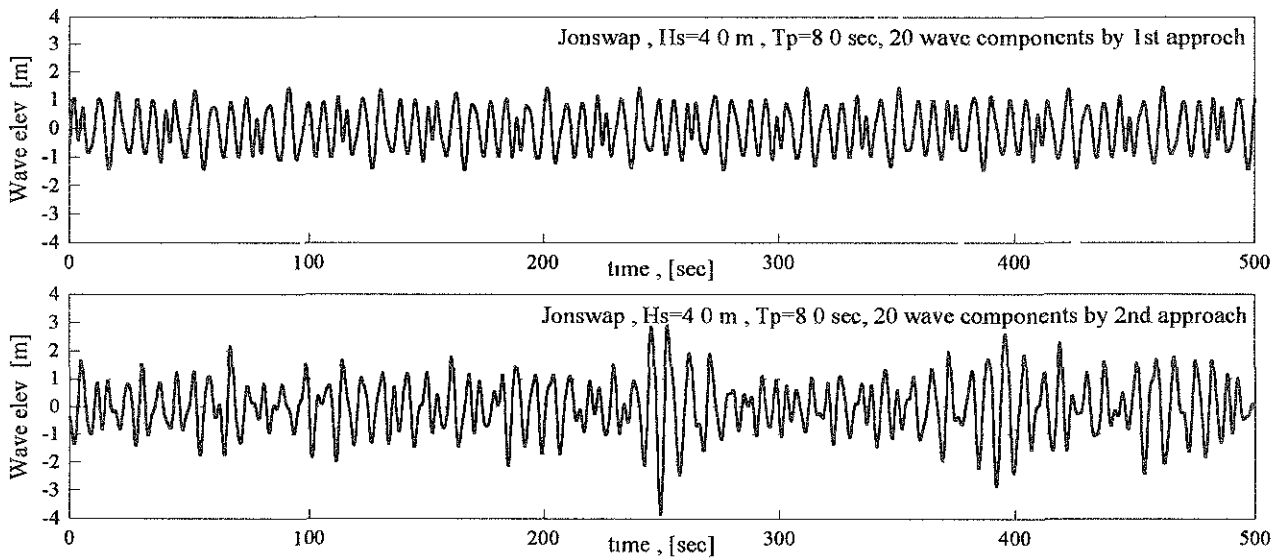


Fig 4 Incident wave records - Comparison of results

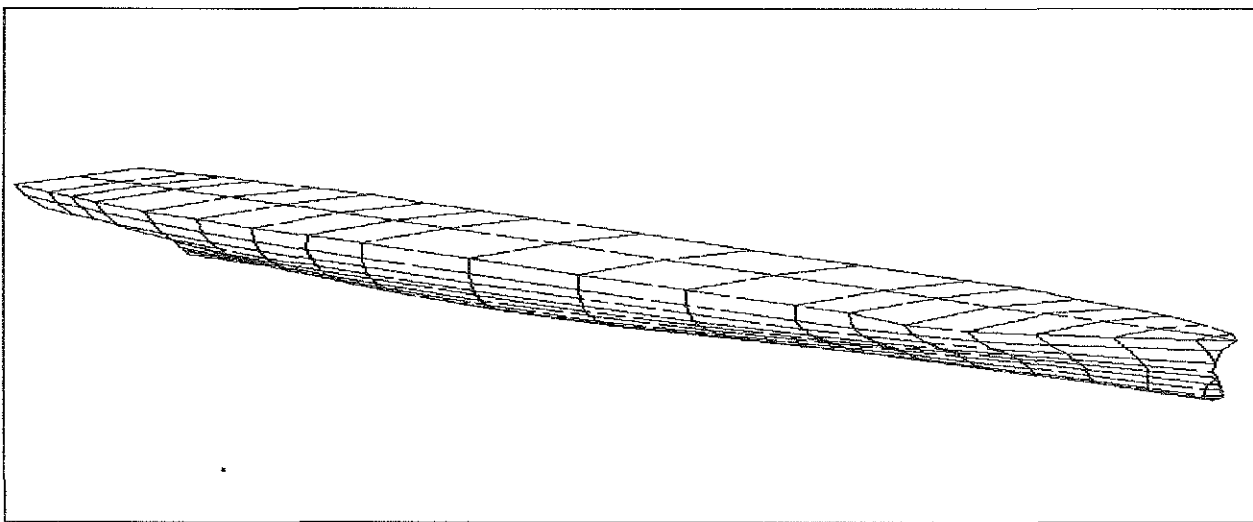


Fig 5 Test ship discretization (2x177 panels)

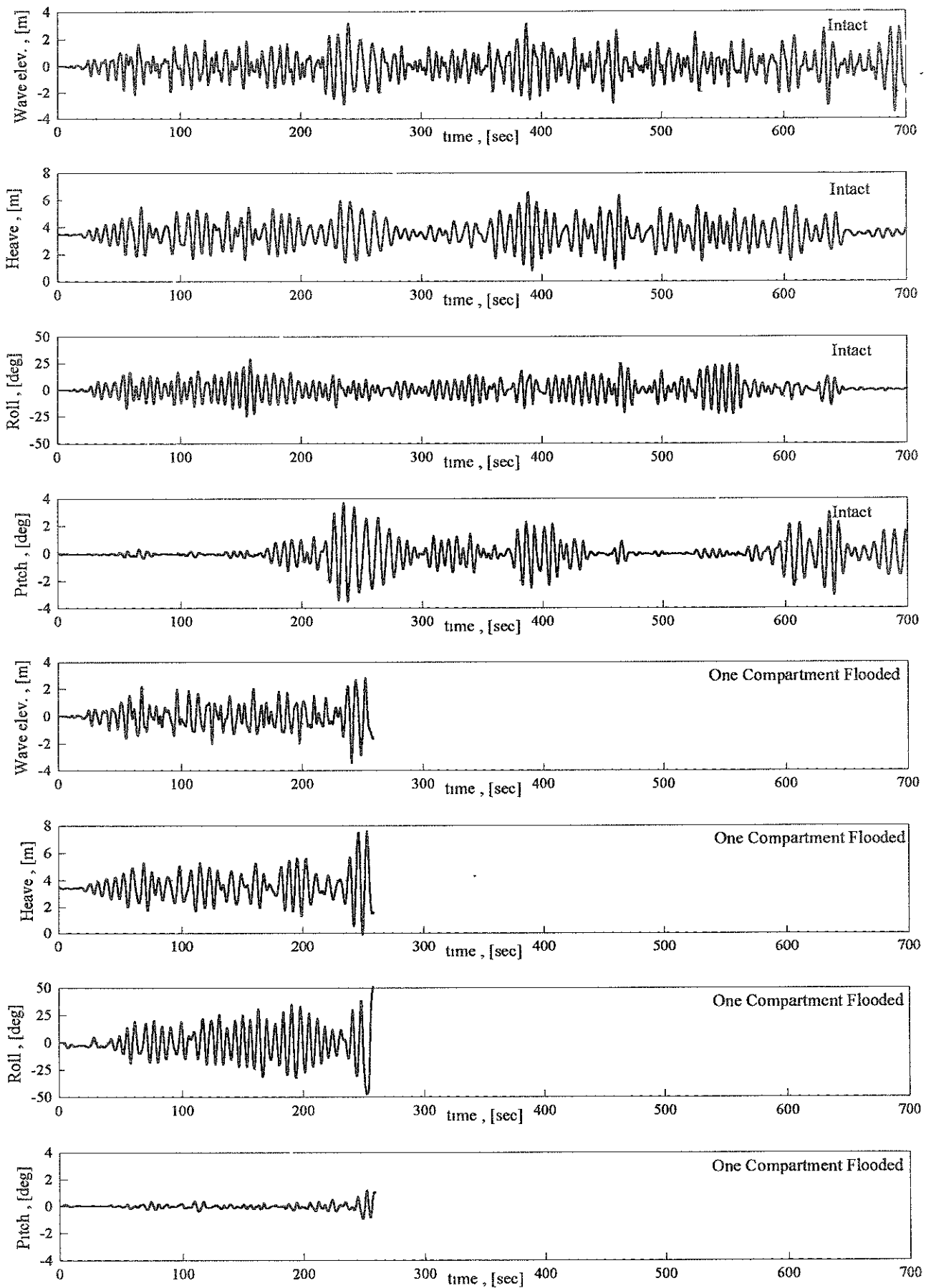


Fig. 6 Simulated records Intact case - Flooded case

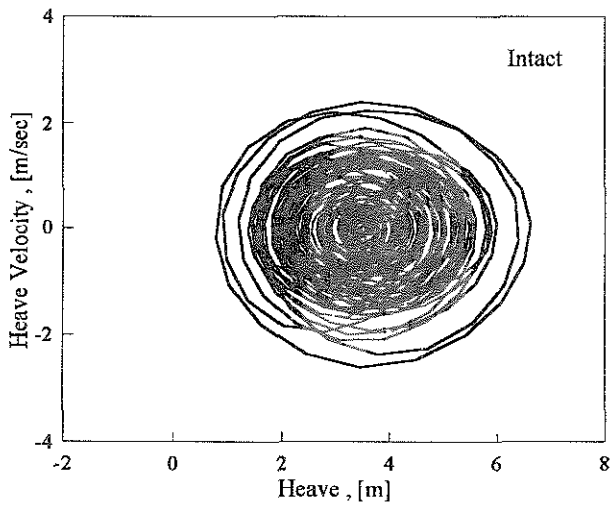


Fig. 7. Heave phase diagram, intact case

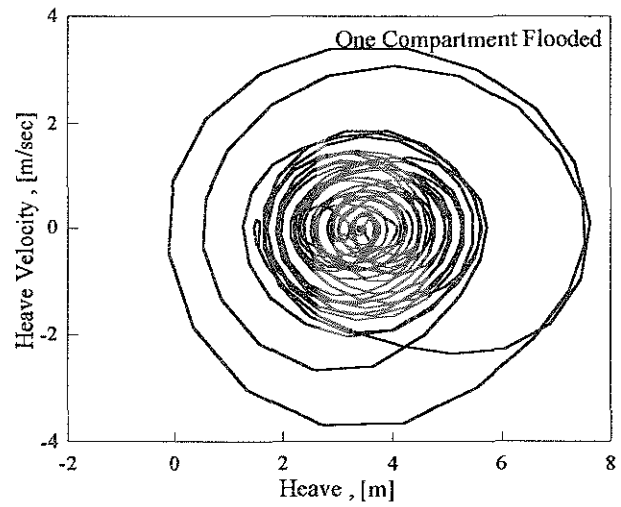


Fig. 8. Heave phase diagram, flooded case

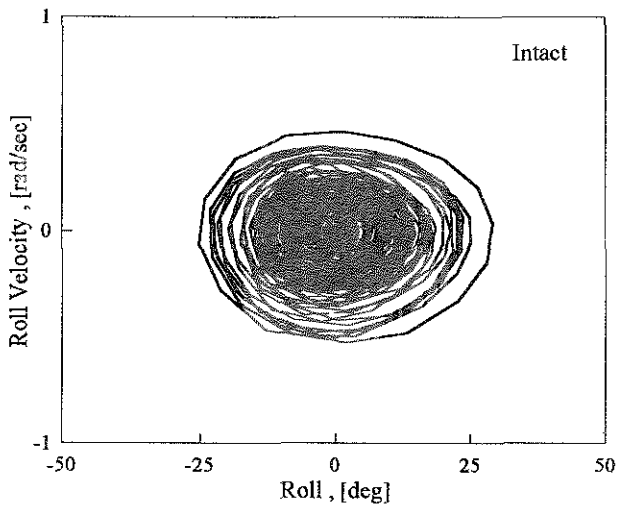


Fig. 9. Roll phase diagram, intact case

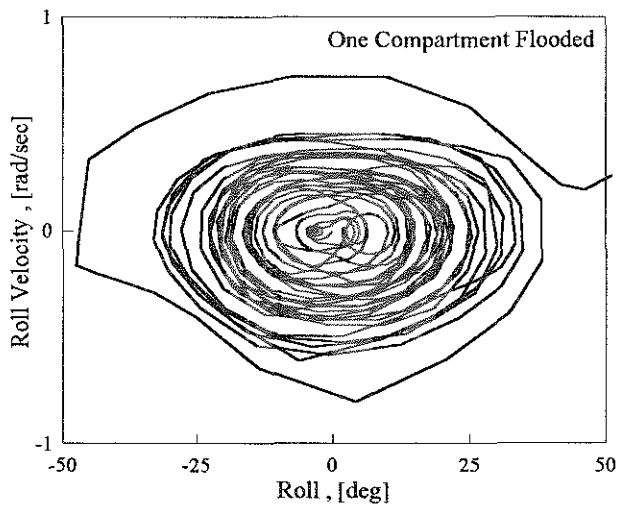


Fig. 10. Roll phase diagram, flooded case

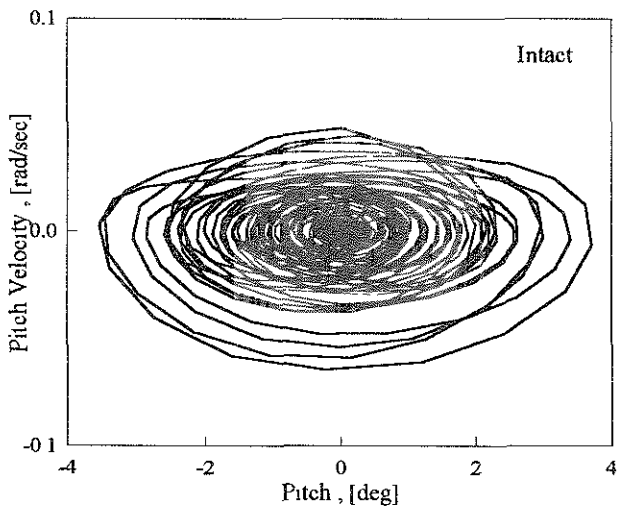


Fig. 11. Pitch phase diagram, intact case

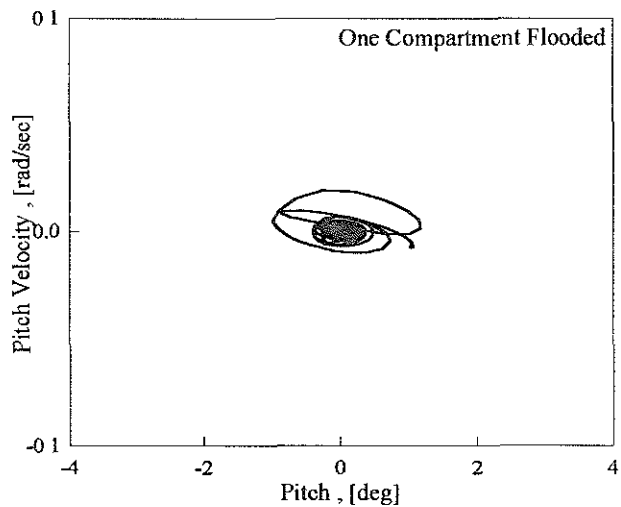


Fig. 12. Pitch phase diagram, flooded case

# A Study of the Safety of Small Fishing Boats for the Scallop Hanging Culture on Fishing Operations in Severe Conditions

Nobuo KIMURA\*, Kiyoshi AMAGAI\* and Kimihiko UENO\*\*

\* Hokkaido University, 3-1-1, Minato, Hakodate, 041, Japan

\*\* Tokyo University of Fisheries, 4-5-7, Minami, Minato, 108, Japan

## ABSTRACT

Lots of small fishing boats for the scallop hanging culture on the coastal area in *Funk-Bay, Hokkaido* have been sometimes compelled to work under the severe sea condition since it is actually main producing season in winter. To secure a safety of fishing operation, there should be great needs of an accurate criterion for judging sea condition, in addition to the sufficient seakeeping qualities.

On basis of tank tests and researches of actual fishing operating condition, it was clarified the stability and the rolling response characteristics of the scallop fishing boats in various working conditions.

In this paper, using wave data measured in the fishing ground, the authors would propose the critical wave height that these fishing boats could be on the sea with safety.

## NOMENCLATURE

$B$  :ship's breadth, m  
 $g$  :gravitational acceleration,  $m/s^2$   
 $GM$  :metacentric height, m  
 $GZ$  :righting arm, m  
 $H_{1/3}$  :significant wave height, m

$k$  :wave number, rad/m  
 $S(\omega)$  :power spectrum,  $m^2 \cdot sec$   
 $\zeta_a$  :wave amplitude, m  
 $\phi$  :rolling amplitude, rad  
 $\phi_{max}$  :maximum rolling amplitude, deg  
 $\lambda$  :wave length, m  
 $\omega$  :wave frequency, rad/sec

## 1. Introduction

The fishing of the scallop culture is one of main fishing since a sum of the fishing production has amounted to about 60% of all of them in this area.

In the fishing ground in winter, the complex wave condition has well happened because of overlapping the short periodical wave generated from the wind blowing from the north-west direction and the long periodical swell transmitted from the *Pacific Ocean*. Moreover, since the facilities of the scallop culture are commonly set on offshore in the range from 1.0 mile to 2.0 miles according to the isobaths that are nearly parallel to the local coast line, the scallop fishing boats are generally under the beam sea condition on the fishing operation.

Then, on the circumstances actually

encountered while the fishing operations, the authors would discuss the safety from the standing point of the rolling angle generated by the characteristic wave in the area.

## 2. Fishing boats for the scallop culture

A scale of the scallop fishing boats is generally very small in the range from 5.0 gross tonnages (*GT*) to 15.0 *GT* with length between perpendiculars being less than 20m, made from *FRP*, and there are specific structural features that have a squarish ship form, a overhang deck, a wide breadth compared with the length, a high bulwarks and small scale freeing ports without prevention system of reversed flow, etc.

A general arrangement of the fishing boat for the scallop culture is shown in Fig. 1. As a bridge is situated on the fore deck and an engine room is located on the after deck, the fishing operation is generally doing on the center area between them.

Because fishermen are usually working used a hydraulic crane equipped on the after deck fixing the right side of the fishing boat to

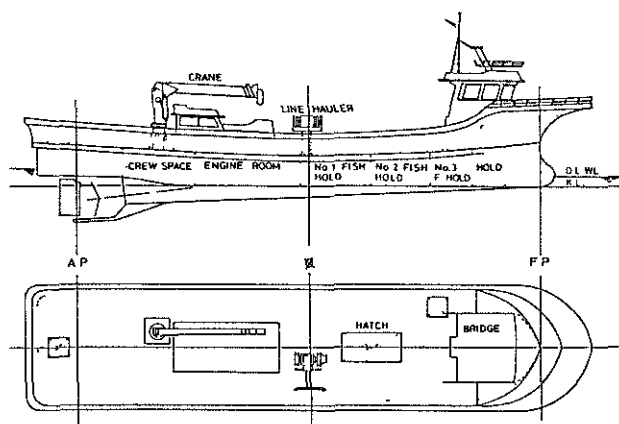


Fig. 1 General arrangement

a main line of the culture facilities, the fishing boat is always fairly inclining to this direction and there is sometimes occurring a lot of free water due to sinking freeing ports under the sea surface. It is said that the inclining angle would exceed 10 degrees in winter when the scallop would completely grow up. It has been reported that the effect of the free water for the small fishing boats is dangerous on the specific conditions because the area of working deck is relatively wide compared with the ship scale [1-2].

## 3. EXPERIMENT

### 3-1 Tank test

A ship model of a 7.9 *GT* fishing boat, that has a typical ship form of a fishing boats for the scallop culture using in this area, reduced in scale by 1/11 was used in the experiment. The rolling tests in the beam sea condition were carried out in the regular waves considering various fishing conditions. The principal particulars of the scallop fishing boat and its body plan are as shown in Table 1 and Fig. 2, respectively. On the basis of the researches of actual fishing operating condition, the loading conditions on the deck were decided as to be 0.0, 2.0, 5.0 and 7.0 tons. they are corresponding to the condition of the departure without the catch, the general catches in the fishing season, the full catches and the maximum catches in the past, respectively. In the table, the rolling angle  $\phi_{bul.}$  (deg) indicates that the bulwark top is even to the sea level and the rolling angle  $\phi_{scu}$  (deg) indicates that the freeing ports are inclining to it, respectively.

### 3-2 The Stability

The stability curves for the each conditions were shown in Fig. 3. In the case of the small fishing boat like this, the rolling angle that sinks the bulwark top into the sea is one of the threshold value so that the stability would change remarkably<sup>[3]</sup>. In this time, the authors would discuss the safety taking notice of the relationship between this angle and wave height. As the  $GM$  is manifestly over 2.0m in the light condition and the  $GM$  is still over 1.5 m even if it is in the worse stability with 5.0 tons loading,

Table 1 Principal particulars of the 7.9GT fishing boat.

ITEM		Loading conditions			
		LIGHT	2 ton	5 ton	7 ton
Lpp	(m)	14.14			
B	(m)	3.63			
D	(m)	1.25			
Disp.	(ton)	13.54	15.54	18.55	20.55
DM	(m)	0.39	0.43	0.49	0.53
TRIM	(m)	0.46	0.42	0.25	0.24
GM	(m)	2.40	2.06	1.65	1.43
KG	(m)	0.95	0.98	1.02	1.05
$\bar{OG}$	(m)	1.41	1.31	1.21	1.17
$\phi$ bul.	(deg)	35.39	34.37	32.83	31.81
$\phi$ scu.	(deg)	18.40	17.06	15.06	13.74

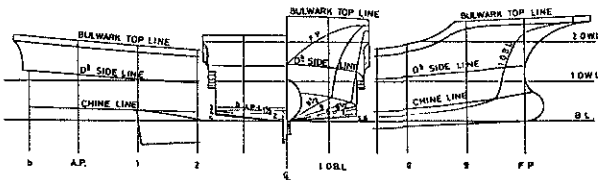


Fig. 2 Lines of the 7.9 GT fishing boat

to say nothing of the size of the  $GZ$ , it would be evident that the ship body generally has the big stability.

### 3-3 The rolling response characteristics

Fig. 4 shows the response characteristics of the rolling motion to the wave in the various loading conditions. A vertical line shows the rolling response function to the wave ( $\phi/k \zeta a$ )

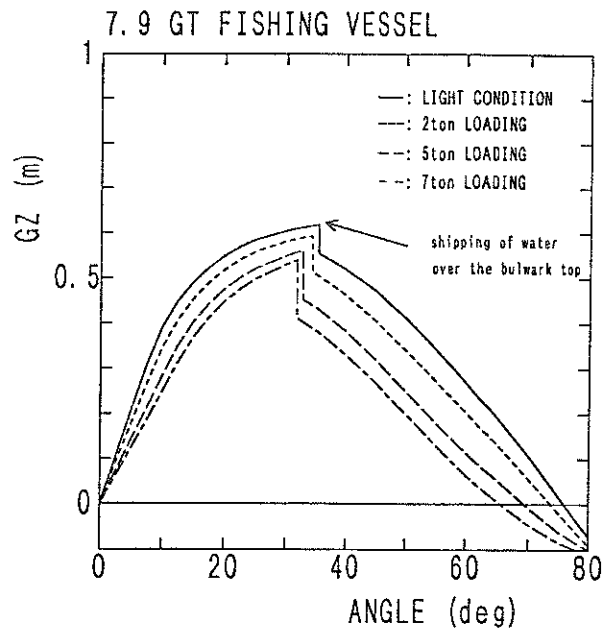


Fig. 3 Stability curve

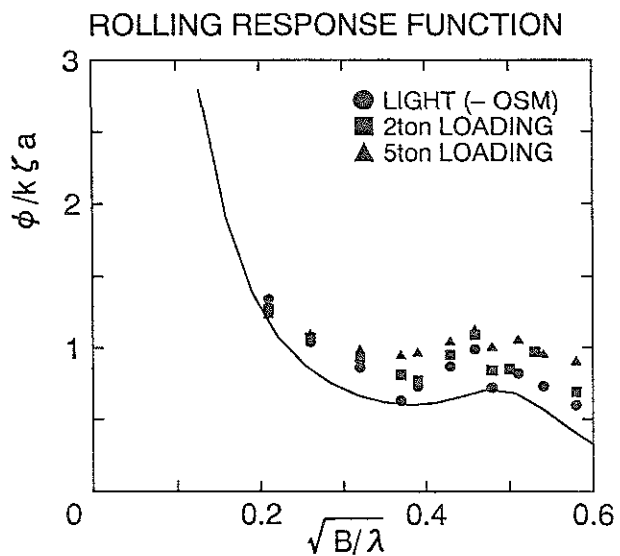


Fig. 4 Rolling response function

and a horizontal line shows the non-dimensional frequency ( $\sqrt{B/\lambda}$ ). Furthermore, a solid line in the figure shows the estimated value due to *ordinary strip method* (OSM) on the no-catch. The responses became slightly greater according to the increases of the scallop catch. It was already clarified that the scallop fishing boat has the maximum rolling response to the wave on the catch with 5.0 tons<sup>[4]</sup>.

The responses fixing the ship body to the culture facilities are shown in Fig. 5. On this condition, the responses without the catch are getting a high values in the range of low frequency.

Fig. 6 is showing the response characteristics on the no-catch using the crane and fixing the ship body to the culture facilities. Fig. 7 is also showing those for the catch with 2 tons.

Mark ● symbolized the rolling response function in the condition of using the crane and mark ○ symbolized those on fixed ship body to the main line of the culture facilities added to

the aforementioned condition. The natural frequency of the scallop with 400 kgw, a unit generally wrapped by a net, lifted by the crane  $\omega_c$  is  $\sqrt{B/\lambda} = 0.23$ .

In the frequency region over  $\sqrt{B/\lambda} = 0.30$ , the response function with use of the crane has a bigger values compared with those values without it. In the cases of fixed the ship body to

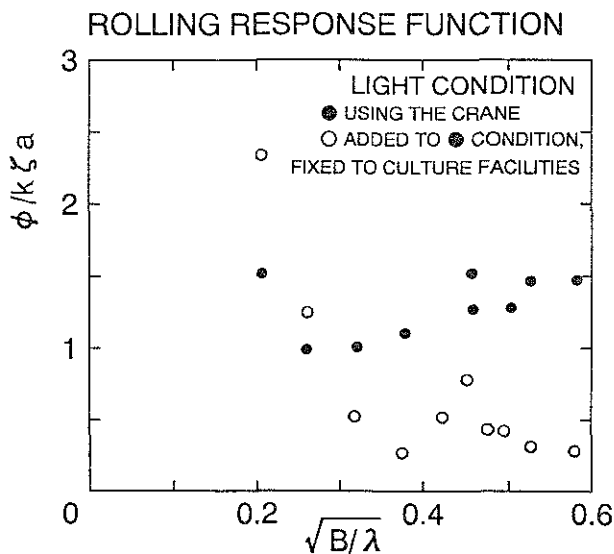


Fig. 6 Rolling response function, light condition

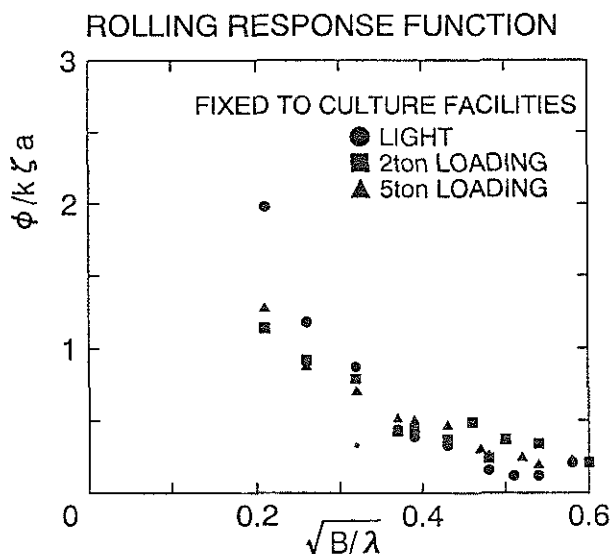


Fig. 5 Rolling response function, fixing the ship body to the culture facilities

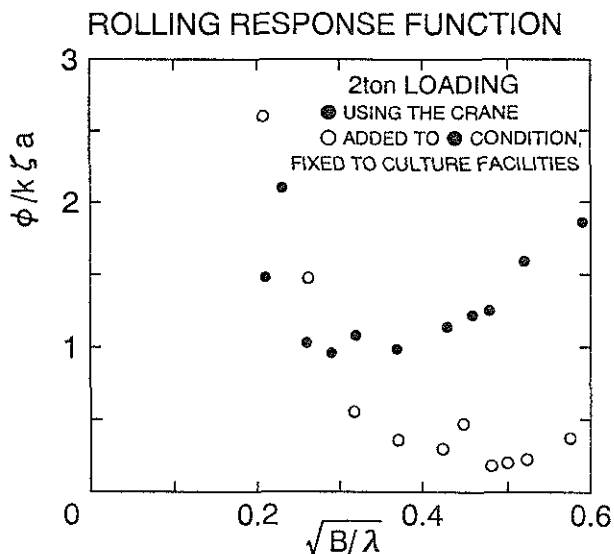


Fig. 7 Rolling response function, 2 tons loading

a main line of the culture facilities adding to the fore condition, the response function becomes very small in the frequency region over  $\sqrt{B}/\lambda = 0.30$  and is conversely big for the long periodic wave under  $\sqrt{B}/\lambda = 0.25$  close to  $\omega_c$ .

As the scallop fishing boat fixes the body to a main line of the culture facilities, the ship

would be doing the asymmetric rolling motion around the stationary inclining angle. The differences of the rolling response for the right side and left side are showing in Fig. 8. In the figure, it is evident that the response for the right side (■) is bigger than that for the other side (▲). As shown in Fig. 9, there is same response characteristics in the case of using the crane. Consequently the scallop fishing boat would get larger rolling on the inclining side while she was under the fishing operation.

### 3-4 Characteristics of wave in the coastal area

In order to clarify the characteristics of wave generated on the coastal area, the authors have carried out the observations of the wave using the microwave doppler radar set on the research ship *Ushio-maru* ( 128 GT ) since 1994. Considering the stationary of wave data, a time of a measurement is 10 minutes and a sampling time is 0.2 sec.

Fig. 10 (a), (b) indicate the examples of the power spectra of the waves measured on December 6th and 19th, 1994 that would be dangerous to the scallop fishing boat because the fishing cooperation demanded all of the ships to a voyage home. Fig. 11 shows the track and positions of these measurements. Nevertheless the sea condition was critical for the small fishing boat, the authors could watch a scallop fishing boat still fishing at point No.1 on December 19th. On December 6th, all of the ships were suspended in the fishing port due to the rough weather.

In the Figures, because of overlapping the short periodical wave generated from the wind blowing from the north-west direction and the

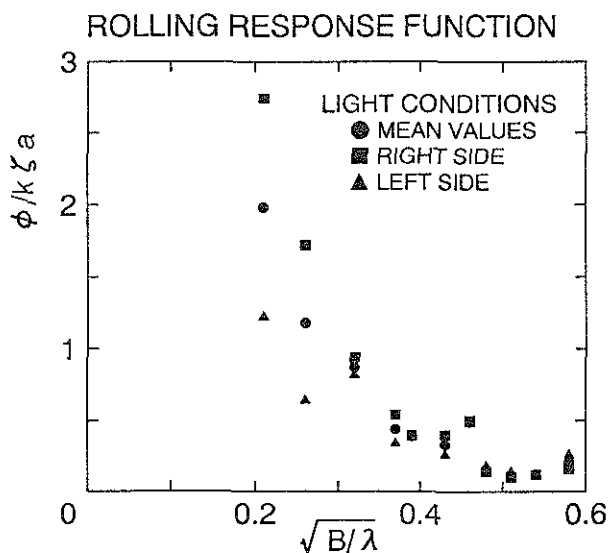


Fig. 8 Rolling response function, light condition

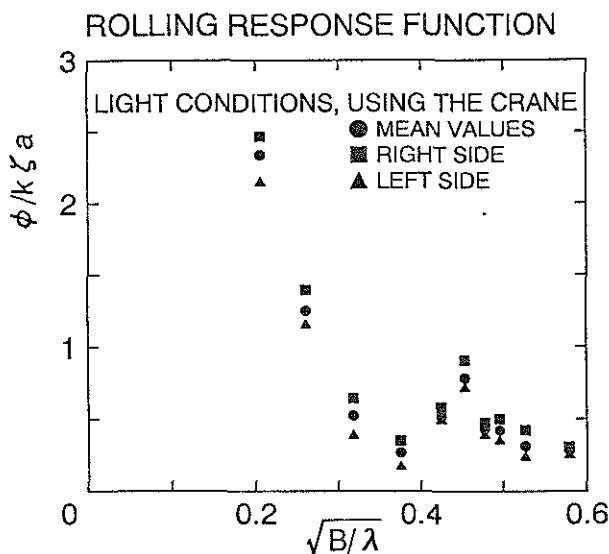


Fig. 9 Rolling response function, light condition, using the crane

long periodical swell transmitted from the *Pacific Ocean*, the characteristic wave having the twin-peaks on each excellent frequency would occur in the fishing ground in this

season. Furthermore, this characteristic would become clearer according as the fetch from the coastal line would be apart longer.

Then, to estimate the appropriate distribution of the wave height generated in this area, the

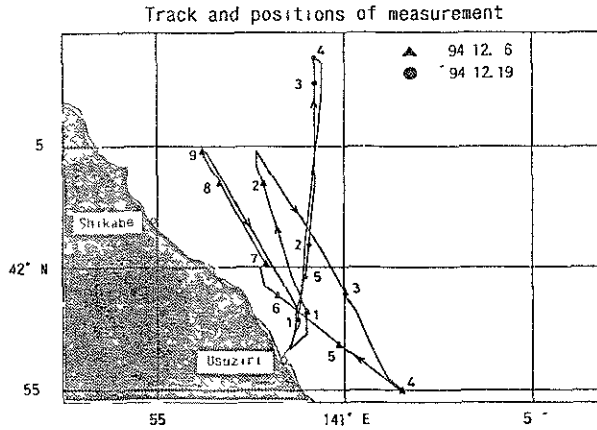
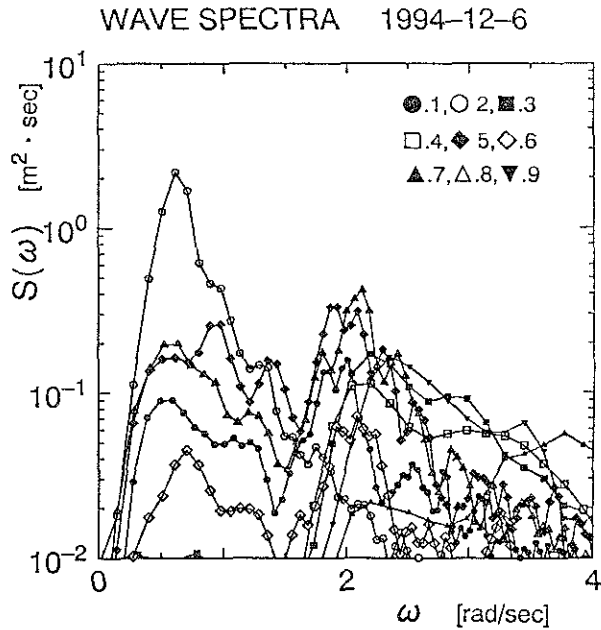


Fig. 10(a) Spectra of the wave in the coastal area, Dec.6<sup>th</sup>, 1994

Fig. 11 The track and positions of the measurements

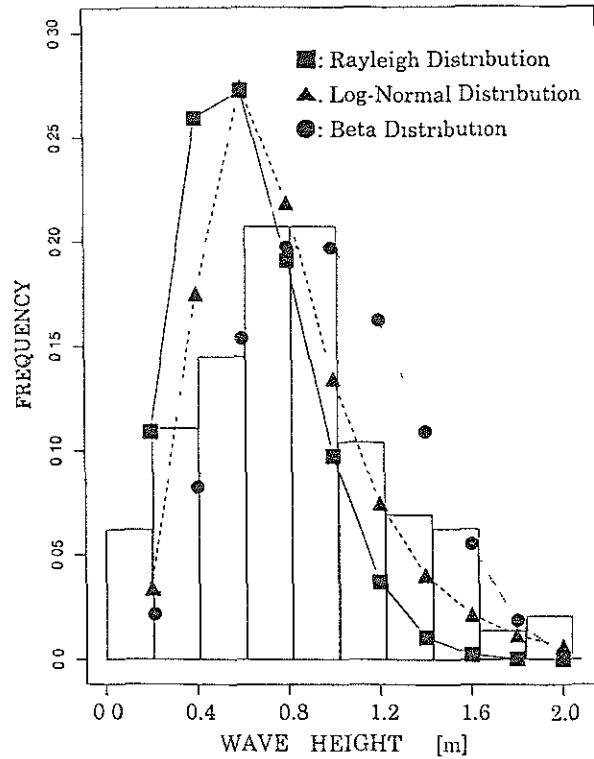
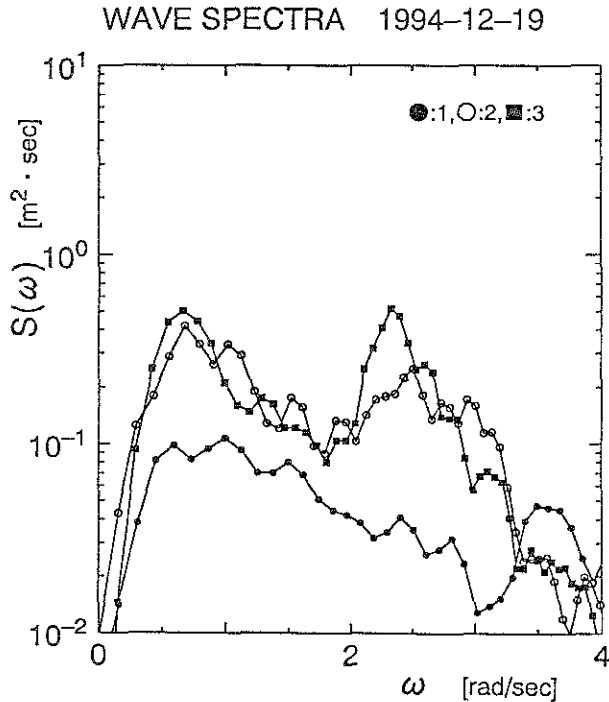


Fig. 10(b) Spectra of the wave in the coastal area, Dec. 19<sup>th</sup>, 1994

Fig. 12 Fitting for the distribution of wave height

authors picked out the three typical distributions and carried out the fitting to the distribution of the wave height processed by the *Zero - up - cross method*. The applied distributions were the traditional *Rayleigh*, the *Log-Normal* and the *Beta* distribution, respectively.

An example of the fitting applied the *Rayleigh* distribution (■), the *Log-Normal* distribution (▲) and the *Beta* distribution (●) to the frequency distribution of the wave height is shown in Fig. 12. The width of each class on the horizontal line is 0.2m in the figure.

The distribution of the wave height could be well approximated by using the distribution of the *Beta* distribution, although the fitting of the distribution functions of the *Rayleigh* distribution and the *Log-Normal* distribution are not successful.

The probability density function of the *Beta* distribution is shown as follows:

$$f(x|p,q) = \frac{1}{B(p,q)} x^{p-1} (1-x)^{q-1},$$

$$= 0 \quad \begin{matrix} p > 0, q > 0, 0 < x < 1 \\ , x < 0, x \geq 1 \end{matrix} \quad (1)$$

where  $B(p,q) = \int_0^1 u^{p-1} (1-u)^{q-1} du$ ,  $p$  and  $q$  are parameters of the distribution, respectively.

The result of the statistical test of the goodness of the fit for the wave data are shown in Table 2. Mark \* indicates that the distribution function is not fitted to the data at 1% significant level. As all cases adapted the *Rayleigh* distribution were significant, it was clear that the distribution was completely different from this. On the contrary, the *Beta*

distributions were indicated stable fitting. With respect to the parameters  $p$  and  $q$ , it is considered that the slight variation is a consequence generated by the configuration of the distribution. However, the parameter  $p$  was constantly equal to 2 was a typical characteristic of the wave height in this area.

If the distribution of the probability density function of the wave height would follow a *Rayleigh* distribution, the rolling amplitude to response would also follow the same distribution. From the standpoint of the safety, it would be important to estimate the rolling in the case that wave height would be around the limit of fishing operation and its configuration of the distribution wouldn't follow a *Rayleigh* distribution.

Table 2 The compatibility test to the frequency distribution of the wave height

DATA POINT	N	(p,q)	Rayleigh	Beta
'941206 01	295	(1,3)	30077.7*	103.7*
'941206 02	150	(1,1)	118.8*	19.1
'941206 03	140	(2,4)	118.5*	15.7
'941206 04	150	(2,4)	598.9*	13.9
'941206 05	220	(2,3)	84.7*	58.4*
'941206 06	260	(2,4)	16259.4*	136.4*
'941206 07	180	(2,6)	891.1*	18.9
'941206 08	192	(2,2)	369.6*	15.7
'941206 09	145	(2,3)	1455.5*	12.9
'941219 01	212	(2,3)	91.1*	126.8*
'941219 02	159	(2,2)	33.8*	21.7
'941219 03	170	(2,2)	31.6*	24.7*
'941219 04	163	(2,3)	607.7*	16.6
'941219 05	120	(2,3)	119.0*	54.4*

\* significant at 1% of the significant level

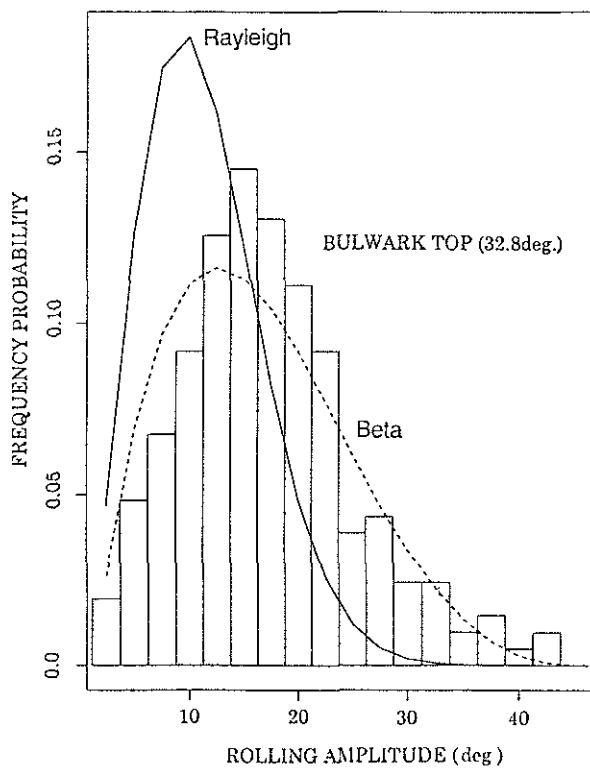


Fig. 13 Estimation of the critical probability of rolling amplitude

In order to estimate the critical probability like the bulwark top would sink into the sea, the authors assumed the above two kinds of distribution functions. The authors show an example of the frequency probability of the rolling amplitude in Fig. 13.

Considering the probability that the bulwark top would be under sea level, the incidental probability is 0.6% estimated by the *Rayleigh* distribution and 2.4% by the *Beta* distribution. As it is evident from this result, the function of the *Beta* distribution could estimate well the probability concerning the safety, although the function of the *Rayleigh* distribution fairly underestimate it.

It's shown an example of the fitting for the rolling amplitude of the scallop fishing boat in

Table 3. As the distributions were all fitted to the *Beta* distribution except one case, it could be suggested that the distribution of the rolling amplitude would follow the *Beta* distribution in case the distribution of wave height would follow this distribution. Then, considering the critical rolling amplitude of the small fishing boats, it's important to grasp the characteristics of wave occurred in fishing ground.

Table 3 An example of the compatibility test for the rolling amplitude

DATA	POINT	CONDITION	N	(p,q)	Rayleigh	Beta
'941206	03	Drift	181	(2,3)	810.4*	19.5
'941206	04	Drift	179	(2,3)	1959.1*	18.4
'941206	07	Drift	207	(2,3)	6966.5*	27.2
'941206	09	Drift	185	(2,2)	963.9*	50.4*

\* significant at 1% of the significant level

### 3-5 Critical wave height for the fishing operation

The authors would suggest one criteria based on the critical wave height related to the  $\phi_{max}$ , because the stability of the scallop fishing boat would rapidly take a turn for the worse when the bulwark top would be under the sea level.

As the wave data on the fishing ground, the authors had carried out 49 measurements of wave, whose  $H_{1/3}$  were above 0.5m, in the fishing season between November and February from 1994 to 1996. The points and number of the measurements in *Funka-Bay* were shown in Fig. 14.

Fig. 15 is showing the estimated values of the  $\phi_{max}$  in the condition with 2 ton's load

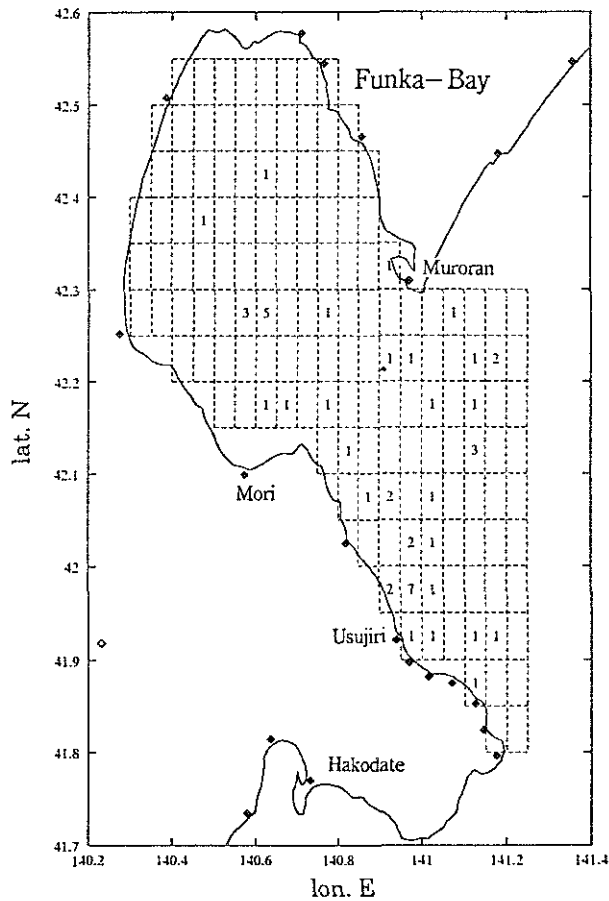


Fig. 14 The points and number of the wave measurements in *Funka-Bay*

using the crane and Fig. 16 is showing those on fixed the ship body to the culture facilities added to the fore condition, respectively.

In the figures, mark  $\circ$  symbolized  $\phi_{max}$  and mark  $\bullet$  symbolized the significant rolling amplitude. The intercept of the vertical line was corresponding to the initial inclining angle  $\phi_{ini}$  (deg) due to fixing to the culture facilities.

To estimate the critical wave height for the fishing operation, it was applied a simple linear regressive equation to the relation between  $H_{1/3}$  and  $\phi_{max}$ . The regressive equation and the 95% confidence interval were also drawn in solid and broken line on the figures, respectively.

The test of goodness of the fitting due to the

linear regressive function were shown in Table 4. Mark \* in the table indicates the goodness of

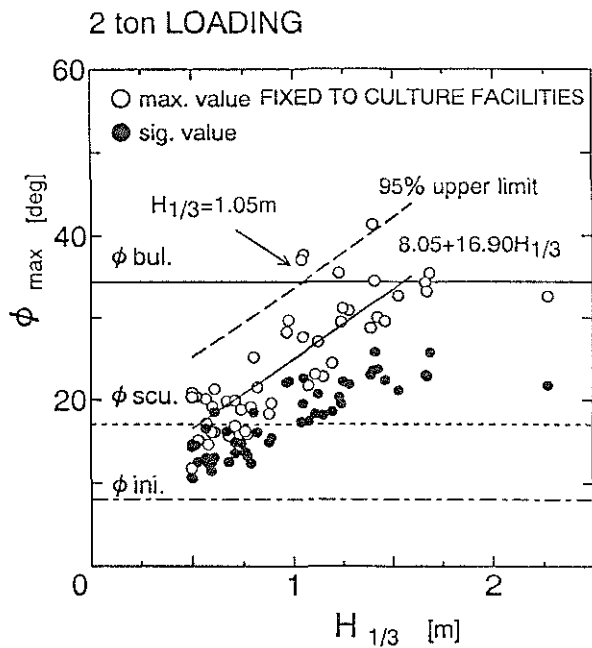


Fig. 15 Estimation of the maximum rolling amplitude, 2 tons loading, using the crane

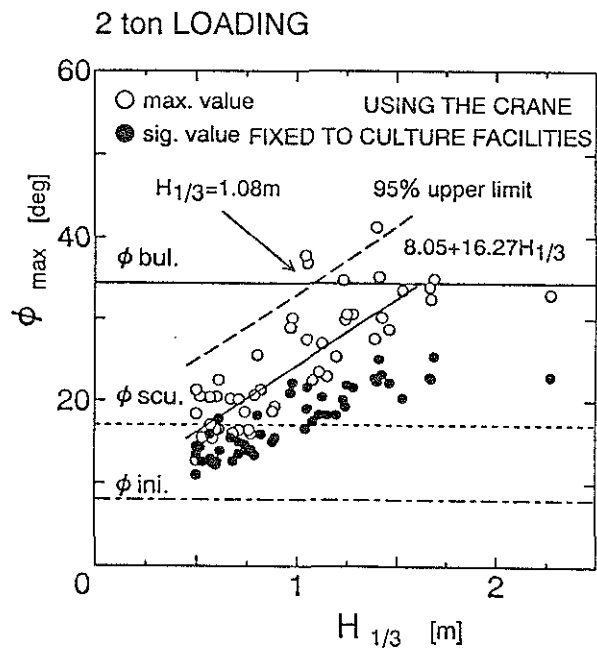


Fig. 16 Estimation of the maximum rolling amplitude, 2 tons loading, using the crane, fixed to the culture facilities

the fitting with significant level at 5% for the regressive equation is significant. As all of the fitting were good and the values of the coefficient of determination  $R^2$  for the regressive function were high ( i.e.  $R^2 = 0.68$  in the case of Fig. 15 and  $R^2 = 0.66$  in the case of Fig. 16 ), it was clarified that  $\phi_{max}$  could be statistically estimated by  $H_{1/3}$ . However, there were fairly difference among estimated critical wave heights according to operating conditions. Considering the general use ( i.e. the catch with 2 tons fixed the ship body to the culture facilities), the authors could suggest that  $H_{1/3} = 1\text{m}$  should be corresponded to the critical wave height for the fishing operation. On the condition without catch, it was dangerous for the scallop fishing boat because of creating fairly big rolling amplitude. Then, the fishermen should take delicate care for the wave condition.

Table 4 Critical wave height for the scallop fishing boat.

Loading conditions	USING CRANE			
	FREE	FIXED	FREE	FIXED
LIGHT CONDITION	0.97m*	0.95m*	0.68m*	0.58m*
2ton LOAD	0.80m*	1.05m*	0.87m*	1.05m*
5ton LOAD	0.72m*	1.31m*		

\* significant at 5% of the significant level

#### 4. CONCLUSION

The main results from this work are summarized as follows;

(1) The characteristic wave having the twin-peaks on the frequency would occur in the

fishing ground because of overlapping the short periodical wave generated from the wind blowing from the coast and the long periodical swell transmitted from the *Pacific Ocean*.

(2) The distribution of the wave height generated on the fishing ground in *Funka-Bay* could be well approximated by using the *Beta* distribution.

(3) If the distributions of the wave height would follow the *Beta* distribution, those of the rolling amplitude would also follow the same distribution.

(4) As the scallop would load on the deck from 0.0 to 5.0 tons, the value of rolling response function would slightly increase.

(5) During the fixing of the ship body to the culture facilities, the rolling responses would force little. Furthermore, the rolling motion to the mooring side would become bigger than that to the opposite side.

(6) On the condition using the hydraulic crane, the rolling responses would fairly increase.

(7) From the viewpoint of the safety for general conditions of the fishing operations, it would be estimated that the scallop fishing boats could do fishing is under  $H_{1/3} = 1\text{ m}$ .

However the authors have studied a safety of the scallop fishing boat under the considerable operating conditions and waves, it would be still the region of a case study. The authors should like to generalize the safety based on the above mentioned standard.

#### 5. REFERENCES

1. K. Amagai et al; On the Practical Evaluation of Shallow water Effect in Large Inclination for

Small Fishing Boats, Fifth International Conference on Stability of Ships and Ocean Vehicles, USA, vol.3, 1-16, 1994.

2. K. Ueno et al; Characteristics of Roll Motion for Small Fishing Vessels with Water on Deck, The Journal of Japan Institute of Navigation, 95, 183-191, 1996.

3. K. Amagai et al; Characteristics of Roll Motion for Small Fishing Boats, Second workshop on stability and operational safety of ships, Osaka, 128-137, 1996.

4. N. Kimura et al; A Study of the Limit of Fishing Operation on a Fishing Boats for the Raising of a Scallop in *Funka-Bay*, The Journal of Japan Institute of Navigation, 94, 273-279, 1996.

#### ACKNOWLEDGMENTS

I would like to express my appreciation to Captain K. Ohkoshi and crewmen of *Ushio-maru* for the measurements of wave in *Funka-Bay*. I also wish to express appreciation to the Captain T. Tukichi of the *Maruto-maru* and Fishermen belonging to the *Shikabe* fishing Cooperation for a lot of support and advice.

# AN INVESTIGATION ON THE INFLUENCE OF STERN HULL SHAPE ON THE ROLL MOTION AND STABILITY OF SMALL FISHING VESSELS

M. A. S. NEVES<sup>1</sup>, M. SALAS<sup>2</sup> and L. VALERIO<sup>1</sup>

<sup>1</sup>Dept. of Ocean Engineering, Federal University of Rio de Janeiro, Brazil

<sup>2</sup>Institute of Naval and Marine Sciences, Austral University of Chile, Chile

## ABSTRACT

In this paper, some relevant aspects of hydrostatic non-linear coupling between symmetric (Heave and Pitch) and anti-symmetric (Roll) motions are discussed. The discussion is presented by comparing the differences in response of two hulls, representatives of typical small fishing vessels. The two hulls are very similar, but their stern arrangements are different; one of the vessels has a transom stern, whereas the other one has a more conventional round stern.

Starting with a complete six degrees of freedom mathematical model, non-linear equations describing the Heave-Roll and Roll-Pitch couplings are used to investigate the dynamic stability of the two ships in regular waves. Attention is focused on the analysis of the differences in geometric aspects of the stability limits of Roll motion of the two vessels and the different role played by each coupling. Connections between these differences and the stern arrangements are then clarified.

## NOMENCLATURE

A Linear added mass matrix.  
 $A_{ij}$  Linear added mass or added inertia in "i" due to "j" mode.  
 $A_0$  Wave amplitude.

$A_w$  Water line area.  
 B Linear damping matrix.  
 $B_{ij}$  Linear damping coefficient in "i" due to "j" mode.  
 $b_{ij}$  Element of linear damping matrix.  
 $B(\dot{\phi})$  Total damping moment  
 $B_{444}$  Non-linear component of damping moment  
 $\overline{BG}$  Distance between centres of gravity and bouyancy at equilibrium  
 C Linear restoring matrix.  
 $C_{ijk}$  Non-linear restoring coefficient in "i" due to "j", "k" modes.  
 D Non-linear restoring matrix.  
 $g$  Gravity  
 $\overline{GM}_t$  Transverse metacentric height  
 $\overline{GM}_l$  Longitudinal metacentric height  
 $I_{ij}$  Mass moment of inertia with respect to i, j axes  
 $I_i$  Area moment of inertia with respect to i axe.  
 m Ship mass  
 $p_{ij}$  Cosine amplitude coefficient of time-dependent restoring matrix element

$q$	Six degrees of freedom displacement vector.
$Qe(t)$	Generalized wave excitation
$q_{ij}$	Sine amplitude coefficient of time-dependent restoring matrix element
$r_{ij}$	Cosine amplitude coefficient of time-dependent damping matrix element
$s$	Finite integer.
$s_{ij}$	Sine amplitude coefficient of time-dependent damping matrix element
$u$	Perturbation superimposed to linear response.
$y_{i,j}$	Elements of generalized displacement vector "y".
$W$	Wave frequency
$W_c$	Encounter frequency
$W_i$	Natural frequency in "i" mode.
$x$	Surge displacement
$\bar{x}$	Surge linear response
$x_f$	Longitudinal centroid of water line
$y$	Sway displacement
$\bar{y}$	Sway linear response
$y_f$	Transversal centroid of water line
$z$	Heave displacement
$\bar{z}$	Heave linear response
$Z_o$	Vertical position of center of mass
$\phi$	Roll angle
$\bar{\phi}$	Roll linear response
$\theta$	Pitch angle
$\bar{\theta}$	Pitch linear response
$\psi$	Yaw angle
$\bar{\psi}$	Yaw linear response
$\rho$	Water density
$\gamma$	Specific density
$\nabla$	ship displacement
$\nabla_o$	ship displacement at equilibrium.

## 1. INTRODUCTION

The stability condition of a ship in waves is very different from that of the same ship in calm water. The difference is due to changes in the geometry of the immersed volume and the altered pressure distribution over the hull when the ship is responding to waves.

In waves, a rigid hull will be excited in six degrees of freedom, and these six modes will be, in many ways, coupled to each other. When the motions are considered to be small, linear equations may be employed to describe the resulting ship motion. In this case, symmetric and anti-symmetric modes may be uncoupled. On the other hand, when large motions are assumed to occur, non-linear equations of motion are required and such uncoupling is not applicable and may not be enforced. In particular, roll motion assumes a strong coupling with the vertical modes.

Parametric resonance may strongly influence the dynamic ship behaviour and stability in waves. This phenomenon has been observed for more than a century. Since Froude observations until nowadays several works have been published on parametric resonance of the roll motion [1,2,4,11,12,16]. These studies usually treat roll motion as an uncoupled motion and the stability analysis may be carried out using the Mathieu equation. This equation may give instabilities when the metacentric height oscillate with a frequency, such as 2, 1, 1/2, 1/4, ..., to the natural frequency of roll motion [1]. Yet, other unstabilizing frequencies may appear when a set of coupled equations with parametric excitation is considered.

In this paper a six degrees of freedom mathematical model is employed in order to study ship stability in quartering seas. Coupling of roll motion with the vertical modes is introduced by deriving hydrostatic force and moments with terms up to second order in the heave, roll and pitch displacements. Stability analysis is made by considering the linear variational equation. A

system of coupled equations with parametric excitation is obtained for the perturbed motions. Distinct effects are found from the heave-roll and roll-pitch couplings. Stability limits corresponding to these couplings are obtained for two vessels.

The discussion is presented comparing the different responses of two hulls. These are representative of typical small fishing vessels. The two hulls are very similar, but their stern arrangements are distinct. One of the vessels has a transom stern, whereas the other has a more conventional round stern. The lines plans of the two vessels, together with other characteristics are given in Appendix A.

The linear responses in the frequency domain of the two vessels are almost identical [8,10,14]. Yet, significant differences in response are obtained when large motions are considered [9]. Differences in stern shape are pointed out as responsible for these differences in the dynamic behaviour of the two small fishing vessels.

## 2. MATHEMATICAL MODEL

A non-linear set of equations of motions in six degrees of freedom is presented in this section.

### 2.1 COORDINATE SYSTEM

Let (oxyz) be a right-handed coordinate system fixed with respect to the mean position of the ship with a vertically upward through the center of gravity of the ship, x in the direction of forward motion, and the origin in the plane of the undisturbed free surface, as shown in Fig. 1.

The ship is supposed to be rigid and to travel with a mean forward speed  $U$  at an angle  $\chi$  to waves incidence, such that  $\chi=0$  stands for astern waves.

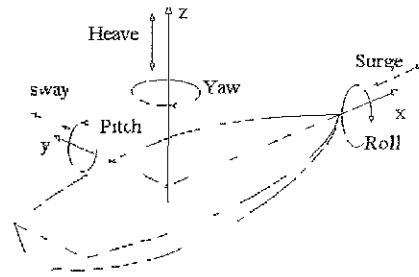


Fig. 1 Coordinate System

### 2.2 EQUATIONS OF MOTION

The non-linear equations may be expressed as:

$$[M+A]\{\ddot{q}(t)\} + B(\dot{q})\{\dot{q}(t)\} + C(z, \phi, \theta)\{q(t)\} = \{Q_e(t)\} \quad (1)$$

The elements  $M_{ij}$  and  $A_{ij}$  in the first two matrices on the left hand side of equation (1) represent generalized masses and added masses. Only linear terms have been retained in the inertia terms. A 3-D panel method has been used in the potential calculations of added masses and potential dampings for zero speed. Speed effects have been introduced in accordance with the Salvesen, Tuck and Faltinsen theory [15]. The hydrodynamic coefficients and exciting terms for the two fishing vessels have been presented in ref. [14].

The matrices B and C represent the damping and the restoring components of the system and contain non-linearities in roll damping and heave-pitch-roll restoring terms, respectively.

#### 2.2.1 ROLL DAMPING

Viscous roll damping has been considered separately and determined by means of Himeno's method, in which the roll damping moment is divided into different components, with explicit consideration of bilge keel effects. The damping components are due to friction, eddy-making, lift, wave generation and bilge keel. The roll damping moment is then expressed in a quadratic form:

$$B(\dot{\phi}) = B_{44}\dot{\phi} + B_{444}\dot{\phi}|\dot{\phi}| \quad (2)$$

Details of the method may be found in reference [5].

### 2.2.1 RESTORING TERMS

The restoring actions in heave, roll and pitch have been obtained from an expansion in Taylor's series up to second order, the following notation being used :

$$C_3(z, \phi, \theta) = C_{33}z + C_{34}\phi + C_{35}\theta + C_{333}z^2 + C_{344}\phi^2 + C_{355}\theta^2 + C_{334}z\phi + C_{335}z\theta + C_{345}\phi\theta \quad (3.a)$$

$$C_4(z, \phi, \theta) = C_{43}z + C_{44}\phi + C_{45}\theta + C_{433}z^2 + C_{444}\phi^2 + C_{455}\theta^2 + C_{443}z\phi + C_{435}z\theta + C_{445}\phi\theta \quad (3.b)$$

$$C_5(z, \phi, \theta) = C_{53}z + C_{54}\phi + C_{55}\theta + C_{533}z^2 + C_{544}\phi^2 + C_{555}\theta^2 + C_{534}z\phi + C_{535}z\theta + C_{545}\phi\theta \quad (3.c)$$

The linear and non-linear coefficients are given in tables 1 and 2 respectively.

Table 1

Linear Restoring Coefficients		
$C_{33} = \gamma A_w$	$C_{34} = 0$	$C_{35} = -\gamma A_w x_f$
$C_{43} = 0$	$C_{44} = \gamma \nabla \overline{GM}_1$	$C_{45} = 0$
$C_{53} = \gamma A_w x_f$	$C_{54} = 0$	$C_{55} = \gamma \nabla \overline{GM}_1$

Derivation of hydrostatic actions is given in Appendix B. The values of the linear and non-linear hydrostatic coefficients for the two vessels are presented in Appendix A. It is important to note that the two hulls display significant differences in some second

order restoring terms, due to geometrical differences in the stern shape.

Table 2

Second Order Restoring Coefficients	
$C_{333} = 2\gamma \frac{\partial A_w}{\partial z}$	$C_{444} = 0$
$C_{334} = 0$	$C_{445} = \gamma \frac{\partial I_x}{\partial \theta}$
$C_{335} = -\gamma \left[ \frac{\partial(A_w x_f)}{\partial z} - \frac{\partial A_w}{\partial \theta} \right]$	$C_{455} = 0$
$C_{345} = 0$	$C_{533} = -2\gamma \frac{\partial(A_w x_f)}{\partial z}$
$C_{344} = 2\gamma \frac{\partial(A_w y_f)}{\partial \phi}$	$C_{534} = 0$
$C_{355} = 2\gamma \frac{\partial(A_w x_f)}{\partial \theta}$	$C_{544} = 0$
$C_{443} = \gamma \left[ \frac{\partial I_x}{\partial z} + \frac{\partial(A_w y_f)}{\partial \phi} \right]$	$C_{535} = -\gamma \left[ \frac{\partial(A_w x_f)}{\partial \theta} - \frac{\partial I_y}{\partial z} \right]$
$C_{433} = 0$	$C_{545} = 0$
$C_{435} = 0$	$C_{555} = 2\gamma \frac{\partial I_y}{\partial \theta}$

### 3. DYNAMIC STABILITY ANALYSIS

In order to investigate the behaviour of the solutions and their qualitative characteristics, a stability analysis of the non-linear equations was carried out.

#### 3.1 LINEAR VARIATIONAL SYSTEM

The stability analysis was determined by means of the variational technique [3].

Consider a solution  $q(t)$  to be of the form ;

$$q(t) = \bar{q}(t) + u(t) \quad (4)$$

where :

$\bar{q}(t)$  is the solution of the linear system

$u(t)$  is a perturbation superimposed to the linear solution

If the solution of the linear system is considered stable, then the solution of the non-linear system near this solution will be stable if a solution of  $u(t) \rightarrow 0$  when  $t \rightarrow \infty$ , and is unstable otherwise [3].

Taking the linear variational system of equation (1), a coupled linear system with time dependent coefficients is obtained.

$$[M+A]\ddot{u}+[B+B_1(t)]\dot{u}+[C+D(t)]u=0 \quad (5)$$

The stability of the non-linear system (1) is then governed by the stability of the solution of the disturbances, as set above in equation (5).

Matrix  $[B_1(t)]$  represent dissipation of energy, and matrix  $[D(t)]$  is composed of oscillatory terms at the excitation frequency and may be expressed as :

$$[D]=\begin{bmatrix} 0 & 0 & 0 & 0 & 0 & 0 \\ 0 & 0 & 0 & 0 & 0 & 0 \\ 0 & 0 & C_{333}\bar{z}+C_{335}\bar{\theta} & C_{344}\bar{\phi} & C_{335}\bar{z}+C_{355}\bar{\theta} & 0 \\ 0 & 0 & C_{443}\bar{\phi} & C_{443}\bar{z}+C_{445}\bar{\theta} & C_{445}\bar{\phi} & 0 \\ 0 & 0 & C_{533}\bar{z}+C_{535}\bar{\theta} & 0 & C_{535}\bar{z}+C_{555}\bar{\theta} & 0 \\ 0 & 0 & 0 & 0 & 0 & 0 \end{bmatrix}$$

where  $\bar{z}(t)$ ,  $\bar{\phi}(t)$ ,  $\bar{\theta}(t)$  are oscillatory solutions to the six-degrees of freedom linear problem of the ship excited by regular waves of arbitrary incidence.

### 3.2 COUPLED EQUATIONS WITH PARAMETRIC EXCITATION

Pre-multiplying the terms of equation (5) by the inverse of inertia matrix, inputting the linear transformation  $u=[T]y$ , where  $[T]$  is the eigenvalues matrix associated to the linear restoring matrix, and expressing the resulting equation in inditial form, gives:

$$\ddot{y}_i + w_i^2 y_i = -A_o \left[ \sum_{j=1}^6 b_{ij} \dot{y}_j + \sum_{j=1}^6 (r_{ij} \cos(w_e t) + s_{ij} \sin(w_e t)) \dot{y}_j + \sum_{j=3,4,5}^6 (p_{ij} \cos(w_e t) + q_{ij} \sin(w_e t)) y_j \right] \quad (6)$$

where  $y_j$  are elements of the generalized displacement vector  $y$ ,  $w_i^2$  represents the square of natural frequencies,  $b_{ij}$  represents the elements of a linear damping matrix,  $r_{ij}$  and  $s_{ij}$  are elements of non-linear damping matrix,  $p_{ij}$  and  $q_{ij}$  are elements of non-linear restoring matrix and  $A_o$  is the wave amplitude.

Equation (6) is a system of *parametrically excited coupled equations*. As shown by Hsu [6] there are many conditions of possible instabilities when a set of Mathieu equations are coupled together. For a system under small parametric excitation and having  $w_i$  ( $i, 1, 2, \dots, n$ ) all distinct, instability may occur at excitation frequencies in the neighbourhoods of,

$$w_e = \frac{w_i \pm w_j}{s}$$

where  $i, j = i, 1, 2, \dots, n$ , and  $s$  is a finite integer.

For each of the above resonant frequencies, criteria for determining limits of stability were obtained by Hsu, for the first approximation.

In the folowing discussion the stability analysis will be restricted to three cases of practical importance, viz.:

$$w_e = 2 w_4$$

$$w_e = w_3 - w_4 \quad (7)$$

$$w_e = w_5 - w_4$$

where  $w_3$ ,  $w_4$  and  $w_5$  are natural frequencies associated with the heave, roll and pitch modes, respectively.

The auto-resonant condition  $w_e = 2 w_4$  has been investigated in a previous paper [10] where it was concluded that in longitudinal waves the main mechanism of energy transfer is the pitch coupling to roll, with heave playing a less relevant role in exciting the roll mode near this resonant condition.

Stability limits for the resonant conditions given in (7) may be investigated by applying the stability criteria established by Hsu [6]. In order to apply the Hsu criterion, and to investigate the assumed couplings in a

qualitative way, the variational system has been uncoupled in two separated systems, the heave-roll and roll-pitch systems.

$$D(t) = \begin{bmatrix} C_{445}\bar{\theta} & C_{445}\bar{\phi} \\ 0 & C_{355}\bar{\theta} \end{bmatrix}$$

### 3.3 COUPLED HEAVE-ROLL SYSTEM

When coupling derives from second order expansions in the restoring terms, and discarding terms of coupling with pitch mode, the equations to stability analysis in the resonance frequency  $w_e = w_3 - w_4$  may be expressed as:

$$[M + A]\ddot{u} + [B]\dot{u} + [C + D(t)]u = 0 \quad (8)$$

where:

$$[M + A] = \begin{bmatrix} m + A_{33} & 0 \\ 0 & I_{xx} + A_{44} \end{bmatrix}$$

$$B = \begin{bmatrix} B_{33} & 0 \\ 0 & B_{44} + B_{444}\bar{\phi} \end{bmatrix}$$

$$C = \begin{bmatrix} C_{33} & 0 \\ 0 & C_{44} \end{bmatrix}$$

$$D(t) = \begin{bmatrix} C_{333}\bar{z} & C_{344}\bar{\phi} \\ C_{443}\bar{\phi} & C_{443}\bar{z} \end{bmatrix}$$

System (8) can be reduced to the canonical form of equation (6), and then the expression for stability limits can be applied to the  $w_e = w_3 - w_4$  condition. Stability limits for the motions near this resonant condition are then obtained in an encounter frequency basis against wave amplitude, as will be given ahead in the next section.

### 3.4 COUPLED ROLL-PITCH SYSTEM

Similarly, the coupled system roll-pitch may be analyzed. In this case, and applying similar reasoning as for the heave-roll coupling, the time-dependent coupling between the two modes may be derived as

On applying the same stability criteria in this case, it is found that the system in this case is always stable. So, the coupling roll-pitch, defined up to second order in the restoring terms, is not able to produce combined parametric instability. Therefore, instabilities in the neighbourhoods of  $w_e = w_5 - w_4$  may be obtained only when considering a system of coupled heave-roll-pitch, such that any energy transfer from pitch to roll at this resonant frequency will occur through the activation of the heave mode.

## 4. RESULTS

Stability limits were calculated for two vessels with different stern arrangements, in several conditions, in order to verify the influence of stern shape. The two vessels have been tested previously by Morral [7], Neves, Pérez and Sanguinetti [8] and Pérez and Sanguinetti [13]. The first ship, here denominated TS, is a typical transom stern fishing vessel. The other one, denominated RS, is a more conventional rounded stern fishing vessel. Principal particulars of the two ships are given in Appendix A.

The influence of transversal metacentric height on stability limits near the  $w_e = w_3 - w_4$  condition were calculated, by considering several values of  $\overline{GM}_t$  (Figs. 2-3). As expected, instability regions are increased when  $\overline{GM}_t$  is reduced. In these figures, the two ships are taking waves by the stern and sailing at 6 knots. Stability limits for the TS hull are more critical than for the RS hull.

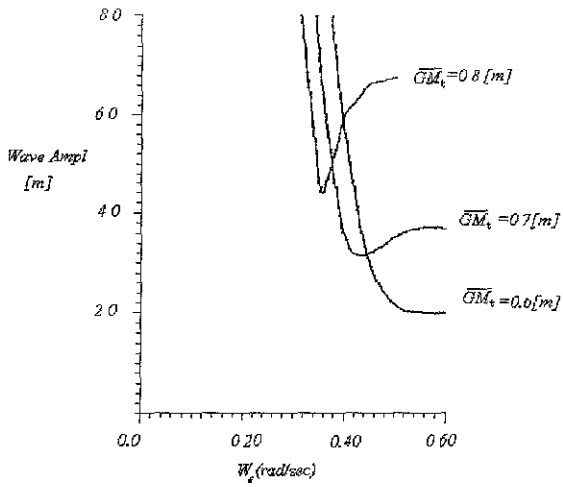


Fig. 2 - Stability Limits, RS ship,  $\chi=30^\circ$ ,  $U=6$  kn.

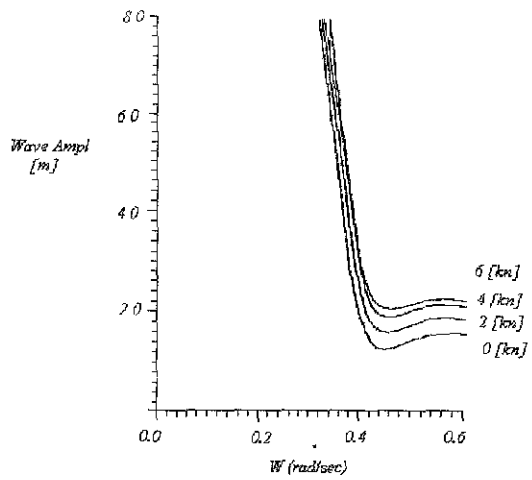


Fig. 5 - Stability Limits, TS ship,  $\chi=15^\circ$ ,  $\overline{GM}_t=0.7$  [m].

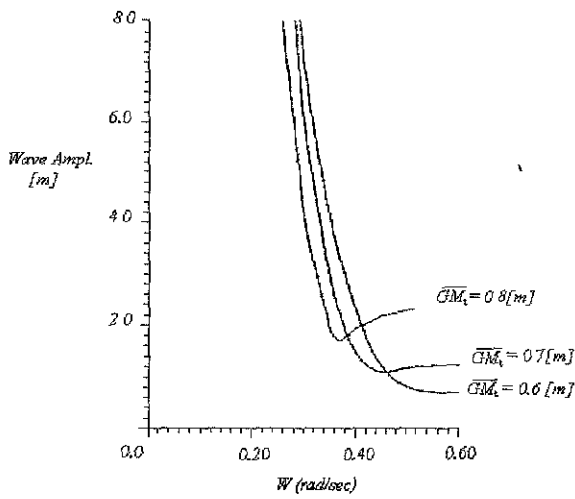


Fig. 3 - Stability Limits, TS ship,  $\chi=30^\circ$ ,  $U=6$  kn.

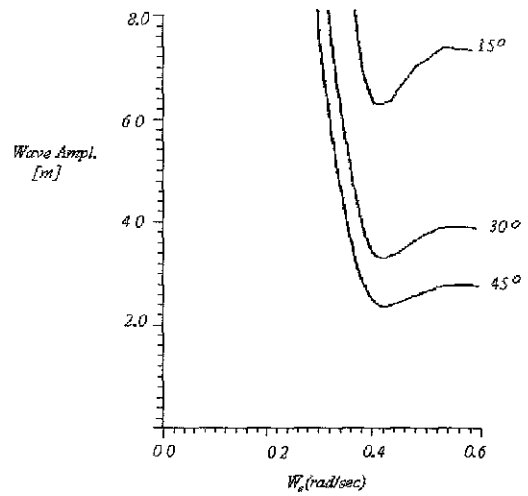


Fig. 6 - Stability Limits, RS ship,  $U=6$  [kn],  $\overline{GM}_t=0.7$  [m].

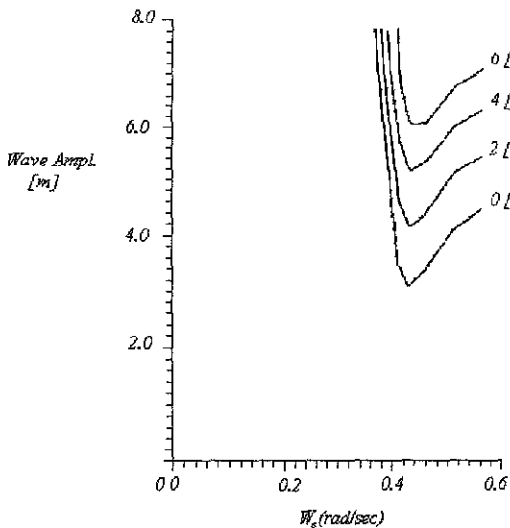


Fig. 4 - Stability Limits, RS ship,  $\chi=15^\circ$ ,  $\overline{GM}_t=0.7$  [m].

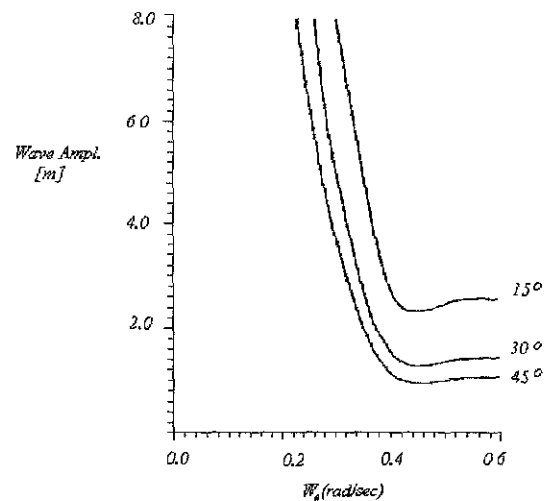


Fig. 7 - Stability Limits, TS ship,  $U=6$  [kn],  $\overline{GM}_t=0.7$  [m].

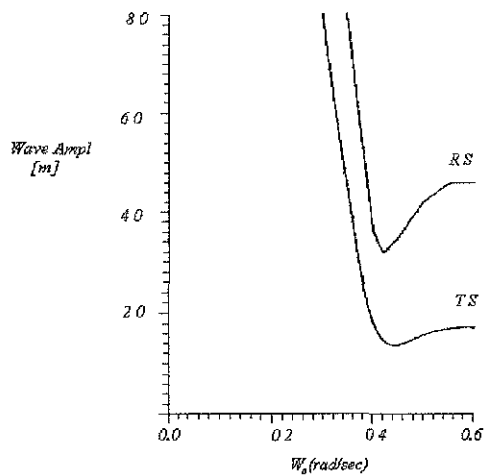


Fig. 8 - Stability Limits,  $\chi=15^\circ$ ,  $U=0$  [kn],  $\overline{GM}_T=0.7$ [m].

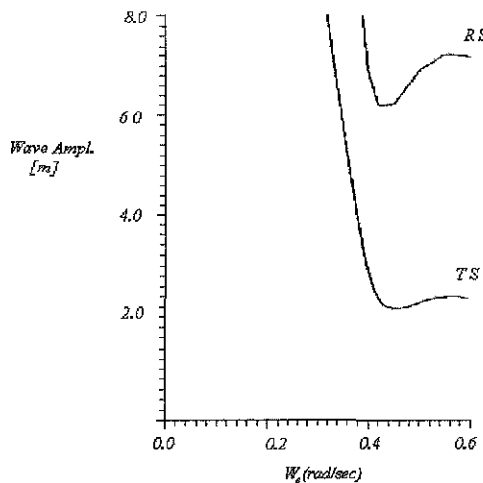


Fig. 9 - Stability Limits,  $\chi=15^\circ$ ,  $U=6$  [kn],  $\overline{GM}_T=0.7$ [m].

Different forward speeds at a heading angle of  $15^\circ$ , are considered in Figs. 4 and 5, both vehicles with a metacentric height of 0.7m. It is seen that increasing speed is a stabilizing action, specially for the RS hull. This is a consequence of the lift damping that increases with speed. Stability limits for different heading angles ( $15^\circ$ ,  $30^\circ$  and  $45^\circ$ ) at 6 knots and metacentric height equal to 0.7m are given in Figs. 6 and 7 for the two vessels. For both ships limits are lower for the 45 degrees wave incidence.

Figs. 8 and 9 show two direct comparisons of stability limits for the two small fishing

vessels, considering the zero speed and 6 knots cases, respectively.

In all cases it can be seen that the RS type vessel is much more stable than the TS type vessel.

#### 4. CONCLUSIONS

A non-linear coupled six degrees of freedom mathematical model for predicting the response of a ship in waves has been described.

The non-linear model presented in this paper permits to study critical stability regions where may occur situations of real risk, depending on the metacentric height of the ship, heading angle of waves, frequency and the hydrostatic restoring properties of the hull.

Introduction of non-linear restoring terms coupling the roll motion to the heave and pitch modes makes it possible for new dangerous conditions of parametric resonance to intervene in the ship dynamics. From the stability point of view, the resonant frequencies that appear are;  $w_e = 2 w_4$ ,  $w_e = w_3 - w_4$  and  $w_e = w_5 - w_4$ . Combined frequencies are particularly interesting to analyse, because they correspond to low frequencies, usually found when the ship sails in stern waves, a situation described by many authors as potentially dangerous.

The theoretical mathematical model presented herein shows that for the level of hydrostatic coupling assumed, heave and pitch modes define distinct mechanisms of parametric excitation of the roll motion. Analyses of the effects of restoring couplings on ship stability are very important, in the sense that they have a direct correspondence with the geometry of hull shape.

Linear hydrodynamic and hydrostatic coefficients are very similar for the two ships. Some second order hydrostatic coefficients, on the other hand, are quite distinct, reflecting the different stern arrangements, and they give

rise to quite different stability limits, indicating that they describe some essential aspects of the ship dynamics in waves.

The model shows that at exciting frequencies near the  $\omega_e = \omega_3 - \omega_4$  tuning the regions of parametric instability are reduced when metacentric height and speed of advance increase. This is in agreement with reports on the occurrence of parametric instability.

## REFERENCES

1. KERWIN, J. E. - "Notes on Rolling in Longitudinal Waves", International Shipbuilding Progress, No. 16, 1955.
2. BLOKI, W. - "Ship Safety in Connection with Parametric Resonance of the Roll". Inter. Shipbuild. Progress., No 306, 1980.
3. CESARI, L. - "Asymptotic Behaviour and Stability Problems in Ordinary Differential Equations", Springer-Verlag, 1971.
4. HUA J. - "A Study of the Parametrically Excited Roll Motion of a Ro-Ro Ship in Following and Heading Waves". Inter. Shipb. Progress, Vol. 39, December 1992, No. 420.
5. HIMENO Y. - "Prediction of Ship Roll Damping - State of Art", Dept. of Naval Architecture and Marine Engineering, The University of Michigan, Report No. 239, Sept. 1981.
6. HSU, C. S. - "On the Parametric Excitation of a Dynamic System Having Multiple Degrees of Freedom". Journal of Applied Mechanics, Sept. 1963.
7. MORRAL, A. - "Capsizing of Small Trawlers". The Royal Institution of Naval, Joint Evening Meeting, Galscow and Rina Spring Meeting, London, 1979.
8. NEVES, M. A.; PÉREZ, N. and SANGUINETTI, C. - "Analitical and Exprimental Study on the Dynamical Stability of Fishing Vessels in Regular Waves". Ingeniería Naval No.639. Spain, 1988 (in Spanish).
9. NEVES, M.A.S. and PERNAMBUCO, T.A.M - "Dynamic Stability of Fishing

It is known that tramson stern type vessels are more vulnerable to parametric resonance than the conventional round stern type vessel. The present study may reveal some explanations for this.

## ACKNOWLEDGMENT

The author's wish to express their thanks to CNPq and CAPES of Brazil for the financial support.

- Vessels in Astern Seas", Proc. XII Congress of Naval Engineering, Buenos Aires, 1991.
10. NEVES, M.A.S. and VALERIO, L. - "Parametric Stability of Fishing Vessels". Proceedings of Fifth International Conference on Stability of Ships and Ocean Vehicles. Florida Tech (U .S. A.), November 1994.
11. PAULLING, J. R. and ROSENBERG, R. M. - "On Unstable Ship Motions Resulting from Nonlinear Coupling". Journal of Ship Research, 1959.
12. PAULLING, J. R.- "The Transverse Stability of a Ship in a Longitudinal Seaway". Journal of Ship Research, No 4 ,1961.
13. PÉREZ, N. and SANGUINETTI, C. - "Experimental Results of Parametric Resonance Phenomenon of Roll Motion in Longitudinal Waves for Small Fishing Vessels". International Shipbuilding Progress, Vol. 42, No. 431, Sept. 1995.
14. PERNAMBUCO, T. A. M. - "Stability of Ships in Oblique Waves", M. Sc. Thesis, Federal University of Rio de Janeiro, Oct, 1990 (in Portuguese).
15. SALVESEN, N.; TUCK, E. O. and FALTINSEN, O. - "Ship Motions and Sea Loads" Det Norske Veritas Publ. no. 75, 1971.
16. SKOMEDAL, N. G. - "Parametric Excitation of Roll Motion and its Influence on Stability". Proceedings, Second International Conference on Stability of Ships and Ocean Vehicles, Tokyo, Oct./1982.

## APPENDIX A

### PARTICULARS OF SHIPS

The main characteristics of the ships used in this paper are listed below, followed by Figs. A1 and A2 which show their lines plans :

Table A.1

PRINCIPAL PARTICULAR OF SHIPS		
denomination	RS	TS
Length [m]	24.36	25.91
Length between perp. [m]	21.44	22.09
Beam [m]	6.71	6.86
Depth [m]	3.35	3.35
Draught [m]	2.49	2.48
Displacement [tons]	162.60	170.30
Water plane area [m <sup>2</sup> ]	102.50	121.00
x - Centroid of A <sub>w</sub> [m]	-0.69	-0.84
Trans. radius of gyration [m]	2.62	2.68
Long. radius of gyration [m]	5.35	5.52
Length of bilge keel [% L <sub>pp</sub> ]	30-80	30-80
Width of bilge keel [m]	0.15	0.15

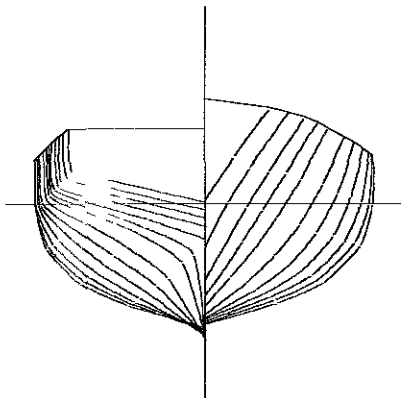


Fig. A. 1 Body plan of transom stern vessel (TS)

Table A.2

Values of Linear Restoring Coefficients		
Coefficient	RS	TS
C <sub>33</sub>	105.06	124.02
C <sub>35</sub>	72.47	103.65
C <sub>53</sub>	72.47	103.65
C <sub>55</sub>	3039.48	3320.92

Table A.3

Values of Second Order Restoring Coefficients		
Coefficient	RS	TS
C <sub>443</sub>	210.32	413.97
C <sub>445</sub>	204.58	1021.46
C <sub>344</sub>	210.32	413.97
C <sub>333</sub>	42.20	77.63
C <sub>355</sub>	2794.47	6346.08
C <sub>335</sub>	106.42	421.83
C <sub>533</sub>	106.42	421.83
C <sub>555</sub>	11449.75	43373.17
C <sub>535</sub>	2794.47	6346.08

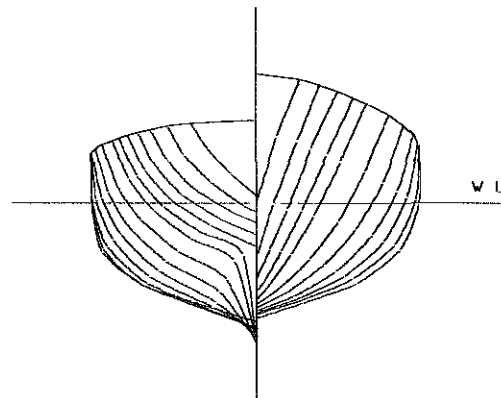


Fig. A. 2 Body plan of round stern vessel (RS)

## APPENDIX B

### NON-LINEAR RESTORING ACTIONS

#### B. 1 EQUATION OF WATER PLANE

Fig. B-1 shows the cross-section of a vessel with two reference axes, AXYZ (inertial system) and Gxyz (fixed system at G). At the equilibrium position the two systems coincide.

Denoting linear displacements of G by  $x_g$ ,  $y_g$  and  $z_g$ , and angular displacement by the modified Euler angles  $\phi$ ,  $\theta$  and  $\psi$ , the coordinates of a point in the AXYZ system are given as

$$X = x_g + a_1x + b_1y + c_1z$$

$$Y = y_g + a_2x + b_2y + c_2z$$

$$Z = z_g + a_3x + b_3y + c_3z$$

where  $a_i, b_i, c_i, i=1,2,3$ , are the directional cosines of axes  $G_x, G_y, G_z$ , respectively, obtained from the ordered rotations defined in sequence as  $\psi, \theta, \phi$ .

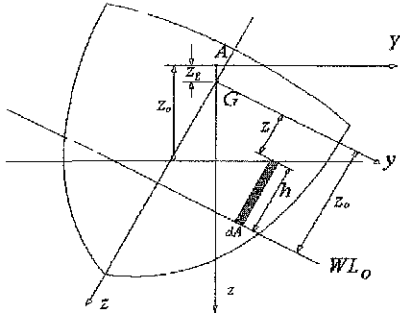


Fig. B-1

The equation of water plane area is:

$$z_o = z_g - x \sin \theta + y \sin \phi \cos \theta + z \cos \phi \cos \theta$$

The water column at each point due to vertical and angular displacements is  $h = z_o - z$ , or

$$h = \frac{z}{\cos \phi \cos \theta} - x \frac{\text{tg} \theta}{\cos \phi} + y \text{tg} \phi \quad (B1)$$

## B. 2 HYDROSTATIC ACTIONS

The bouyancy force acting on the hull is

$$c_3(z_g, \phi, \theta) = -\gamma \nabla_o - \gamma \int_{A_w} h dA \quad (B2)$$

and the moments of this force in the roll and pitch modes are given as:

$$c_4(z_g, \phi, \theta) = -\gamma \int_{A_w} [c_3 y + b_3 h / 2] h dA + b_3 \gamma \nabla_o \overline{BG} \quad (B3)$$

$$c_5(z_g, \phi, \theta) = -\gamma \int_{A_w} [-c_3 x + a_3 h / 2] h dA + a_3 \gamma \nabla_o \overline{BG} \quad (B4)$$

After substitution of (B1) in equations (B2), (B3) and (B4), the following hydrostatic actions, valid for large displacements, are obtained:

$$c_3(z_g, \phi, \theta) = -\gamma \nabla_o - \gamma \left[ \frac{z A_w}{\cos \phi \cos \theta} - \frac{x_f \text{tg} \theta A_w}{\cos \theta} + y_f \text{tg} \phi A_w \right] \quad (B5)$$

$$c_4(z_g, \phi, \theta) = -\gamma [z y_f A_w + \gamma I_{yy} \sin \theta - \gamma I_{xx} \sin \phi \cos \theta + \gamma A_w - \gamma \frac{1}{2} \sin \phi \cos \theta \left[ -\frac{x_f \text{tg} \theta}{\cos \phi} + y_f \text{tg} \phi \right]^2 A_w - \gamma \sin \phi \cos \theta \nabla_o \overline{BG}] \quad (B6)$$

$$c_5(z_g, \phi, \theta) = \gamma [z x_f A_w - I_{yy} \sin \theta + I_{xy} \cos \theta \sin \phi] - \gamma \frac{1}{2} \sin \theta \left[ -x_f \frac{\text{tg} \theta}{\cos \phi} + y_f \text{tg} \phi \right]^2 A_w + \gamma \sin \theta \nabla_o \overline{BG} \quad (B7)$$

In the above expressions,  $x_f$  and  $y_f$  represent planar coordinates for centroid of waterplane area.

## B. 3 HYDROSTATIC COEFFICIENTS

The expressions for the hydrostatic actions given above (equations (B5, B6 and B7)) may be expanded in Taylor series up to second order terms. Equations (3a, 3b, 3c) in the main text are then obtained, where, in accordance with the nomenclature introduced :

$$C_{ij} = -\frac{\partial C_i}{\partial n_j} \Big|_o ;$$

$$C_{yjk} = -\frac{\partial^2 C_i}{\partial n_j \partial n_k} \Big|_o \quad \forall j \neq k$$

and

$$C_{\text{ill}} = -\frac{1}{2} \frac{\partial^2 C_i}{\partial n_l^2} \Big|_o$$

## ON THE STABILITY SAFETY OF THE SHIPS

G. Boccadamo, P. Cassella, A. Scamardella  
Dipartimento di Ingegneria Navale  
University "Federico II" of Naples  
via Claudio, 21 - 80125 Naples (ITALY)

### ABSTRACT

As it is well known the ships safety against capsizing depends not only on the intact stability of the ships but also on the operative conditions and on the crew ability.

As a matter of fact, while on one hand some dangerous situations of capsizing, such as deck in water, water on deck, poor stability in very severe environmental conditions can be avoided mainly by means of ship's stability characteristics, on the other hand other dangerous situations can be avoided only by means of the ability of the ship master to escape from them.

The paper deals with.

- an useful tool to satisfy the stability criteria in the preliminary design stage by means of geometrical similarity laws and of regression analysis technique applied to systematic series of the hulls

- the necessary measures in order to reduce the danger of the ship capsizing due to particular combinations of operative situations and of environmental conditions.

### 1. INTRODUCTION

Many theoretical and experimental researches carried out during the last thirty years allow nowadays a good understanding of the various causes of ships capsizing, but it is not possible

to transfer all the results of these researches into simple regulations.

Nowadays for all types and sizes of the ships, having length of 24 m and over, the safety against capsizing should be given by the IMO stability criteria (statistical criteria and weather criterion).

These criteria, by considering only the geometrical characteristics of the ship, the loading conditions and some very simple operational conditions, should establish a same standard level of safety against capsizing for any ship.

However the I.M.O. stability criteria do not take into account various possible dangerous situations of the ship at sea, such as: stability reduction on wave crest, influence of deck in water, influence of water on deck, surf-riding, and consequently possible broaching-to, dynamic rolling resonance in beam sea, parametric rolling resonance in following and in quartering sea, bifurcation phenomenon, poor stability in very severe conditions, concentration of a dominant part of wave energy in a narrow band of encounter wave frequency, load shifting on board due to severe environmental conditions, etc.

Moreover, the stability criteria do not consider that the same environmental conditions for small vessels, and especially for the fishing vessels, are more severe than for the other ships

## 2. DIFFERENT SIZE AND TYPE OF THE VESSELS: CASUALTIES AND LOSSES OF HUMAN LIVES

The comparison of the casualties among the fishing vessels, the oil tankers and the gas carriers is shown by the histograms from fig 1 to fig.3 obtained by Lloyd's Register data

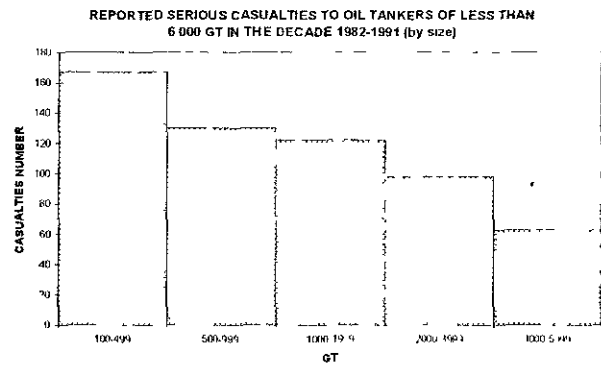


FIG. 1

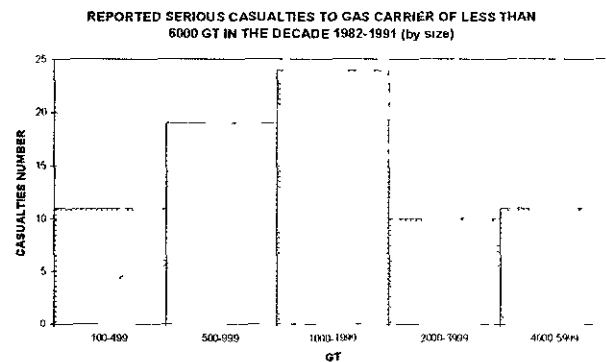


FIG. 2

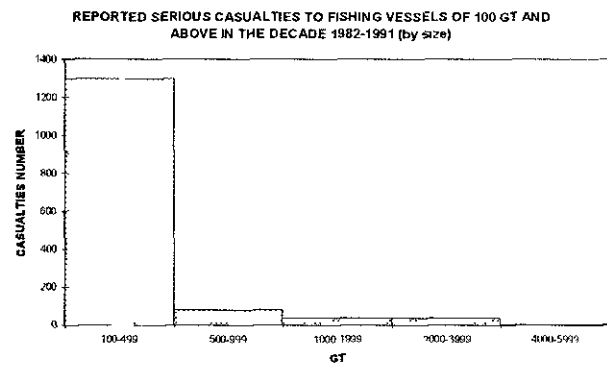


FIG. 3

Another comparison of the human lives lost among the fishing vessels, the oil tankers and the gas carriers is shown by the histogram of fig 4 obtained by the same data

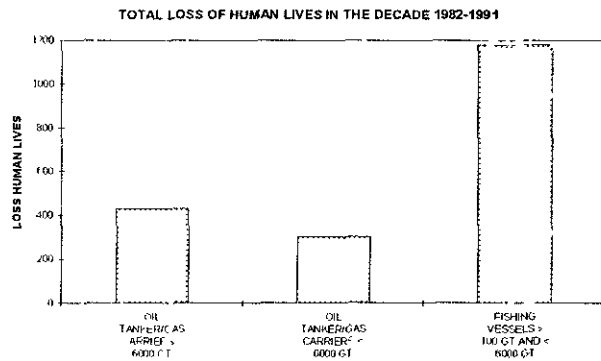


FIG. 4

The above mentioned comparisons are given for ships having gross tonnage between 100 and 6000, and they point out the necessity to improve the safety at sea of the small ships, especially the fishing vessels.

By the Lloyd's Register data we obtained also the following histograms for ships with gross tonnage between 100 and 6000

- the total loss of human lives in one decade subdivided by the size of the vessel (fig.5);
- the number of serious casualties in one decade subdivided for type of casualty (fig.6);
- the number of human lives lost in one decade for type of casualty (fig.7).

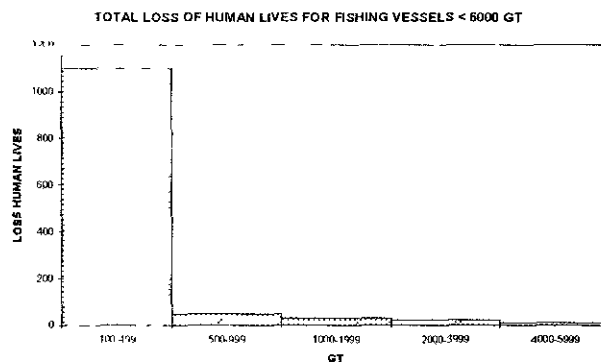


FIG. 5

TOTAL NUMBER OF ACCIDENTS HAPPENED IN THE DECADE 1982-1991 TO FISHING VESSELS

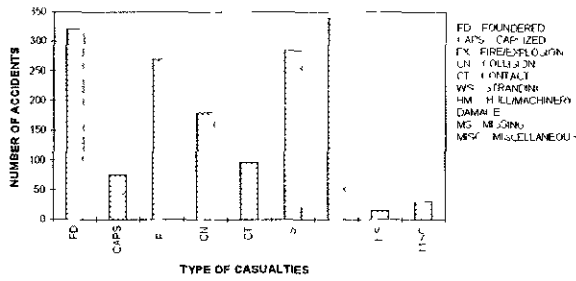


FIG 6

TOTAL LOSS OF HUMAN LIVES IN THE DECADE 1982-1991 FOR FISHING VESSELS SUBDIVIDED FOR CASUALTIES

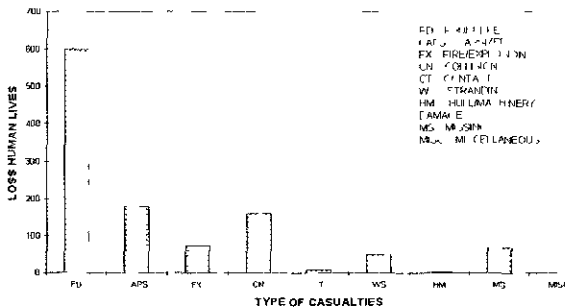


FIG 7

For the smallest fishing vessels, we have no data of casualties, but it is well known the dramatic situation of the many disasters and of human lives lost at sea.

However the safety against capsizing, not only of the fishing vessels, should be improved, but of all the small ships by means of the improvement of the stability characteristics, of the training of the crew and of guidance to the Master for ship navigating in rough sea

By means of the analysis of the systematic series of the hulls the paper shows the possibility of

- analyse methodically the influence both of the ship form and geometry and of loading conditions on the I M O stability indices,
- furnish the ships designer with an useful tool in order to check I M O stability criteria in the preliminary design stage and to use automatic procedures for a quick optimisation of ship's stability characteristics;
- check quickly the stability of the operative ships in different loading conditions;
- make a comparison among the various stability indices,

- verify if the compliance to I.M.O. criteria could imply undesired consequences as bad characteristics and operational conditions on board

### 3. CHECK OF THE I.M.O. STABILITY CRITERIA

In previous papers [1], [2], [3], [8], the theoretical background of hull's geometrical similarity and its application to the systematic series hulls have already been discussed.

Particularly if we consider many different combinations of hulls geometrical characteristics and loading conditions, by means of geometrical similarity and of regression analysis it is possible to have the following polynomial expressions for the stability indices:

$$C_{\varphi_s} = \frac{B}{T} \operatorname{tg} \varphi_s = \sum_1 a_i C_p^m C_v^n \left(\frac{B}{T}\right)^p \left(\frac{f}{B}\right)^q \left(\frac{KG}{D}\right)^r \quad (1)$$

$$I = \sum_1 a_i C_p^m C_v^n \left(\frac{B}{T}\right)^p \left(\frac{f}{B}\right)^q \left(\frac{KG}{D}\right)^r (\nabla_0)^s \left(\frac{L}{\nabla^{1/3}}\right)^t \quad (2)$$

$$\frac{b}{a} = \sum_1 a_i C_p^m C_v^n \left(\frac{B}{T}\right)^p \left(\frac{f}{B}\right)^q \left(\frac{KG}{D}\right)^r (\nabla_0)^s \left(\frac{L}{\nabla^{1/3}}\right)^t \left(\frac{A_s}{LT}\right)^u \left(\frac{h_s}{T}\right)^v \quad (3)$$

being

B, T and D the moulded beam, mean draught and moulded depth respectively;

$\varphi_s$  the angle at which the righting lever GZ is maximum,

I is the generic statistical stability index (GM,  $GZ_{30^\circ}$ ,  $GZ_{40^\circ}$ ,  $E_{40^\circ}$ ,  $E_{40^\circ} - E_{30^\circ}$ );

b/a is the index considered by the weather criterion,

f the design freeboard at midship;

$C_{\nabla} = \frac{\nabla}{\nabla_0}$  the ratio between the real and the design displacement volume;

$C_p$  (or  $C_b$ ) the prismatic (or the block) coefficient;

KG the vertical position of the centre of gravity;

$A_s$  the superstructures area;

$h_s$  the vertical distance from the centre of the windage area to the centre of the underwater lateral area.

Then the maximum allowable  $KG^*/D$  value which fulfils each index can be obtained by solving the previous equations with respect to  $KG^*/D$  and by substituting for  $C_{\varphi}$ ,  $I$  and  $b/a$  the minimum values required in the IMO recommendations

So, these  $KG^*/D$  values can be expressed by means of the regression analysis in the form:

$$\frac{KG^*}{D} = \sum_i b_i C_p^m C_v^n \left(\frac{B}{T}\right)^p \left(\frac{f}{B}\right)^q \quad (4)$$

$$\frac{KG^*}{D} = \sum_i b_i C_p^m C_v^n \left(\frac{B}{T}\right)^p \left(\frac{f}{B}\right)^q \nabla_0^s \left(\frac{L}{\nabla^{1/3}}\right)^t \quad (5)$$

$$\frac{KG^*}{D} = \sum_i b_i C_p^m C_v^n \left(\frac{B}{T}\right)^p \left(\frac{f}{B}\right)^q \nabla_0^s \left(\frac{L}{\nabla^{1/3}}\right)^t \left(\frac{A_s}{LT}\right)^u \left(\frac{h_s}{T}\right)^v \quad (6)$$

where the first  $KG^*/D$  value satisfies the  $\varphi_c$  criterion, the second one satisfies simultaneously all the other statistical indices and the third one satisfies the weather criterion.

The previous polynomial expressions, by means of the flow diagram shown in fig. 8, give us the possibility to use automatic procedures in order:

- to check the influence of ship's form and dimensions on the different stability indices and to furnish the ship designer with an useful tool for the optimisation of ship's stability characteristics;

- to furnish the ship master with a simple tool in order to check the operative ship's stability in any load condition by means of computer on board;

- to check that the GM value, in order to verify all the stability indices, does not assume excessive value with very low rolling period of the ship and consequently bad seakeeping characteristics and operational conditions on board.

#### 4. CONSIDERATIONS ON THE SHIP'S SAFETY AND ON THE NECESSARY MEASURES TO IMPROVE IT

Every ship has its individual characteristics and responds to environmental conditions in its own way. Therefore the ship should be designed so that it can survive in the extreme environmental conditions which are expected to encounter in the life time.

But the stability safety is a very complex problem and it is at present not possible and we think that will be not possible in the future to have stability criteria, which take into account all the different possible causes of ship capsizing

At present we can consider two groups of dangerous situations relating respectively to ship stability in beam sea and to combination of speed, direction and sea condition in following and in quartering sea.

##### 4.1 - Ship in beam sea

The safety against capsizing of the ship in beam sea should be given mainly in the ship design by means of standard stability characteristic. This is the main aim of the I.M.O stability criteria which furnish a standard safety against capsizing taking into account some considerations due to the experience and especially to the possibility of the ship to survive in severe beam wind and wave.

However in order to have the same standard safety for to all the ships these criteria should take into account also the different types and the different sizes of the ships, and the different effective operative and environmental conditions in the geographic area in which the ship will operate during its life.

Moreover we think that it is necessary to improve the I.M.O criteria with the following additional measures:

- to fix a minimum allowable value of  $f/B$ , and consequently the angle of the deck edge immersion in order to avoid the heeling moment due to water on deck.

# FLOW DIAGRAM

CHECK THE INFLUENCE OF SHIP'S FORM AND DIMENSIONS  
ON THE DIFFERENT STABILITY INDICES

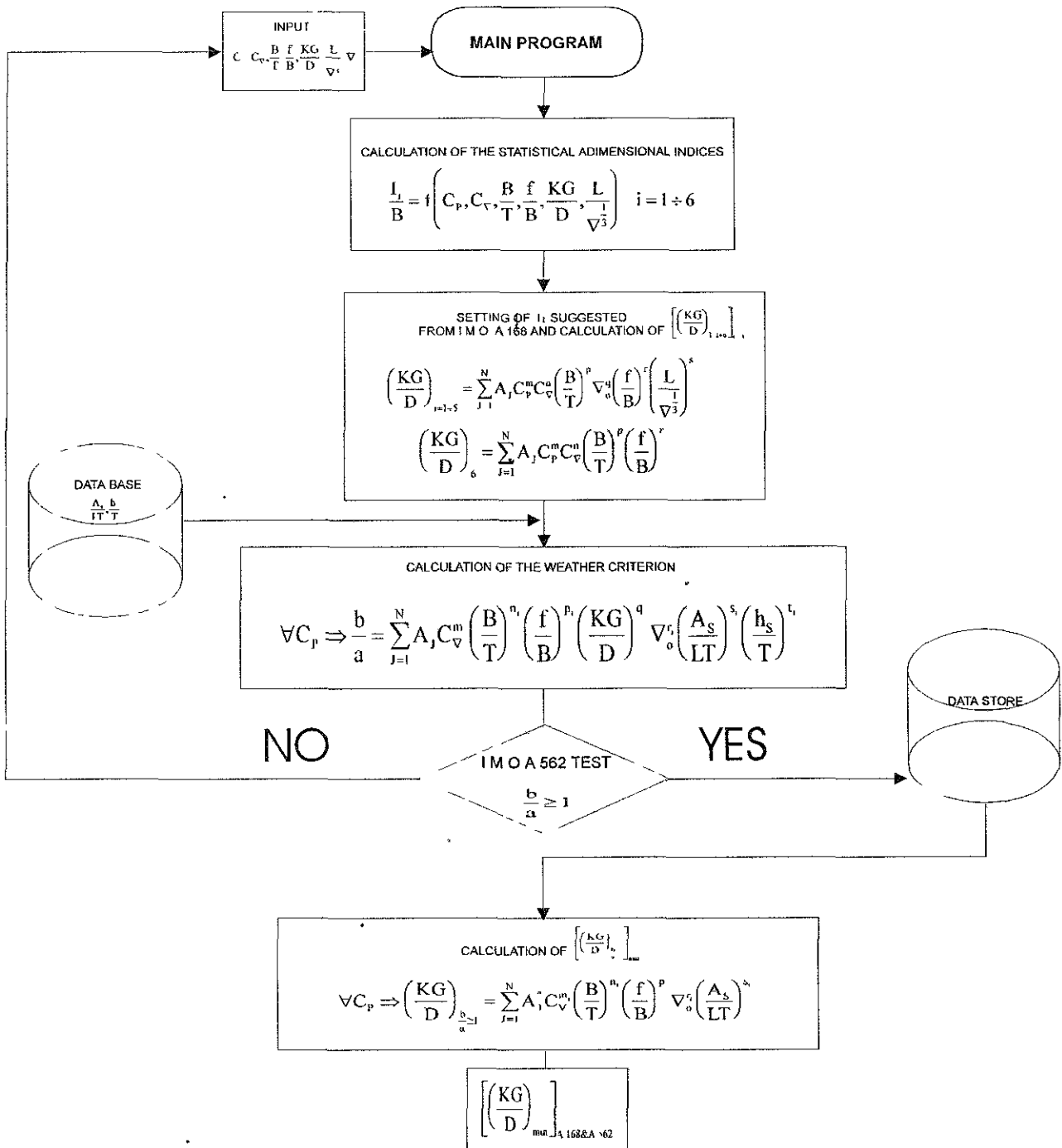


FIG 8

- to fix not only a minimum allowable of GM, but also a maximum value of GM to beam ratio, being this value an indicator of the natural rolling period of the ship and consequently of the inertia forces, which influence the comfort and the operational conditions on board.

- to fix a maximum value both of the ratio of windage area to underwater lateral area and of the wind heeling lever in order to avoid the danger of capsizing due to heeling moment both of the wind and of the wave action in very severe beam sea.

- to use a procedure which includes the variation of the wind velocity at different heights above the waterline in order to have a more realistic determination of heeling moments due to wind

- to consider a velocity of overturning wind related to a fixed risk level in the geographic operational area of the ship in order to have a sufficient stability margin against heeling moment due to the wave pressure effect, water on deck etc

#### 4.2 Ship in following and in quartering sea

Theoretical researches and especially towing tank model tests highlight the various dangerous situations of the ship's capsizing in following and in quartering sea: pure loss of stability on wave crest, surf riding and broaching to, parametric rolling resonance, high concentration of wave energy in narrow band of encounter wave frequency

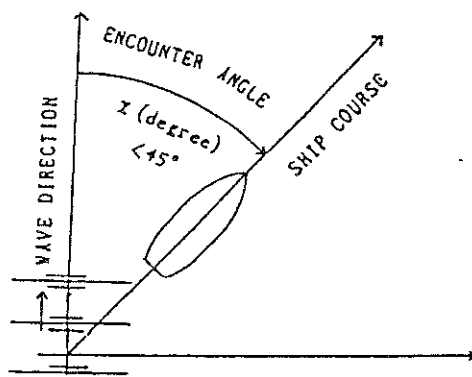
At present it is well known that these dangerous situations are due to a specific range of combination of ship speed, encounter angle and sea condition; as the ship capsizing can be avoided if the ship runs out of this range, it is necessary to furnish the ship master with a guidance for avoiding the dangerous situation in following and in quartering sea

Particularly the master should be provided with a set of simple basic provisions which could be used by him in order to escape from them in a rapid and effective manner.

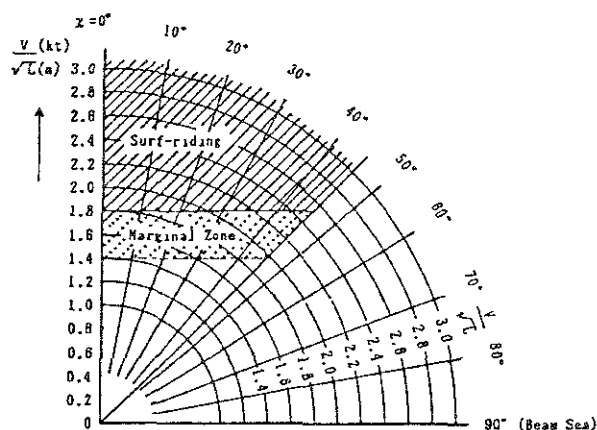
To this aim, the polar diagrams (figs. 9 and 11), suggested by working group of Intact Stability at thirty-ninth session of IMO SLF Sub-Committee held in London on March 1995, could be very useful, as guidance to the master.

These diagrams show the dangerous zones due to surf-riding and to concentration of dominant part of wave energy in narrow band of encounter wave frequency and consequently to successive high wave attack, by means respectively of  $V/\sqrt{L}$  and  $V/T$  diagram versus wave encounter angle, being  $V$  the speed of ship in knots,  $L$  the length of ship in meters and  $T$  the mean wave period.

When the operational conditions of the ship are out of the dangerous zone due to broaching and to successive high wave attack, it is necessary to determine by means of the fig 10 the encounter wave period, and if it is nearly equal to natural rolling period of the ship or its half the speed of the ship must be reduced in order to avoid respectively synchronous rolling motion and parametric rolling motion



Definition of encounter angle  
Fig. 9



Dangerous zone due to surf-riding  
FIG 10

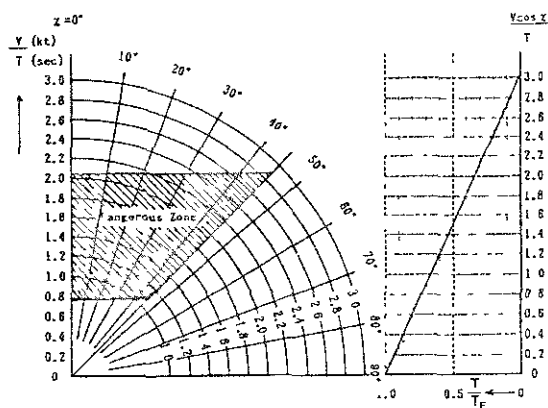


Fig 11

Dangerous zone to encounter to high wave group and relation between mean wave period and encounter wave period in following and quartering seas

### 3.3 The human error

The human error is the main source of the ship's disaster. Particularly the disaster can be due to loading and ballasting errors, to water-tight doors open, to wrong manoeuvres, etc. As ascertained by the conclusions of various Inquiry Committees the human error is the source of almost 80% of the ship's disasters. Therefore, it is necessary to reduce the probability of disaster due to human error.

To this aim:

- The stability criteria and the loading manual should be as simple as possible and should foresee an adequate safety margin in order to enable eventual loading and ballasting errors;
- the crew, and particularly the Officers, should have a deep knowledge of the ship operative dangerous situations due to the various types of error or negligence.

## 5. CONCLUSIONS

The intact stability of a ship is one of the most important elements to consider in the design stage. The ship's safety against capsizing in fact depends on its stability degree.

Many theoretical and experimental researches carried out in the last thirty years allow nowadays a good understanding of the various possible causes of ship's capsizing: insufficient intact stability with particularly severe inclining actions; resonance between rolling motion of ship and inclining actions period; parametric resonance in following sea; deck wetness or shipping water on deck, effect of the sliding weights, pure stability loss on wave crest, successive high wave attack, surf-riding and broaching-to, bifurcation, etc.

On the other hand the human error is the main source of the ship's disaster, consequently we have to concentrate most of our effort on tasks: "how to assist the master in order to reduce the probability of human error".

First of all we consider that it is necessary a better training of the crew and particularly of the officers, as they have a good understanding of the various possible causes of ship's capsizing and a deep knowledge of the operative dangerous range.

As far as the foreseeable modifications of the stability criteria are concerned in the next future, we should first all consider that each ship has its own dynamic characteristics on which the reaction to the effecting meteorological action depends.

Therefore, in order to avoid the frequent loss of small ships we should have different values of the stability indices for different ship's size.

and for different geographic operative area. Particularly the stability criteria should be most severe for small ships, as the fishing vessels.

Really each ship should have appropriate stability criteria, which could take into account all the dangerous situations of the ship at sea.

However the manifold possible operative of ship scenarios give us till now, but perhaps in the future too, no possibility to obtain ship individual criteria. Such criteria should be obtained both by means of mathematical models and of ship model tests. The models adopted till now are very simplified and therefore do not give us the desired goal. Some phenomena involved in extreme wave conditions still await their mathematical representation.

However, even though we are far from obtaining satisfactory mathematical models of the ship in its own effective operative situation, this direction could provide the solution of the problem, solution which modelled by computer would allow the ship's master to avoid the capsizing by taking the necessary decision thanks to a computer on board.

If will not be possible to consider all the different operative situations of the ship by a mathematical model, however the well known dangerous situations deriving from beam sea and from the quartering and the following sea could be avoided by satellite observation of the meteorological conditions on the ship course. In this case a computer on board with the obtained data could change automatically speed and course of ship so to avoid the dangerous capsizing situations.

At last it would be necessary to create in each seaport navigational aids centres for all the ships and especially for the small ships, as for example the small fishing vessels, whose crew is made of fishermen who don't have a satisfactory training.

## 6. ACKNOWLEDGEMENTS

This paper is part of a research on the ship's safety sponsored with the financial support of the C.N.R. (Italian National Research Council) and MURST [Ministry of the Scientific and Technological Research (40% funds)].

## 7. REFERENCES

1. Campanile A., Cassella P.: "Form Stability Reduction Among Waves For Series 60 Hulls" Ocean Engineering vol.16 1989.
2. Boccadamo G., Cassella P.: "Ridgely-Nevitt Fishing Vessels Series Stability In Longitudinal Waves" STAB'90 Napoli (Italy) 1990.
3. Boccadamo G., Cassella P., Russo Krauss G., Scamardella A.: "Analysis of IMO Stability Criteria by Systematic Hull Series and by Ship Disaster", STAB '94, Melbourne (U.S.A.), 1994
4. Grochowalski S., Archibald J B., Connolly F J., Lee C.K., "Operational Factors in Stability Safety of Ships in Heavy Seas", STAB '94, Melbourne (U.S.A.), 1994
5. Kobylinski L., "Methodology of the Development of Stability on the Basis of Risk Evaluation", STAB '94, Melbourne (U.S.A.), 1994
6. Takaishi Y., "Dangerous Encounter Wave Conditions for Ships Navigating in Following and Quartering Seas", STAB '94, Melbourne (U.S.A.), 1994
7. Report of the I.M.O. Working Group on the Intact Stability SLF 39/WP3/Add1
8. Cassella P., "I.M.O. Stability Criteria: Analysis and Considerations", AQUAMARINE'95, Maritime Engineering Conference, Perth, Australia, 1995

# A REVIEW OF DESIGN CHARACTERISTICS OF SOME FISHING VESSELS OPERATED IN TURKEY

G. ÖZMEN<sup>1</sup>, A.D. ALKAN<sup>2</sup>, and S. ISHIDA<sup>3</sup>

<sup>1</sup> Faculty of Marine Sciences, Karadeniz Technical University, Trabzon, Turkey

<sup>2</sup> Department of Naval Architecture and Marine Engineering, Yildiz Technical University, Istanbul, Turkey

<sup>3</sup> Ship Research Institute, Ministry of Transport, Tokyo, Japan

**Keywords:** fishing vessel design-stability-traditional vessel

## ABSTRACT

The commercial fishing fleet of Turkey is experiencing sudden changes in economic strategies so that the design and use of fishing vessels require new approaches that should produce a better efficiency in their exploitation. Since the great majority of present vessels are built using traditional methods, there is a very little collected information on their design data as well as current stability levels within commercial fishing fleet.

In this paper, basic design characteristics of some selected fishing vessels, operating in Turkish waters, are studied with different scopes such as quality of design properties and safety levels. These levels are described by comparing the present vessels with the ones designed by using rational engineering tools.

## NOMENCLATURE

ITTC Standard Symbols and Terminology in SI units are used.

## 1. INTRODUCTION

In this study, a general view was carried out on some particular traditional fishing vessels operated in Turkish waters. Their basic design characteristics were studied in different scopes by comparing with some other vessels designed using engineering knowledge.

The traditional Turkish vessels in this study are all craftsman designs and operated in purse-seine applications. Their stability and seaworthiness capability were compared with some competitive vessel designs whose quality already justified through model tests. Although a large quantity of computations were carried out, the results were converted to practical figures in order to make a practical comparison among all vessels.

According to the results obtained by using basic naval architecture tools, the designed vessels clearly showed better stability quality than traditional ones. As far as the seakeeping quality on vertical motions were considered, traditional vessels seem to be superior with the advantage of large beam to draught ratio. However, their operating experience reveals that the traditional vessels in general are not strong enough to perform fishing activities in extreme weather conditions.

## 2. TURKISH FISHING VESSELS

The Turkish fishing fleet has about 10,000 coastal fishing vessels, most of which purse seiners and trawlers, catching 1,200,000 tones per year according to the statistics of 1995. As regards to this figure, Turkish vessels are competitive with respect to the catch quantity per vessel. The overall lengths of vessels employed in professional fishing is varying from 20 to 45 metres, in addition, in recent years, some larger vessels built whose length reached

Table 1  
Number of fishing vessels in different regions [1].

Vessel Type	East Black Sea	West Black Sea	Marmara Sea	Egean Sea	Mediterranean Sea
Purse-seiner	130	132	129	83	35
Trawler	53	113	30	40	123
Carrier	78	21	11	24	6
Other	2,783	945	1,731	2,182	1,061
<b>TOTAL</b>	<b>3,044</b>	<b>1,211</b>	<b>1,901</b>	<b>2,329</b>	<b>1,225</b>

62 metres with 16 metres of breath. Table 1 shows the distribution of different vessel types with respect to the sea regions.

### 3. SELECTED VESSELS AND THEIR DESIGN PROPERTIES

In this study, 7 traditional purse-seiner vessels and some other fishing vessels previously designed by the professional designers were selected. The traditional vessels (T23, T30, T34, T40, T41, T62, KTU27) are presently operated in Turkey, all are monohull, steel built by the local craftsmen. The vessel KTU27 represents a typical Black Sea vessel was used as parent form in a hull form optimization study [2].

In order to define relative design features of the traditional hulls, the data-base of some other vessels possessing naval architecture designs were also used, those are C.1482 designed for Mediterranean fishing [3]; ITU148/1B, parent form of Istanbul Technical University small fishing vessel family and ITU148/8B and ITU148/4K from the same family [4].

Sectional views of the investigated vessels is shown in Figure 1, and Table 2 contains their detailed hydrostatic characteristics in design loading condition.

#### 3.1 Stability Properties of the Vessels

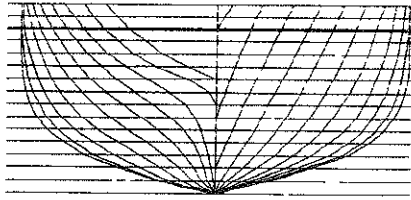
For the purpose of investigating preliminary design characteristics of the fishing vessels, stability computations were performed in calm

sea and in waves. Stability in waves was considered in two different wave positions relative to vessel, wave crest and wave trough amidships. In both cases the wave length was set equal to the vessel length between perpendiculars.

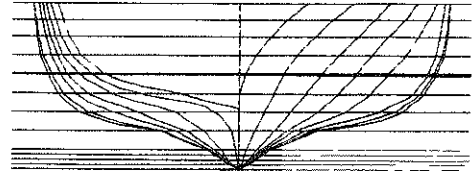
The restoring levers were divided by the breath of each vessel in order to provide a sensible comparison. The computation of the restoring levers were carried for heel angles up to 80 degrees where the most competitive vessel reached its maximum potential restoring. Stability computations in waves was performed for a wave amplitude equals to  $L_{pp}/40$  where  $L_{pp}$ , the length between perpendiculars, varying for each vessel.

As regards to the stability characteristics in calm sea shown in Figure 2, the traditional vessels showed relatively higher restoring levers in the range of smaller heel angles. However, the 'designed vessels' demonstrated their superiority in larger heel angles. As shown in Figure 3 and Figure 4, as far as the stability in waves are considered, the designed vessels showed their superiority particularly in the case of the wave trough amidships.

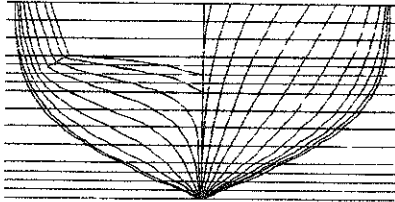
Considering the same relative height of the centre of gravity, the engineering designs demonstrate better restoring capabilities at large angles of heel where the probability of capsizing is higher both for calm sea and waves.



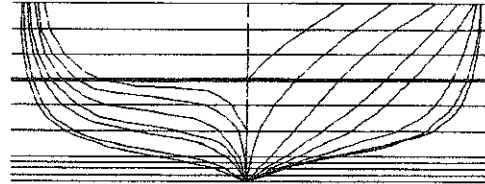
C.1482



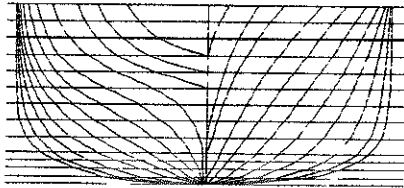
T30



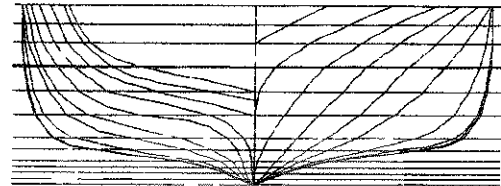
ITU 148/1-B



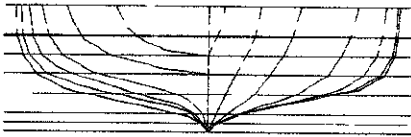
T34



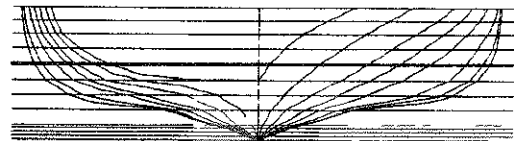
ITU 148/4-K



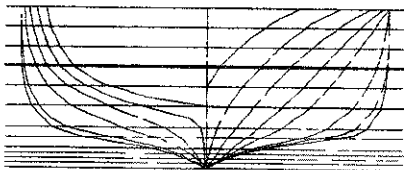
T40



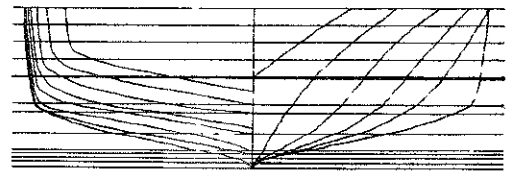
KTU27



T41



T23



T62

Fig 1 Sectional views of the vessels

Table 2  
Hydrostatic properties of the vessels at design waterline.

Vessel	$L_{PP}$	B	T	L/B	B/T	D	$C_B$	$C_P$	$C_{WP}$	$C_M$	$L/\nabla^{1/3}$
C.1482	28.01	6.75	2.87	4.150	2.352	4.650	0.468	0.581	0.745	0.805	4.489
148/1B	20.00	5.71	2.29	3.500	2.500	3.220	0.378	0.560	0.728	0.673	4.329
148/4K	20.00	5.71	2.29	3.500	2.500	3.250	0.490	0.553	0.740	0.877	3.968
T23	22.00	6.90	2.00	3.188	3.450	2.800	0.503	0.676	0.822	0.745	4.115
T30	26.10	8.10	2.00	3.222	4.050	3.504	0.429	0.755	0.832	0.567	4.612
T34	34.01	9.15	2.20	3.717	4.159	4.050	0.473	0.694	0.819	0.681	4.950
T40	39.91	10.5	2.50	3.800	4.200	3.660	0.465	0.629	0.768	0.738	5.074
T41	37.45	11.7	2.00	3.200	5.850	3.800	0.416	0.728	0.811	0.572	5.241
T62	59.35	15.5	3.20	3.829	4.844	5.800	0.485	0.732	0.871	0.663	5.270
KTU27	27.00	8.00	2.00	3.375	4.000	2.940	0.453	0.713	0.793	0.635	4.650

Vessel	$\nabla$ ( $m^3$ )	$\Delta$ (kN)	$A_{ws}$ ( $m^2$ )	$A_{WP}$ ( $m^2$ )	$A_M$ ( $m^2$ )	$x_{CF}$ (m)	$x_{CB}$ (m)
C.1482	239.5	2407.8	226.5	132.7	15.6	-1.218	-0.581
148/1B	98.6	991.0	135.5	83.2	8.8	-1.800	-0.869
148/4K	128.1	1287.9	138.5	84.5	11.6	-0.602	-0.035
T23	152.8	1536.9	171.2	124.7	10.3	-0.691	-0.279
T30	181.2	1822.0	218.8	175.8	9.2	-1.095	-0.577
T34	324.4	3262.2	323.3	324.2	13.7	-1.653	-0.619
T40	486.6	4893.1	416.7	321.8	19.4	-2.339	-1.021
T41	364.8	3668.6	411.3	355.2	13.4	-1.575	-1.042
T62	1428.6	14365.0	985.3	801.3	32.9	-4.552	-1.565
KTU27	195.8	1920.7	223.8	171.2	10.2	2.022	2.787

(minus values of  $x_{CF}$  and  $x_{CB}$  shows aftward)

Vessel	KM (m)	KB (m)	$BM_T$ (m)	$BM_L$ (m)	$T_1$ (kN/cm)	$M_1$ (kNm/cm)
C.1482	3.338	1.784	1.554	22.301	13.35	20.34
148/1B	3.290	1.510	1.780	18.183	82.09	88.44
148/4K	2.687	1.366	1.321	15.014	8.50	9.67
T23	3.966	1.290	2.676	24.864	12.53	17.94
T30	5.806	1.370	4.436	42.322	17.66	29.53
T34	5.933	1.448	4.485	58.143	25.68	55.62
T40	6.548	1.608	4.940	58.479	32.35	71.70
T41	10.120	1.369	8.752	87.731	35.72	85.95
T62	12.131	2.143	9.988	131.417	80.57	318.09
KTU27	4.942	1.346	3.597	39.798	1.755	29.02

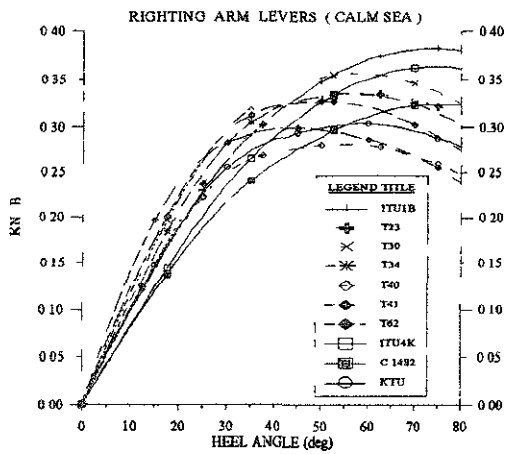


Fig 2 Relative restoring arm curves at calm water

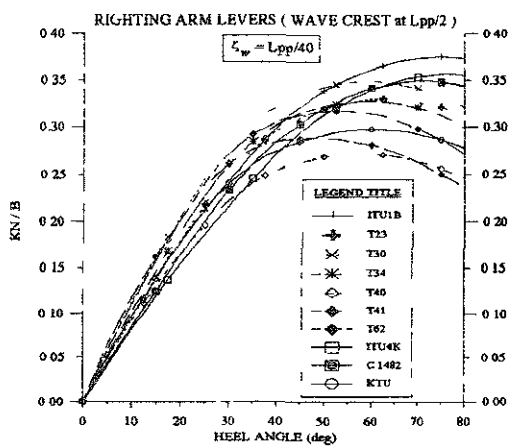


Fig. 3 Relative restoring arm curves on wave crest amidships

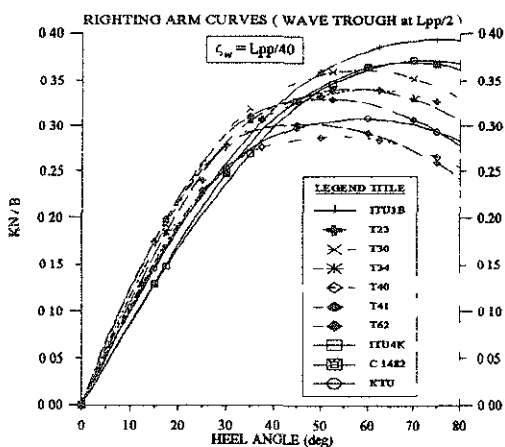


Fig 4 Relative restoring arm curves on wave trough amidships

### 3.2. Motion of the Vessels

Seaworthiness capabilities of the vessels were studied by considering coupled heaving and pitching motion. Using the statistical output of response amplitudes of the vessels, the operability index computations were carried out in order to compare the seakeeping performance trends of the vessels.

For this aim some significant seakeeping phenomena which limit the fishing vessels' operability were taken into consideration [5]. The operability index for absolute bow acceleration, slamming and deck wetness probability of occurrences were computed. The wave statistics were used in the computations contain the data of East Mediterranean seaway area [6].

As seakeeping limit criteria, the following limit criteria for the fishing vessels were used:

- absolute vertical bow acceleration (at station 0)  $0.5 \times 9.81 \text{ m/s}^2$ ,
- slamming (at station 17) 6%,
- deck wetness (at station 0) 10%,

where station means that the length between perpendicular was divided into 20 sections and station 0 and 20 refer bow and stern, respectively.

The operability indices of the vessels for absolute vertical bow acceleration, slamming and deck wetness are shown in Figures 5, 6 and 7 respectively. The operability indices were computed as percentage for the same non-dimensional Froude numbers.

Regarding to absolute bow acceleration from Figure 5, larger vessels in length demonstrated higher operability. The highest operability was of vessel T62, which has the largest size in the vessel group under investigation. It is remarkable that this vessel has very high form coefficients and length to displacement ratio. On the other hand, bow acceleration of small hulls were very sensitive to the speed of

advance, so that for the Froude numbers higher than 0.20, their operability decreased gradually.

The effect of size was slightly appeared also in slamming and deck wetness operability indices. T62, T41 and ITU4K had higher slamming performance where ITU1B and ITU8B showed worse values. The vessel ITU8B was selected in order to insert a larger vessel from the ITU family which was derived from ITU1B with  $L_{pp}=28.7$  metres [4, 7]. As deck wetness operability index is concerned, Figure 7 shows that, apart from KTU27 and T40 which has worse deck wetness operability, all vessels performed fair deck wetness operability. The vessel T62 is also the best at this performance measure because of her stiff motion characteristics for the given seakeeping limits.

The most important difference in the motion characteristics of the traditional vessels relative to the designed ones is due to their wide and shallow sections which produce larger restoring and damping for vertical motions.

### 3.3. Power Estimation

There are several power estimation methods in the literature, however, these estimations gave some difficulties because of the exceptional hull form geometry of the traditional forms. In this application, the algorithm proposed by Darwin which reasonably predicts the effective power of the vessels was used [8]. The algorithm was checked with the tank test results of the designed vessels and the error level was found acceptable for the preliminary design purposes.

As seen from Figure 8, for the same Froude number, the effective power of the vessels were transformed to a dimensional ratio, *i.e.* effective power (kW) divided by the displacement (kN).

The vessels ITU1B and ITU4K gave the best powering characteristics in the whole Froude number range, while the other vessels needed much more power to maintain in the same

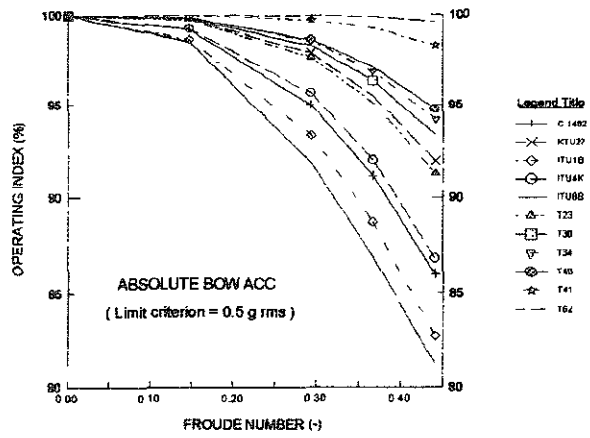


Fig. 5 Bow acceleration operability index

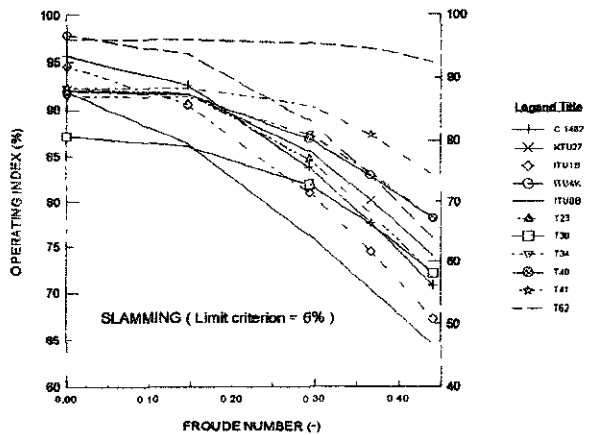


Fig. 6 Slamming operability index

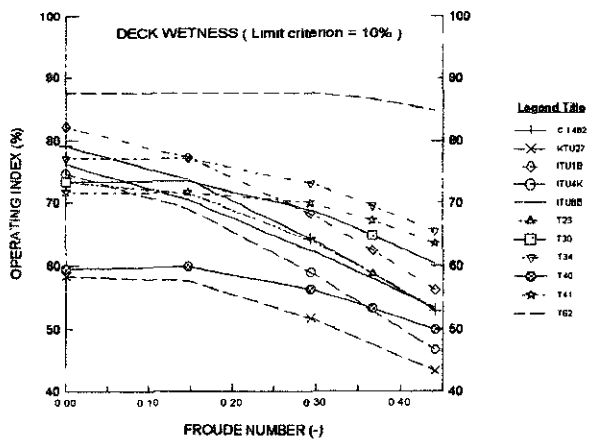


Fig. 7 Deck wetness operability index

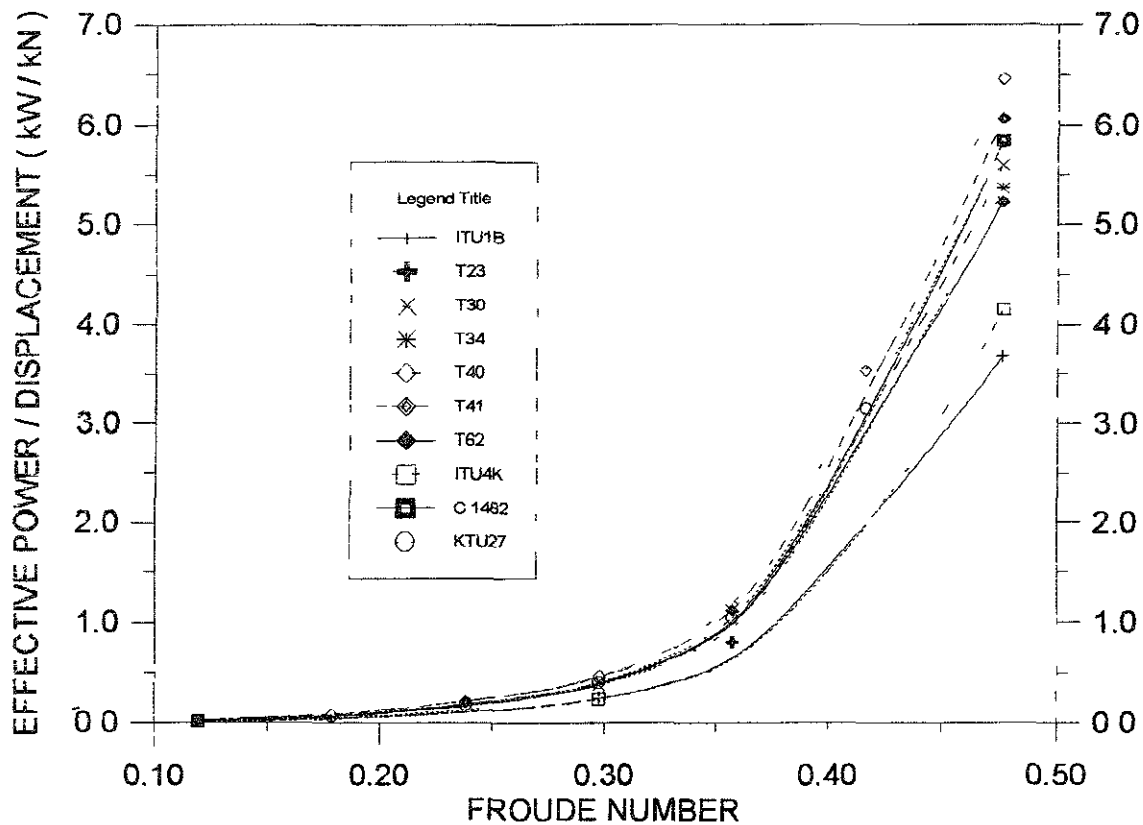


Fig 8 Relative powering characteristics of the vessels for the same Froude number

Froude number Certainly, almost all traditional vessels operated in Turkey are over powered because of the lack of engineering practice in the concern of hull form, resistance and propulsion design

The vessel C.1482 required much power since this vessel was designed for trawling operation and had fish hold. The traditional ones were without fish hold, in fact they use fish carrier to transfer the catch

#### 4. CONCLUSIONS

On the point of the results obtained from this study, the traditional Turkish fishing vessels need hull form modifications particularly in order to reach satisfying safety at sea. The special hull form of these vessels should be investigated further, namely, by considering dynamic stability in critical motions, capsize

mechanisms caused by rolling and motions in beam and following seas

#### ACKNOWLEDGEMENTS

The support given by The Turkish Fishing Foundation for Research, Development and Recovery is gratefully acknowledged.

#### REFERENCES

1. *Turkish Fisheries Statistics*, State Institute of Statistics, 1995
2. Ozmen, G, "Hull Form Optimisation of Fishing Vessels with Respect to Seakeeping", PhD Thesis, University of Glasgow, Scotland, 1995
3. Messina, G, "Definition of Fishing Vessel Type for Mediterranean Fishing" (in Italian), Research Report for the Ministry of Merchant Marine, Ancona, 1984

4. Kafali, K., "Investigation of Fishing Vessel Hull Forms" (in Turkish), Publication of Turkish Shipbuilding Research Institute, Technical University of Istanbul, No. 25, 1980, pp. 6-8.
5. Chilò, B. and Sartori, G., "Seakeeping Merit Rating Criteria Applied to Ship Design", *International Shipbuilding Progress*, Vol. 26, No. 304, 1979, pp. 299-313.
6. *Global Wave Statistics*, British Maritime Technology Limited, Feltham, 1986.
7. Alkan, A.D., "Hydrodynamic Analysis of ITU Series of Fishing Vessels", Report No. 79, University of Trieste, Trieste, 1992.
8. Messina, G. and Susat, L., *Propulsive Power of Marine Vehicles* (in Italian), Ancona, 1993.

# Dynamic Simulation of Capsizing for Fishing Vessels with Water on Deck

Z. J. (Jerry) Huang and C. C. Hsiung

Centre for Marine Vessel Design and Research  
Faculty of Engineering  
Dalhousie University  
P. O. Box 1000, Halifax, Nova Scotia, Canada, B3J 2X4

## Abstract

The time-domain analysis of non-linear ship motion in waves has been carried out and applied to study the capsizing phenomenon of fishing vessels with water flow on deck. The nonlinear effects from the Froude-Krylov forces, water flow on deck, viscous forces, and maneuvering forces on the ship motion are included. Motions with water on deck and the capsize of fishing vessels which have low length-to-beam ratio and shallow draft are computed. A numerical switch for turning on/off the wave force on deck as well as the deck flow force is designed so that when the deck submerges or emerges either one of these two force components is correctly applied on the deck.

## Introduction

Water on deck is a very important factor to affect the safe operation of fishing vessels. For small fishing vessels, the amount of water shipped on deck may be 20% to 30% of the vessel's intact displacement (Caglayan and Storch, 1982).

Dillingham (1981) initiated the numerical

computation of the nonlinear shallow water flow on a two-dimensional deck using the Random Choice method. Pantazopoulos (1988) extended this method to a three-dimensional deck space. Huang and Hsiung (1996a) introduced the Flux-Difference Splitting method to tackle the problem of shallow-water flow on deck and obtained stable results. Based on this approach, the effect of water flow on deck on the ship motions was investigated by Huang (1995).

Lee and Adee (1994) computed the motions of a cylinder in sway, roll and heave including the free water on deck. The equations of ship motion with the frequency-domain coefficients were solved in the time domain in regular beam seas. The hydrodynamic forces on the hull were obtained from a 2-D strip theory in the frequency domain. In their work, the forces due to water flow on deck were obtained by using the 2-D Random Choice method (Dillingham, 1981).

Lin and Yue (1994) extended the time-domain Green function method to large amplitude ship motion problem. The exact hull surface boundary condition was satisfied on the instantaneous wetted surface under the incident wave profile. Another approach was adopted by de Kat and Paulling (1989), in

which the Froude-Krylov force and restoring force were calculated based on the instantaneous wetted hull surface under the incident wave profile while linear radiated and diffracted wave forces were employed. They applied this method to analyze ship capsizing. An extensive capsizing model test was carried out by Grochowwalski (1989). The effect of water shipping on deck and deck in water were studied in his work.

In this study, the nonlinear effects are from: (i) the Froude-Krylov forces and hydrostatic restoring forces which are computed at the instantaneous hull position in the incident waves; (ii) forces due to water flow on deck; (iii) viscous damping, resistance, cross-flow drag; (iv) rudder and maneuvering forces; and (v) the nonlinear equation of ship motion.

Ship motions of six-degrees-of-freedom have been considered in the numerical computation of the deck flow. The forces and moments caused by the water flow on deck are computed by integrating the pressure over the deck area. A numerical switch for turning on/off the wave force on deck and the deck flow force is designed so that when the deck submerges or emerges either one of these two force components is correctly applied to the deck. An autopilot is adopted for coursekeeping of the vessel in waves. It has been found from the simulation that a bias rudder angle should be assigned. The rudder is activated about this bias angle which is determined by the wave heading and also the forward speed of the vessel. Without such a bias rudder angle, the vessel will advance with a mean drift angle in waves.

Numerical simulation shows that the water flow on deck is a very important factor affecting the stability safety of small fishing vessels in waves. The water flow on deck can cause a large heel angle and even deck submergence. These conditions together with a large wave acting on the vessel's broadside may lead to ship capsizing. This research work is being

applied to the development of stability safety criteria for shallow draft fishing vessels.

## The Nonlinear Ship Motion in the Time Domain

Three coordinate systems are employed for the ship motion analysis as shown in Fig. 1.

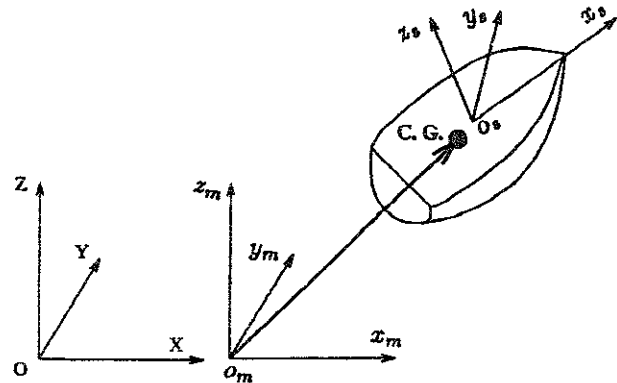


Fig. 1 Coordinate Systems for Ship Motions

$OXYZ$  is the space-fixed coordinate system with the  $OXY$ -plane on the calm water surface and the  $OZ$ -axis is positive upwards. The second coordinate system  $o_m x_m y_m z_m$  is a moving system which moves with the same steady forward speed as the ship in the  $OX$ -direction. The  $o_m x_m y_m$  plane always coincides with the  $OXY$ -plane, the  $o_m x_m$ -axis is in the same direction as the  $OX$ -axis, and the  $o_m z_m$ -axis is positive upwards. The third coordinate system  $o_s x_s y_s z_s$  is fixed on the ship with the  $o_s x_s y_s$ -plane coincident with the  $OXY$ -plane when the ship is at its static equilibrium position, and the  $o_s z_s$ -axis is positive upwards.

The oscillatory ship motions are described in the  $o_m x_m y_m z_m$  system. The ship motions are represented by  $(\xi_1, \xi_2, \xi_3, e_1, e_2, e_3)$ , in which,  $(\xi_1, \xi_2, \xi_3)$  are the displacements of the centre of gravity, and  $(e_1, e_2, e_3)$  are the Eulerian angles of the ship in space. The Eulerian angles are measurements of the ship's

angular motions about the axes which pass through the centre of gravity of the ship. The instantaneous translational velocities of ship motion in the directions of  $o_s x_s$ ,  $o_s y_s$  and  $o_s z_s$  are  $u_1$ ,  $u_2$  and  $u_3$ , respectively, and the angular velocities about axes parallel to  $o_s x_s$ ,  $o_s y_s$  and  $o_s z_s$  and passing through the centre of gravity are  $u_4$ ,  $u_5$  and  $u_6$ , respectively. The equations of ship motion are:

$$[m_{kj}] \begin{pmatrix} \dot{u}_1 \\ \dot{u}_2 \\ \dot{u}_3 \\ \dot{u}_4 \\ \dot{u}_5 \\ \dot{u}_6 \end{pmatrix} + \begin{pmatrix} m\vec{\Omega} \times \vec{u} \\ \vec{\Omega} \times ([I]\vec{\Omega}) \end{pmatrix} = \begin{pmatrix} F_1 \\ F_2 \\ F_3 \\ F_4 \\ F_5 \\ F_6 \end{pmatrix} \quad (1)$$

where  $\vec{u} = (u_1, u_2, u_3)$ ,  $\vec{\Omega} = (u_4, u_5, u_6)$ ,  $[m_{kj}]$  is the generalized mass matrix:

$$[m_{kj}] = \begin{bmatrix} m & 0 & 0 & 0 & 0 & 0 \\ 0 & m & 0 & 0 & 0 & 0 \\ 0 & 0 & m & 0 & 0 & 0 \\ 0 & 0 & 0 & I_{11} & 0 & -I_{13} \\ 0 & 0 & 0 & 0 & I_{22} & 0 \\ 0 & 0 & 0 & -I_{13} & 0 & I_{33} \end{bmatrix} \quad (2)$$

and  $[I]$  is the moment of inertia matrix

$$[I] = \begin{bmatrix} I_{11} & 0 & -I_{13} \\ 0 & I_{22} & 0 \\ -I_{13} & 0 & I_{33} \end{bmatrix} \quad (3)$$

in which  $m$  is the mass of the ship,  $I_{kk}$  ( $k = 1, 2, 3$ ) denotes the moments of inertia of the ship, and  $I_{kj}$  ( $k \neq j$ ) are the products of inertia of the ship. The total external forces on the ship are

$$F_k(t) = F_k^{Rs}(t) + F_k^{FK}(t) + F_k^{Dif}(t) + F_k^{Ra}(t) + F_k^\nu(t) + F_k^{Dk}(t) + F_k^H(t) + F_k^{Rud}(t) \quad (4)$$

for  $k = 1, 2, \dots, 6$

where  $F_k^{Rs}$  are the restoring forces;  $F_k^{FK}$  are nonlinear Froude-Krylov forces;  $F_k^{Dif}$  the diffracted wave forces;  $F_k^{Ra}$  the radiated wave forces;  $F_k^\nu$  the viscous forces including viscous

roll damping moment, resistance and cross-flow drag;  $F_k^{Dk}$  the nonlinear forces due to water flow on deck;  $F_k^H$  the hull maneuvering forces; and  $F_k^{Rud}$  the rudder force. Computation of these force components will be discussed in other sections of this paper, and the details can be found in Huang (1995).

The motion displacements  $(\xi_1, \xi_2, \xi_3)^T$  and  $(e_1, e_2, e_3)^T$  are solved from:

$$\begin{pmatrix} \dot{\xi}_1 \\ \dot{\xi}_2 \\ \dot{\xi}_3 \\ \dot{e}_1 \\ \dot{e}_2 \\ \dot{e}_3 \end{pmatrix} = \begin{bmatrix} [R] & 0 \\ 0 & [B] \end{bmatrix} \begin{pmatrix} u_1 \\ u_2 \\ u_3 \\ u_4 \\ u_5 \\ u_6 \end{pmatrix} \quad (5)$$

where matrices  $[B]$  and  $[R]$  are defined as follows:

$$[B] = \begin{bmatrix} 1 & s_1 t_2 & c_1 t_2 \\ 0 & c_1 & -s_1 \\ 0 & s_1/c_2 & c_1/c_2 \end{bmatrix} \quad (6)$$

$$[R] = \begin{pmatrix} c_2 c_3 & s_1 s_2 c_3 - c_1 s_3 & c_1 s_2 c_3 + s_1 s_2 \\ c_2 s_3 & s_1 s_2 s_3 + c_1 c_3 & s_1 s_2 s_3 - s_1 c_3 \\ -s_2 & s_1 c_2 & c_1 c_2 \end{pmatrix} \quad (7)$$

and  $c_i = \cos e_i$ ,  $s_i = \sin e_i$ , and  $t_i = \tan e_i$  for  $i = 1, 2, 3$ .

The ship motions in the time domain are solved simultaneously from twelve equations in both (1) and (5).

**Nonlinear Froude-Krylov Forces:** The nonlinear Froude-Krylov forces are computed based on the instantaneous position of the ship in the incident waves. At each time instant, the ship motions  $(\xi_1, \xi_2, \xi_3, e_1, e_2, e_3)$  are solved from equations (1) and (5). Making use of the Eulerian angles  $(e_1, e_2, e_3)$ , the coordinates of the nodes on the ship's hull is determined in the ship-fixed coordinate system. Then, the wave profile  $\zeta_0(X, Y, t)$  is computed at all the nodal points. The position of nodal points are compared with the incident wave

surface as shown in Fig. 2.

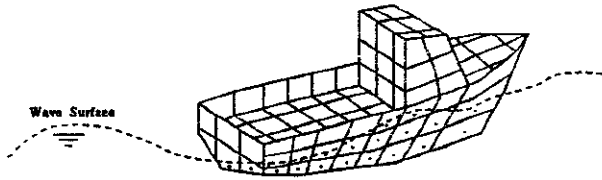


Fig. 2 The wetted hull surface below the wave surface

The pressure at the nodes under the incident wave surface is computed and the Froude-Krylov forces (both dynamic and static parts) are evaluated by integrating the pressure over the instantaneous wetted hull surface (Huang, 1995).

In this work, statistical wave data in the Nova Scotia Shore, Area 5 are selected to determine the incident wave (Eid et al, 1991). The statistical data are from wave buoy measurements covering a time interval from 1970 to 1988. Based on the wave data, the Ochi-Hubble six parameter wave spectrum was used in the computation.

**Forces due to the Radiated and Diffracted Waves:** Linear radiated and diffracted wave forces are used in the simulation. They are computed using the 3-D panel method. The detailed description was given by Huang and Hsiung (1996).

**Viscous Roll Damping:** Roll decay model test have been carried out for shallow draft fishing vessels (Huang, 1995). The roll damping coefficients have been determined from those tests. However, when test data are not available, semi-empirical formulae would be used. For large amplitude ship motions, the linear-plus-quadratic model is used:

$$F_4^v(\dot{e}_1) = (\alpha_1^v + \alpha_2^v|\dot{e}_1|)\dot{e}_1 \quad (8)$$

where  $\alpha_1^v$  and  $\alpha_2^v$  are the viscous roll damping coefficients. Empirical formulae such as those given by Schmitke (1978) are suggested. It should be pointed out that all existing empirical formulae are expressed in the frequency domain, i.e. they are functions of roll amplitude and frequency. In the time-domain simulation, we need to express the roll damping as a function of the instantaneous roll velocity.

A method converting the frequency-domain roll damping into the time-domain is given in this study. Fig. 3 shows the computed roll damping coefficients for a ship at  $F_n = 0.2$  with various roll amplitudes and frequencies. Based on the roll amplitude and frequency, we can work out the roll velocity. From this family of curves, it can be found that at the same roll velocity, the roll damping coefficients are the same regardless of the combination of the amplitude and frequency of roll. This indicates that the damping coefficients depend on roll velocity only. Therefore, we fit the damping coefficient by a quadratic polynomial, and the coefficients of the polynomial are the coefficients of the roll damping which can be used in the time-domain motion simulation. The fitted damping curve is shown in Fig. 4. It can be seen that the fitted curve is very close to the one predicted by Schmitke's formula.

#### Resistance and Cross-Flow Drag:

Resistance is important to surge, sway and yaw in the time-domain motion simulation. For Nova Scotia inshore fishing vessels, resistance tests have been carried out (Lacy, 1995). Fig. 5 shows the resistance coefficient curves for the nine tested ship models covering a broad range of such type of vessels.

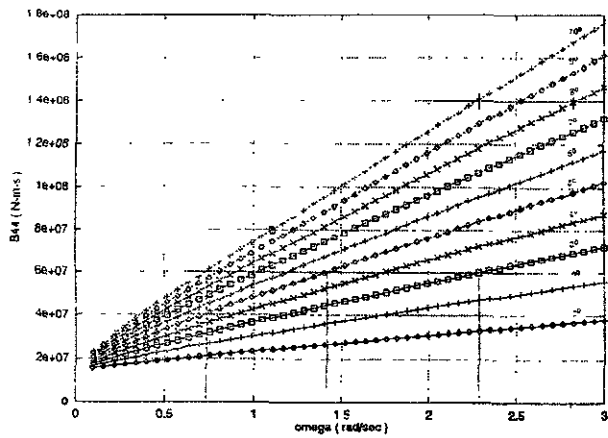


Fig. 3 Roll damping computed in the frequency domain

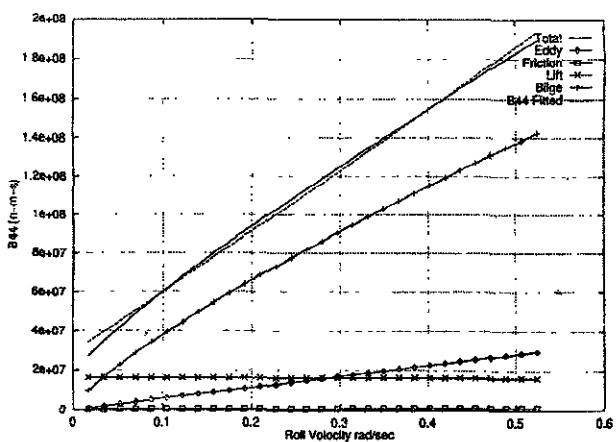


Fig. 4 The fitted roll damping coefficients

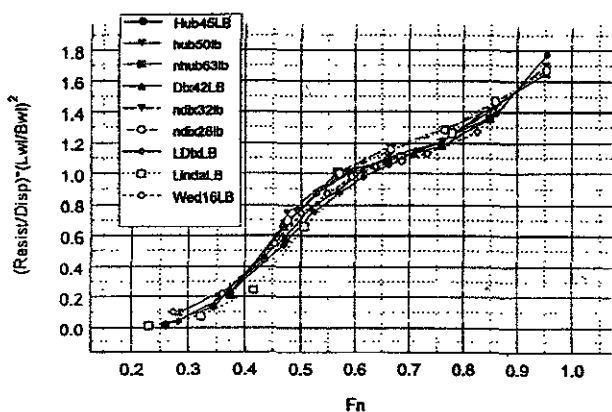


Fig. 5 Resistance of shallow-draft fishing vessels

Four fishing vessel models were also towed transversely in the tank in order to measure the cross-flow drag (Huang, 1995). The test results as shown in Fig. 6 indicate that the four fishing boats have similar transverse drag.

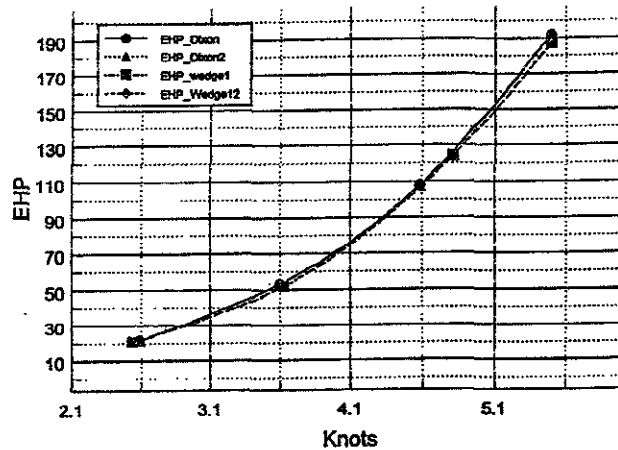


Fig. 6 Cross-flow drag for shallow-draft fishing vessels

Fig. 7 shows the the simulated sway motion with and without the cross-flow drag.

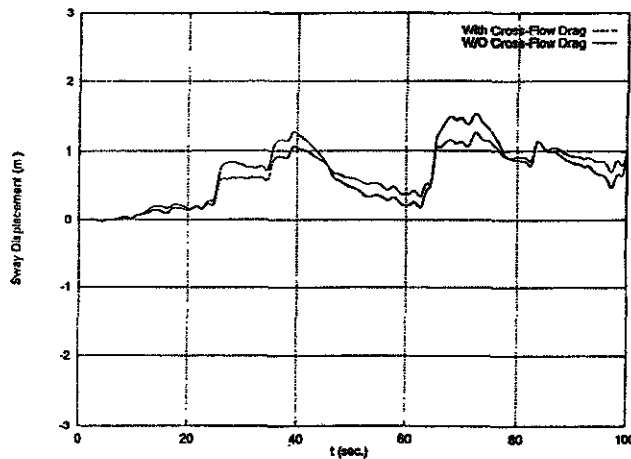


Fig. 7 Sway motion with and without cross-flow drag,  $\beta = 90$  deg,  $H_s = 1.5$  m,  $U = 6.37$  kts

**Hull Maneuvering Forces, Rudder Forces and Autopilot:** Hull maneuvering forces and rudder forces are included in the time-domain ship motion simulation. They

are computed using the formulae given by Kijima et al.(1990). In this work, we are particularly interested in an autopilot that can keep the course of the ship during simulation. Comparisons between the motion simulations with and without the hull maneuvering and rudder forces have been given by Huang (1995).

The following formula is used for the autopilot:

$$\delta(t) = \begin{cases} \alpha_0^r - \alpha_1^r e_6(t) - \alpha_2^r \dot{e}_6, & \text{if } e_6 > \delta_0 \\ 0, & \text{if } e_6 \leq \delta_0 \end{cases} \quad (9)$$

where  $\alpha_0^r$  is a bias rudder angle about which the rudder responds to the yaw motion based on the autopilot,  $\alpha_1^r$  is the yaw gain,  $\alpha_2^r$  is the yaw rate gain, and  $\delta_0$  is the threshold value of yaw beyond which the rudder is activated. Fig. 8 shows the yaw motion of a fishing vessel with the bias rudder angle  $\alpha_0^r = 0$  deg and  $\alpha_0^0 = -6$  deg. It can be seen that with the bias rudder angle, the vessel can maintain its heading in waves.

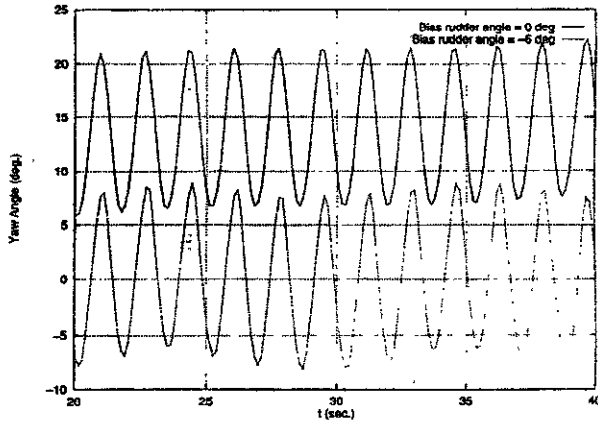


Fig. 8 Yaw motion simulation with  $\alpha_0^r = 0$  deg and  $\alpha_0^r = -6$  deg

## Water Flow on Deck

The ship motions of six degrees of freedom have been considered in the numerical computation of the deck flow. The coordinate

system  $oxyz$  for water flow on the three-dimensional deck is shown in Fig. 9. It is fixed on the deck space with  $oxy$  attached on the deck bottom plane. The  $oz$ -axis is positive upward and the origin  $o$  is at the centre of the deck.

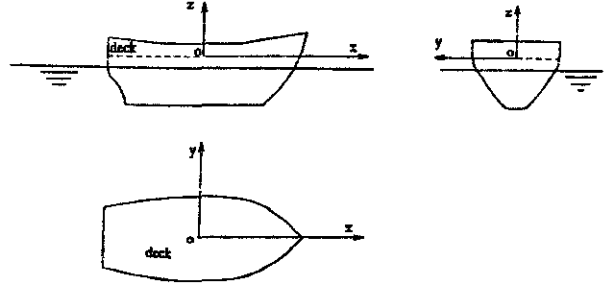


Fig. 9 Coordinate system for water flow on deck

The continuity equation and Euler's equations of motion can be written as follows:

$$\frac{\partial u}{\partial x} + \frac{\partial v}{\partial y} + \frac{\partial w}{\partial z} = 0 \quad (10)$$

$$\begin{aligned} \frac{\partial \vec{u}}{\partial t} + (\vec{u} \cdot \nabla) \vec{u} = & \vec{f} - \frac{1}{\rho} \nabla p - \vec{u} - \vec{\Omega} \times \vec{r}_d \\ & - 2\vec{\Omega} \times \vec{u} - (\vec{\Omega} \cdot \vec{r}_d) \vec{\Omega} \\ & + (\vec{\Omega} \cdot \vec{\Omega}) \vec{r}_d \end{aligned} \quad (11)$$

where  $\vec{u} = (u, v, w)^T$ ,  $u$ ,  $v$  and  $w$  are velocity components of the water particles in  $x$ -,  $y$ - and  $z$ - directions, respectively;  $p$  is the pressure; and  $\vec{f}$  is the body force.  $\vec{r}_d = (x - x_g, y - y_g, z - z_g)^T$ , and  $(x_g, y_g, z_g)$  is the coordinate of the centre of gravity of the ship in the  $oxyz$ -system.

Once the water depth and the water particle velocity are computed, the pressure on deck can be obtained as follows:

$$\begin{aligned} p(x, y, t) = & \rho \{ \zeta [g \cos(e_1) \cos(e_2) + \dot{u}_3 \\ & + 2(u_4 v - u_5 u) + (u_4 u_6 - \dot{u}_5)(x - x_g) \\ & + (u_5 u_6 - \dot{u}_4)(y - y_g) + (u_4^2 + u_5^2) z_g] \\ & - \frac{1}{2} [(\zeta - z_g)^2 - z_g^2] (u_4^2 + u_5^2) \end{aligned} \quad (12)$$

Then forces and moments caused by water flow on deck are calculated by integrating the pressure over the deck area, i.e.,

$$F_i^{Dk}(t) = - \int_{S_{Dk}} n_i p(x, y, t) dS \quad (13)$$

where  $S_{Dk}$  is the wetted surface of the deck and  $n_i$  is the outward unit normal of  $S_{Dk}$ .

The numerical model based on the Flux-Difference Splitting method has been extensively validated against published test data of water sloshing in the deck well (Huang, 1995).

A validation example of water sloshing in a swaying tank is given in Fig. 10. The tank is 0.4 m wide with a mean water depth of 2.0 cm. The sway amplitude is 2 cm and the frequency is 3.471 rad/sec. The time history of wave motion agrees well with the test data from Iwamoto's (1991) work.

A model test for water sloshing on deck was conducted by the authors. The purpose of the test was to measure the wave motion in the tank and the sloshing moment. Time histories of the computed and measured wave motions are shown in Fig. 11 where the roll amplitude is 3 deg, the frequency is 3.769 rad/sec, and the mean water depth is 3.2 cm. The time histories of sloshing moment are shown in Fig. 12 which correspond to  $\omega = 2.2$  rad/sec and  $a_4 = 10$  deg. The mean water depth is 2.5 cm. The figures show that for the time histories of wave motion and sloshing moment. A very good agreement has been achieved between the computed results and the test results. Fig. 13 shows the amplitude of the sloshing moment in a tank of 1 m wide and with water depth  $h_0 = 6$  cm. The model test data are from Van den Bosch and Vugts (1966).

The wave motion under the excitation of six-degrees of freedom of ship motions are more complicated than those under roll excitation only. An example of the wave motion is shown in Figs. 14(a) and 14(b) for a deck well of 0.35 m by 0.35 m with the water depth

3.5 cm. The rotation pivot is assumed to be located at the centre of the deck. The frequency of excitation is 3.94 rad/sec. A three-dimensional rotating bore can be clearly observed. The corresponding sloshing moments in roll and pitch are shown in Fig. 15.

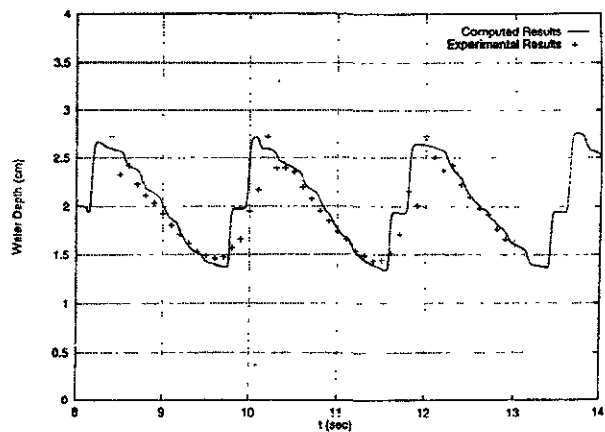


Fig. 10 Time history of wave motion for  $\omega = 3.471$  rad/sec,  $a_2 = 0.5$  cm

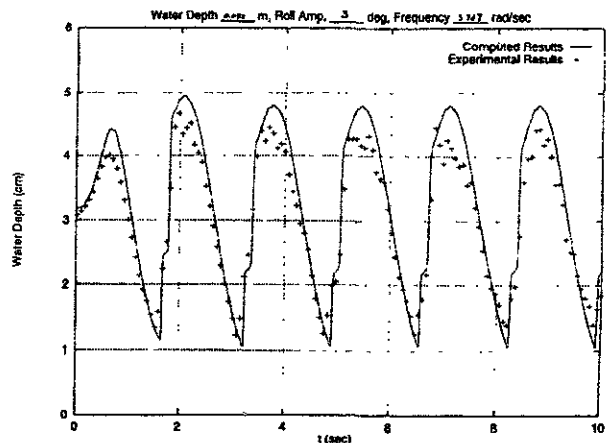


Fig. 11 Time history of wave motion for  $\omega = 3.769$  rad/sec,  $\phi = 3$  deg

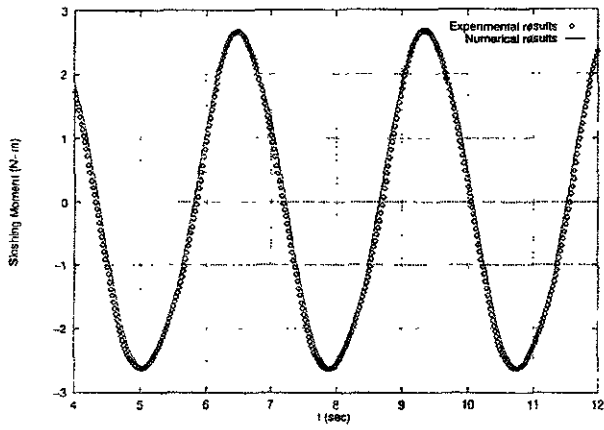


Fig. 12 Sloshing moment at  $\omega = 2.2$  rad/sec,  $\phi = 10$  deg

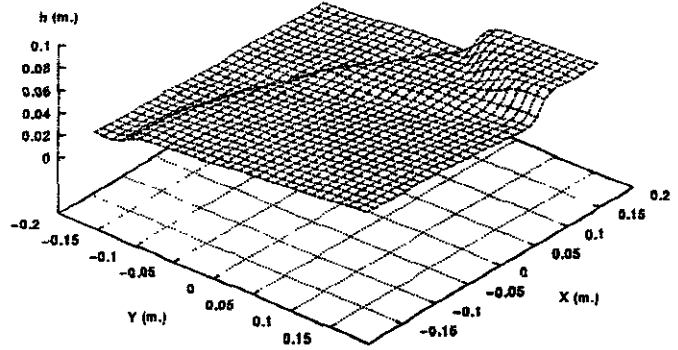


Fig. 14(b)  $t = 7.6$  sec

Fig. 14, Wave profile due to six-DOF motions

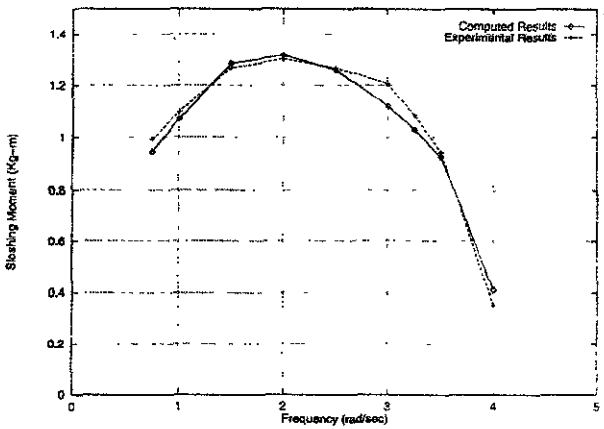


Fig. 13 Sloshing moment amplitude,  $h_0 = 6$  cm,  $\phi = 5.73$  deg

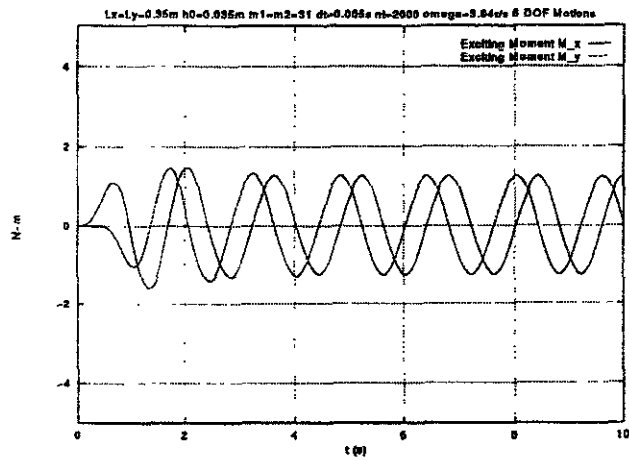


Fig. 15, Sloshing moments in roll and pitch, corresponding to Fig. 14

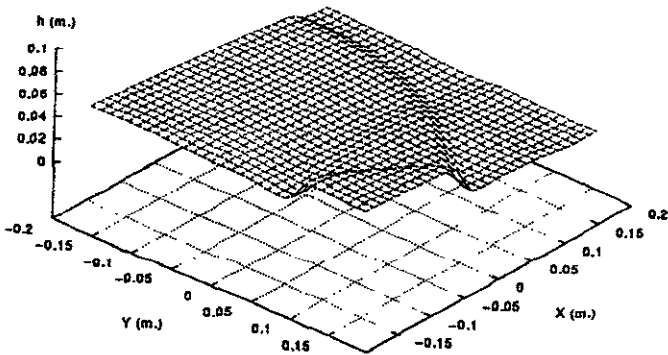


Fig. 14(a)  $t = 7.2$  sec

## Simulation of Motions

A model test has been conducted for a shallow draft fishing vessel. Details of the validation results have been reported (Huang and Hsiung, 1996a, Hsiung and Huang, 1996). An example of the validation is given in Fig. 16 and Fig. 17 for the wave spectra and the roll

response spectra, respectively.

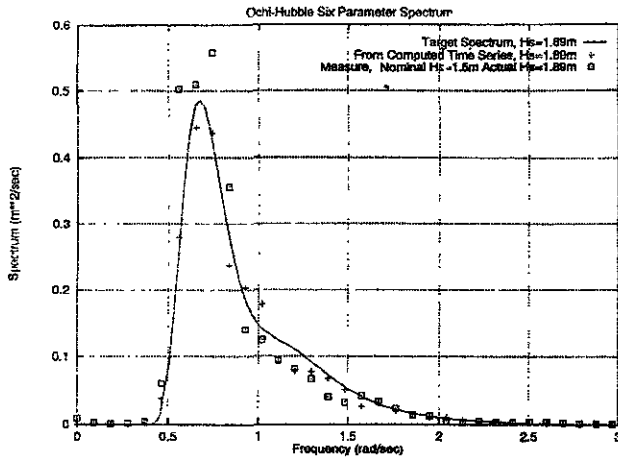


Fig. 16 Measured and computed wave spectra

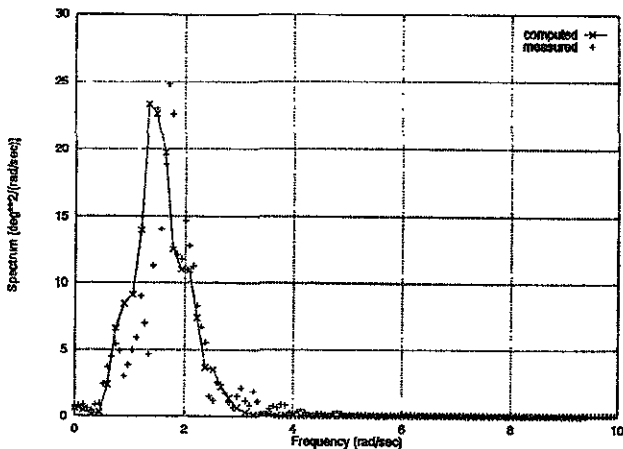


Fig. 17 Computed and measured roll spectra,  $\beta = 90^\circ$ ,  $H_s = 1.5$  m,  $U = 6.33$  kts

Water trapped on the deck can result in an increase or a reduction in roll depending on the sea conditions. A shallow draft fishing vessel, Wedge 1, is used in the simulation with water on deck. The lines of this vessel are shown in Fig. 18. This vessel has a very shallow draft with a large skeg and flat bottom near the stern, as well as a low length to beam ratio. It is very stiff in waves, the typical full-scale natural period is only about 3 sec.

The motion simulation starts with the vessel in an upright position. When water on

deck is considered, the amount of water is gradually added up to the desired amount, e.g. 4 tons, within 50 time steps. Even though the simulation was carried out for six-degrees-of-freedom ship motion, we mainly concentrate on the roll motion.

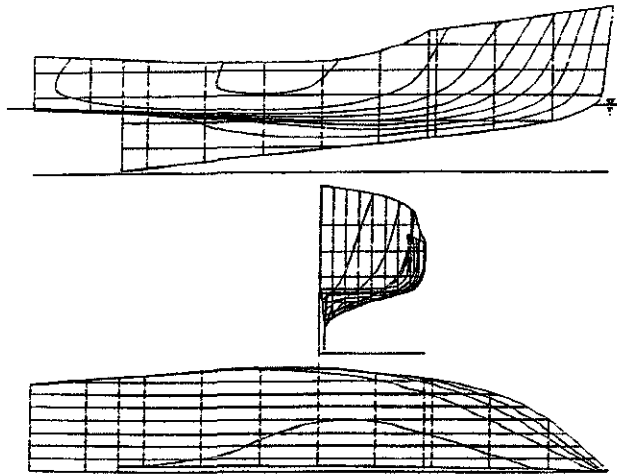


Fig. 18 Lines of fishing vessel Wedge 1

Motion simulation at zero speed, with beam seas, and  $H_s = 1.5$  m has been carried out. The roll motions with and without 4 tons of water trapped on the open deck are shown in Fig. 19. This amount of water corresponds to about a mean depth of four inches across the deck. It can be seen that the roll motion with water on deck is smaller than that without water on deck. In this case, water on deck acts as a stabilizer. When the wave height is increased to  $H_s = 2.5$  m (Fig. 20), the roll motion with water on deck is greater than that without water on deck. It is quite clear from this analysis that the effect of water on deck on the boat's motions depends on sea conditions prevailing at the time. The effect of water on deck on roll motion in regular beam seas is shown in Fig. 21. Without water on deck, the roll motion has a mean bias angle due to the nonlinear effect of hydrodynamic forces and the nonlinear terms in the equation of ship motion. With water on deck, the roll angle is magnified and the mean position

of roll is varying with time.

on deck, we switch off the water flow on deck force and the wave force is used.

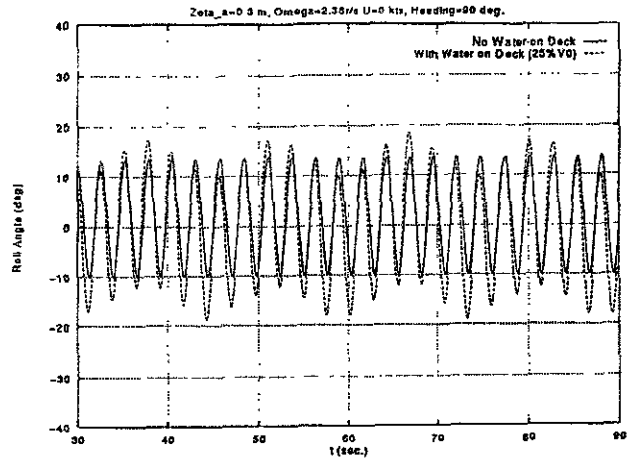
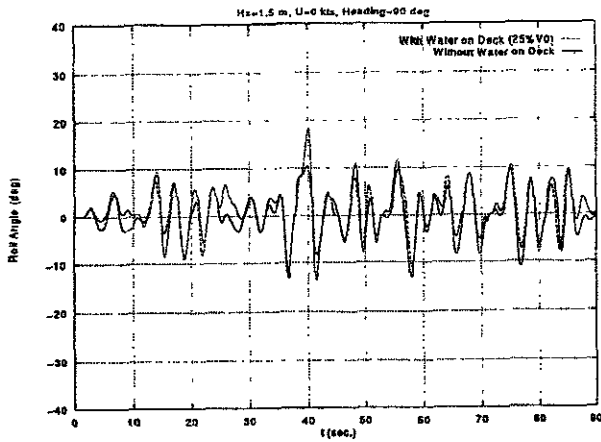


Fig. 19 Roll motion in beam sea,  $H_s = 1.5$  m

Fig. 21 Effect of water on deck on roll motion

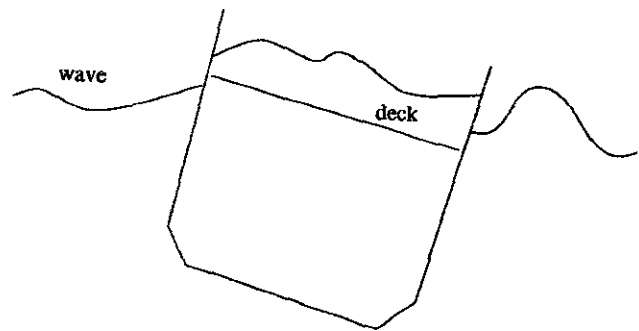
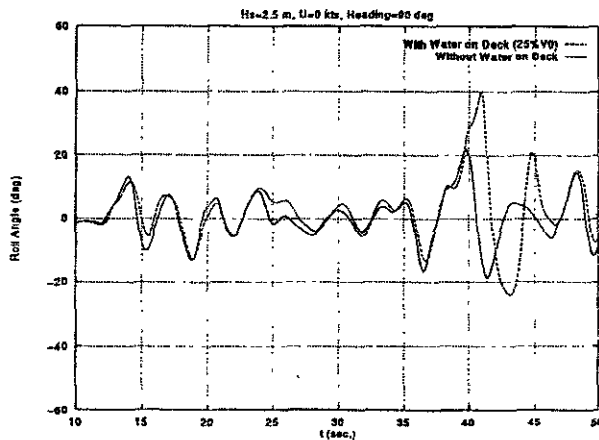


Fig. 22 Trapped water sloshing on deck

Fig. 20 Roll motion in beam sea,  $H_s = 2.5$  m

When the vessel's deck is deeply submerged in waves, the deck is subjected to the wave force instead of the water sloshing on the deck. These two scenarios are shown in Fig. 22 and Fig. 23, respectively. A switch has to be designed properly in the simulation to select the correct hydrodynamic force. In the computation, we assume that if the heeling angle is exceeding a threshold angle  $\phi_{cr}$  or the volume between the deck and the wave surface is greater than that of the trapped water

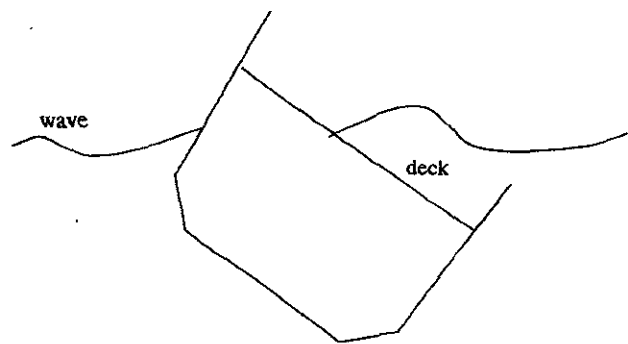


Fig. 23 Deck deeply immersed

An example of capsizing is shown in Fig. 24 for the fishing vessel, the significant wave height is  $H_s = 2.5$  m, heading  $\beta = 90$  degree and the vessel is at zero forward speed. The weight of water on deck is approximately 25% of the intact displacement of the boat. Details of the boat capsize scenario are given in Figs. 25(a) to 25(e). This series of pictures shows the heave, roll and the relative position of the boat to wave profile at various time instants. By studying Figs. 25(a) to 25(e), the capsize event can be clearly analyzed. Fig. 25(a) starts to show that the deck is submerged at the wave trough. Then, a wave crest travelling from right to left meets the boat and forces it to roll to the lee side as shown in Fig. 25(b). The boat then rides on the wave crest, and tends to roll back to the weather side as given in Fig. 25(c). However, a large part of the deck is now deeply submerged and the wave crest pushes against the weather side hull of the boat (Fig. 25(d)). At this moment, the righting moment of the boat is reduced as the boat is on the wave crest, and eventually the boat capsizes (Fig. 25(e)).

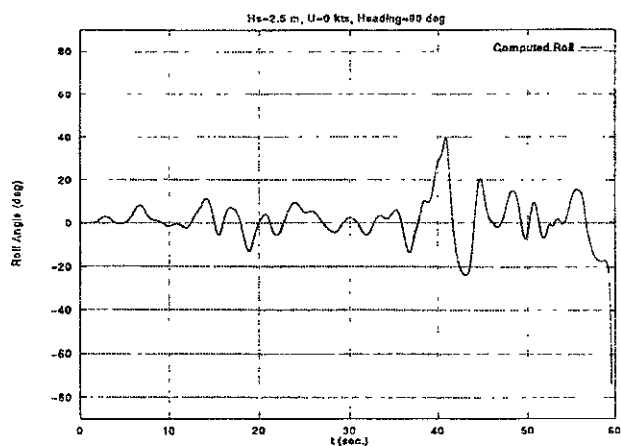


Fig. 24 Time history of a capsize event,  $H_s = 2.5$  m,  $\beta = 90^\circ$ ,  $U = 0$  kts with 4 tons of water on deck

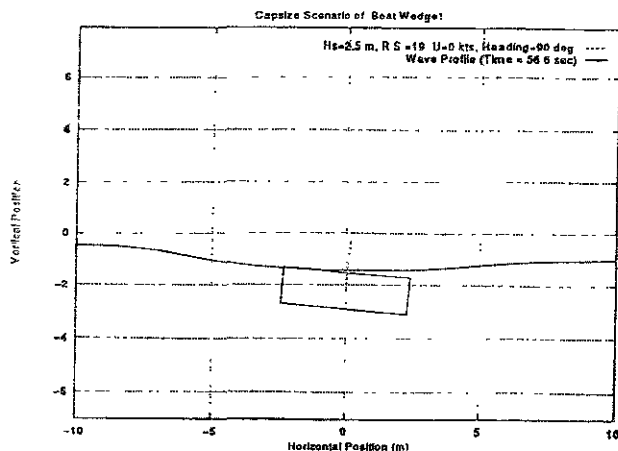


Fig. 25(a)

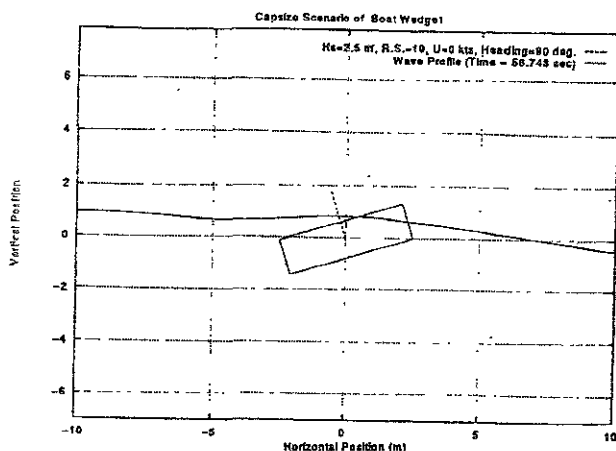


Fig. 25(b)

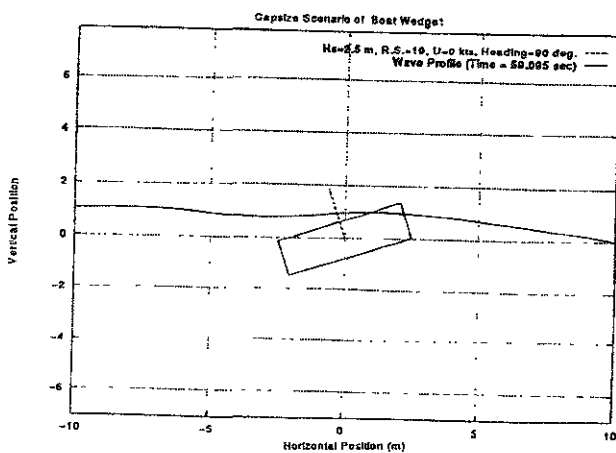


Fig. 25(c)

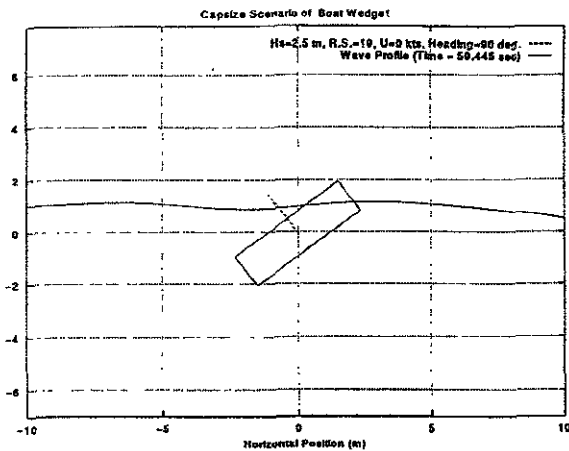


Fig. 25(d)

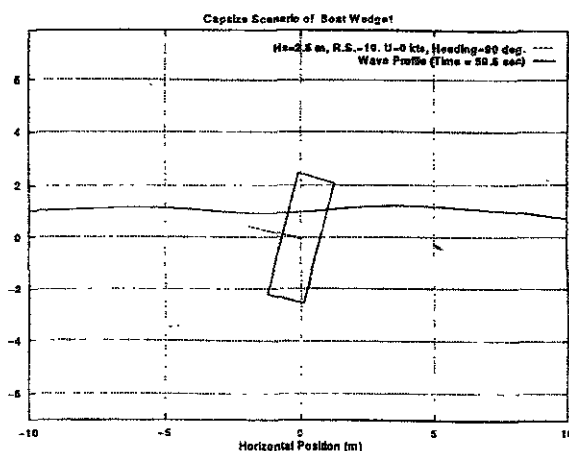


Fig. 25(e)

Fig. 25 Capsizing Scenario,  $H_s = 2.5$  m,  $\beta = 90^\circ$ ,  $U = 0$  kts with 4 tons of water on deck.

## Conclusions

A method for simulating the nonlinear ship motion has been developed for shallow-draft fishing vessels with water shipped on deck. Validation work has been completed for ship motion without water on deck, as well as water flow on deck and its induced heeling moment on the vessel. All of these are used to predict the capsizing events of vessels in waves. In this work, the simulation is carried out by

using a constant mass of water on deck, and the effect of water on deck on the ship motion is investigated. It has been found that the effect of water on deck on the roll motion depends not only on the amount of water but also on the wave condition, while the traditional investigation was limited to the linear theory in which the roll motion with water on deck was independent on the incoming waves amplitude. A numerical switch has been considered in the simulation to select the correct forces acting on deck. This is very important to the capsizing simulation. The tuning of the switch is being refined by numerical and experimental analyses.

## Acknowledgements

The authors are grateful for the research supports from Transport Canada, and Natural Sciences and Engineering Research Council of Canada. They also appreciate the valuable discussions on the effect of the deck in water with Dr. Stefan Grochowalski of the Institute for Marine Dynamics, National Research Council of Canada.

## Reference

- Caglayan, I. and Storch, R.L., "Stability of Fishing Vessels with Water on Deck. A Review", *Journal of Ship Research*, Vol. 26, No. 2, June 1982.
- de Kat, Jan O. and Paulling, J.R., "The Simulation of Ship Motions and Capsizing in Severe Seas," *Transactions, SNAME*, Vol. 97, 1989.
- Dillingham, J., "Motion Studies of a Vessel with Water on Deck", *Marine Technology*, Vol. 18, No. 1, 1981.
- Eid, B, Morton, C., Calnan, C. and Cardone, V., "Wind and Wave Climate Atlas", Transport Canada Publication No. TP 10820 E,

- 1991.
- Grochowalski, S., "Investigation into the Physics of Ship Capsizing by combined Captive and Free Running Tests", Transactions, SNAME, 1989.
- Hsiung, C. C. and Huang, Z. J., "Validation of Numerical Method to Compute Motions of Shallow-Draft Vessels in Waves", the 21st International Towing Tank Conference, Bergen and Trondheim, Norway, September 1996.
- Huang, Z. J. and Hsiung, C. C., "Nonlinear Shallow-Water Flow on Deck Coupled with Ship Motion", Proceedings of the 21st Symposium of Naval Hydrodynamics, Trondheim, Norway, 1996a.
- Huang, Z. J. and Hsiung, C. C., "Nonlinear Shallow-Water Flow on Deck", Journal of Ship research, Vol.40, December 1996b.
- Huang, Z. J., Nonlinear Shallow Water Flow on Deck and Its Effect on Ship Motion, Ph. D. Thesis, Technical University of Nova Scotia, Halifax, Nova Scotia, 1995.
- Iwamoto, S., Numerical Analysis of Shallow Water Dynamics on Deck. Journal of Ship Research, 86, 111-129, 1994
- Kijima, K., Katsuno, T., Nikiri, Y. and Furukawa, Y., "On the Maneuvering Performance of a Ship with the Parameter of Loading Condition", Journal of the Society of Naval Architects of Japan, Vol. 168, 1991.
- Lacy, G., "Comparison of the Resistance Characteristics of Five Inshore Fishing Vessels", The Third Canadian Marine Hydrodynamics and Structure Conference, Halifax, Nova Scotia, Canada, 1995.
- Lee, K. and Adey, B., "Numerical Analysis of a Vessel's Dynamic Responses with Water Trapped on Deck", Proceedings of the Fifth International Conference on Stability of Ships and Ocean Vehicles, Melbourne, Florida, 1994.
- Lin, W. M. and Yue, D. K., "Large Amplitude Motions and Wave Loads for Ship Design", Proceedings of the Twentieth Symposium on Naval Hydrodynamics, Santa Barbara, California, 1994.
- Pantazopoulos, M. S., "Three-Dimensional Sloshing of Water on Deck", Marine Technology, Vol. 25, 1988.
- Schmitke, R. T., "Ship Sway, Roll and Yaw Motion in Oblique Seas", Transactions SNAME, Vol. 86, 1978.
- Van den Bosch, J. J. and Vugts, J. H., "On Roll Damping by Free-Surface Tanks", Transactions, RINA, Vol. 108, 1966.

# ANALYSIS OF A GENERAL CARGO SHIP LOST IN FRONT OF THE CATALONIA COAST

Prof. Ricard Marí Sagarra, Ph. D.

Prof. Juan Olivella Puig, Ph. D.

Department of Nautical Science and Engineering  
UNIVERSITAT POLITÈCNICA DE CATALUNYA  
Barcelona, SPAIN

## ABSTRACT

A general cargo ship sank in front of the Tarragona coast, just a short time after leaving the port of Vilanova, being the meteorological conditions excellent.

The general information of the ship was used to verify several parameters related with her last trip, taking into account, moreover, some data from the port authorities, service companies involved in the load ship activity, and also from the master and crew of the ship. This checking showed the need to inquire into the load distribution and the ballast tanks. At this stage, the study of the flotability and the stability of the ship was made in order to determine the conditions in the actual moment of losing her and how it happened.

The analysis of the studies carried out allowed to deduce that the deficiency of stability could be the main circumstance of the ship's loss. The evidences given by the crew explaining the sinking of the ship are in good agreement with the hypothesis of the ship's instability.

## 1. SUMMARY OF THE EVENTS

A general cargo ship of 2.085 metric tons of dead weight, with two holds and built in 1984, sank in front of the Tarragona coast two hours after leaving the port of Vilanova i la Geltrú

with destination to Oran (Algeria).

The last cargo ports were Barcelona and Vilanova. The ship arrived to the Barcelona port with ballast (the tanks with ballast are unknown) and with 31 containers of 20 feet in the holds, which were discharged, and loading 289,5 metric tons of chemical products stowed on 350 pallets and distributed into the two holds. In the Vilanova port she shipped 1.514 metric tons of calcic carbonate, also in pallets, distributed into the holds and on deck, with a high of two pallets situated on each hatch.

During the sailing from Vilanova to her fatal destination, (Fig. 1), the weather was fine, fact that has been corroborated by the Meteorological Service Information as well as by the statement of the fourteen crew members, who remained about twenty seven hours adrift in a lifeboat until they were finally rescued, presenting symptoms of cold, dehydration and tiredness, but fortunately without any serious injuries.

## 2. SHIP GENERAL INFORMATION

To know better the lost ship, tables 1 to 3 contain the more important characteristics and the data of her load lines with the corresponding displacements, and the tank capacities. Figure 2 also shows the diametral and horizontal planes with the location of the holds and the tanks of the ship.

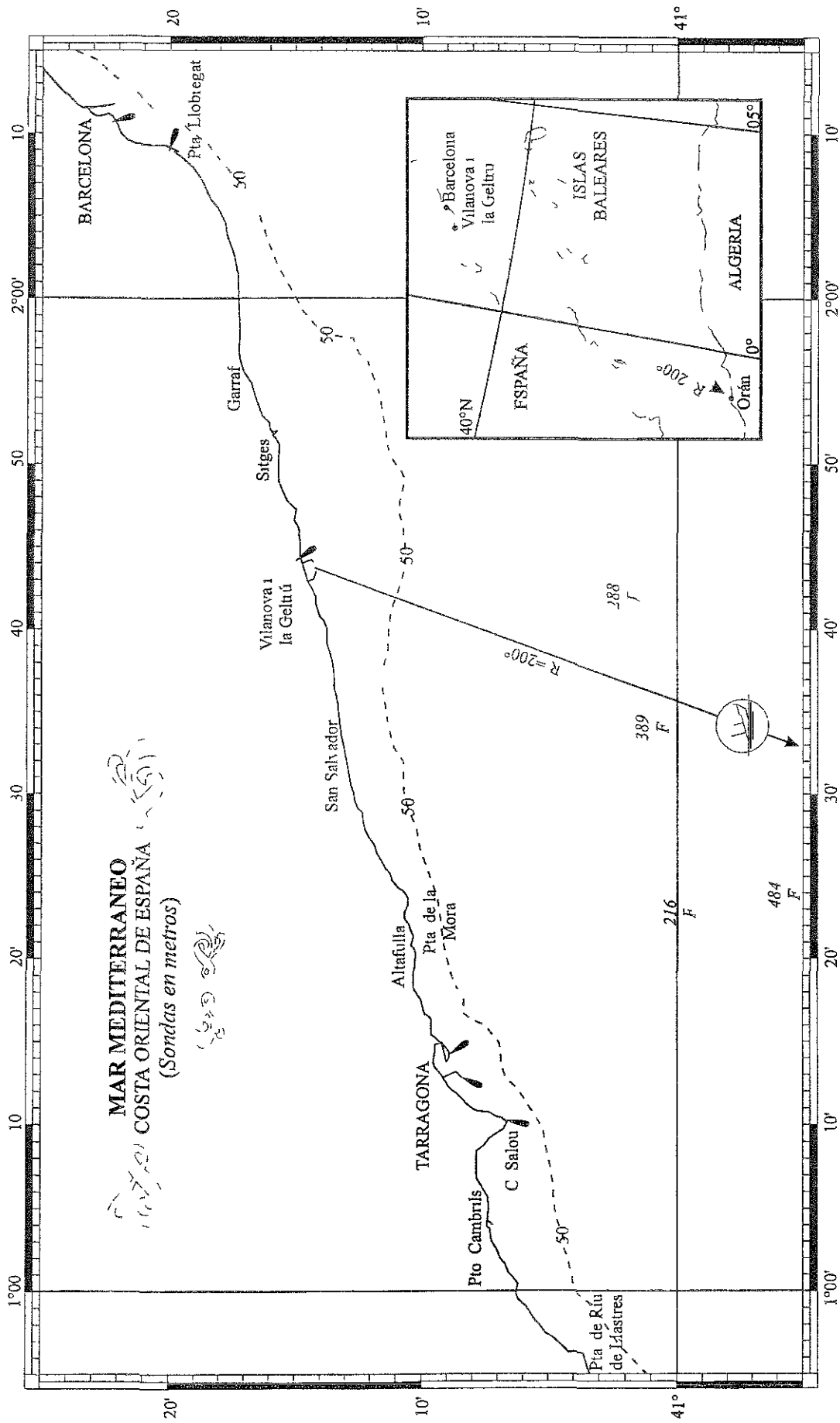


Figure 1. Ship course

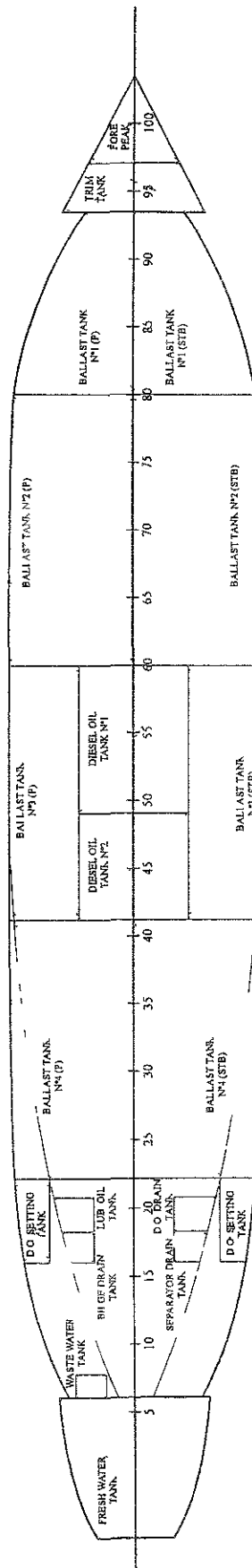
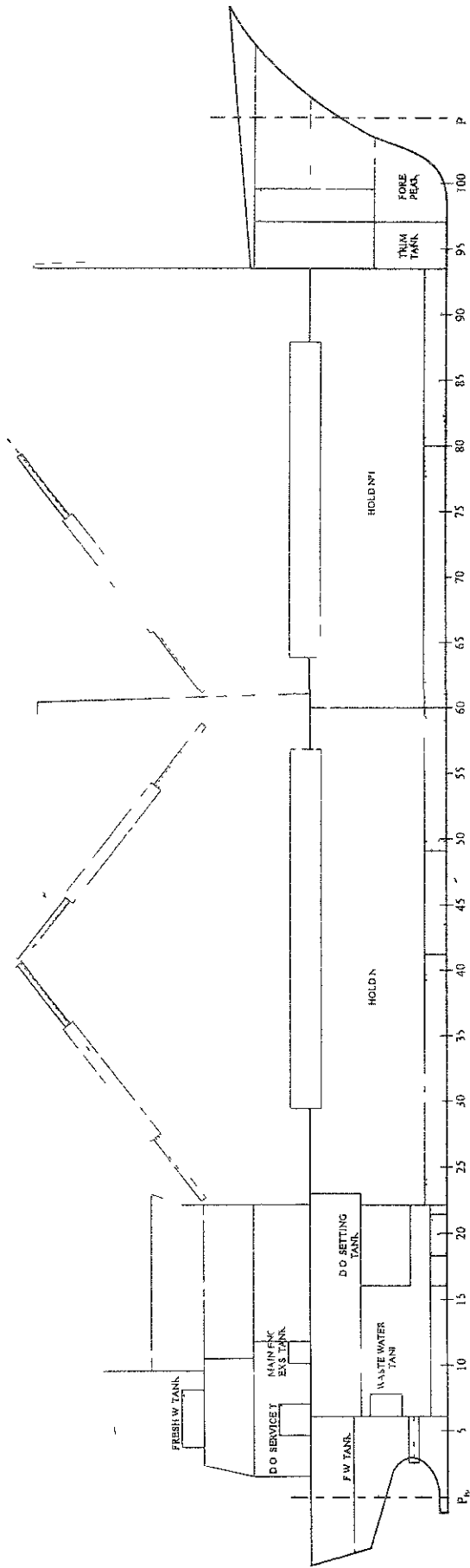


Figure 2. General ship distribution

Table 1. Ship characteristics

Length between perp.	63.00 m
Moulded breadth	10.80 m
Depth	6.10 m
Draught	5.18 m
Displacement	2785.00 Tm
Dead weight	2085.00 Tm
Gross tonnage	1171.00 Tm

Table 2. Freeboard draught and displacement

Freeboard	Draft mm	Displacement Metric Tons
Tropical FW	5.397	2.860
Summer FW	5.289	2.785
Tropical FW	5.287	2.860
Summer FW	5.179	2.785
Winter SW	5.071	2.706

Table 3. Tank capacities

Description	Volume m <sup>3</sup>	Weight Metric Tons
Ballast	412,670	422,987
FW tanks	26,029	26,029
DO tanks	91,453	76,820
Lub oil	4,910	4,419

### 3. CARGO CONDITION AT THE DEPARTURE FROM THE VILANOVA PORT

The information about the cargo shipped in the ports of Barcelona and Vilanova was got and

verified from the partial weights of the trailers recorded in the reception dock, the shipping controls, the operation reports and the cargo plans from the stevedoring companies, the freight/cargo manifest presented to the Customs Administration, and the information given by the master and officers of the ship.

Part of the load, a total of 340,6 metric tons, was stowed in the deck upon the hatches of the two holds, having the deck load a high of 2,20 m. Table 4 indicates the cargo distribution and figure 3 shows the general cargo plan. The ship also had on board 25 metric tons of fresh water in the afterpeak tank and 24 metric tons of diesel oil. According to a document signed by the master of the ship the departure draught were 5,45 m aft and 5,25 m forward. The ship was upright.

Table 4. Cargo distribution

Location	Total Metric Tons
Hold n° 1	655,3
Deck load	114,8
Hold n° 2	807,6
Deck load	225,8
TOTAL	1.803,5

### 4. ANALYSIS OF THE CARGO CONDITIONS

A first analysis of the ship cargo condition was carried out with the help of the hydrostatic curves, and it allowed us to get the following evidences:

- The ship displacement was 2.574,4 metric tons computed according to the cargo stowed in the holds and on the deck, plus the values of fresh water and diesel oil. To this displacement corresponds a mean draught of 4,86 m, a quantity below the mean draught of 5,35 m to

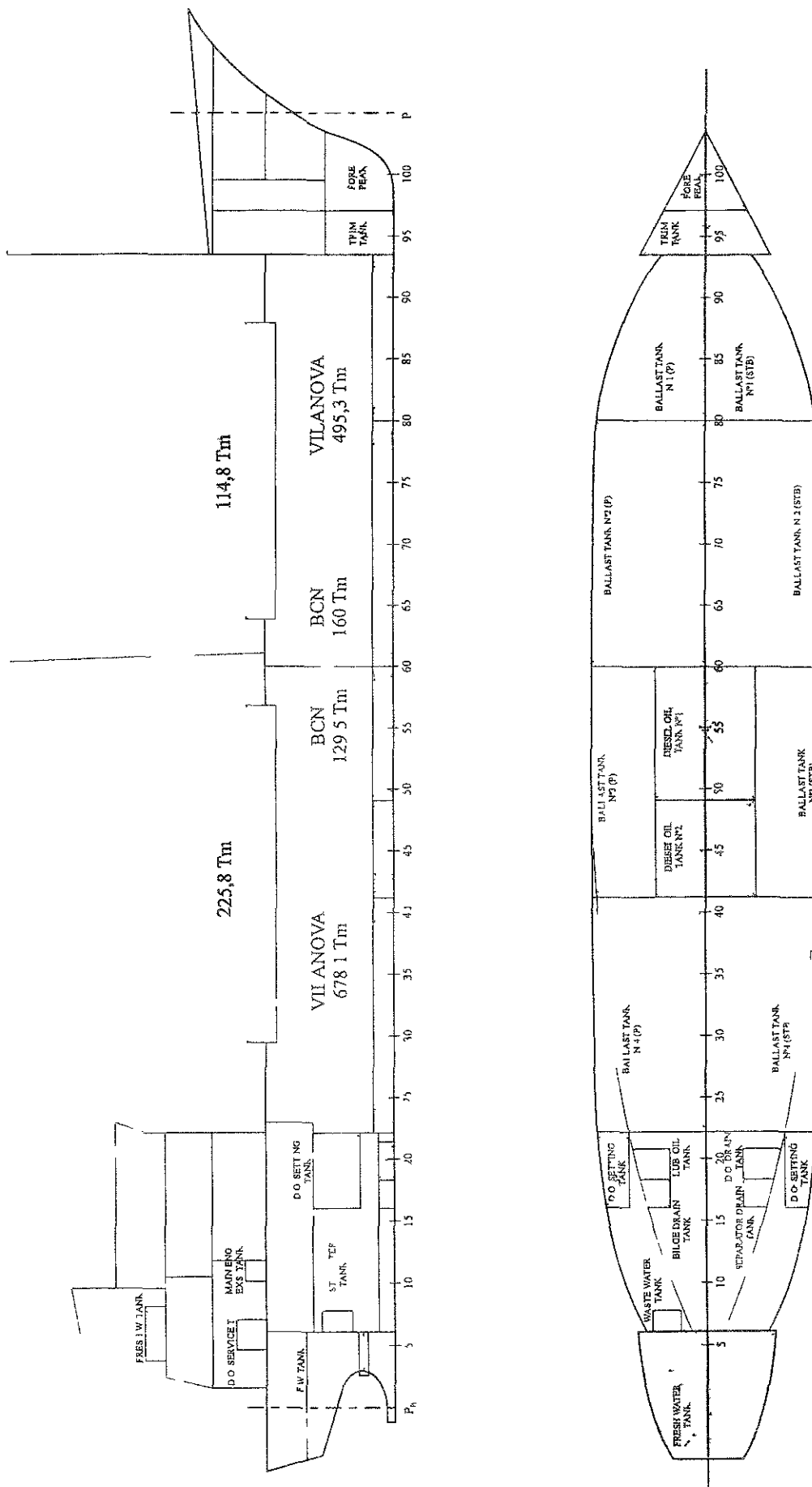


Figure 3. Cargo plan

the departure of the last port.

- The difference between the displacements corresponding to these two mean draughts indicate a deficiency of about 370 metric tons without the appropriate documented justification.

- The allowable draught by freeboard zone and date, according to the international load lines regulation, for summer draught was 5,289 m for this ship.

## 5. STUDY OF THE HOLDS OCCUPATION

As an approximation to the problem it was carried out a study of the cargo occupation in the holds.

Table 5. Cargo capacities

Location	Grain m <sup>3</sup>	Bale m <sup>3</sup>
Hold N° 1	1.030,00	973,00
Hold N° 2	1.205,00	1.142,00
Hatch N° 1	147,96	147,96
Hatch N° 2	172,62	172,62
TOTAL	2.555,58	2.435,58

Table 6. Cargo volumes in the holds

Item	Location	Holds (m <sup>3</sup> )	Cargo (m <sup>3</sup> )	Diff. (m <sup>3</sup> )
1	Hold & Hatch 1	1.121	770,48	350,52
2	Hold & Hatch 2	1.314	887,92	426,08
	10% stowage loss			
3	Hold & hatch 1	1.121	847,50	273,50
4	Hold & hatch 2	1.314	976,80	337,20

With this aim, it was considered on the one hand the grain and bale volumes of the holds, (Table 5), and also the volumes of the cargo shipped in each hold according with the stowage factor of each kind of product, (Table 6).

In table 6, items 1 and 2 give the cargo values in terms of the stowage factors, and in items 3 and 4 it is considered, too, a loss of ten per cent for the operation of stowing the cargo on the holds in these particular case. Important differences between the bale volume and the theoretical volume to be occupied in each hold have been noticed. If it is considered that the holds were filled up to the beams, then it may also be considered that there was a bigger loss of stowage. To verify this circumstance, e.g., that the ship's holds were full according to the cargo plan, we need a better knowledge of the form of the ship's holds and the stowage, than the one available for this study.

## 6. HYPOTHESIS ABOUT THE LOAD CONDITION OF THE SHIP

The hypothesis studied were stated as objective as possible, based in the cargo documentation of the ship and with the evidences of the crew and related people, not always into agreement. Anyway, what is clear is that the ship was overloaded at the departure, and so the research should be directed to the search and justification of the weight before appointed of the extra 370 metric tons that the ship had on board.

Furthermore, as it will be seen, this weight has a special implication in the posterior loss of the ship.

In the different hypothesis stated, the ballast of the ship was always in mind for two reasons: firstly, due to the assumption that the ship arrived with ballast to the Vilanova port, given the little quantity of load charged in Barcelona, and, secondly, due to the existence of references denoting that the ship was unballasting while she was sailing in the midchannel of the port just after undocking. It seems that the ballast is the hypothesis most reasonable to justify the true displacement of the ship.

Following this idea, some computations were done with different combinations of the ballast tanks, being a feasible alternative that the double bottom tanks, port and starboard, were still with ballast at the moment of the ship's departure, (Table 7).

Table 7. Ballast tanks

Location	Weight Metric Tons
Fore peak	22,220
Trim peak	30,136
Nº 1 Ballast T. P/Stb	61,275
Nº 2 Ballast T. P/Stb	140,088
Nº 3 Ballast T. P/Stb	86,387
Nº 4 Ballast T. P/Stb	81,646
Sea water service T.	1,055
<b>TOTAL</b>	<b>422,987</b>

## 7. SHIP BUOYANCY AND STABILITY COMPUTATIONS

A previous question to be pointed out was the unavailability of the calculations effected on board, if so. The process was set out starting from the data of the ship's inclining experiment.

Special reference is to be made to the following computations, due to their influence on the conclusions of the investigation.

1. Starting from the light displacement and the position of the center of gravity of the ship and according to the information of the inclining experiment, the computation of the displacement and the centre of gravity is made for the ship including fresh water, diesel oil, lubricant, crew and divers, that is, without cargo and/or ballast.

2a. Ship's buoyancy and stability calculations in the assumption of the holds being full as seen in the cargo plan indications.

2b. Buoyancy and stability calculations of the ship loaded, as seen in the cargo plan, plus the double bottom tanks of ballast full.

3a. Buoyancy and stability calculations of the ship with the holds loaded according to the volumes indicated in table 6 (including ten per cent of stowage lost).

3b. Buoyancy and stability of the ship as in case 3a, plus the full ballast tanks of the double bottom.

## 8. TRANSVERSE STABILITY ANALYSIS

In the computations according to the conditions expounded in the previous section (2a, 2b, 3a, and 3b), the IMO stability criteria have been verified and, moreover the curve of Rahola has been included in the graphics of the right levers, due to the significance of its relative position with regard to each lever curves.

Some considerations about the more important incidences in every four cases under analysis, are commented below.

### *Computation 2a*

Ship loaded according to the cargo plan.

Displacement, D	2.574,4 t
Mean draught, Cpm	4,860 m
Metacentric height, $GM_c$ (corrected for free surfaces)	0,100 m
Heel, $\theta$	0°

- The mean draught has a less value than the departure mean draught.

- The metacentric height corrected for free surface has a critical value, below the IMO minimum.

- The area contained by the curve of GZ arms (dynamical stability) has a very little value, (Fig. 4).

- This cargo condition does not fulfil the IMO criteria. Furthermore, in this particular case, it does not satisfy any of their conditions.

#### Computation 2b

Ship loaded according to the cargo plan plus ballast.

Displacement, D	2.940,7 t
Mean draught, Cpm (in the mean perpendicular)	5,353 m
Mean draught, Cm (in the centre of flotation)	5,362 m
Metacentric height, $GM_c$ (corrected for free surfaces)	0,405 m
Heel, $\theta$	0°

- The mean draught is practically equal to the mean draught of the departure port.

- Both the metacentric height ( $GM_c$ ) and the right lever (GZ) increase considerably as compared with the case of computation 2a, (Fig. 4). However, this cargo condition does not observe the IMO criteria, except for the metacentric height which is superior to the minimum requested.

#### Computation 3a

Ship loaded according to the cargo volumes.

Displacement, D	2.574,4 t
Mean draught, Cpm	4,860 m
Metacentric height, $GM_c$ (corrected for free surfaces)	0,384 m
Heel, $\theta$	0°

- As in computation 2a, the mean draught does not reach the mean draught of the departure port.

- Concerning the transverse stability, the centre of gravity of the holds cargo descends, as it was considered a void in the upper part of the holds. This improves appreciably the conditions predicted in case 2a. In spite of this, the cargo plan 3a does not reach the IMO stability criteria, (Fig. 5).

#### Computation 3b

Ship loaded according to the cargo volumes plus ballast.

Displacement, D	2.940,7 t
Mean draught, Cpm (in the mean perpendicular)	5,353 m
Mean draught, Cm (in the centre of flotation)	5,362 m
Metacentric height, $GM_c$ (corrected for free surfaces)	0,654 m
Heel, $\theta$	0°

- The mean draught corresponds to the departure of the ship, due to the presence of the ballast weight of the double bottom tanks.

- The ship's stability has for this cargo distribution the most favourable condition with respect to the other cases. Nevertheless, it does not comply with all points of the IMO criteria, (Fig. 5).

### 9. HEELING MOMENT DUE TO THE ACTION OF THE RUDDER

From the several possibilities of external and internal forces than could have created a heeling moment, it was investigated with special

attention the one produced by the action of the rudder over one side, which normally causes immediately a heel to the same side.

A simplified equation got from the IMO stability criteria, was worked out to calculate this moment. This gives as a result the heeling lever caused by the rudder,

$$l_h = 0,02 \frac{V^2}{L} \left[ KG_c - \frac{Cm}{2} \right]$$

being,

- $l_h$  heeling lever in metres
- $V$  ship speed in m/s
- $L$  waterline length in metres
- $KG_c$  vertical coordinate of the centre of gravity of the ship in metres
- $Cm$  mean draught in metres

The heeling arm was computed for the load condition 2a, that is, the ship loaded according to the stowage plan, (Fig. 3), and no ballast on board. Its value is,

$$l_h = 15,2 \text{ mm}$$

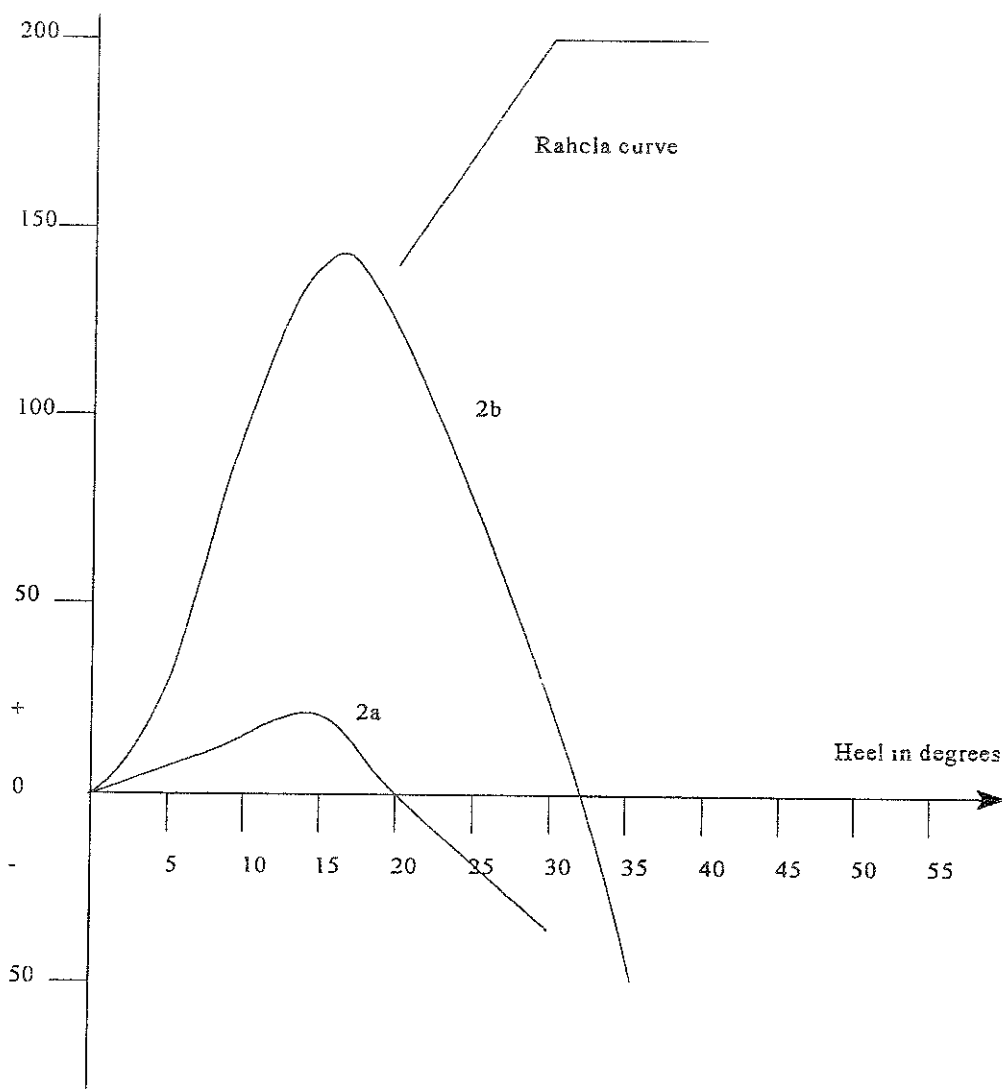


Figure 4. Curves GZ from computations 2a and 2b

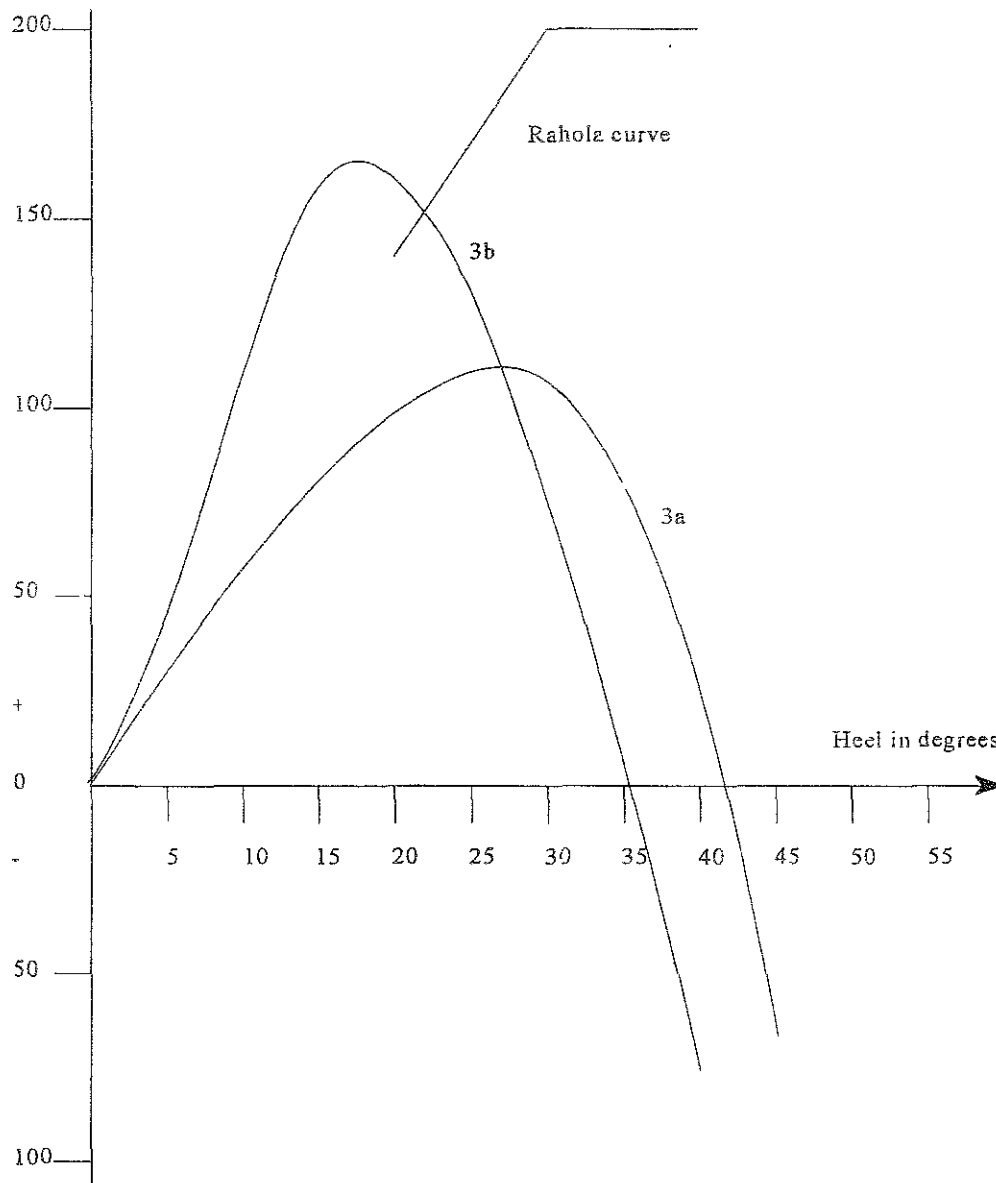


Figure 5. Curves GZ from computations 3a and 3b

## 10. CONCLUSIONS

Starting from the hypothesis made through the present study, the following sequence of the possible events is made:

1. The ship left the last port loaded according to the stowage plan and with ballast in the double bottom, (computation 2b). Under these conditions the ship was overloaded for the periodical navigation zone imposed by the IMO load regulations, with a mean draught slightly

below the fresh water tropical draught. It is known that the weather was fine, without appreciable sea and/or wind. The transversal stability in this condition did not reach the minimum of the criteria established by the IMO.

2. It was assumed, by means of testimonies, that during the departure manoeuvre the ship was making unballasted operations which are considered to have continuity until the double bottom tanks were completely unballasted.

3. After the unballast, the ship remained in the condition 2a, loaded according to the cargo plan presented by the stowage company.

4. The helmsman indicates that it was changed from the automatic pilot to the manual steering, which it is very important, and that the rudder was full over one side. It is unknown for us the cause of this change, as well as if the close of the rudder to one side was voluntary or fortuitous.

5. In table 8 it is showed the values of right levers for the condition 2a, and the heeling levers due to the rudder hard to one side.

Table 8. Righting and heeling arms

Heel degrees	Rightings arms (mm)	Heeling arms (mm)
0	0,0+	15,2
5	11,3+	15,1
10	13,2+	15,0
15	21,4+	14,7
20	1,4+	14,3
30	36,0 -	13,2
40	176,3 -	11,6
45	269,1 -	10,7
60	511,0 -	7,6
75	3.935,2 -	3,9

6. In table 8, again, it is observed the small reserve of stability. Even considering the difficulties of the appreciation of the ship data, which means that the values must be regarded as approximates, there is no place for the optimism.

7. The testimonies indicate a little heel at the beginning of the disaster, of which the ship did not recover. It followed a progressive heel, which made the ship careened and eventually sunk, which can be understood as a clear lack of stability.

## BIBLIOGRAPHY

INTERNATIONAL MARITIME ORGANIZATION. **Recommendation on intact stability for passenger and cargo ships under 100 metres in length.** London: IMO, 1983.

MARÍ SAGARRA, Ricardo. **Maniobra de los buques.** 2da. ed. Barcelona: Edicions UPC, 1995.

OLIVELLA PUIG, Juan. **Teoría del Buque. Flotabilidad y estabilidad.** 2da. ed. Barcelona: Edicions UPC, 1995.

OLIVELLA PUIG, Juan. **Teoría del Buque. Estabilidad, varada e inundación.** Barcelona: Edicions UPC, 1995.

ORGANIZACIÓN MARÍTIMA INTERNACIONAL. **Convenio Internacional sobre líneas de carga, 1966.** Londres: IMO, 1966.

# ON CAPSIZING RISK FUNCTION ESTIMATION DUE TO PURE LOSS STABILITY IN QUARTERING SEAS

V.L. Belenky

National Research Institute of Fisheries Engineering,  
Ebidai, Hasaki, Kashima, Ibaraki, 314-04, Japan

## ABSTRACT

The paper is focused on possibility of generalisation of piecewise linear approach for the case of quartering seas. The consideration devoted mainly to assumptions that are necessary to build an algorithm for capsizing risk calculation. It is shown that combination of superposition method with piecewise linear presentation of the  $GZ$  curve allows to solve the problem if assume independence of external excitation and restoring moment. It is shown also that this assumption is equivalent in some sense to the method of slowly changing amplitudes.

## NOMENCLATURE

$B$	breadth of a ship
$GM$	metacentric height
$GZ$	stability curve
$f$	probability density function
$f_E$	excitation process
$f_R$	restoring term
$h_w$	wave height
$I_x$	moment of inertia
$k_{Fi}$	slope coefficient of range $i$ in piecewise presentation on $GZ$ curve
$L$	length of a ship
$M_{44}$	added moment of inertia
$m_h$	mean value of wave heights
$m_\lambda$	mean value of wave lengths

$v$	speed of a ship
$V_w$	variance of wave elevation process
$\delta$	roll damping coefficient
$\varepsilon_w$	initial phase of wave
$\lambda$	risk function
$\lambda_w$	wave length
$\lambda_{1,2}$	eigen values
$\omega$	true wave frequency
$\omega_E$	encounter frequency
$\omega_\phi$	natural roll frequency
$\phi$	roll angle
$\chi$	course relative to general direction of wave proliferation

## 1. INTRODUCTION

The probabilistic approach to ship stability standard based on reliability theory [1], [2] supposes consideration of different assumed situations that could occur during ship operation.

The numerous number of factors describing assumed situation can be significantly decreased by dividing them into meteorological and operational [3], [4]. While meteorological factors can be somehow related with the geographical region where ship is sailing, the operational ones are human decision. According to [3], [4] these operational factors could be limited by two parameters speed and course of a ship.

Assuming to have all the meteorological information, it is not difficult to retrieve a value of angle between vector of ship speed and general direction of wave proliferation. So the basic assumed situation for intact stability assessment can be described as «sailing with certain speed and course in certain geographical region». There are several scenarios of capsizing in such situation described in [4]: impact of breaking wave, pure loss stability, surf riding and broaching to, green water shipping, etc.

This paper is particularly devoted to one of them - capsizing due to pure loss stability, including consideration of heeling moment of waves and wind and changing of the  $GZ$  curve caused by quartering seas. The last factor cannot be excluded if the course angle relative to general direction of wave proliferation is arbitrary. Our consideration is limited by these factors and does not reflect any other phenomena that are possible while sailing in quartering seas: surf riding and parametric resonance.

There is a comprehensive literature devoted to stability in following and quartering seas: the phenomenon of changing stability caused by following waves action was discovered at the end of the XIX century, however systematic research was started in 50s. Scope of this paper does not allow to place even a brief review of the literature on this matter.

Mechanics of capsizing is quite complicated nonlinear matter even in beam seas. The method to be chosen for capsizing investigation depends on what kind of capsizing definition is adopted. Here we used Sevastianov definition [5] «capsizing is a transition to stable state oscillation in vicinity of equilibrium that is dangerous from practical point of view». Direct application of this definition lead the author to developing piecewise linear method that allows to keep topology of phase plane [6]. Further

study of this matter, however, showed that Sevastianov definition is equivalent to classic one [7], because we can neglect influence of external excitation after roll angle crosses the level of  $GZ$  curve maximum. It makes outcomes of piecewise linear method as least comparable with the results obtained by the methods considering capsizing as a cross of separatrix [8].

Further study of the piecewise linear systems allowed the author to develop practical method of capsizing risk function estimation in beam seas [9]. The main goal of this paper is to highlight obstacles in generalisation of piecewise linear methods for assessment stability in quartering seas.

## 2. MATHEMATICAL MODEL OF SHIP ROLLING AND CAPSIZING

Since we are trying to reach methodological purposes we consider the simplest mathematical model of a ship sailing in quartering seas:

$$\ddot{\phi} + 2\delta\dot{\phi} + \omega_{\phi}^2 f_R(\phi, t) = f_E(t) \quad (1)$$

We assume ship speed constant and, therefore, we can consider external excitation as stationary ergodic stochastic process. Due to arbitrary course of a ship relative to general direction of wave proliferation, the restoring term is a function of time.

The restoring term is a deterministic function of two stochastic arguments: time and roll angle. There is evident probabilistic relationship between external excitation and restoring term, but we neglect this dependence for the first expansion.

This assumption allows to use different presentation of stochastic processes for external excitation and restoring term. External excitation includes wave and wind heeling moments presented here by Fourier series, amplitudes of which are calculated in accordance of corresponding spectra and initial

phases are considered as independent stochastic value with uniform distribution in the range  $[0;2\pi]$ , see [9]:

$$f_E(t) = \sum_{i=1}^N b_i \sin(\omega_i t + \varphi_i) + \sum_{i=1}^N c_i \sin(\omega_i t + \psi_i) \quad (2)$$

Contrary to the above, bend line presentation of irregular wave is used for the wave in the restoring term.

$$\zeta_w(t) = \frac{h_w}{2} \cos(\omega t + \varepsilon_w) \quad (3)$$

There are three stochastic values here: wave height, wave frequency and initial phase.

Using equation (3), and recommendations [11], restoring term can be presented as follows:

$$f_R(\phi, t) = f_{R0}(\phi) + f_{RA}(\phi) \cos(\omega_E t + \varepsilon_w) \quad (4)$$

Here:  $f_{R0}(\phi)$  is a mean value of restoring term it; it can be expressed via  $GZ$  curves on wave crest and trough:

$$f_{R0}(\phi) = \frac{GZ_T(\phi) + GZ_C(\phi)}{2 \cdot GM} \quad (5)$$

Amplitude of the restoring term chaining due to quartering wave action can be expressed as:

$$f_{RA}(\phi) = \frac{GZ_T(\phi) - GZ_C(\phi)}{2 \cdot GM} \quad (6)$$

Values of the  $GZ$  curve on wave crest and wave trough can be calculated by any appropriate method. The author used Nechaev method [11] based on comprehensive series of model tests. According to this method (see appendix), the  $GZ$  curves on crest and trough of a wave can be evaluated as some addition to the calm water  $GZ$  curve. These figures are functions of: wave characteristics, angel of heel, speed and course relative to waves:

$$GZ_C(\phi) = GZ(\phi) + \Delta GZ_C(\phi, h_w, \lambda_w, \chi, \nu) \quad (7)$$

$$GZ_T(\phi) = GZ(\phi) + \Delta GZ_T(\phi, h_w, \lambda_w, \chi, \nu) \quad (8)$$

Encounter frequency  $\omega_E$  is related with true frequency of wave:

$$\omega_E = \omega - \frac{\omega^2}{g} \nu \cos \chi \quad (9)$$

The true frequency depends on wave length:

$$\omega = \sqrt{\frac{2\pi g}{\lambda_w}} \quad (10)$$

Therefore:

$$\omega_E = \omega_E(\lambda_w, \nu, \chi) \quad (11)$$

Summarising all above we can state that restoring term is a deterministic function of roll angle, stochastic characteristics of wave and given parameters of ship heading;

$$f_R(\phi, t) = f_R(\phi, h_w, \lambda_w, \varepsilon_w, \nu, \chi) \quad (12)$$

Stochastic characteristics of wave can be considered as slowly changing figures in comparison of wave elevation, wave slope or rolling. It allows to rewrite equation (12) as (we are keeping stochastic arguments only):

$$f_R(\phi, \tau) = f_R[\phi(\tau), h_w(\tau), \lambda_w(\tau), \varepsilon_w(\tau)]$$

We see that above assumption on neglecting probabilistic relationship between external excitation and restoring term is equivalent to introducing another independent variable. This independent variable is another time scale for slowly changing stochastic processes, what partially excuses the above assumption.

To determine a moment of capsizing we used piecewise linear approach [9], that supposes the broken line presentation of the decreasing part of  $GZ$  curve, see fig. 1

The piecewise linear approach to stability assessment in beam seas was developed in previous author's works [6], [7], [9] [10]. It concentrates on consideration of system's behaviour at decreasing part of the  $GZ$  curve.

Each range of broken line allows to build linear solution within itself:

$$\phi(t) = Ae^{\lambda_1 t} + Be^{\lambda_2 t} + p(t) + \phi_v \quad (13)$$

where  $p(t)$  is a partial solution that could be ignored due to its comparatively small contribution [7] into the whole solution (13),  $\lambda_{1,2}$  are eigen values, one of each is always positive and the other vice versa:

$$\lambda_{1,2} = -\delta \pm \sqrt{\omega_\phi^2 k_{R1} + \delta^2} \quad (14)$$

$A$  and  $B$  are arbitrary constants that are dependent on initial conditions. Whether capsizing happen or not during this semi period of oscillation is determined by sign of the arbitrary constant  $A$  at last range of the broken line. If the constant is positive the solution is unlimited and angle of heel will increase until a ship reach upside down equilibrium.

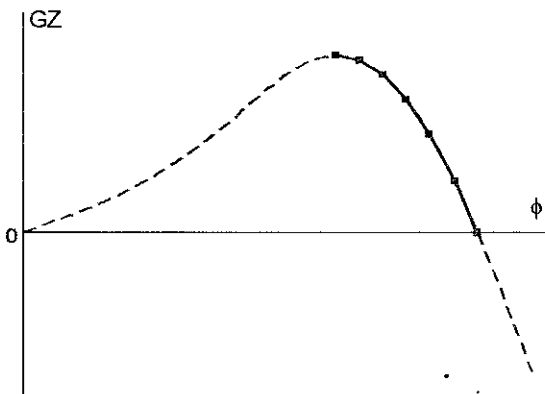


fig.1 Piecewise presentation of the GZ curve

There is a special iterative procedure that allows to calculate initial angular velocity of crossing the level of  $\phi_{max}$  to provide positive value of the arbitrary constant  $A$  at the last range, see [9]. Such value of the roll velocity was called «critical» there -  $\dot{\phi}_{cr}$ . The critical roll velocity depends on history of oscillations at increasing part of the  $GZ$  curve and can be calculated by conventional methods of rolling calculation.

So, according to piecewise linear approach a capsizing can be determined as an event of crossing level of  $\phi_{max}$  with the roll velocity exceeding  $\dot{\phi}_{cr}$ :

$$X = \{\dot{\phi} > \dot{\phi}_{cr} | \phi > \phi_{max}\} \quad (15)$$

The main advantage of piecewise linear approach is the simplicity of handling such a nonlinear phenomenon as capsizing. This simplicity is reached due to clear and vivid linear solution that was used as a main component of the piecewise linear approach. Unfortunately an attempt to generalise this method for cases when the restoring term is a function of time leads to Mathieu type equation even within the most simple assumption. Solution of Mathieu type equation hardly can be called «simple» or «vivid». So direct generalisation of piecewise linear approach for stability assessment in quartering seas leads to losing mentioned above advantage. Therefore a superposition method was used here.

### 3. PROBABILITY OF CAPSIZING

The essence of superposition method is dividing the phenomenon into some quantity of elementary incompatible events that covers all possible space of outcomes. Then we solve the problem for each of these elementary events. The probability of the phenomenon can be calculated further by total or whole probability formula. This method is quite common, its description can be found in any manual on theory of probability, see, for example [14].

We are looking for the probability of capsizing of a ship in quartering seas. The solution is known for the given constant restoring term [9] and it is possible to find  $GZ$  curve changes due to quartering seas at any moment of time [11].

Let's divide time in certain ranges, small enough that we can neglect stability changes during each of them. So our elementary event takes

time from  $\tau_j$  till  $\tau_{j+1} = \tau_j + \Delta\tau$  and during this event:

$$E_j = \left\{ \tau \in [\tau_j; \tau_j + \Delta\tau] \mid h_w, \lambda_w, \varepsilon_w \right\} \quad (16)$$

This allows us to calculate probability of capsizing, using whole probability formula.

$$P(t = \Delta\tau \cdot K) = \sum_{j=1}^K P(X|E_j)P(E_j) \quad (17)$$

Let's consider probability of elementary event:

$$P(E_j) = P\left\{ \tau \in [\tau_j; \tau_j + \Delta\tau] \mid h_w, \lambda_w, \varepsilon_w \right\} = P_\tau(h_w, \lambda_w, \varepsilon_w) \quad (18)$$

This is a probability to encounter a wave with certain height and length in certain phase at any moment of time  $\tau_j$ . We can assume that phase  $\varepsilon_w$  is independent on other parameters and its probability distribution constant in the range  $[0; 2\pi]$ . This assumption is reasonable because moment  $\tau_j$  is arbitrary and does not connect with any other event in our mathematical model:

$$P(E_j) = P(h_w, \lambda_w) \cdot P(\varepsilon_w) \quad (19)$$

Combined probability of wave heights and lengths is investigated in oceanography quite well and can be considered as known.

$$P(h_w, \lambda_w) = f(h_w, \lambda_w) dh_w d\lambda_w \quad (20)$$

Finally:

$$\begin{aligned} P(E_j) &= P\left\{ \tau \in [\tau_j; \tau_j + \Delta\tau] \mid h_w, \lambda_w, \varepsilon_w \right\} = \\ &= P(h_w, \lambda_w, \varepsilon_w) = P(h_w, \lambda_w) \cdot P(\varepsilon_w) = \\ &= f(h_w, \lambda_w) \cdot f(\varepsilon_w) \cdot dh_w d\lambda_w d\varepsilon_w \end{aligned} \quad (21)$$

Substitution of the equation (21) into formula (17) followed by transition to infinite small values yields:

$$\begin{aligned} P(t) &= \\ &= \int_0^\infty \int_0^\infty \int_0^{2\pi} P(X|t) f(\lambda_w, h_w) f(\varepsilon_w) d\varepsilon_w dh_w d\lambda_w \end{aligned} \quad (22)$$

If we are interested in the risk function, we should calculate equation (22) with  $t=1$ , having in mind that conditional probability of capsizing with the elementary event transforms into the risk function calculated for the given GZ curve

$$P(X|t=1) = \lambda(GZ) \quad (23)$$

and

$$\lambda = \int_0^\infty \int_0^\infty \int_0^{2\pi} \lambda(GZ) f(\lambda_w, h_w) f(\varepsilon_w) d\varepsilon_w dh_w d\lambda_w \quad (24)$$

The question arises: how do we take into account that long waves take more time than short ones? May be we should introduce some statistic weight coefficient regarding period of wave?

In fact, time of certain wave action is already taken into account in Nechaev algorithm because encounter frequency is present in formula (4). Some more details on Nechaev algorithm as well as brief description of risk function calculation with the given GZ curve can be found in appendixes.

#### 4. CONCLUSIONS AND COMMENTS

Direct generalisation of the piecewise linear method to the stability of ship in quartering seas leads to significant mathematical difficulties related with the necessity to consider transition process in Mathieu equation.

However, the problem of capsizing risk function estimation in quartering seas can be solved within frames of the piecewise linear approach using method of superposition.

Application of superposition method requires adoption of an assumption on independence of stochastic processes of restoring terms and external excitation.

The assumption on independence of stochastic processes of restoring terms and external excitation is equivalent to consideration of wave length and height as slowly changed parameters.

Problems to be solved at the second expansion: adequacy and margins of applicability of the above assumption, using of up-to-date oceanographic data on the wave elements distribution.

## REFERENCES

1. Sevastianov, N.B. An algorithm of probabilistic stability assessment and standards, *Proc. of 5th STAB conference*, Vol. 5. Melbourne, Florida, 1994
2. Kobylinski, L. Stability standards and probability of capsizing - philosophical aspects, *Proc. of Int. Symp. on Ship Safety in a Seaway: Stability, Maneuverability, Nonlinear Approach (SEVASTIANOV SYMPOSIUM)*, Vol. 1, Paper 1, Kaliningrad 1995
3. Mordachev, S.V., Sevastianov, N.B. and Belenky, V.L. Assumed situations in probabilistic norms of stability, *Proc. of 5th STAB conference*, Vol. 6. Melbourne, Florida, 1994
4. Mordachev, S.V. Assumed situations and human factor in probabilistic approach to stability assessment *Proc. of Int. Symp. on Ship Safety in a Seaway: Stability, Maneuverability, Nonlinear Approach (SEVASTIANOV SYMPOSIUM)*, Vol. 1, Paper 8, Kaliningrad 1995
5. Sevastianov N.B. and Pham Ngock Hoeh Boundary between the domains of stable and unstable free ship motion in drift-rolling regime, *Trans. of Kaliningrad Technical Institute "Seakeeping of Fishing Vessels"*, Kalininrgad, 1979, Vol. 81, PP. 17-25 (in Russian)
6. Belenky, V.L. A new method of statistical linearization in severe rolling and capsizing problem, *Proc. of 18th SMSSH*, Varna 1989
7. Belenky, V.L. A capsizing probability computation method, *Journal of Ship Research*, Vol. 37, No. 3, Sept. 1993, pp 200-207
8. Umeda, N., Yamakoshi, Ya. and Tsuchiya, Ts. Probabilistic study on ship capsizing due to pure loss of stability in irregular quartering seas, *Proc. of 4th STAB Conference*, Naples, 1990
9. Belenky, V.L. Piece-wise linear methods for the probabilistic stability assessment for ship in a seaway, *Proc 5th STAB Conference*, vol. 5, Melbourne, Florida, 1994
10. Belenky, V.L. Some problems of stochastic dynamics of piecewise linear and nonlinear, *Report on seminar at University of Michigan*, 13 March 1997
11. Nechaev, Yu.I., Modelling of ship stability in waves, Sudostroenie, Leningrad, 1989, 240 p., (in Russian)
12. Boroday, I.K., Morenschildt, V.A., Vilensky G.V., and others, *Applied Dynamic of Ship in a Seaway*, edited by I.K. Boroday, Leningrad, "Sudostroenie", 1989, 259 p. (in Russian)
13. Boroday, I.K., Netsvetaev, Yu.A. Ship motion in a seaway, Sudostroenie, Leningrad, 1969, 432 p. (In Russian)
14. Ventsel, E.S and Ovcharov, L.A. Theory of probability and its engineering applications, Moscow, Nauka, 1988 (in Russian)
15. Belenky, V.L., Degtyarev, A.B., Boukhanovsky, A.V., Probabilistic qualities of nonlinear stochastic rolling, *Ocean Engineering*, 1997, Vol. 25, pp. 1-25 in press
16. Belenky, V.L., Degtyarev, A.B., Boukhanovsky, A.V., Probabilistic qualities of severe ship motions, *Proc 6th STAB Conference*, Varna, 1997 to be printed
17. Sveshnikov, A.A., Applied methods of stochastic function theory, "Nauka" Moscow, 1968., (in Russian)

## ASKNOWLEDGEMENT

This work was supported by the Polish Committee of Scientific Research under Grant KBN nr 9 T12C 046 08 «Zintegrovany system

oceny bezpieczeństwa statku na szalowanym morze przy użyciu metod probabilistycznych», supervisor J. Bielanski. Participation of the author in this work was in frame of international scientific cooperation between Kaliningrad State Technical University (Russia) and Technical University of Gdansk (Poland). The authors are grateful to Professor Lech Kobylinski and Doctor Jan Bielanski for discussions and help provided in the course of this work. The contents of this paper is based on reports of Technical University of Gdansk No 49/95, 6/96 and 21/96

## APPENDIX 1 NECHAEV METHOD

The method is based on series of model test in hydrochannel of Kaliningrad Technical Institute. Results of these experiments were presented in a form of regression polynoms and were published in [11]. Using this polygons, it is possible to estimate  $GZ$  curves on wave crest and on wave trough, if the length of wave is not very far from length of the ship with taking into account course angle:

$$\lambda_w = L \cos \chi \quad (A1)$$

Usage of this figures is limited by he following values of ship parameters:

$$3.2 \leq L/B \leq 8.00 \quad 0.5 \leq C_B/C_w \leq 0.92$$

$$2.0 \leq B/T \leq 4.2 \quad 0.5 \leq C_B/C_M \leq 0.85$$

$$1.05 \leq H/T \leq 2.2 \quad 0.15 \leq Fn \leq 0.45$$

The  $GZ$  curve when ship is located on wave crest is expressed as:

$$GZ_c(\phi) = GZ(\phi) + B \left( F_c(\phi) + \sum_{i=1}^{17} A_i f_{c_i}(\phi) \right) \quad (A2)$$

where  $GZ_c(\phi)$  is stability diagram on wave crest;  $F_c(\phi)$ - basic values for wave crest (see appendix);  $f_{c_i}(\phi)$  is influence function;  $A_i$  is a set of numbers expressing influence of ship parameters that are differ from the basic model:

$$\begin{aligned} A_1 &= L/B - 4.82 & A_7 &= A_1^2 & A_{13} &= A_2 A_4 \\ A_2 &= B/T - 2.67 & A_8 &= A_2^2 & A_{14} &= A_1 A_6 \\ A_3 &= H/T - 1.3 & A_9 &= A_3^2 & A_{15} &= A_1^3 \\ A_4 &= C_B/C_w - 0.7 & A_{10} &= A_5^2 & A_{16} &= A_2^3 \\ A_5 &= C_B/C_M - 0.692 & A_{11} &= A_6^2 & A_{17} &= A_3^3 \\ A_6 &= Fn - 0.28 & A_{12} &= A_1 A_2 \end{aligned}$$

Here  $L, B, H, T$  are main dimensions of a ship and  $C_B, C_w, C_M$  are form coefficients. The  $GZ$  curve, when ship is on wave trough, can be expressed as:

$$GZ_T(\phi) = GZ(\phi) + B \left( F_T(\phi) + \sum_{i=1}^{17} A_i f_{T_i}(\phi) \right) \quad (A3)$$

where  $GZ_T(\phi)$  is stability diagram on wave trough;  $F_T(\phi)$ - basic values for wave trough (see[11]);  $f_{T_i}(\phi)$  is influence function.

If the wave length is different from the length of the ship, the following correction function can be introduced:

$$Corr(\lambda_w / L) = 1 + k_1 \cdot \bar{\lambda}_w - k_2 \cdot \bar{\lambda}_w^2 - k_3 \cdot \bar{\lambda}_w^3 \quad (A4)$$

where,  $\bar{\lambda}_w = \lambda_w / L - 1$  is dimensionless relative wave length,  $k_i$  is coefficients set that could be found in [11] along with the other numerical figures that are necessary for calculation of stability in quartering seas

## APPENDIX 2 ESTIMATION OF RISK FUNCTION WITH THE GIVEN GZ CURVE

As it was mentioned above capsizing event could be associate with up-crossing of the level  $\phi_{max}$  and an angular velocity of such up-crossing exceeds some critical value. So the probability of capsizing can be expressed as follows:

$$P(X) = P(\phi > \phi_{max}) P(\dot{\phi} > \dot{\phi}_{cr}) \quad (A5)$$

Calculation of the critical angular velocity is considered in [9] in details. To calculate the second probability, we should know distribution

of roll velocities. This distribution could be assumed as Gaussian for comparatively low build vessels with «conventional»  $GZ$  curve only [15] Contrary to, the distribution of roll velocities of high free board vessels with S-shaped  $GZ$  curve may differ from Gaussian type significantly. According to the author's knowledge the only way to get the distribution in this case is numerical simulation. Due to cyclic non-stationary quality [16] of nonlinear rolling, the distribution estimate cannot be done by generating one realisation of the process, but some ensemble of independent realisations should be simulated

Probability of the up-crossing event can be estimate if we consider up-crossings as Poisson flow of rare random events [6], [7], [9]

$$P(\phi > \phi_{\max}) = 1 - \exp(-\xi t), \quad (\text{A6})$$

where  $\xi$  is intensity of up-crossings. It is expressed as follows for Gaussian rolling distribution that is limited by «conventional» type of  $GZ$  curve:

$$\xi = \frac{1}{2\pi} \sqrt{\frac{V_{\dot{\phi}}}{V_{\phi}}} \cdot \exp\left[-\frac{\phi_{\max}^2}{2V_{\phi}}\right] \quad (\text{A7})$$

Variances of rolling  $V_{\dot{\phi}}$  and rolling velocities  $V_{\phi}$  can be obtained using linearization of nonlinear terms with further application of spectral methods [12], [13] Because we consider ship motion in quartering seas calculation on 3D waves is preferred

$$V_{\dot{\phi}} = \int_{-\frac{\pi}{2}}^{\frac{\pi}{2}} \int_0^{\omega_{\max}} S_{\dot{\phi}}(\omega, \varepsilon) d\omega d\varepsilon \quad (\text{A8})$$

If the  $GZ$  curve has S-shaped form the probability distributions of roll angles and roll velocities should be obtained using numerical simulation Intensity of up-crossing in this case is expressed and following integral :

$$\xi = \int_0^{\infty} \dot{\phi} \cdot f(\phi = \phi_{\max}) f(\dot{\phi}) d\dot{\phi}. \quad (\text{A9})$$

# ON PROBABILITY OF SHIP CAPSIZING DUE TO BREAKING WAVES ACTION

V.L. Belenky

National Research Institute of Fisheries Engineering,  
Ebidai, Hasaki, Kashima, Ibaraki, 314-04, Japan

S.V. Mordachev

Kaliningrad State Technical University  
1 Sovetsky Avenue, Kaliningrad, 23600, Russia

## ABSTRACT

The paper is devoted to theoretical background of estimation of risk function of ship capsizing due to encounter breaking wave. Because mechanics of breaking wave action on a ship is practically unknown in general, an energetic method was used. A main idea of this method here is that a work of heeling moment could not be greater than whole wave energy. So we assumed that wave uses all its energy for ship capsizing with a reduction coefficient that can be found from a model test. Risk function that is probability of capsizing derived using energy balance equation and upcrossing theory

## NOMENCLATURE

$a(t)$  amplitude vs. time - bend line  
 $A_B$  work of heeling moment caused by breaking wave  
 $A_D$  work of damping moment  
 $A_W$  work of external excitation  
 $b$  parameter of Weibull distribution  
 $E_B$  energy of break wave on the length of a ship  
 $E_{bcr}$  critical energy of break wave on the length of a ship that causes capsizing  
 $E_F$  full energy of ship rolling  
 $h_w$  wave height  
 $h_{cr}$  the breaking wave height that causes capsizing

$I_x$  moment of inertia  
 $\Delta K$  changing of kinetic energy  
 $m_h$  mean value of wave heights  
 $m_\lambda$  mean value of wave lengths  
 $m$  effective moment of inertia  
 $M_{44}$  added moment of inertia  
 $M_R$  restoring moment  
 $M_D$  damping moment with taking into account changing damping caused by heel  
 $M_B$  heeling moment caused by breaking wave  
 $M_W$  roll excitation moment caused by irregular waves and gusty wind  
 $\Delta P$  changing of potential energy  
 $P_T$  probability of at least one capsizing during time  $T$   
 $P_B$  probability of wave to be broken  
 $P_C$  probability of capsizing after time  $T$ , if broken wave was encountered  
 $T_m$  mean value of period of irregular seas  
 $V_W$  Variance of wave elevations process  
 $V_\lambda$  Variance of wave lengths  
 $W$  weight displacement  
 $\kappa_B$  reduction coefficient breaking wave energy  
 $\Omega(t)$  stochastic phase in bend line presentation of sea waves  
 $\phi$  roll angle

## 1. INTRODUCTION

The probabilistic approach to ship stability standard based on reliability theory [1] [2] supposes consideration of different assumed situations that could occur during ship operation. Breaking wave action on a ship in beam position is significant one for small vessels. The classic example of a stability casualty is the capsizing of m/s Helland-Hansen [3] Lack of reliable mathematical model of breaking waves makes theoretical study of the subject really difficult, therefore experimental approach is a main tool in such kind of research.

It seems that the first attempt to estimated ship stability in breaking waves was made in Sankt-Petersburg in the early 60s; it was initiative of S. Blagoveshchensky. The breaking wave were generated by the floating bottom that was used as a local submersible obstacle [4]. Pressure transducers were located on the deck and side of the model that was able to drift and roll. Mathematical model of capsizing under action of breaking was developed [5],[6]. The model was based upon an assumption that the heeling moment is generated by impact of breaking wave According to this model a ship is capsized when her kinetic energy generated by the impact exceeds her potential energy. Further research of ship behaviour in breaking waves in shallow water was carried out in Leningrad Shipbuilding Institute and reflected in [7].

A comprehensive study of deep water breaking waves dynamics and their action on ship was carried out in Norwegian Institute of Technology in Trondheim [10]. Experiments with the model of mentioned above m/s Helland-Hansen carried out by E.Dahle and J. Kjeldsen [3] These experiments showed primary role of inertia in ship-breaking wave interaction, see also [11], [12].

Ship dynamics in deep water breaking waves was studied in towing tank of Kaliningrad Technical Institute under supervision of

N.Sevastianov [7], [8], [22]. Breaking wave was obtained by generating a special sequence of waves with continuously increasing period These wave interfered due to difference in phase velocity. The resulting wave becomes too steep and breaks A particular purpose of the study was to investigate influence of architecture type on ship stability in breaking waves. The outcome was that the ship architecture elements like superstructures and even bulwarks are involved in the interaction with breaking wave and might be significant for stability in this situation. The other significant conclusion was that it is impossible to deal with the breaking wave stability using just deterministic methods.

Probabilistic approach to ship stability in breaking waves was applied in series of Norwegian research devoted to probability of capsizing in steep waters [13] and risk analysis [14], [15].

## 2. APPROACH ADOPTED

Our main purpose is to estimate a risk function value, or in other words, to find probability of capsizing per unit of time. Taking into account factor of time seems to be quite significant for probabilistic approach based upon reliability theory, (for more detail see [1]). So a scheme of capsizing probability determination should include clear relationship with the time.

We consider sea waves as a stochastic process. Usually such a process is assumed to be stationary ergodic and Gaussian. We also shall use these assumptions as quite common and convenient.

Output of a dynamic system describing a ship also is stochastic. It is assumed to be stationary and Gaussian. The last assumption means that we limit ourselves by ships with conventional (not S-shaped) GZ curve, see [16] or [17]. This limitation does not interfere so much: breaking waves are dangerous for relatively small ships

that has S-shape form of the GZ-curve quite rare. We do not use here ergodic assumption concern non-linear rolling: it was shown in [17] that such non-linear stochastic rolling process possesses cyclic non-stationary quality.

So let's imagine a ship that meet breaking wave from the side: it seems that breaking waves from the other directions are not so dangerous. Further we shall consider only beam position of ship.

Taking into account all mentioned above we can consider kinetic and potential energies of ship rolling as stochastic processes. Full energy of wave is also stochastic process for irregular seaway. So capsizing due to breaking wave action can be considered as a random event that wave has been broken at the same place where the ship is located and the sum of potential, kinetic and accepted wave energy exceeds whole amount of ship potential energy (the is defined by area under GZ curve).

$$P_T(X) = P_B \cdot P_C(T) \quad (1)$$

Here:  $P_B$  is a probability that next wave will be broken and  $P_C(T)$  is a probability of capsizing after time  $T$  if the previous condition was satisfied.

### 3. PROBABILITY OF WAVE TO BE BROKEN

To describe a wave we used hypothesis of small waves in the first expansion. The approach adopted allows to use more complicated models of wave, however for the first expansion simplicity was preferred in order to develop the methodology of research and highlight the problems appear.

To find the probability of a wave to be broken we use bend presentation of irregular wave.

$$\zeta_w(t) = a(t) \cdot \sin \Omega(t) \quad (2)$$

The amplitude  $a(t)$  or a bend line is a stochastic process that has Rayleigh distribution [18]. The

random phase value  $\Omega(t)$  has constant distribution in the range  $[0; 2\pi]$ . Taking into account evident relationship between wave amplitude and height, we can express the distribution of wave height as follows:

$$f_h(h_w) = \frac{\pi}{2m_h} \cdot \frac{h_w}{m_h} \cdot \exp\left[-\frac{\pi}{4} \cdot \left(\frac{h_w}{m_h}\right)^2\right] \quad (3)$$

Mean value of the wave height is related with the wave elevations variance  $V_w$  as follows:

$$m_h = \sqrt{2\pi V_w} \quad (4)$$

As it is known wave length and wave height are not independent stochastic values. However, here we assume their independence - to develop the methodology we need the most simple figures. Real distribution can be used for the second expansion. So we use Rayleigh distribution for the wave lengths [19,20]:

$$f_\lambda(\lambda) = \frac{\pi}{2m_\lambda} \cdot \frac{\lambda}{m_\lambda} \cdot \exp\left[-\frac{\pi}{4} \cdot \left(\frac{\lambda}{m_\lambda}\right)^2\right] \quad (5)$$

Mean value of the wave lengths can be obtained using Neumann spectrum and the value of mean period of irregular seas  $T_m$ . The variance of the wave length can be find using changing coefficient that is known from seas statistics

$$m_\lambda = \frac{2}{3} \cdot \frac{gT_m^2}{2\pi} \quad v_\lambda = \frac{\sqrt{V_\lambda}}{m_\lambda} \approx 0.461 \quad (6)$$

As we assumed above, height and lengths are independent:

$$f(h_w, \lambda) = f_h(h_w) \cdot f_\lambda(\lambda) \quad (7)$$

General appearance of the distribution (7) is shown in fig. 1.

Using the most simple geometrical criterion of breaking  $h_w/\lambda = 1/7=0.142$  we can easily calculate probability of breaking wave in any given point:

$$P_B = \iint_{h_w/\lambda > 0.142} f(h_w, \lambda) dh_w d\lambda \quad (8)$$

This method is also just a sample Breaking is a marginal situation for the wave, so the probability of wave to be broken deserves separate study. Breaking wave is a nonlinear matter, and any method proposed requires investigation of its adequacy

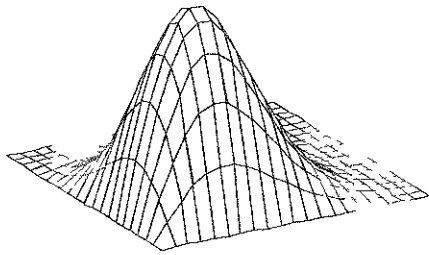


Fig. 1 Combined distribution of wave lengths and heights

#### 4. MATHEMATICAL MODEL OF SHIP MOTION

Let us consider ship rolling under action of irregular waves and gusty wind

$$\begin{aligned} (I_x + M_{44})\ddot{\phi} + M_D(\dot{\phi}, \phi) + M_R(\phi) = \\ = M_B(t) + M_W(t) \end{aligned} \quad (9)$$

According to Energy/Work balance method we should rewrite this equation in first integrals:

$$\begin{aligned} \int_{\phi_0}^{\phi} (I_x + M_{44})\dot{\phi} d\dot{\phi} = \\ = \int_{\phi_0}^{\phi} M_B(t) d\phi + \int_{\phi_0}^{\phi} M_W(t) d\phi - \\ - \int_{\phi_0}^{\phi} M_D(\dot{\phi}, \phi) d\phi - \int_{\phi_0}^{\phi} M_R(\phi, t) d\phi \end{aligned} \quad (10)$$

We have got the equation in first integrals, which reflects a balance of changing energies and works at any time during the range from  $t_0(\dot{\phi}_0, \phi_0)$  till  $t(\dot{\phi}, \phi)$ . Using special symbols for the terms of the equation it can be rewritten in compact view:

$$\begin{aligned} \Delta K + A_D(t_0, t) + \Delta P = \\ = A_B(t_0, t) + A_W(t_0, t) \end{aligned} \quad (11)$$

Here we consider several significant assumptions in order to simplificate problem to make possible first expansion solution.

**The First** We assume that work of damping moment is equal to the work of wave excitation moment

$$A_D(t_0, t) = A_W(t_0, t). \quad (12)$$

Strictly speaking, this assumption is quite rough: it is true for linear system only in stable state regime.

**The Second.** We substitute the work of heeling moment caused by breaking wave by the whole amount of wave energy in the length of the ship with some reduction coefficient. This reduction coefficient takes into account that only some part of the wave energy is transferred to ship rolling. Because we do not know mechanism of breaking wave action on a ship, this coefficient is estimated from the model test [13].

$$A_B = \kappa_B E_B \quad (13)$$

**The Third.** We assume that the whole amount of breaking wave energy is the same that a small wave with the same height has. This assumption is accepted in order to simplify the first expansion. As it will be seen from the further consideration, it is possible to use formula for whole energy of Stocks wave as well.

Other assumptions considered further are important but have not such principle influence on the problem solution as these three

mentioned above. Finally we have energy/work balance equation in the following view:

$$-\Delta K + \Delta P = \kappa_B E_B \quad (14)$$

We reorder terms in (14) to have in left side all terms concerning time  $t_0$ , the moment of breaking wave action begins. Right side of equation (14) contains terms concerning time  $t$  when maximal dynamic angle of heel is achieved (roll velocity equals zero at maximum roll angle):

$$K(\dot{\phi}_0) + P(\phi_0) + \kappa_B E_B = P(\phi) \quad (15)$$

Following traditional approach adopted for energy/work balance method, we consider capsizing to be occur when dynamic angle of heel exceeds the angle of vanishing stability:

$$K(\dot{\phi}_0) + P(\phi_0) + \kappa_B E_B = P(\phi_v) \quad (16)$$

A value of potential energy at the angle of vanishing stability can be easily interpreted geometrically: it is a value of the area under the  $GZ$  curve:

$$P(\phi_v) = W \cdot \int_0^{\phi_v} GZ(\phi) d\phi \quad (17)$$

Let's consider the first two terms of (16) in detail; to do it let's examine energy balance equation before the breaking wave action:

$$\int_{\phi_0}^{\phi} (I_x + M_{44}) \dot{\phi} d\dot{\phi} = \int_{\phi_0}^{\phi} M_W(t) d\phi - \int_{\phi_0}^{\phi} M_D(\dot{\phi}, \phi) d\phi - \int_{\phi_0}^{\phi} M_R(\phi) d\phi \quad (18)$$

Taking into account (12):

$$\int_{\phi_0}^{\phi} (I_x + M_{44}) \dot{\phi} d\dot{\phi} = - \int_{\phi_0}^{\phi} M_R(\phi) d\phi \quad (19)$$

Calculating integrals (18), we got

$$K(\dot{\phi}) - K(\dot{\phi}_0) = -P(\phi) + P(\phi_0) \quad (20)$$

We are considering two moments of time: moment  $t_0$  with roll angle  $\phi_0$  and roll velocity  $\dot{\phi}_0$ , and moment  $t$  with roll angle  $\phi$  and roll velocity  $\dot{\phi}$ . The first moment is arbitrary; the second one is be chosen regard to the problem considered. When we were considering the problem of dynamic angle of heel, the second moment corresponds to amplitude value of roll angle and zero value of roll velocity:

$$K(\dot{\phi}_0) + P(\phi_0) = P(\phi_{\max}). \quad (21)$$

We can also choose this moment when roll velocity reaches its maximal value and roll angle is equal to zero:

$$K(\dot{\phi}_0) + P(\phi_0) = K(\dot{\phi}_{\max}). \quad (22)$$

However, because the total amount of energy should be kept:

$$K(\dot{\phi}_0) + P(\phi_0) = K(\dot{\phi}_{\max}) = P(\phi_{\max}). \quad (23)$$

Therefore equation (16) can be substantially simplified.

$$K(\dot{\phi}_{\max}) + \kappa_B E_B = P(\phi_v). \quad (24)$$

## 5. EXPERIMENTAL VALIDATION: REDUCTION VALUE

As we have pointed out above a value of breaking wave energy is assumed to be equal to small wave energy on ship length.

$$E_B = \frac{1}{8} \rho g h_w^2 \lambda L, \quad (25)$$

Taking into account that wave is breaking and using well known criterion of breaking, we can rewrite formula (25) as follows:

$$E_B = \frac{7}{8} \rho g h_w^3 L. \quad (26)$$

To validate such approach and to find above 'reduction' value model rest results should be used. Here we have taken the results were obtained in Trondheim [13] in relation with capsizing M/S Helland Hansen. These results

were presented in a form of the border between 'safe' and 'unsafe' areas in coordinate system breaking wave height (critical height for the border) and whole amount of ship potential energy  $P(\phi_v)$ , see fig 2. Two curves are presented there for ship with a rail and for ship with a bulwark.

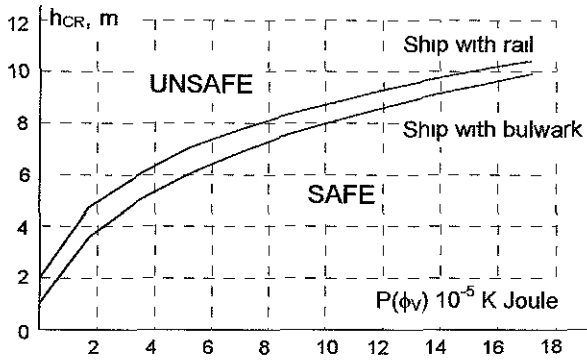


Fig. 2 Safe and unsafe regions as found from model test of M/S Helland Hansen, taken from [15]

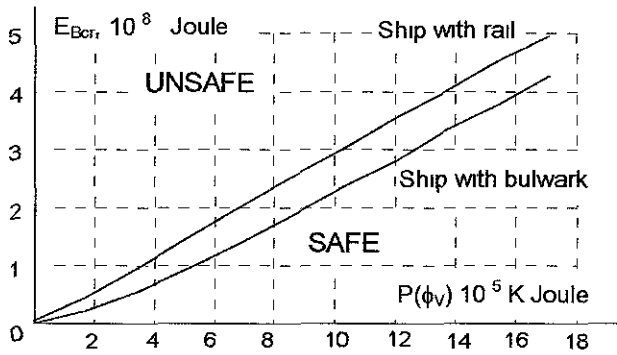


Fig 3 Critical energy of the braking wave as a function of whole amount of a ship potential energy

To validate our approach we should recalculate these curves to the other coordinate system instead critical wave height the breaking wave the critical energy should be used. If the formula (26) can be used for capsizing action estimation, then these curves should be converted into straight lines. If such effect takes place, so amount of energy of breaking wave that is used for capsizing is constant and does not depend on the particular GZ curve. As it can be seen from fig 3 existence of this effect is not disproved.

A picture like shown in fig 3 allows to estimate a value of the reduction coefficient  $\kappa_B$ . It is an angular coefficient of the lines, approximating curves at fig 3. In our example for the ship with  $L=50$  m the following values were obtained:

ship with rail  $\kappa_B=0.003422$

ship with bulwark  $\kappa_B=0.004231$

## 6. RISK FUNCTION OF CAPSIZING CAUSED BY BREAKING WAVE

As we have indicated above, capsizing is associated with a random event that the sum of current potential, kinetic energy and full wave energy are greater than full ship potential energy. Risk function is an intensity of flow of such events. We can consider this sum as the following stochastic process:

$$P_R(t) = K(\dot{\phi}_{\max}) + \kappa_B E_B \quad (27)$$

Then we can connect capsizing with the upcrossing of the level  $P(\phi_v)$  by the stochastic process  $P_R(t)$ . A general formula for upcrossing intensity exists:

$$\xi = \int_0^\infty \dot{P}_R \cdot f(P_R = P(\phi_v), \dot{P}_R) d\dot{P}_R \quad (28)$$

here  $f(P_R, \dot{P}_R)$  is a combined distribution of process  $P_R(t)$  and its derivative by time.

So, it can be clearly seen that to solve the problem we need to know the combined distribution of process  $P_R(t)$  and its first derivation by time. Theoretically this problem is not a difficult one; it is a well-known problem of calculation of distribution of deterministic functions of several random arguments. To solve it we need first to know distributions of arguments that are stochastic processes of energies and their derivatives.

So we are starting from the investigation of the breaking wave energy. Taking into account formula (26) (here we include reduction in the

formula of breaking wave energy for the sake of simplicity):

$$E_B(t) = k_{red} h_w^3(t); \quad (29)$$

where

$$k_{red} = \frac{7}{8} \rho g L \kappa_B \quad (30)$$

Using well known (see, for example [21]) formula for the distribution of deterministic monotone function of a stochastic argument, we can express the distribution density of the breaking wave energy:

$$f_{EB}(E_B) = f_h(h_w(E_B)) \cdot |h'(E_B)| \quad (31)$$

Here  $h_w(E_B)$  is the inverse function relative to formula (29).

$$h_w(E_B) = \sqrt[3]{\frac{E_B}{k_{red}}}, \quad (32)$$

$$h'_w(E_B) = \frac{1}{3\sqrt[3]{k_{red} E_B^2}} \quad (33)$$

Substitution of (32) and (33) into (31) yields.

$$f_{EB}(E_B) = f_h\left(\sqrt[3]{\frac{E_B}{k_{red}}}\right) \cdot \left| \frac{1}{3\sqrt[3]{k_{red} E_B^2}} \right|; \quad (34)$$

and after the simplification:

$$f_{EB}(E_B) = \frac{1}{12V_w \sqrt[3]{k_{red}^2 E_B}} \times \exp\left(-\frac{1}{8V_w} \sqrt[3]{\frac{E_B^2}{k_{red}}}\right) \quad (35)$$

The next step is derivation of the combine distribution of the breaking wave energy and its derivative. To do it conditional distribution of the derivative of the wave energy is required:

$$f_{EB}(E_B, \dot{E}_B) = f_{EB}(E_B) f_{EB}(\dot{E}_B | E_B); \quad (36)$$

here:  $f_{EB}(\dot{E}_B | E_B)$  is the conditional distribution of the derivative of the breaking wave; it is the distribution of the derivative with the condition that the energy of the breaking wave has reached a certain value  $E_B$

To find conditional distribution we differentiate the formula (29) by the time as any other complicate function:

$$\dot{E}_B = 3k_{red} h_w^2 \dot{h}_w \quad (37)$$

There are two stochastic values in equation (37) height of waves  $h_w$  and its derivative  $\dot{h}_w$ . A formula for distribution density of the last figure has been derived in the theory of stochastic processes [18]:

$$f_{\dot{h}_w}(\dot{h}_w) = \frac{1}{\sqrt{8\pi V_w (\omega_2^2 - \omega_1^2)}} \times \exp\left(-\frac{\dot{h}_w^2}{8V_w (\omega_2^2 - \omega_1^2)}\right) \quad (38)$$

where:  $\omega_1$  and  $\omega_2$  are the first and the second wave spectrum moments correspondingly:

$$\omega_1 = \frac{m_1}{V_w}; \quad \omega_2 = \sqrt{\frac{m_2}{V_w}}; \quad (39)$$

$m_1$  and  $m_2$  are corresponding wave spectrum moments.

Let's express the derivative of the breaking wave energy as function of the breaking wave energy and the derivative of the wave height using formulae (29) and (37).

$$\dot{E}_B(\dot{h}_w) = 3 \cdot \sqrt[3]{k_{red} E_B^2} \cdot \dot{h}_w, \quad (40)$$

and then, let's find the inverse function:

$$\dot{h}_w(\dot{E}_B) = \frac{\dot{E}_B}{3 \cdot \sqrt[3]{k_{red} E_B^2}}. \quad (41)$$

The conditional distribution of the derivative of the breaking wave energy can be found as the

distribution of monotone deterministic function of one stochastic argument  $\dot{h}_w$ .

$$f_{EB}(\dot{E}_B|E_B) = f_{dh}(\dot{h}_w(\dot{E}_B)) \cdot \left| \frac{\partial \dot{h}(\dot{E}_B)}{\partial \dot{E}_B} \right| \quad (42)$$

Substitution of formula (41) into (42) and its further simplification yields:

$$f_{EB}(\dot{E}_B|E_B) = \frac{1}{12\sqrt[3]{k_{red} E_B^2} \sqrt{\pi V_w (\omega_2^2 - \omega_1^2)}} \times \exp\left(-\frac{\dot{E}_B^2}{72V_w (\omega_2^2 - \omega_1^2) \sqrt[3]{k_{red} E_B^4}}\right) \quad (43)$$

Having formulae (35) and (43) it is not difficult to derive formula for required the combine distribution of the breaking wave energy and its derivative.

The other term of the (27) is the kinetic energy of a ship when she reaches maxima of roll velocity. It is described by the following equation:

$$E_F(t) = K(\dot{\phi}_{max}) = \frac{1}{2}(I_x + M_{44})\dot{\phi}_{max}^2 = \frac{1}{2}mQ(t)^2 \quad (44)$$

The distribution density of the kinetic energy can be obtained by the same way that above:

$$f_{EF}(E_F) = \frac{1}{4mV_\phi} \exp\left(-\frac{E_F}{4mV_\phi}\right) \quad (45)$$

as well as the combined distribution density of the ship roll kinetic energy and its derivative:

$$f_{EF}(E_F, \dot{E}_F) = \frac{1}{16\sqrt{\pi m^3 V_\phi^3 (\omega_{Q2}^2 - \omega_{Q1}^2)} E_F} \times \exp\left(-\frac{\dot{E}_F^2}{16mE_F V_\phi (\omega_{Q2}^2 - \omega_{Q1}^2)} - \frac{E_F}{4mV_\phi}\right) \quad (46)$$

Where:  $\omega_{Q1}$  and  $\omega_{Q2}$  are the first and the second relative moments of the roll velocities spectrum, that should be calculated as above and  $V_\phi$  is the variance of the roll velocities.

Our next purpose is to find a combine distribution of the process  $P_R$  and its derivative  $\dot{P}_R$ . Taking into account (27) and our further stipulations, it is not difficult to see that:

$$P_R = E_B + E_F; \text{ and } \dot{P}_R = \dot{E}_B + \dot{E}_F. \quad (47)$$

It will be convenient to present the process  $P_R$  and its derivative as components of some stochastic vector:

$$\vec{P}_R = (P_R, \dot{P}_R); \text{ and } \vec{P}_R = \vec{E}_B + \vec{E}_F \quad (48)$$

As it is known (see, for example [21]) a distribution density of sum of two stochastic vectors can be expressed as:

$$f_P(\vec{P}_R) = \int_{-\infty}^{+\infty} \int_0^{P_R} f_{EB}(\vec{E}_B) f_{EF}(\vec{P}_R - \vec{E}_B) dE_B d\dot{E}_B \quad (49)$$

or, in scalar form:

$$f_P(P_R, \dot{P}_R) = \int_{-\infty}^{+\infty} \int_0^{P_R} f_{EB}(E_B, \dot{E}_B) \times f_{EF}(P_R - E_B, \dot{P}_R - \dot{E}_B) dE_B d\dot{E}_B \quad (50)$$

Limits of the integration are to be chosen with taking into account that energies are not negative figures:

Upper limit is maximal value of  $P_R - E_B$ ; evidently it is  $P_R$ ;

Low limit is minimum value of  $P_R - E_B$ ; evidently it is 0.

Let's consider an expression under integral symbols in formula (50) in more detail:

$$f(E_B, \dot{E}_B, P_R, \dot{P}_R) = f_{EB}(E_B, \dot{E}_B) f_{EF}(P_R - E_B, \dot{P}_R - \dot{E}_B) \quad (51)$$

taking into account all above consideration this figure can be presented as:

$$f(E_B, \dot{E}_B, P_R, \dot{P}_R) = \frac{1}{2304\pi a_{red} E_B \sqrt{m^3 V_\phi^3 V_\zeta^3 (\omega_2^2 - \omega_1^2) (\omega_{Q2}^2 - \omega_{Q1}^2)}} \times \exp \left( - \frac{\dot{E}_B^2}{72 V_\zeta (\omega_2^2 - \omega_1^2) \sqrt[3]{a_{red}^2 E_B^4}} - \frac{1}{8 V_\zeta \sqrt[3]{a_{red}^2}} \left( \frac{(\dot{P}_R - \dot{E}_B)^2}{16 m V_\phi (\omega_{Q2}^2 - \omega_{Q1}^2) (P_R - E_B)} - \frac{(P_R - E_B)}{4 m V_\phi} \right) \right) \quad (52)$$

Formula (52) is quite complicate, while the internal integral in (50) can be found in elementary functions. However expression obtained is too complicate to be analysed symbolically. The external integral in formula (50) can be obtained only numerically.

The last step is numerical calculation of the intensity of upcrossing of the process  $P_R$  through level  $P(\phi_v)$  in accordance with formula (28) that is a value of the risk function of capsizing due to breaking wave if such a meeting has been taken place.

## 7 CONCLUSIONS AND COMMENTS

The main idea that allows to estimate risk function of ship capsizing caused by breaking wave action is energetic one: energy of breaking wave - ship interaction could not exceed full energy wave before breaking. Energy/work balance approach allows to model phenomena physics of which is not investigated completely yet.

The energy of interaction could be expressed as full energy of wave with from equal to ship length and taken with some reduction coefficient that expresses other factors of energy consumption. Numerical value of the coefficient can be obtained from available experimental data. The coefficient does not depend on the GZ curve and does depend on the ship architecture (where ship has bulwark or rail).

Despite of the above comments, the solution described can be considered as some illustration due to severe simplifications, authors have to implement in order to get the formulae. To get practical method it would be useful to study adequacy of the mathematical model of nonlinear ship motion in form of equation of first integrals, where balance of works of damping and excitation moment considered independently.

As it was pointed out the probability of a wave to be broken is a separate problem that deserves separate study.

The other step to the second expansion could include using Stocks wave instead of small wave hypothesis. The probabilistic scheme also could be improved by consideration of the probability of the wave to be broken as a function of time.

At the same time even the first expansion allows to go step-by-step through the estimation procedure of risk function of ship capsizing due to breaking waves action.

## REFERENCES

1. Sevastianov, N.B. An Algorithm of Probabilistic Stability Assessment and Standards, *Proc. of 5th STAB conference*, Vol. 5. Melbourne, Florida, 1994
2. Kobylinski, L. Stability Standards and Probability of Capsizing - Philosophical Aspects, *Proc. of Sevastianov Symposium*, Vol. 1, Paper 1. Kaliningrad Technical University, Kaliningrad 1995
3. Dahle, E.Aa. and Kjeldsen, J. The capsizing of m/s Helland-Hansen, *Naval Architect*, RINA, March, 1980, No.2
4. Balitskaya, E.O. Some results of investigation of ship behaviour in shallow breaking waves, *Tr. of the Register of USSR "Theoretical and practical problems of stability and unsinkability"*, Transport,

- Moscow - Leningrad, 1965, pp.147-165 (in Russian)
5. Kholodilin, A.N. On small ship stability regulations, *Tr. of the Register of USSR "Theoretical and Practical Problems of Stability and Unsinkability of Sea Vessels"*, Morskoy Transport, 1963, pp.45-51 (in Russian)
  6. Kholodilin, A.N. and Tovstikh, E.V. The model experiment for the stability of small ships in erupting waves, *Proc. 12th ITTC*, Rome, 1969, pp. 795-797
  7. Kholodilin, A.N. and Mirokhin, B.V. The action of the erupting shallow water waves upon the models of ships, *Proc. of 13th ITTC*, 1972
  8. Sevastianov, N.B. Practical and scientific aspects of stability problem for small fishing vessels, *Proc. of Int. Conf. on Design Considerations for Small Crafts*, RINA, London, 1984, pp.13-15
  9. Cerka, J and Batuev, A.D. Influence of superstructures and deck houses on capsizing probability, *Tr. of Nikolaev Shipbuilding Institute*, Nikolaev, 1985, pp.48-56 (in Russian)
  10. Kjeldsen, S.P. and Myrhaug, D. Kinematics and dynamics of breaking waves, Part 4 of Report "Ship in Rough Seas" of River and Harbour Laboratory at Norwegian Institute of Technology, Report No STF60 A78100, Trondheim, 1978
  11. Nechaev, Yu.I., Modelling of ship stability in waves, Sudostroenie, Leningrad, 1989, 240 p., (in Russian)
  12. Sevastianov, N.B. Experiment and theory in applied hydromechanics, *Tr. of Krylov society "Problems of Seakeeping of Ships and Ocean Vehicles"*, Vol. 515, Sudostroenie, Leningrad, 1991, pp.4-9 (in Russian)
  13. Dahle, E.Aa., Myrhaug, D. And Dahl, S.J. Probability of capsizing in steep and high waves from the side in open sea and coastal waters, *Ocean Engineering*, Vol. 15 1988, pp 139-151
  14. Dahle, E.Aa., Myrhaug, Risk analysis applied to capsize of smaller vessels in breaking waves, *Proc. Hornafjordur International Coastal Symposium, at Hofn, Hornafjordur, Iceland, 1994*, pp 629-636
  15. Dahle, E.Aa., Enerhaug, B. and Myrhaug, D. Risk analysis applied to capsize of smaller vessels in breaking waves with examples from Russian waters, *Proc. of Sevastianov Symposium*, Vol.1, paper 2, Kaliningrad Technical University, Kaliningrad 1995
  16. Belenky, V.L., Degtyarev, A.B. and Boukhanovsky, A.V., Probabilistic qualities of severe rolling, *Proc. of Sevastianov Symposium*, Vol.1, paper 7 Kaliningrad Technical University, Kaliningrad, 1995.
  17. Belenky, V.L., Degtyarev, A.B., and Boukhanovsky, A.V., Probabilistic qualities of nonlinear stochastic rolling, *Ocean Engineering*, 1997, Vol. 25, pp. 1-25 in press
  18. Sveshnikov, A.A., Applied methods of stochastic function theory, "Nauka" Moscow, 1968., (in Russian)
  19. Boroday, I.K., Netsvetaev, Yu.A. Seakeeping of ships, Sudostroenie, Leningrad, 1982, 288 p. (in Russian)
  20. Boroday, I.K., Netsvetaev, Yu.A. Ship motion in a seaway, Sudostroenie, Leningrad, 1969, (In Russian)
  21. Ventsel, E.S and Ovcharov, L.A. Theory of probability and its engineering applications, Moscow, Nauka, 1988 (in Russian)

22. IMO doc. SLF/28 11 Jan 1984, Intact stability of fishing vessels in breaking waves Results obtained on small trawlers, Submitted by USSR

### **ASKNOWLEDEGEMENT**

This work was supported by the Polish Committee of Scientific Research under Grant KBN nr 9 T12C 046 08 «Zintegrovany system oceny bezpieczenstwa statku na sfalowanym morze przy uzyciu metod probabilisticznych», supervisor J. Bielanski

Participation of the authors in this work was in the frame of international scientific cooperation between Kaliningrad State Technical University (Russia) and Technical University of Gdansk (Poland) The authors are grateful to Professor Lech Kobylinski and Dr. Jan Bielanski for discussions and help provided in the course of this work The contents of this paper is based on reports of Technical University of Gdansk No 3/96 and 11/96

**APPLICATION  
OF EXPERT SYSTEMS  
AND ON-BOARD COMPUTERS  
FOR STABILITY MONITORING  
AND CONTROL**

# SPECIALIZED SOFTWARE FOR STABILITY CONTROL ON BOARD RO-RO SHIPS

V Rakitin, V Chalakov, R. Kischev, *Bulgarian Ship Hydrodynamics Centre, Varna, BULGARIA*  
N. Lyutov, *Varna Free University, Varna, BULGARIA*

## ABSTRACT

Development and operational features of an on-board computer system for Ro-Ro ship loading, stability and strength control is described. An important novelty in the system structure is the inclusion of ship behaviour prediction in real seas. Trial runs proved its compatibility with acting regulations and standards, and it is recently installed for regular operation on board four Ro-Ro ships under Bulgarian ensign.

## 1. INTRODUCTION

After detailed examination of the expedience of computerized system's utilization for stability, strength and seakeeping control as well as tendencies of their elaboration and operational requirements stated by customers, an advanced version of PC based on-board system for operational control has been developed at BSHC [1], [2]. Its universality enabled quick adaptation to different ship types, such as bulkcarriers, containerships, multipurpose ships, etc. Recently, the same basic algorithms were utilized to extend the applicability of the system to Ro-Ro ships.

The RO-RO MASTER program package assists for convenient and quick estimation of ship statics, stability, girder forces and hull deflections at given realistic case of loading. It also permits elaboration of sample cargo plan variants and their assessment from the view point of stability, strength and seakeeping criteria imposed. The program modules operate utilizing exact hull form description and calculations in real time of hydrostatics, load distribution curves and buoyancy. Even if the

procedure does not replace official documents such as "Information on stability" or "Calculations on ship strength", it appears as an instrument for facilitating of ship operation and multiplies application of standard documentation by its possibility to create and assess variety of situations arising at reality.

The compound program modules for calculations on statics, stability, strength and seakeeping are based on classical theoretical methods certified by Bulgarian Register of Shipping (BRS), use is also made of operational data taken from ship's documentation, as well as some systematic model test's results.

The system operation and service is made user-friendly, not requiring specialized knowledge on computers, which make it especially attractive to crew members.

## 2. GENERAL STRUCTURE OF THE PROGRAM PACKAGE

The RO-RO MASTER program package consists of following general modules:

\* **Initialization** - Input and organization of all necessary data concerning ship particulars, construction, ownership, classification, etc.

\* **Input Data** - Detailed hull form description, light ship load distribution, disposition and geometry of cargo holds, fuel, ballast and other tanks, location of single cargo units, etc.

\* **Initial Calculations** - Cargo plan compilation and static calculations. Ship static parameters are evaluated instantaneously after any change in loading status during preparation or check-up of the current cargo plan.

\* **Stability** - Evaluation of actual initial stability, as well as operational stability. Calculations are performed parallel with static calculations using exact hull form description and accounting for actual trim and heel. Stability evaluations follow IMO Resolutions A 562 (14), A 167 (ES.IV) and A.206 (VII), as well as methods approved by BRS.

\* **Strength** - Evaluation of current ship girder loadings in still water and at real operational conditions. Calculations follow BRS recommendations and are in conformity with Lloyd's Register Rules, Chapter 4 - Longitudinal strength.

\* **Seakeeping** - Prediction of ship behaviour in real environment. Calculations are based on a precipitated version of the strip theory and where applicable model and full scale test results are utilized for calibration. For convenience, observed wave height and course angle are used as input.

### 3. SYSTEM FUNCTIONS

The RO-RO MASTER program package has following functional abilities:

\* Elaboration of ship cargo plan - new compilations as well as recalling of stored cases. Ship loading is evaluated step by step starting with light ship parameters and proceeding with every load item - service and ballast tanks, cargo decks, etc. Adding, removing or shifting cargo units (trailers) is envisaged during compilation and water density could be changed, thus giving to the procedure freedom for variational compiling and check-up of actual cargo plans.

\* Instantaneous (real time) evaluation of ship displacement, draft, trim, heel and CG position after any single change in loading elements.

\* Instantaneous estimation of stability (metacentric height, static stability arm, free surface's influence, wind action influence, etc.).

\* Instantaneous estimation of ship loading, shearing force, bending moment and hull deflection distributions along the ship length.

\* Seakeeping predictions (natural periods of motion, roll, pitch and heave amplitudes and accelerations, wave shearing forces and bending moments, deck wetness, slamming, expected speed loss)

\* Real time visualization of status describing values such as ship displacement, draft aft, fore and middle, static heel, trim, CG position, metacentric height

\* One-button-touch visualization of load distribution curve, shearing force, bending moment and hull deflection distribution.

\* One-button-touch visualization of polar diagrams of calculated seakeeping parameters.

\* Preparation and printing of standard documents such as:

- Loading condition general particulars;
- Disposition plan for loading units and their particulars (the program allows introduction of different unit sizes and deck arrangements but accounts for actual deck plan);
- Current filling of service and ballast tanks (available stores and ballast);
- Protocol of actual stability parameters and static arm diagram;
- Protocol of actual hull strength;
- Data sheet of seakeeping calculations and predictions.

### 4. SYSTEM OPERATION

The user-friendly system operation utilizes hierarchical menu organization with memorizing of interruption points and screen images mobility

#### 4.1 Main Options

The main menu comprises of following items:

\* **Ship Initial Data** - gives ship registration data, her main particulars and light ship information,

\* **Corrections** - affords alternative corrections in water density, free surfaces, trim and dead loads characteristics;

\* **Destination** - introduces information for the route parameters,

\* **Service Tanks** - describes parameters of service tanks for heavy and diesel oil, lubrication oil, fresh water, etc, according to their current status (filling) and visualize their position on the screen plan by blinking (Fig 1),

\* **Water Ballast** - describes general particulars of the water ballast tanks and their current status, and visualize their position on the screen plan by blinking,

\* **Stores** - keeps and renew when necessary information about crew and its luggage, stores, etc ,

\* **Cargo Operations** - a basic item in the main menu, which allows introducing trailer's weight, length, distances at positioning, identification info, etc The selected unit is visualized on the screen (Figs 2 and 3) by its position on the deck, and in the same time the data are transferred to a table systematizing current info about trailers - total number, weight total, etc ,

\* **Graphic Options** - visualize diagrams of load distribution, girder loads distribution and stability arm curve, parameters of which are calculated in real time during compilation of current cargo plan (Figs 4,5,6),

\* **Seakeeping Predictions** - estimates ship behaviour (periods and amplitudes of motion, speed loss, slamming and deck wetness probability) in current loading status at conditions identified by visual wave parameters, heading and speed of advance, builds and visualize corresponding polar diagrams (Figs 7, 8),

\* **Print-Outs** - prints all requested output documentation,

\* **Saved Conditions** - saves up to 15 variants of loading and supplies them by request,

\* **Program Stop** - quit loading case compilation with or without saving

## 4.2 Cargo Plan Creation

Cargo plan compilation makes use of hierarchic submenus, renewable screen images of loading areas and renewable table presentation of

keyed-in information The operator is free to choose the order of introducing new cargo units, and to save or delete current status of loading At any new entrance, instantaneous values of ship static are calculated and showed on the screen All this makes the procedure user-friendly, convenient and fast, useful for training as well as for preliminary preparations

## 4.3 Control Messages

To ease operator's action and to avoid failures, the program modules perform control functions also, concerning logic and feasibility of keyed-in instruction Control messages appear on the screen and inform for

- \* lack of space or access to accomodate a trailer at selected position,
- \* invalid trailer parameters,
- \* exceeding of actual tank volume,
- \* dangerous decrease of instantaneous initial metacentric height,
- \* total loss of stability during loading,
- \* exceeding allowable hull stresses, shea-ring forces or bending moments,
- \* exceeding allowable seakeeping criteria
- \* quitting cargo plan compilation without specifying the case, etc.

Screen messages are cancelled by simple strocke of any key

## 4.4 Output Documents

After completing of loading or discharge operations (completing of current cargo plan), following documents could be issued.

\* **Trim & Stability Book** - generalized data for current ship displacement, draft and stability, to be signed by the authorized operator,

\* **Ship Condition** - data for ship loading and stability in table form,

\* **Deck Cargo Plan** - plan for cargo units arrangement in rows on upper, main and car decks, including table of trailers weights and identification numbers,

\* **Service Tanks** - data tables for available quantities stored into service tanks,

\* **Ballast** - data tables for available water quantities stored into ballst tanks,

\* **Ship Stability Data** - initial ship stability data, such as metacentric height and corrections, stability arms, heeling angles, etc ,

\* **Ship Strength** - actual values of still water shearing forces, bending moments and hull deflections under current loading,

\* **Seakeeping** - predictions of ship behaviour in waves under current loading, including motion amplitudes, accelerations wave shearing forces and bending moments, probabilities of occurrence of slamming and deck wetness, speed loss, etc

## CONCLUSIONS

Judging from the functional abilities of the on-board computer system RO-RO MASTER created at BSHC, following main operational advantages covering ship owner's interests in effective ship operation could be pointed out

\* Possibilities for full utilization of ship loading capacity and speeding the time for loading/discharging,

\* Possibility for loading control,

\* Obtaining of actual parameters of ship stability and strength,

\* Control of ship behaviour at sea and possibility for selecting safe and efficient operational regime,

\* Possibility of personnel training,

\* No special knowledge on computers is required, the system operation being user-friendly,

\* Possibilities for upgrading and modifications to match different customer requirements, for example mixed loading, extention or rearrangement of cargo decks, etc

The RO-RO MASTER package has successfully passed three monts trial runs on board "Sredetz" Ro-Ro ship sailing under Bulgarian ensign, and it is recently installed for regular operation on other sisterships of the series

## REFERENCES

1 Lyutov N , Kischev R , Chalakov V , Rakitin V - *Program Aspects in Developing an On-Board Computer System for Ship Stability and Strength Control* - Paper No 27, ACMBUL'93 International Conference, Varna, 1993

2 Rakitin V , Kischev R , Lyutov N , Chalakov V - *The CONSTABLE Program Package as a Basis for Generation of Computerized On-Board Systems for Ship Stability and Strenght Control* - International Conference on Computer Application on Board Ships, Varna, 1995

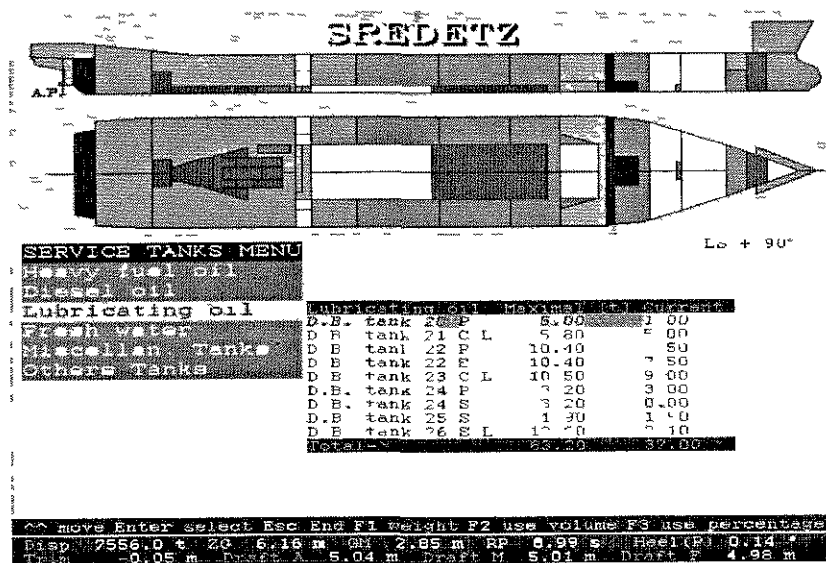


Fig. 1 Screen image of the lubricating oil tanks situational plan

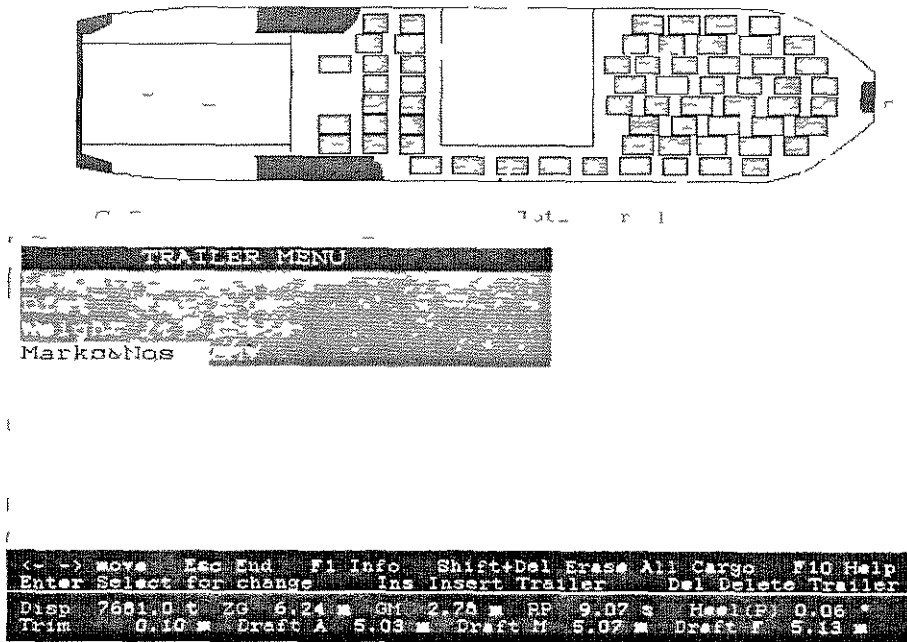


Fig 2 Screen image of the car deck situational plan



Fig 3 Screen image of the upper deck situational plan

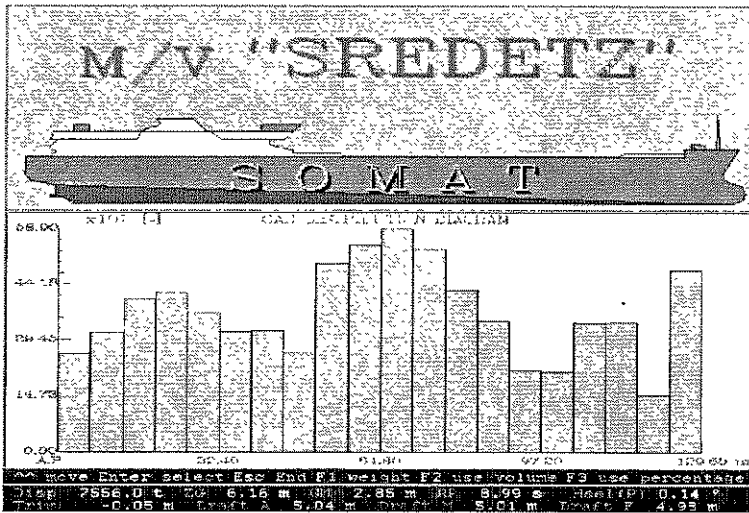


Fig. 4 Screen image of the load distribution curve

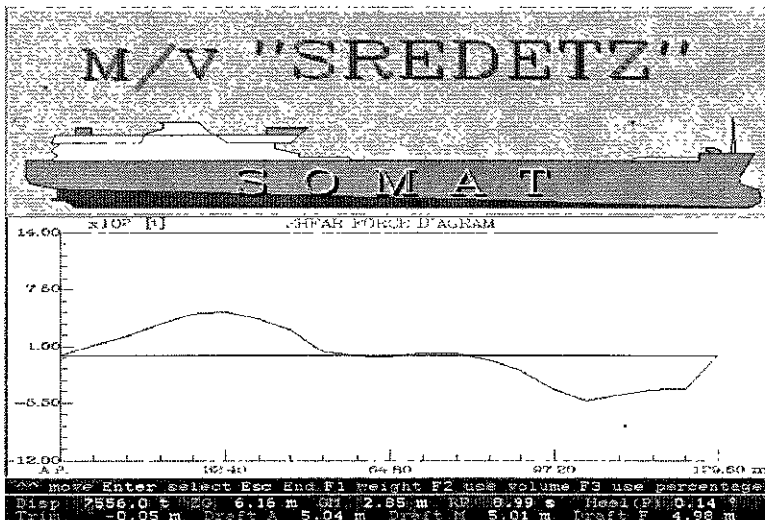


Fig. 5 Screen image of the shearing force distribution curve

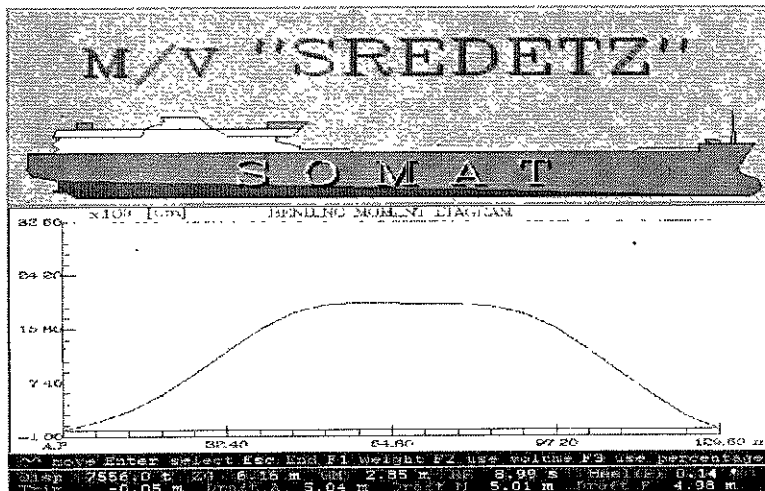


Fig. 6 Screen image of the bending moment distribution curve

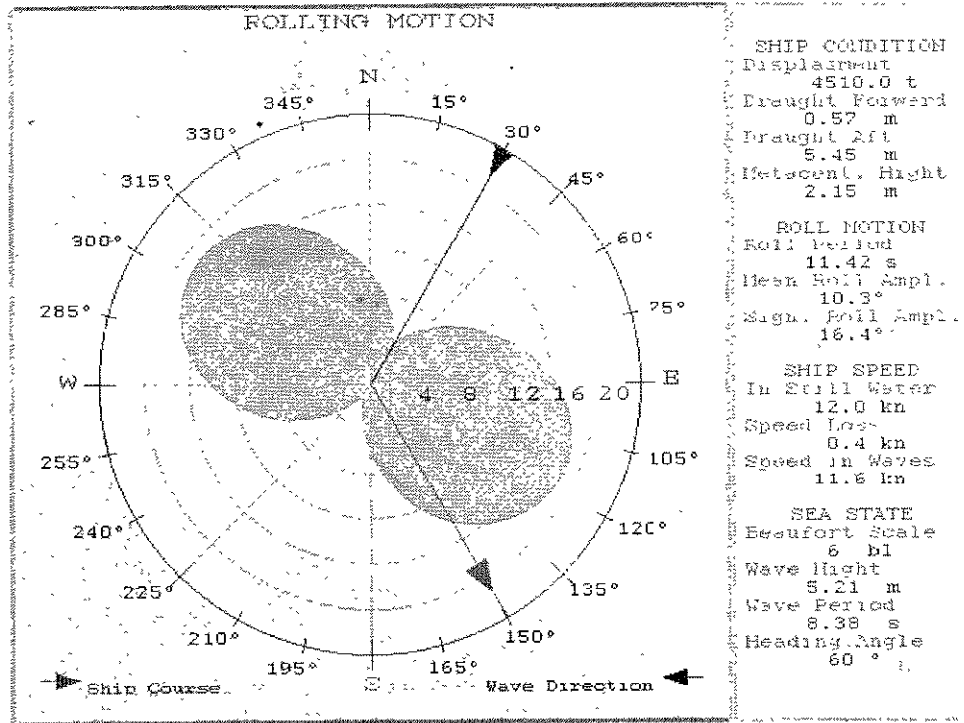


Fig. 7 Roll angles diagram

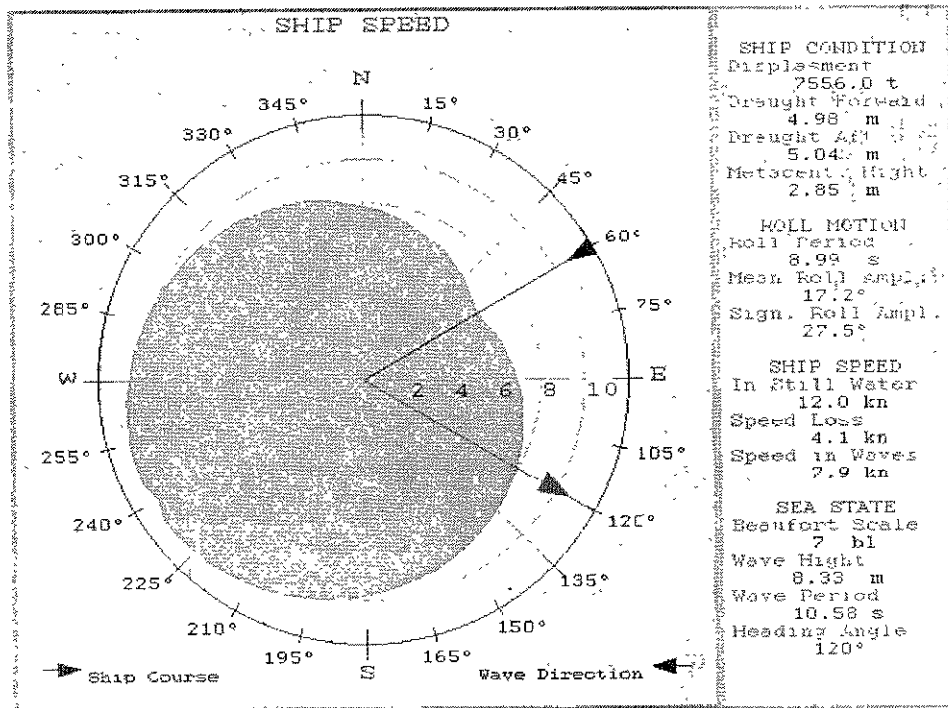


Fig. 8 Attainable operational speed diagram

## THE FULL-SCALE TEST OF THE INTELLIGENCE SYSTEM OF THE SHIP SEAWORTHINESS ANALYSIS AND PREDICTION

V I Alexandrov, D M Rostovtcev, A P Matlakh,  
Yu I Nechaev, V I Polyakov  
State Marine Technical University,  
State Enterprise «Admiralty Shipyard»,  
Saint-Petersburg, Russia  
E-mail: polestar@mail.wplus.net

### ABSTRACT

The full-scale test results of the intelligence system (IS) for providing the ship seaworthiness are discussed. The experiment has been carried out under various hydrometeorological situation on a small boat, containership and tanker for checking the system operation under various conditions of service and the interaction of human-computer in decision making.

### INTRODUCTION

The ship dynamics on waves is one of the most complex problems dealing with the interaction of the ship and environment in storm conditions. The uncertainty of the initial information and data incompleteness about the physical pictures of interaction result comprehensive investigation of the ship behavior features on seas as a non-linear dynamic system with various characteristics of external disturbances. Accumulation of these data will give sound reasons to solve the safe navigation problem by means of operative seaworthiness estimation and to make sound decisions by means of intelligence system.

The stored in IS knowledge is much more than the navigator memory possibilities. It is not available from the ship documentation and is not only the theory of ship and experimental hydromechanics achievements, but it is data reflecting original approaches

for the processing, analysis and representation of the actual information about the ship seaworthiness changes, and also the professional experience of the highly skilled experts.

Of special practical interest are measurements data of the seas parameters, stability and the damaged ship grounding (heel trim equilibrium angles, emergence metacentric height, stability diagram), their processing and analysis are made in real time scale. This allows to essentially increase the situation estimation certainty and the quality of decisions made in the ship survivability.

There are other, more important reasons for IS developing. First, this is the problem position about the estimation of ship dynamics on seas. The problem is complex and scantily investigated, the seaworthiness estimation requirements (especially of a damaged ship) are various and sometimes contradictory, all this makes the operative practical problems solution very difficult in the conditions of time limit, uncertainty of external forces and ship dynamic characteristics on the basis documentation at the navigator's disposal.

The ship damages analysis shows the navigators' miscalculations and errors in decision making under the emergency situations. Unlike others, the IS has a quality to quickly response to the continuously changing environment and explain the navigator the rules according to which the

proposes recommendation has been worked out.

The results of the IS «Seaworthiness» full-scale test carried out on various stages of outer disturbances on ship of different purposes are discussed in the paper. Special attention has been paid to estimation the efficient operation of the knowledge base (KB) declarative and procedure component and the interaction human- computer in the situations analysis and decision making.

## 1. THE SYSTEM CHARACTERISTICS

The IS «Seaworthiness» is an intelligent assistant for the navigator and is intended to provide the seakeeping capabilities of ships and floating technical vehicles used for the ocean exploration under various service conditions, including emergencies. The system operation is provided by computer software in the real-time scale [1-4]

Operations, performed by IS, contain control and prediction of the seas, ship seaworthiness estimation, evaluation and prediction of stability in the conditions of increasing storm intensive icing, the choice of the optimum heading angle and speed depending on the requirements of stability, oscillation, propulsion and strength on waves, estimation and prediction of ship fouling effect and producing practical recommendations as to ship steering in storm. The system gives the navigator the unique information that is not available in the ship documentation.

Fig. 1 shows the structural scheme of the IS «Seaworthiness»

Knowledge representation in the contents is conventional for complex system using the artificial intelligence technology. Peculiarities of the searching space and the subject field resulted in the IS architecture, this is typical for the consultative type systems, operating on the basis of data measurements, simulation and structural knowledge base (NB).

The basis of the developed NB model, containing declarative and procedure components, is the logic structure that includes models of situation evaluation and

condition identification of the complex hierarchic system under conditions of

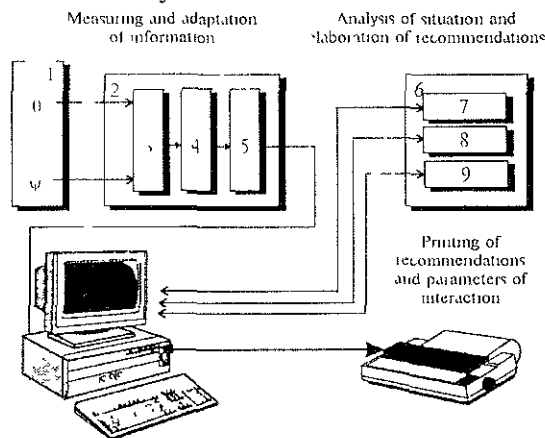


Fig. 1. The structural scheme of the IS «Seaworthiness»: 1 - Sensor block, 2 - module of transformation initial data, 3 - commutator, 4 - analog-digital transformer, 5 - interface, 6 - expert system, 7 - data base, 8 - knowledge base, 9 - conclusion machine

incompleteness and uncertainty information. Models for the making decision are aimed of actual measurements data of the interaction processes of the floating object and the environment.

The formalized knowledge system was created by conceptual modeling methods by means of the knowledge analysis, systematization and structurization about the ships dynamics under various operational conditions. As a model of knowledge representation we use the production rules that are formal structure which controls knowledge, allows to provide knowledge organization modeling, rules independence and enables to separate the controlling and subject knowledge. The output mechanism suggests using obscure considerations. The obscure aims concept is the methodological base for designing decision makes the procedures under these circumstances. Along with the symbol includes quite a number of operations that need numerical and algorithm methods. All this allows to increase the decision making process efficiency under extreme situations.

The information technology requirements are generally stated as follows:

1. The knowledge representation is in the form of structures reflecting the general output rules, storing and modifying of which is

independent of the used algorithms and programs, all this secures

- software flexibility.
  - completeness of the data forming and analysis problem.
- 2 Composition of the applied simulation should provide its component correction in accordance with the systems adaptation to various operation conditions.
  - 3 KB operation in the IS is independent of the applied information volume in the confidence probability range 0.80 - 0.95.

## 2. RESULTS OF THE EXPERIMENTS

The IS full-scale tests have been carried out aboard the tanker in the Baltic sea, of the container ship in a voyage in the Mediterranean and the Atlantic on a small ship in the Black sea. The most complete investigation of the IS operation was checked on the small ship, where the ship motions on waves were chosen according to specially developed program.

In the course of the test operation the dynamic characteristics measurements, this system adaptation and finishing, receiving new knowledge about the ship behavior on seas and their integration with the old ones were carried out. The following factors were of special practical interest: testing the working capacity of the applied methods for estimating and predicting the seas parameters, the transverse stability characteristics and the KB reaction on the standard and non-standard situations arising in the seaway. All this allowed is to correct the mathematical models of the interaction of the ship and environment, the mechanism of logical output and the procedure of decision making on the basis of fuzzy aims and limitations.

The test proved the possibility of practical evaluation and prediction of the dynamic characteristics, the reliability of KB operation under various conditions of service.

The displacement of the containership was 15 000 tons, of the tanker – from 25 000 to 40 000 tons and that of the small ship was 160 - 200 tons. The sea waving was 6 numbers and more in the containership trials

and 3-5 numbers for the small ship. The tanker trials were on moderate sea (up to 3 numbers) and aimed exercising the IS reaction to the operations resulting from appearing external disturbance forces and moments (circulation, anchor trials, ballasting, etc.).

Waves conditions were characterized by the spectrum density the approximation of which with the adequate practical accuracy was achieved also by using the Barling spectrum.

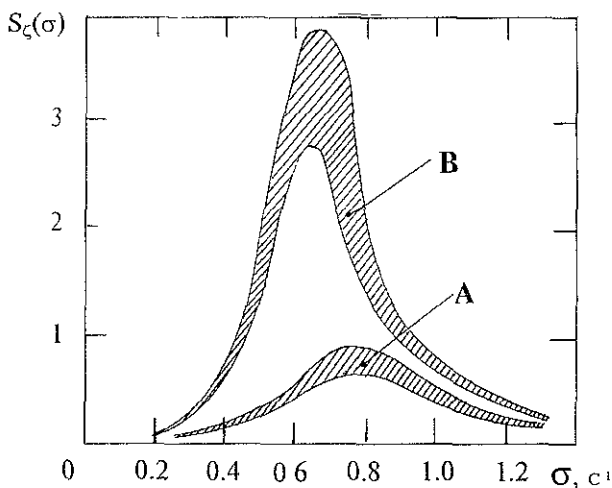


Fig. 2. Areas of changing spectral characteristics of wave: A - 5 balls; B - 6 balls

Fig. 2 shows the fields of changing spectrum components in the limits of the fixed numbers for the 5-6 numbers seas.

Table 1 shows the comparative data about the different ways of measuring seas parameters [5], where you can see that the IS method applied to the seas estimation on the basis of identification method gives good results that coordinate with the actual the measurement data received by means of standard wave-meters and systems (string wave recorder, laser sensor, wave recorder GM-32).

The seas parameters prediction was carried out by the adaptive model with the 4 and 8 hours advance (Fig. 4). These data control by independent measurements demonstrate the working ability of the applied adaptation procedure considering the prediction model class

The oscillation regimes observed in the trials, covered different frequency conditions, due to combinations of ship speed and the wave heading angle

It is interesting to note that for the small ship the rolling was observed generally in the field of the main resonance (Fig. 3A) or the containership this behavior was observed only for pitching. However, during the containership trials we could record parametric resonance under the action of three-dimensional waves packets during ship movement with the heading angle on the astern seas (Fig. 3B).

Table 1. Wave height measurement (3% providing, m)

Wave force, (balls)	Laser sensor	Wave recorder GM-32	String wave recorder	Designed algorithm	Max Div, %
3	-	-	1,17	1,23	5,1
4	1,80	1,74	1,76	1,85	6,3
5	3,28	3,17	-	3,40	7,2
6	5,72	5,61	-	5,83	3,9

The operative control of the transverse metacentric height is done by two methods by using gradually more complex regression models [4] and on the basis of direct measurements of variable cargoes liquid levels. As you can see on Fig. 5, in both cases the received estimates are not beyond the 5 percent confidence interval.

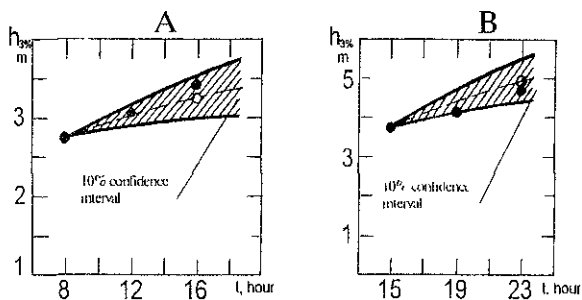


Fig. 4 Wave height prediction (3% providing)

A - small ship; B - containership (• - measurement results, o - predict results)

Table 2 gives the general characteristics of the selected test conditions and the received results.

During the run trials of the tanker the IS was used for checking the ship reaction on the outer disturbances ( forces and

moments), arising in the carrying out of conventional operations according to planned program. In particular, the applied methods for the estimating elements of

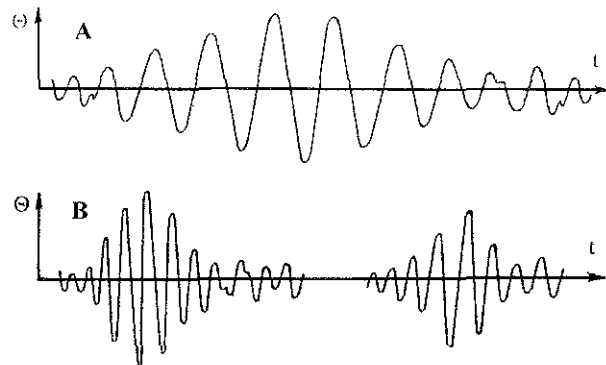


Fig. 3. Time curve characterizing regime of main (A) and parametric (B) resonance

buoyancy and stability (the ship grounding parameters, the initial metacentric height, diagrams of the static and dynamic stability, etc.) have been checked in various ship loading, also dynamic characteristics, determining the ship heel on turning and

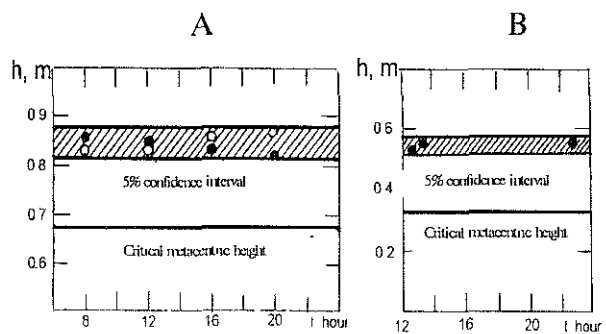


Fig. 5. Metacentric height estimate:

A - small ship; B - containership (• - measurement results, o - predict results)

other maneuvers have been recorded.

Table 2. Comparison characteristics of seaworthiness (selective data)

Ship's type	Small ship		Containership		Tanker	
Ship's velocity, kn.	6	0	14,5	14,0	5	5
Head angle, deg.	45	90	10	10	0-360	0-360
Draught, m	2,2	2,1	7,64	7,65	11,3	7,5
Wave length, m	20	26	43,4	67,5	22	23
Wave period, sec.	4,3	5,0	5,6	8,1	4,6	4,7
Wave height 3%, m	1,75	2,3	3,96	5,00	1,9	2,0
Rolling 3%, deg.	12	16	5,6	6,5	-	-

Pitching 3%, deg	2,8	1,9	1,3	1,5	-	-
Actual metacentric height, m	0,84	0,83	0,530	0,525	0,8	1,8
Critical metacentric height, m	0,50	0,49	0,328	0,327	0,6	1,0
Heel on circulation, deg	-	-	-	-	3,2	9,6
Loss of speed, kn	3	1	2,3	2,8	-	-

In the full-scale conditions the information process models which reflected the situation dynamics in KB operating were being developed. Many useful advises and proposals which have been considered in improving the graphic interface in the KB system were given to the navigator

## CONCLUSION

The test carried out demonstrate the IS reliability and the necessity of its application in the practical evaluation of ship seaworthiness under various service conditions. The received data are an important information for improving methods of dynamic characteristics operative control, determining the ship seaworthiness, for increasing safe navigation.

The full-scale experiment provide the possibility of applied the developed methods of estimating seas parameters and stability control in IS of real time.

The visual presentation of the information on the display screen by means of graphic images made it possible to create a convenient device for reflecting the complex structured data. This allows the navigator to expand his image-intuition thinking, especially in the stages of situation identification and decision making for ensuring safety of the ship and the crew.

## REFERENCES

1. Alexandrov V.L., Rostovtcev D.M., Matlakh A.P., Nechaev Yu.I., Polyakov V.I. The Intelligence System of Analysis and Prediction of Tankers Seaworthiness. Proceedings of the International Symposium «Marine Intelligence system» St -Petersburg, Russia, 1996.
2. Nechaev Yu.I. Full-scale tests of the marine expert system for the ship seaworthiness in extreme situations. Transactions of the conference on artificial intelligence. 1 ver. 1992, pp. 67-68.
3. Nechaev Yu.I. Vessel's Expert Systems - Conception, Problems, Perspective. November 7-11. Florida, USA. 1994. STAB'94. Proceedings Volume 2.
4. Nechaev Yu.I., Dubovik S.A. The estimate of probability of the ships capsizing on a seaway. - Processing of the international symposium Ship safety in a seaway: stability, maneuverability, non-linear approach. Kaliningrad, 15 - 19 May, 1995. Vol 1, Paper 6.
5. Pospelov D.A. Semiotic models in control systems// Architectures for semiotic modeling and situation analysis in large complex systems: Proceedings of the 1995 ISIC Workshop - the 10<sup>th</sup> IEEE International symposium on intelligent control, Aug 27-29, 1995, Monterey (Cal) USA, p.p. 6-12

# ANALYSIS OF EXTREMAL SITUATIONS AND SHIP DYNAMICS IN SEAWAY IN INTELLIGENT SYSTEM OF SHIP SAFETY MONITORING

Yu.I.Nechaev<sup>1</sup>, A.B.Degtyarev<sup>2</sup>, A.V.Boukhanovsky<sup>3</sup>

<sup>1</sup> -- Professor, Dr.Sc., <sup>2</sup> -- Associate Professor, Ph.D., <sup>3</sup> -- Research Fellow, Ph.D.  
Marine Technical University, 3 Lotsmanskaya str., 190008 St.Petersburg, Russia  
Institute of High-Performance Computing and Data Bases,  
PO Box 71, 194291 St.Petersburg, Russia  
deg@fn.csa.ru, nonlin@fn.csa.ru

## ABSTRACT

Approach to analysis and prognosis of extremal situations and ship dynamics in intelligence systems of real time scale is discussed. Concrete data about system testing with the help of special design of instrumental means are given. The report is accompanied by computer illustrations of situations consistency and graphics output information.

## INTRODUCTION

Development of intelligence systems (IS) of ships and offshore safety ensuring is connected with solving different complicated technical problems. These problems depend on variety of fulfilled functions, impossibility of full control of state-vector components, strict requirements to reliability of accepted decisions. These problems are most important in development of real-time intelligence systems. Appearance of such IS in considered problem field is connected with state of the art in analysis and forecast of seaworthiness in exploitation conditions. Complexity of the problem and conflict-

ing requirements make decision very difficult for navigator [1].

IS presents to navigator unique data that could not be received with the help of technical documentation on the ship including information about ship's stability. Based on the data the system carries out situation analysis and generates practical recommendations for choice of the best seagoing conditions in complicated hydrometeorological situation.

The results of investigation of IS knowledge base performance with the help of mathematical modelling data are discussed in this paper. Extremal situation imitation and ship behaviour modelling in different external conditions are fulfilled on the basis of instrumental tool described in [2].

## 1. SEA WAVES MODELLING

Imitation of such phenomena as sea waves, wind, current, sea level variation is extremely difficult. It is connected with stochastic of external excitations. We cannot use only 1D model [4] for adequate sea object behaviour modelling, since external excitation are multidimensional. Moreover, all considered phenomena are cyclic nonstationary. Therefore

they should be considered as polimodulating probability processes and fields [3]. Vector field autoregressive model could be offered for such objects modelling. This model is generalisation of classical 1D autoregressive model [5] Principles of this model are based on passing of white noise through linear vector partial differential equation. Coefficients of this equation are identified with the help of statistical and correlation characteristics of original vector field and depend on modulating field.

Discreet analogue of this equation is defined as

$$\begin{aligned} \overset{r}{V}(x, y, t) &= \sum_{i=1}^N \sum_{j=1}^M \sum_{k=1}^L \Phi_{ijk}(p, \Omega) \overset{r}{V}(x - i\Delta_x, \\ & y - j\Delta_y, t - k\Delta_t) + \overset{r}{\varepsilon}(x, y, t) \\ \overset{r}{W}(x, y, t) &= \overset{r}{Y}(\overset{r}{V}(x, y, t)) \end{aligned} \quad (1)$$

$$\Phi_{ijk}(p, \Omega) = \begin{bmatrix} \Phi^{11}_{ijk}(p, \Omega) & \Phi^{1K}_{ijk}(p, \Omega) \\ \Phi^{K1}_{ijk}(p, \Omega) & \Phi^{KK}_{ijk}(p, \Omega) \end{bmatrix}$$

$$K = \dim(\overset{r}{W})$$

Matrix coefficients of (1) are estimated by the following matrix system solution:

$$\begin{aligned} \sum_{i=0}^N \sum_{j=0}^M \sum_{k=0}^L \Phi_{ijk}(p, \Omega) \cdot K_{\downarrow}(X - i\Delta_x, Y - j\Delta_y, \\ \tau - k\Delta_t | p, \Omega) = K_{\downarrow}(X, Y, \tau | p, \Omega) \end{aligned} \quad (2)$$

However, (1) equation solution has the same distribution law as white noise distribution only in Gauss' case. Modelling of vector fields with any distribution law could be carried out in two ways:

1. Inertialess Gauss field transformation in field with any distribution law [6]. It is admissible only for scalar fields. So this method is efficient when correlation between vector components is in-

significant (for example, wind waves and wind in quasistationary interval).

2. White noise with boundless divided distribution law in equation (1) using [4]. This approach is more difficult, but it could be applied for vector fields

Any external excitations model requires appropriate verification. Evidently only coincidence of statistical and spectral characteristics of elements that are not used for model identification could be verification criteria. For example for 3D waves modelling in quasistationary interval wave spectrum is initial data. So in this case verification parameters are heights, periods, lengths, slopes, 3D-indexes and wave hill heights [3].

Results of verification of 2D and 3D waves, wind and currents models are presented in papers [3, 4, etc.].

## 2. IMITATION MODELLING OF EXTREMAL SITUATIONS

Monte-Carlo method was adopted for analysis of ship's dynamics. The goal of the modelling is rolling statistical characteristics calculation. First rolling was considered as stationary process. This way corresponds to case of nondamaged ship. We investigated both severe rolling [7] and parametric ship oscillations [8,9]. But in all these papers the diagram of transverse righting moment was nonlinear, symmetric and with positive metacentric height. If it is necessary to explore extremal situations and ship dynamics (it is very important for IS learning) such modelling is inadequate. It is essential to model accident process when character of stability diagram is changing due to progressive flooding. We can train IS to recognise accident character based on the results of such modelling. So the goal of mathematical modelling of damaged ship is to investigate evolution of statistical characteristics of nonstationary rolling

when righting moment is changing in some boundaries that are determined by typical accident situations.

We consider five different 10 minutes evolution from initial nondamaged to damaged condition. Progressive flooding is characterised only by changing of stability diagram. Initial diagram and five final diagrams are shown in fig.1

Autoregressive technique was used for exiting forces modelling. Spectral approximation of 2 ICSS [10] with parameters  $\bar{h} = 2.8$  m.,  $\bar{\tau} = 8$  s. was used for waves modelling

All calculations are presented in form of histograms of rolling (fig.2), diagrams of evolution of estimations of mean roll angle, standard deviation (fig.3), std. skewness (fig.4), std. kurtosis (fig.5) and rolling recurrence (fig.6).

On the basis of the results of mathematical modelling we can make the following conclusions:

1. Distribution law in first scenario remains normal. Only motion intensity is changed due to metacentric height changing.
2. Quasinormal distribution law and variance keeping are typical for second scenario of progressive flooding. Rolling population mean is slowly changed.
3. Distribution density becomes double modal in 3rd progressive flooding scenario. At first motion decreases with metacentric height reduction and increase when stability diagram becomes third type. Std. skewness, kontrakurtosis and entropy coefficient vary essentially.
4. Accident situations IV and V can have double development. When static heeling moment is big the system begins to motion only in region of energy depression with high level (e.g. near static heeling angle). Such situation is very similar to second type. Or, when static heeling moment is not big, the system can oscillate with some probability in two stable positions. In this

case distribution density becomes double modal and essentially nonsymmetric. Std. skewness, kontrakurtosis and entropy coefficient vary essentially.

5. Insignificant difference of std. skewness and std. kurtosis from zero could be caused not only by some stable system state but also by S-shape of stability diagram [7].

As shown in fig.7 mathematical modelling of different scenarios of progressive flooding permits to classify different situations in terms of kontrakurtosis and entropy coefficient.

## CONCLUSION

Modelling and interpretation are the main tools of complicated processes analysis in real-time IS. Considered approach for initial data analysis have been realised in IS of control and forecast of seaworthiness and unsinkability of 28400 t DWT tanker. Seakeeping testing of this tanker was carried out in the Baltic Sea. Algorithms of buoyancy and stability estimation in different load conditions that were applied in IS were checked up during these experiments. Dynamic characteristics that define heel in turning and other manoeuvres were marked. As a result models of information processes that describe situation dynamics in knowledge base performance were corrected.

Thus effective performance of knowledge base of seaworthiness IS was developed during imitative modelling and full-scale testing.

## ACKNOWLEDGEMENT

The research is performed with financial support of Goscomitet of Russian Federation of Higher Education, Grant A-446.

## REFERENCES

1. Nechaev Yu.I. Ship-borne intelligence systems: conception and the special features of information, calculation and measuring technology. *Transaction of International symposium "Marine intelligence systems"*, St.Petersburg, June 3-9, 1996. pp.480-489
2. Boukhanovsky A.V., Degtyarev A.B. The instrumental tool of wave generation modelling in ship-borne intelligence systems. *Transaction of International symposium "Marine intelligence systems"*, St.Petersburg, June 3-9, 1996. pp.464-469
3. Boukhanovsky A.V., Degtyarev A.B. Probabilistic Modelling of Stormy Sea Fields. *Proceedings of International Conference "Navy and Shipbuilding Nowadays"*, St.Petersburg, 26-29 February, 1996, Section A, Vol.2, paper A2-29, 10 pp. (in Russian)
4. Rozhkov V.A., Trapeznikov Yu.A. Probabilistic models of oceanological process. L., Hydromet. Ed., 1990 (in Russian)
5. Box D., Jenkins G. Time series analysis. M., Mir, 1974 (in Russian)
6. Shelukhin O.I., Belyakov I.V. Non-gaussian process. SPb., Politechnika, 1992 (in Russian)
7. Belenky V.L., Degtyarev A.B., Boukhanovsky A.V. Probabilistic Qualities of Severe Rolling. *Proceedings of International Symposium "Ship safety in a seaway: stability, manoeuvrability, nonlinear approach"*, Kaliningrad, 15-19 May 1995, Vol.1, paper 7
8. Degtyarev A.B., Boukhanovsky A.V. On the Estimation of the Ship Motion Stability in Real Sea. *Proceedings of International Symposium "Ship safety in a seaway: stability, manoeuvrability, nonlinear approach"*, Kaliningrad, 15-19 May 1995, Vol.2, paper 8
9. Boukhanovsky A.V., Degtyarev A.B. Nonlinear Stochastic Ship Motion Stability in Different Wave Regimes. *Transaction of International Conference CRF-96, St.Petersburg, June 3-9, 1996. pp.296-306*
10. Davidan I.N., Lopatukhin L.J., Rozhkov V.A. Wind Waves in the World Ocean. Leningrad, Hydrometeorol. Ed., 1985, 256 p. (in Russian)

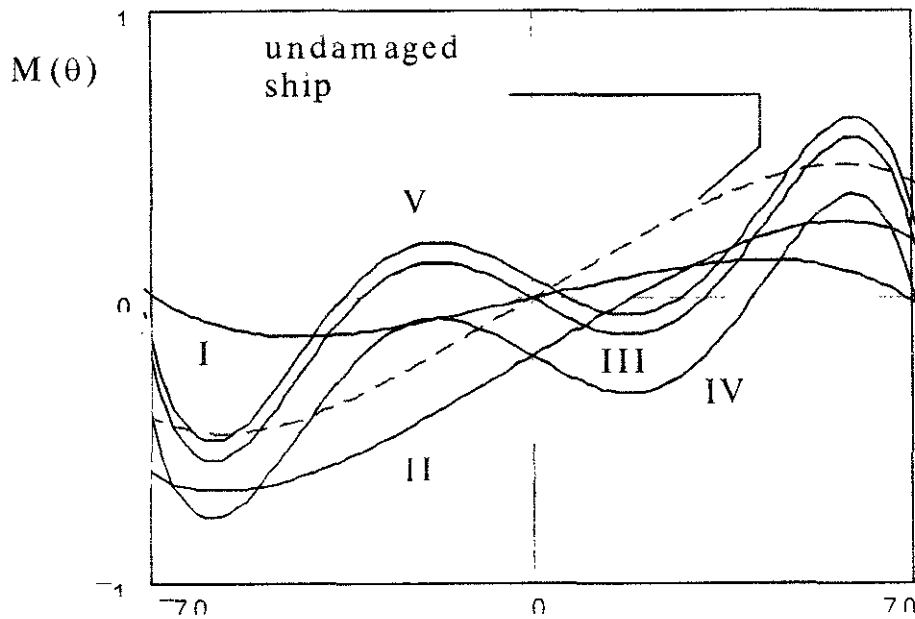


Fig.1. Stability diagrams for initial situation (undamaged ship) and five final (I-V) situations for different scenarios of progressive flooding.

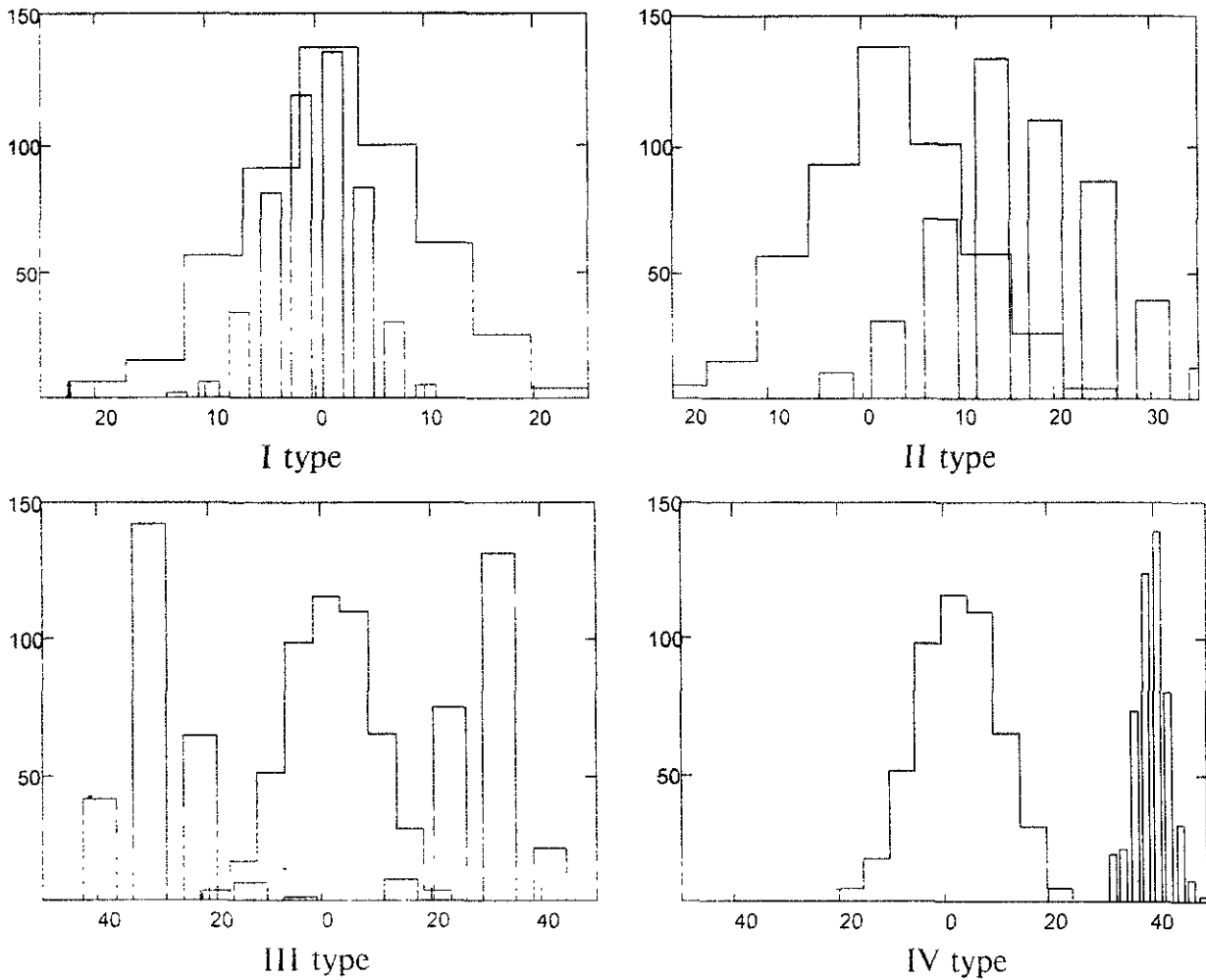
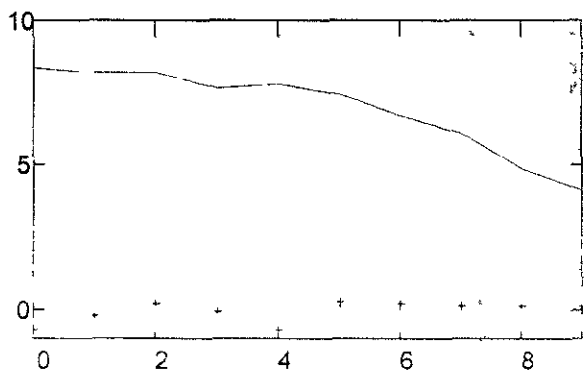
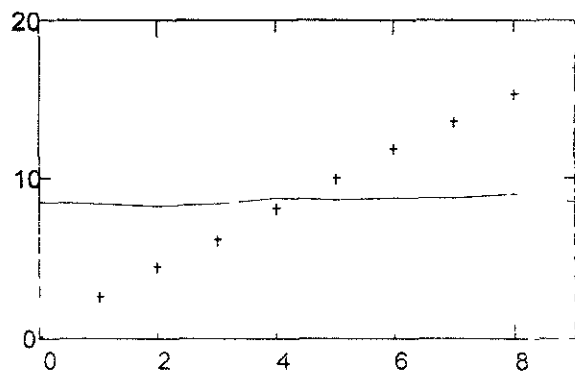


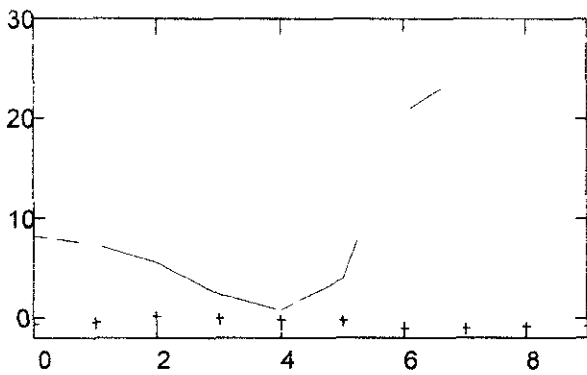
Fig.2 Estimations of roll distribution in initial (step line) and final (histogram) moments for different scenarios of progressive flooding (I-IV types)



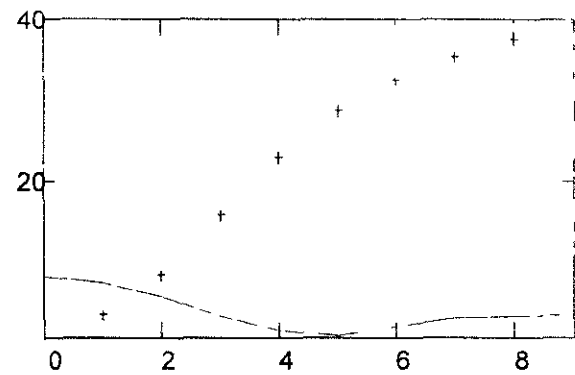
I type



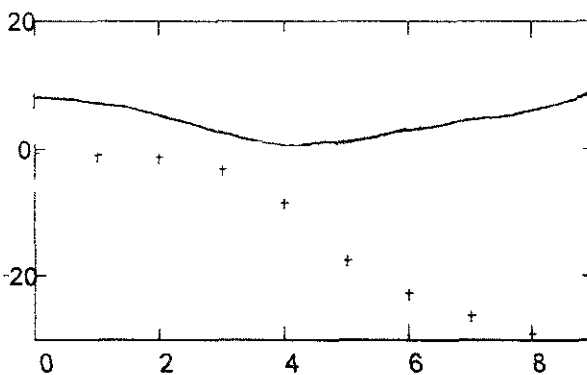
II type



III type

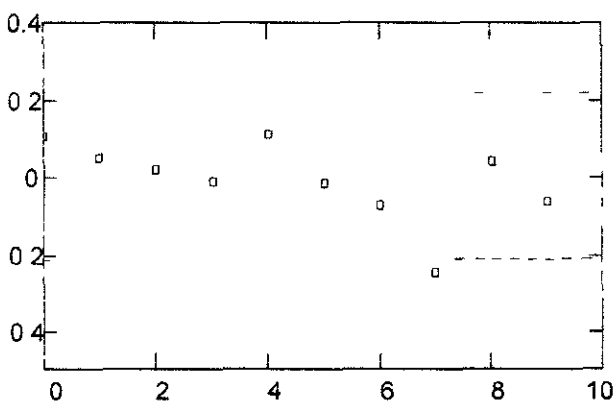


IV type

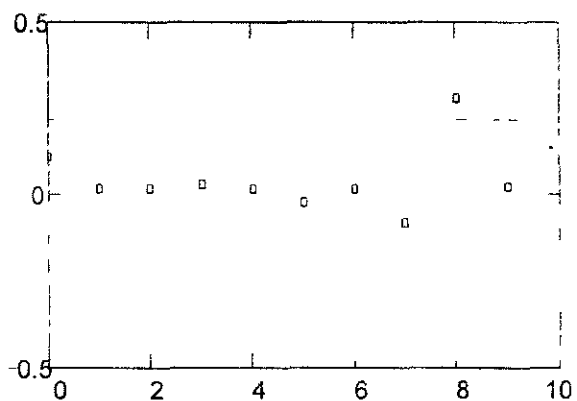


V type

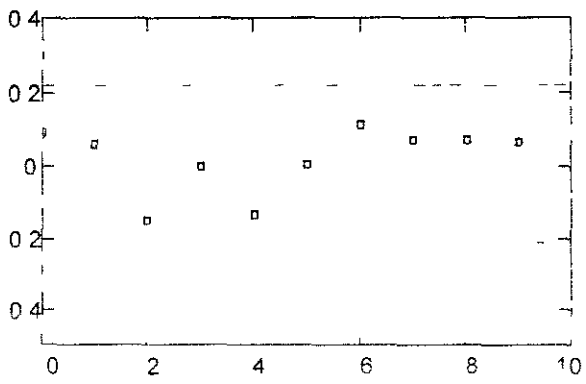
Fig.3 Evolution of mean roll angle ( $\bar{\theta}(t)$  - points (+)) and standard deviation ( $\sigma_{\theta}(t)$  - solid line) estimations for different scenarios of progressive flooding (I-V types). (rolling - degrees, time - minutes)



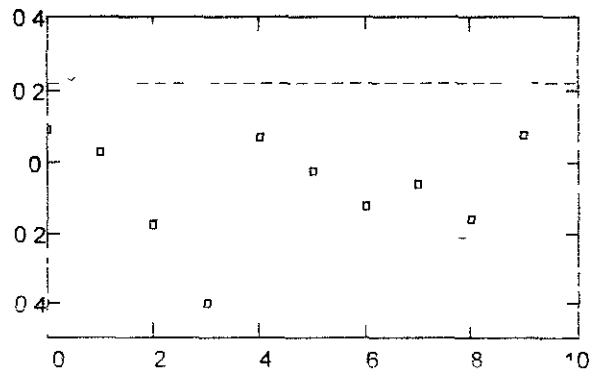
I type



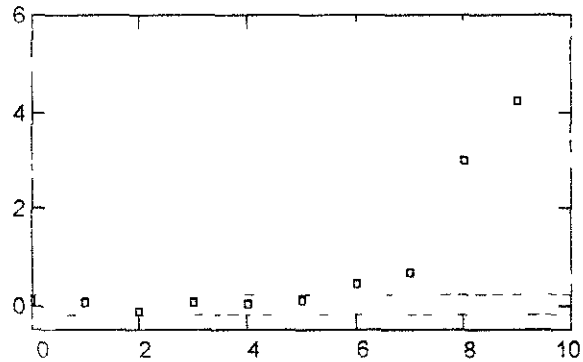
II type



III type

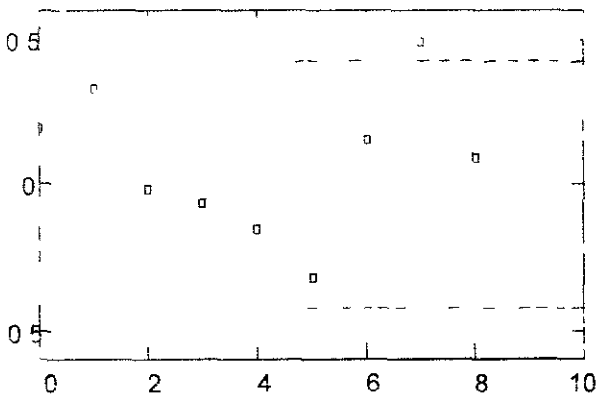


IV type

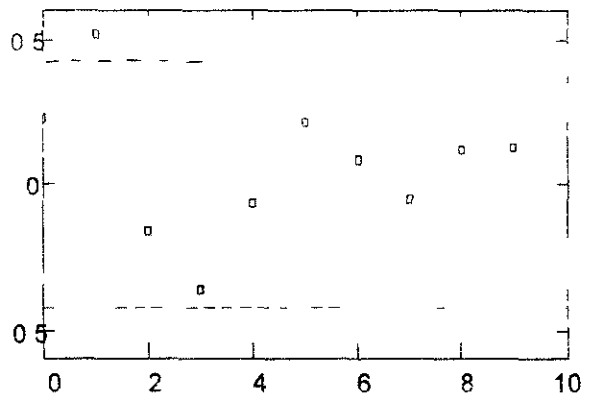


V type

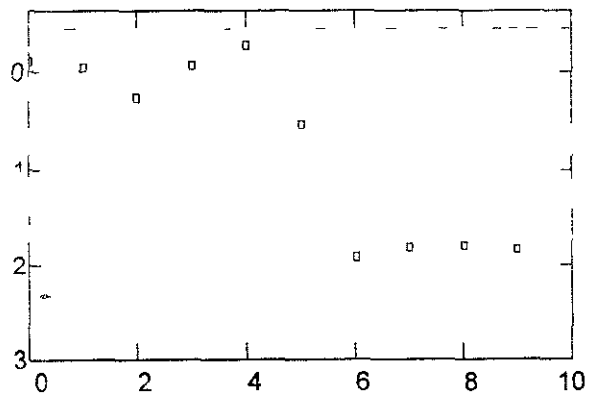
Fig.4 Evolution of std. skewness estimation (points), dash - boundaries of 95% gaussian confidence interval



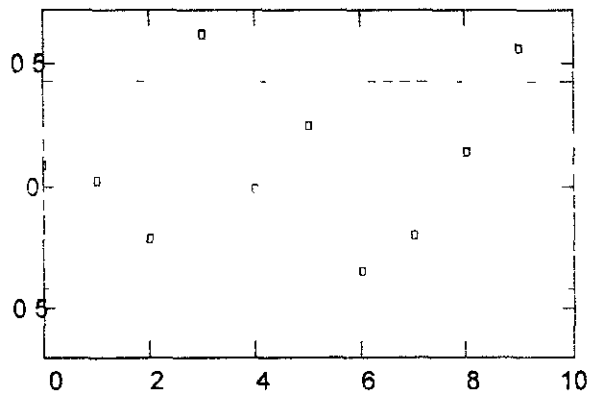
I type



II type



III type



IV type

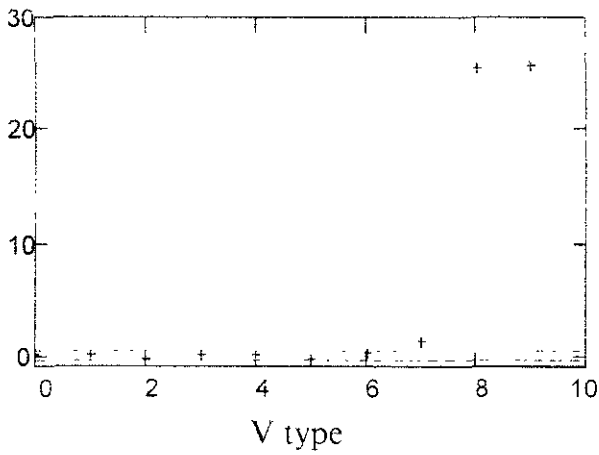
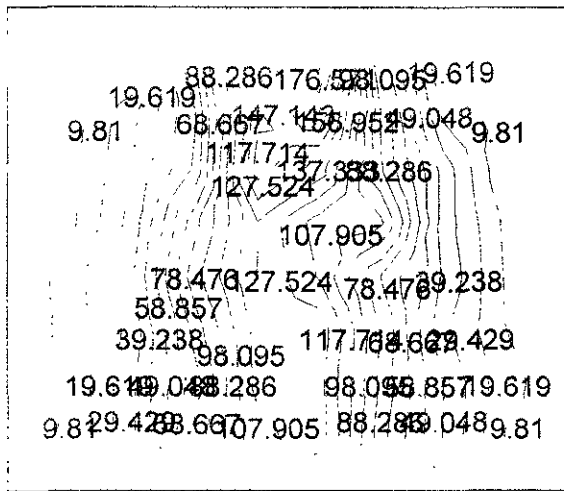
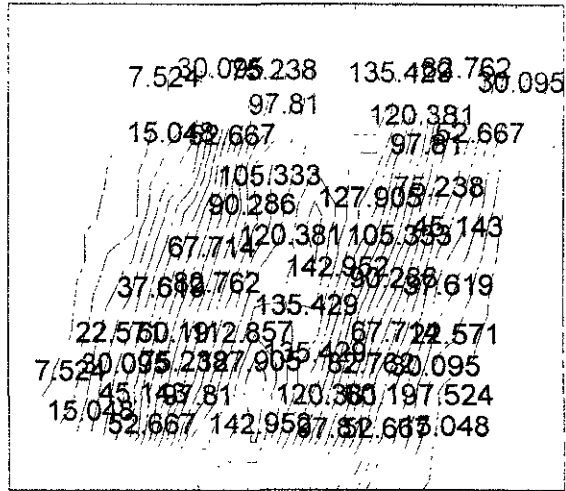


Fig. 5 Evolution of std. kurtosis estimation (points), dash — boundaries of 95% gaussian confidence interval.



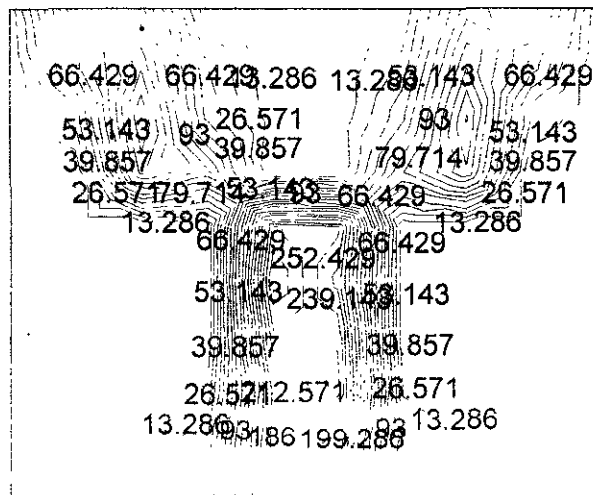
E

I type



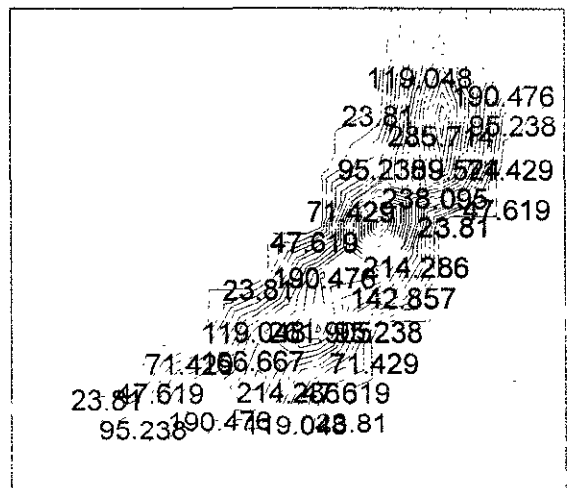
E

II type



E

III type



E

IV type

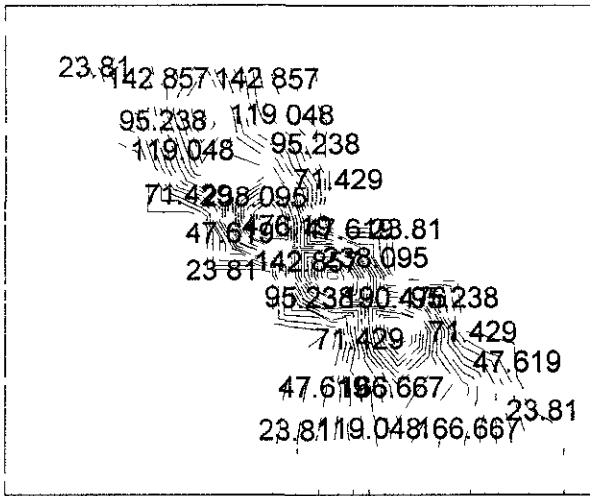


Fig.6 Evolution of rolling recurrence estimation for different scenarios of progressive flooding (I-V types).

E

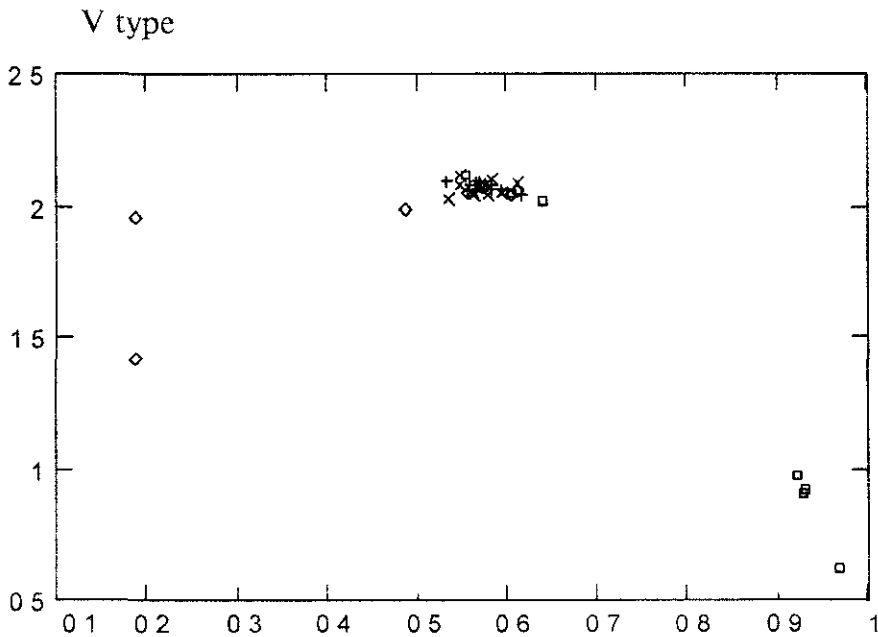


Fig.7 Distribution laws of rolling under all sections in terms of contrakurtosis (ordinate) and entropy coefficient (abscissa) (+ - type I; x - type II, □ - type III, ◇ - type V)

# EXPERIENCES WITH ON BOARD COMPUTER (EXPERT) SYSTEMS FOR STABILITY AND STRENGTH; OBJECTIVES FOR THE COMING YEARS.

R. Kleijweg  
Scheepsbouwkundig Advies en RekenCentrum SARC BV  
The Netherlands

## ABSTRACT

The Scheepsbouwkundig Advies en RekenCentrum (Naval Architectural Software and Engineering Centre) SARC BV since 1980, holds a leading position on the development and sale of software for the marine industry and on the execution of complex engineering tasks in the field of, among other things, stability, damage stability, longitudinal strength, hull design and production fairing.

LOCOPIAS, a derivative of the PIAS shipdesign system, is specially designed for on board use. The first chemical tanker was equipped with LOCOPIAS in 1993, because of classification society requirements regarding damage stability. More and more ship-owners and shipmanagers discover the qualities of LOCOPIAS. It is now, in 1997, installed on board of 75 various types of vessels, with various specific requirements.

This paper will discuss the market requirements as well as the governmental directives, with respect to onboard expert systems for (damage) stability control.

## 1. HISTORY

Since the beginning of the 1970's computers have been introduced for the calculation of stability on board of ships. Loading manuals, which included standard loading conditions, hydrostatic particulars, stability particulars

and tank particulars, were used to calculate the current loading condition. The resulting vertical centre of gravity (VCG) of this loading condition was compared with a maximum allowable VCG-curve according to IMCO regulations.

Options were SOLAS-74 calculations for grain stability. The numerical functions and the shipdata were programmed in a PROM. Results were displayed on a monitor and printed on a sort of cash slip.

Since the personal computer (PC) has become common good, they have also been introduced for on board use. Accordingly, the computer programmes have been adapted to the possibilities of the PC.

Apart from the hardware evolution, more and more requirements from the authorities and the industry have lead to the contemporary high standard in on-board computer (expert) systems.

## 2. GENERAL REQUIREMENTS

General requirements for on board computers can be distinguished in the following groups :

- i) Stability and strength requirements, by legislation
- ii) Quality Assurance (QA) requirements, by legislation and industry
- iii) Program function requirements, by ship owner and ship operator

In many cases the requirements of the diffe-

rent groups overlap.

### 3. STABILITY AND STRENGTH

The contemporary international requirements from the International Maritime Organization (IMO) and the requirements from the classification societies imply the software requirements. These requirements concern :

1. Calculation methods
2. Program operation
3. Presentation of the results

#### 3.1 Technical requirements of the calculation methods

The high speed of the personal computers have made it possible to apply more sophisticated calculation methods, which result in more accurate and physically more correct results. The classification societies and the authorities have adapted the regulations accordingly. This means that contemporary computer applications must include the following functions :

For the intact stability :

- calculation of the hydrostatics with the actual list and trim of the vessel
- calculation of the dynamic stability with the free to trim effect (constant longitudinal centre of gravity LCG)
- calculation of the weather criteria (heeling moment due to wind)
- correction for free surface moments (FSM) of tank contents based on the actual level in each tank, with the actual list and trim of the vessel
- as an option the centre of gravity and the actual FSM of the tank contents may shift as the vessel inclines. This gives an even better simulation of the behaviour of the ship.

For the longitudinal strength :

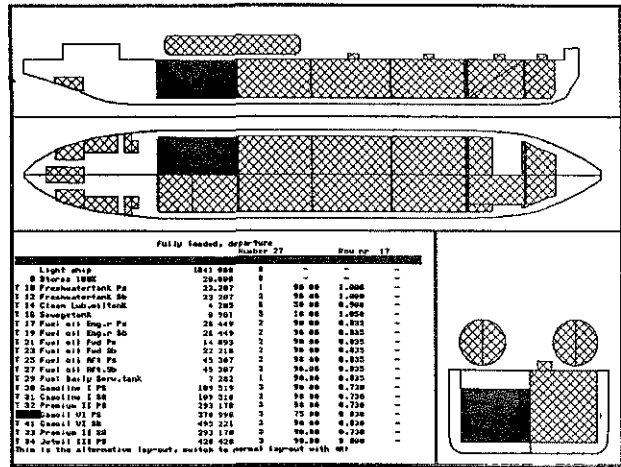
- numerical integration of the actual weight loading
- numerical integration of the buoyancy based on the actual list and trim
- calculation of shearforce, hogging moment, sagging moment at a variable number of

fixed locations, the so called readout points [1].

For the damage stability :

- direct calculations, without the use of maximum allowable VCG curves, see par.3.1.2.
- calculation of the sinkage based on the hull geometry taking into account (partial) deck immersion

In order to be able to place the above technical requirements in the perspective of marine safety and pollution prevention, the traditional calculation methods are set against the contemporary methods. In order to cover all aspects of the requirements a chemical tanker is used as an example.



Chemical tanker

Fig.1

To cope with an infinite number of loading conditions present interpretations of the IMO regulations require that tables or diagrams of maximum allowable Vertical Center of Gravity (VCG) are calculated for every combination of draft, trim, percentage of filling of each cargotank and specific weight of contents of each cargotank. With those tables or diagrams of maximum allowable VCG the master of the ship is able to verify whether the actual VCG' (corrected for free surface effects) of an actual loading condition is less than the maximum allowable VCG for the

*draft, trim, rate of tankfilling and specific cargoweight of that loading condition.*

This manual process of verification is laborious, time consuming and error-prone, so adequate assistance of computer technology is indispensable in the light of contemporary requirements of quality assurance and marine safety.

### 3.1.1 Traditional calculation methods

Basically the traditional methods of calculation may lead to two kinds of inaccuracies :

i) As mentioned before the actual VCG of an actual loading condition is corrected for free surface effects. Traditionally this correction is made on basis of the free surface moments (FSM) of all partially filled tanks (so including all cargotanks, because complete filling of cargotanks is prohibited). Correction with the FSM's assumes implicitly that correction is constant over all angles of inclination. At higher percentages of filling (about 60% to 70% and more) for cargotanks this leads to an overcorrection at angles of inclination of more than about 5 degrees. So the standard method of correction for free surface effects may lead to the conclusion that the vessel does not comply with (damage) stability criteria, while a more precise method of calculation may indicate that the vessel does comply. ***This may lead to sub-optimal loading of the vessel !***

ii) IMO interpretations require maximum allowable VCG tables or diagrams to be made for *every* combination of draft, trim, rate of filling and specific weight of contents of each cargotank. It is common practice that maximum allowable VCG tables or diagrams are calculated for combinations of some *fixed* values of draft, trim, rate of filling and specific weight, while to decrease the number of calculations it is often assumed that neighbouring cargotanks do have equal

rate of filling and specific weight.

All these simplifications decrease calculation accuracy of course and may also lead to sub-optimal loading.

Even in these days of high-performance computing occasionally a so-called envelopped curve of maximum allowable VCG is used, which represents the *minimum* of all maximum allowable VCG's. While this envelopped curve is more convenient to use for the master, its accuracy is so low that it certainly leads to non-optimal loading.

### 3.1.2 Contemporary calculation method

Contemporary computer programs are based on the geometry of hullform and compartments. This allows for all calculations to be made by *direct* calculations, so the program does not need precalculated tables of hydrostatics, stability or maximum allowable VCG'. Optionally the correction for free surfaces can be performed on basis of the *actual* shift of the liquid at every angle of inclination. The shift of all liquids should be calculated both in transverse and longitudinal direction, because the trim will change as the longitudinal centre of buoyancy (LCB) changes when the heeling angle of the vessel changes.

### 3.2 Program operation

In order to obtain a reliable software program, certain parts have to be protected against accidental changes. Furthermore the program has to be accompanied by a thorough manual. Lloyd's Register has been the precursor in defining directives for loading computer software [2].

A number of aspects are to be considered along with the software :

i) Security; the software program as well as the basic shipdata (hull form, light ship weight, compartments, non-watertight openings etc.) must be stored in binary code in order to avoid any easy changes. On top of that the software program must check the validity of the shipdata all the time, and reject calculations if the check fails. Future changes to the shipdata or

the program must only be possible by the manufacturer.

In order to check the computer hardware on malfunctioning the software must include a test procedure which results in a known outcome, which is calculated by the manufacturer.

- ii) Crew training; there should be a thorough training for the crew along with the delivery and installation of the software. If the crew changes from ship regularly, the total crew of the fleet should follow a training.
- iii) Manual; a so called Operation Instruction Manual (OIM) must accompany the software. This OIM is a reference book for the operation of the program, the input data of the loading computer program and the test conditions.
- iv) The supplier of the loading computer has to ensure continued service and support also after installation.

### 3.3 Presentation of the results

A number of requirements are described concerning the presentation on paper of the results of the damage stability, intact stability and longitudinal strength calculation.

**Intact stability :** light ship weight fixed in each loading condition, specified list of all deadweight items, hydrostatic particulars, initial stability, dynamic stability, statical angle of heel, calculation of wind moments, calculation of maximum allowable VCG' and the conclusion whether the loading condition complies with the stability criteria.

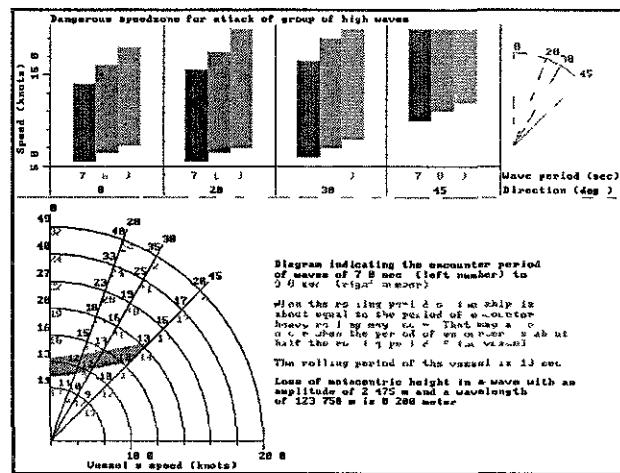
**Damage stability :** for the above loading condition all anticipated damage cases have to be calculated. These damage cases are fixed in the software and not editable. Apart from that it must be possible to calculate each anticipated damage case. Statical angle of heel, trim, initial stability G'M, range of the righting lever curve must be presented. A certificate of compliance can be printed as an option.

**Longitudinal strength :** graphs of maximum allowable and actual shear forces, sagging moments and hogging moments. Calculation

of the ratio between actual and permissible values at fixed locations.

### 3.4 Individual requirements

Dependent on the type of vessel specific requirements may be applicable. These requirements are mainly initiated by the ship owner. Items one could think of are: crane loading, container loading, import and export of loading conditions for electronic mailing, seastate diagrams (Fig.2), connection with tank measuring systems, grain loading and stability according to the Graincode, simulation of roll on roll off operations, stability of a grounded ship, functions for administration, production of special reports etc.



Seastate diagram

Fig.2

## 4. RESUMING THE OBJECTIVES

The main objectives of the loading computer on board can be listed as follows :

- i) increment of control room efficiency
- ii) increment of loading capacity, specially in the case of ship types with critical stability behaviour
- iii) increment of ship's safety, both for the stability as the strength aspect
- iv) eventually better insight in avoiding accidents
- v) by uniformity in requirements for the loading computer and the presentation of the results, the local authorities have a

better insight in the safety of the ship.

The question should be asked if above goals are achieved. They can be achieved if the following conditions are met :

- i) a protocol must be available for the ship's crew, that describes the procedures to follow. This procedure must be checked at regular intervals. The mainframe for certain procedures is given in the ISM code [4], however this code does not describe the filling in of these procedures. This is exactly the bottleneck of the working of the ISM code. How the procedures can be incorporated in the daily process is amongst others described in [5]. A ship owner and ship operator should apply an administration system and train the ship's crew in order to secure a continuous standard of quality. Only few ship owners currently work according to this ISM code, although it will become effective not later than 1 june 1998.
- ii) For the ship owners and the manufacturers of the loading computers, the classification societies and the local authorities should unify their requirements on all subjects described in par.3. Nowadays all are working with their own directives, which makes it very hard to satisfy them all. Off course this is also caused by the fact that the ISM code mainframe has to be filled in by the local authorities, the classification societies all have their own interpretation of guidelines from the International Association of Classification Societies (IACS). Attaining general class approved loading computer software is therefore a laborious and uncertain job. Especially in the case of damage stability the ship's crew could profit an advantage when using type approved software. In the case of a chemical tanker each loading condition in combination with each damage case is determined by direct calculation. A conclusion is drawn whether the loading is safe or not. Without the use of a computer this is

impossible, see par.3. Lloyd's Register has described a procedure for the damage stability calculation in [2], but has withdrawn this section in [3] in the paragraph 3.5 describing : *"The damage stability component of a loading program is not included in the general approval"*. In the light of the quality assurance (QA) and the ISM code this is to be regretted. Especially since Germanischer Lloyd does not have a guideline for loading computer software, but does have an approval procedure for damage stability nowadays. Technically everything is possible, but the authorities and classification societies should draw one line in order to achieve the goals.

- iii) In terms of efficiency the contemporary computer programs have proven their worth. Once the ship's crew has discovered the abilities, they tend to use the loading computer more and more. The use of the loading computer becomes self-evident, if parts of the software are tailor made to the requirements of the ship owner. Many ship owners have discovered the advantages of a modern computer program in terms of higher efficiency, higher quality, more safety and higher payloads. In this sense the introduction of the on board loading computer meets the expectations.

## 5. DEVELOPMENTS FOR THE YEARS AHEAD

The filling in of the ISM code, with respect to the on board computers for stability monitoring, should be centrally coordinated. The local authorities can then use these general directives for a national directive.

The body of the IACS could be used to make one uniform guideline for the classification societies. This improves the level of quality and marine safety. Currently the interpretations of a classification society depend fully upon the personal taste of the examiner.

## 6. RESUME

In the case that all direct calculations are incorporated in an on board expert system this will allow the crew to concentrate on the actual loading of the vessel and monitor the effects of the loading which is in progress by checking the stability at regular intervals. Specialized ship-type dependent software programs even raise the on board safety to a higher level.

In the coming years efforts have to be made to set a global standard and a uniform interpretation of the ISM code and the classification society requirements. Only then the sophisticated technical opportunities are reclaimed to a maximum and will contribute to a higher level of marine safety. Apart from all technical solutions the human factor remains essential; without applying the proper procedures, the computer has no value.

## REFERENCES

1. Procedure for approval of multipoint loading instruments, Lloyd's Register, may 1988.
2. Lloyd's Register's procedure for approval of loading instruments with stability computation capability, final rev.1, april 1994.
3. Approval of longitudinal strength and stability calculation programs, Lloyd's Register, january 1997.
4. International management code for the safe operation of ships and for pollution prevention, (International Safety Management ISM code ), IMO resolution A.741(18), 4 november 1993.
5. Code of shipmanagement standards (ISMA code), International Ship Managers Association, issue 2, september 1994